Laboratory modelling of soil collapsibility

Okwedadi, Chinyelugo

Award date:
2015

Awarding institution:
Coventry University

Laboratory Modelling of Soil Collapsibility

By

Anne Chinyelugo Okwedadi

PhD

August 2015

Laboratory Modelling of Soil Collapsibility

By

Anne Chinyelugo Okwedadi

August 2015

A thesis submitted in partial fulfilment of the University's requirements for the Degree of Doctor of Philosophy

DECLARATION

I declare that the work in this research project entitled “Laboratory Modelling of soil Collapsibility” has been performed by me in the Department of Computing and Engineering under the supervision of Dr Samson Ng’ambi and Dr Eshmaiel Ganjian. The information derived from the literature has been duly acknowledged in the text and list of references provided.

DATE: _

Anne Chinyelugo Okwedadi

ABSTRACT

Collapsible soils covers naturally over 10% of the earth's surface. This makes it a global problem and it is essential that engineers identify and control collapsibility prior to construction. Hence in this thesis, a study on identification, evaluation and control of soil collapsibility is undertaken.

Four geologically different soils have been tested at five compactive variables from optimum moisture content (OMC). The soils tested include: Brown inorganic silty clay of low plasticity (A); White inorganic silt with slight plasticity (B); Red inorganic clay of intermediate plasticity (C); and Brown sand-clay mixtures with inorganic clay of low plasticity (D). The soils were each compacted at moisture variations 60% - 80%, 80% - 95%, 95% - 105%, 110% - 125% and 125% - 150% respectively representing 'Low Dry OMC', 'High Dry OMC', 'At OMC', 'Low Wet OMC' and 'High Wet OMC'.

The major causes of collapsibility of soil and the geomorphological processes that gives the pedogenesis of collapsible soils, is highlighted and great emphasis is placed on the adverse effect of collapsible soils.

The experimental results from particle size distribution, Atterberg, compaction, triaxial and double oedometer tests showed that the soil's percentage fine with the fines material (silt or clay), coefficient of uniformity, optimum moisture content, Atterberg limits, and stress-strain properties affect the metastability of the soils and they can be compared to the soil's collapse potential when pressures and moisture content are applied on the soils.

Results obtained showed that the soil's collapse potential is directly proportional to 1) percentage fines, 2) the difference between the silt and clay percentage, 3) the Atterberg limits (liquid limit, plastic limit and plasticity index), and 4) internal friction angle; and

inversely proportional to 1) coefficient of uniformity, 2) initial moisture content, 3) cohesion and finally 4) peak deviator stress. Each soil's geological property proved to have an adverse effect on the metastability of the soils especially the dry of optimum moisture content.

The most interesting results were obtained from the oedometer test. Results of the critical pressure varied with each soil and their compactive variable; Most of the soils at their 'dry OMC' had the highest collapse potential. In general, the lower the critical pressure the higher the collapse potential of the soil.

The experimental data obtained herein were checked with the past research collapse indexes and found the results agreeing with just two research work out of eighteen examinations.

Finally models for identifying soil collapsibility are generated with relationship between parameters from sieve, Atterberg, proctor compaction and triaxial. Laboratory data and data from twelve research work were used to verify the models and they show that the models work. After the verification of these formulas with past research data collected, the best models were three compactive variable models. The models give a collapsibility index in terms of percentage fines, initial moisture content, initial degree of saturation and initial dry density.

ACKNOWLEDGEMENT

I am most grateful to God Almighty, for helping me complete this thesis successfully and for good health of mind and body through this period and always.

To my family, for all their support, love, care and provision given me, I say thank you. May God richly bless each one of you. I love you all.

I express my profound gratitude to my thesis supervisors, Dr Samson Ng'ambi, Dr Eshmaiel Ganjian and Prof Ian Jefferson for their selfless dedication to this thesis. Their patience, guidance, motivation and his professional criticisms strengthened me and brought out the very best in me.

I am also indebted to all my colleagues in the Department of Computing and Engineering whose inspiration, encouragement and support has brought me thus far, especially Mr Terry Teeling, Mr Kieran Iehane, Mr Alan McDonald Mr Ian Breakwell and Mr Alain Binga. I'm really grateful.

To my personal advisors and friends, for all your time, concern and care, I can never thank you enough; Theodore Ubah, Muriel Iten, Florence Osugo, Inalegwu Ella and Felix Jojo. May God grant all your heart desires and bless you. I will miss you all.

Special thanks go to the love in my life. I bless God for bringing you my way. Your support has been uncanny. You've made me believe in myself every step of the way. Thank you. Mr Theodore Ubah. I love you more every single day.

NOMENCLATURE

CP - Collapse potential, Collapse index, Coefficient of collapsibility, subsidence index

Cu – Coefficient of uniformity

Cc – Coefficient of curvature

D10 - Maximum size of the smallest 10%

D30 - Maximum size of the smallest 30%

D60 - Maximum size of the smallest 60%

Gs - Specific gravity

MC – Moisture content

W_0 – Initial/natural state water content

W_{max} – Moisture content at saturation

ρ_w – Density of water '1g/cm^3'

ρ_{bulk} – Bulk density

L_L – liquid limit, water content at liquid limit

P_I is the plasticity index,

P_L- plastic limits

A – Area of sample

γ_d - Dry unit weight,

γ_{dn} - natural dry unit weight

γ_w - Unit weight of water. '9.81kN/m^3'

ρ_w – Density of water '1g/cm^3'

ΔP – change in pressure

P_{cr} - critical pressure

P_w – Pressure at wetting

d - Thickness of the soil layer

σ - Total stress

τ_f – Shear strength

C' – Effective cohesion

φ'– Effective internal angle of friction

θ – angle between major principal plane and the plane of failure

σ_1' – Effective principle stress 1

σ_3' – Effective principle stress 2

σ_f' – Effective normal shear at failure

σ_{max} – Peak deviator stress

$(\sigma_n - u_a)$ = net normal stress;

$(u_a - u_w)$ = matric suction; and

(χ) = is a parameter dependent on the degree of saturation. It varies from 1 for fully saturated soil to 0 for totally dry condition.

H – Sample height

H_s – Height of solid particles

H_o – initial sample height

Δh_i – Initial change in sample height

Δh – change in height

e – Void ratio

e_0 – Void ratio at initial moisture content, natural moisture content, before saturation

e_f – Final void ratio

Δe = Void ratio reduction

$e_{m,max}$ – Void ratio macro pores

e_L – Void ratio at liquid limit

$_d$ –Before inundation

$_w$ - After inundation

Sr - Degree of saturation

Sr_0 – Natural/Initial degree of saturation

$D = \frac{1}{Sr}$ - Deficiency of saturation

M_s – Mass of solids

M_t – Mass of soil in ring

DS_{70} – Maximum derivative stress at 70 kPa confining pressure

DS_{140} – Maximum derivative stress at 140 kPa confining pressure

DS_{280} – Maximum derivative stress at 280 kPa confining pressure

e_{pL} – Void ratio at plastic limit

e_p – Void ratio at total vertical loading from overburden pressure at certain depth

e'_p – Void ratio at same pressure after wetting and collapse

n_0 - natural porosity

t_{90} – Value corresponding to the D_{90} point on the square root time curve graph

Mv – Coefficient of volume compressibility

Vs – Volumetric strain

Cv – Coefficient of consolidation

K – Coefficient of permeability.

TABLE OF CONTENTS

LIST OF TABLES

LIST OF FIGURES

1 INTRODUCTION

1.1 Research background

Collapsible soils, which cover naturally over 10% of the earth's surface, represent a global problem (Evans et al 2004; Northmore et al 2008). Collapsible soils in general are unsaturated soil that goes through a radical rearrangement of particles causing loss of volume due to seismic activities, or/and wetting, with or without additional loading. Collapsible soils are typically silt and sand size with a small amount of clay, pedogenesis via dry alluvial (water) fan, colluviums (gravity) and Aeolian (wind-blown) deposits; They are porous soil structures that show relatively high apparent strength (cohesion) in their dry state, have low density, and are susceptible to large settlement upon wetting; their collapse severity is affected by the extent of wetting, depth of the collapsible soil deposit, the load from overburden weights (e.g. structure) and the collapse potential of the subsoil (Pereira and Fredlund 2000; Houston, Lawrence 2002; Evans et al 2004; Rafie, Moayed, Esmaeli 2008; Northmore et al 2008; Frye 2009; Jefferson and Rogers 2012).

The most common collapsible soil known is the loess soil. Loess was first formed when glaciers covered the earth; the warm temperatures melted the glaciers creating flows of water down into valleys or rivers, fluvial transportation from the piedmount region and out into the desert exposing the mud; when dried, strong winds blew the exposed debris and gathered the finer materials from the flood plains into huge clouds of dust, which were deposited into banks and higher piles of loess form; with each individual glacier deposit and post-deposition a palaeosol of loess soil is produced (Derbyshire and Meng 2005; Smalley et al 2006).

With the recent occurrences, sinkhole is one of the most common and most hazardous collapses. This subsidence is most commonly caused by changes in ground water levels and processes of erosion; they are found worldwide. The mechanism that is responsible for the appearance of sinkholes is the disintegration of soluble rocks and the creation of subsurface cavities that collapse when not adequately supported (Martinez et al., 1998; Gutierrez and Cooper, 2002; Waltham et al., 2005; Parise, 2008; Shalev and Lyakhovshy 2012).

1.2 Motivation for this study

Several failures from collapsible soils have caused millions of dollars' worth of damage to public facilities e.g. schools, roads, water tanks and other infrastructure and so have an adverse effect on living and even lives. The damages are from shear failure of cementation bonds when dry (due to loading which transcends the soil's critical pressure), soil liquefaction due to hydro-collapse, or differential settlements (Das 2004) which was not anticipated for, at the design and construction stages. This is and has been a challenge on the developer, designer and engineer in charge of such a site; so prior to construction, determination and identification of collapse potential of a soil is important.

1.3 Key past studies

In the class of collapsible soil several researchers have classified soil collapsibility; each one based their criteria on different parameters. The parameters are shared into four categories, namely:

- Atterberg with soil properties parameters,
- Void ratios of the soil parameters,

- Numerical limit parameters (like dry density, clay content, critical pressure, and moisture content at liquid limit and saturation),
- And the graph category for dry density and liquid limit.

1.3.1 In the 'Atterberg with soil properties parameters' category, for collapse:

Batygin (1937) $\frac{W_0}{L_L} * \frac{1}{Sr} > 1$ *Equ 1.1*

Denisov (1951) $\frac{L_L}{\frac{\gamma_w}{\gamma_d} - \frac{1}{Gs}} < 1$ *Equ1.2*

Priklonskij (1952) $\frac{L_L - W_0}{L_L - P_L} < 0.5$ *Equ1.3*

Feda (1966) $\frac{\frac{W_0}{Sr_0} - P_L}{L_L - P_L} > 0.85$ *Equ1.4*

Gibbs & Bara (1962) and Handy (1973) $\frac{W_{max}}{L_L} \geq 1$ *Equ1.5*

1.3.2 In the 'soil's void ratios' category, for collapse:

Abelev (1948), Jenning & Knight (1975) and Hormdee, Ochiai, & Yasufuku (2004) propsed the criteria

$\frac{\Delta e}{e_0+1}\% > 2\%$, 6% and 10% respectively *Equ1.6*

Denisov (1951) $\frac{e_l}{e_0} < 1$ *Equ1.7*

Lehr (1967) $\frac{e_0 - e_l}{1 + e_0} > -0.1$ *Equ1.8*

1.3.3 In the numerical limit category:

Clevenger (1958) - Dry density is less than 1.28Mg/m^3,

Larionov (1959) - Critical pressure is less than 0.15MPa,

Handy (1973) - Clay content is less than 16%,

Grabowska-Olszewska (1988) – natural moisture content less than 6%,

1.3.4 And for the graph category:

Gibbs & Bara (1962) and lutennegger & saber (1988) – graph of dry density against liquid limit of which at 25% liquid limit, the soil is collapsible. See Figure 1.1.

Figure 1.1: Collapsibility based on Gibbs and Bara (1962) and Lutennegger and Saber (1988) study

1.4 The research question and gaps

The initial literature study by the author revealed that most of the studiesthat have been carried out in the past on collapsible soils, have focused on areas that are not naturally collapsible. Ironically, many cases of collapse related geotechnical problems have been observed for soils not considered to be the classical collapsible soils.

In the light of this review, this study poses the following research question: “should study on collapsibility be limited only to soils classified as ‘collapsible soils’ or to all

soils that exhibit the nature of collapsible soils?". The author believes the answer is an ensured **YES.**

This study has identified the following gaps in knowledge:

- In the identification and classification of collapsibility (ability to recognize and establish related properties of the soil that makes it collapsible),
- In the estimation of collapsiblility critical indexes for geological properties of a soil represented in groups of soil type (fabric properties), compactive variables (factors of soil samples prepared at varying moisture content) and critical pressures (the pressure at which a maximum collapse is observed).
- In the assessment of the effects of inundation, pressure and compactive variables on collapsible soil structure.
- And in a design factor of safety to be applied as a check prior to construction to prevent the damages caused by soil collapsibility.

1.5 Aims and Objectives

This research aims to:

- Give an elaborate review of collapsible soils
- Simulate and investigate the geological factors that control collapsibility of the soils.

The objectives of this research include:

- Study the influence of soil type on collapsibility by testing four geologically different soils.
- Investigate the effect of compactive variable (moisture content, density, degree of saturation) varied by synthesizing the four soils at five moisture variations each producing structures to study the metastabilty of a soil structure.

- Determine the impact of critical pressure applied on a soil structure when in its as-compacted state and in its saturated state.
- Produce a collapse index for identifying collapse-susceptible states of a soil.

1.6 Methodology of the research

In this research all the objectives are put into consideration and studied using four geologically different soils (depending on the soil fabric). These soils are prepared at five varying soil structures which is a percentage of the individual soil's optimum moisture content (compactive variables). Each soil structure is tested for its collapse potential by finding the volumetric strain difference between its as-compacted state and its inundated state. The pressure at the point of collapse gives the critical collapse pressure. From the data obtained a collapsibility index is generated to give a factor of safety guide.

To achieve the aim of this research, the following steps are followed:

1. Discern the effects of the geomorphological processes (pedogenesis) of collapsible soils, by:
    - Describing the processes that occur in the generation of fabrics with metastable properties (provenance, erosion / transportation, deposition and post-depositional changes);
    - Stating the outcome of these processes in the evident geological properties of the soil;
    - Discussing the features in features and mechanism in collapsibility;
    - Mentioning the areas collapsible soils are typically found.
2. Prepare and observe synthesized metastable soils by:
    - investigating into knowledge of the properties of a typical collapsible soil;

- Selecting four geologically different soils, which are sieved through to maintain soil grain size less than 2 mm.
- Classifying these soils using sieve analysis, hydrometer, Atterberg and compaction test.
- Synthesizing metastable structured soils by using five moisture ranges at particular percentages from the optimum moisture content.

3. Investigate the effects of the different geological soil properties on collapsibility. These are measured in three features of:
    - Soil type (fabric, size and nature of the soil grains),
    - Compactive variable (bonding state-parameters such as density, degree of saturation, void ratio, water content) and
    - Critical pressure (soil's overburden pressure)
4. Discuss and compare past research work with results acquired from laboratory tests.
    - The past research work done is explored and categorized into groups of soil property.
    - Results obtained from the laboratory are used to check for collapsibility using the past research findings on factors controlling collapsibility.
5. The laboratory results attained are used for identification and modelling of collapsibility of soils:
    - The analyzed results are used for identifying the controlling effects collapsibility has on a soil structure
    - Results are used also to obtain a collapsibility index
    - The collapsibility index is checked with past research data.

1.7 Structure of Thesis

This thesis consists of six chapters:

Chapter 1 is the introduction. It gives an insight into the:

- Research background,
- Gap in knowledge of collapsibility of soils,
- Aims and objectives of this research,
- Method for achieving the aim of the research and
- Structure of the thesis.

Chapter 2 is the literature review. It covers the investigations in the:

- Geomorphological processes involved in a natural collapsible soil and the areas they are found.
- Features in collapse mechanism and the processes involved in the mechanism of collapse.
- Geological properties of collapsible soils: collapse predictors, factors that affect the severity of collapse, typical soil fabrics found with collapsible soils and matric suction a factor that has a close relationship with collapse in soil.
- Assessment and investigations on collapsibility of soils, from reconnaissance, field testing to laboratory test involved.
- Past research knowledge in coefficient of collapse.

Chapter 3 is the methodology chapter. It indicates the processes involved in the:

- Experimental work, where the technique for producing a metastable soil is discussed, procedures for soil classification tests, triaxial test and oedometer test are outlined and the standard codes are mentioned.
- Guides to the analysis of soil properties that affect soil collapsibility; this is looked at in the topics of Soil type, compactive variable and critical pressure.
- Quantifying collapsibility based on past studies.

Chapter 4 presents the laboratory test results and analysis. It gives an elaborate description of the data, graphs and tables obtained and analysed. The group results recorded include:

- Soil classification – particle size distribution (PSD), Atterberg and compaction test.
- Triaxial test
- Oedometer test.

Chapter 5 presents the discussion and modelling of collapsibility. This includes:

- Scrutiny of the laboratory results and their behavioral pattern with collapsibility of soils. They are looked at in the categories of soil classification, shear strength parameters and consolidation properties.
- Identification of collapsibility of soil in the classes of soil type, compactive variable and load. These would include collapse predictive models.
- Comparing the new collapse indexes with the past research's data.

Chapter 6 presents the conclusion and recommendations.

2 LITERATURE REVIEW

Soil collapsibility is brought about by changes in state parameter of an open structured soil. The classic collapsible soils are natural materials in which particle types and sedimentation mechanism combine to produce collapsibility. The metastable soil is seen as stable until its structure is triggered and then it becomes unstable and collapses.

One might be thinking the probability of a metastable soil collapsing is very low, but the triggers can be from minor earthquakes or wetting which can be caused by changes in surface and groundwater regimes, resulting from urbanization, cultivation, weather e.t.c.; often bringing significant increases in soil moisture contents and overburden pressure resulting in changes like stability, strength, matric suction, bonds and density which could lead to the collapse of the soil structure. The inevitable trigger is from inundation of the soil structure since it could happen naturally (from rainfall) or accidentally (from burst of pipe), from the top (e.g. Surface runoff and percolation of rain-water, irrigation, poor drainage and flooding), the bottom (e.g. Rise in groundwater table and capillary rise from the water table) or even within the soil layers (e.g. leaks from pipes, underground storage tank). This goes to show water-induced-collapse is of high possibility in the life span of the structure on the collapsible soil.

In essence, soil collapsibility is the loss of volume of open structured soil due to the influence of factors such as water, seismic activity, or/and stress. Collapsible soils need to be observed and identified so as to prevent the intended damages that could happen. Understanding the geomorphological formation, geological history and mechanical properties of a typical metastable soil would go a long way in aiding

identification, observation and prevention of the catastrophes that could befall the site in question.

2.1 Geomorphological Processes

Geomorphological is the study of the nature and origin of landforms and the processes that shape and give soils their properties. The natural creation of meta-stable soils is revealed as the formation process is observed.

Geomorphological changes are caused by physical (consolidation), chemical (changes like mineral addition, removal or transformation), biological agents (roots, worms, termites and various micro-organisms) or a combination of these agents. These changes can increase or decrease the jeopardy affiliated with collapse such that the deposition and post-depositional processes may increase or decrease soils shear strengths, denseness or sensitivity.

Figure 2.1: A classification of collapsible soils (Rogers 1995)

The natural process of particle generation (particle type and sedimentation mechanism) and the geology of the source region to which a soil is formed is what result in collapsibility (Derbyshire, et al. 1995; Derbyshire and Meng 2005) and the type of collapsible soil. Figure 2.1 shows the various types of naturally formed collapsible soils.

In this sub-chapter, understanding the processes involved in the pedogenesis of collapsible soil is investigated by looking at the interactions in weathering (disintegration), erosion (transportation and deposition) and the historical formation of loess soil which is a combination of these processes. Loess soil represents all forms of naturally formed collapsible soils, since it is the most commonly found and the most investigated.

2.1.1 Weathering processes

Weathering is the primary process in soil formation. It is the change and breakdown of rock minerals. The types of weathering processes include Physical, chemical and biological weathering processes and the location of their occurrence is dependent solely on the climate.

The physical weathering results into the mechanical disruption of rocks and its processes dominate in cold and dry climates (e.g. granular disintegration, exfoliation, joint block separation, shattering by changes in temperature or pressure) (Hong kong Geology 2009). This weathering produces soils that are angular-shaped of which more transportation and weathering could increase the roundness of the soil particle. Although, the history and type of source rock dictates the minimum size attainable during natural crushing and abrasion (Derbyshire and Meng 2005). Weathering which occurs immediately after deposition is often essential to the meta-stability of the soil (Rogers 1995).

Chemical weathering consists of processes of decay of rock forming minerals caused by water, temperature, oxygen, hydrogen and mild acids mineral; it dominates in warm and humid climates. During weathering like those of the granitic sands of south Africa, (Rogers 1995: 11-12) where the weathering process is geochemically controlled and is manifested by weathering of feldspar leaving a sub-rounded sand with an open

structure (loosely packed); the fabric encircling the primary mineral particles is altered to produce the meta-stable structure.

Biological weathering process is a supporting process caused by the presence of vegetation (root wedging), lesser extent animals, and the production of organic acids. They tend to be more active in warm and humid climates.

2.1.2 Erosion (Transportation and deposition)

Erosion is the movement of weathered rock materials away from their original site of weathering. Erosion processes are driven by the force of gravity, by a flowing medium such as water (e.g. rivers), and ice (e.g. glaciers), or gravity may act alone (e.g. rockfalls) or by wind movement (e.g. deflation).

Erosion processes are commonly considered under four groups (Hong kong Geology 2009): Mass Wasting: the processes that occur on slopes, under the influence of gravity, Fluvial: the processes that involve flowing water, which can occur within the soil mass (e.g. soil piping), over the land surface (e.g. rills and gullies), or in seasonal or permanent channels (e.g. seasonal streams and rivers). Wind: the processes that involve the action of rapidly moving air streams in dry areas, which can be cold or hot deserts. Glacial: the processes that involve the presence of ice, either in the soil (e.g. solifluction), or as the transporting medium (e.g. glaciers).

The different formations of collapsible soils can be based on their transportation and deposition formation. The mechanisms include:

- Alluvial (water deposited)
- Colluvial (gravity deposited)
- Aeolian (wind deposited) basically loess

Erosion is one of the main concerns in geomorphological process since its process of movement can set the stage for other factor to trigger the collapse or the collapse can be trigger collapse immediately (Torrance 1995:295).

The determination of the depositional, transportation and weathering history of the soil may provide an appropriate range of thickness and likely behaviour of specific collapsible soil units; also the behavioural properties are affected by the past and present climatic conditions. As observed “Wentworth (1933) favoured the transport mechanism as the major determinate of the grain size; Assalay et al (1998), that particle formation is as important determinant of the grain size of silts as the transportation process; Tsoar and Pye (1987) assert that wind transportation is the sorting mechanism; Fookes and Best (1969) affirm that processes operating during deposition as the principal determinant of the engineering properties of a soil; and Derbyshire and Meng (2005) states that the dominant control on thickness may be largely attributable to post-depositional events, since the loess accumulates to a thickness that effectively mask some or all of the morphology of the underlying terrain.” (Derbyshire and Meng 2005).

2.1.3 The Pedogenesis Events

2.1.3.1 Loess

Loess which is a wind deposit collapsible soil is the most widely distributed collapsible soil; covers approximately 10% of the earth’s land surface (Derbyshire and Meng 2005; Northmore et al 2008). Loess soil is a classic type of collapsible soil that is used herein to describe typical geomorphological processes. This is because it’s the most studied and the most encountered naturally (Jefferson et al 2001) in the area of collapsible

soils. The origin of deposition and formation of loess soils is from several different deposit formations which involve Eluvial, proluvial, Deluvial, Alluvial and Aeolian; but the worldwide paradigm theory is that of Aeolian deposition formation (Smalley et al. 2006).

In the formation of Primary loess deposits, Smalley, 1966 states 4 critical stages / events: provenance events for formation of silt-sized material (P), events for transportation of the silt particles (T), deposition of these particles (D1) and post-depositional changes (Wright 2001a).

Figure.2.2 shows the Loess material made in the mountains is carried out into the desert; perimontane and peridesert regions interact. T4 event cause widespread loess material distribution.

The events as explained by Smalley et al. 2006; are summarised in the following paragraphs.

P: making the material: The Pye and Sherwin (1999) diagram (Figure.2.2) locates the deposits in their piedmont (near foothills /footpath of a mountain range) position and suggests that the lower part of the deposit is alluvial and the upper part Aeolian material returned by the wind via a later event in the sequence.

T1: the first defined transportation event: The abundant fine material, produced in the mountains is moved down to the piedmont region.

D1: initial significant deposition: Mixed deposit is formed in the foothills region, which means that apparent D1 is actually D1 with a layer of D3 on top.

T2: The key second stage transportation activity could be putting the fine particles into large rivers for onward transportation out into the desert region.

T3: out into the desert: T3 allows these rivers to move the material away from the piedmont regions and out into the dry deserts. This is a key event in the formation of a “desert” loess deposit.

D2: Relatively uniformly sorted deposits are formed in particular of particles in the size range 10 - 50µm. These are the raw material for desert loess and it is the rivers which place them in the desert setting as D2 alluvium. Figure.2.2 shows their location.

Figure.2.2: The Tashkent 1978 model illustrated by Pye and Sherwin (1999). Cited Smalley et al. 2006)

T4: Aeolian action: Although the sorted deposits has a relatively high stability their desert situation exposes them to erosion by sand grain impact and this injects silt-sized particles into the atmosphere (Smalley 1970, Jefferson and Smalley 1999) and they are transported in suspension . The D2 deposits form a source for dust.

D3: Loess deposit formation: T4 particles can fall in a whole range of places; many could stay in the deserts for a long time acting as a reservoir of silt particles which can be released as climate conditions allow, to form loess deposits. No significant P1 action in dry deserts. Depositions at deserts fringes can bring the D3 particles back towards source regions to form deposits on top of D1 deposits, as shown in Figure.2.2. The D3 events give loess its chief characteristics (Fookes and Parry 1993 cited in Houston and Lawrence 2002; Derbyshire and Meng 2005):

- Open meta-stable macro-pores structure
- With porosity of 0.5 or greater
- A void ratio of 1.0 or more
- low dry unit weights ranging from 11kN/m3 – 14 kN/m3
- weakly plastic
- Allows tendency to collapse when loaded and wetted, hence high meta-stability and a proclivity (tendency) for hydroconsolidation.

D4: Subsequent post-deposition changes: The arrival of meta-stability may be a D3 phenomenon but the formation of collapsibility should be D4 activity, since true collapsibility maybe introduced by a fairly complex interaction of carbonates and clay (Milodowski et al. 2012) due to post-deposition action, concentrating clay material at the inter-particle contacts.

The Milodowski et al. (2012) observations suggested that in an airfall loess there is an early formation of inter-particle contacts via calcite crystals which form a sort of scaffolding connecting the major primary mineral units; This scaffolding is constructed from linear crystals of calcite and perhaps similar carbonate minerals and when the linkages are complete they act

as nets to catch clay mineral particles and to build up a clayey connection between the major structural units (Smalley et al. 2006). It can be seen as acting to produce a clay bridge (see Figure 2.9) which allows collapse to take place; hence truly characteristic collapsibility is developed by post-deposition action.

A high percentage of loess deposits are made of silt sized quartz. Quartz is very common in igneous and metamorphic rocks at a mean size of approximately 700µm that is crystalline rock (Livingstone and Warren 1996), however the mean size of the earth's detrital quartz that is loess quartz is 60µm (Blatt 1970). The geomorphic mechanisms capable of producing silt quartz include Aeolian abrasion, fluvial comminution, glacial grinding, salt weathering and frost weathering (Wright 2001a). These silt producing mechanisms were studied in the lab by Wright, Smith and Whalley 1998 the result indicated that fluvial and Aeolian activities are highly effective. Table 2.1 shows the result of the laboratory experiment.

Table 2.1:The relative effectiveness of silt-producing mechanisms calculation of the theoretical maximum amount of silt produced from 1 kg of the original sample (Wright, Smith and Whalley 1998).

2.1.4 Areas where collapsible soils have been found

The actuality of collapsible soils has been revealed all over the world. Typically, they are found in arid and semi-arid climate areas, due to the nature of the environment which aids the formation of collapsible soils (Houston, et al 2001). They have been found in large parts of Eastern Canada, the central and north-western parts of United States, in Europe including western Russia, central Asia and in eastern China (Derbyshire, Dijkstra and Smalley 1995: vii; Rogers 1995; Houston, et al 2001; Derbyshire and Meng 2005; Northmore, et al 2008). In Iran they are located in central and eastern desert (Rafie, Moayed, Esmaeli 2008).

Less common are collapsible silt-rich deposits of sands found in South America and Sahara Fringes (Nigeria, Tunisia, Libya, and Israel); also are the volcanic ash of Japan and New Zealand and quickclay of Scandinavia and Canada (Rogers 1995; Derbyshire and Meng 2005; Wright 2001a; Wright 2001b) “In addition, thin, discontinuous loess drapes are found in many mountain regions of the world especially in High Asia (eg the karakoram (Owen et al. 1992) and the Anyemaqen Mountains of north-eastern Tibet) but also including loess in sub-Andean montane basins as in north-west Argentina (eg Sayago 1995; Iriondo 1997); Finally a loessic silt component has been detected in some surface soils outside such generally recognised loess regions (eg Catt 1978; 2001)” (Derbyshire and Meng 2005).

Figure 2.3 illustrates over 4 feet (about 1.2 m) of displacement of a residential roadway after a water main broke beneath it. Note the settlement and downward deflection of the sidewalk and use of a boulder as an additional in Colorado and warped sidewalk due to collapsing soils near Meeker, Colorado.

Figure 2.3: Differential settlement in walking pavements

2.2 Collapse Mechanism

Collapse mechanism has been studied by several researchers, where the state change from meta-stability to unstable is studied. To better understand the collapse mechanism, the dictions are explained first before the process involved in the collapse mechanism.

2.2.1 Features in Collapse mechanism

To grasp the mechanism of collapse, one must first understand the dictions that are associated with the mechanism of soil collapse.

State parameters: such as load (stress), water content, porosity, time, temperature e.t.c. defines a set of physical boundary within which the soil structures exist, their change results in the transition of the soil structure into another. Collapse is therefore intimately connected with state parameters and their variables. When state parameters are changed, soil structure gets first into metastable stage and then collapses in an attempt to restore its stability under the new set of state parameters (Feda 1995). For example: A soil with original water content (WC) 14.3% with degree of saturation 41.5%, upon wetting, rose to WC 30% and being in a metastable equilibrium (high initial porosity of 47.4%) collapsed when bonding ceased to strengthen the soil skeleton (Feda 1995). The governing state parameter is water content, which triggered the collapse. Of secondary importance is the load – if high enough, the structure is compressed before wetting and even at low initial water content it stops to be metastable when wetted (Feda 1995).

Collapse – any abrupt, sudden change of stability; Collapse of soil structure means a partial or total loss of its ability to carry the load resulting in a sudden drop of its mechanical characteristics (Feda 1995).

Local collapse (Figure 2.4): is of smaller extent being confined to weak regions of the soil structure – typical for cemented clays. It has to do with 'homogenization' formed by a structure having different state parameters (Feda 1995).

Total collapse (Figure 2.5): results in a complete failure of the system which cannot find equilibrium without complete rebuilding of its structure. New forms are emerging and a new dissipation mechanism comes with a new state boundary surface (Feda 1995). The system is hence completely another one.

Structural systems:

Soils represent a system consisting of interacting particles and are defined by the: Geometry of their contacts, bonding of various kinds and Flow of different forces (Feda 1995).

Soils belong to a set of structured systems whose thermodynamical behaviour should be identical (i.e. having same state parameters). Typical soil behaviour as observed is a combination of segments of smooth behaviour with sharp transitions (collapses) at their boundaries of the structured system. The interruption represents a transition from one equilibrium position to another. In this connection, one uses the term "Fluctuation" which can be applied to the present analysis of smooth and interrupted transitions, affects structures and in the limit case brings about change. Small fluctuations in a stress strain graph results in Local collapses gradually finding the stage of thermodynamic equilibrium. Large fluctuations are impulses for the creation of thermodynamically new structure. This corresponds to total collapse that can be seen from initial laboratory tests carried out by the author in Figure 2.4 and Figure 2.5.

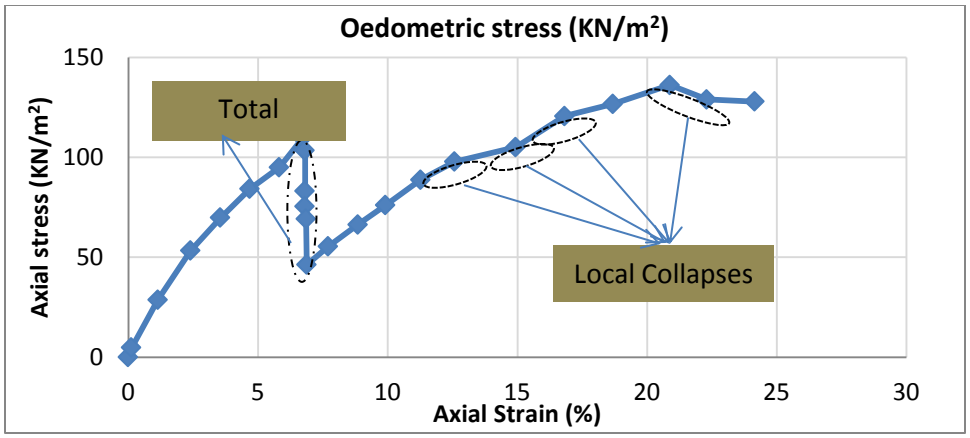

Figure 2.4: Evidence of local and total collapse from an Oedometer test.

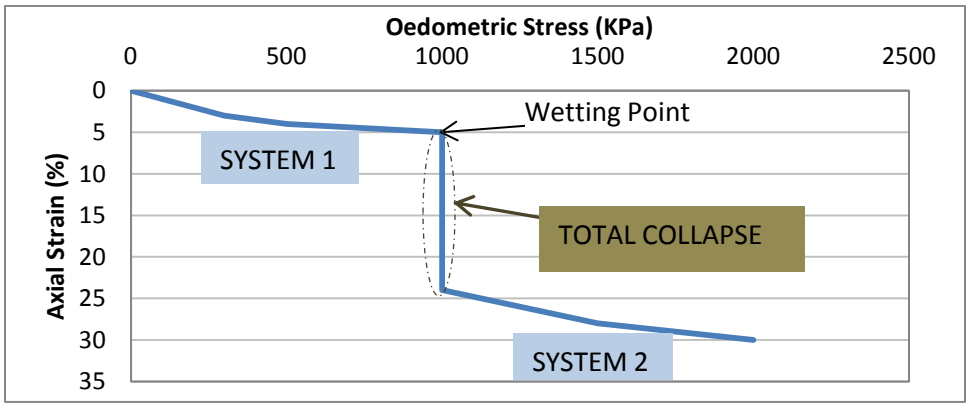

Figure 2.5: Typical Oedometer test of collapse by wetting.

2.2.2 Mechanism of collapse

2.2.2.1 Debonding:

Often, loess collapse is speculated to originate in dissolving of bonding material like calcium; if the bonding material is relatively dry its stormy deterioration occurs more probably due to wetting effect (Feda 1995). The soil is metastable until it approaches saturation, then it turns unstable. Low inter-particle bond strength from capillary tension or binding agent (like carbonates) supplies a loose bulky structured (metastable) soil with high dry strength (Dudley 1970, Barden et al. 1973 & Mitchell 1976). The capillary tension (soil suction) that is present in

the semi saturated soils seems to vanish (capillary pressures approaching zero) after soil voids saturates (Holtz and Hilf 1961; Rafie, Moayed and Esmaeli 2008).

Most cementation consists of dried clay binding the coarser particles together with chemical precipitates (see Figure 2.9). Cementation-like effects results from the high soil suction that exists in the soil in their natural dry state (Houston & Lawrence 2002).

Figure 2.6: Progressive debonding (Feda 1982)

As seen in Feda (1995), the collapse mechanism of collapsible soil when loaded is depicted in two phases (Figure 2.6); in the first phase, the more stress applied on the soil the higher the bond strength, till it gets to the critical load where there is bond failure. The phase 2 starts when the bond is failing and friction is becoming the main composite strength; this is the total collapse stage where the soil structure attempts to restore stability. At the phase 3, the bond has been destroyed and the soil is more compact forming a new set of physical boundaries and having friction with no bond as its means of stability. Here the relevant change in state parameter is the load (stress). Collapse from debonding is most times a total collapse.

In both cases, the debonding leads to the soil grains shifting and shearing against each other into a denser configuration of which causes settlement or subsidence (Burland 1965; Frye 2009).

2.2.2.2 Inundation

Sensitive binding agents which are water sensitive easily breaks, soften, disperse or dissolve when in contact with water. When the load is kept constant, the intensity of collapse is due to the amount of strain-softening, typical of unsaturated loess or expansive clay (Feda 1995). The governing parameter is the water content (Matric suction). A collapse surface can be constructed by combining stress, degree of saturation and the value of collapse.

2.2.2.3 Critical load:

Collapse triggered by the critical load is the most common of all the collapses, with regards total collapse, a detrimental effect takes place (brittle behaviour), it's measured using stress-strain curve (Feda 1995). The critical load has been explained in the debonding shown in Figure 2.6. High enough stress (load) cause the structure to be meta-stable (Dudley 1970, Barden et al. 1973 & Mitchell 1976). Collapse would occur at any stress level greater than that at which the soil has been previously wetted (Houston & Lawrence 2002).

2.2.2.4 Grain crushing and Fabric:

Grain breakage could cause collapse from high compression stresses, where each compression curve consists of segments as seen in Figure 2.7. Within each segment, strain-hardening occurs up to the local collapses which are indicated by a corner on the compressive curve. Each

subsequent segment of compression curve indicates higher compressibility than the former one. (Feda 1995)

A simple sieve analysis may prove that coarser grains of equal diameters are broken more easily than a mixture of grain sizes. This can be explained by the decrease of the value of contact forces of individual grains. Well graded materials better resist crushing than poorly graded ones. Load, water and time also affect collapse potentials of soils. Crushing of grains increases with time due to stress redistribution, this is responsible for the collapse.

Figure 2.7: Grain crushing, Isotropic compression curve (Feda 1982)

2.2.2.5 Softening-hardening:

For softening-hardening, collapses are expressed more by stress-strain curve than by pore-water pressure changes (CIUP test). It is typical of fissured clay. Figure 2.8 shows the shape of collapse and the graph of the collapse. (Feda 1995). Collapse of the soil is associated with localised shear failures rather than an overall shear failure of the soil mass (Maswoswe 1985).

Figure 2.8: Softening-hardening effect as revealed by triaxial specimens of fissured saturated neogene (young) clay (Feda 1995).

2.2.2.6 Time:

Collapse induced by time (creep) as a state parameter is a simple case where the crushing of grains increasing with time (due to stress redistribution, time-dependent resistance of shale (rock fissile of consolidated clay) e.t.c.) (Feda 1995).

2.2.2.7 Pore water pressure

Collapse due to pore water pressure increase happens in two possibilities (Feda 1995):

1. Where the pore water pressure increase is independent of the soil deformation like in piping, hydraulic fracturing, drop in suction e.t.c. (ie external source).
2. When the breakdown of the soil skeleton induces (under poorly drained and saturated conditions) an increase in pore water pressure (internal source).

2.2.2.8 Structural unit

A typical collapsible structure is described as an open silty skeleton with contact bonds enabling its stability, this concept strictly apply to unsaturated soil (Feda 1995).

Liquefaction of quick clay and effect of particle crushing (Cluster) are normal soil collapse behaviour (Feda 1995). From the pass studies, it is shown that a common basic collapse mechanism applies to the different types of soil ranging from sand to clay. In the case of clay, it is assumed that the cause of collapse must lie in an open flocculated structure; it might also be due to an effectively granular structure, with the grains composed of aggregates of clay plates (Barden, McGown & Collins 1973).

2.2.2.9 Stress - strain

During saturation process of a collapsible soil, there is both a gradual increase in compressibility and gradual decrease in shear strength this change causes the collapse (Jennings & Burland 1962, and Barden et al 1973). During wetting-induced collapse, under constant vertical load and under Ko-oedometer conditions, soil specimen undergoes an increase horizontal stresses (Maswoswe 1985). As the degree of saturation increases, soil collapse progresses; this process continues to a ‘critical degree of saturation’ for a given soil above which collapse is negligible regardless of the wetting (Jennings & Burland 1962, and Houston et al. 1993) as seen in Table 2.2.

The collapse phenomenon are apparently a contradiction of the principle of effective stress, since wetting increases pore pressure and decreases effective stress and hence is expected to cause heave rather than settlement; But the mechanism indicates that collapse was due to local shear failure between soil grains and hence compactable with the principle of effective stress (Barden, McGown & Collins 1973).

Table 2.2: Steps of collapse mechanism by Pereira & Fredlund (2000) cited in Jefferson & Rogers 2012

Under Triaxial stress state, the amount of volumetric strain from a change in stress state (loading) or wetting depends on the mean normal total stress volumetric strain component (Axial and Radial strains) (Pereire & Fredlund 2000).

- Therefore for a given mean normal total stress: The magnitude of axial collapse increases and the magnitude of radial collapse decreases with an increasing stress ratio.
- Volumetric strain is independent of the principal stress ratio.

$$\text{Principal stress ratio}=\frac{\text{Axial stress}}{\text{Radial stress}}$$

2.3 Geological Properties

Geological properties are the properties that give the soil its structure, its mechanical ability and its stability. The properties of the soil that affects its collapse potential are vital to the investigation and identification of collapsible soils. Here in is found observations made about the geological properties of collapsible soil; the asperity of collapse relating to the soil's geology and how the geological properties of a soil fabric relate to the metastable state of a soil.

2.3.1 Collapse predictions

Soil collapse form major hazard in the environment which can be averted if suspected or identified. The knowledge of a soil's potential to collapse can go a long way in preventing the destruction of building, roads and properties in general.

Criteria for identifying collapsible soils have been described by Habibagahi & Taherian (2004), Rogers (1995: 5); Dudley (1970); Beckwith (1995); Lin (1995); Barden et al. (1973); Mitchell (1976); Houston et al (2001); Rafie, Moayed & Esmaeli (2008); Steven & Pawalak, (n.d.) and they are as followings:

- Open, partially unstable structure unsaturated fabric: most collapsible soils are unsaturated open structures, of which a degree of loading, density and wetting can cause an immediate collapse.
- High silt content (more than 30% and sometimes more than 90%) and sand size with a small amount of clay: collapsible soils are known for their small range of particle sizes which is formed from detrital quartz of 60μm mean size.
- Low density, high porosity (more than 40%) and low saturation (less than 60%): these properties make the soil structure meta-stable.

- Show relatively high apparent strength (cohesion) in their dry state and susceptible to large settlement upon wetting: collapsible soils have bonding or cementing agent that stabilizes the soil in its unsaturated state but fails when wetted.
- All fills are collapsible: Beckwith (1995) suggests that Holocene (geologically young or recently altered) deposits should be assumed to be collapsible unless a comprehensive testing program demonstrates otherwise.
- Local site geology, depositional processes also climatological data: all can cause a soil to be collapsible as seen in the pedogenesis of collapsible soils.
- Geographical and geological information is strongly correlated with collapsibility and collapse potential; the engineering experience and geological evidence are also essential element of the site characteristics.

Soil properties that affect the collapse potential of the soil according to Habibagahi & Taherian (2004) are listed in descending order: Initial dry density, Pressure from wetting and initial water content, Atterberg limits, Coefficient of uniformity and clay content, Coefficient of curvature (Cc). These show the apparent strength of the soil in their natural state and aid in the identification of which soil samples has the potential of collapse.

2.3.2 Severity of collapse

Collapsibility of soil is identified as non-elastic deformation so the collapse starts when the applied stress exceeds soil structural pressure value (Reznik 2007).

Knowledge of the severity of the collapse gives one an insight into how devastating the damages caused from the collapse could be. Below is a list of some different factors that the severity of collapse is dependent on (Jennings & Burland 1962; Barden et al. 1973; Hodek & Lovell 1979; Houston et al 1988 and El Sohby & Rabba 1984):

- Soil grains (Percentage of soil grain sizes and clay content)
- Initial water content
- Initial dry density
- Depth of the deposit
- Loading from overburden weight and structure
- Collapse potential of the soil
- Extent of wetting and wetting front
- Energy and process used in compaction

Basma and Tuncer, (1992) from their research on Evaluation and Control of collapsible soils, concluded from their results that well-graded soils tend to collapse more than poorly graded ones under similar situations; they also added that collapse potential decreases with an increase in, the difference between the sand and clay percentages; compaction water content and initial dry unit weight, while increasing with pressure at wetting.

2.3.3 Soil Fabrics

We may wonder how collapsible soils particles are kept from forming closer packing naturally. This is due to natural formations like Clay Bridge, Carbonates and Gypsums (Rogers, 1995: 6) as described in the geomorphology (the pedogenesis events – D4) and collapse mechanism (debonding) chapters above. A compacted and meta-stable unsaturated soil structure is kept stable by bonds that are highly dependent on capillary action, such that the soil's bonds have strength to hold the soil structure as long as the soil has a low degree of saturation; at a critical degree of saturation the bonds fail and the soil collapses (Jennings and Knight 1957, & Barden et al 1973).

There are several varieties of bonding agents in collapsing soils some of which are (Rodgers 1995 and Barden, McGown & Collins 1973):

- Capillary tension
- Fine Silt bond
- Aggregated clay bond or clay onion-skin bond
- Flocculated clay bond buttress
- Mud flow type of separation
- Clay bridge structure

Figure 2.9: Bonding agents in collapsing soil. (Rodgers 1995:13)

In soil collapse, the bonding agents that come into play are seen in Figure 2.9. These bonding agents can be put into 3 categories of formation; they include matric suction from capillary force, chemical bonds from the soil's minerals and silt clay bonds. In the silt clay bonds, the fine silts and clay-sized grains making up the aggregates are drawn to pore margins by pore water menisci, yielding fine-particles bridges, buttresses and adhering aggregates (Derbyshire 1984).

In the nature of bonding, the lower the water content the greater the bond strength. It's never clear how much the effects of electro-chemical and capillary is, (Barden, McGown & Collins 1973) but bonding failure between bulky grains of collapsing soil (open structure) can involve: an immediate drop in strength experienced from capillary suctions, clay buttresses is rather slower and chemical cementing has a very slow loss of strength. Jefferson and Rogers (2012), rather affirms that silt clay bonds would fail first since the particles are removed by inundation. But the fact is the difference would depend on the force at which the soil is inundated.

Another important factor is the clay content. El Sohby & Rabba (1984) discovered effects of clay content in a soil fabric. Their result showed that 10% to 45% of clay content in a soil mixture would cause a collapse but above 50% would have a swelling effect; also that a silt-clay mixture collapses at a lower clay content (10% - 20%) than a fine sand-clay mixture (30% - 40%).

2.3.4 Matric suction

Matric suction is defined as the difference between pore air pressure and pore water pressure.

In cases of soil collapse, at least one type of bond failure occurs and in other cases, there will be complex interaction, but in all, they get weakened by the addition of water. During inundation shear strength and volume change of unsaturated soils is controlled two stress state variables (Houston et al. 2001):

Pore pressure (μ) = Total stress (σ) – effective stress (σ^1).

Net normal stress = Total stress (σ) – air-pore pressure (μ_a)

Matric suction = air-pore pressure (μ_a) – water-pore pressure (μ_w)

Matric suction of a soil reduces greatly by wetting as indicated in the Soil Water Characteristic Curve (SWCC) of Figure 2.10, but reduction of matric suction under load, causes compression.

Figure 2.10: Typical soil-water characteristic curve (SWCC) (Fredlund et al. 1998)

The predicted SWCCs shown in Figure 2.10 were developed by Houston et al. 2001 using correlations between the fitting parameters of the Fredlund and Xing (1994) SWCC (Soil water characteristic curve) equation with well-known soil properties such as the diameter D_{60} for non-plastic soils for plastic soils, the soil index properties used were the plasticity index PI and percentage passing 75μm sieve P_{200} (Zapata 1999). Also a large database from various labs and literature sources has been developed for estimating SWCCs (Fredlund et al. 1998).

The shaded portion in Figure 2.10 shows the range of SWCCs for the collapsible soil (encountered in the Western USA, China, Italy and Brazil) used in predicting this moisture-suction characteristics; they are shown in Table 2.3; its believed to be representative of most naturally occurring collapsible soils encountered in the field.

Table 2.3: Naturally occurring collapsible soils (Houston et al. 2001)

Name	**D60 (mm)**	**P200 (Decimal)**	**PI (%)**	**wPI***	**source**
Silt A: Weak cementer gray silt, AZ	0.05	0.74	0	0	1
Silt B: Cemented silt with sand, AZ	0.063	0.62	0	0	1
Silt C: Gray sandy silt, AZ	0.18	0.20	0	0	1
Northern Scottsdale, AZ soil (I)	-	0.65	1	0.7	2
Northern Scottsdale, AZ soil (II)	-	0.67	3	2	2
Price Club silt, Arizona	0.085	0.54	4	2.2	3
Loess from Missouri Basin*	0.06	0.93	9	8.4	4
Lanzhou Province Loess, China*	0.02	0.78	12	9.4	4
Loess from Shaansi Province, China	-	0.8	10	8	4
Malan loess – Gansu Province, China	-	0.92	7.1	6.5	5
Lishih loess - Gansu Province, China	-	0.92	7	6.4	5
Wucheng loess - Gansu Province, China	-	0.96	7.4	7.1	5
Petronila – Pernambuco, Brazil	-	0.59	10	5.9	6
Sta Maria ds Boa Vista - Brazil	-	0.29	9	2.6	6
Carnaiba - Pernambuco, Brazil	-	0.36	22	7.9	6
Recife - Pernambuco, Brazil	-	0.80	36	28.8	6
Cl from Parecis – Western Brazil	-	0.91	11	10	7
Metramo dam soil - Italy		0.38	13.3	5.1	8

Sources:

[1]Houston and El-Ehwany (1991); [2]Houston et al. (1988); [3]Zapata (1999); [4]Bell (1992);

[5]Fookes and Parry (1994); [6]Ferreira and Lacerda (1998); [7]Conciani et al (1998);

[8]Rampino et al (1998) * Average values; wPI = P200 x PI

2.4 Investigations and assessments on collapsibility of soils

Collapsibility criteria from past researchers give a clear yardstick for which a conclusion can be drawn on whether a soil is a threat to a foundation/construction or not. They are estimations by which collapse-prone soils can be categorized, particularly with regards to increase in soil water content.

2.4.1 Reconnaissance

The soil type is one of the influential variables affecting collapsibility. Using visual examination, simple tests, observation of site conditions, and geological information (origin, formation and mineralogy) e.t.c., one can assess the properties of the soil by describing the physical nature and state of the soil. However, the use of material properties and distributions alone is not effective in determining whether a soil is collapsible or not.

Some of the physical properties of the soil which controls the geotechnical and geophysical responses includes: Particle size, Mineralogy, Fabrics, Inter-particle bonding, Density, and Water content.

Reconnaissance process should be followed includes:

- Planning and Procurement
- Description and Classification of Soils and Rocks
- The desk study and walk-over survey
- Subsurface Exploration: Engineering Geophysics
- Subsurface Exploration: Boring, Drilling, Probing and Trial Pitting
- Sampling and Sample Disturbance
- Undisturbed Sampling Techniques

- Laboratory testing
- In Situ Testing (field testing)
- Basic Field Instrumentation for Site Investigation

Methods like Trial pits, excavation or boring and Geological variations in bedrock surface (i.e. Hollows in filled channels), would aid the study, identification and classification of the soil.

2.4.2 Field testing

Field testing is approached using two methods of geotechnical and geophysical.

Under geotechnical approach, the methods include: Standard Penetration Tests, Seismic Cone Penetration Tests, Dilatometer Tests, and Pressure-meter Tests.
These tests provide the design engineer with information that can be used to develop a rationale for accepting or rejecting data and for resolving inconsistencies between data provided by different laboratories and field tests.

Geophysical survey techniques (it's at its early stage) can be successfully employed if properly selected and applied (Northmore et al 2008). They can establish areas and thickness distributions of loess deposit across engineering sites; Provide a significant role in identifying zones of metastable collapse prone sequences; and Geophysical techniques offer a huge potential to characterise the lateral and vertical extent of a range of deposits and can provide useful insight in their behaviour (Northmore et al 2008).
Geophysical testing including

- Shear wave profiling,
- Seismic Refraction (P and S wave methods),

- Spectral Analysis of Surface Waves method,
- Reflection Microtremor method,
- Electromagnetic (EM31 and EM34):
- Electrical resistivity surveys

Geophysical techniques + calibration with geotechnical collapse data (both field and laboratory testing) + lithological (physical characteristic i.e. geology) sequencing, together is essential to complete a full characterisation of a site and its profile (lateral and vertical extent), once established the real power of geophysical approach is its enhanced ability to accurately determine the true depth and lateral spread of particular deposit (Northmore et al. 2008).

2.4.3 Laboratory testing

Laboratory testing includes the testing of soils obtained disturbed or undisturbed from the field. The testing is done to know and analyse the properties of the soil that makes it behave in a particular way, and what makes the soil metastable (collapse).

2.4.3.1 Soil Classification Tests

Soil classification plays an important role in knowing the properties of the soil. These tests include Moisture determination, sieve analysis, Atterberg limits and Compaction.

- Moisture content determination

For many soils, the water content may be a prominent index used for determining the link between the way a soil behaves and its properties. Especially when it comes to the collapsibility of soil, the initial moisture content in soil affects greatly the degree of collapse when saturated also; there is a direct relationship between natural moisture content and the soil's potential stability (Grabowska-Olszewska 1988).

- Sieve analysis and Sedimentation

In conjunction with other tests; the grading of soil is a powerful quality control and quality acceptance tool. Like the grading indicates collapsibility, as Basma and Tuncer, (1992) observed - well-graded soils tend to collapse more than poorly graded ones under similar situations. Also the percentage of fines (Jennings & Burland 1962), amount of clay content (Handy 1973, and Habibagahi & Taherian 2004) and type of bond like clay buttresses (Rodgers 1995 and Barden, McGown & Collins 1973) are deciding factor on the collapse severity of a meta-stable soil.

- Atterberg limits

The objective of the Atterberg limits test is to obtain basic index information about the soil used to estimate strength and settlement characteristics (Manion 2010). The amount of water that takes it from one state to another is an important factor in the examination of the severity of collapse.

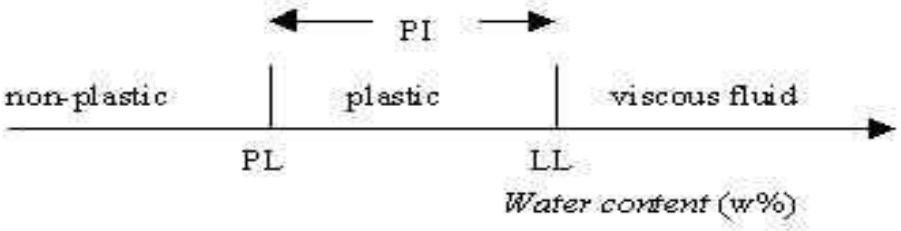

Figure 2.11: Atterberg limit illustration

With reference to Figure 2.11, when moisture content increases, it gets to points of plastic limit (PL) and then liquid limit (LL). Most empirical formulas in the study of soil collapse make use of these parameters such studies as formulas by Batygin (1937); Denisov (1951); Priklonskij (1952); Gibbs and Bara (1962); Feda (1966); Darwell and Denness (1976); Lutennegger and saber (1988) and much more (seen in section 2.5 below).

- Compaction

The objective of the compaction test is to obtain the moisture content – dry density relationship for a soil and thereafter to determine the optimum moisture content and maximum dry density as schematically illustrated in Figure 2.12. This helps to know the degree of collapse (Clevenger 1958). The lower the density of the soil the less dense the soil structure (open structure) would be.

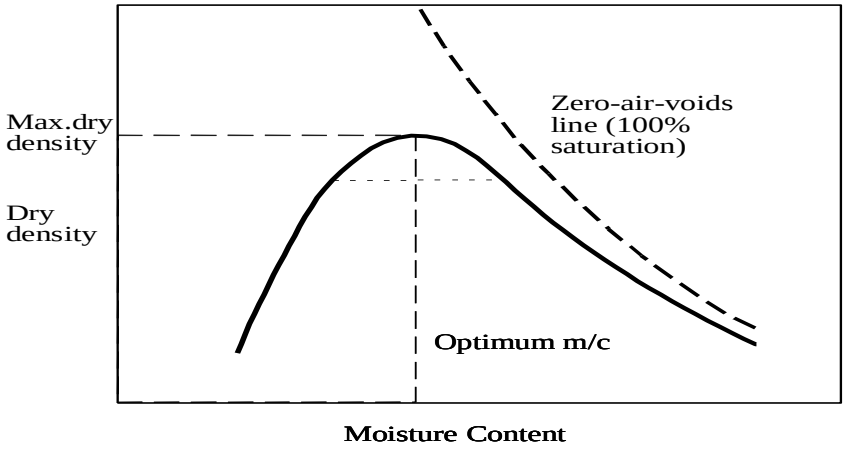

Figure 2.12: Compaction characteristics

2.4.3.2 Oedometer Test

Oedometer test is the most used method of laboratory testing of collapse potentials of soil, authors like Abelev (1948); Jennings & Knight (1975); Mansour, Chik & Taha (2008); Nouaouria, Guenford & Laffi (2008); Northmore et al. (2008) have used it and found it most effective.

- Single Oedometer collapse test:

This method of collapse test follows the step below, and is seen in Figure 2.5:

- Loading the specimens incrementally to a specific state of vertical stress and allowing the sample to come to equilibrium under the applied pressure

- Stress level ranging between 200 and 400 kPa
- The sample is then wetted and the deformation (collapse) measured
- Results are Analyzed using Abelev (1948), Jennings & Knight (1975). These are discussed below in the Correlation coefficients of collapse numbers 5 and 12 respectively.

➢ Double Oedometer collapse test

This is very similar with the single oedometer test, except the following are considered during testing; also Figure 2.13 shows a typical result of double oedometer test:

- One tested at in-situ natural water content
- Second tested at fully saturated level before test begins
- Both at identical loading
- Collapse potential can be determined at any required stress level
- Critical stress (σ_{cr}) represents the stress level at which the dry sample loose structure breaks down.

➢ Limitations for the oedometer test:

Oedometer test is applicable for the soils that do not include high percentage of soluble minerals in its matrix; Soils with high percentage of soluble minerals could be an under estimation of the collapse potential since the amount of water might not be enough to dissolve all the present salts and the water get salt saturated (Mansour, Chik & Taha 2008). In this case leaching out of these salts shall be carried out prior to or during testing. Figure 2.14 shows the graph of underestimation of the collapse as observed by Mansour, Chik & Taha 2008. In the light of the oedometer test limitations Mansour, Chik & Taha (2008) created the Rowe cell, where leaching process could be performed as well as consolidation and permeability test. The load in this cell is applied hydraulically.

Figure 2.13: Typical result from Double Oedometer Test (Mansour, Chik & Taha 2008)

Figure 2.14: Collapse potential of clay soil- Dead Sea-Jordan (Mansour, Chik & Taha 2008)

2.4.3.3 Triaxial Testing

The volume change behavior for unsaturated collapsing compacted soil can be defined using the triaxial permeameter cell developed by Huang (1994). Triaxial can be independently control by: the total stress (σ), the pore-air pressure (μ_a) the pore-water pressure (μ_w). The triaxial testing system can measure the total volume changes.The experimental ranges used by Jose, Pereire and Fredlund 2000 for triaxial testing is explained below:

- matric suction is 0 – 90kPa

- net normal stress (ie $\sigma - \mu_a$) is 20–200kPa

The degree of saturation of two identical soils with same matric suction are always different if one is on drying path and another one is on wetting path (Uchaipichat 2010). Therefore, the areas within the void affected by matric suction of these two soils are also different as seen in Figure 2.15 below. This causes difference in the effective stress which controls volume changes and loading collapse curve.

Figure 2.15: typical soil water characteristics curve (Uchaipichat 2010)

2.4.3.4 Soil Synthesis methods

The study of collapsible soils from undisturbed samples is difficult to retrieve since the open metastable fabric is disturbed during the sampling process; to overcome these shortcomings, artificial cemented specimens was used in Medero, Sehnaid and Gehling (2009) study.

The laboratory scheme focuses on defining the mechanical behaviour of the residual soil at dry-of-optimum water content condition and at low dry density. This condition forms a structure

which is capable of further densification, resulting in a collapsible soil (Derbyshire, Dijkstra and Smalley 1995: vii Pereire and Fredlund 2000).

A double-oedometer test in Pereira and Fredlund (2000) paper illustrated that:

- The residual soil compacted at optimum conditions of standard AASHTO energy did not present any collapsing behavior.
- There is Low collapsibility when loaded under unsaturated conditions
- A meta-stable soil can be saturated without collapse of its structure under low net confining stress.

Medero, Sehnaid, Gehling (2009) carried out a laboratory testing program which exhibits the physical characteristics of natural deposits of High void ratio, low cementation content and suction level and unsaturated conditions prior to the induced wetting; the basic requirement for producing a metastable specimen is achieved by a mixture of: Soil, Poland cement, Water and Particles of expanded polystyrene (EP). The small particles of EP act as voids and allow samples with very low density.

During Medero, Sehnaid, Gehling (2009) experiment, the following 2 conditions had to be met to justify the inserting of the polystyrene into the soil:

- First, the polystyrene stiffness and shear strength should be very small when compared to those of the soil skeleton: this ensures that the mixture does not modify the mechanical behavior of the soil.
- Then, at a given void ratio, a soil sample and a soil polystyrene sample should present similar values of hydraulic conductivity.

2.5 Correlation coefficients of collapse

Collapsibility has been quantified using a number of criteria. These criteria are based on correlation between easily determined Physical – Mechanical indices and collapsibility. They are all explained and summarised in the following sections.

2.5.1 Batygin (1937):

He introduced the coefficient of collapsibility (P) as (Minkov 1984:146) shown in Equ2.1.

$$P = \frac{W_0}{L_L} * D \qquad \textit{Equ2.1}$$

Where (deficiency of saturation)$D = \frac{1}{Sr}$

Sr = Degree of saturation

W_0 = Nature water content

L_L = Liquid limit

Batygin states that for collapsibility, P > 1.

2.5.2 Tokar (1937):

He had the first published criterion for the coefficient of macroporosity (m_p) of a soil with the formula in Equ2.2. He stated that $m_p < 1$ shows the loess is collapsible and $m_p \geq 1$ is non-collapsible (Minkov (1984)).

$$m_p = \frac{e_p^{'}}{e_p} \qquad \textit{Equ2.2}$$

Where ep – void ratio for the total vertical loading at certain depth

And e'p – void ratio at the same pressure after wetting and collapse

2.5.3 Soviet Building Code (1948):

This code is called the relative settlement (i_m), having the same parameters as those used by Tokar (1937) cited in Minkov (1984). The Equ2.3 below shows that the soil is collapsible when i_m is greater than 0.02.

For collapse $$i_m = \frac{e_p - e_p^{'}}{1 - e_p} > 0.02 \qquad \textit{Equ2.3}$$

2.5.4 Priklonskij (1952):

He was the first to suggest a criterion identifying with the strength of a soil, and relating to natural moisture content and the Atterberg limits. (Darwell and Denness 1976) His parameter (K_d) can be compared with the liquidity Index (L_L). See Equ2.4 to Equ2.6.

For collapse $$K_d = \frac{L_L - W_0}{L_L - P_L} < +0.5 \qquad \textit{Equ2.4}$$

And $$P_I = \frac{W_0 - P_L}{L_L - P_L} \qquad \textit{Equ2.5}$$

But $$L_L - P_L = P_I \qquad \textit{Equ2.6}$$

Where P_I is the plasticity index, and W_0, L_L and P_L are the moisture contents in the natural state and at the liquid and plastic limits respectively.

2.5.5 Feda (1966 op.cit.):

Like Priklonskij (1952) his parameters are based on related natural moisture content and the Atterberg limits. Feda produced probably the most comprehensive criterion and based his research on evolving a parameter related to the sensitivity of a soil (Darwell and Denness 1976). The sensitivity is the ratio of the undisturbed and remoulded strengths under same conditions so that a very sensitive soil would therefore seem to be structurally unstable. Therefore Feda established a relationship between sensitivity and the liquidity index just like

Skempton and Northey(1952). Feda proposed that a soil is meta-stable if KL > 0.85 as seen in Equ2.7.

$$K_L = \frac{\frac{W_0}{Sr_0} - P_L}{P_I} > 0.85 \qquad \textit{Equ2.7}$$

Where K_L is the subsidence index and W_0, Sr_0, P_L and P_I are as previously defined.

Feda imposed two constraints on the criterion, firstly that the natural porosity n_0>40%, and secondly that the soil should be subjected to sufficient enough load for structural collapse to happen in wetting (Darwell and Denness 1976 and Bell 2004:310).

2.5.6 Darwell and Denness (1976):

The criterion is an adaptation of Feda's criterion; it can be rearranged to include values for the natural dry density (γ_{dn}) and the specific gravity (Gs). See Equ2.8 to Equ2.12 below.

For Collapse $$\frac{\frac{W_0}{Sr_0} - P_L}{L_L - P_L} > 0.85 \qquad \textit{Equ2.8}$$

Or $$\frac{e_0 - e_{Pl}}{e_L + e_{Pl}} > 0.85 \qquad \textit{Equ2.9}$$

But $$\frac{W_0}{Sr_0} = \frac{\gamma_w}{\gamma_d} - \frac{1}{Gs} \qquad \textit{Equ2.10}$$

So $$\frac{\gamma_w}{\gamma_d} - \frac{1}{Gs} - P_L > 0.85(L_L - P_L) \qquad \textit{Equ2.11}$$

Or $$L_L + \frac{3}{17}P_L < \frac{1}{0.85}\left(\frac{\gamma_w}{\gamma_d} - \frac{1}{Gs}\right) \qquad \textit{Equ2.12}$$

2.5.7 Abelev (1948):

Introduced maximum coefficient of macro pores ($e_{m,max}$) as seen in Equ2.13.

$$e_{m,max} = e_n - e_L \qquad \textit{Equ2.13}$$

e_n - Void ratio in natural condition

e_L – Void ratio at liquid limit

He proposed that $e_{m,max}$ < 0.03 shows non-collapsible, $e_{m,max}$ > 0.07 is collapsible and in-between the 0.03 and 0.07 is a transitory state (Minkov 1984:146).

Abelev (1930) is the first researcher who proposed a criterion for evaluation of soil collapsibility potential (Rafie, Moayed and Esmaeli, 2008) with the use of direct loading test to determine the influence of wetting. The collapsibility coefficient equation could be written as seen in Equ2.14.

$$Ie = \frac{\Delta e}{e_1 + 1}\% \qquad \textit{Equ2.14}$$

Δe = Void ratio reduction resulting from soil saturation

e_1 = Void ratio before soil saturation

Regarding the above criterion if Ie is greater than 2 percent (Ie > 2%) then the soil will be susceptible to collapse. Abelev (1948) used stress level of 300 KPa While, Jennings and Knight (1975) recommended the using of stress level of 200 KPa, and calculating the collapse potential with the Equ2.15 below (Mansour, Chik and Taha 2008).

$$Ie = \frac{\Delta \mathrm{e}}{1 + e_0} \qquad \textit{Equ2.15}$$

e_o: natural void ratio

The stress level of 200 kPa was adopted by (ASTM D 5333-96, 2000) to classify the severity of the collapse problem (Day, 2001).

2.5.8 Denisov (1951):

Amongst the first to identify the potential subsidence of soils using the soil's natural porosity is Denisov (1951). His criterion was also based on a consideration of the voids ratios at the natural moisture content and the liquid limit (Darwell and Denness 1976).

He therefore suggested that a soil may be meta-stable if Equ2.16 occurs.

$$\frac{e_l}{e_0} < 1 \qquad \textit{Equ2.16}$$

Where e_L and e_0 are void ratios at the liquid limit and natural moisture content respectively

This criterion can be rewritten (Darwell and Denness (1976)) in terms of the natural dry density and the liquid limit as in Equ2.17 and Equ2.18.

$$e_0 = w_0 * Gs = Gs\,(\frac{\gamma_w}{\gamma_d} - \frac{1}{Gs}) \qquad \textit{Equ2.17}$$

And $$e_l = L_L * Gs \qquad \textit{Equ2.18}$$

So that Denisov's criterion becomes Equ2.19.

$$\frac{L_L}{\frac{\gamma_w}{\gamma_d} - \frac{1}{Gs}} < 1 \qquad \textit{Equ2.19}$$

Where W_O and L_L are the moisture contents in the natural state and at the liquid limit, Gs is the specific gravity of the grains, γ_d is the natural dry density, and γ_w is the density of water.

2.5.9 Soviet Building Code criterion (1962):

This is like that of Denisov (1951), since it compares only parameters related to the porosity of a soil (Darwell and Denness 1976), hence the criterion states that meta-stability may be present if Equ2.20 is likely.

$$\frac{e_0 - e_l}{1 + e_0} > -0.1 \qquad \textit{Equ2.20}$$

This may be compared with the coefficient of subsidence (R) which is given by Equ2.21.

$$R = \frac{e_1 - e_2}{1 + e_1} \qquad \textit{Equ2.21}$$

Where e_1 and e_2 are the void ratios before and after wetting, the Soviet Code is adequate when the natural degree of saturation (S_0) does not exceed 0.6.

2.5.10 Clevenger (1958):

In his research suggested that the collapsibility of a soil is dependent on the dry density (Bell 2004:310). Giving the ranges as:

Dry density < 1.28Mgm^{-3} - collapsible

Dry density > 1.44 Mgm^{-3} - has small collapse

And 1.44Mgm^{-3} > Dry density > 1.28Mgm^{-3} - is of transitional settlement.

2.5.11 Handy (1973):

Recommended that collapsibility could be determined either by the percentage of clay content; or from the ratio of Liquid limit to saturation moisture content (Bell 2004:310). The ranges are as follows:

Clay content < 16% - high probability of collapse

Clay content between 16% and 24% - Probably collapsible

Clay content between 25% and 32% - Probably less than 50% collapse

And Clay content > 32% - are non-collapsible

Then, soils with ratio of Liquid limits and Saturated Moisture content < 1- collapsible

And ratio of Liquid limits and saturated moisture content > 1 - non- collapsible.

2.5.12 Zur, Wiseman (1973):

They applied the dry densities of a soil at natural moisture content (ρ_d) and liquid limits (ρ_{dL}) to acquire a collapsibility criterion which is seen in Equ2.22 (Minkov (1984).

For collapse $$\frac{\rho_d}{\rho_{dL}} < 1.1 \qquad \textit{Equ2.22}$$

2.5.13 Grabowska-Olszewska (1988):

Suggestion for collapsibility was based on the natural moisture content (Bell 2004:310) in Table 2.4.

Table 2.4: Natural moisture content vs. Potential stability

If natural moisture content < 6%	the soil's potentially unstable (collapsible)
Natural moisture content between 6% and 19%	soil with intermediate behavior
And Natural moisture content > 19%	It is a stable (non-collapsible) soil.

2.5.14 Larionov et al (1959):

Recommended collapsibility established on the bases of a certain critical pressure (P_{cr}) (Minkov 1984:148).

If Pcr > 0.15MPa – non-collapse

0.1MPa < Pcr < 0.15MPa - Slightly collapsible

Then Pcr ≤ 0.1MPa - Highly collapsible

2.5.15 Jennings and Knight (1975):

They quantitatively identified the collapse nature of soil basing their prediction on their experience with collapsible Aeolian soils in South Africa (Williams and Rollins 1991:8) defined a collapse potential as the percentage strain at a loading intensity of 200KPa as shown in Table 2.5. The collapse potential is a useful indicator of severity of collapse, but it is not a design value for predicting collapse (Williams and Rollins 1991:8).

Table 2.5: collapse potential Jennings and knight (1975) (cited in Williams and Rollins 1991).

2.5.16 Hormdee, Ochiai and Yasufuku (2004):

With the Knowledge that the single and double consolidation test is usually performed to investigate collapsibility of undisturbed or compacted soils, Hormdee, Ochiai and Yasufuku connected the collapsibility investigations in terms of collapse index (Ic) determined at 200KPa and collapse potential (Ic) determined at any stress level (Hormdee, Ochiai and Yasufuku 2004:2).

The briefly method is to apply load up to a pressure then increase the moisture content until saturation is reached. The collapse index and collapse potential can be calculated with a formula given as:

$$Ic = \frac{100\,\Delta e}{1 + e_0} = \frac{100\,\Delta h}{h_0} \qquad \textit{Equ2.23}$$

Where Δe and Δh are the changing Void ratio and Sample height due to inundation at the same applied pressure. e_0 and h_0 are initial void ratio and initial sample height. The classification of the degree of collapsibility is shown in Table 2.6.

Table 2.6: classification of collapsibility of soil (Hormdee, Ochiai and Yasufuku 2004:2)

Settlement of a soil layer for the applied vertical stress is obtained by:

$$Ic * \frac{d}{100} \qquad \textit{Equ2.24}$$

Where d is the thickness of the soil layer.

This test method may be used to find the collapse potential at a particular vertical stress or the collapse index at an applied vertical stress of 200KPa (Hormdee, Ochiai and Yasufuku 2004:2).

2.5.17 Gibbs and Bara (1962):

This is based on a simple identification method for collapsible soils, for which there is a correlation between the liquid limit and dry density. In the criterion, he stated that any soil having a dry density high enough to achieve (upon saturation) moisture content equals or higher than the liquid limit would be collapsible (Jardine, Potts and Hingins 2004). In other words if the volume of water at saturation (W_{max}) exceeds the liquid limit's water volume (L_L) then the soil is susceptible to collapse. Hence for collapsibility can be expressed as Equ2.25 and Equ2.26.

$$W_{max} \geq L_L \qquad \textit{Equ2.25}$$

$$\frac{L_L}{W_{max}} \leq 1 \qquad \textit{Equ2.26}$$

According to Handy (1973) (cited in Minkov 1984:152) this criterion is like a factor of safety against collapse, where the more higher the ratio $\frac{L_L}{W_{max}}$ exceeds 1, the safer the structure.

With this in mind, Gibbs and Bara (1962) defined a relationship in a graph of dry density against liquid limits show in the Figure 2.16.

Figure 2.16: Collapsibility according to Gibbs and Bara (1962) (cited in Jardine, Potts and Higgins 2004:425)

Prokopovich (1984) (cited in Williams and Rollins 1991:8) resolved that this relationship proposed by Gibbs and Bara (1962) was not always dependable since collapse can occur when water content of the saturated soil is well below the liquid limit. So to decide on the usefulness of this test, the test would have to be executed to establish a correlation between soil collapsibility liquid limit and dry density. Also cited in Williams and Rollins 1991:8 is Owen (1988) who used the criteria of Figure 2.16. His results were scattered due to the difficulty of acquiring quality undisturbed samples in collapsible soil. For these reasons this criterion is not applicable for cohesion less soils such as silty sands and non-plastic sandy silts which establish a large percentage of collapsible soils.

2.5.18 Lutennegger and saber (1988):

The amount of volume change that occurs when soil undergoes collapse is obtained from oedometer test. Once the geotechnical engineer recognizes the probability of collapsible soils present, then prediction is done depending on the density and consistency limits measurements as shown in Figure 2.17 (Mansour, Chik and Taha 2008:4).

Figure 2.17: Commonly used criterion for determining collapsibility (Lutenegger and Saber 1988 cited in Mansour, Chik and Taha 2008:4)

2.5.19 Basma and Tuncer (1992):

A collapse prediction model from utilizing the experimental data obtained from influences of soil type (Percentage of fines and coefficient of uniformity), compaction parameter (initial dry density and initial moisture content) and of pressure at wetting, gave rise to equations that predicts the response of undisturbed samples. Using the guide by Jennings and Knight (1975), the potential severity of collapse is noted.

$$CP = 48.496 + 0.102\ Cu - 0.457w_i\ - 3.533\gamma_d\ +\ 2.80l_n(p_w) \qquad \textit{Equ2.27}$$

$$CP = 47.506 + 0.072(S - C) - 0.439w_i\ - 3.123\gamma_d\ +\ 2.851l_n(p_w) \qquad \textit{Equ2.28}$$

Where CP – collapse potential (%)

Cu – Coefficient of uniformity

w_i – Initial water content (%)

γ_d – Compaction dry unit weight (kN/m3)

p_w – Pressure at wetting (kPa)

(S-C) – Difference between sand and clay content (%)

2.5.20 Reznik (2000):

Collapse is the sudden volume decrease due to water content increase under unchanging total vertical stresses is a phenomenon quantified by a collapse potential (CP).

$$cp = \frac{h_{\sigma d} - h_{\sigma w}}{h_0} = \frac{\Delta h_{\sigma w} - \Delta h_{\sigma d}}{h_0} \qquad \textit{Equ2.29}$$

The right side of equation above can be rewritten as:

$$CP = \left(\frac{e_0 - e_\sigma}{1 + e_0}\right)_w - \left(\frac{e_0 - e_\sigma}{1 + e_0}\right)_d \qquad \textit{Equ2.30}$$

When σ = 0, then $h_{\sigma d} = h_0$ ($\Delta h_{\sigma d} = 0$).

3 METHODOLOGY

Undisturbed collapsible soil samples retrieved from the field are difficult to study due to disturbance of the open metastable fabric that can occur during the sampling process (Medero, Sehnaid, Gehling 2009). To overcome these challenges, metastable soil samples are synthesised and tested to simulate the behavioural properties of a compacted field soils. This compacted soil simulates the condition of a site before commencing construction.

Several factors affect the collapse potential of a soil. These include the soil's fabric (size and nature of the soil's grains), bonding agent, and state-parameters like density, matric suction, degree of saturation, void ratio, water content and loading (both overburden and applied load). All these elements work together to make the durability, strength and stability of the soil structure. This thesis investigates these different factors to understand the role that each factor plays in the stability of the soil structure as far as the mechanism of collapse is concerned.

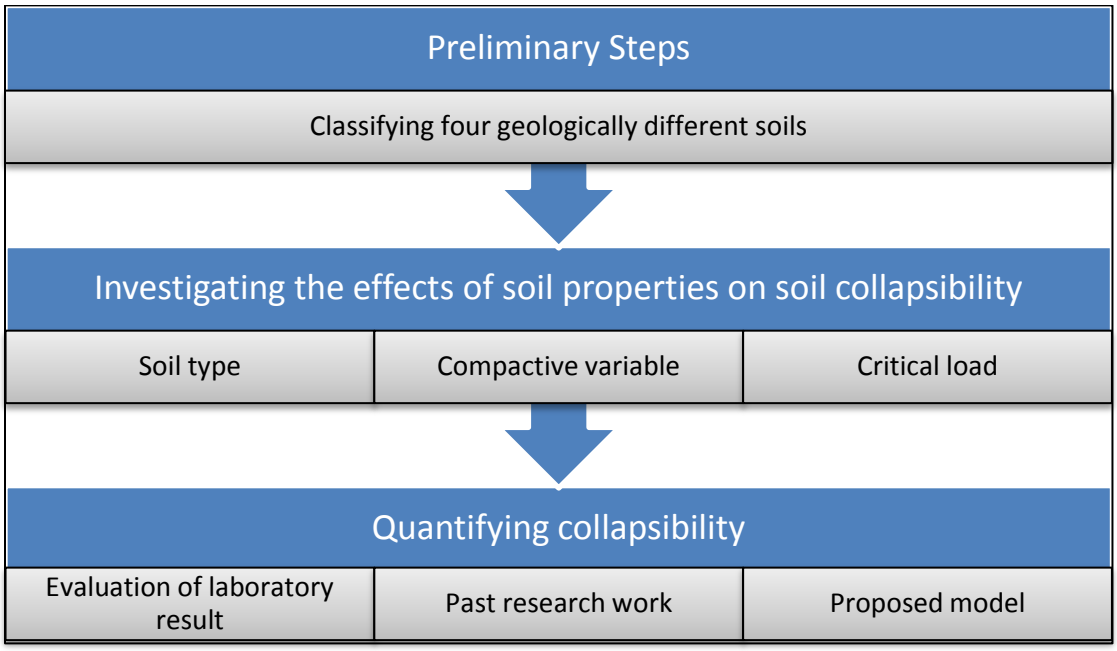

Figure 3.1: Methodology summary

The relationship between a soil's fabric and state-parameters that make the soil metastable would be incorporated in the preparation, observation and study of collapsible soils.

The steps to be followed are shown in Figure 3.1, these include:

- Preliminary step: Preparation, classification and observation of meta-stable soils
- Investigation of the effects of geologically and structurally different soil properties on collapsibility
- Quantification of soil collapsibility from critical monitoring of the soil structure.

3.1 EXPERIMENTAL STEPS

Geological factors such as, particle size distribution (PSD), maximum dry density (MDD), optimum moisture content (OMC), degree of saturation (Sr) and pressure will be observed to note their effect on the soil's collapse potential when the structural properties are reconditioned. Sets of specimens will be constructed such that the physical and mechanical properties are tested and then analysed to ascertain their collapse potential as a structure.

3.1.1 Meta-stable soils

The classic collapsible soils are natural material which particle type and sedimentation mechanism combines to produce collapsibility (Derbyshire, Dijkstra, and Smalley 1995). So this physical properties pertaining to the fabric of the soil will be selected from soils with varying PSD and bonding properties. In preparing the soil for synthesis into meta-stable state, different soil gradations will be selected to conform to a desirably different specification of which would be identified during the classification of the soils. Their description, percentage passing and sedimentation by weight would be used to specify. The plasticity indexes of the soils are particularly important in the fabric bonding of the soil and stability of the soil structure. This would be also considered in the specification selection.

3.1.2 Soil classification and Property identification

Different laboratory tests are carried out to classify the structure of the soil and test the mechanical properties. To achieve these, the laboratory tests included:

- Sieve Analysis and sedimentation test to identify the soil's fabric makeup
- Atterberg and compaction among others for classification

- Triaxial and oedometer test to check the mechanical properties, shear strength, consolidation properties and measure the collapse potential of the soil.

Table 3.1 shows a summary of the test materials and functions and Figure 3.2 gives the flow chart of the experimental test.

Table 3.1: Laboratory Tests guide

Test	***Factors Acquired***	***Materials***	***Reason***
Sieve analysis	Grading of the soil, Particle size distribution (PSD)	Set of sieves, Oven, Trays, Spatulas, wire brush and scale.	Soil gradation classification
Hydrometer analysis test	Grading of the fines, Part of the PSD. Coefficient of uniformity (Cu) Coefficient of curvature (Cc)	Soil hydrometer, Dispersion reagent (sodium oxalate and sodium hexametasphate), 2 graduated cylinders (1000 ml and 100 ml capacity), Stop-watch, Moisture can, Oven, Trays, Glass rod.	To realize the distribution of fine (silt/clay) in the soil
Atterberg	Liquid limit Plastic limit Plasticity index	Cone penetrometer, Distilled water, Moisture can, Oven, Trays, Spatulas, Scale, 3mm diameter rod.	Particle bonding properties and analysis of collapsibility
Compaction	Maximum Dry Density (MDD) Optimum Moisture Content (OMC)	Standard proctor mould with base plate and collar, Rammer, Trowels, Wash bottle, Moisture can, Oven	Realize the durability of the synthesized soil
Tri-axial	Total stress Cohesion Internal friction Shear strength	Tri-axial cell, compression test machine, rubber membrane,	For analysis of collapsibility
Oedometer	Collapse Potential, Settlement criteria and Critical stress	Consolidation test set-up, Set of weights to load samples, 2 porous stones to place on top and bottom, Dial gauge	Collapsibility check

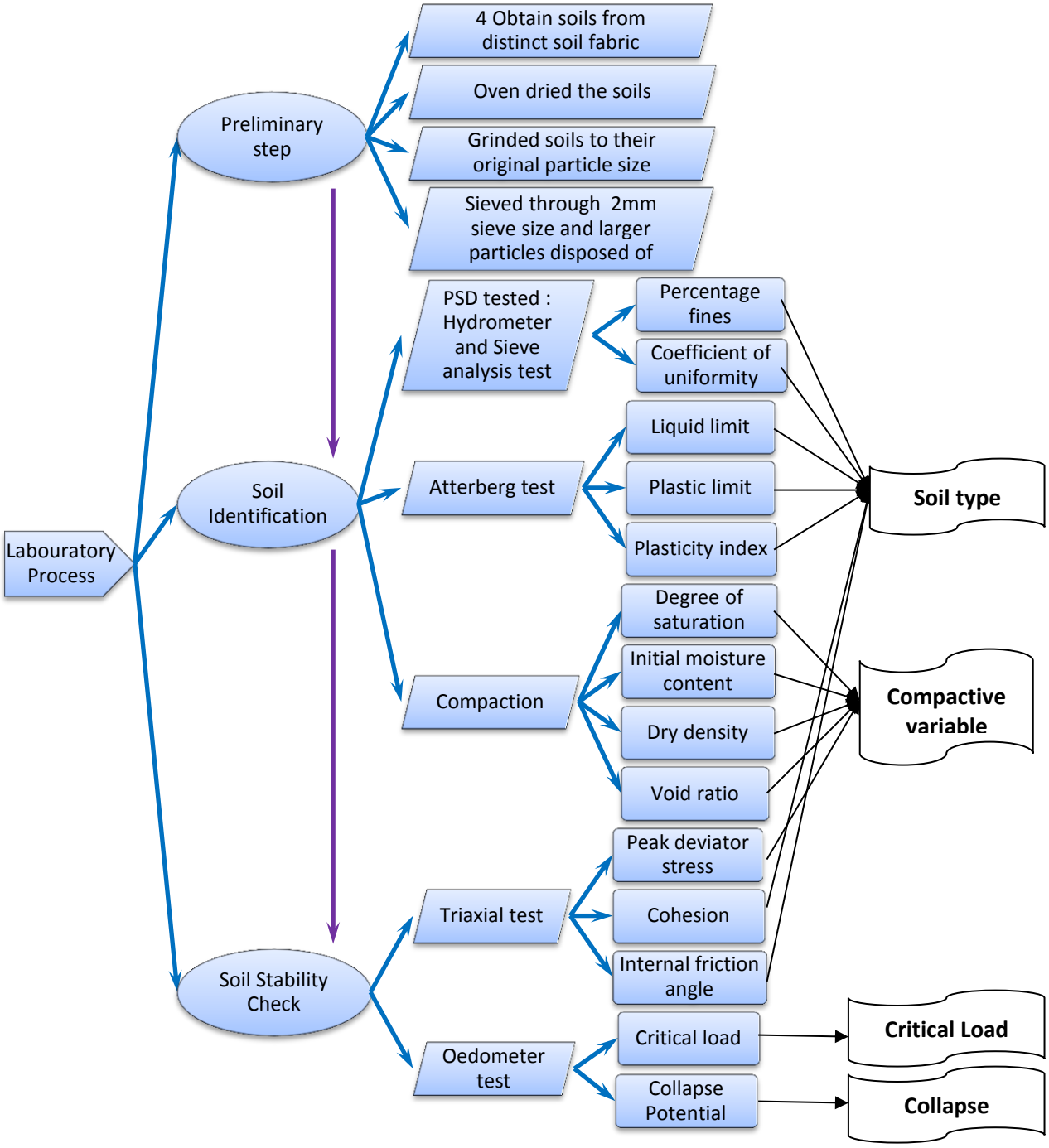

Figure 3.2: Laboratory test and the acquired parameters

3.1.3 Triaxial and oedometer Test

Triaxial and oedometer tests were carried out to measure collapsibility. The triaxial test was performed on the unsaturated samples prepared at the different moisture variations. The same samples were then used for an oedometer test at the prepared state and again at an inundated state, hence testing the samples when unsaturated and then when saturated. These processes define the densification of the soils caused by changes in the initial stability state of the soils structure induced by addition of water at constant total vertical stress. The total tests performed here are drawn out in **Error! Reference source not found.**.

3.1.3.1 Triaxial testing

Standard test procedure for unconsolidated-undrained (UU) is described in BS1377, part 7; and ASTDM D2850. The setup used is the T_{10} model (1.5”) standard cells.

The sample was compacted using the standard proctor compaction test, pushed in 3 tubes of 38mm diameter and extracted. Samples were then cut to a 78mm height approximately using the split tube former.

The sample for this test was not inundated. Confirming pressures of 70kPa, 140kPa and 280kPa were used to test the effect on the total shear strength of the soil.

3.1.3.2 Oedometer testing:

For the standard test procedure used, see BS 1377, part 5; Eurocode 7, Part 2 and ASTM D2435.

The prepared sample was prepped using the standard proctor compaction method to compact a layer of 25 blows with the 2.5kg force. The ring was pushed into the soil with the help of the jack and setup for a consolidation test. This was done twice to prep 2 specimens for the oedometer test. Specimen measurement is approximately 76mm diameter and 19mm height. One of the

specimens was used to run the oedometer test for as-compacted properties and the other was soaked for 24 hrs to produce a saturated sample, and then tested for collapse.

This test method was used to observe the effects of the loading and wetting on the sample with time. Unlike the standard method of testing for 24hrs, this oedometer test was run for 30mins, since the instantaneous reduction of volume was what was required to be measured.

The volumetric strains for as-compacted and inundated samples were obtained from the oedometer tests. The as-compacted volumetric strain represents the coming to equilibrium of the soil sample under the applied vertical stress whilst the inundated volumetric strain represents deformation induced by the change in state parameter (wetting), which is independent of the loading-wetting sequence.

3.1.4 Procedure

Samples from the field were collected; tested to know their mechanical and physical properties (soil fabric) and then tested to check their collapse potential. The soils were also prepared and pretested to identify their geological properties for soil structure synthesis.

3.1.4.1 Soil Selection

Four soils were selected by physically observing the fines portion of the soils since collapsibility occurs in the fines fraction of a soil composition. Literature on properties of a typical collapsible soil has been discussed in sub-chapter 2.3.1 on page 32. In this research identification of collapsibility is of focus. Hence the selected soils were not natural collapsible soils; they were selected to cover the range of physical fine grain size particles. They include silty clay, silty fine sand, clayey soil and finally clayey sand. The two of the four soils have silt, one with clay mix and the other with fine sand mix. One is completely clay and the last soil is a clay and sand mix.

3.1.4.2 Soil Preparation

The soil samples were dried in the oven for at least 24 hours and then fines were grinded to their original particle sizes. The soil fabrics selected were ensured to contain only fine sand, silt and/or silt particles, hence larger particles were disposed of. This was due to the fact that in the study on soil collapsibility, the fines were of utmost importance and is thus focused on in the research.

3.1.4.3 Preliminary tests

Preliminary testing concerned synthesised soils for their geological properties. Dry sieve analysis and sedimentary test were conducted on the soil samples to identify the particle size distribution of the samples. For the soil description, the standards used were BS 5930 (1999) and ASTM D2487-1 (2011).

Next, the Atterberg limit test was carried out to specify the characteristics of the fines and obtain values for liquid limit, plastic limit and plasticity index of the soils. The standards used here were BS 1377, part 2 (1990), and ASTM D4318 (2010)

Finally mechanical properties of the different soils are tested for the MDD and OMC using the standard proctor compaction test. Detail for this test is given in BS1377-4 and ASTM D698, D1557 and D7382.

All the tests are listed and explained in Table 3.1.

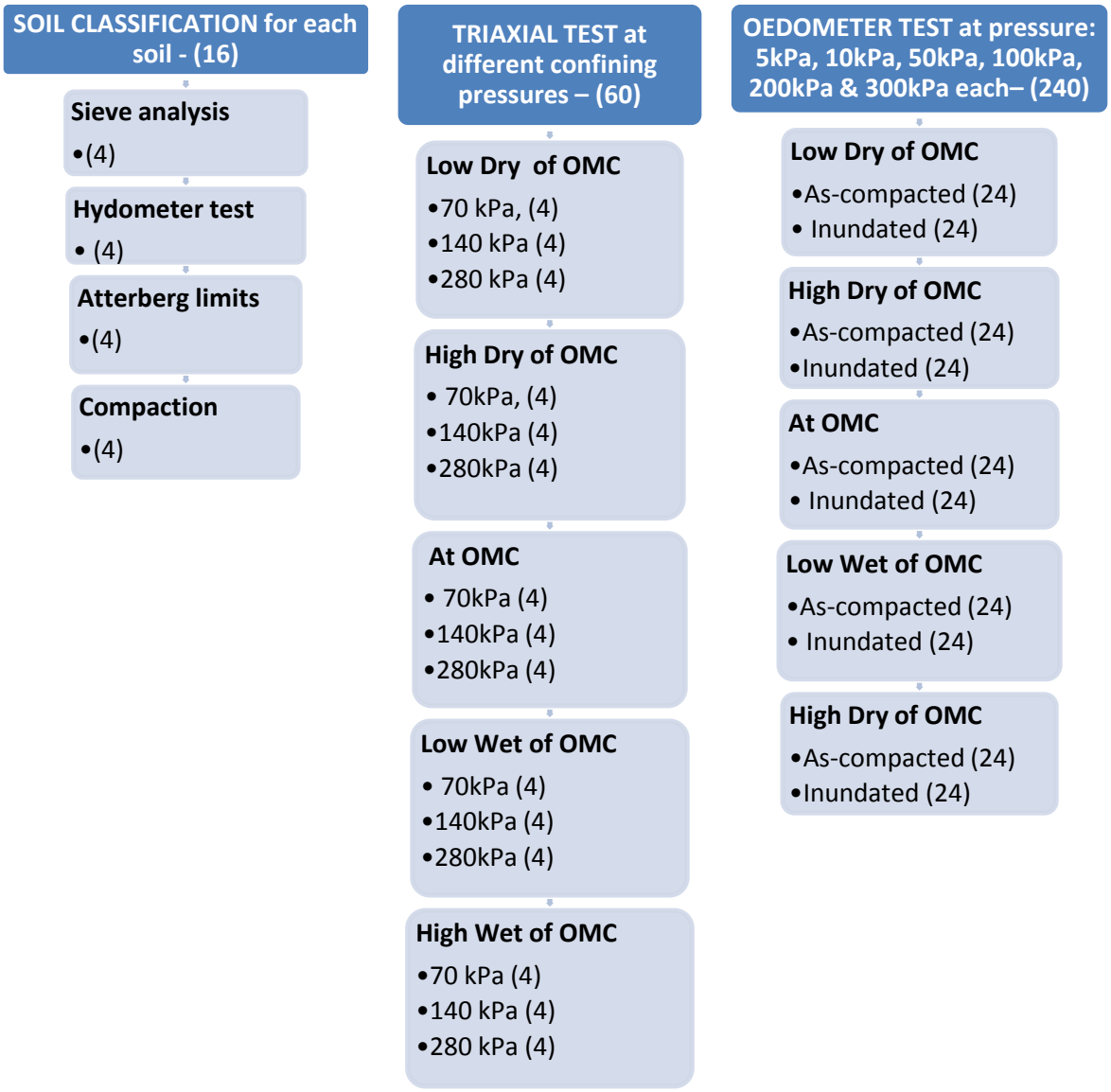

Figure 3.3: Experimental tests to be carried out

3.2 EFFECT OF SOIL PROPERTIES ON SOIL COLLAPSIBILITY

Once the physical and mechanical properties have been tested; the soils' geological factors are adjusted, modified and observed to note their effect on the collapse potential of the soil. Various specimens are prepared at varying soil structure and then tested to ascertain their collapse potential. In the preparation of metastable structured soils, the following factors will be observed:

- Soil type: Particle size distribution (PSD) and bonding property of the soil.
- Compactive variable: Initial moisture content initial dry density and degree of saturation
- Critical pressure

During the modification of the soil mechanical properties and collapse potential: the soil fabric were selected with soil gradation in mind; where, the initial moisture content which is a percentage of the optimum moisture content as show in Table 3.2 and Initial dry density obtained from the compacted sample (standard proctor compaction) at this stated initial moisture content (MC) are acquired. The degree of saturation was identified at state of the compacted soil sample. The prepared sample was loaded at several stresses for as-compacted MC (which is same as initial MC) state and inundated state to identify the critical pressure. The degrees of these factors varied produce different soil structures which were tested to reveal their effect on the soil's collapsibility.

The triaxial apparatus is used, with the aim of quickly obtaining a measure of compressive strength for the soils in an unsaturated state and oedometer test was conducted to check the collapse potential of the prepped soil samples.

3.2.1 Soil type

Soil fabric play a fundamental role in particle bonding, this is influenced mainly in their particle size distribution (PSD) and bonding ability of the soil's fabric. PSD has been considered and tested in the preliminary stage of soils testing. The classified soils will be tested and scrutinized for their effect on collapsibility by comparing factors like the soil's percentage of fine, fines material, and coefficient of uniformity, Atterberg limits, peak deviator stress, cohesion, and internal friction angle, to the soil's collapse potential.

Al-Shayea (2001); Lawton et al. (1992); and Basma and Tuncer (1992), each give guides to this analysis where each looks into the contributions a remoulded (compacted) unsaturated soil have in collapsibility of soils. Al-Shayea (2001) investigated into the effects of soil type by varying the clay content of the soils, he established the determining power of consistency limits, stress-strain relationship and hydraulic conductivity to volume change characteristics (collapsibility). Lawton et al. (1992) also varied the clay content of the soils to explore the effects on collapsibility by discussing the factors of moisture, solids and stress, relative compaction and principal stress ratio parameters. Basma and Tuncer (1992) on the other hand investigated eight soils with different geological properties focusing on divulge the effect of difference between sand and clay, and coefficient of uniformity (Cu).

3.2.2 Compactive Variables

Water content plays a huge role in collapsibility of a soil. The compactive variable is simply the preparing of a soil sample with all its state parameters formed from a proctor compaction test. For this thesis, the soil samples were prepared with an initial moisture content that is a percent of its OMC; the varying moisture content in Table 3.2 gives a series for creating different soil structure. The initial MC, initial dry density and void ratio acquired during compaction were used to compare the soil's degree of collapse, drawing their effects on soil collapsibility. Studies

carried out by Reznik (2007); Alawaji (2001); and Basma and Tuncer (1992) were based on the same approach.

At this point the soils have been tested for the MDD and OMC, and the performances of each soil type categorized. The soils prepared at the different moisture variation (Table 3.2) produced a series of five structurally different soil samples for each soil. These samples are observed to check the effect of compactive variables on degree of collapse using triaxial and oedometer test.

Table 3.2: Moisture content variation

Moisture rate	**Percentage range of moisture content of the fabric mix**
Low dry of OMC (**1**)	65 - 80% of the optimum moisture content (OMC)
High dry of OMC (**2**)	80 – 95% of OMC
At OMC (**3**)	95% - 105% of OMC
Low wet of OMC (**4**)	110% - 125% of OMC
High wet of OMC (**5**)	≥125% of OMC

The properties of the compactive variables of the different soils are analyzed; drawing a comparison between each sample's collapse potential against their degree of saturation, percentage from OMC, and initial moisture content. Important past research for guidance included Pereira et al (2005), Reznik (2007) and Houston et al (2001).

3.2.3 Critical Pressure

The critical loading were surveyed at pressures 25kPa, 50kPa, 100kPa, 200kPa and 300kPa using the oedometer test for as-compacted MC and inundated MC. Past research that involved critical pressure include Pereia J.H.F and Fredlund D.G. (2000) and Lawton et al (1991). The

prepared samples were tested each for 30mins at each loading, tested continuously for all the loads.

3.3 QUANTIFYING COLLAPSIBILITY

The factors that affect the stability of the soil have been drawn out at this point of the investigation. Experimental evaluations were compared with the past research work to factor out the relevance of these factors to collapsibility so as to draw analogies.

3.3.1 Quantifying collapsibility based on past studies

Factors in the parameters column of Table 3.3 are found from the test results of the synthesised soil geological properties as seen in the literature chapter. This is to check the collapse potential of the synthesised soil according to the past researchers. These aim to identify the critical points of the key parameters at which a soil structure is metastable and the degree of metastability.

Table 3.3: Past Reviews

No.	***Researcher / Year***	***Parameters***	***Method of testing***
1	Batygin (1937) Denisov (1951) Priklonskij (1952) Feda (1966) Darwell and Denness (1976)	W_o, L_L, P_L, S_r, γ_d, γ_w, G_s (Moisture content, Atterberg and density)	Classification - Atterberg - compaction
2	Abelev (1948) Denisov (1951) soviet building code criterion (1969) Jenning and Knight (1975) Hormdee, Ochiai and Yasufuko (2004)	e_l, e_0/e_1, e_2, Δe, (Void ratios)	Triaxial and Classification
3	Clevenger (1958) Larionov et al (1959) Gibbs and Bara (1962) Handy (1973) Grabowska – Olszewska (1988) Lutennagger and saber (1988) Basma and Tuncer (1992)	Dry density variations, Critical pressure, Moisture contents, Clay content, and Graph of Dry density and Liquid limit.	- Compaction - Sieve analysis - Atterberg - edometer, - Triaxial and - Classification

4 TEST RESULTS AND ANALYSIS

The experimental results and analysis reported in this chapter are compiled in form of tables and graphs. Four soils termed *A*, *B*, *C*, and *D* are considered in this study; they were collected naturally by a geotechnical company in the UK at different sites, depths and using different methods of extraction. They were sieved through a 2mm sieve to suit the desired geological characteristics for testing and observation. This was done because, the stability and metastability of a soil structure is dependent on the soil particles being less than 2mm.

The soils used in this study are geologically different. They were first classified and identified using methods of dry sieve analysis, sedimentation and compaction to identify each soil's maximum dry density and optimum moisture content.

In order to check for the collapse potential of a soil, the soils were prepared at five moisture variations at a percentage of their optimum moisture content (OMC); these include Low Dry of OMC (65% - 80%), High Dry of OMC (80% - 95%), At OMC (95% - 105%), Low Wet of OMC (110% - 125%), and High Wet of OMC (≥125%), denoted as 1, 2, 3, 4 and 5 respectively. Each sample was then analysed to identify the collapse potential using triaxial and oedometer test methods.

4.1 SOIL CLASSIFICATION

Classification of the soils involved in this study was carried out in accordance with the Unified soil classification systems (USCS). The classification results include Particle size distribution (PSD), Atterberg limits and Compaction test. PSD curve and plasticity chart are shown in Figure 4.1 and Figure 4.2 respectively. The compaction result is presented in Table 4.4 and Figure 4.3.

4.1.1 Particle size distribution (PSD)

The grading curves in Figure 4.1 reveal that the fines vary between the soils. A, B and C soils possess 78%, 93%, and 97% fines respectively and soil D had the least with 39% fines. All four samples are well graded soils with no possible gap in the particle size distribution (PSD).

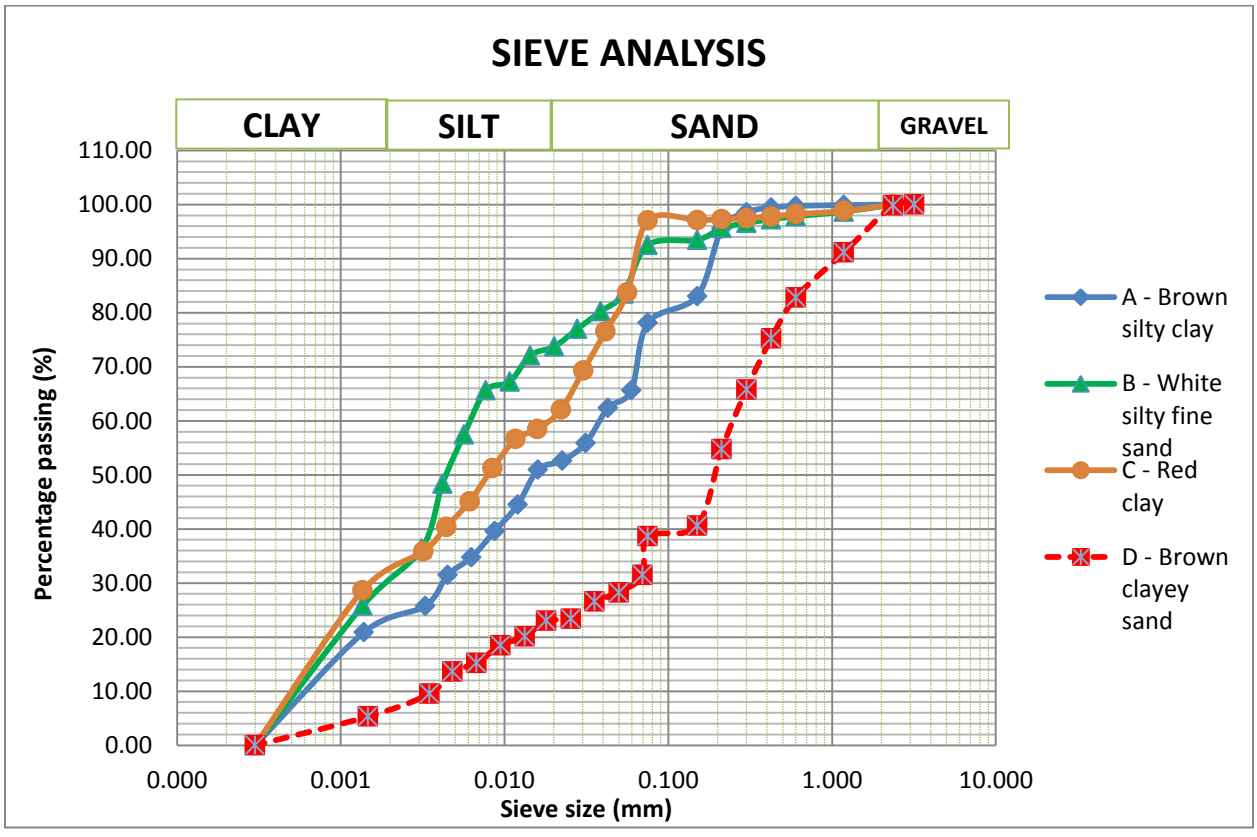

Figure 4.1: PSD curves of the four soils

Table 4.1 shows the soils grading summary, which includes the determined coefficient of uniformity (Cu) and coefficient of curvature (Cc) of each soil. The PSD curve and the Cu and Cc calculated show all four samples are well graded soils with no possible gap in the particle size distribution (PSD).

Table 4.1: Grading summary

Soils	GRADING (%)			VALIDATORY VALUES				
	SAND	Fines		D_{10} (mm)	D_{30} (mm)	D_{60} (mm)	CU	CC
		Silt	Clay					
A	21.90	52.34	25.76	0.00062	0.0040	0.045	72.58	0.57
B	7.48	56.17	36.35	0.00046	0.0022	0.007	15.65	1.46
C	2.94	61.22	35.84	0.00051	0.0020	0.020	39.22	0.39
D	61.40	29.11	9.51	0.00310	0.0450	0.340	109.68	1.92

4.1.2 Atterberg limits

Table 4.2 and Figure 4.2 show the analysed test data and corresponding plasticity chart for the four samples. *A*, *B*, and *D*, are of low Plasticity with Liquid limit lower than 35%, and *C* has an intermediate plasticity.

Table 4.2: Atterberg limits values

Soils	ATTERBERG LIMITS (%)		
	LIQUID LIMIT	PLASTIC LIMIT	PLASTICITY INDEX
A	30.10	23.50	6.60
B	25.70	22.66	3.04
C	36.80	26.01	10.79
D	23.40	17.13	6.27

The plasticity chart in Figure 4.2 gives representative characteristics of the plasticity of the soils. Each symbol is explained in the USCS of which is obtained the characteristic description of each soil. Soils A and C are found on the A-line at a position that gives a characteristic symbol of CL which represents inorganic clay of low to medium plasticity. Soils B and D characteristic symbol is ML which represents inorganic silts or clayey fine sands with slight plasticity. With the position from the A-line, B is silt and D is clay. From visual examination and experimental identification of the results, the four soils are observed looking at the percentage and category of its fines, uniformity of grading and plasticity is vital to the collapsibility of soils.

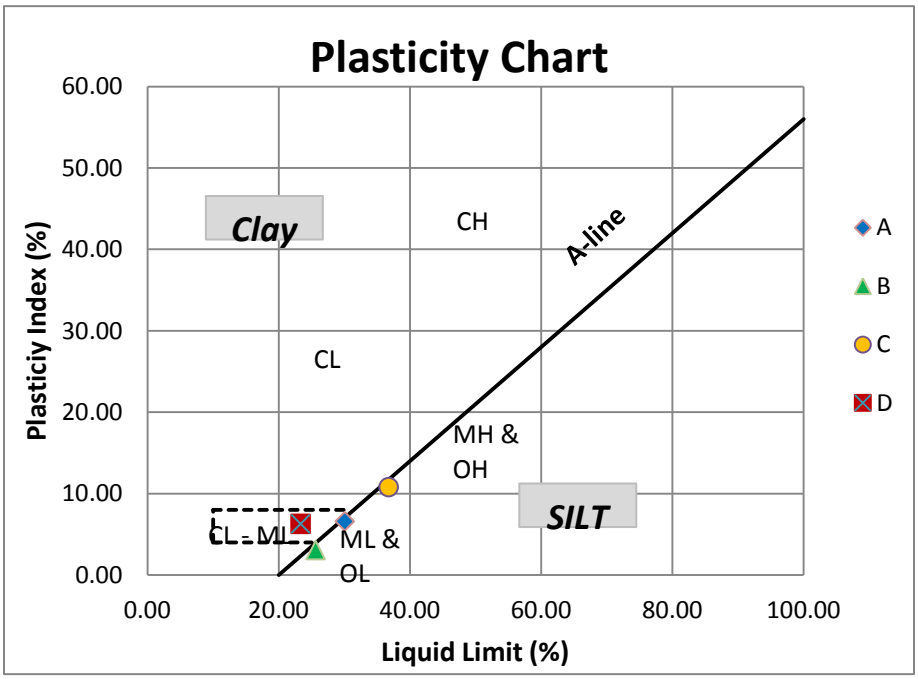

Figure 4.2: Plasticity chart of the different soil

Hence, the soils are classified as follows:

A - Brown inorganic silty clay of low plasticity

B - White inorganic silty fine sand with slight plasticity

C - Red inorganic clay of intermediate plasticity

D - Brown clayey sand with inorganic clay of low plasticity

Table 4.3 show the full description of these soils.

Table 4.3: Description and classification of the four soils

Soil	***Description***	***Grading***	***Plasticity***	***Dry strength (crushing Characteristics)***	***Dilatancy (reaction to shaking)***	***Toughness (consistency with PL)***	***Compressibility and Expansion***	***Drainage characteristics***	***Value for foundation***
A	Brown inorganic silty clay	Well graded	Low plasticity	Medium	Very slow	Medium	Medium	Almost impervious	Good to poor bearing value
B	White inorganic silty fine sand	Well graded	Slightly plasticity	Slight	Quick to slow	None	Slight to medium	Fair to poor	Very poor; susceptible to liquefaction
C	Red inorganic clay	Well graded	Intermediate plasticity	High	Almost none	Medium	Medium	Impervious	Good to poor bearing value
D	Brown clayey sand with inorganic clay	Well graded	Low plasticity	Medium	Slow	Slight	Slight to medium	Poor to impervious	Good to poor bearing value

The following conclusions were also drawn from the tables and figures

- All four soils are well graded since the values for Cu are > 5 and those of Cc are between 0.5 and 2.
- The Effective sizes of the soils which are the maximum size of the smallest 10% of the soil (D10) are for A – 0.62um, B – 0.46um, C – 0.51um and D – 3.1um.
- The soils C with 97% fines, B with 92% fines, A with 78% fines and D with 39% fines give the order from low to high amount of fines comprising of silty fines and clayey fines.
- The soils made of clay fines (C and D) have more stability than soils A and B which are of silt fines; this is because clay bonds has a higher stability than those of silt. The D should be more metastable because of the sand mix and it's very high Cu factor; but the present of clay bonds gives it a more stable potential. Note that particles of clay can be measured as silt in the PSD, and vice versa; hence the plasticity properties (from Atterberg limits) are used to classify the fines are silty or clayey.
- The liquid limit result of the soil gives the 'C' an intermediate plasticity and the other three soils low plasticity; this incites the stability of 'C' over the others.

From the classification of the soils, it can be predicted that of all the soils, Soil B would be the most prone to collapse because of the high presence of silty particles; next prone is the soil A with less silty particles mixed with clay particles. D with a high percentage of sand grains would show low densification, hence low collapse; also the presence of clay bond in the mix would give it a more stable potential. Soil C which is made of high amount of clay bonds could be of high collapse since clay has a high volumetric strain when saturated.

4.1.3 Compaction

Standard compaction tests were carried out on the different soils to obtain the dry density and optimum moisture content (OMC). From the recorded values of mass, volume and moisture content of the sample, the bulk and dry densities are calculated using formulas in Equ4.1 and Equ4.2.

$$\rho_{\text{bulk}}(g/cm^3) = \frac{Mass\ of\ compacted\ sample\ (g)}{Volume\ of\ mould\ (cm^3)} \qquad \textit{Equ4.1}$$

$$\rho_d(g/cm^3) = \frac{\rho_{\text{bulk}}\ (g/cm^3)}{1 + MC} \qquad \textit{Equ4.2}$$

The degree of saturation (Sr) for each sample is also calculated using formula in Equ4.3.

$$Sr = \frac{\rho_{bulk}(1+e)}{\rho w * e} - \frac{Gs}{e} \qquad \textit{Equ4.3}$$

The moisture variations of the soils are 65% - 80%, 80% - 95%, 95% - 105%, 110% - 125%, and ≥125%, respectively representing 'Low Dry of OMC', 'High Dry of OMC', 'At OMC', 'Low Wet of OMC' and 'High Wet of OMC' denoted as 1, 2, 3, 4 and 5 respectively.

Table 4.4 show the analysed compaction data for all four soils and Figure 4.3 shows the compaction graph for each soil plotted as dry density against corresponding moisture content, and each soil's moisture variation. Factors for the soils compiled from the PSD test, Atterberg limit test and compaction test are summarised in Table 4.5.

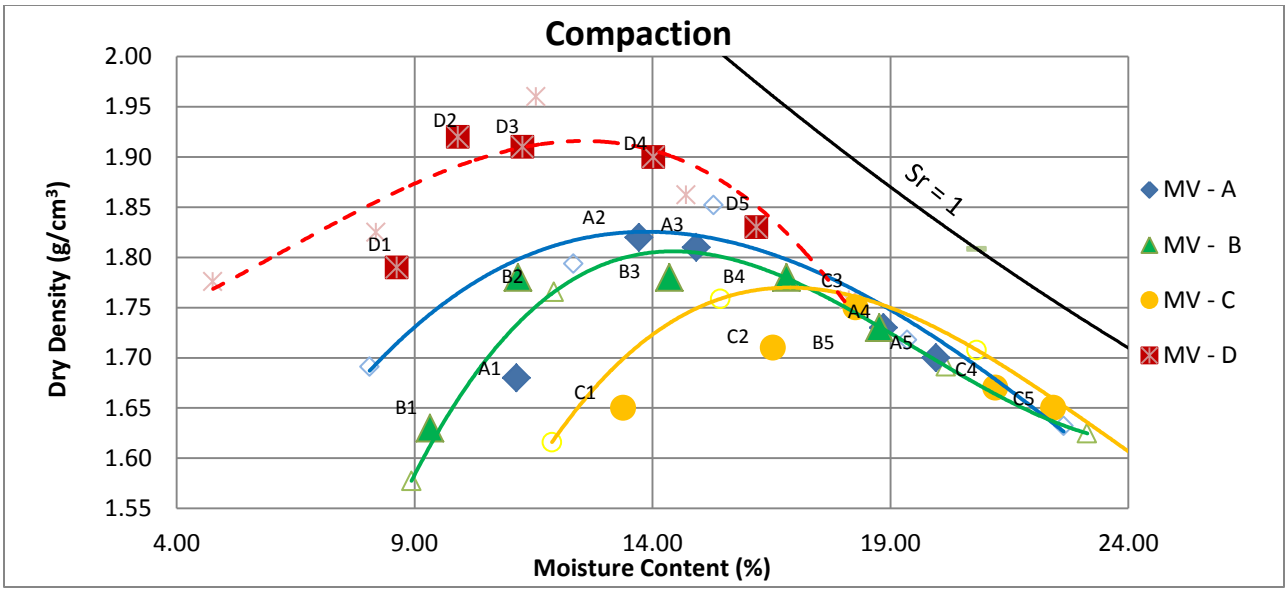

Figure 4.3: Compaction curve of the four soils with the moisture variation points (MV)

Table 4.4: Compaction result

SOILS	*Optimum Moisture Content 'OMC' (%)*	*Maximum Dry Density 'MDD' (g/cm³)*	*Degree of Saturation 'Sr'*
A	15.600	1.860	0.809
B	14.600	1.840	0.735
C	17.750	1.770	0.806
D	11.200	1.960	0.677

Comparing the compaction results and the previous PSD and Atterberg limit test, the following deductions can be made:

- The compaction results (Table 4.4) reflect the effect of the fines and plasticity of the soil. Soil C, which possess the highest percentage of clay fines and plasticity has the highest OMC, but the least MDD. And at the least amount of OMC the *D* gets to a MDD higher than A, B and C with the least degree of saturation, percentage of fines and plasticity.

This shows that soils with high percentage of clay fines attain their MDD at a high OMC and have a lower MDD than other soils. The opposite is the case when the soil is made of high percentage of fine sand.

- The higher the initial moisture content at compaction, the lower the collapsibility of the soil, this is because the initial bond from the fines is already weakened hence reduced metastable forces; so the remaining forces to be reduced completely by wetting is significantly less. Hence less collapse occurs.
- The higher the density of the soil, the more compact the structure, hence a less metastable structure. Since high density would give very little chance for volume change.
- The void ratio has an inverse relationship with the density. The denser the structure, the lower the void ratio, which causes less volumetric loss of the soil structure.
- The OMC of a soil gives a guide to how much moisture content a soil can absolve. Soils with the potential to absolve high amount of water tend to collapse more than those with less, since this high water content in the soil reduces its stability. Also low OMC give limited range of change in moisture content. The compaction curve gives a guide on collapsibility, since samples prepared dry of OMC are of higher collapse potential than those of At-OMC and wet of OMC.

It is difficult to predict which of the soil is most metastable from observation of the compaction result; but picking the related parameters, a prediction can be made. From the MDD, C with the least value is most likely to collapse but the clay bonds have a stabilizing effect on the structure; and from the degree of saturation, D is the most probable to be metastable except for the presence of clay bonds, high MDD and low OMC which would make it a more stable soil.

Table 4.5: Classification of soils A, B, C and D

Parameters			***A***	***B***	***C***	***D***
Percentage of Fines			78.10	92.52	97.52	38.62
Void ratio	*e*		0.56	0.58	0.64	0.48
Bulk density		*(g/cm³)*	2.15	2.11	2.08	2.18
Degree of saturation	*Sr*		0.81	0.73	0.80	0.68
Porosity	*n*		0.36	0.37	0.39	0.32
Specific Volume	*v*		1.56	1.58	1.64	1.48
Air voids	*A*	*(%)*	6.65	9.69	7.70	10.46

4.2 TRIAXIAL TEST

Four soils termed A, B, C and D were prepared at Low Dry of OMC', 'High Dry of OMC', 'At OMC', 'Low Wet of OMC' and 'High Wet of OMC' denoted as 1, 2, 3, 4 and 5 respectively. For each soil, triaxial tests were carried out to investigate the stress-strain effects of each soil at confining pressures 70kPa, 140kPa and 280kPa.

The triaxial data for the partially saturated soil samples were obtained using unconsolidated-undrained triaxial test, and analysed using formulas in Equ4.4 to Equ4.7.

$$\tau_f = c' + \sigma_f' tan\phi' \qquad \textit{Equ4.4}$$

$$\theta = 45^0 + \frac{\phi'}{2} \qquad \textit{Equ4.5}$$

$$\tau_f = \frac{1}{2}(\sigma_1' - \sigma_3')sin2\theta \qquad \textit{Equ4.6}$$

$$\sigma_f' = \frac{1}{2}(\sigma_1' + \sigma_3') + \frac{1}{2}(\sigma_1' - \sigma_3')cos2\theta \qquad \textit{Equ4.7}$$

Where τ_f= shear strength;

c' = effective cohesion;

σ_f' = effective normal stress at failure;

ϕ' = effective internal angle of friction;

θ = theoretical angle between the major principal plane and the plane of failure; and

σ_1' and σ_3' = effective principal stresses.

In unsaturated condition, the matric suction influences the shear strength of the soil. Equ4.8 represents the equation by Terzaghi (1936) for the shear strength of a soil; and Equ4.9 gives the formula for shear strength for unsaturated soil by Bishop (1959).

$$\tau_f = C' + (\sigma_n - \mu_w)tan\phi' \quad \textit{Equ4.8}$$

$$\tau_f = C' + (\sigma_n - \mu_w)tan\phi' + (\mu_a - \mu_w)[(\chi)tan\phi'] \quad \textit{Equ4.9}$$

Where τ_f, c' , ϕ', as previously described;

$(\sigma_n - u_a)$ = net normal stress;

$(u_a - u_w)$ = matric suction; and

(χ) = is a parameter dependent on the degree of saturation. It varies from 1 for fully saturated soil to 0 for totally dry condition.

4.2.1 A - Brown inorganic silty clay

The analysed values for A are represented in the stress – strain graphs for A1, A2, A3, A4 and A5 shown in Figure 4.4 below. The results from the curves are summarised in Table 4.6.

The following distinct features could be observed from the curves and summary table:

- Higher initial moisture content (MC) of the soil, produced far reduced deviator stress. Hence A5 with the highest Initial MC has the least shear strength of the other samples (A1, A2, A3 and A4).
- The higher the confining pressure applied on the soil, the higher the shear strength of the soil. A1 has the highest difference between the shear strengths of the samples under the 3 confining pressures (70kPa, 140 kPa and 280kPa). A2 and A4 have a similar trend of the shear strength with an average change in the confining pressure. Finally, A3 and A5 have shear stresses for the three confining pressures varying at similar trends with little difference between them. This is due to the compact nature of the sample A3 and the almost saturation point of A5. All these observations are evident from Figure 4.4.
- As the moisture variables of the soil increase, the internal friction angle reduces (from 43.15^o to 33^o to 16.64^o to 16.56^o to 5.71^o). See Table 4.6.

- At OMC cohesion has the highest value with 138 kPa at A3 and then reduces as the soil is away from the OMC. It decreases towards the dry of OMC with values of 115 kPa and 50 kPa for A2 and A1 respectively. In the wet of OMC direction it decreases with values of 63 kPa and 52 kPa for A5 and A4 respectively (Table 4.6).

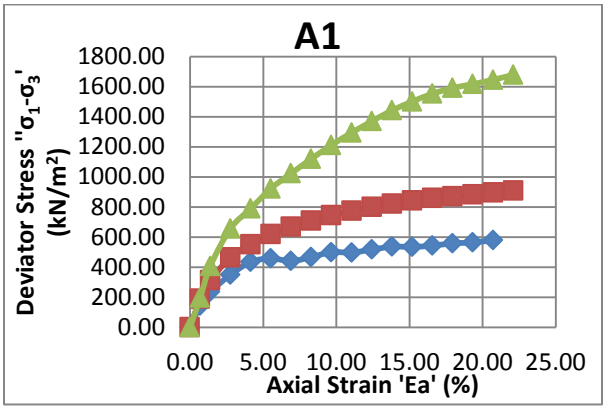

A1

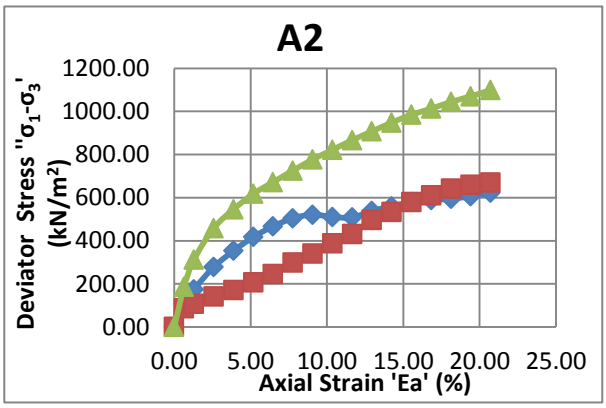

A2

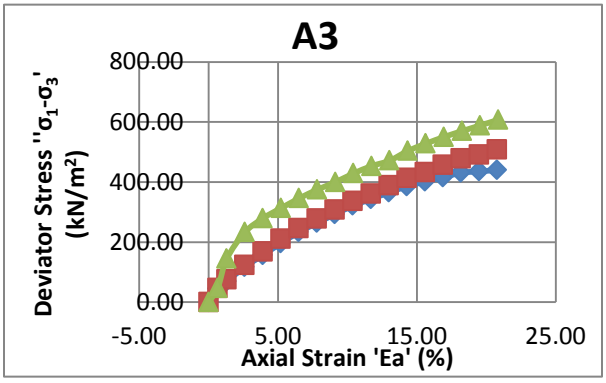

A3

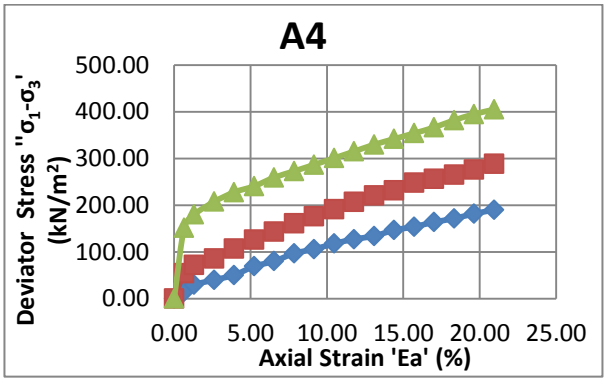

A4

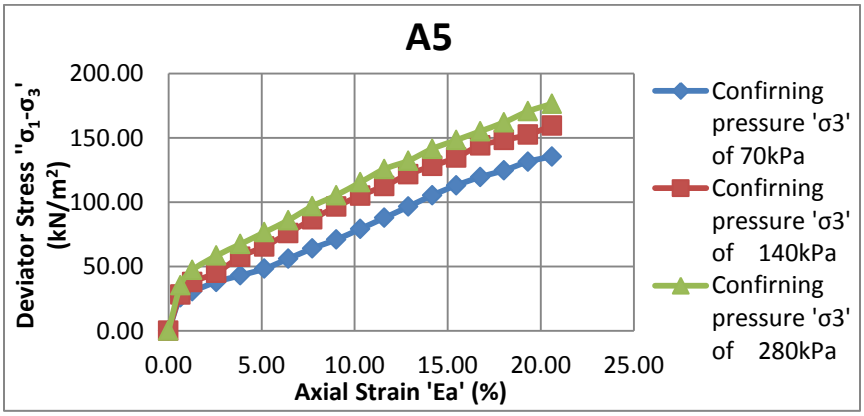

A5

Figure 4.4: Triaxial stress-strain curves for A.

Table 4.6: Stress-strain result for A

Result from graph	A1			A2			A3			A4			A5		
Confining pressure / Normal stress 'σ3'	70 kPa	140 kPa	280 kPa	70 kPa	140 kPa	280 kPa	70 kPa	140 kPa	280 kPa	70 kPa	140 kPa	280 kPa	70 kPa	140 kPa	280 kPa
Deviator stress (max) 'σ1-σ3' (kPa)	580	900	1650	625	676	1100	440	510	610	190	288	402	136	159	178
Axial stress 'σ1' (kPa)	650	1040	1930	695	816	1380	510	650	890	260	428	682	206	299	458
Internal angle of friction (^{o})	43.15			33.00			16.64			16.56			5.71		
Cohesion (kN/m^2)	50			115			138			63			52		

4.2.2 B - White inorganic silt

A summary of the analysed values for B can be observed in the stress – strain graphs for B1, B2, B3 B4 and B5 shown in Figure 4.5 below. The results from the curves are summarised in Table 4.7.

The following distinct features can be observed from the curves and summary table:

- Like soil A the higher the confining pressure applied on the soil, the higher the deviator stress of the soil. Increase in the initial moisture content of the soil, causes reduction in the soil's shear strength except for B2. At low moisture content silty soil particles form a loose soil structure with negligible cohesion and slight frictional force between their particles. Hence at this state, addition of load would cause the sample to crumble. Giving B2 a shear strength higher than B1.
- The effect of the confining pressures in B1, B2 and B3 produced high difference between the shear stresses of the samples. However for B4 and B5 the shear stresses under the confining pressures of 70kPa, 140 kPa and 280 kPa increase with a slight difference between them. This is evident from Figure 4.5.
- Here the increase in moisture content caused an initial increase in the internal friction angle from 41.99^{o}, 42.77^{o} and then reduction to the last value (39.5^{o} to 30.8^{o} to 11.31^{o}). Shown in Table 4.7 .
- The maximum cohesion is found at B4. The other cohesion values of B reduce as the moisture contents move away from the low wet of OMC (ie. B4). For samples drier than B4 these values are 135kPa for B3, 120 kPa for B2 and 85 kPa. Sample B5 with a higher MC have cohesion of 120 kPa (Table 4.7).

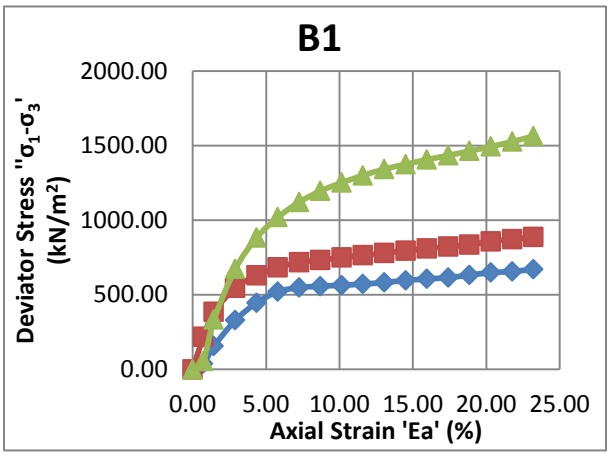

B1

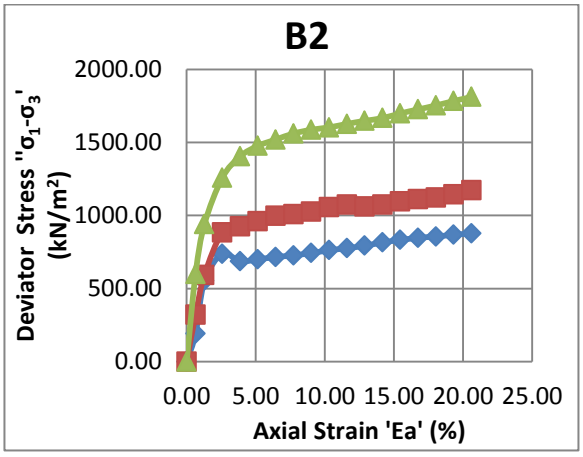

B2

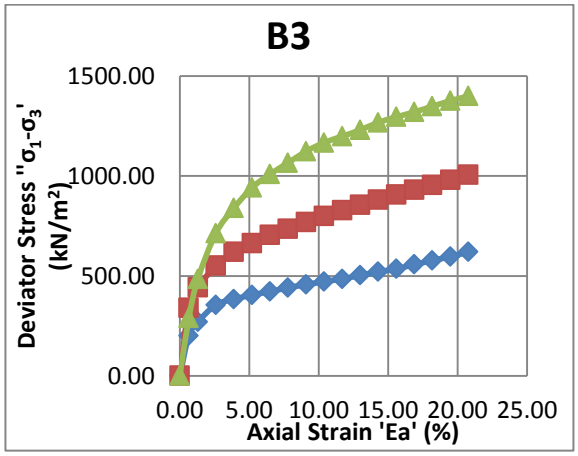

B3

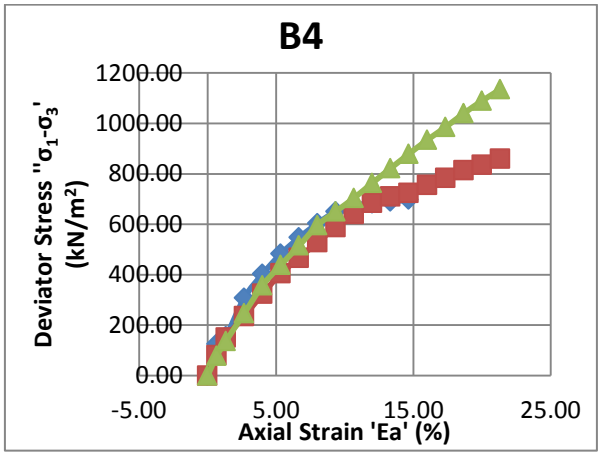

B4

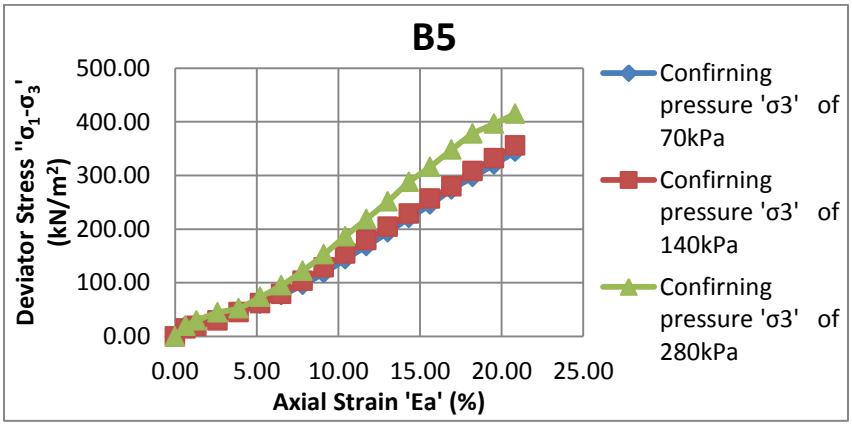

B3

Figure 4.5: Triaxial stress-strain curves for B.

Table 4.7: Stress-strain result for B

Result from graph	B1			B2			B3			B4			B5		
Confining pressure / Normal stress 'σ3'	70 kPa	140 kPa	280 kPa	70 kPa	140 kPa	280 kPa	70 kPa	140 kPa	280 kPa	70 kPa	140 kPa	280 kPa	70 kPa	140 kPa	280 kPa
Deviator stress (max) 'σ1-σ3' (kN/m^2)	670	880	1560	880	1165	1800	620	1005	1400	695	860	1124	341	354	413
Axial stress 'σ1' (kN/m^2)	740	1020	1840	950	1305	2080	690	1145	1680	765	1000	1404	411	494	693
Internal angle of friction (^{o})	41.99			42.77			39.52			30.84			11.31		
Cohesion (kN/m^2)	85			120			135			150			120		

4.2.3 C - Red inorganic Clay

The analysed values for C are represented in Figure 4.6 (stress – strain curves for C1, C2, C3, C4 and C5). The results from the curves are summarised in Table 4.8.

The following distinct features can be observed from the curves and summary table:

- Like soils A and B the higher the confining pressure applied on the soil, the higher the deviator stress of the soil; and increase in the initial moisture content of the soil, causes reduction in the soil's shear strength.
- The effect of the 70 kPa confining pressure in samples C1 and C2 produced high peak axial stress point at low axial strain, and then fails. This is typical of clay soils with low initial moisture content applied with low confining pressure. Samples C3, C4 and C5 have the shear stresses at confining pressures of 70kPa, 140 kPa and 280kPa increasing at similar trends with a decreasing difference between them. This is also the sign of a classic clay soil with average to high moisture content. This is evident from Figure 4.6.
- As the moisture contents increase, the internal friction angle reduces (41.28^{o}, 29.17^{o}, 16.65^{o}, 14.04^{o} and 5.71^{o}), as shown in Table 4.8.
- Sample C2 has the highest cohesion of 170 kN/m^2. Increased MC samples give reduced cohesions of: C3 – 137 kPa, C4 – 108 kPa and C5 – 60 kPa, and then the less MC sample C1 also has a lesser cohesion of 83 kPa. (Table 4.8).

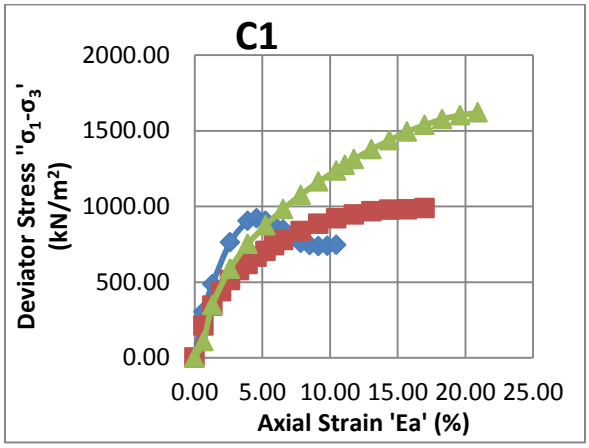

C1

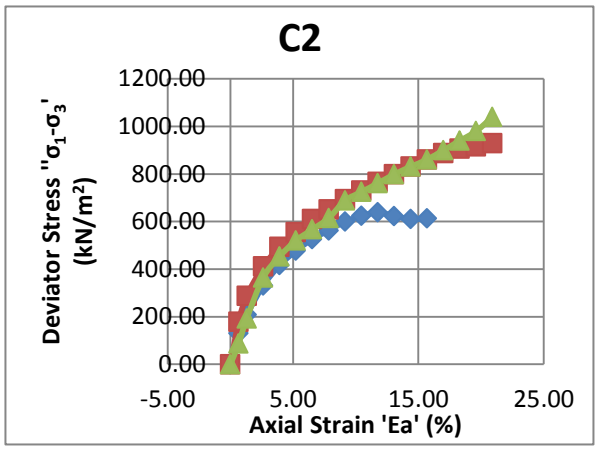

C2

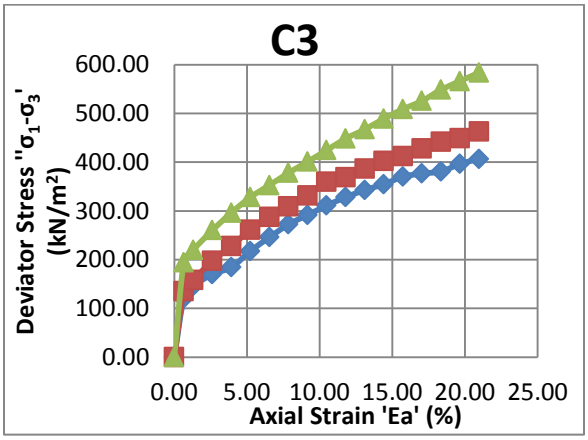

C3

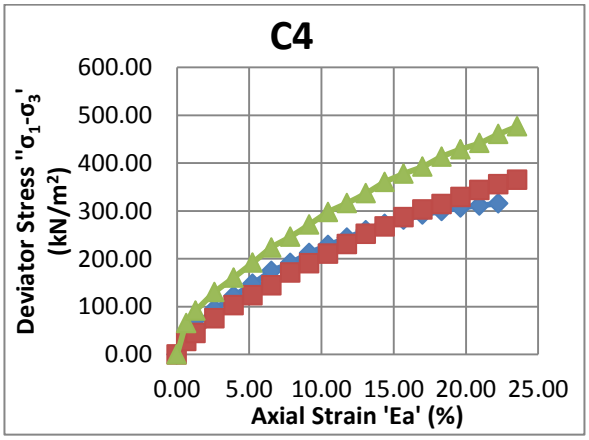

C4

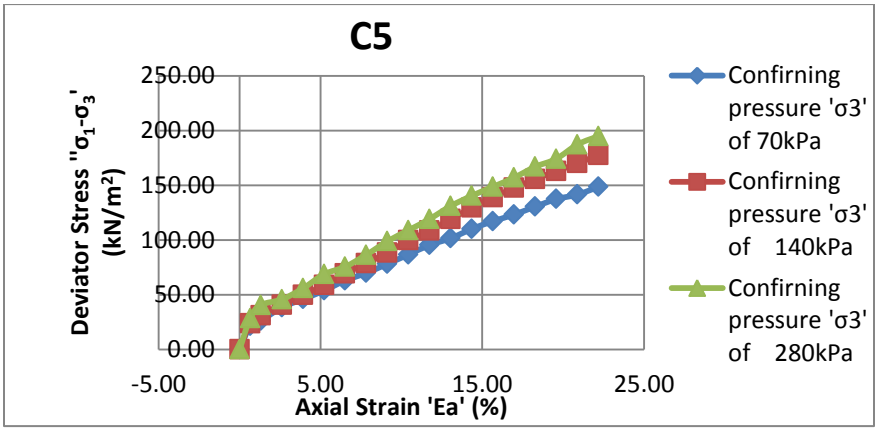

C5

Figure 4.6: Triaxial stress-strain curves for C.

Table 4.8: Stress-strain result for C

Result from graph	C1			C2			C3			C4			C5		
Confining pressure / Normal stress 'σ3'	70 kPa	140 kPa	280 kPa	70 kPa	140 kPa	280 kPa	70 kPa	140 kPa	280 kPa	70 kPa	140 kPa	280 kPa	70 kPa	140 kPa	280 kPa
Deviator stress (max) 'σ1-σ3' (kN/m^2)	720	990	1620	640	920	1040	408	460	580	318	355	460	148	177	194
Axial stress 'σ1' (kN/m^2)	790	1130	1900	710	1060	1320	478	600	860	388	495	740	218	317	474
Internal angle of friction (^{o})	41.28			29.17			16.65			14.04			5.19		
Cohesion (kN/m^2)	83			170			137			108			60		

4.2.4 D – Brown Sand-Clay mixtures

The analysed values for D represented in the stress – strain graphs for D1, D2, D3, D4 and D5 are shown in Figure 4.7 below. The results from the curves are summarised in Table 4.9.

The following distinct features can be observed from the curves and summary table:

- Like the other soils the higher the confining pressure applied on the soil, the higher the deviator stress of the soil; and increase in the initial moisture content of the soil, causes reduction in the soil's shear strength.
- The effect of the confining pressures in D1, D2 and D3 produced significant difference between the shear stresses of the samples. The soil with the combination of clay and fine sand gives the samples with low MC a high volumetric change (low density) as the confining pressure is increased. Although with higher MC, the soil sample approaching saturation (reduced voids) would cause a little volumetric change as the confining pressures increase. This is observed with sample D4 and D5 which varies at similar trends with slight difference between the shear stresses of the confining pressures. This is evident in Figure 4.7.
- The internal friction angles of samples D1 and D2 are the same (38.66^o, 38.66^o), and then as the moisture variables increase, the internal friction angle reduces (36.87^o, 1.91^o and 1.82^o). Shown in Table 4.9.
- Increase in moisture content caused an initial increase in the cohesion from D1 to D2 (105 kN/m^2 to 110 kN/m^2) and then a decrease in the cohesion as the MC continues increasing (D3 – 100 kN/m^2, D4 – 82 kN/m^2, and D5 – 74 kN/m^2). This is displayed in Table 4.9. Note that D2 has the highest cohesion.

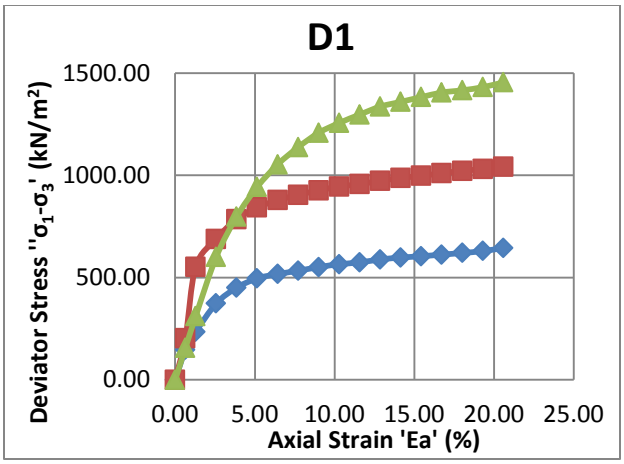

D1

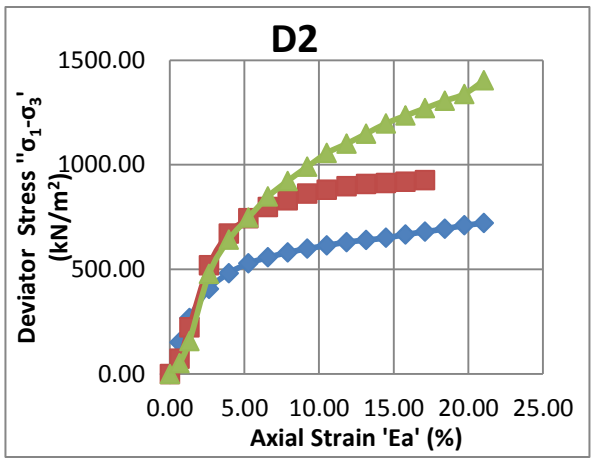

D2

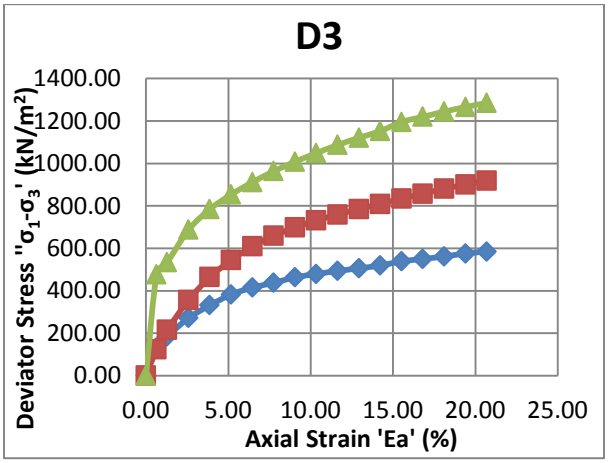

D3

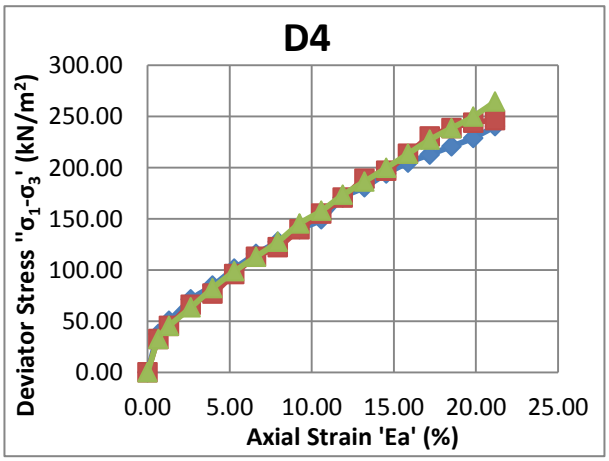

D4

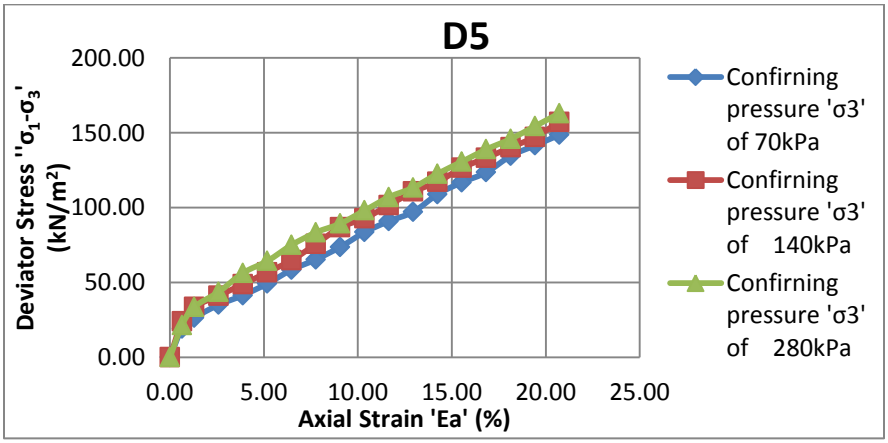

D5

Figure 4.7: Triaxial stress-strain curves for D.

Table 4.9: Stress-strain result for D

Result from graph	D1			D2			D3			D4			D5		
Confining pressure / Normal stress 'σ3'	70 kPa	140 kPa	280 kPa	70 kPa	140 kPa	280 kPa	70 kPa	140 kPa	280 kPa	70 kPa	140 kPa	280 kPa	70 kPa	140 kPa	280 kPa
Deviator stress (max) 'σ1-σ3' (kN/m^2)	640	1040	1450	720	925	1400	598.5	920	1280	240	247	263	149	157	162
Axial stress 'σ1' (kN/m^2)	710	1180	1730	790	1065	1680	668.5	1060	1560	310	387	543	219	297	442
Internal angle of friction (^{o})	38.66			38.66			36.87			1.91			1.82		
Cohesion (kN/m^2)	105			110			100			82			74		

The stress-strain curves and data obtained from the triaxial tests of the four soils reveal that with other factors kept constant increase in shear stress of a soil is affected by an increase in the confining pressure and decrease of the soil's initial moisture content. See Figure 4.4 to Figure 4.7. Although silty soils would require certain moisture content below which the shear strength would increase as the moisture content increases. The peak deviator stresses of the soils are found in A1 for soil A, then B2, C1 and D1 for their individual soils.

The shear strength parameters (cohesion and internal friction angle) of the individual soils are affected by the propotion of fines (clay, silt or fine sand) of the soil. Clay soils have a high resistance (shear strength) increase with confining pressure when moisture content is about or less than the OMC point. This is reflective in the internal friction and cohesion where the maximum points of these factors are seen. See Table 4.6 to Table 4.9.

The internal friction angle reduces as the soil's MC increases. In some cases for soils with higher silt or fine sand content, there is an initial increase before a continuous decrease in internal friction angle as the MC increases. The maximum points for the internal friction angle for the soil are A1, B2, C1, and D1.

Cohesion of a soil increases as the soil's MC increases, only to a point of which further increase in the soil's MC causes a reduction in cohesion of the soil. The maximum point of the cohesion factor is found within 80% to 110% of the soil's OMC. Although for soils with high percentage of silty or fine sand component, their max cohesion value could be above this range like in soil B. The maximum cohesion points of the soils used herein are A3, B4, C2 and for D, D2.

4.3 OEDOMETER TEST

As previously mentioned, Four soils termed A, B, C and D were prepared at 'low dry of OMC', 'high dry of OMC', 'At OMC', 'low wet of OMC' and 'high wet of OMC', denoted as subscript 1, 2, 3, 4 and 5, respectively. For each triaxial test carried out, an oedometer test was done on the same samples to determine their compressibility characteristics and the effects of various parameters and properties on the collapse potential. These samples were loaded at 'As-compacted' state and after 24 hours inundation under pressures of 5kPa, 10kPa, 25kPa, 50kPa, 100kPa, 200kPa and 300kPa. Collapse was quantified by taking the difference of the volumetric strains (%) between the as-compacted and inundated specimens.

The oedometer test were analysed using Equ4.10 - Equ4.16.

$$M_s = \frac{M_t}{W_0 + 1} \qquad \textit{Equ4.10}$$

$$H_s = \frac{M_s}{A * G_s * \rho_w} \qquad \textit{Equ4.11}$$

$$e_0 = \frac{H_0 - H_s}{H_s} \qquad \textit{Equ4.12}$$

$$M_v = \left(\frac{1}{1 + e_0}\right)\left(\frac{e_0 - e_f}{\Delta P}\right) \qquad \textit{Equ4.13}$$

$$V_s = \frac{\Delta h_i}{H} * 100\% \qquad \textit{Equ4.14}$$

$$C_v = \frac{0.848 * d^2}{t_{90}} \qquad \textit{Equ4.15}$$

$$K = C_v * M_v * \gamma_w \qquad \textit{Equ4.16}$$

Where Ms – Mass of solids;

Mt – Mass of soil in ring;

W_0 – Initial moisture content;

Hs – Height of solid particles;

A – Area of sample;

Gs – Specific gravity;

ρ_w – Density of water (1g/cm^3);

E_0 – Initial void ratio;

E_f – Final void ratio;

H – Sample height;

H_0 – initial sample height;

Δh_i - Initial change in sample height;

Mv – Coefficient of volume compressibility;

ΔP - Change in pressure;

Vs – Volumetric strain;

Cv – Coefficient of consolidation;

d – Thickness of the soil layer;

T_{90} – Value corresponding to the d_{90} point on the square root time curve graph; and

K – Coefficient of permeability.

4.3.1 Analysis for soil A - Brown inorganic silty clay

Figure 4.8, Figure 4.9, Figure 4.12 and Figure 4.15, give the graphical representation of pressure and void ratio, volumetric compressibility, volumetric strain and collapse respectively for the moisture variations of A. Figure 4.10, Figure 4.11 and Figure 4.13 represent void ratio, volume compressibility and volumetric strain plots against pressure for the moisture variations of B for as-compacted and inundated states. Figure 4.14 shows a column representation of volumetric strain of each pressure for the five moisture variations of A.

From the graphs and curves, the following can be observed:

- Increase in pressure caused a corresponding decrease in void ratio (Figure 4.8 and Figure 4.10), volume compressibility (Figure 4.9 and Figure 4.11) and volumetric strain (Figure 4.12 and Figure 4.13), but for the collapse plot, increase in pressure first caused an increase in collapse and then a decrease for A1 and A2 and the others samples show a linear collapse curve. See Figure 4.15.

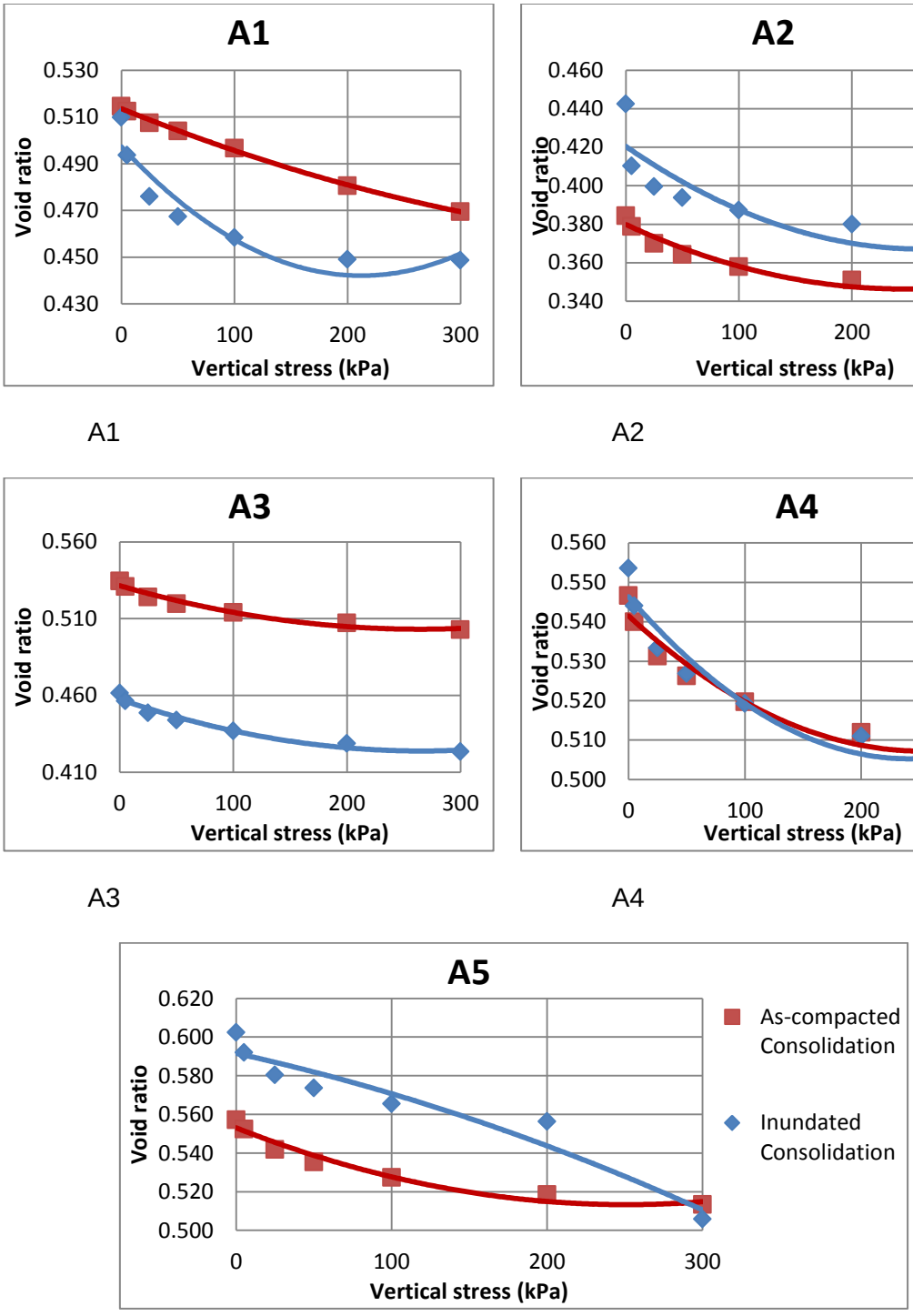

A1 A2

A3 A4

A5

Figure 4.8: Change in void ratio with increase in pressure for soil A and its moisture variations.

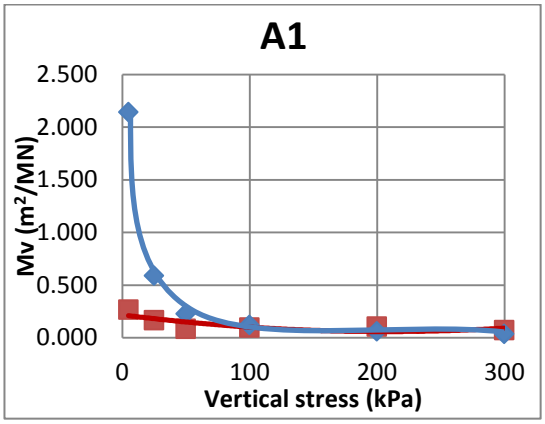

A1

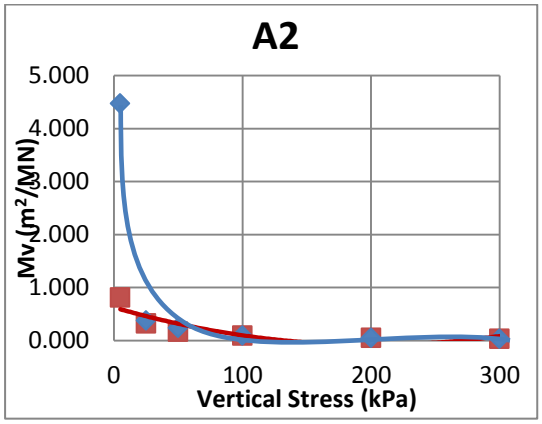

A2

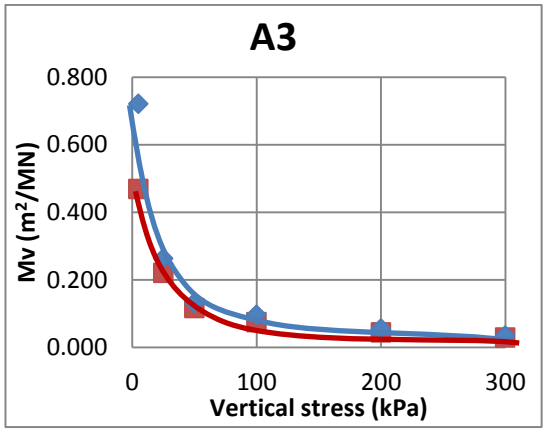

A3

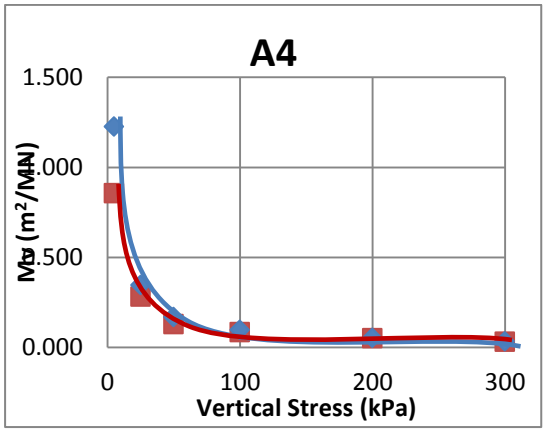

A4

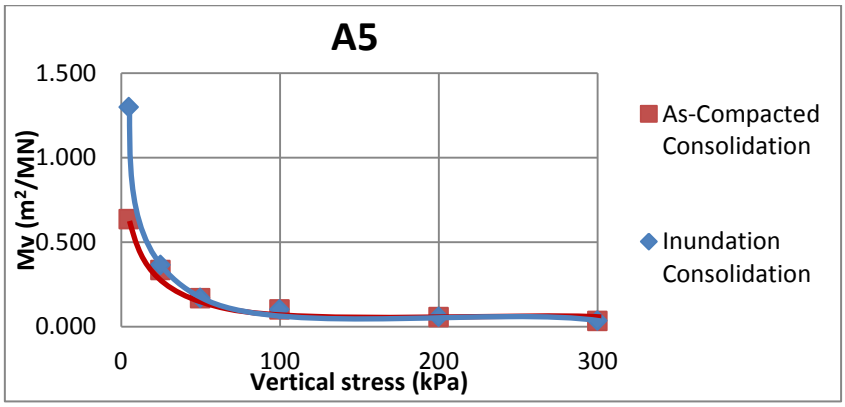

A3

Figure 4.9: Array of volume compressibility versus vertical stress of A moisture variations at As-compacted and Saturation state.

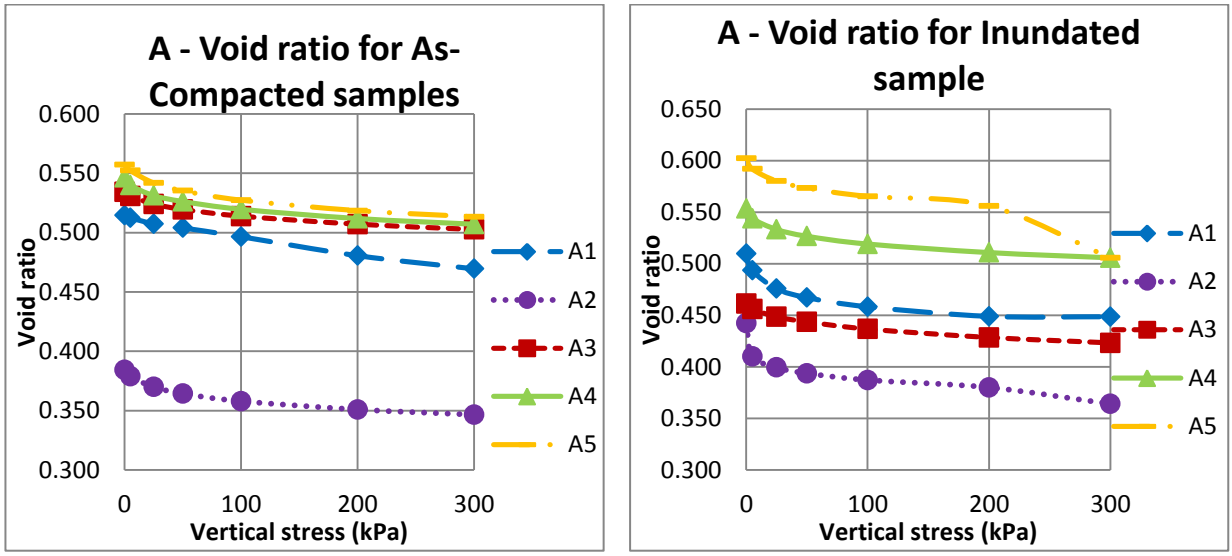

Figure 4.10: Soil A change in void ratio as pressure increases for both as-compacted and inundated samples.

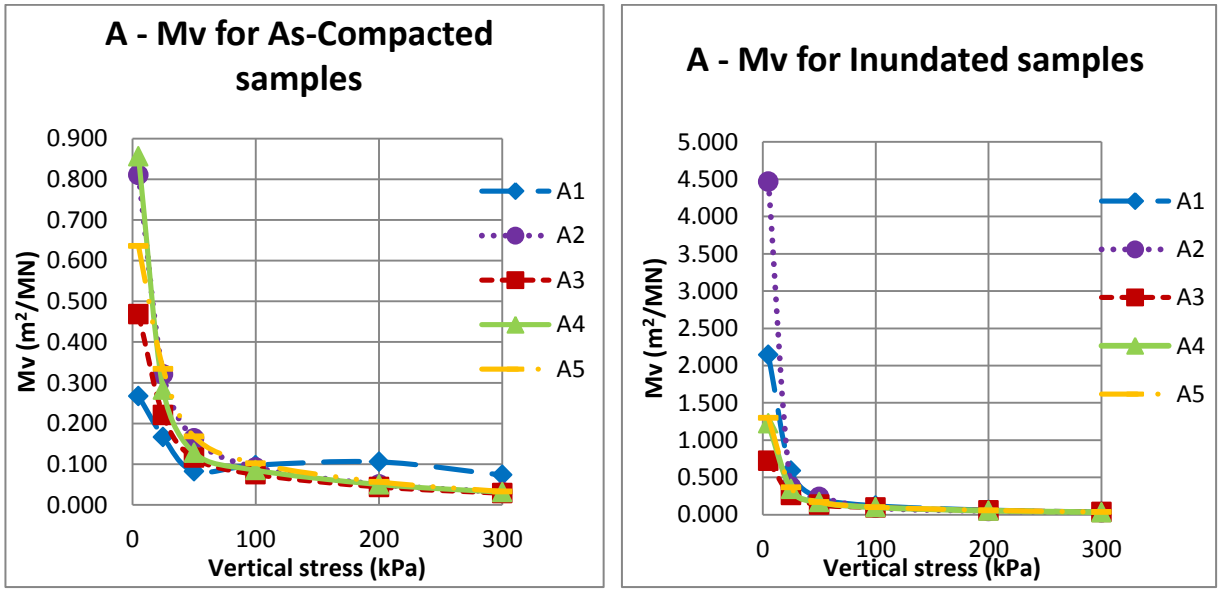

Figure 4.11: Soil A change in volume compressibility as pressure increases for both as-compacted and inundated samples.

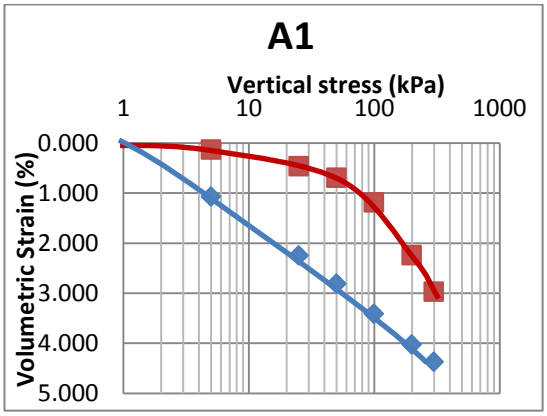

A1

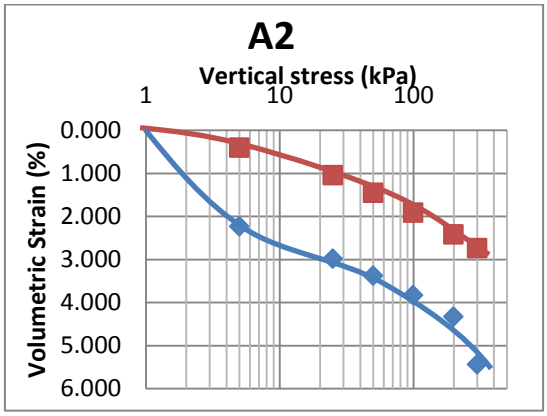

A2

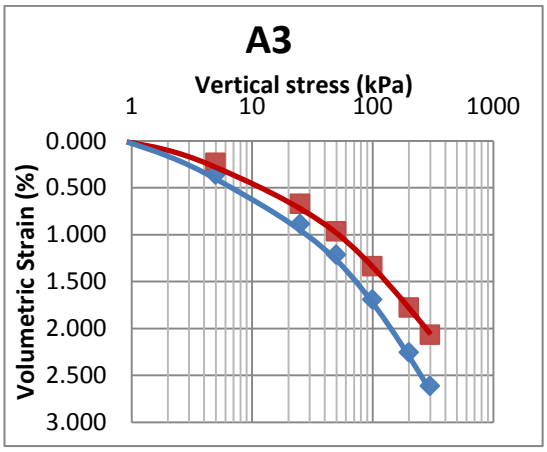

A3

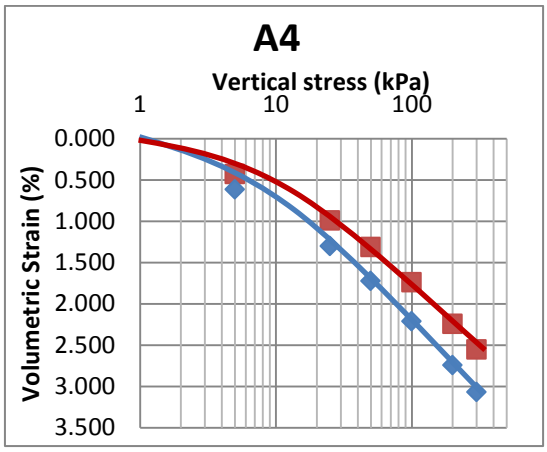

A4

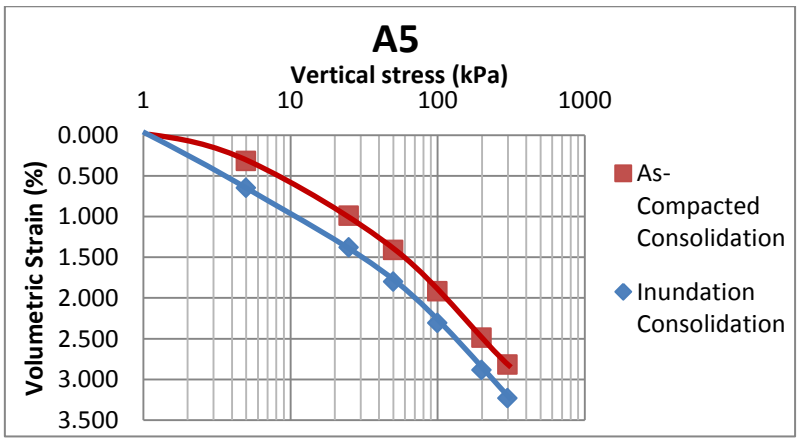

A5

Figure 4.12: Double-Oedometer tests result for the different moisture variations for soil A

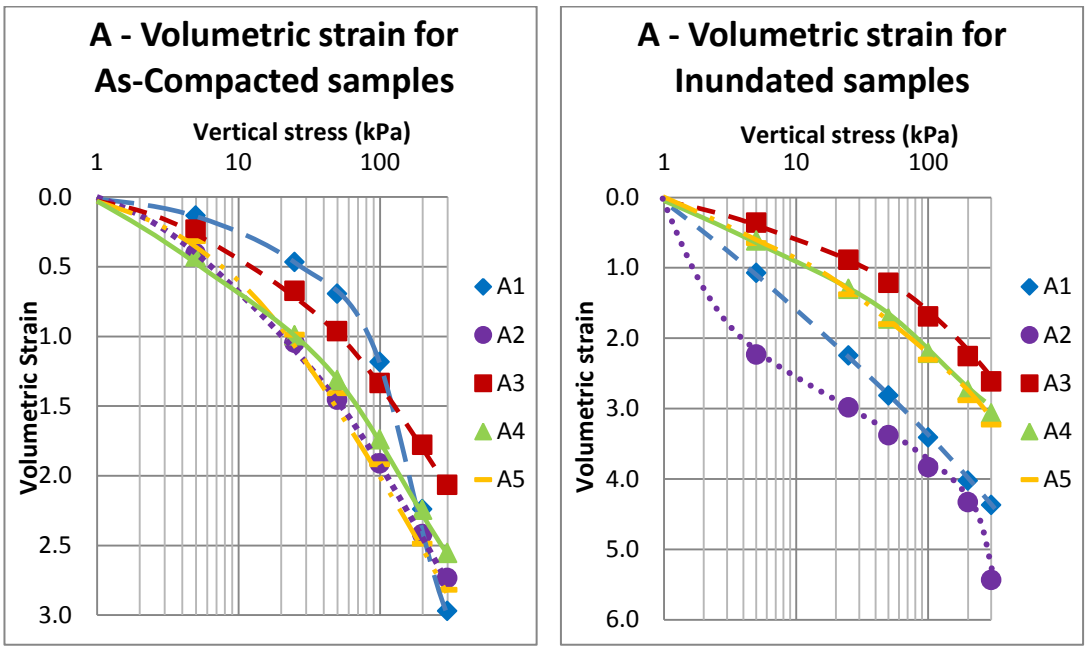

Figure 4.13: Soil A change in volumetric strain as pressure increases for both as-compacted and inundated samples.

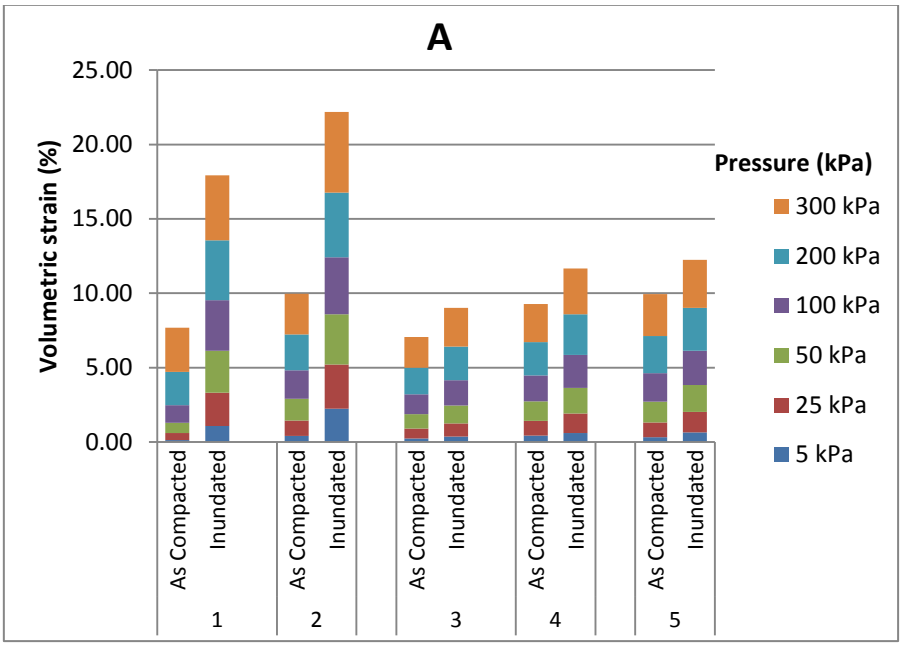

Figure 4.14: Column representation of the volumetric strain of each pressure in kPa at as-compacted and saturated states for soil A.

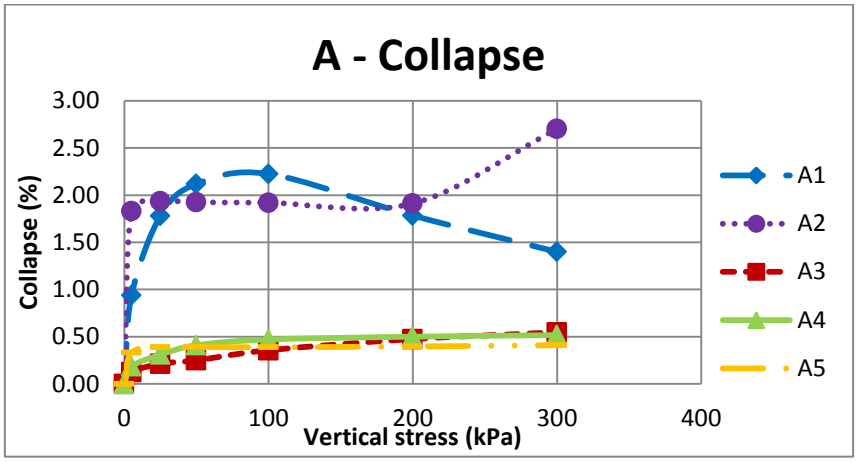

Figure 4.15: Collapse plot at various pressures for soil A

- For the graph of void ratio against pressure, the initial positions of the as-compacted and inundated samples are affected by the compaction during preparation stage. A1 has the as-compacted graph higher than the inundated sample, with line trend close together at low pressure then diverges at mid-point and converges at higher pressure. A2 and A3 have both of their curves (from as-compacted and inundated samples) gradually flowing downwards at an almost parallel pattern with the as-compacted sample higher. Sample A4 has both curves flowing stiff to gentle rate with a cross point at 100kPa pressure. For A5, as the pressure increases, the void ratios flow of both as-compacted and inundated converge with the inundated sample higher. Therefore for A, as the pressure increases the curves for as-compacted is of a steep flow for highly dried samples and it becomes gentler for higher moisture content. For the inundated samples with dry of OMC (A1) at initial pressures, have a steep flow which gentles out as the pressure increases to much higher pressure. With higher MC, the curves of inundation samples are as gentle as the as-compacted samples. Shown previously in Figure 4.8.
- The graphs for void ratio against pressure of as-compacted state and inundated state moisture variation for soil A (Figure 4.10) show that, the

inundated samples each have similar flow pattern with A5 having the highest initial point and A2 having the least. As the pressure increases A2 and A5 flow gradually reducing until 200 kPa where there is a sharp drop, showing a tangible drop in void. The samples in their as-compacted state all have a gradual reduction in void ratio as the pressure increases.

- For the graph of volume compressibility against pressure, the as-compacted and inundation soils at zero loading have the first point of the as-compacted higher. And as vertical stress increases, the points merge to a single flow of points as both approaches zero. A1 and A2 have the highest volume compressibility factor at zero vertical stress than A3, A4 and A5. Hence, the closer to saturation the as-compacted soil is the lower the volume compressibility and the more convergence of the points. The inundated samples of all the specimens have low initial volume compressibility. Although individually the A1 has the least initial volume compressibility; being with the least MC, it's prone to absorb the most moisture during inundation. As shown previously Figure 4.9.
- The flow pattern for volume compressibility of the moisture variation for soil A at as-compacted state and inundated state shown in Figure 4.11. As the pressure increases the volume compressibility steep drop, and then gentile flow approaching zero. In the samples in the as-compacted states, the steep drop ends at 50 kPa whiles for the inundated samples, 25 kPa makes the end of the steep drop.
- Graphs of volumetric strain against pressure (Figure 4.12) have trend lines for inundated curves at higher volumetric strain than those of the 'As-compacted' volumetric strain. Samples dry of OMC (A1 and A2) have the curves of as-

compacted samples and inundated samples more apart than those at-OMC (A3) and wet of OMC (A4 and A5).

- Comparing the volumetric strain against pressure of the individual moisture variations for soil A, in their as-compacted and inundated states is shown Figure 4.13; The curves for as-compacted state, are all having similar flowing with A1 having the most arch. Hence it experiences low change in volumetric strain at low pressures and higher change in volumetric strain beyond 50 kPa. For the inundated state curves, the samples have different flow path with A3 having the least decline. A2 and A1 have the most increase in volumetric strain as pressure increase.
- In Figure 4.14 the column representation of the volumetric strain is displayed showing the stack of inundated sample's volumetric strain is higher than those of the as-compacted for the pressure sum. Pressures 200 kPa and 300 kPa unlike the other pressures have the most volume change in all the moisture variations and their as-compacted and inundated samples.
- The collapse of each moisture variation of A at each pressure is shown in Figure 4.15. The curves for A3, A4 and A5 are very similar with the first most increased collapse at 25 kPa, and the subsequent minimal increase as the pressures increase. A1 and A2 have very high collapses as the pressure increases. A1 has a continuous increase in collapse to the peak collapse at 100 kPa, after which increased pressure made it collapse less. A2 has an instantaneous increased collapse at 25 kPa pressure which is maintained till 200 kPa; after which at 300 kPa, the collapse is increased to the peak.

4.3.2 Analysis for soil B - White inorganic silt

Figure 4.16, Figure 4.17, Figure 4.20 and Figure 4.23, gives the graphical representation of pressure against void ratio, volumetric compressibility, volumetric strain and collapse respectively of the moisture variation of B. Figure 4.18, Figure 4.19, and Figure 4.21 represents void ratio, volume compressibility and volumetric strain plots against pressure of the moisture variations of B for as-compacted and inundated states. Figure 4.22 shows a column representation of volumetric strain of each pressure for the five moisture variations of B.

From the graphs and curves, the following can be observed:

- Like A, B has a similar relationship between the Increasing pressure causing the decrease in void ratio (Figure 4.16 and Figure 4.18), volume compressibility (Figure 4.17 and Figure 4.19) and volumetric strain (Figure 4.20 and Figure 4.21).
- For the graph of void ratio against pressure, as the pressure increases the B1 and B2 have their curves similarly aligned. The as-compacted curves flowing in a gentle manner while the inundated curves have an initial steep flow and then a gentle end from pressure 100 kPa. Samples B3 and B4 have their curves parallel. As the pressure increases the B5 has the curves converging towards each other showing that the inundated curve is flowing downwards at a faster rate than the as-compacted curve. This response is similar to these of soil A. as shown in Figure 4.16.
- In the graphs for void ratio of as-compacted state and inundated state moisture variation for soil B (Figure 4.18), the inundated samples each have similar flow pattern. B1 has the highest initial point and B2 has the least. As the pressure increases B1 and B5 flow gradually reducing until 200 kPa where there is a

sharp drop, showing a massive drop in void as compacted to the other B samples. The samples in their as-compacted state all have a gradual reduction in void ratio as the pressure increases.

- For the graph of volume compressibility against pressure, the same observation can be seen as that of A with the inundated samples having higher volume compressibility than as-compacted sample. B2 has the farthest initial as-compacted sample curve point from the inundated sample curve. Whiles sample B1 has its first as-compacted curve point farther than B and B3. As shown in Figure 4.17.
- The pattern of flow for volume compressibility of the moisture variation for soil B at as-compacted state and inundated state are displayed in Figure 4.19. As the pressure increases the volume compressibility steep drop, and then gentile flow approaching zero. In the samples of as-compacted states, the steep drop ends at 50 kPa whiles for the inundated samples, 25 kPa makes the end of the steep drop, same as in the soil A.
- Like Soil A, the graphs of volumetric strain against pressure for soil B in Figure 4.20 have trend lines for inundated curves at higher volumetric strain than those of the 'As-compacted' volumetric strain. Also, the samples dry of OMC (B1 and B2) have the curves of as-compacted samples and inundated samples more apart than the other moisture variations (B3, B4 and B5). Although, B2 has the most space between the as-compacted sample and the inundated sample.

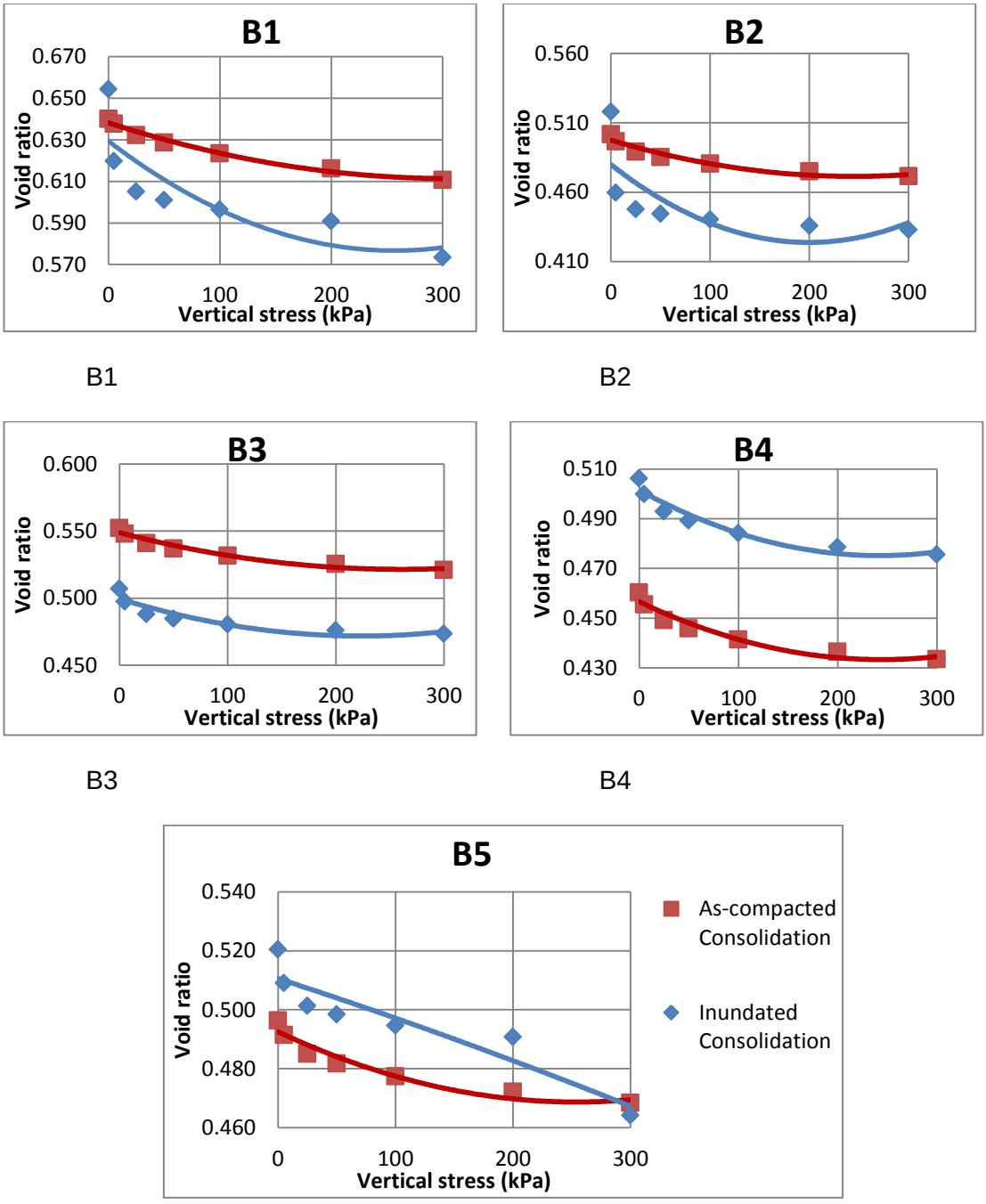

Figure 4.16: Change in void ratio with increase in pressure for soil B and its moisture variations.

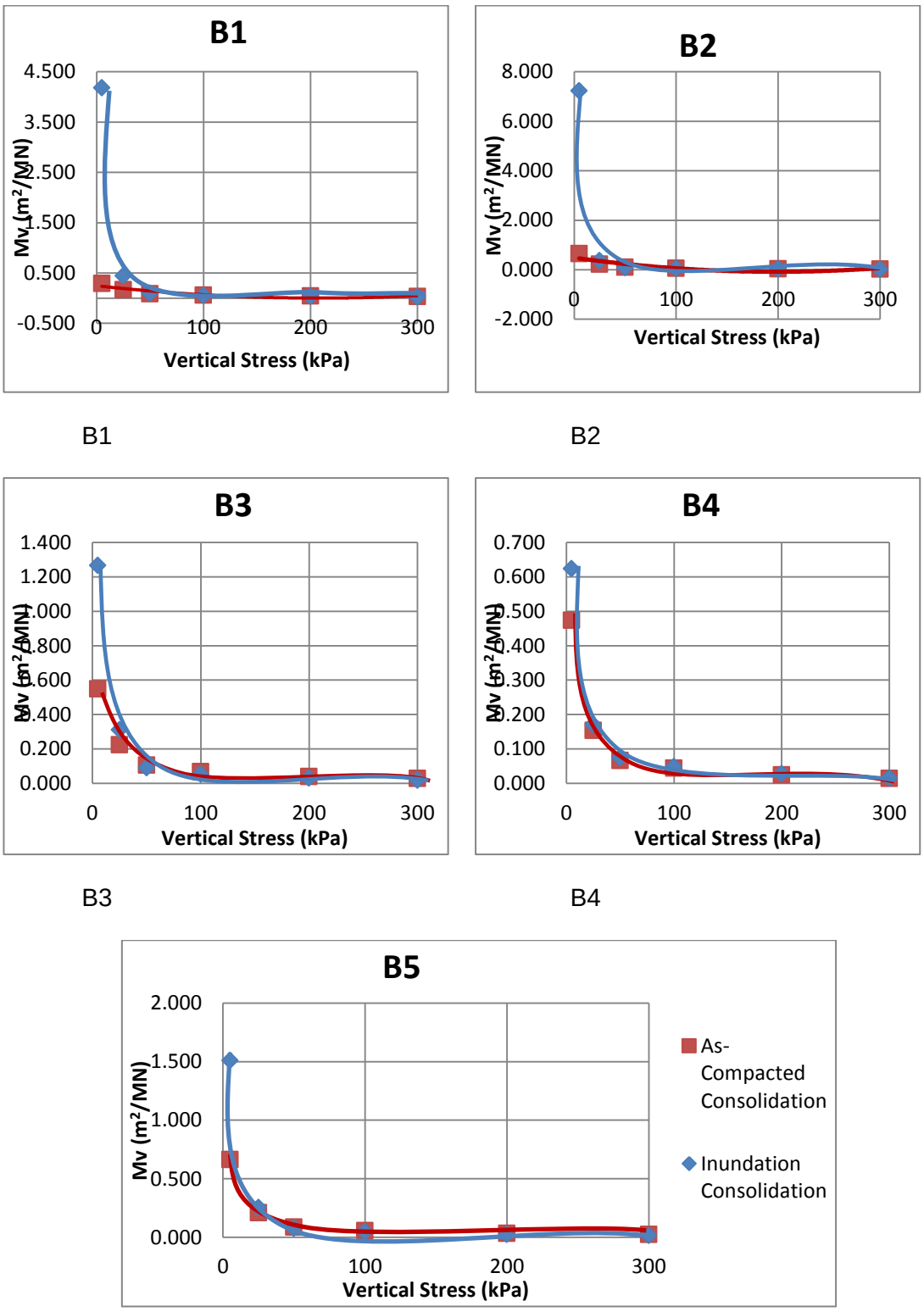

Figure 4.17: Array of volume compressibility versus vertical stress of B moisture variations at as-compacted and Saturation state.

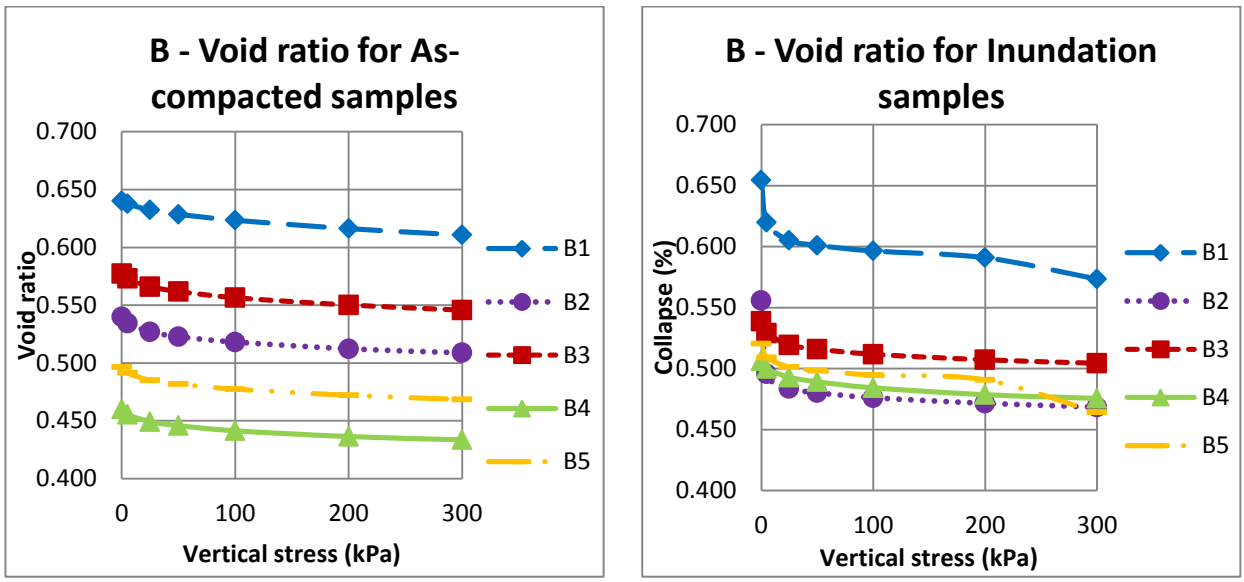

Figure 4.18: Soil B change in void ratio as pressure increases for both as-compacted and inundated samples.

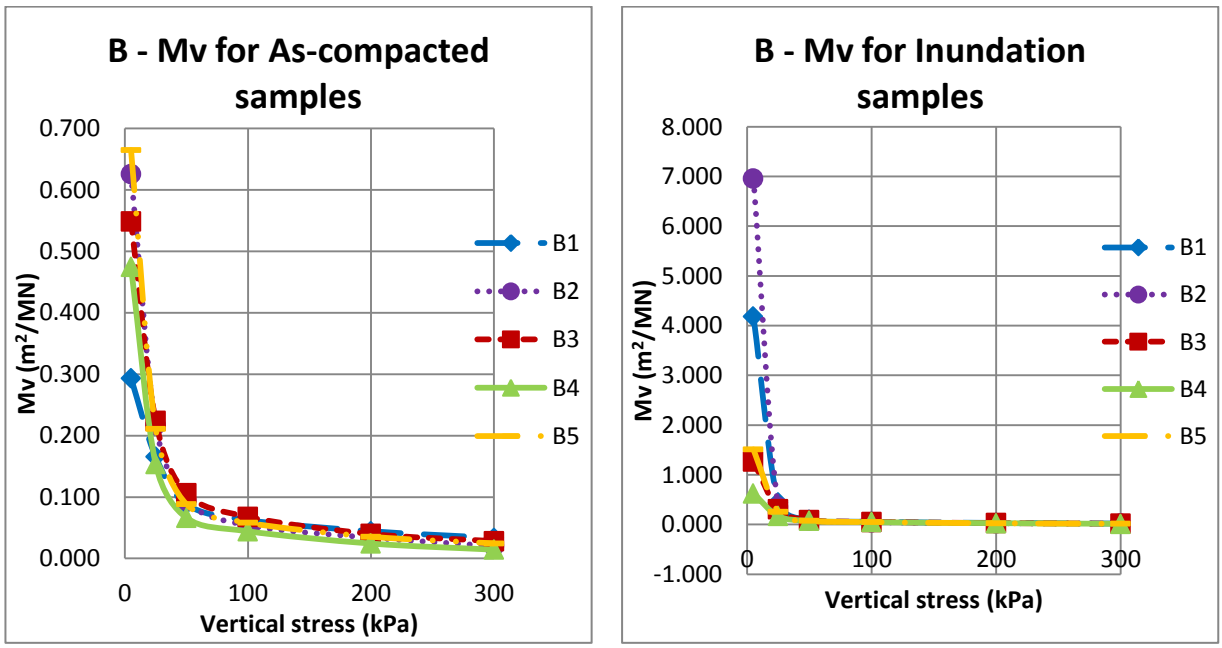

Figure 4.19: Soil B change in volume compressibility as pressure increases for both as-compacted and inundated samples.

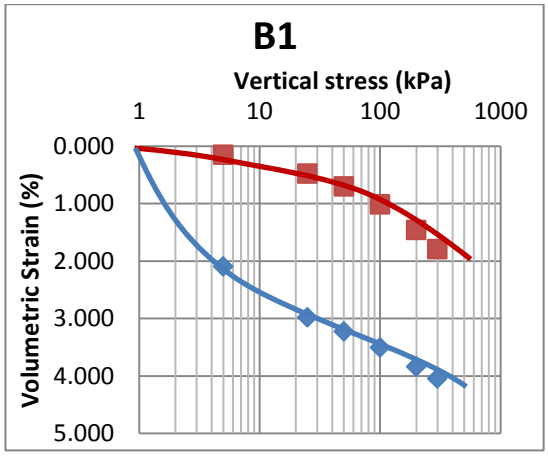

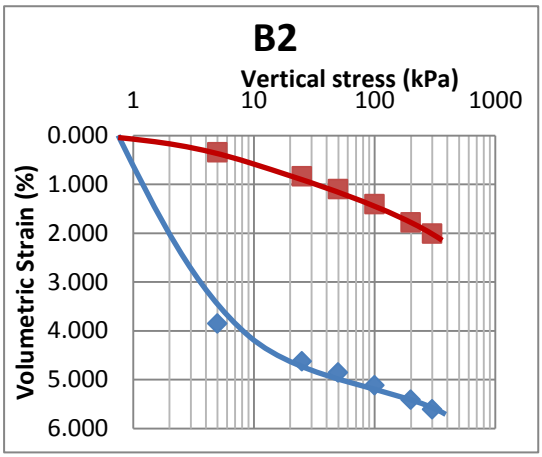

B1 B2

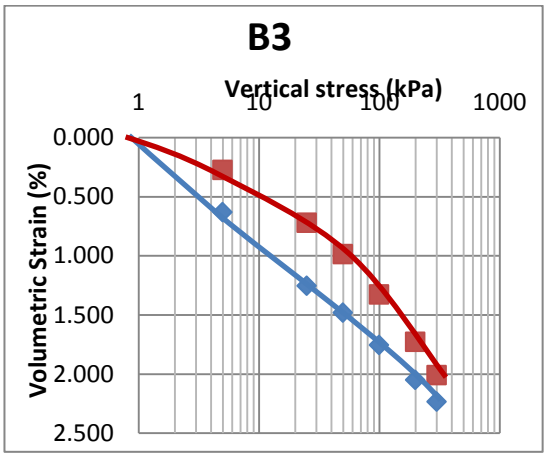

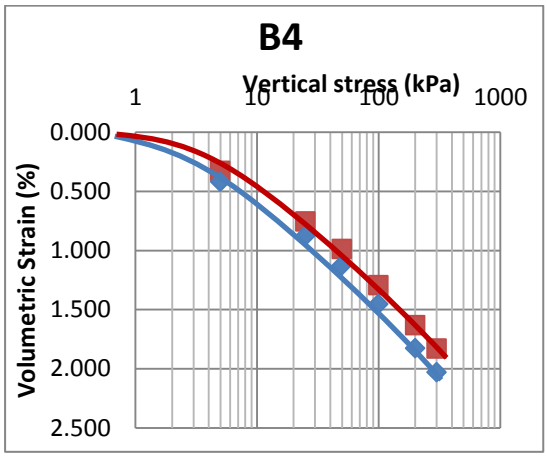

B3 B4

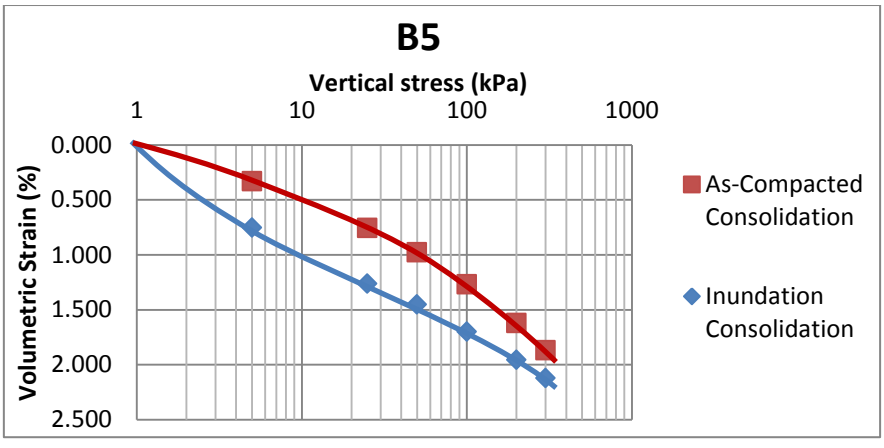

B5

Figure 4.20: Double-Oedometer tests result for the different moisture variations for soil B

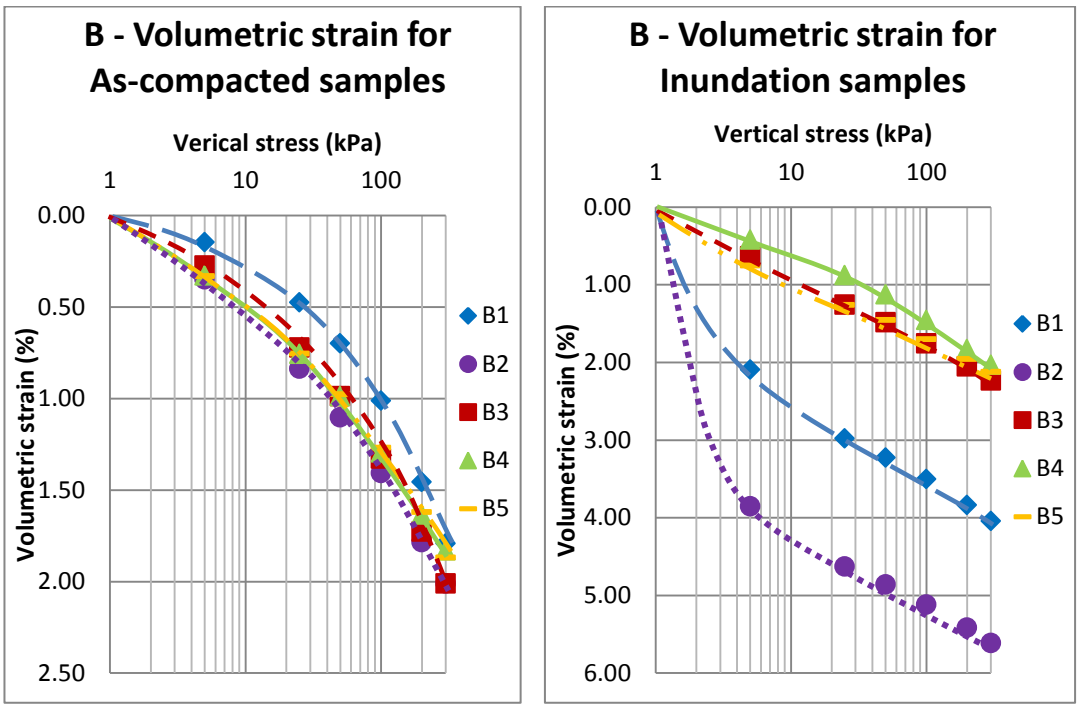

Figure 4.21: Soil B change in volumetric strain as pressure increases for both as-compacted and inundated samples.

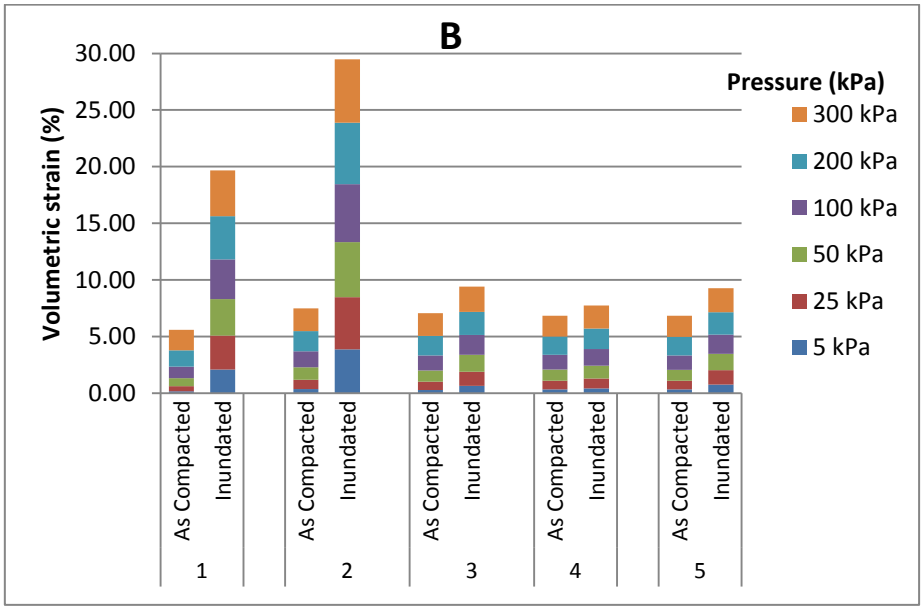

Figure 4.22: Column representation of the volumetric strain of each pressure in kPa at as-compacted and saturated states for A, B, C and D.

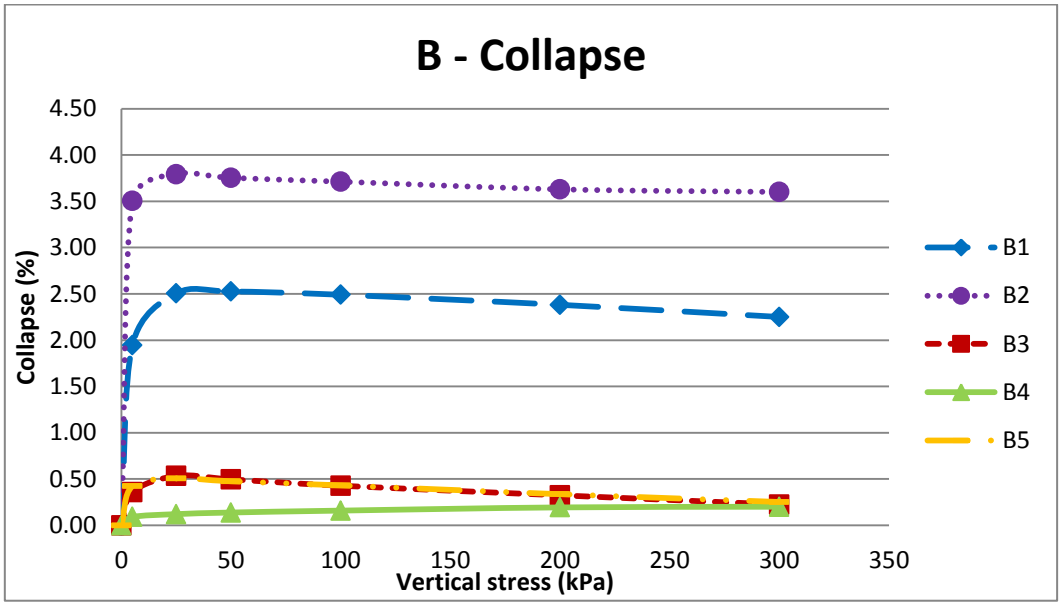

Figure 4.23: Collapse plot at various pressures for soil B

- Comparing the individual moisture variations for soil B, in their as-compacted and inundated states for the volumetric strain is as shown in Figure 4.21. The curves for as-compacted state all have similar flowing curves as the pressure increases. For the inundated state curves, the samples have different flow path, B3, B4 and B5 all have the least decline. B2 and B1 have the most loss in volumetric strain as pressure increased. The steep fall from both samples are found between 0 kPa and 5 kPa pressures.
- In Figure 4.22 the column representation of the volumetric strain showed that pressures 200 kPa and 300 kPa have the most volume change for all the moisture variations and their as-compacted and inundated samples; also, the column escalade show that the inundated sample show higher stack than the as-compacted.
- Collapse of the moisture variation of B at each pressure is shown in Figure 4.23. B2 has the highest collapse for the all the pressures while B4 has the least. The curves for B3, B4 and B5 are almost the same with low collapse and samples B1 and B2 have very high collapse.

4.3.3 Analysis for soil C - Red inorganic clay

Figure 4.24, Figure 4.25, Figure 4.28 and Figure 4.31, gives the graphical representation of pressure and void ratio, volumetric compressibility, volumetric strain and collapse respectively of the moisture variation of C. Figure 4.26, Figure 4.27 and Figure 4.29 represents void ratio, volume compressibility and volumetric strain plots against pressure of the moisture variations of C for as-compacted and inundated states. Figure 4.30 shows a column representation of volumetric strain of each pressure for the five moisture variations of C.

From the graphs and curves, the following can be observed:

- With the Increase in pressure, the void ratio (Figure 4.24 and Figure 4.26), volume compressibility (Figure 4.25 and Figure 4.27) and volumetric strain (Figure 4.28 and Figure 4.29) decreases.
- For the graph of void ratio against pressure, it can be observed that, as the pressure increases the curve of the C1 and C2 have their inundated curve flowing from steep at lower pressures to a more gentle flow at much higher pressures. For C3, C4 and C5 the curves for as-compacted and inundated are both flowing at a similar flow. As shown in Figure 4.24.
- In the graphs of void ratio against pressure of as-compacted state and inundated state moisture variation for soil C (Figure 4.26), the inundated samples each have similar flow pattern same as soils A and B. C4 has the highest initial point and C2 has the least. The samples in their as-compacted state and inundated state, all have a gradual reduction in void ratio as the pressure increases.
- For the graph of volume compressibility against vertical stress, C2 has the highest difference between the volume compressibility for the as-compacted

and inundated samples. C1 and C2 have a much higher difference than C3, C4 and C5. Shown in Figure 4.25**.**

- The flow pattern for volume compressibility against pressure of soil C moisture variation at as-compacted state and inundated state are displayed in Figure 4.27. The flow pattern is the same as soils A and B, having the samples in their as-compacted state, reduce at a steep drop rate ending at 50 kPa and for the inundated samples, steep drop rate ending at 25 kPa of pressure before concluding the flow at a gentle flow path towards zero volumetric compressibility.
- Graphs of volumetric strain against pressure shown in Figure 4.28 have the inundated curves higher in volumetric strain than those of the 'As-compacted'. The differences between the inundated curves are much higher in C1 and C2 as compared to C3, C4, and C5. Although C2 has the highest volumetric strain difference.
- Comparing the volumetric strain for soil C moisture variations in their as-compacted and inundated states are shown Figure 4.29. The curves for as-compacted state like in soils A and B, all have similar gentle flowing curves with C1 having the most arch seen in low volumetric strain at initial pressures but then experiences high volumetric strain from 100 kPa pressure to 300 kPa. For the inundated state curves, the samples B1, B3, B4 and B5 all have the least decline. B1 has the most volumetric strain as pressure increased. The steep fall is found between 0 kPa and 5 kPa pressures.

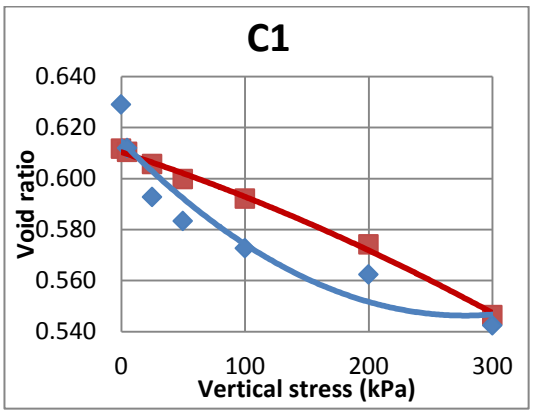

C1

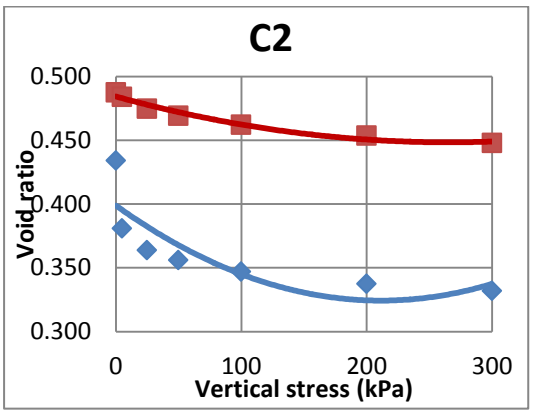

C2

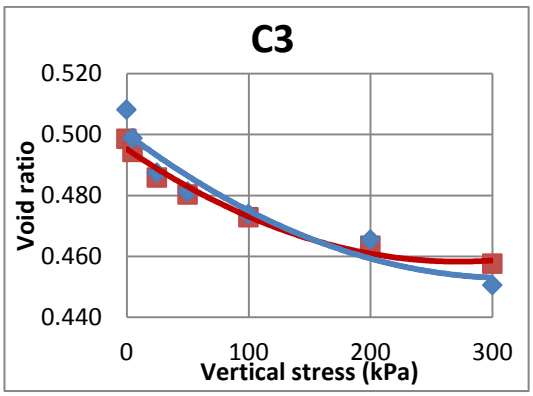

C3

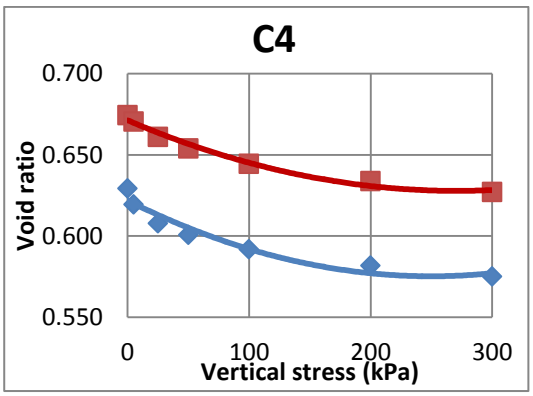

C4

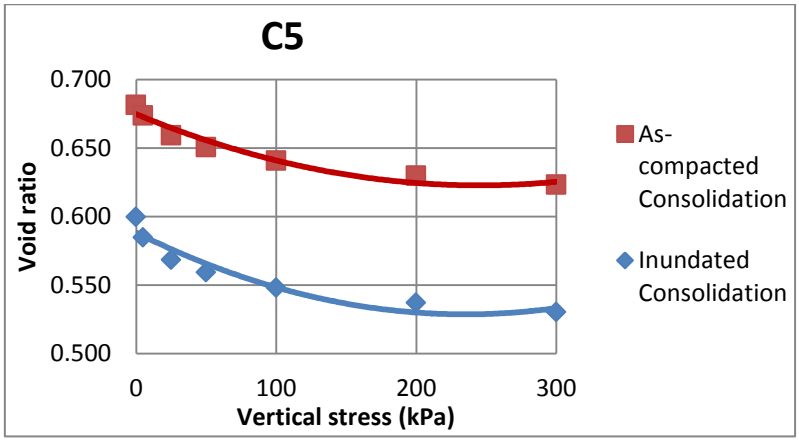

C5

Figure 4.24: Change in void ratio with increase in pressure for soil C and its moisture variations.

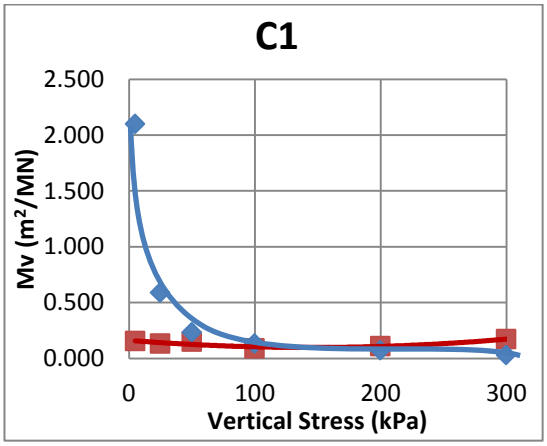

C1

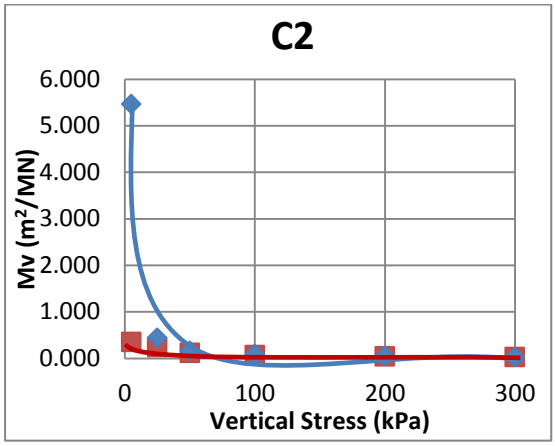

C2

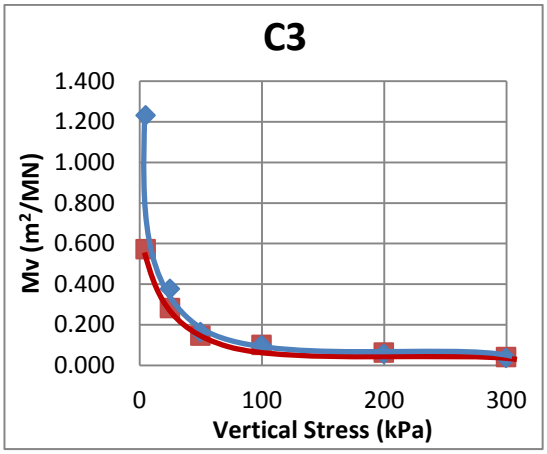

C3

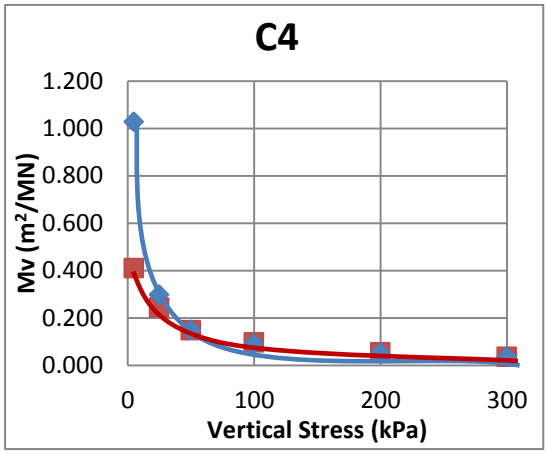

C4

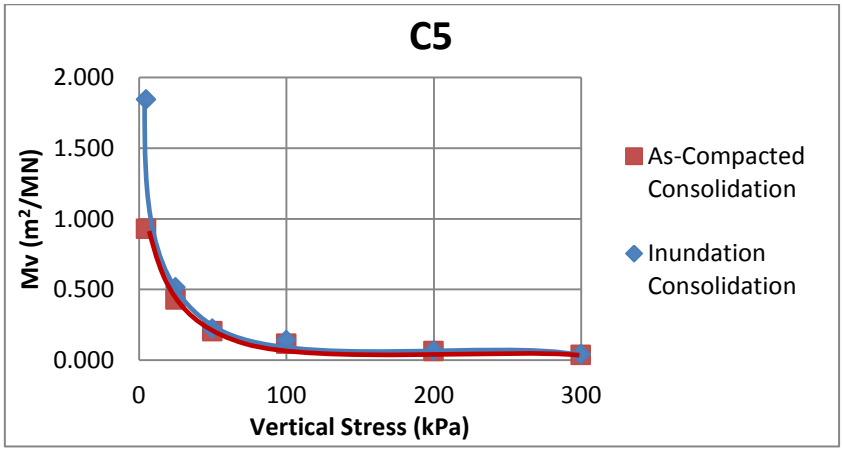

C5

Figure 4.25: Array of volume compressibility versus vertical stress of C moisture variations at as-compacted and Saturation state.

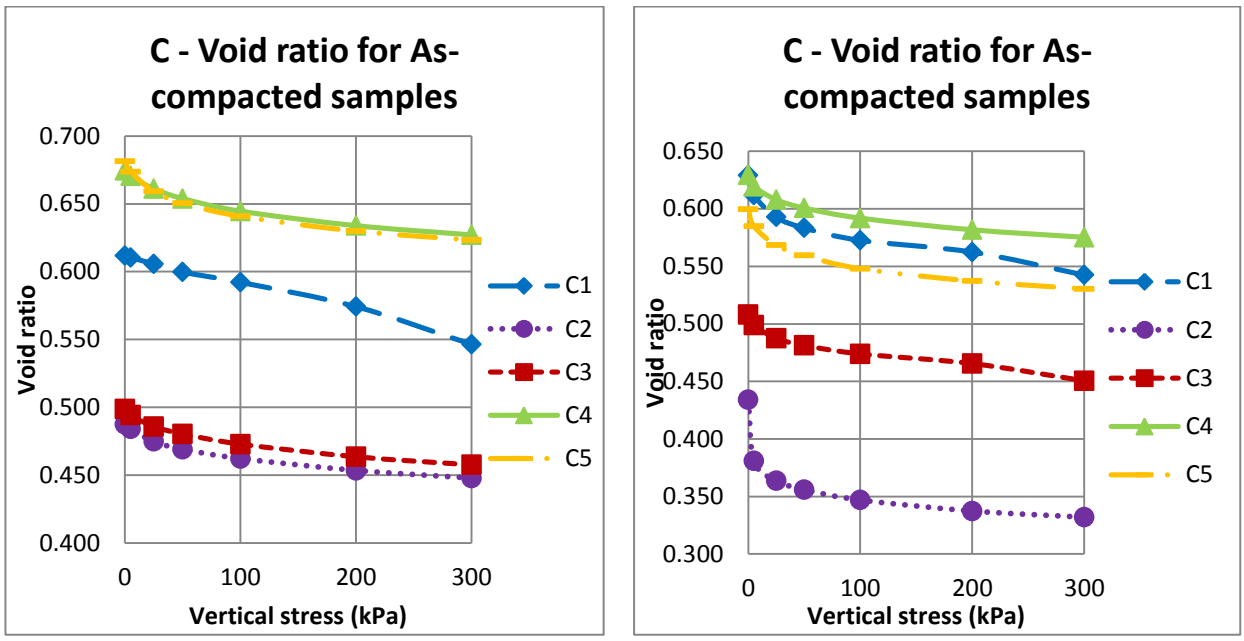

Figure 4.26: Soil C change in void ratio as pressure increases for both as-compacted and inundated samples.

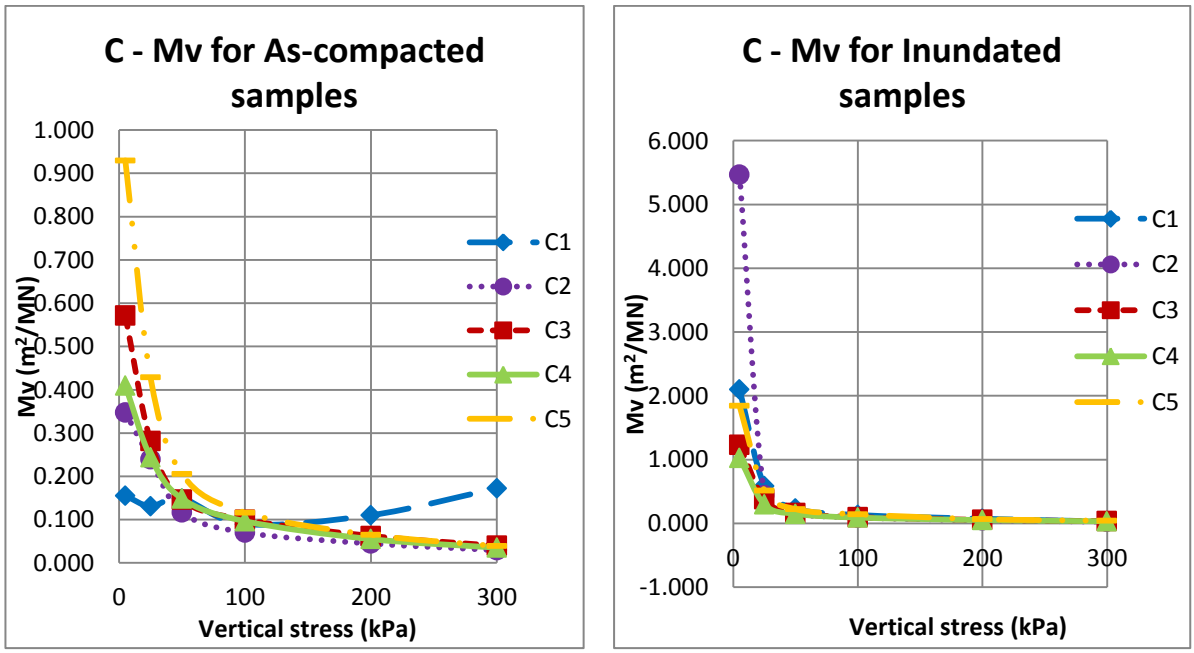

Figure 4.27: Soil C change in volume compressibility as pressure increases for both as-compacted and inundated samples.

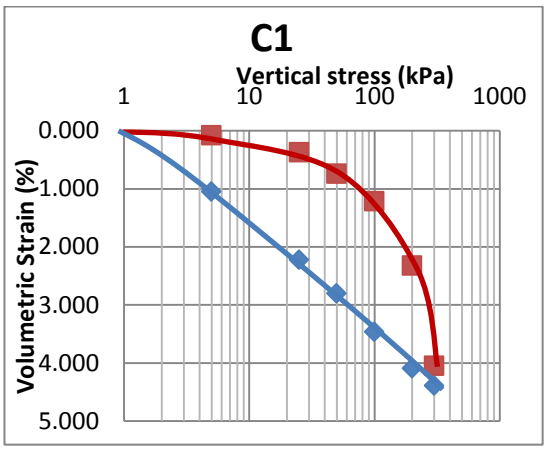

C1

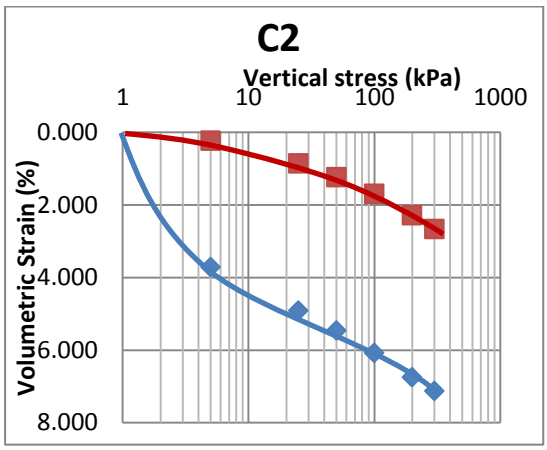

C2

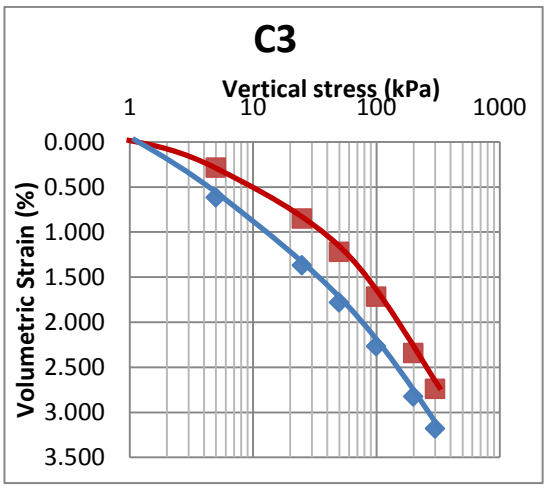

C2

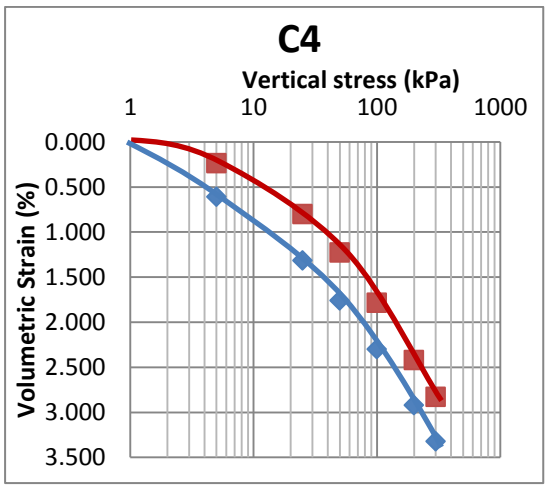

C4

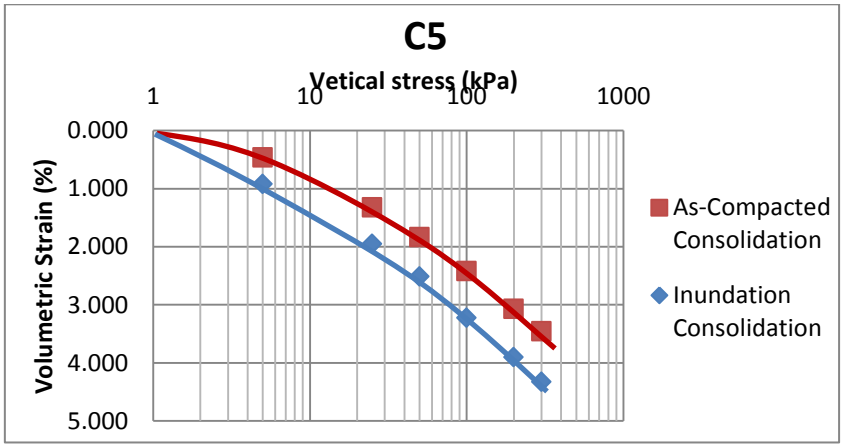

C5

Figure 4.28: Double-Oedometer tests result for the different moisture variations for soil

C

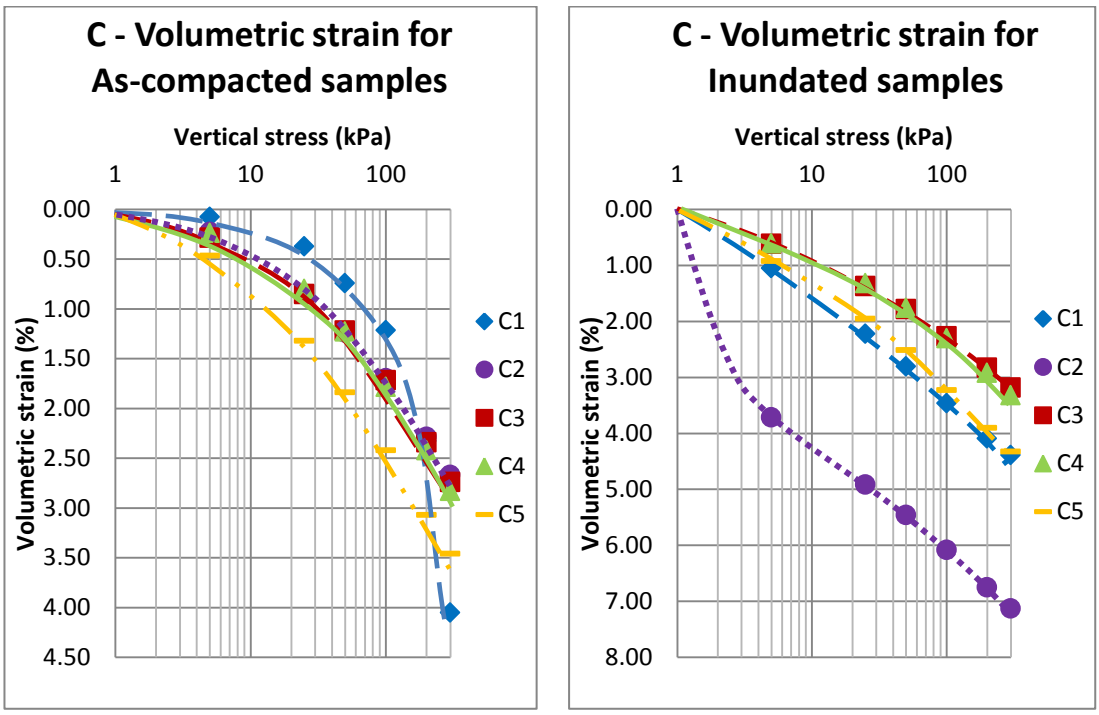

Figure 4.29: Soil C change in volumetric strain as pressure increases for both as-compacted and inundated samples.

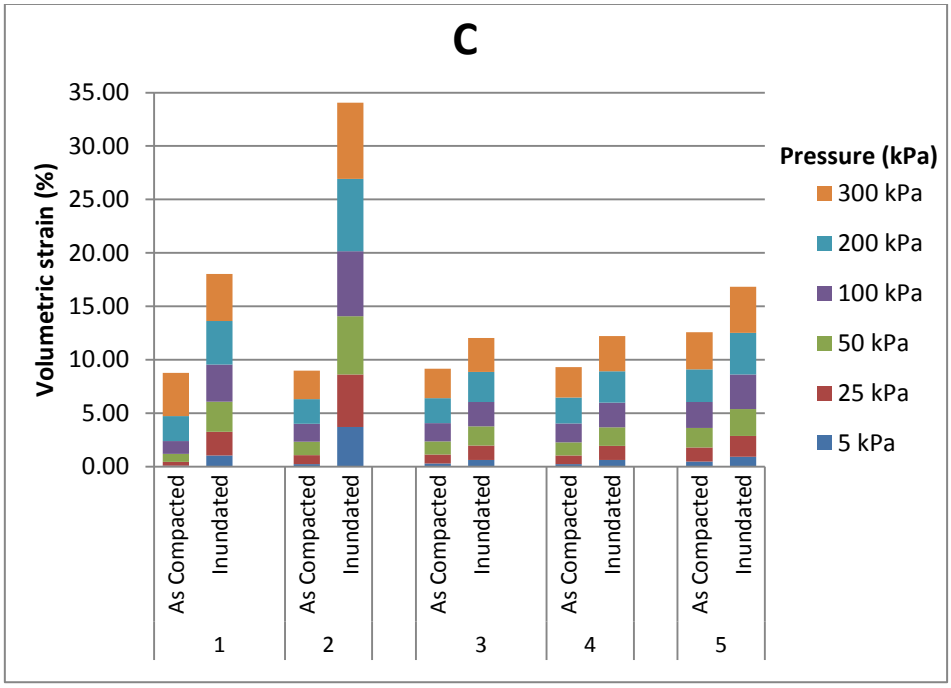

Figure 4.30: Column representation of the volumetric strain of each pressure in kPa at as-compacted and saturated states for A, B, C and D.

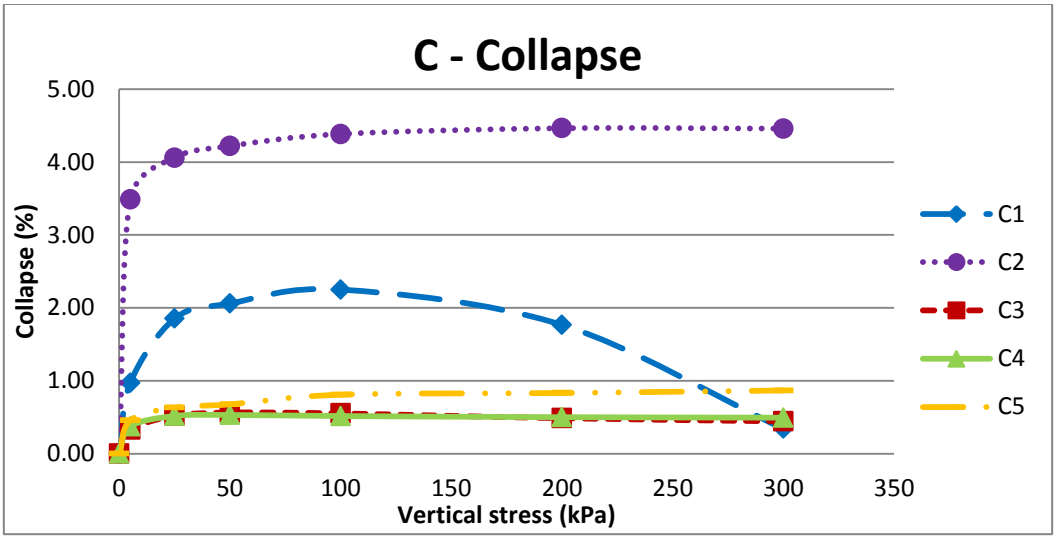

Figure 4.31: Collapse plot at various pressures for soil C

- The column representation of the volumetric strain for soil C is shown in Figure 4.30. The inundated samples for each moisture variations of soil C have a higher stack of volumetric strain at each pressure than those of as-compacted samples. C2 has the highest inundated sample column. For the as-compacted stack C5 has the highest and the others have roughly similar high of column. Pressures 200 kPa and 300 kPa have the highest volumetric pressures of all the samples.
- The collapse of each moisture variation of C at each pressure is displayed in Figure 4.31. For the plot of collapse, increase in pressure first caused a huge increase in collapse for C2, which was maintained as the pressure was increased. C1 has a high increase at the first pressure also, but it progressively increases till 100 kPa after which it reduces in collapse as the pressure increase. C3 and C4 have the initial increase and then maintains it to the last pressure. C5 have the sharp increase at 5 kPa also, but instead continues to increase gradually.

4.3.4 Analysis for soil D - Brown Sand-Clay mixtures

Figure 4.32, Figure 4.33, Figure 4.36 and Figure 4.39, gives the graphical representation of the effect of pressure on void ratio, volumetric compressibility, volumetric strain and collapse respectively of the different moisture variation of D. Figure 4.34, Figure 4.35 and Figure 4.37 represents void ratio, volume compressibility and volumetric strain plots against pressure of the moisture variations of D for as-compacted and inundated states. Figure 4.38 shows a column representation of volumetric strain of each pressure for the five moisture variations of D.

D has a similar relationship between the Increase in pressure and decrease in void ratio (Figure 4.32 and Figure 4.34), increase in pressure and decrease in volume compressibility (Figure 4.33 and Figure 4.35) and increase in pressure and decrease in volumetric strain (Figure 4.36 and Figure 4.37) as soils A, B, and C.

From the graphs and curves, the following can be observed:

- For the graph of void ratio against pressure, it can be observed that as the pressure increases, the D1, D2, D4 and D5 the curves have a parallel gentle flow as the void reduces. But for sample D3, the inundated sample has an initial steep decrease in void ratio as the pressure increase, although as the pressure reaches 100 kPa the reduce flows in a gentle rate as the void ratio reduces. The as-compacted D3 sample has however a more gentle flow all through the increase in pressure. As shown in Figure 4.32.
- In the graphs of void ratio against pressure of as-compacted state and inundated state moisture variation for soil D (Figure 4.34), the inundated and as-compacted samples each have similar flow pattern. They all have a gradual reduction in void ratio as the pressure increases.

- For the graph of volume compressibility against pressure, all the moisture variations of D have same curve flow and the difference between each moisture variation sample is approximately the 1 m^2/MN except for D4 which has the least with about 0.25 m^2/MN of volume compressibility. Shown in Figure 4.33.
- The flow pattern for volume compressibility against pressure of soil D moisture variation at as-compacted state and inundated state are shown in Figure 4.35. The flow pattern is the same as soils A, B and C, having the samples in their as-compacted state, reduces at a steep drop rate ending at 50 kPa, except for soil D, the inundated samples, steep drop rate ending at 50 kPa of pressure before flowing gently towards zero volumetric compressibility.
- Graphs of volumetric strain against pressure shown in Figure 4.36 have similar trend lines for all the samples. As the pressures are increased, the as-compacted and inundated samples flow closely downwards signifying little difference between both as the volumetric strain increases. Sample D3 slightly differs from the other samples that have a much higher difference between the inundated and as-compacted samples.
- The volumetric strain for soil D in their as-compacted and inundated states is shown in Figure 4.37. The curves for both as-compacted and inundated states all have similar gentle flowing curves where increase in pressure is caused by increase in volumetric strain.
- Unlike soils A, B and C, the column representation of the volumetric strain of D has the highest total volumetric strain in sample D3. The difference between the samples dry of OMC and wet of OMC are closely increasing as the pressure is increased. Shown in Figure 4.38.

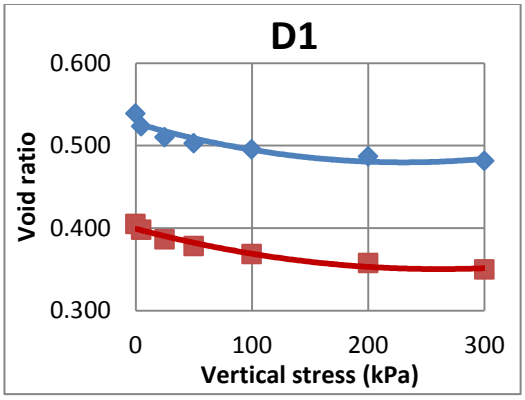

D1

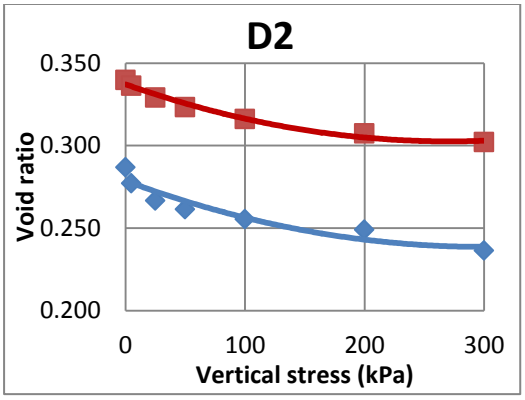

D2

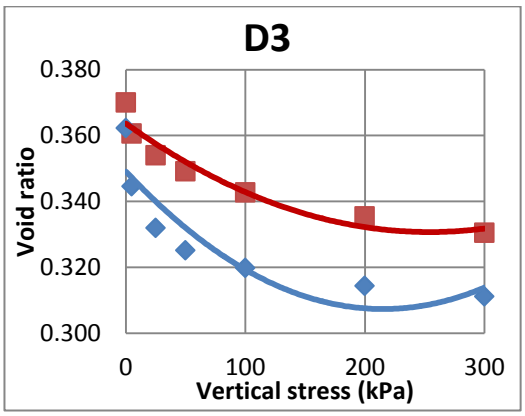

D3

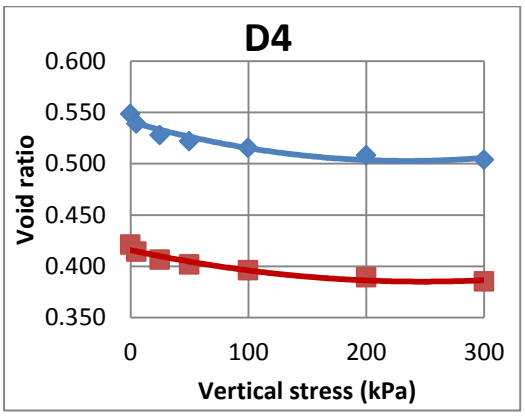

D4

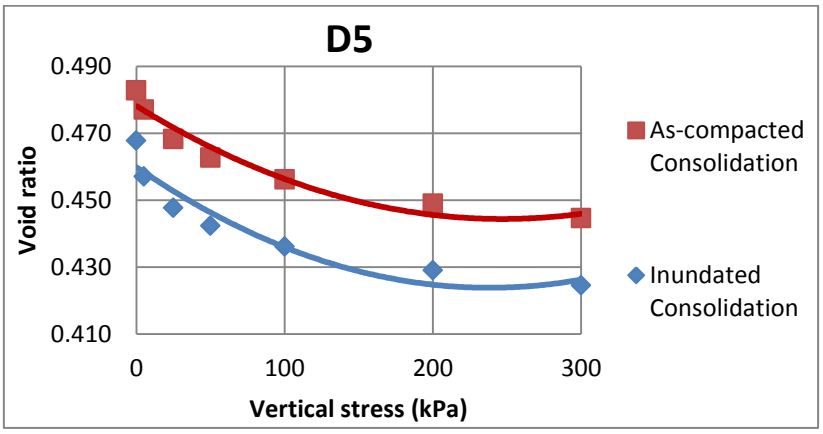

D3

Figure 4.32: Change in void ratio with increase in pressure for soil D and its moisture variations.

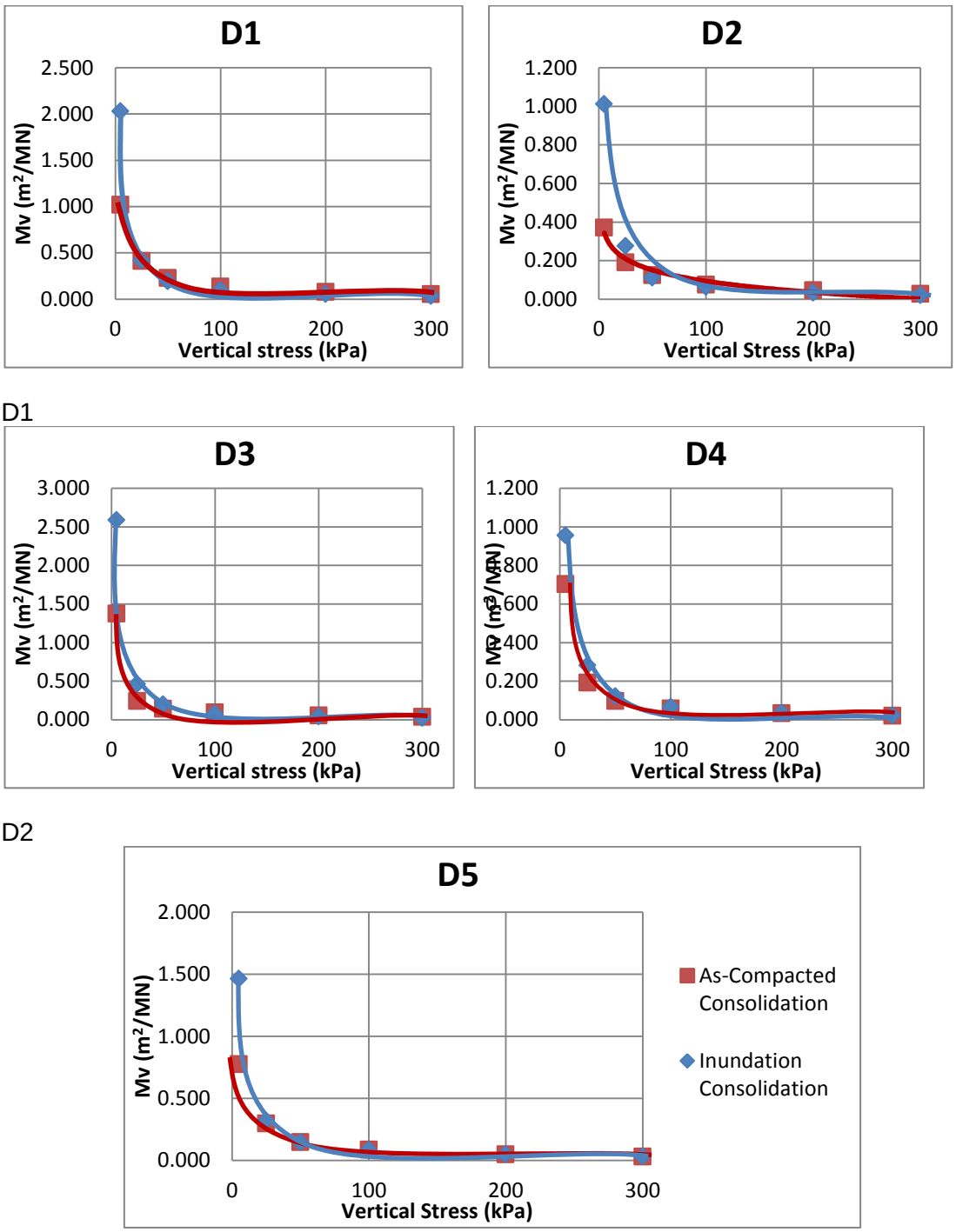

D1

D2

D3

Figure 4.33: Array of volume compressibility versus vertical stress of D moisture variations at as-compacted and Saturation state.

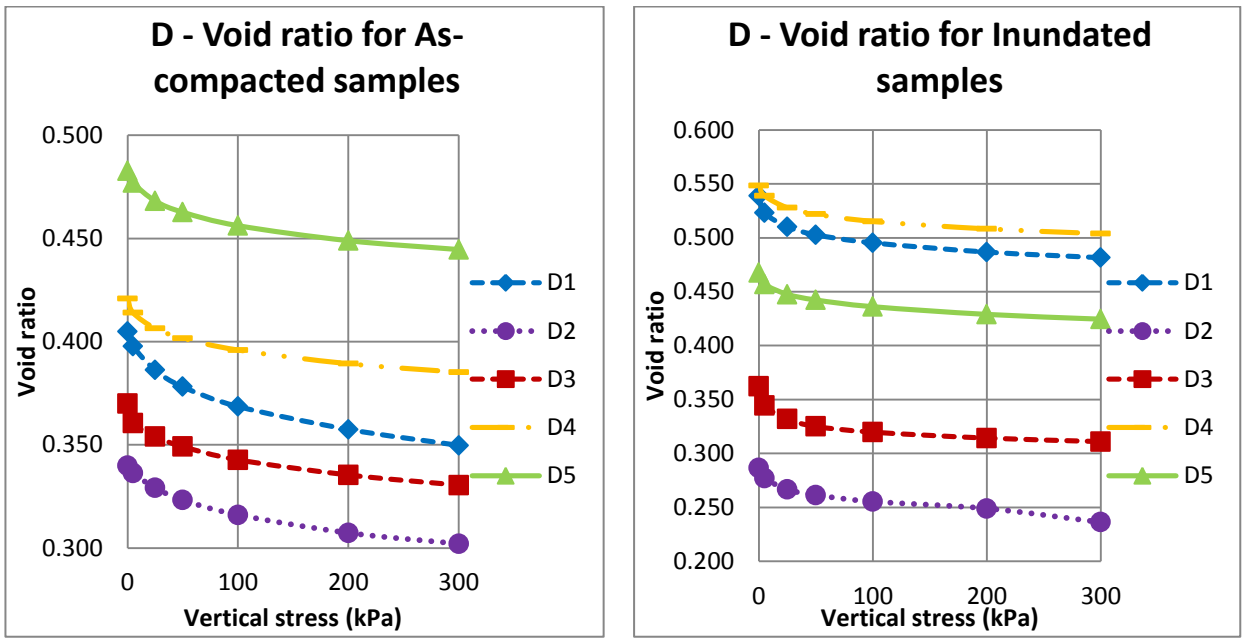

Figure 4.34: Soil D change in void ratio as pressure increases for both as-compacted and inundated samples.

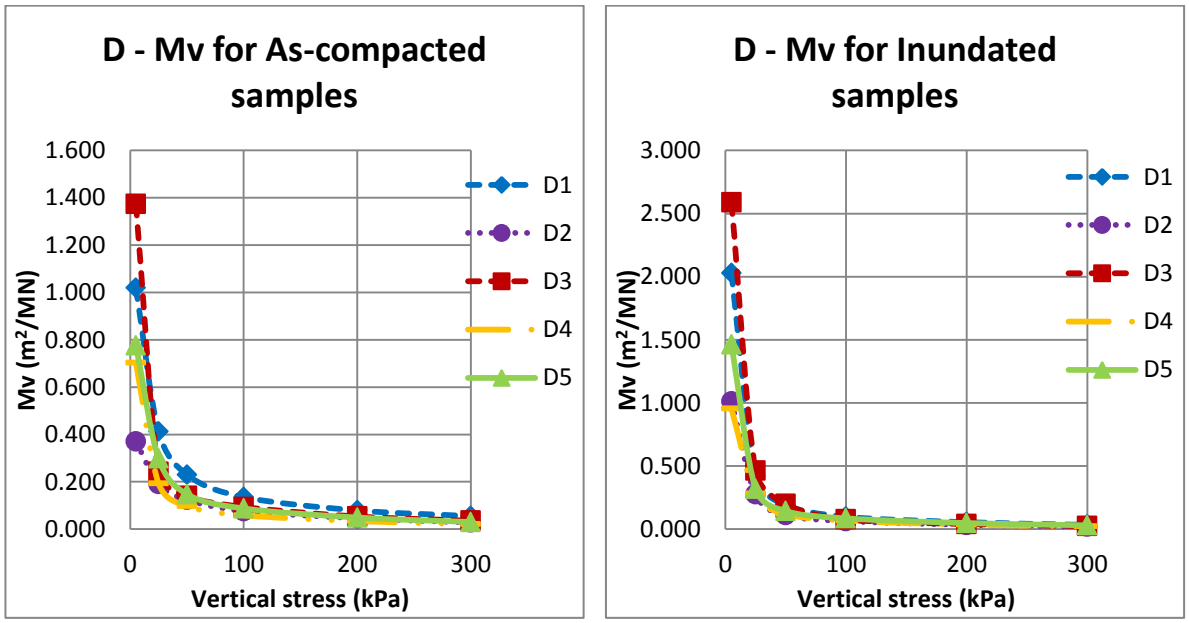

Figure 4.35: Soil D change in volume compressibility as pressure increases for both as-compacted and inundated samples.

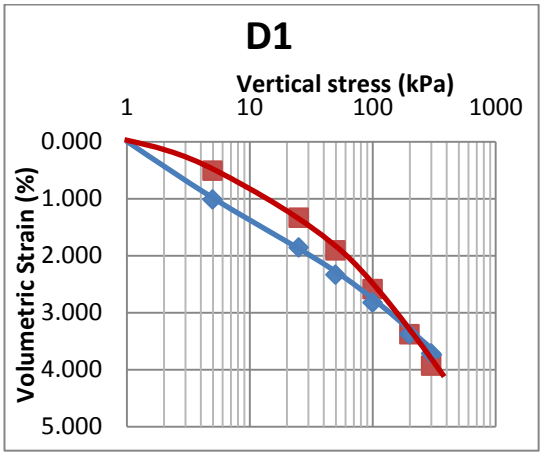

D1

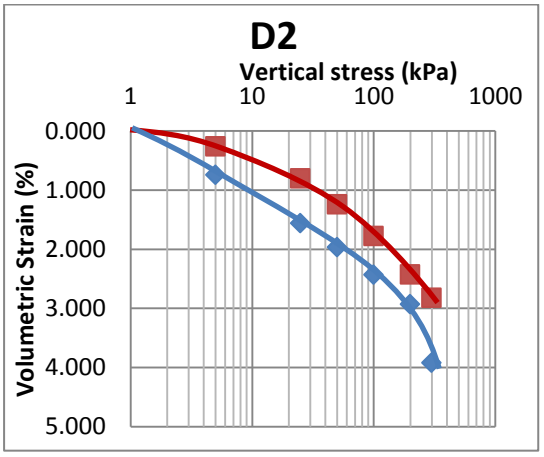

D2

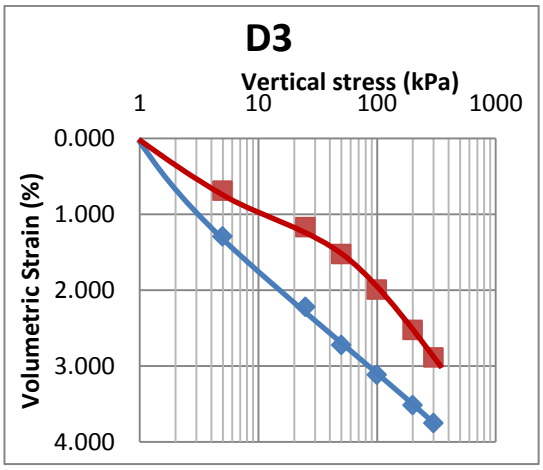

D3

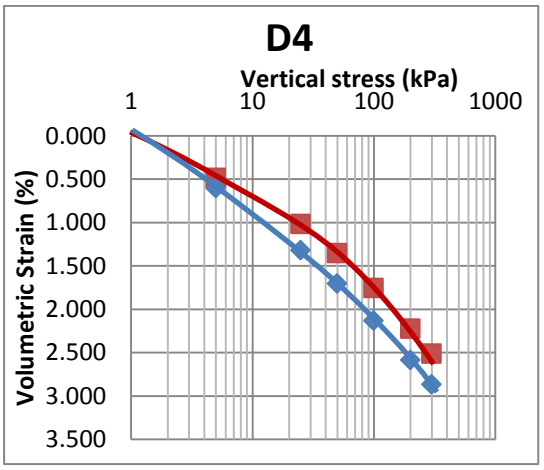

D4

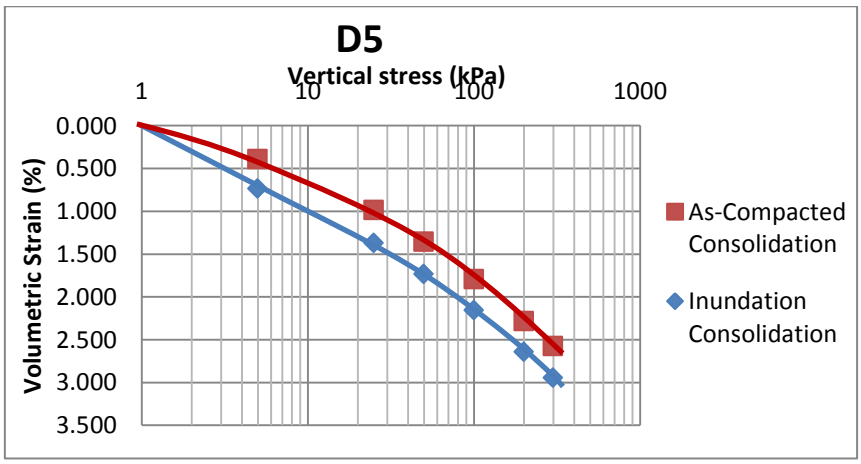

D5

Figure 4.36: Double-Oedometer tests result for the different moisture variations for soil D

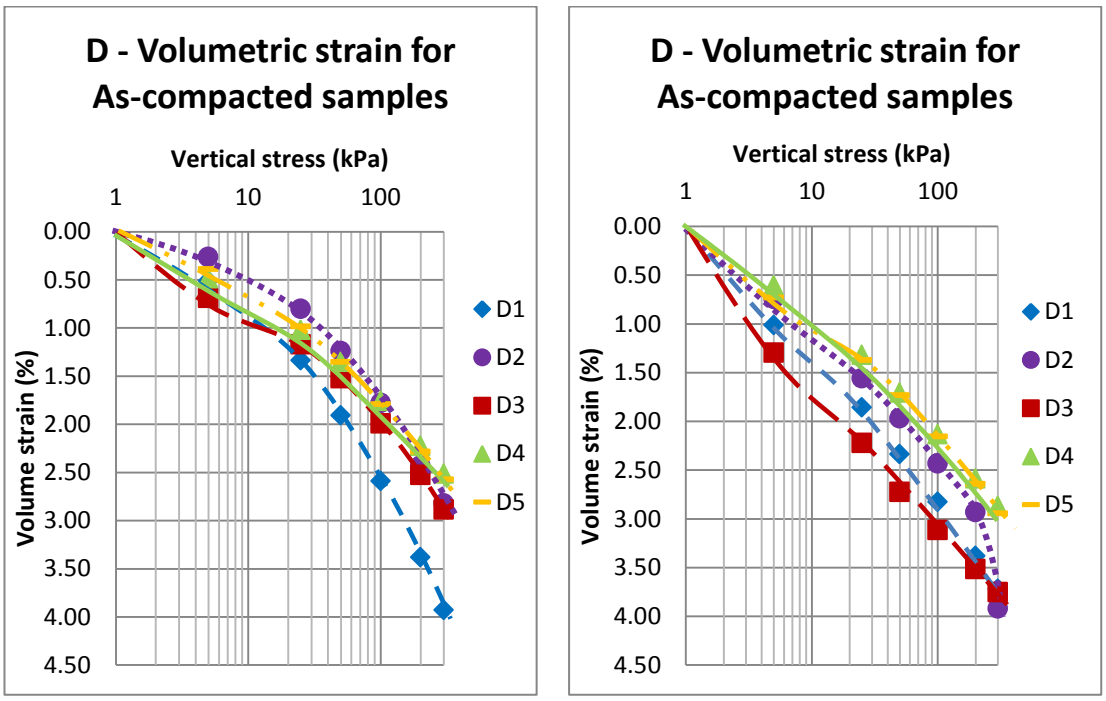

Figure 4.37: Soil D change in volumetric strain as pressure increases for both as-compacted and inundated samples.

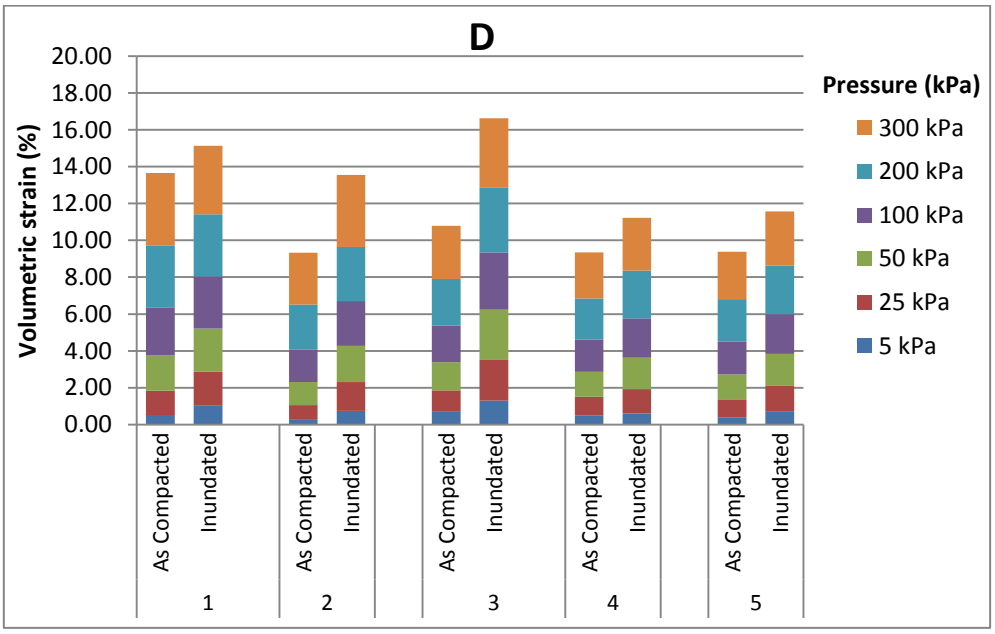

Figure 4.38: Column representation of the volumetric strain of each pressure in kPa at as-compacted and saturated states for A, B, C and D.

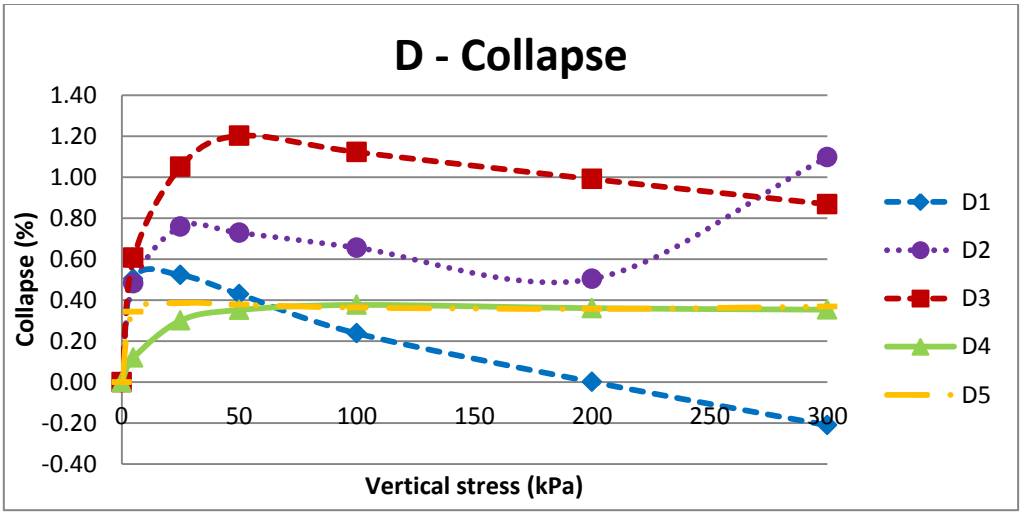

Figure 4.39*: Collapse plot at various pressures for soil D*

- The collapse of each moisture variation of D at each pressure is shown in Figure 4.39. The flows of the curves are absolutely different from the other soils. First, the highest curve of collapse is seen in D3, secondly, the increase in collapse of most of the samples are not instantaneous and thirdly, D2 has an unexpected increase at pressure 200 kPa to 300 kPa. The collapse curves of D4 and D5 flow on the same horizontal line from pressure 50 kPa to 300 kPa, although D5 gets to the horizontal point at the first applied pressure (5 kPa). The curves for D1 and D3 hit the highest collapse at 50 kPa and then they both fall with D1 falling at a higher rate than D3 as the pressure increases. D2 on the other hand has the highest collapse.

4.3.5 General summary

4.3.5.1 Void ratio

The graphs of as-compacted state and inundated state for the void ratio against pressure for soils A, B, C and D are shown in Figure 4.10, Figure 4.18, Figure 4.26 and Figure 4.34. The graphs of void ratio against pressure with each pair of as-compacted and inundated samples for each soil's moisture variations of the soils A, B, C and D are shown in Figure 4.8, Figure 4.16, Figure 4.24 and Figure 4.32 respectively. The graphs reveal that the inundated samples have a steeper flow of void ratio (high change in void ratio) as the pressure increases, than the as-compacted samples. This steep flow changes gradually to a gentle flow as the pressure continues from 100 kPa to 300 kPa. This is the case for most of the moisture variations mostly for the dry of OMC. The others however have a parallel gentle flow for both the inundated sample and as-compacted sample. This is common in the wet of OMC. Although for Soil D all of the moisture variations follow this pattern except for the D3 of which the inundated samples flow at a steeper rate than as-compacted samples. The samples with high change in void ratio are more prone to collapse than those with gentle flow in change in void ratio.

4.3.5.2 Volume compressibility

The volume compressibility against pressure for soils A, B, C and D at as-compacted state and inundated state are seen in Figure 4.11, Figure 4.19, Figure 4.27 and Figure 4.35. The flow pattern for the soil is such that the samples in their as-compacted state have a steep flow for the first pressures up to 50 kPa, and the inundated samples, have the steep flow rate to 25 kPa of pressure before the curve flattens to gently flow towards zero volumetric compressibility. This is so for all the soils except soil D, which has the steep flow ending at 50 kPa of pressure.

The inundated samples have higher volume compressibility than the samples of as-compacted samples. The graphs of each pair of as-compacted and inundated states for volume compressibility against vertical stress for soils A, B, C and D are observed in Figure 4.9, Figure 4.17, Figure 4.25 and Figure 4.33. The highest volume compressibility difference between the inundated sample and the as-compacted sample of the moisture variation is found in the high dry of OMC for all the soils (A2 – 4 m^2/MN; B2 – 7 m^2/MN; and C2 – 5 m^2/MN) except soil D. The soil D has however it's highest difference at OMC (D3) with about 1.2m^2/MN. Low dry of OMC has the next obvious high difference for all the soils (A1 – 2 m^2/MN; B1 – 4 m^2/MN; C1 – 2 m^2/MN and D1 – 1 m^2/MN). The other samples for the soils have volume compressibility less than 1 m^2/MN. The soils and their samples with the difference of volume compressibility high at the start of pressures shows that the soil is probable to high collapse than those with much less difference if volume compressibility between the as-compacted sample and inundated sample.

4.3.5.3 Volume strain

The volumetric strain for soils A, B, C, and D in each as-compacted and inundated state is shown in Figure 4.13, Figure 4.21, Figure 4.29 and Figure 4.37. The curves for as-compacted state have similar flowing curves where increase in pressure causes increase in volumetric strain. It was noticed that low dry of OMC (1) at low pressures (A1 < 50 kPa, B1 < 100 kPa, C1 < 100 kPa and D1 < 25 kPa) has the least volumetric strain, but at higher pressure there is a high increase in the volumetric strain. The inundated state have different flow path. In soil A, B, and C, the dry of OMC (A1, A2, B1, B2, C1, and C2) have the most volumetric strain as pressure increased.

The inundated samples have a higher volumetric strain than the as-compacted samples. See Figure 4.12, Figure 4.20, Figure 4.28 and Figure 4.36 for graph of each pair of as-compacted and inundated states for soil A, B, C and D respectively. The

highest difference in volumetric strain between the inundated and as-compacted samples of each soil is revealed in the dry of OMC (A1, A2, B1, B2, C1, and C2) of the soils. This is so for all the soils except for soil D, of which the highest is rather noticed at OMC (D3).

4.3.5.4 Collapse Potential

Collapse potential which is the difference between the volumetric strains of inundated and as-compacted samples are shown previously in Figure 4.15, Figure 4.23, Figure 4.31 and Figure 4.39 for soils A, B, C and D respectively. Each graph shows the collapse each pressure causes when applied on the sample. The flow of the collapse points for each set of wet of OMC samples in all the soils have a drastic increase in the first pressures up to 50 kPa, and then maintains that level of collapse with little changes as the pressure continues to increase to the 300 kPa pressure. Soils A, B and C have the highest collapse at high dry of OMC (A2, B2 and C2) while D at OMC (D3). The D soil reveals that the factors of fine sand in the make-up contributes to resisting high volumetric strain since further densification of the soil when loaded and wetted occur at a limited rate. Hence, at OMC for D (D3) gives the highest collapse potential because it has the highest resistance to the pressures applied.

5 DISCUSSION AND MODELLING

The relationship between related parameters of the soils is discussed and modelled. The collapse potential of four soils tested at their compactive variables which are percentage of each soil's optimum moisture content, are also discussed. The results are hence discussed under laboratory corollary, identification of soil collapsibility and past research works, to achieve a new collapse predictive model.

5.1 LABORATORY COROLLARY

Studied herein are the experimental soil result properties discussed under three headings:

- Soil classification properties
- Shear properties
- Consolidation properties

Table 4.5 shows the soil properties of the four soils and in Table 5.1, Table 5.2, Table 5.3, and Table 5.4 the parameters obtained from the laboratory studies for the five moisture variations of the four geologically different soils are tabulated.

5.1.1 Soil Classification Properties

Figure 5.1 shows the change of degree of saturation as the moisture content of the four soils is varied. This shows that the degree of saturation (Sr) increases with an increase in moisture content (MC). As the degree of saturation approaches saturation (Sr = 1), the curve gentles out to an almost flat line. This is because as the limited remaining air voids of 100% saturation is approached, it is more difficult for the air to be replaced by MC, due to the denseness (particle arrangement) of the soil and the lost suction force which aided in the pull of water into the voids between the soil

particles. This shows that at a low Sr, little addition of MC would cause a rapid increase in Sr, and as saturation is approached, large increase in the MC would cause little change in Sr. Here Sr gives a much clearer measure of moisture content on the structural stability of the soil (because it measures the capacity of water with regards to the soil's voids).

Void ratio of the soils plotted against moisture content is represented in Figure 5.2. With increase in moisture content, the void ratio decreases to a certain point beyond which it starts to increase. This is an inverse representation of dry density against moisture content (Figure 4.3). Hence void ratio is inversely proportional to dry density. This is expected since the density represents how closely packed soil's particles are and the void ratio represents how much space is contained between the soil's particles. When the soil is of very low saturation the increase in MC increases the soil's suction. Upon soil compaction the suction gives it the pulling force to create a denser structure than when with less moisture content. This causes the increase in the dry density of the soil as the moisture content increases. When the soil reaches saturation greater than 80% (as seen in Figure 5.1), more MC would cause the soil suction to drop to zero, causing the soil particles to disperse creating more space for the increased MC. At this point the void ratio increases because of the excessive amount of MC. Compaction of such sample would not be possible since all the voids are filled, hence producing a lower density.

Table 5.1: Laboratory tests summary result for soils A and B, triaxial test.

Parameters		A					B				
		1	**2**	**3**	**4**	**5**	**1**	**2**	**3**	**4**	**5**
Intended MC (%)		10.0	13.5	15.0	18.3	20.0	10.0	12.3	14.5	17	20.0
MC at compaction (%)		11.14	13.72	14.92	18.86	19.96	9.33	11.18	14.36	16.82	18.77
% of MC from OMC (%)		71.39	87.96	95.65	120.92	127.96	63.90	76.60	98.36	115.21	128.56
Dry Density (g/cm^3)		1.68	1.82	1.81	1.73	1.70	1.63	1.78	1.78	1.78	1.73
Void ratio 'e_0'		0.73	0.59	0.60	0.67	0.71	0.78	0.63	0.63	0.63	0.67
Degree of saturation 'Sr' (%)		44.20	67.38	71.64	81.68	81.71	34.74	51.57	65.96	77.27	80.93
Triaxial Max shear stress (kN/m^2)	70 kPa	580	625	440	190	136	670	880	620	695	341
	140 kPa	900	676	510	288	159	880	1165	1005	860	354
	280 kPa	1650	1100	610	402	178	1560	1800	1145	1124	413
Initial angle of friction (^{o})		43.15	33.00	15.64	19.44	5.71	41.99	42.77	39.52	30.84	11.31
Cohesion (kN/m^2)		50	115	138	48	52	85	120	135	150	120

Table 5.2: Laboratory tests summary result for soils A and B, oedometer test.

Parameters	A					B				
	1	**2**	**3**	**4**	**5**	**1**	**2**	**3**	**4**	**5**
As - compacted										
Final MC (%)	9.95	11.67	13.31	14.12	14.51	8.29	12.06	10.836	13.61	15.24
Initial Void ratio 'e_0'	0.51	0.38	0.53	0.55	0.56	0.64	0.50	0.58	0.46	0.50
Initial Degree of saturation	0.57	1.00	0.81	0.97	1.00	0.38	0.62	0.69	1.00	1.00
Inundation										
Initial MC (%)	17.58	15.26	15.91	19.09	20.77	22.56	17.86	18.58	17.45	17.95
Final MC (%)	16.03	15.01	13.16	14.61	14.52	20.07	16.86	17.50	14.76	16.39
Initial Void ratio 'e_0'	0.51	0.44	0.46	0.55	0.60	0.65	0.52	0.54	0.51	0.52
Initial Degree of saturation	1.00	1.00	1.00	1.00	1.00	1.00	1.00	1.00	1.00	1.00
Both										
Max collapse (%)	2.22	2.70	0.55	0.51	0.41	2.53	3.79	0.53	0.20	0.51
Load max collapse (kPa)	100	300	300	300	300	50	25	25	300	25
Total collapse (%)	10.24	12.22	1.97	2.39	2.31	14.10	21.99	2.37	0.90	2.43
Critical Load (Moderate) kPa	25	25	300	300	300	25	5	200	-	200
Critical Load (M. severe) kPa	100	100	-	-	-	50	25	-	-	-
Critical Load (Severe) (kPa)	300	300	-	-	-	200	50	-	-	-
Difference in Sr (%)	0.43	0.00	0.19	0.03	0.00	0.62	0.38	0.31	0.00	0.00

Table 5.3: Laboratory tests summary result for soils C and D, triaxial test.

Parameters		C					D				
		1	**2**	**3**	**4**	**5**	**1**	**2**	**3**	**4**	**5**
Intended MC (%)		12.0	15.5	17.0	20.8	23.0	7.00	9.7	11.0	13.1	16.0
MC at compaction (%)		13.39	16.54	18.27	21.21	22.43	8.63	9.91	11.27	14.20	16.19
% of MC from OMC (%)		75.44	93.18	102.93	119.51	126.37	77.05	88.45	100.63	126.77	144.55
Dry Density (g/cm^3)		1.65	1.71	1.75	1.67	1.65	1.79	1.92	1.91	1.90	1.83
Void ratio 'e_0'		0.76	0.69	0.66	0.74	0.76	0.62	0.51	0.52	0.53	0.58
Degree of saturation 'Sr' (%)		51.30	69.30	80.27	83.61	86.19	40.58	55.88	63.18	78.28	80.64
Triaxial Max shear stress (kN/m^2)	70 kPa	720	640	408	318	148	640	720	599	240	149
	140 kPa	990	920	460	355	177	1040	925	920	247	157
	280 kPa	1620	1040	580	460	194	1450	1400	1280	263	162
Initial angle of friction (^{o})		41.28	29.17	16.65	14.04	5.19	38.66	38.66	36.87	1.91	1.82
Cohesion (kN/m^2)		83	170	137	108	60	105	110	100	82	74

Table 5.4: Laboratory tests summary result for soils C and D, oedometer test.

Parameters	C					D				
	1	**2**	**3**	**4**	**5**	**1**	**2**	**3**	**4**	**5**
As - compacted										
Final MC (%)	12.47	14.74	14.72	17.63	16.25	8.90	9.96	10.77	10.39	11.39
Initial Void ratio 'e_0'	0.61	0.49	0.50	0.67	0.68	0.41	0.34	0.31	0.42	0.48
Initial Degree of saturation	0.61	0.95	1.00	0.93	0.96	0.65	0.89	0.88	0.96	0.95
Inundation										
Initial MC (%)	21.69	14.97	17.52	21.70	20.68	18.58	10.89	12.49	18.91	16.13
Final MC (%)	15.94	14.90	16.48	18.78	15.23	11.92	10.68	11.63	11.37	12.43
Initial Void ratio 'e_0'	0.63	0.43	0.51	0.63	0.60	0.54	0.29	0.36	0.55	0.47
Initial Degree of saturation	1.00	1.00	1.00	1.00	1.00	1.00	1.00	1.00	1.00	1.00
Both										
Max collapse (%)	2.25	4.46	0.56	0.53	0.87	0.52	0.76	1.20	0.38	0.39
Load max collapse (kPa)	100	200	50	50	300	25	25	50	100	25
Total collapse (%)	9.24	25.07	2.89	2.93	4.27	1.48	4.23	5.84	1.86	2.20
Critical Load (Moderate) kPa	25	5	200	200	100	-	100	50	-	300
Critical Load (M. severe) kPa	100	25	-	-	-	-	-	-	-	-
Critical Load (Severe) (kPa)	-	50	-	-	-	-	-	-	-	-
Difference in Sr (%)	0.39	0.05	0.00	0.07	0.04	0.35	0.11	0.12	0.04	0.05

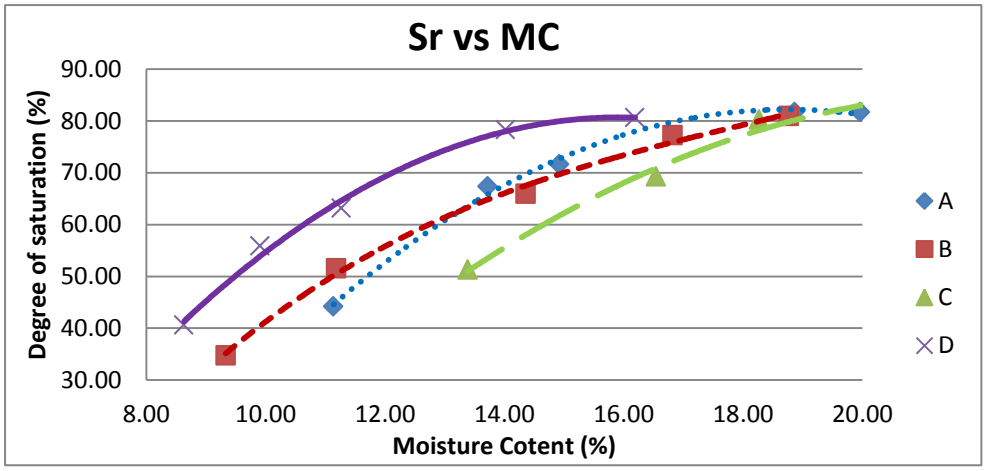

Figure 5.1: Degree of saturation vs. Moisture content for the various soils

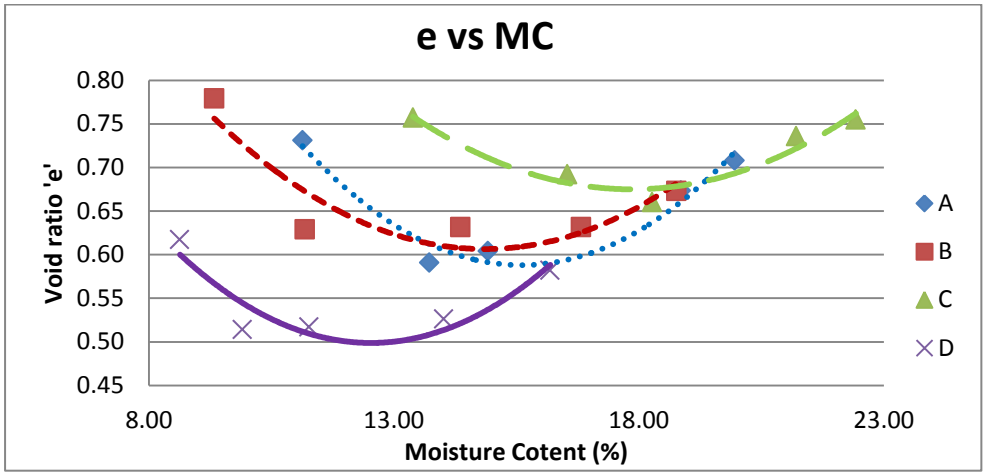

Figure 5.2: void ratio for the different soils vs. moisture content.

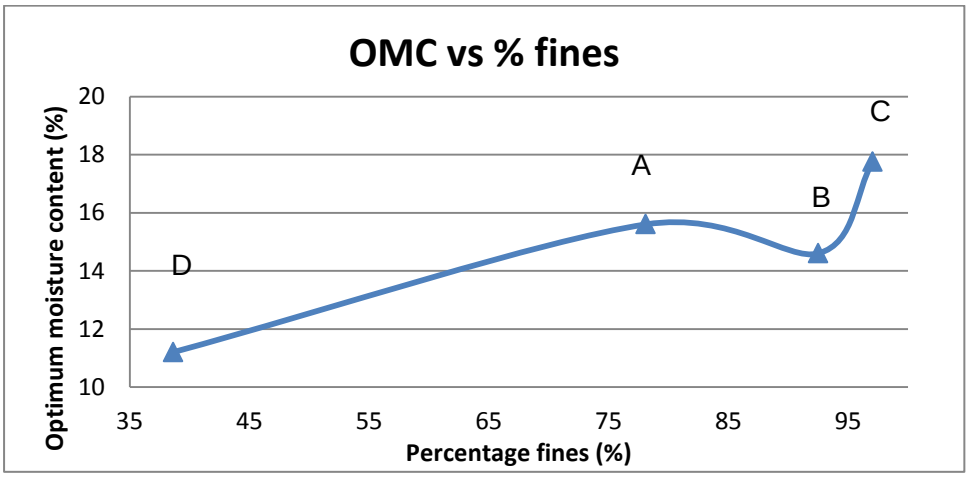

Figure 5.3: Optimum moisture content versus percentage fines of the four soils

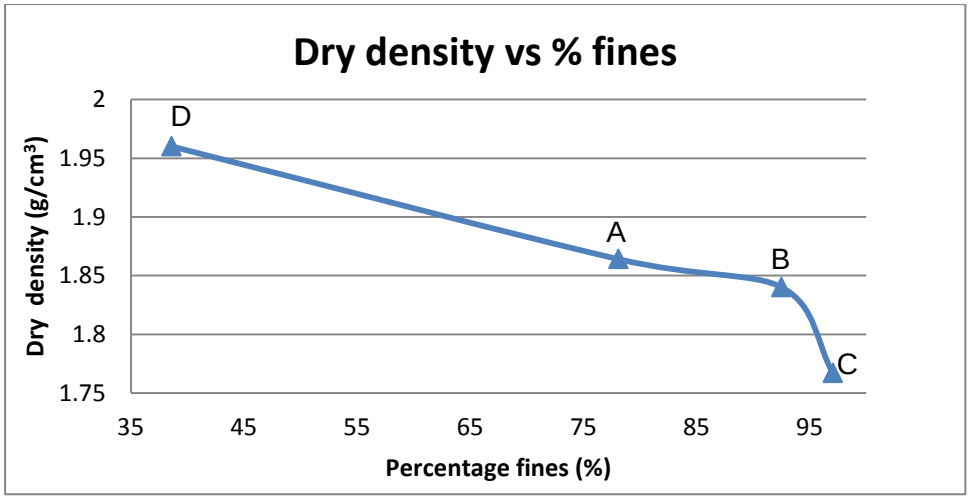

Figure 5.4: Dry density versus percentage fines of the four soils

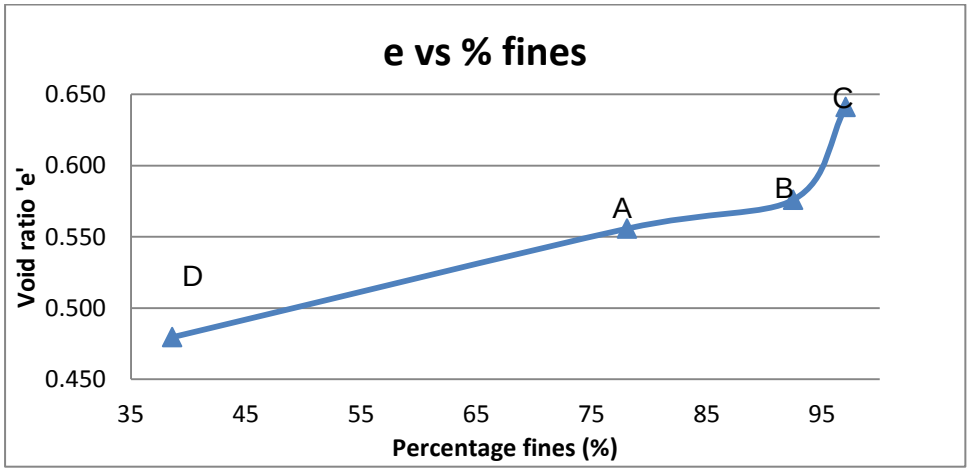

Figure 5.5: Void ratio versus percentage fines of the four soils

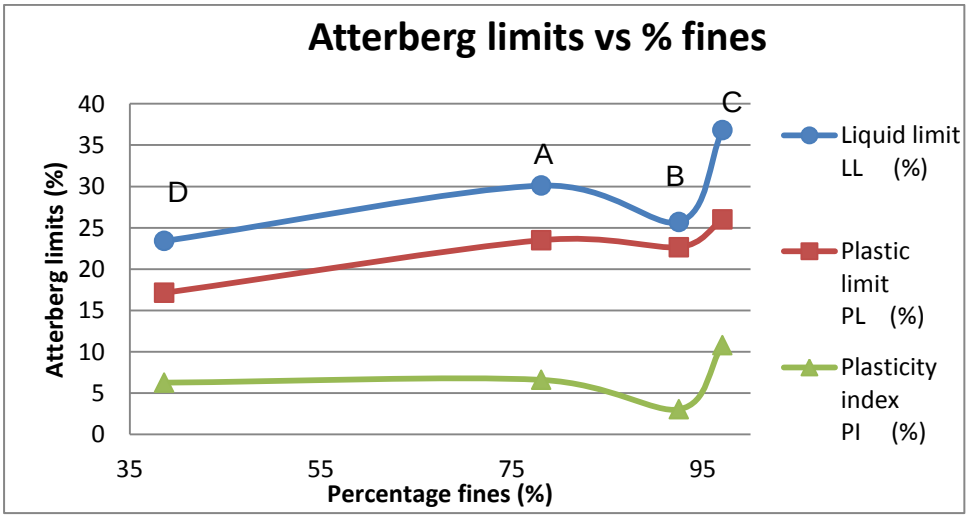

Figure 5.6: Atterberg limits versus percentage fine of the four soils

Figure 5.3, Figure 5.4, and Figure 5.5 show the graphical representation of optimum moisture content (OMC), dry density, and void ratio respectively, each against percentage fines. OMC and void ratio are both directly proportional to percentage fines whiles dry density is inversely proportional to percentage fines. The more the fines the higher the probability of the soil to absorb moisture due to increased surface area, and so for moisture content that give the best performance – OMC, the soil would need a higher amount of OMC to amass for the high percentage of fines. See Figure 5.3.

From the graphs of dry density and void ratio against percentage fines (Figure 5.4 and Figure 5.5), its observed that with an increase in percentage fines, dry density decreases and void ratio increases, this is because soils with less percentage fines would be made of larger grains. Well-graded soil can be easily compacted to relatively high densities which result in higher strengths and stiffness'. Furthermore soils with high percentage of fines have a relatively uniform grade which when compacted would have less density. Hence, soils with lower percentage fines have a higher density and lower void ratio and vice versa. Wang, Chan, and Lam (2009) who achieved the same result discussed this behaviour to be due to the intruding of the fine grained particles into the inter-particle space of the larger particles causing a denser structure.

Figure 5.6 shows the graphs for liquid limit (LL), Plastic limit (PL) and plasticity index (PI) against percentage fines. Since consistency limits is a factor of moisture content, it's clearly shown that the more the fines, the higher the limits, due to the intake of water. The makeup of the fines is another factor that affects this graph, since soils with high clay fraction would have a higher Atterberg limit than those with silt. The B soil being a silty soil with little or no clay fraction has a lower point on the straight line graph. The soil's B being off the straight line graph is observed in all the graphs shown in Figure 5.3, Figure 5.4, Figure 5.5 and Figure 5.6.

5.1.2 Shear Strength Properties

Figure 5.7 and Figure 5.8 show the stress-strain curves and the peak deviator stresses respectively of the four soils and their five moisture variations. The deviator stresses of the moisture variation for the soils are all similar in flow pattern as the deviator stresses increase with axial strain (see Figure 5.7). The deviator stresses are observed to increase in such a manner that samples prepped at low initial moisture content have a steep increase for the first few axial strains and then continues at a gentle linear curve. This is because at low moisture content, the soil is of high stiffness depicting high resistance to the continuous increasing pressure applied. This continues until it gets to the point where this stiffness is eliminated as detected in the shallow gradient part of the curve. At this point the strength of the soil is limited. For samples prepped at higher moisture content, the increase in deviator stress is not as high, and the curves have shallow gradient all through. Here the sample is of low stiffness causing this curve pattern.

It is observed further that the flow of the peak deviator stresses is such that the samples compacted at low initial moisture content (Dry OMC) have steep gradient as the confining pressures increase (see Figure 5.8), showing a more steep variation. And then the samples with lower peak deviator stresses (high moisture content) have little change in their peak deviator stress as the confining stress increases. From this it is concluded that samples prepared at Dry-OMC (with initial low moisture) have a high varying increase in peak deviator stresses (see Figure 5.9); samples prepped At-OMC have a medium varying path and finally the Above-OMC prepped samples have a very gentle flow path, where little or no chance in peak deviator is noticed as the confining pressure increases. This is true for all the soils except for B, where the highest peak deviator stresses are B2. Despite this discrepancy, the B2 of the B moisture variation has the highest shear strength; because of the silty makeup, the

dryer preparation of the soil collapses at the least pressure, but with a little increase in MC, the soil is made more compact hence having more strength.

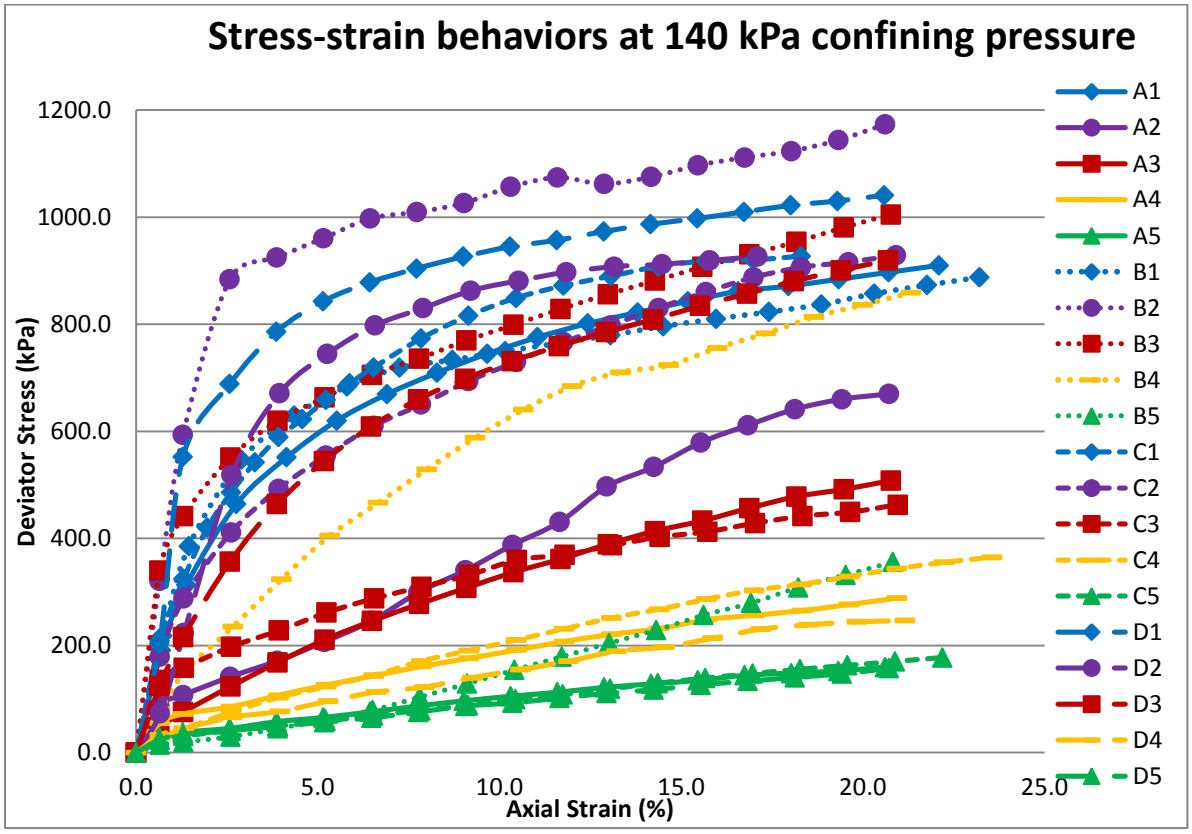

Figure 5.7: Shear-strain behaviour at 140 kPa confining pressure of the 4 soils at 3 varied moisture state

Figure 5.9 is the graph of peak deviator stress plotted against initial moisture content of the soils A, B, C and D at confining pressures 70 kPa, 140 kPa and 280 kPa. For each soil it is noticed that as the moisture content increases, the peak deviator stress decreases and as the confining pressure increases, the peak deviator stress increases. This is due to the lubrication caused by the addition of water to the soil, hence reducing the cohesion and internal friction angle present which in turn reduces the shear strength of the soil. More insight is given by Gu et al. (2014) which confirms this trend.

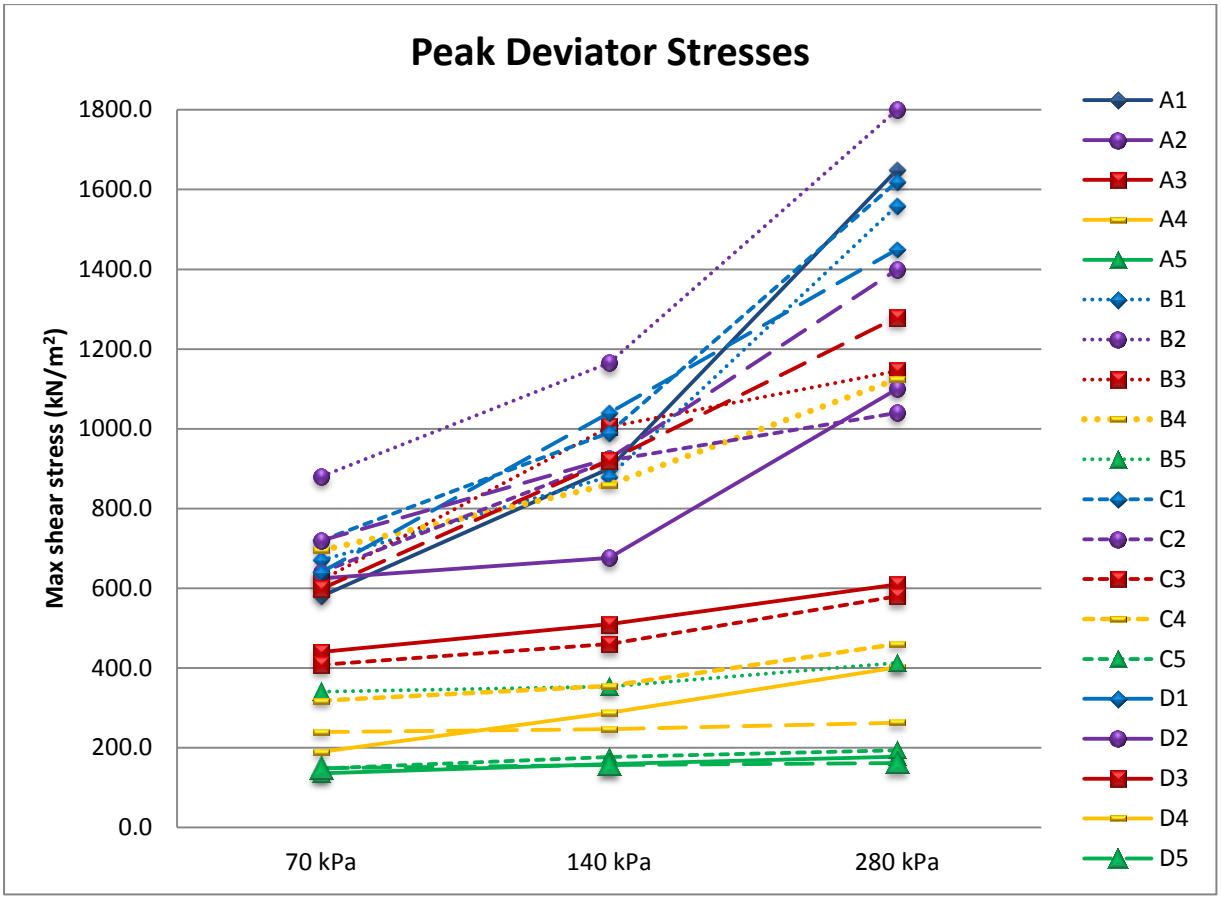

Figure 5.8: Peak deviator stress consecution points of confining pressures 70 kPa, 140 kPa and 280 kPa for the 5 moisture variations of the soils A, B, C and D.

Cohesion and internal friction angle sequacity for the five moisture variations of the four soils are shown in Figure 5.10. The cohesion of soils increases with an increasing moisture content, but only to a limit, beyond which cohesion decreases with a continuous increase in moisture content identical to the shape of the compaction curve. The initial increase in cohesion is due to the cementation and adhesion forces which are increasing with moisture content, only to that point, of which more water become excessive and these forces decrease, such that the distance between the soil particles increase and the electrostatic and electromagnetic attraction (van der waals) forces between them decreases, causing the fall in cohesion. Mitchell 1993; Al-Shayea 2001; and Gu et al 2014 confirm this

findings. This is the same to the capillary suction between the particles, which decreases as the moisture content increases to saturation condition. From the results obtained, the maximum cohesion limit falls in the range of the optimum moisture content (OMC) of the soil. The highest cohesion for each soil is seen in the mid-range of the moisture variation.

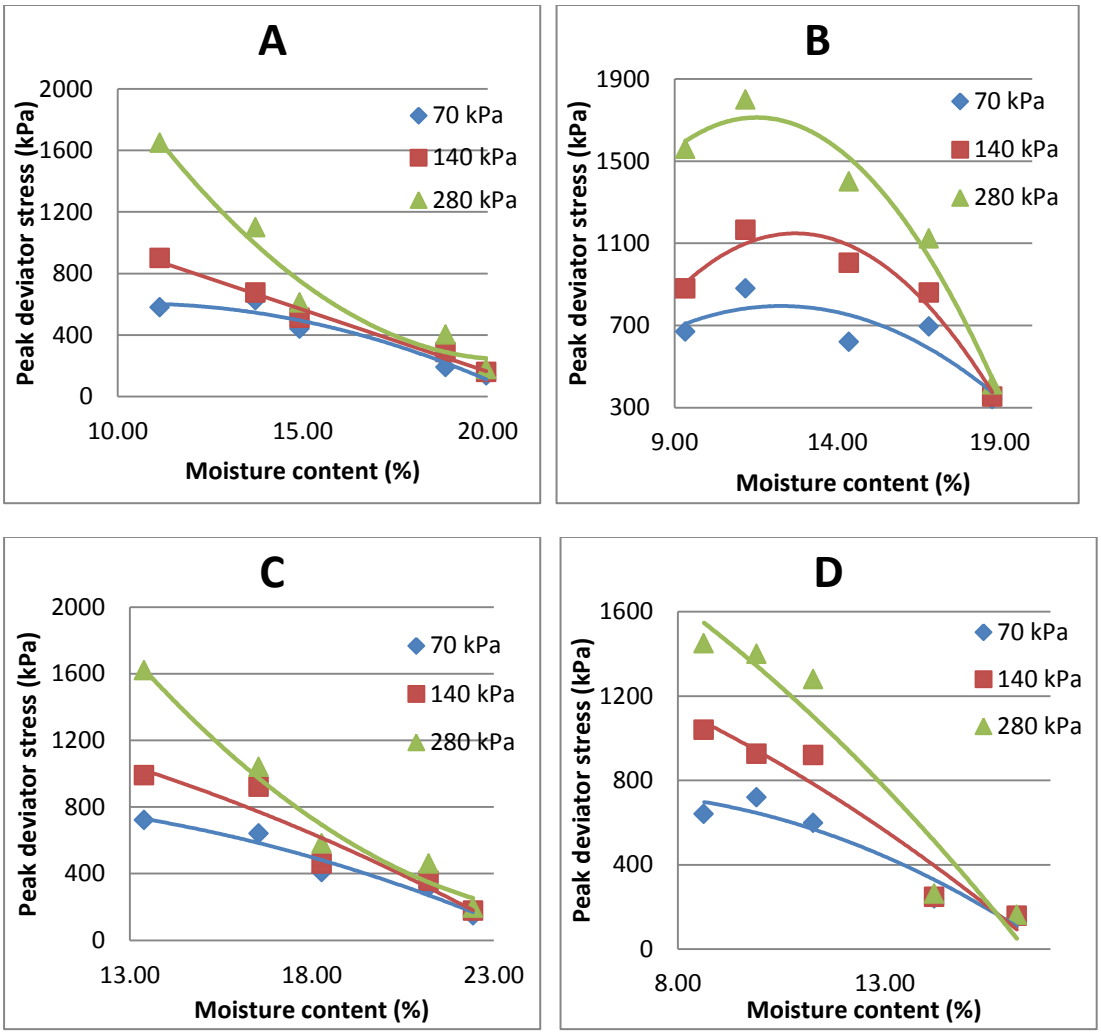

Figure 5.9: Peak deviator stresses for the soils A, B, C and D versus moisture content (MC) for confining pressures 70 kPa, 140 kPa and 280 kPa.

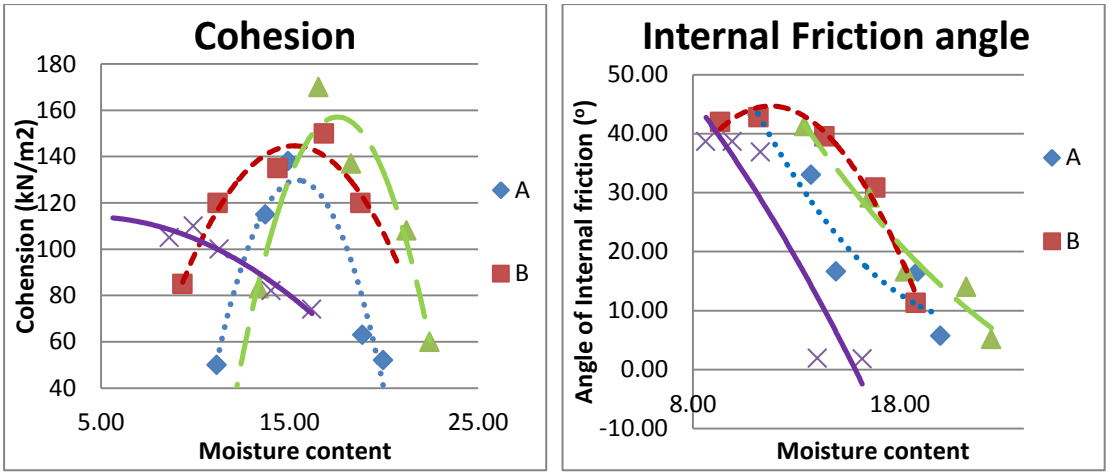

Figure 5.10: Shear-stress cohesion and internal friction angle results sequacity for the five moisture variations of the soils A, B, C and D.

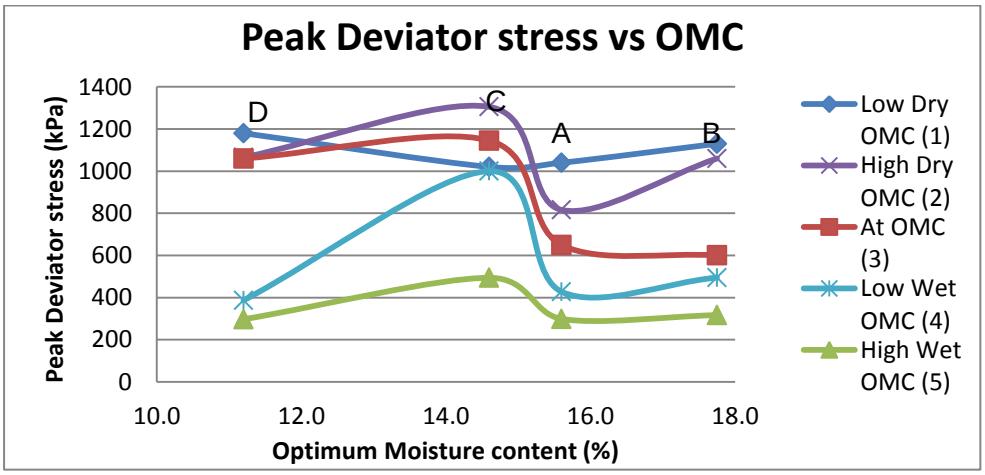

Figure 5.11: Peak deviator stresses for the various soil types versus Optimum moisture content (OMC) uniformity prepped at dry-of-OMC, At-OMC and Above-OMC

For the internal friction angle, increase in moisture content causes a drop in friction angle (Figure 5.10). The decrease in the internal friction is due to the increased lubrication of the soil particles from the increase in the moisture content. Horn and Deere (1962), Mitchell (1993) and Al-Shayea (2001) also have observed this lubricating effect of the soil fabric.

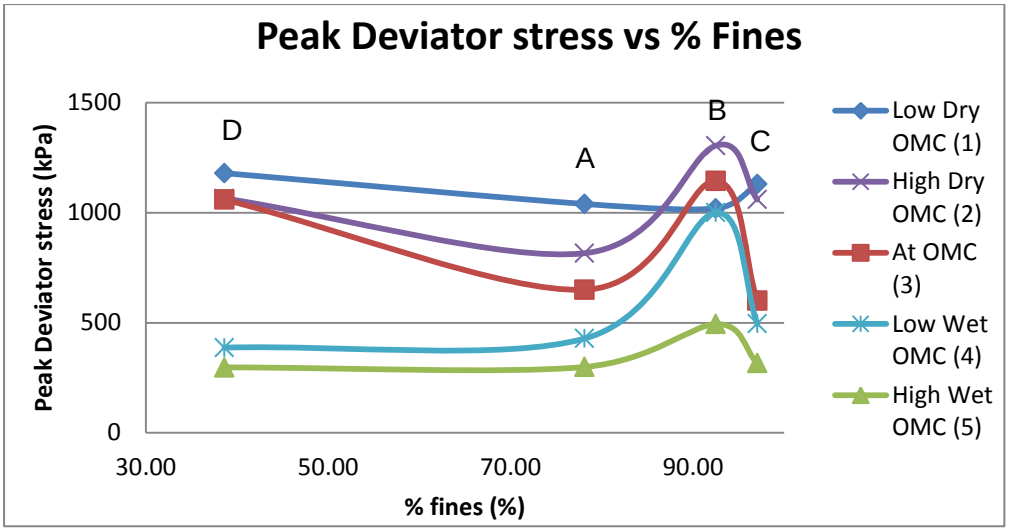

Figure 5.12: Peak deviator stresses for the various soil types versus percentage fines prepped at dry-of-OMC, At-OMC and Above-OMC

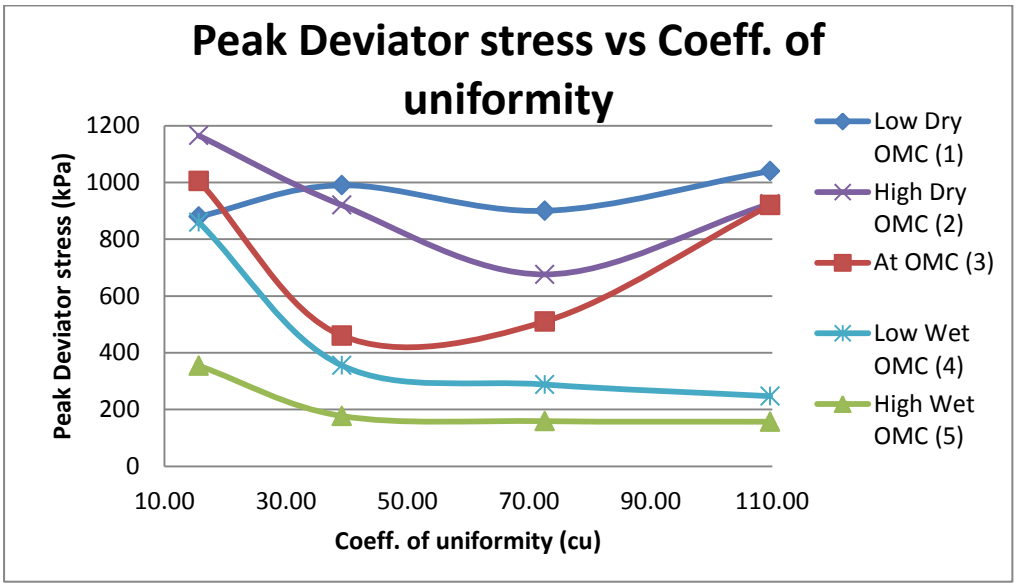

Figure 5.13: Peak deviator stresses for the various soil types versus coefficient of uniformity

Figure 5.11 shows the graph of peak deviator stress against optimum moisture content (OMC) for the four soils at varying initial moisture content. The points for each of the soils follow in such a way that as their OMC increases their peak deviator stresses decreases. As much as the component of each of the soils affect the OMC values, they also affect the deviator stress behaviour as the initial moisture content

moves from dry OMC to wet OMC. The C soil which is a clayey soil has a higher point on the curves which shouldn't be so, since clay particles would cause a lower deviator stress, but the sticky nature of the clay in the soil causes the soil to be denser during the preparation stage (compaction of the soil) giving it the higher deviator stress as the initial MC increases to At-OMC.

In the graph of peak deviator stress against percentage of fines in Figure 5.12, as the percentage fines increases the peak deviator decreases. The proportion of these fines also has an effect on this graph. Here the off soil in the curve is the soil's B which is a silt soil. As the silt particles change from dry of OMC to wet of OMC, they have a higher deviator stress than the other soils, even with a lower percentage fines.

For both graph representations shown in Figure 5.11 and Figure 5.12 for peak deviator stress against OMC and percentage fines respectively; the dry of OMC gives a proper graph curve, but with a wetter of OMC preparation of the soils, the other soil property conspicuously affects the graph flow. Also, it's noticed that a proper At-OMC would have the steepest flow than dry of OMC and wet of OMC, and proper wet of OMC would have an almost flat flow.

The graph of peak deviator stress $(\sigma_1 - \sigma_3)_{max}$ against coefficient of uniformity (Cu) shown in Figure 5.13, shows that higher Cu of a soil causes a decrease in the soil's shear strength. This flow pattern is observed in all the moisture variations except for the At-OMC. The accurate pattern is seen clearly in the wet of OMC, where there is a steep drop in $(\sigma_1 - \sigma_3)_{max}$ at low Cu. Cu which represents how well graded the particle size distribution of the soil is. This shows that soils of high well-grading (high Cu) tend to have low peak deviator stress. This is due to the ability of the particles to rearrange, causing the soil to exhibit less shear strength.

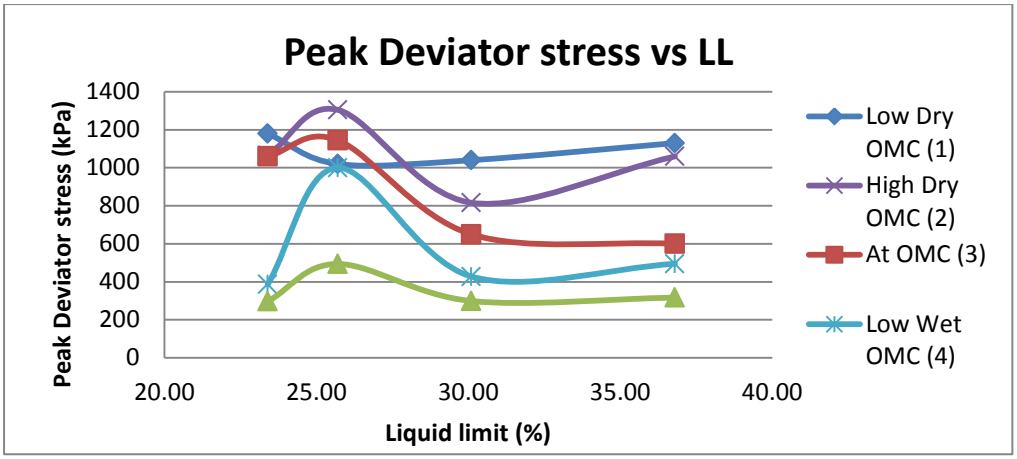

i. LL

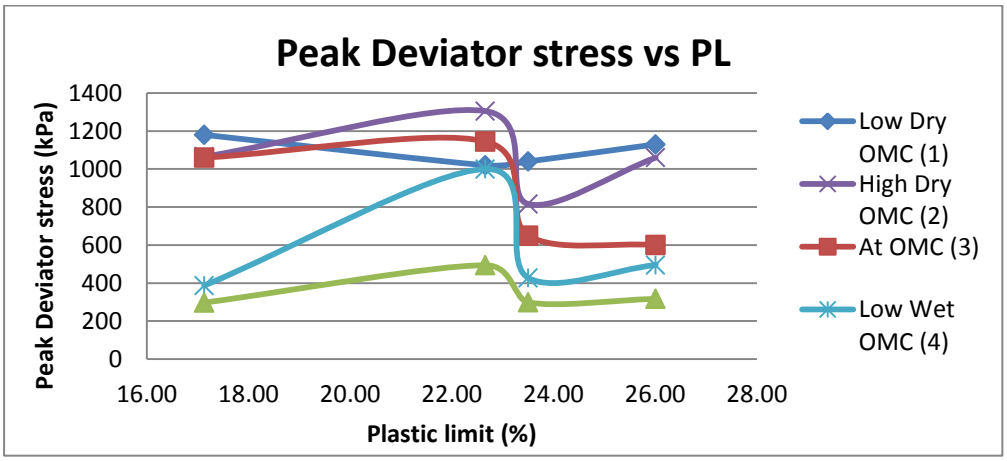

ii. PL

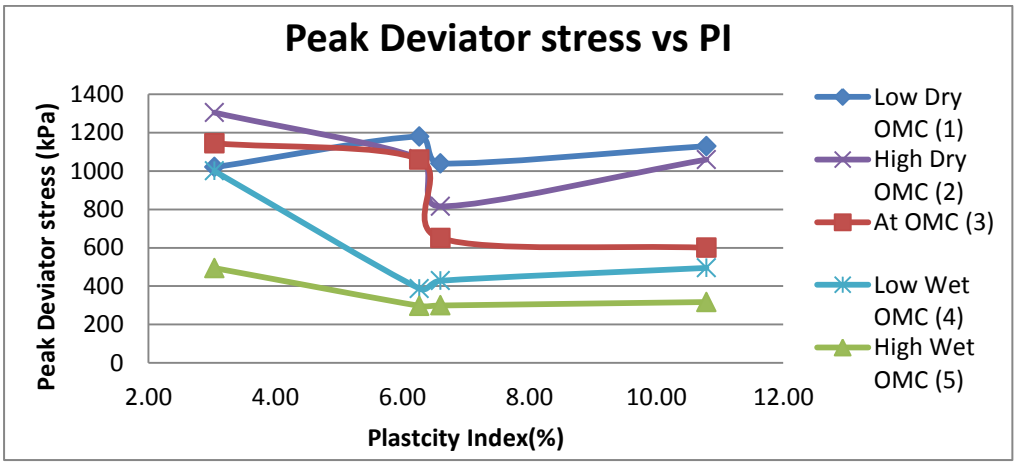

iii. PI

Figure 5.14: Effect of the consistency limits and moisture variation on the peak deviation stress: (i) LL, (ii) PL and (iii) PI.

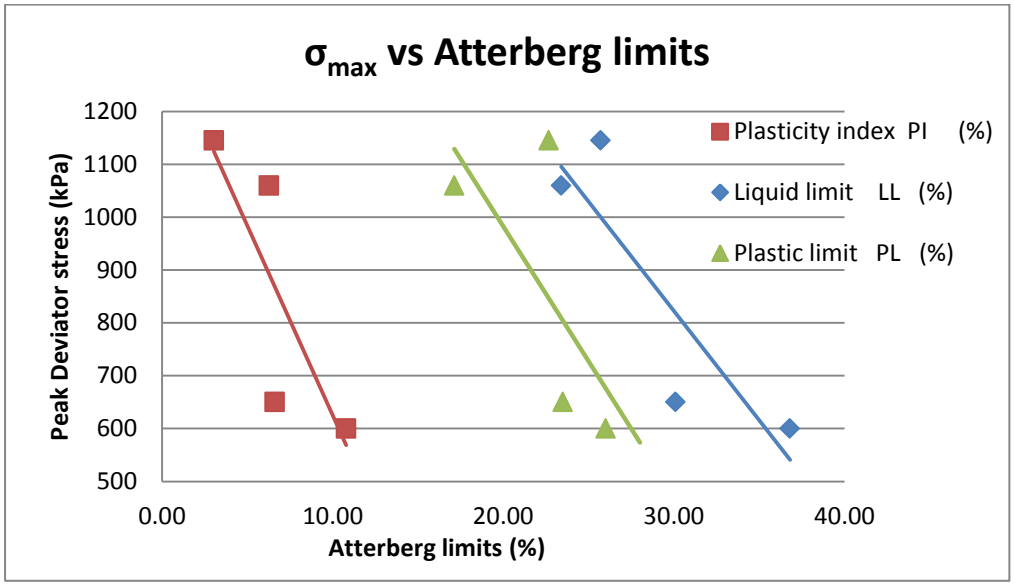

Figure 5.15: Peak deviator stress against Atterberg limits of the different soils

Figure 5.14 shows the peak deviator stresses for the various soil types versus the consistency limits – liquid limit (LL), plastic limit (PL) and plasticity limit (PI) for each soil prepped at dry-of-OMC, At-OMC and wet of OMC. Increase in the Atterberg limits cause a decrease in the peak deviator stress. The gross fine-sand element of the D soil and the gross silty component of the B soil cause the lower consistency limits as compared to the soils A (less of silt make-up) and C (clayey) soils. The higher the clay content in a soil, the higher the Atterberg limits and so the lower the peak deviator stress. This is true for all five moisture variations. Al-Shayea (2001) also found this in his study.

The soils' prepped at At-OMC of peak deviator stress against Atterberg limits show the curves of LL, PL and PI are represented in Figure 5.15 they all follow the same pattern previously discussed.

5.1.3 Consolidation Properties

Figure 5.17 shows the effect of pressure on collapse for the four different soil types prepared at five different moisture variations. The difference between the as-compacted and inundated curves points give the collapse potential value.

Figure 5.16 shows the full volumetric strain of all the soils at their five moisture variation each at as-compacted properties and inundated states. It is noticed that inundated samples are susceptible to larger volumetric strains than the as-compacted samples. Of all the samples inundated C2 sample has the highest volumetric strain. Followed are the inundated B2 and A2 and then inundated B1, C1, A1 and C5 before the first D samples (D3). The dry of OMC for soils A, B and C, have their inundated volumetric strain a lot higher than samples at as-compacted state, but for soil D, as much as the inundated samples have a higher volumetric strain, the as-compacted samples are with only a maximum of about 5% less than the inundated samples.

The densities at the moisture variations 2 and 3 (low dry of OMC and at-OMC respectively) for each of the soils are less than 0.04 g/cm^3 apart and yet the volumetric strain of these samples are well apart. These show that the main deciding factors are the moisture content and the position of the sample from the OMC. Samples with high percentages of clay content are receptive to moisture content. As-compacted at dry of OMC acquired really low volumetric strain, and when inundated to approaching saturation increased drastically to an immense volumetric strain.

The difference between the volumetric strain of the inundated and as-compacted states of each moisture variation samples result in the calculated collapse potential for each sample. The cumulative collapse (i.e. sum of collapse potential of each sample) at each pressure is shown in Figure 5.17 and the collapse at each pressure is shown in Figure 5.18. The order at which the samples collapse from high to low are C2, B2, B1, A2, A1, C1, D3, C5, D2, B4 and so on.

Looking at Figure 5.18, most of the samples have a high collapse at the first two pressures. The samples at low dry of OMC (A2, B2, C2, and D2) have increased collapse as the pressure increase, they maintain this increase, except for A2 and D2, which reduced a little at pressures 100 kPa and 200 kPa and then shoots up again at 300 kPa. In contradiction, samples 'high dry of OMC' (A1, B1, C1 and D1) show increase at the initial pressure till it reaches 50 kPa, of which there is a continuous decrease in the collapse as the pressure increases. For the at-OMC (B3, C3, and D3), low wet of OMC (A4, B4, C4 and D4) and high wet of OMC (A5, B5, C5 and D5), the samples all increase gradually and moderately as the pressure increases to 50 kPa and then maintains this amount of collapse. A3 retains a progressively moderate increase in collapse throughout the increase process of the pressure.

Habibagahi and Taherian (2004); Rabbi et al. (2014) had similar curve of collapse potential against pressure at wetting, where increase in pressure caused an increase in collapse.

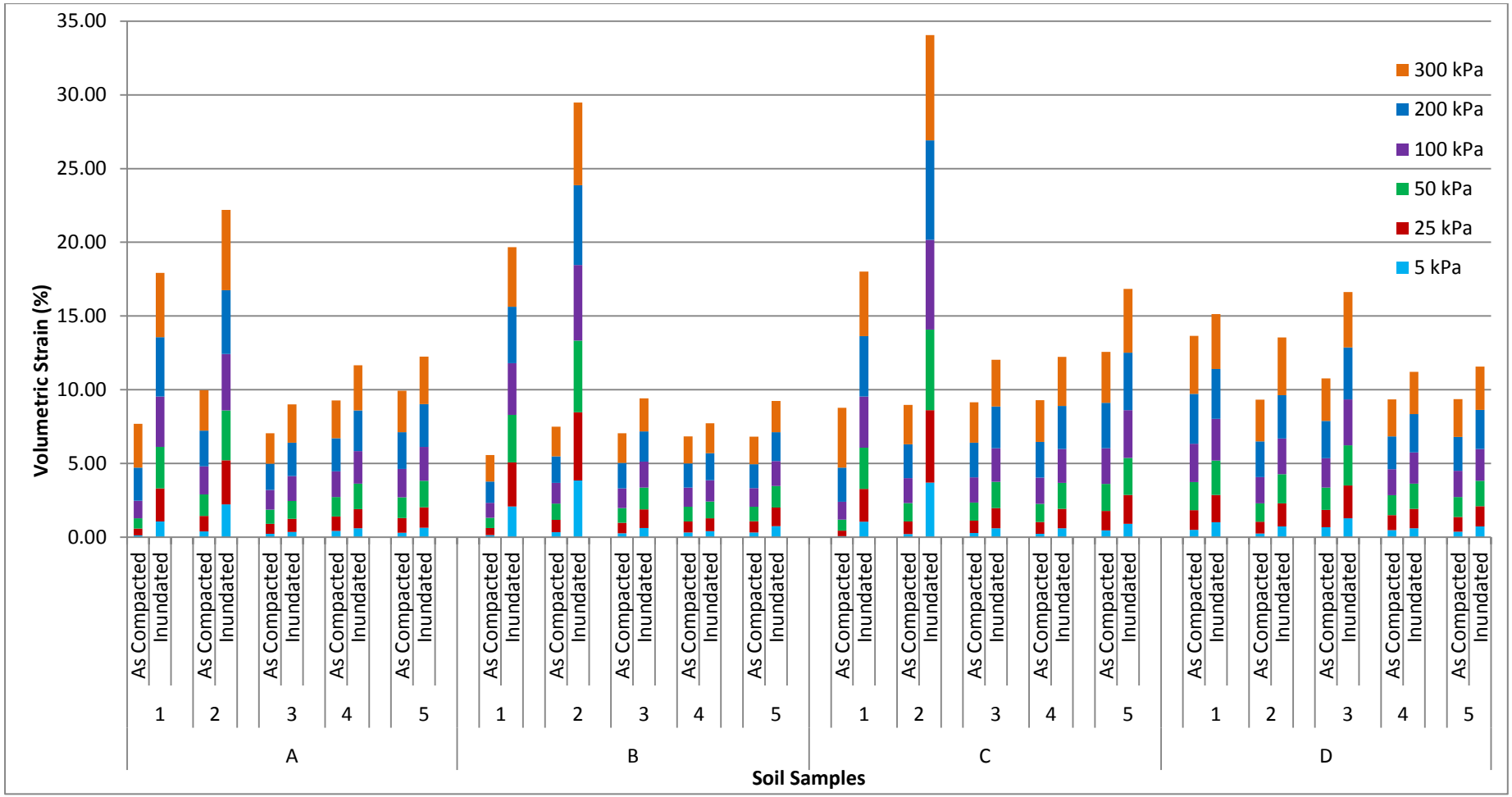

Figure 5.16: Column representation of the volumetric strain of each pressure in kPa at as-compacted and saturated states for soil A, B, C and D.

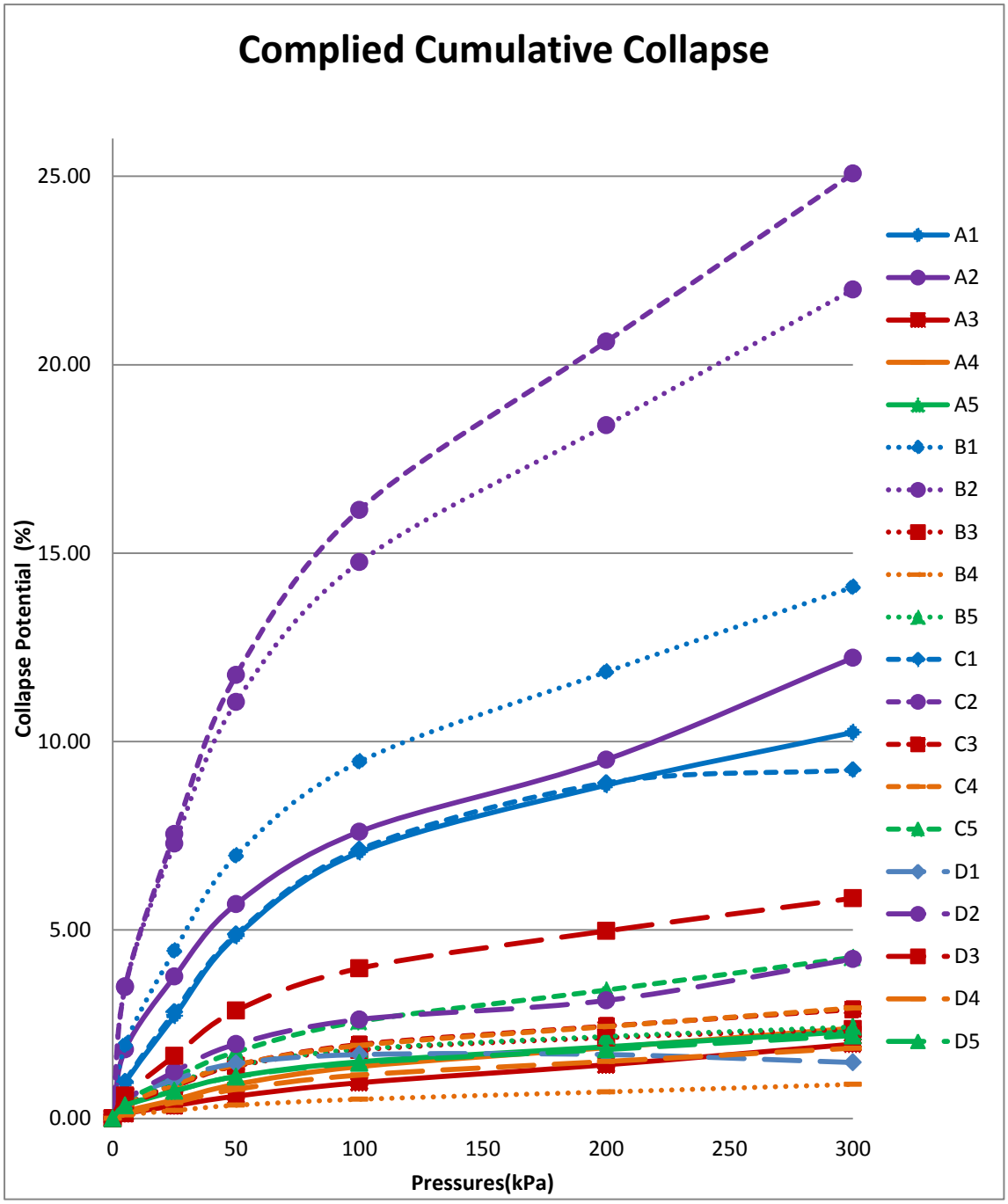

Figure 5.17: Cumulative collapse potential of the twenty samples at increasing pressures

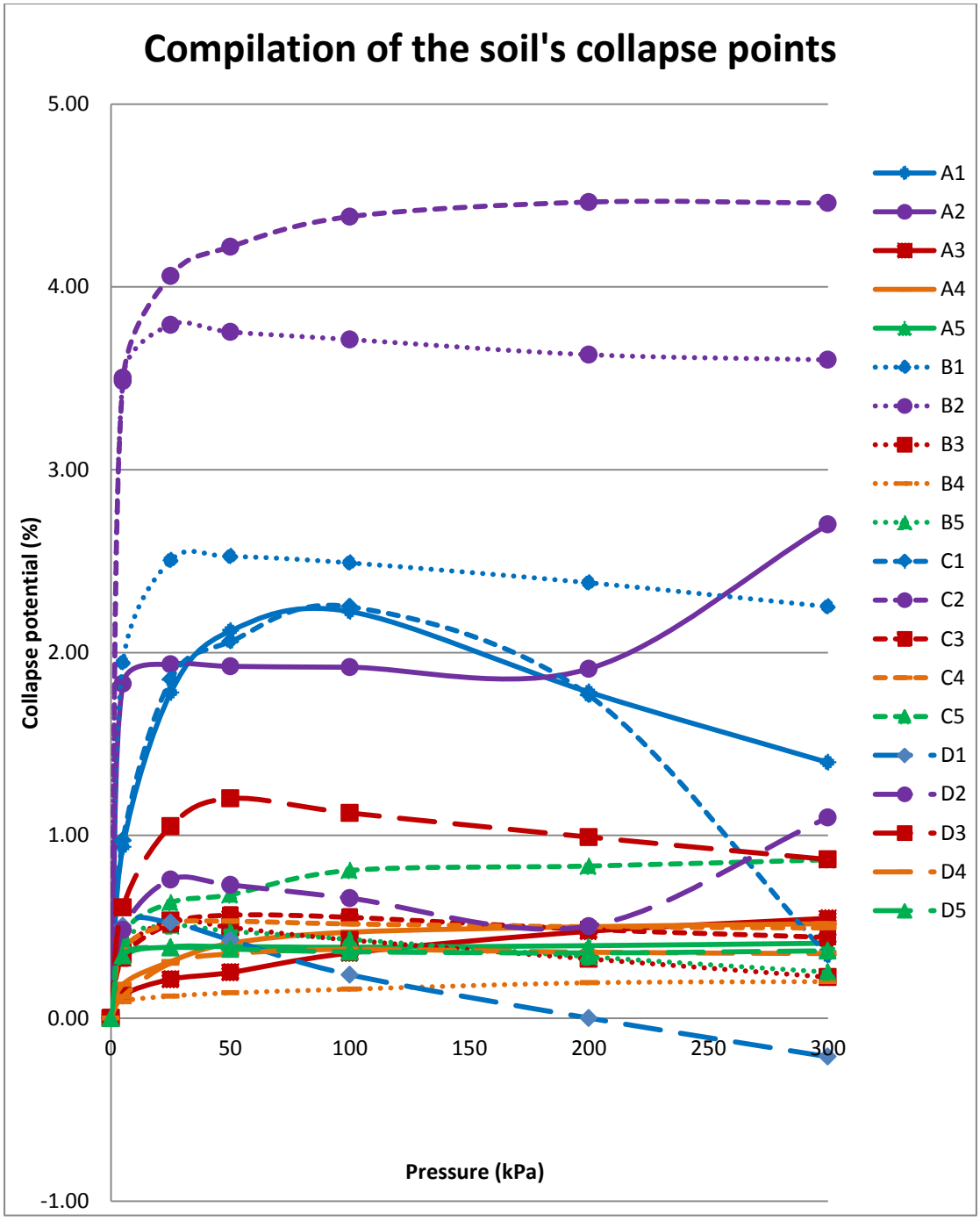

Figure 5.18: Collapse potential of the twenty samples at increasing pressures.

5.2 IDENTIFICATION AND PATTERNS FOR IDENTIFICATION OF SOIL COLLAPSIBILITY

From the complied result and analysis, collapsibility can be identified and described under three captions namely:

- Soil type
- Compactive variables and
- Critical pressure

5.2.1 Soil type

From the graphical representation of the four geologically different soils the relationship between collapse potential (CP) against Particle size distribution (PSD) parameters, Atterberg limits, and shear strength properties are observed and discussed. Graph of CP vs PSD (Percentage of fines and coefficient of uniformity) is shown in Figure 5.19; graph of CP vs Atterberg limits (LL, PL, PI) is shown in Figure 5.20; and graph CP vs Shear strength properties (angle of friction and cohesion) is in Figure 5.21.

From the graph of collapse against percentage fines and coefficient of uniformity (Cu) (Figure 5.19), it is noticed that percentage fines are directly proportional to collapse whereas Cu is inversely proportional to collapse. This behaviour is in correlation with compaction mechanism (Figure 5.4); where soils with lower percentage fines have higher Cu (more well-graded) of which produces higher dry density, since they tend to compact more by particles rearrangement and densification causing a stable system. The higher the Cu is, the more well-graded the soil will be; what this means is, that the particle composition of the soil is approaching a more balanced range of particle size content, with inter-particle filling of the space between the larger

particles by the tiny particles is high. Research result by Wang et al. (2009) concurs with this when they examined the microstructure of soils. They found that the fine grained particles move randomly in the pores space of larger particles. These void spaces cause the high volumetric strain when wetting and pressure is applied on the soil. Hence high percentage fines and lower Cu soils (not so well-graded) would collapse more. This result however, disagrees with Basma and Tuncer (1992)'s conclusion, where they stated that higher Cu correlates with higher CP; however their result was more pronounced in the wide ranges of particle sizes where the D10 and D60 had values from clay range and sand range respectively. The denser (lower percentage fines and higher Cu) the soil is, the lower the void ratios are, thus less collapse upon wetting and loading. The denseness of the soil reduces the metastability of the soil and even if wetting reduces the soil resistance, the volumetric change is considerably less.

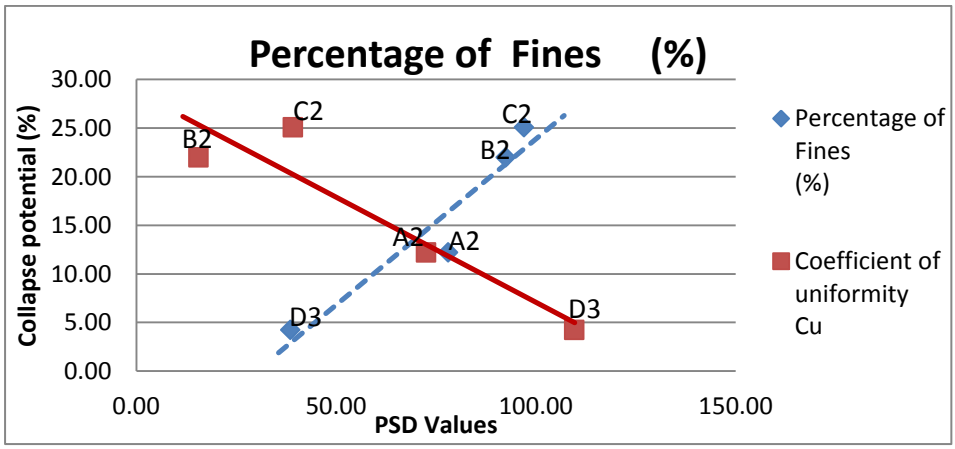

Figure 5.19: Relationship between collapse potential against percentage fines and against coefficient of uniformity

The collapse potential of a soil is also dependent on the existence of bonding materials. This is where the Atterberg results play an important role. Soils C and D have clay as their binder, which should have lower collapse potential than A and B with silt bond (Figure 5.20). Rogers, 1995 and Basma and Tuncer 1992 state that

'collapsible soils are typically characteristics of silty soils', therefore soils with their binder as clay are more stable soils than those with silt fines as discussed. Although in this research it came across that a sample with high clay content would have high collapse due to the ability of the clayey sample to amass higher volumetric strain when saturated as compared to its as-compacted state. This is highly dependent on the percentage of clay content in the PSD. Khattab et al (2006) and Lawton et al (1992) agree to this in their studies. Their results showed that increase in clay content caused an increase in collapse potential.

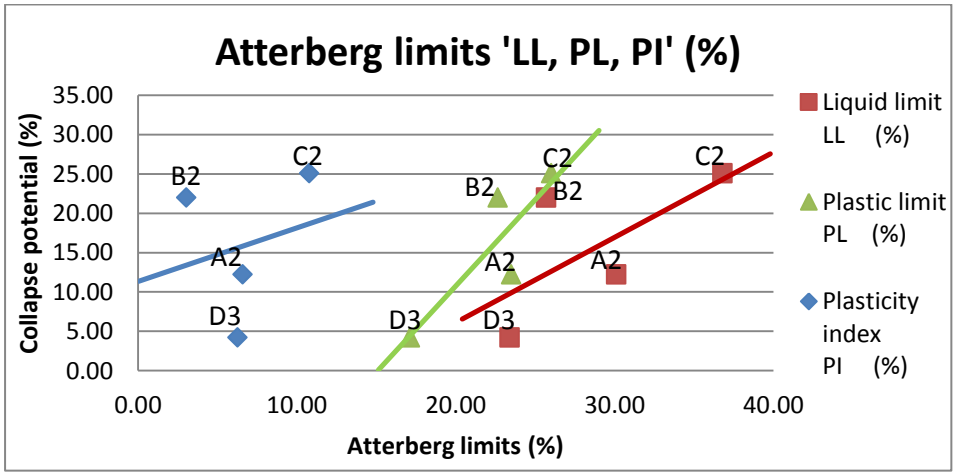

Figure 5.20: Effects of liquid limit, plastic limit and plasticity index on collapse potential

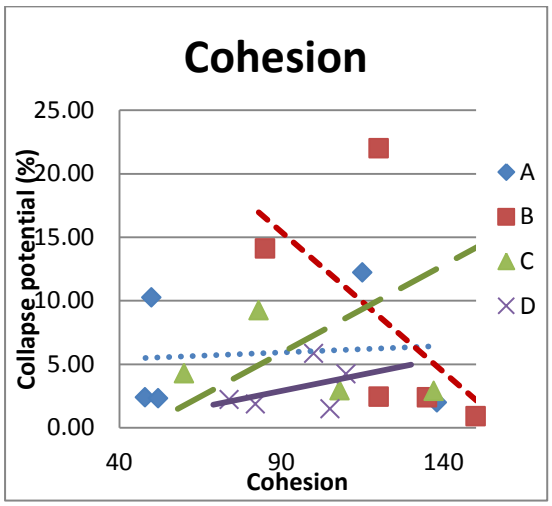

I. Angle of friction

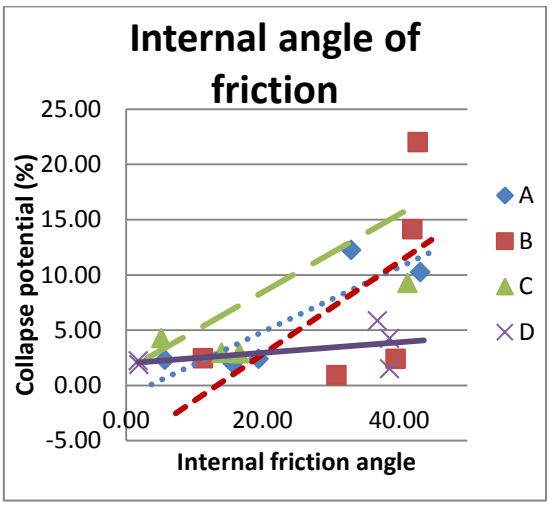

II. Cohesion

Figure 5.21*: Collapse potential against shear-stress properties*

Collapse against Atterberg limits is shown in Figure 5.20. The trend of the points of graph of collapse potential against liquid limit, plastic limit and plasticity index are similar for three of the soils, where increase in all three causes an increase in collapse potential of the soils. B on the other hand doesn't fit into the trends because of its silty particles. Al-Shayea (2001) from his investigation of the effect of clay content on the consistency limit concluded that increase in clay content causes an increase in the consistency limit; and then Basma and Tuncer (1992) concluded also that higher clay content in comparison to sand content results in higher collapse potential. Hence in correlation, increase in Atterberg limit would bring about higher collapse potential. Further correlations can be drawn from observation of Figure 5.6, where percentage fines and Atterberg limits are directly proportional and then again in Figure 5.19, percentage fines are directly proportional to collapse. So considering its direct link with the percentage fines, Atterberg limit would be directly proportional to collapse.

Figure 5.21 shows collapse against angle of friction and collapse against cohesion. The graph of collapse potential against angle of friction shows that with higher angle of friction, collapse is more. As explained previously from the graph Figure 5.10, the increasing of water content in the soil cause a reduction in internal friction due to the sliding and slipping of the soil particles (Al-Shayea 2001 and Gu et al. 2014); also in Figure 5.24 (which is yet to be discussed), the higher the initial moisture content, the lower the collapse potential of the soil. This combined pattern just shows that with higher moisture content; the internal friction would be reduce causing a decreased collapse; since the slipping and sliding of the particles creates an already collapsed soil (an even more compact soil) at prior stage. The different soils thus collapse in the order of soil C and B with the steepest of the four soils have more collapse

potential then soil A and D which have a gentle flow curve. Hence C with the highest point and steepest line is predicted to be the most collapsible next to B, A and then soil D.

The graph of collapse potential against cohesion gives no discernible trend, but with the factors involved an analysis can be drawn. The response of soil cohesion to water is the same as dry density to water as seen in Figure 5.10 and Figure 4.3 respectively; this is due to the increasing cementation and adhesion due to compaction with increasing water content, only to a point, beyond which more water content causes decreasing cohesion and density from separation distance between the soil particles. Thus the denser a soil is, the higher the cohesion of that soil. Therefore, since denser soils (high initial dry density) collapse less, soils with high cohesion would collapse less. Because even when the cohesion factors of: cementation and adhesion, electrostatic and electromagnetic attraction and capillary suction losses their strength, the collapse would be low due to the denseness of the soil (limited voids to collapse to). Al-Shayea (2001) result from testing the effect of moistures content on cohesion gives a supporting result.

A characteristic observation of the peak deviator stresses can be evaluated from comparing the graphs of moisture content and coefficient of uniformity for each soil. Soils with high coefficient of uniformity for each soil exhibits lower peak deviator stress (Figure 5.13) and reduced collapse potential (Figure 5.19). Also relationship between peak deviator stress and collapse can be determined from graphs of peak deviator stress against moisture content in Figure 5.9 and moisture content against collapse potential in Figure 5.24. Increase in moisture content causes a decrease in both peak deviator stress and collapse potential of the soil. Therefore this shows a trend that peak deviator stresses of the soils are directly proportional to collapse.

Conceding to this also is the phenomenon in collapse and peak deviator stress of a soil. Both phenomena deal with the ability of a soil to resist failure (shear strength) and to show failure (collapse), of which the same factors would represent. Hence increases in peak deviator stress would reflect a higher collapse potential.

5.2.2 Compactive variation

The significance of initial dry density, initial void ratio, and initial moisture content (MC), on collapse are illustrated in Figure 5.22, Figure 5.23 and Figure 5.24 respectively. The compactive variable in this research is made up of properties that the soil has its structural ability produced from five moisture variations which are a percentage of the optimum moisture content (see Table 3.2). They include moisture content, dry density, void ratio and degree of saturation. Each soil compacted at percentage of its optimum moisture content had varying properties, of which the farther away from the OMC, the compacted soil is found to have lower dry density. Compaction curves in Figure 4.3 are evident of this.

The trend lines for the CP verses void ratio (Figure 5.23) and CP against dry density (Figure 5.22) are inversely similar, like a split mirror graphs of one another. This is expected since void ratio is inversely proportional to dry density. Figure 5.22 indicates that for a compacted soil at a particular moisture content and compaction intensity, increasing initial dry density causes decrease in the collapse potential of the soil. The higher the density of the soil the less profound effects of the metastable forces are on the soil. this is in line with conclusions drawn by Basma and Tuncer 1992. When the particles of the soils are heavily packed (high density), the probability for these particles to rearrange to form a closer packed structure is less; hence less collapse of the soil. Also, the denser a soil (higher the initial dry density), the lower the initial void ratio, consequently the more stable the soil structure (lesser

the CP). Results that agree with this were achieved by Basma and Tuncer (1992); Tadepalli and Fredlund (1991); Habibagahi and Taherian (2004); Seleam (2006); Benchouk et al. (2013).

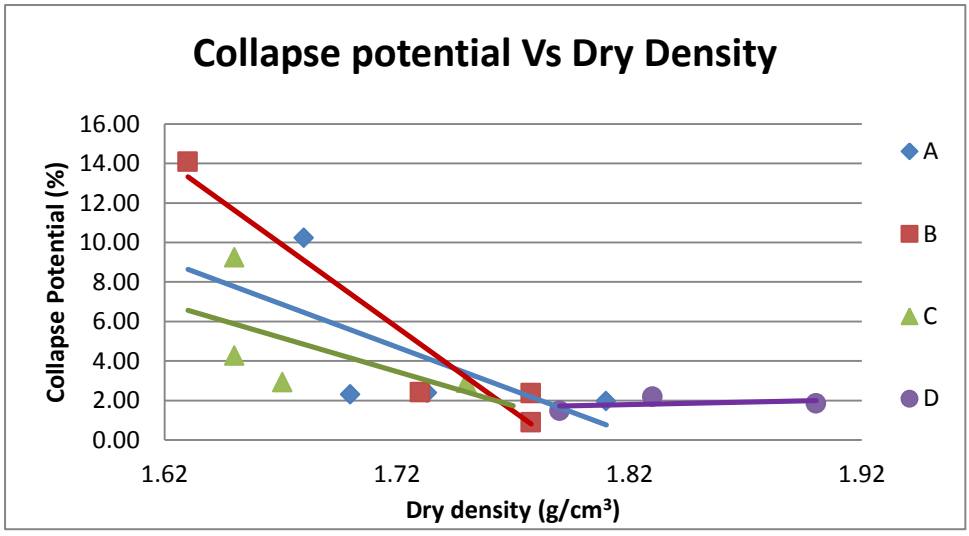

Figure 5.22: Relationship between collapse potential and initial dry density

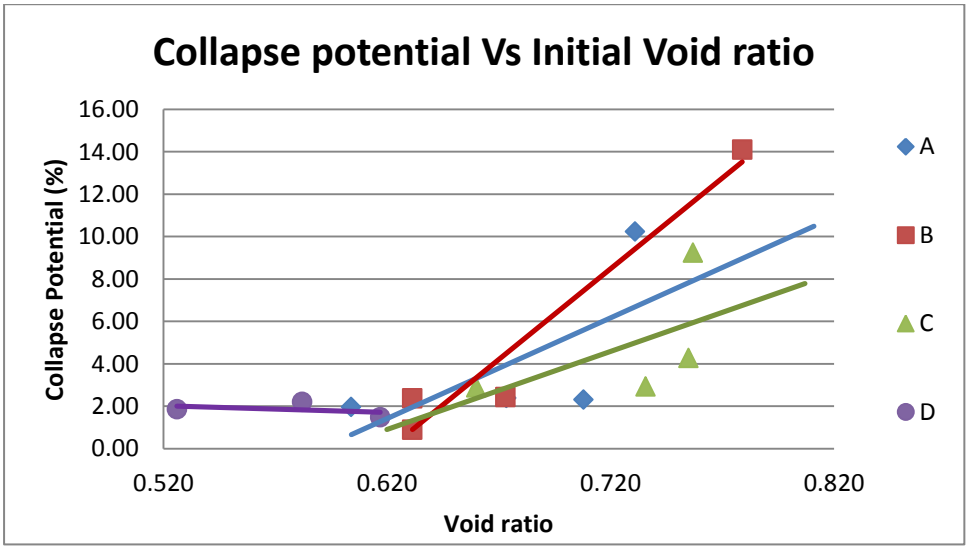

Figure 5.23: Relationship between collapse potential and initial void ratio

Graphs in Figure 5.22 and Figure 5.24 reveal similar trends in the graphs of CP against initial dry density and CP against initial MC respectively. Figure 5.24 divulges the influence of initial MC on collapse potential. The initial moisture content of the compacted soil is inversely proportional to collapse with the related initial dry density.

The reduction in CP is due to the the initial bonds from fine fractions which are weaken due to higher initial MC. The same was found in Bamas and Tuncer (1992) study. The matric suction which acts as a bond also reduces in strength as moisture content increases. Hence increase in the initial moisture content reduces the matric suction breaking the bonds and causing the collapse occurrence, but this time before the testing, thus creating a more stable soil. Similar result has been obtained in the effect of initial MC to collapse by Tadepalli and Fredlund (1991); Basma and Tuncer (1992); Habibagahi and Taherian (2004); Seleam (2006); Ayadat and Hanna (2008); Gaaver (2012); Benchouk et al. (2013); Rabbi (2014).

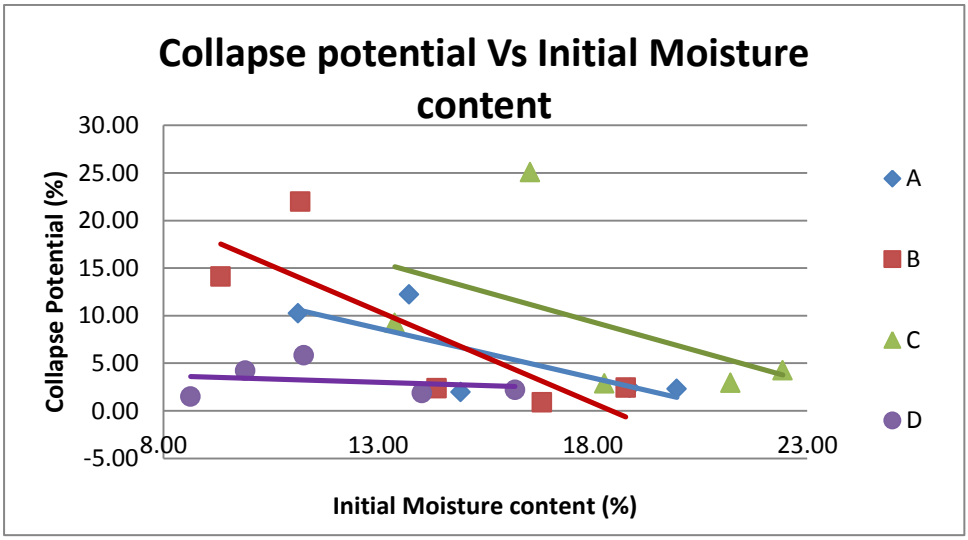

Figure 5.24: Relationship between collapse potential and initial moisture content

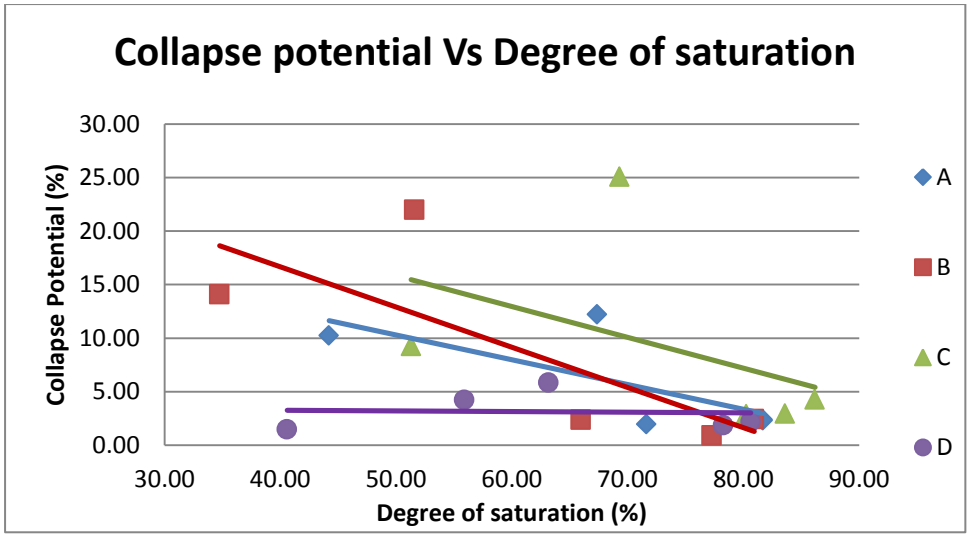

Figure 5.25*: Effect of degree of saturation on collapse*

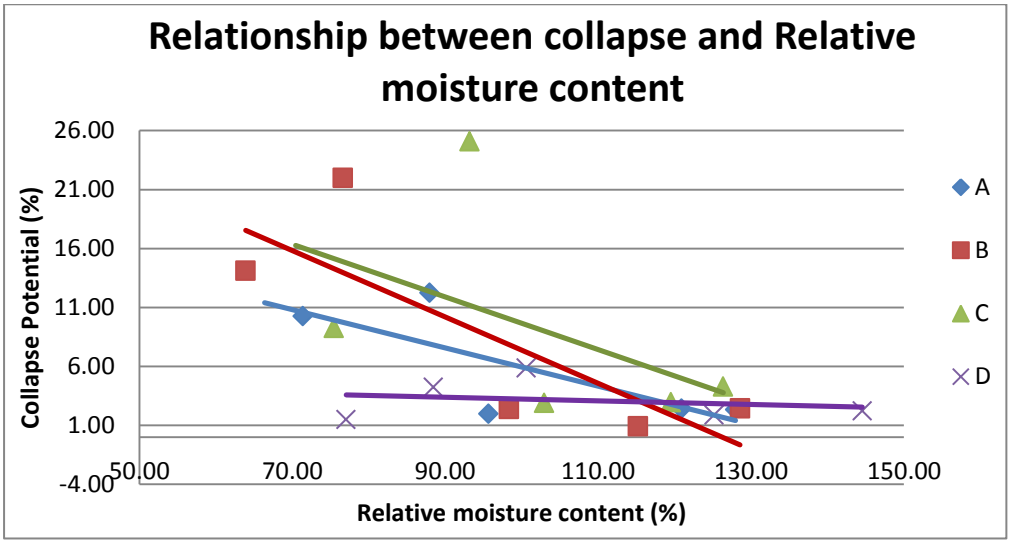

Figure 5.26: Relationship between *percentage from OMC and collapse*

Figure 5.25, and Figure 5.26 show the effects degree of saturation (Sr), and relative moisture content respectively have on collapse. Relative moisture content (RMC) is the ratio of initial moisture content and OMC in percentage. Graphs of collapse potential against Initial MC, degree of saturation, and relative moisture content have a similar flow chart. See Figure 5.24, Figure 5.25 and Figure 5.26 respectively. Here, Initial MC, Sr and RMC are inversely proportional to collapse. Hence increase in all 3 parameters would cause a decrease in collapse. As the moisture content increases, the voids between soil particles are filled with water, which is simply the increasing of

the degree of saturation (and increase in RMC). This process reduces the susceptibility for collapse; since the initial bonds from fine fractions are already weaken due to higher initial MC (and Sr and RMC).

5.2.3 Critical Pressure

The critical pressure (P_{cr}) of a soil is the pressure at which cumulatively gives the soil the term collapsible. And for this research, soils with collapse greater than 6% are qualified as collapsible. 6% is chosen based on previously reviewed literature (refer to Table 2.5 and Table 2.6 in pages 55 and 56 respectively). In practice structures that have undergone that amount of collapse would have exceeded their serviceability limit due to extensive damage.

The graph plots include:

- Figure 5.27 - curve representation of each soil and their moisture variables;
- Figure 5.28 - collapse of each soil with increase in pressure;
- Figure 5.29 – relationship between vertical pressure and relative moisture content;
- Figure 5.30 represents the cumulative stack of pressures plotted with collapse for the soils and their moisture variation;
- Figure 5.31 displays the critical load at the range of collapse severity (moderate – 2%, moderately severe – 6%, severe – 10%) of the soils and their moisture variations and
- Figure 5.32 exhibits critical pressure points and the corresponding collapse potential of the soils at moderately severe collapse.

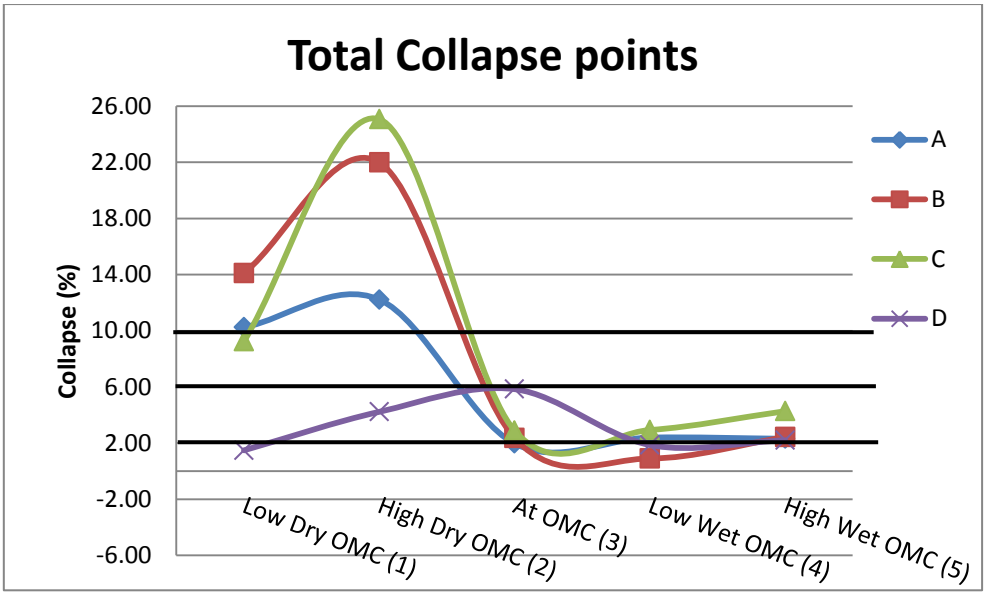

Figure 5.27: Total collapse - C*ollapse flow trend of the different soil states.*

Collapsibility threshold was checked at 2%, 6% and 10% collapse as stated by Abelev (1948); Jenning and Knight, (1975); and Hormdee, Ochiai and Yasufuku, (2004) respectively as the appropriate point for collapsibility. All the soils and their moisture variation have a moderate (2%) collapse potential except for the D1. At the point of severe (10%) and moderately severe (6%) collapse, only the A1, A2, B1, B2, C1 and C2 are found (Figure 5.27).

From this, it is deduced that when soils are inundated and loaded, the samples dry of OMC' (1 & 2) have a much higher collapse potential than the other compactive variations, and the 'At OMC' has the least. However, soil D has a different effect; the exact opposite is rather the case. This was due to the initial shear strength of the 'At OMC' which is much higher than the other compactive variation for soil D, of which at saturation the degree of densification of the other compactive variables is not high enough to compete with At OMC. In all the soils nonetheless, the wet of OMC (4 & 5) for each soil have the least collapse potential, which tallies with the analysis on effect of initial moisture content on the soil's collapse potential (Figure 5.24).

For the effects of the pressures of individual collapse shown in Figure 5.28, most of the soils have a gradual increase up till it hits the highest collapse point (the critical load) and then gradual drop. D1 has the trend from high to low with the most collapse at 5kPa pressure and then declines; this elucidates that inundation is the primary collapse trigger. The moisture content breaks the bond which gives the soil structure its stability. Since its collapse, forming a denser structure, higher pressure would only cause very limited collapse. Soils with moisture sensitive bonds would typically act this way.

Soils A5, B1 - B5, C2, C3, C4, D4 and D5 collapse trends illustrated in Figure 5.28, reveals the collapse as approximately constant through the changes in pressure. This can be interpreted as loading and inundation working together at an almost equal rate to cause the collapse in this compactive variation. The soil samples found here are those with relative moisture content greater than OMC of approximately >100% (that is moisture content wet of OMC). Soil samples that are not as moisture sensitive also fall in this range.

Due to the compact nature or/and near saturation of the samples A3, A4, C5, (Figure 5.28) the collapse sequence is from low to high as the pressure increases, hence inundation is having very little effect and the collapse is mainly due to the increase in load.

Samples like A1, C1, D3, with an increasing pattern, and then at a point, it begins to drop. The point where higher pressure does not cause increase in collapse shows the sample's critical point. All the different samples with the different flow trends all have this critical point, except they are not as visible as this. This set of samples is the same with those with little effect from the inundation, except they have a lower critical pressure point.

Other samples like A2 and D2 (Figure 5.28) with a normal format flow that is just disrupted by an irregular increase in collapse can be explained by the pressure

applied causing the immediate increase. This pressure might have been caused by crushing of the sand particles.

Observing the pressure at which the soils and their compactive variations collapse moderately, the relative moisture content increases with an increase in moderate collapse pressure (see Figure 5.29). Samples dry of OMC (at lower percentage from OMC) samples are more prone to collapse by little pressure since the degree of densification is lower at this point. Hence movement of particles to form a denser structure is apparent and achievable at low pressure. The increase in pressure would continue to the point where further increase in the pressure would produce negligible collapse. That pressure point is the critical pressure of that soil. This is because the sample becomes saturated and at its maximum densification. Similar finding was acquired by Basma and Tuncer (1992); Habibagahi and Taherian (2004); Nouaouria and Lafifi (2008). The flow curve graph of the soils can be seen in Figure 5.18.

In Figure 5.30, the pressure at which the collapse at moderate (2%), severely moderate (6%) and severe (10%) occur is seen where the descriptive line cuts through in the graph. It gives a clear visual of all the soils and their compactive variables in columns where each stake represents the thickness of collapse potential expelled by each pressure.

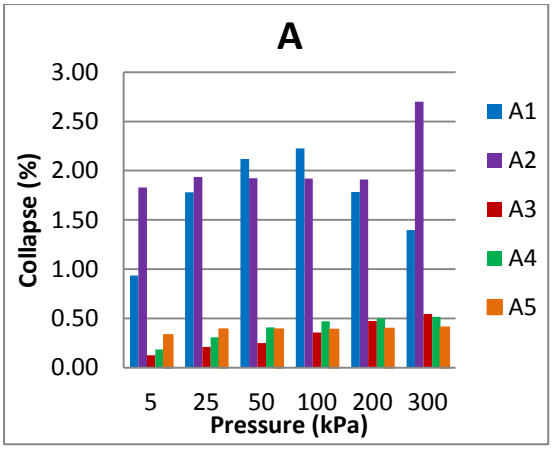

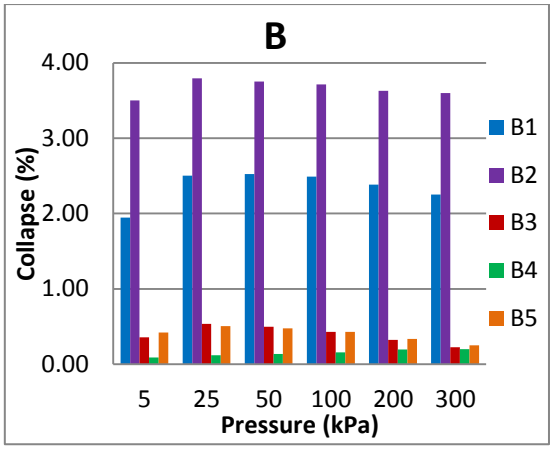

i) *A* *ii)* *B*

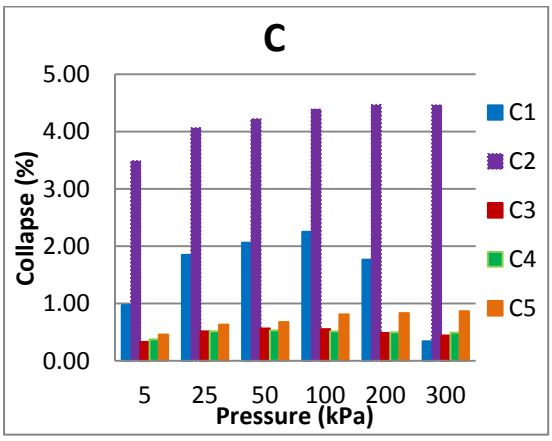

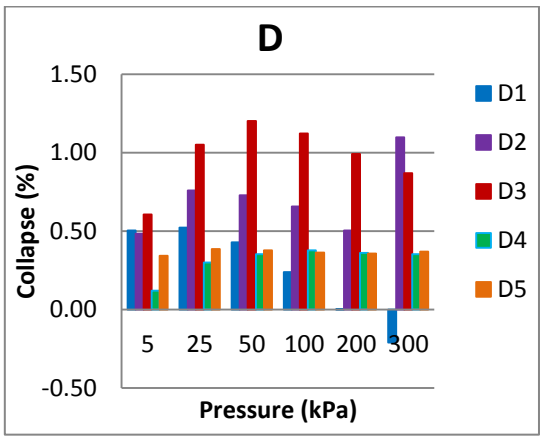

iii) *C* *iv)* *D*

Figure 5.28: Effect of pressure on collapse for each soil and their compactive variation

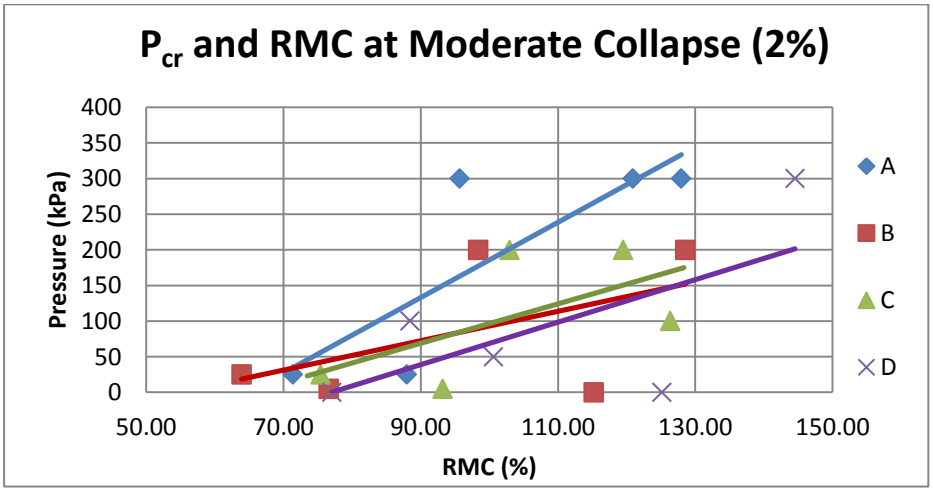

Figure 5.29: Relationship between RMC and pressure at moderate collapse (2%)

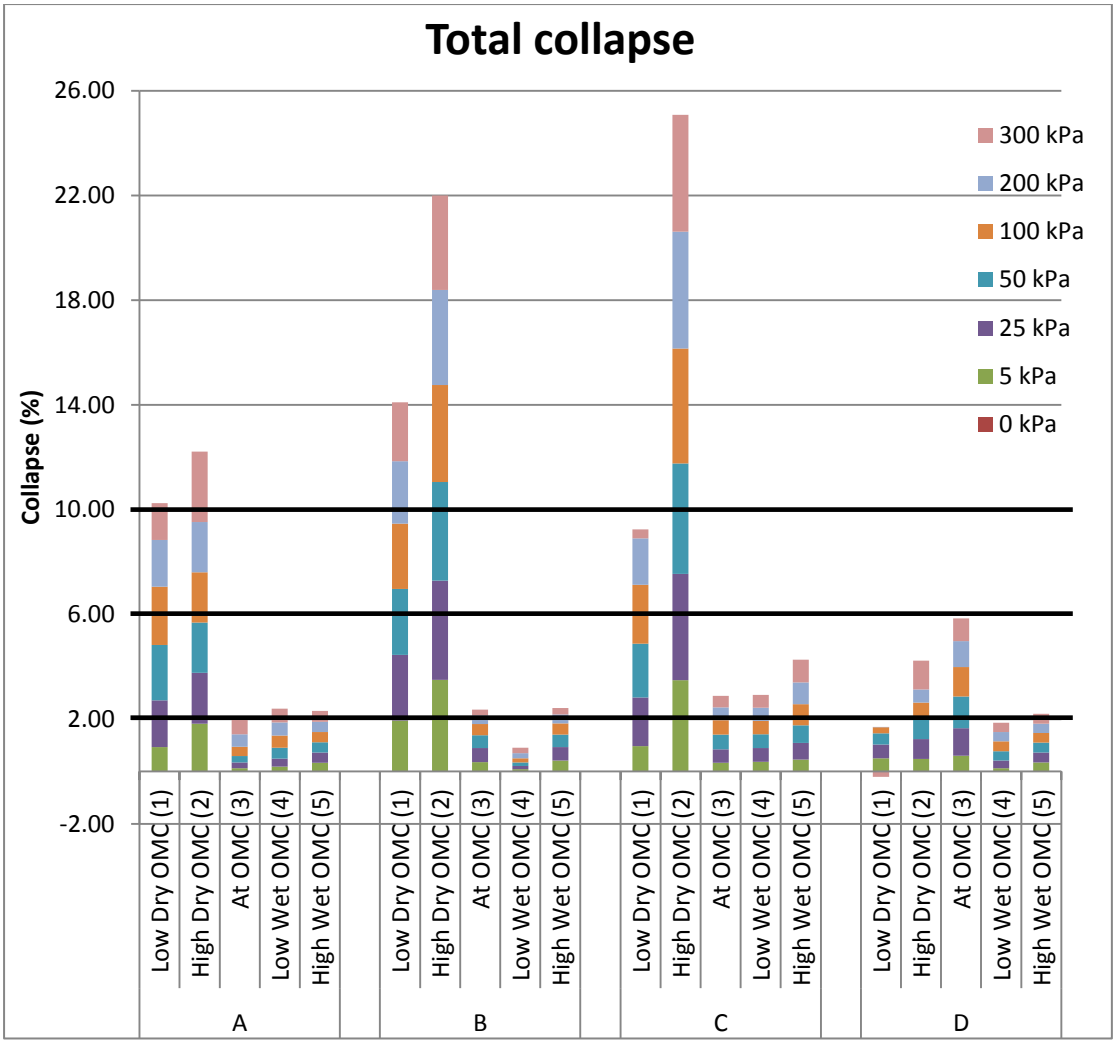

Figure 5.30: Representation of collapse against cumulative stacking of pressure for each soil and their compactive variables.

The critical pressures at moderate collapse (at 2%), moderately severe collapse (at 6%) and severe collapse (at 10%) have been drawn in Figure 5.31. The behavioural pattern is in such a way that samples at OMC (3) have the highest critical pressures as seen, except in cases where there are 0 kPa of pressure; This is because the soils at OMC (3) are the most compact of the compactive variables. Graph of moderate collapse (Figure 5.31) has this as a fact for A1, A2, B1, B2, C1 and C2, but the D had the exact opposite with D3 having the highest collapse but not as high as the moderately severe sensitivity check. Graphs for moderately severe and severe;

show pressures for only soils A1, A2, B1, B2, C1 and C2. This shows that at much higher sensitivity, the dry of OMC of a soil is most probable to be found.

The 0 kPa pressures are for the compactive variables that have not collapse at the percentage sensitivity check. Showing they would need pressure greater than 300 kPa for the sensitivity to be reached.

For the aim of this study, the moderately severe sensitivity gives the soil's critical pressure. Hence the pressure at critical pressure is same as the pressure reached for moderately severe collapse.

Figure 5.32 shows the critical pressure points of each soil at moderately severe collapse. Sample C2 has the most collapse potential at 25 kPa critical pressure. It is the most collapsible of the four soils. Sample B2 has a lesser collapse potential but with the same critical pressure of 25 kPa. Next is B1 with 50 kPa of critical pressure. A2 A1 and C1 have the highest critical pressure of 100 kPa. Thus A2 is more collapsible than the A1 and A1 than C1. D is however not moderately collapsible, making it the least collapsible of the four soils.

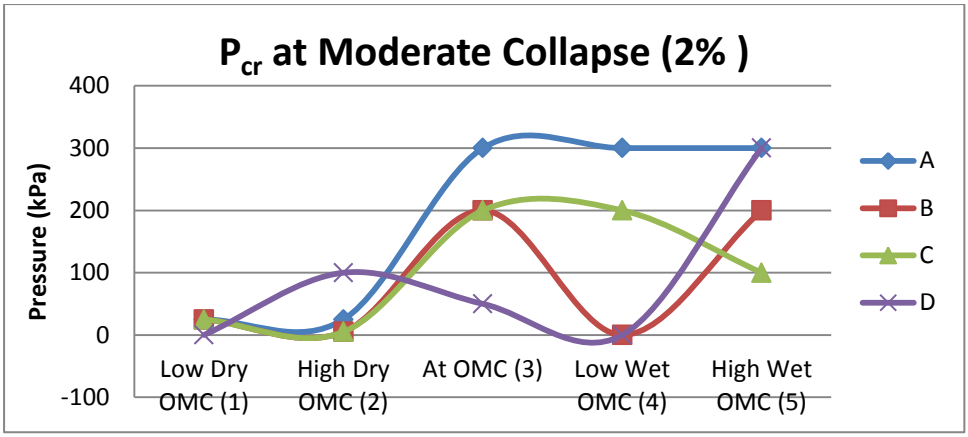

i. Moderate collapse

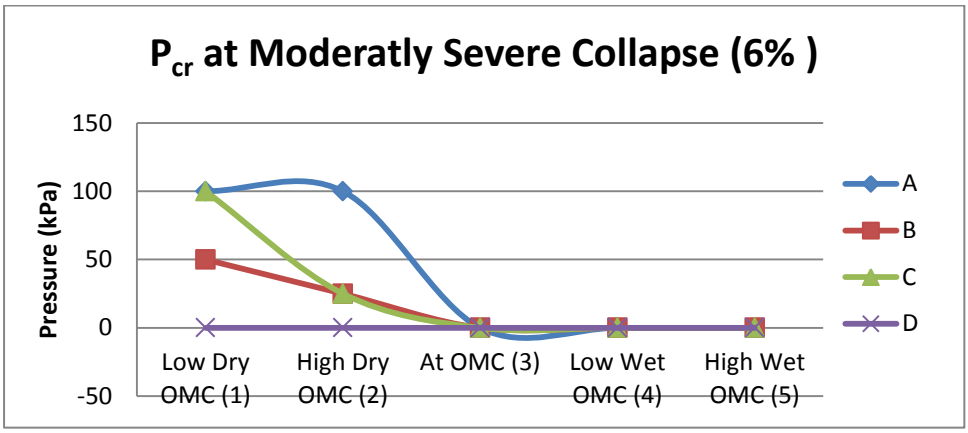

ii. Moderately severe collapse

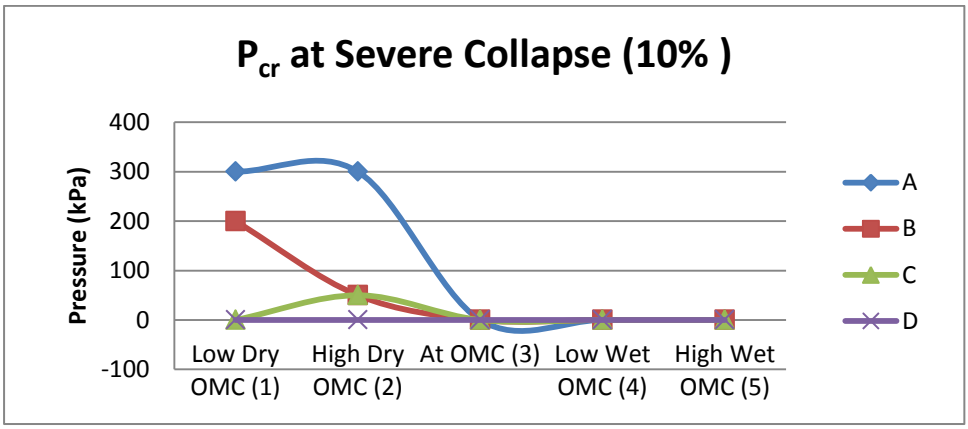

iii. Severe collapse

Figure 5.31: Critical load at the range of severity of the soils and their compactive variations

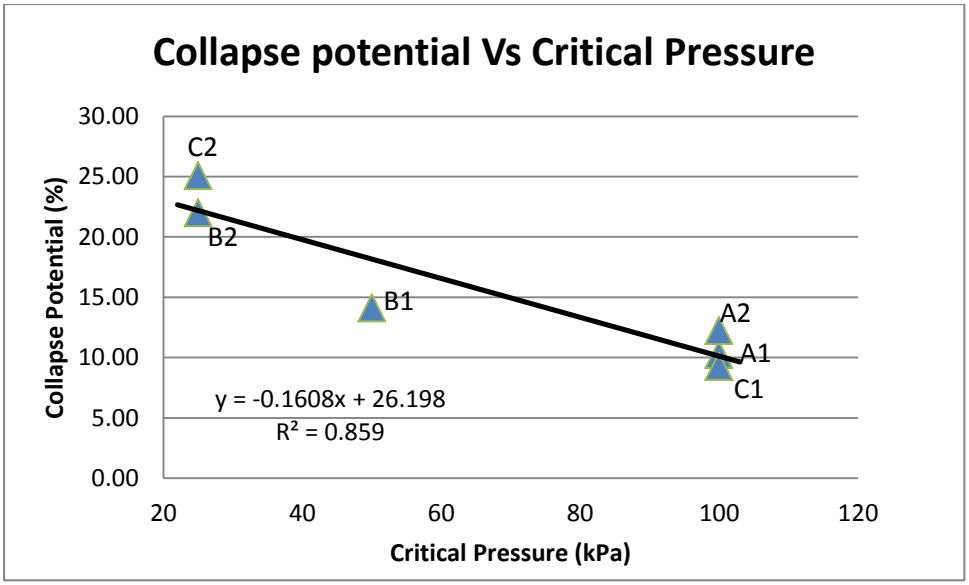

Figure 5.32: Critical pressure points verse collapse potential of the soils at moderately severe collapse

The graph in Figure 5.32 is inverse to the graph of collapse against wetting pressure as earlier discussed. it shows that critical pressure points for soils with high collapse potential tend to attain low pressures since soils most prone to collapse would collapse at the slightest of pressures. Hence, the higher the critical pressure a soil has, the less prone to collapse that soil would be. Also, looking at the critical pressures of each of the samples, they all fall under 150 kPa of pressure. This conforms to Larionov (1959) who stated that critical pressure of a collapsible soil should be less than 0.15MPa.

5.2.4 Past research work

Figure 5.33 shows Gibbs and Bara (1962); and Lutennegger and Saber (1988) collapsibility check graph and the four soils and their compactive variable, Table 5.5 gives the experimental laboratory data used for analysing the past research collapse indexes and Table 5.6 gives the solutions of the past research formula of collapsibility.

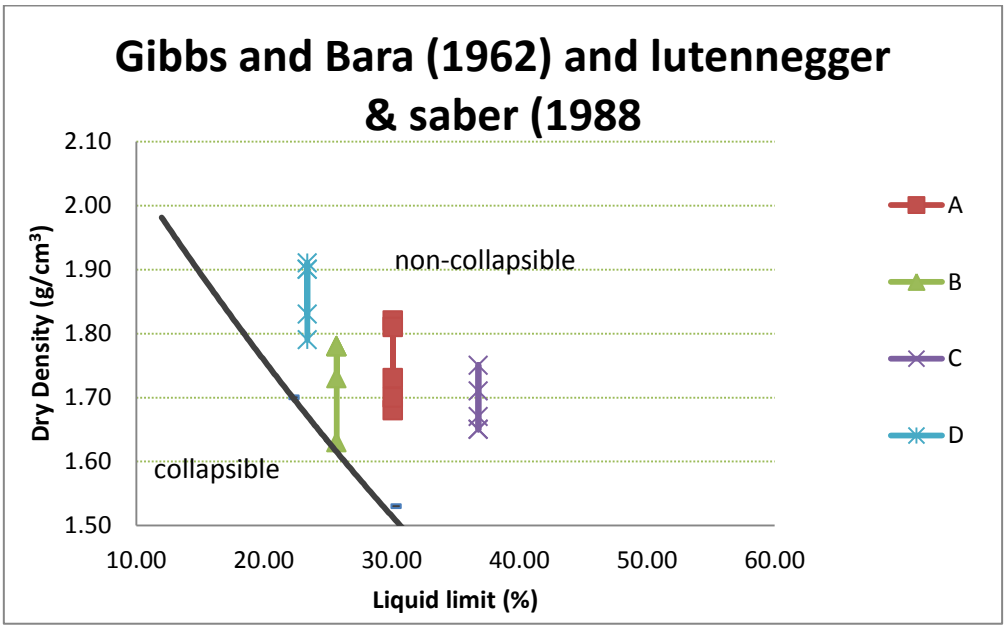

Figure 5.33: Gibbs and Bara (1962); and Lutennegger and Saber (1988) collapsibility check

From the graph of Gibbs and Bara (1962); and Lutennegger and Saber (1988) in Figure 5.33, the only collapsible sample is the B1.

The solutions of the past research formula of collapsibility given in Table 5.6, show the collapsible samples from the samples indicated in the bold red text. The table reveals:

- Tokar (1937), Soviet (1948) and Basma and Tuncer (1992) equations found the twenty experimental samples as collapsible.

- Handy (1973) with the measure of clay content established soil D as collapsible.
- Abelev (1948) found all the samples except samples A3, B4, D1 and D4 as collapsible.
- Jenning and Knight (1975) found the following values as greater than 6% collapse – A1, A2, B1, B2, C1 and C2.
- Hormdee et al. (2004) all the samples found 6% (Jenning and Knight 1975) collapse except for C1.
- Soviet (1967) found all the samples for soil B, sample A1, D1 and D5 to be collapsible.
- Zur Wiseman (1973) found samples B5 and D1 as collapsible.
- Batygin (1937), Priklonskij (1952), Feda (1966), Clenvenger (1958) with dry density parameter, Grabowska-Olszewska (1988), and Denisov (1951) research work found the samples to be non-collapsible.
- Larionov (1959) prediction secures A1, A2, B1, B2, C1 and C2, as collapsible.

Out of the 18 research work stated here, three of them found the samples to be collapsible, other eight researchers found some of the samples as collapsible and the others found the samples non-collapsible. This could be due to the fact that most of these researchers studied soil collapsibility using naturally collapsible soils, not considering normal compacted soils. And so with the four soils used in this research, the rules for predicting soil collapsibility don't always apply and in this case didn't apply.

Since in this research, from the table of severity (Table 2.5), a soil is termed to be collapsible when it exceeds 6% collapse, the samples found to be collapsible tallies with Jenning and Knight (1975). The results in this research also tallies with Larionov (1959), whose prediction works perfectly with the results herein.

From result here in A1, A2, B1, B2, C1 and C2 had moderately severe collapse which agrees with just two research works out of eighteen examinations. This goes to agree with Rogers (1995) who concluded that all soils should be suspected of collapse unless proved otherwise.

Table 5.5: Factors from experimental data used for the solutions of the past research formula for collapsibility

Parameters	A					B					C					D				
	1	2	3	4	5	1	2	3	4	5	1	2	3	4	5	1	2	3	4	5
Clay content (%)	25.8	25.8	25.8	25.8	25.8	36.4	36.4	36.4	36.4	36.4	35.8	35.8	35.8	35.8	35.8	9.5	9.5	9.5	9.5	9.5
Sand (%)	21.9	21.9	21.9	21.9	21.9	7.5	7.5	7.5	7.5	7.5	2.9	2.9	2.9	2.9	2.9	61.4	61.4	61.4	61.4	61.4
Coefficient of uniformity Cu	72.6	72.6	72.6	72.6	72.6	15.7	15.7	15.7	15.7	15.7	39.2	39.2	39.2	39.2	39.2	109.7	109.7	109.7	109.7	109.7
Initial Moisture Content 'W_o' (%)	11.1	13.7	14.9	18.9	20.0	9.3	11.2	14.4	16.8	18.8	13.4	16.5	18.3	21.2	22.4	8.6	9.9	11.3	14.0	16.2
Optimum moisture content 'OMC' (%)	15.6	15.6	15.6	15.6	15.6	14.6	14.6	14.6	14.6	14.6	17.8	17.8	17.8	17.8	17.8	11.2	11.2	11.2	11.2	11.2
Relative moisture content 'RMC' (%)	71.4	88.0	95.7	120.9	128.0	63.9	76.6	98.4	115.2	128.6	75.4	93.2	102.9	119.5	126.4	77.1	88.5	100.6	125.2	144.6
Final MC 'W_{max}' (%)	16.0	15.0	13.2	14.6	14.5	20.1	16.9	17.5	14.8	16.4	15.9	14.9	16.5	18.8	15.2	11.9	10.7	11.6	11.4	12.4
Dry Density (g/cm^3)	1.7	1.8	1.8	1.7	1.7	1.6	1.8	1.8	1.8	1.7	1.7	1.7	1.8	1.7	1.7	1.8	1.9	1.9	1.9	1.8
% dry density from Max dry density (%)	90.1	97.8	97.1	93.0	91.2	88.6	96.8	96.6	96.6	94.0	93.4	97.0	99.0	94.5	93.4	91.3	97.7	97.4	97.0	93.4
Plasticity Index PI (%)	6.6	6.6	6.6	6.6	6.6	3.0	3.0	3.0	3.0	3.0	10.8	10.8	10.8	10.8	10.8	6.3	6.3	6.3	6.3	6.3
Liquid limit LL (%)	30.1	30.1	30.1	30.1	30.1	25.7	25.7	25.7	25.7	25.7	36.8	36.8	36.8	36.8	36.8	23.4	23.4	23.4	23.4	23.4
Plastic limit PL (%)	23.5	23.5	23.5	23.5	23.5	22.7	22.7	22.7	22.7	22.7	26.0	26.0	26.0	26.0	26.0	17.1	17.1	17.1	17.1	17.1
Void ratio 'e_0'	0.7	0.6	0.6	0.7	0.7	0.8	0.6	0.6	0.6	0.7	0.8	0.7	0.7	0.7	0.8	0.6	0.5	0.5	0.5	0.6
Degree of saturation 'Sr' (%)	44.2	67.4	71.6	81.7	81.7	34.7	51.6	66.0	77.3	80.9	51.3	69.3	80.3	83.6	86.2	40.6	55.9	63.2	78.3	80.6
Critical Load (Moderate) (kPa)	25.	25.	300	300	300	25.	5.0	200	300	200	25.	5.0	200	200	100	300	100	50.	300	300

	0	0	.0	.0	.0	0		.0	.0	.0	0		.0	.0	.0	.0	.0	0	.0	.0
Critical Load (Moderately severe) (kPa)	100.0	100.0	-	-	-	50.0	25.0	-	-	-	100.0	25.0	-	-	-	-	-	-	-	-
Collapse Potential at 300 kPa load (%)	10.2	12.2	2.0	2.4	2.3	14.1	22.0	2.4	0.9	2.4	9.2	25.1	2.9	2.9	4.3	1.5	4.2	5.8	1.9	2.2
initial Void ratio 'ei'	0.5	0.4	0.5	0.6	0.6	0.7	0.5	0.5	0.5	0.5	0.6	0.4	0.5	0.6	0.6	0.5	0.3	0.4	0.5	0.5
final void ratio ' ef'	0.4	0.4	0.4	0.5	0.6	0.6	0.4	0.5	0.5	0.5	0.6	0.3	0.5	0.6	0.5	0.5	0.2	0.3	0.5	0.4
difference in void ratio 'Δe'	0.1	0.1	0.0	0.0	0.0	0.1	0.1	0.0	0.0	0.0	0.1	0.1	0.0	0.0	0.1	0.1	0.0	0.0	0.0	0.0
Void ratio liquid limit 'e_L' (LL*Gs)	0.9	0.9	0.9	0.9	0.9	0.7	0.7	0.7	0.7	0.7	1.1	1.1	1.1	1.1	1.1	0.7	0.7	0.7	0.7	0.7
Dry density at liquid limit (ρ_w*Gs)/(1+el) (g/cm^3)	1.5	1.5	1.5	1.5	1.5	1.6	1.6	1.6	1.6	1.6	1.4	1.4	1.4	1.4	1.4	1.7	1.7	1.7	1.7	1.7
Maximum MC 'Wmax' (e0/Gs*100) (%)	25.2	20.4	20.8	23.2	24.4	26.9	21.7	21.8	21.8	23.2	26.1	23.9	22.8	25.4	26.0	21.3	17.7	17.8	18.1	20.1

Table 5.6: Gives the solutions of the past research formula of collapsibility

Researcher	Collapsibility indices	A					B					C					D				
		1	2	3	4	5	1	2	3	4	5	1	2	3	4	5	1	2	3	4	5
Batygin (1937) - Equ2.1	>1	0.8	0.7	0.7	0.8	0.8	1.0	0.8	0.8	0.8	0.9	0.7	0.6	0.6	0.7	0.7	0.9	0.8	0.8	0.8	0.9
Priklonskij (1952) - Equ2.4	< 0.5	2.9	2.5	2.3	1.7	1.5	5.4	4.8	3.7	2.9	2.3	2.2	1.9	1.7	1.4	1.3	2.4	2.2	1.9	1.5	1.1
Tokar (1937) - Equ2.2	< 1	**0.9**	**0.9**	**0.9**	**0.9**	**0.9**	**0.9**	**0.8**	**0.9**	**0.9**	**0.9**	**0.9**	**0.8**	**0.9**	**0.9**	**0.9**	**0.9**	**0.9**	**0.9**	**0.9**	**0.9**
Feda (1966) - Equ2.7	> 0.85	0.2	0.2	0.2	0.2	0.2	0.2	0.1	0.1	0.1	0.2	0.2	0.2	0.2	0.2	0.2	0.2	0.1	0.2	0.2	0.2
Abelev (1948) - Equ2.14	> 2%	**10.24**	**12.22**	1.97	**2.39**	**2.31**	**14.10**	**21.99**	**2.37**	0.90	**2.43**	**9.24**	**25.07**	**2.89**	**2.93**	**4.27**	1.48	**4.23**	**5.84**	1.86	**2.20**
Jenning & Knight (1975) - Table 2.5	> 6%	**10.2**	**12.2**	2.0	2.4	2.3	**14.1**	**22.0**	2.4	0.9	2.4	**9.2**	**25.1**	2.9	2.9	4.3	1.5	4.2	5.8	1.9	2.2
Hormdee et al. (2004) - Table 2.6	> 10%	**10.2**	**12.2**	2.0	2.4	2.3	**14.1**	**22.0**	2.4	0.9	2.4	**9.2**	**25.1**	2.9	2.9	4.3	1.5	4.2	5.8	1.9	2.2
Denisov (1951) - Equ2.19	< 1	1.3	1.6	1.5	1.4	1.3	1.0	1.3	1.3	1.3	1.2	1.5	1.6	1.7	1.5	1.5	1.2	1.4	1.4	1.4	1.2
Soviet building code (1948) - Equ2.3	> 0.02	**0.1**	**0.1**	**0.1**	**0.1**	**0.1**	**0.2**	**0.2**	**0.1**	**0.1**	**0.1**	**0.2**	**0.2**	**0.1**	**0.1**	**0.2**	**0.1**	**0.1**	**0.1**	**0.1**	**0.1**
Soviet building code (1967) - Equ2.20	> -0.1	**-0.1**	-0.2	-0.2	-0.1	-0.1	**0.0**	**-0.1**	**-0.1**	**-0.1**	**0.0**	-0.2	-0.2	-0.2	-0.2	-0.2	**0.0**	-0.1	-0.1	-0.1	**-0.1**
Clenvenger (1958) - Dry density	< 1.28 Mg/m^3	1.7	1.8	1.8	1.7	1.7	1.6	1.8	1.8	1.8	1.7	1.7	1.7	1.8	1.7	1.7	1.8	1.9	1.9	1.9	1.8
Handy (1973) - clay content	< 24%	25.8	25.8	25.8	25.8	25.8	36.4	36.4	36.4	36.4	36.4	35.8	35.8	35.8	35.8	35.8	**9.5**	**9.5**	**9.5**	**9.5**	**9.5**
Zur Wiseman (1973) - Equ2.22	< 1.1	1.1	1.2	1.2	1.2	1.1	1.0	1.1	1.1	1.1	**1.1**	1.2	1.3	1.3	1.2	1.2	**1.1**	1.1	1.1	1.1	1.1

Grabowska-Olszewska (1988) - Table 2.4	< 6%	11.1	13.7	14.9	18.9	20.0	9.3	11.2	14.4	16.8	18.8	13.4	16.5	18.3	21.2	22.4	8.6	9.9	11.3	14.0	16.2
Larionov et al (1959) - Critical pressure	< 0.15MPa	**100.0**	**100.0**	-	-	-	**50.0**	**25.0**	-	-	-	**100.0**	**25.0**	-	-	-	-	-	-	-	-
Gibbs and Bara (1962) & Handy (1973) - Equ2.26	<= 1	1.2	1.5	1.4	1.3	1.2	**1.0**	1.2	1.2	1.2	1.1	1.4	1.5	1.6	1.5	1.4	1.1	1.3	1.3	1.3	1.2
Basma and Tuncer (1992) -	Equ2.27	**53.9**	**52.2**	**58.7**	**57.1**	**56.7**	**49.1**	**43.2**	**52.1**	**52.1**	**50.2**	**49.6**	**43.4**	**52.8**	**51.7**	**49.3**	**65.4**	**61.3**	**58.7**	**62.5**	**61.8**
	Equ2.28	**18.8**	**17.2**	**23.8**	**22.3**	**21.9**	**-160.4**	**-166.2**	**-157.1**	**-157.0**	**-158.9**	**-191.2**	**-197.4**	**-187.8**	**-188.8**	**-191.2**	**428.0**	**423.9**	**421.4**	**425.3**	**424.6**

5.3 COLLAPSE PREDICTIVE MODEL

Analysed laboratory results were used to generate a model that can be used in the identification of soil collapsibility. Model generation was done using SPSS (Statistical Package for the Social Sciences) software. The formulation was done in groups of different testing methods listed below. Common to all the formulas is the 'difference between the initial degree of saturation and inundated (final) degree of saturation' (Diff.Sr) and initial moisture content (MCi). The groups of testing for model formulation include:

- Proctor compaction test – Optimum moisture content (OMC), Maximum dry density (MDD) and Relative moisture content (RMC) shown in Equ5.1.

RMD $$\frac{MCi}{OMC} * 100\% \qquad \textit{Equ5.1}$$

- Atterberg test – Liquid limit (LL), Plastic limit (PL) and Plasticity index (PI)
- Sieve test – Percentage fines (%fines) and Coefficient of uniformity (Cu)
- Triaxial test – Maximum derivative stress (Ds_{70}, Ds_{140}, Ds_{280}), Internal friction angle (φ) and Cohesion (C).
- Compactive variables – initial moisture content (MCi), Initial dry density (Ddi), Initial degree of saturation (Sri) and 'difference in saturation between the as-compacted and the inundated' (Diff.Sr).

20 values from 20 soil samples of analysed laboratory tests were inputted in SPSS with their variables. These values and variables are shown in Table 5.7 and

Table 5.8. For the best of formula generating, a model summary is presented.

Table 5.7: SPSS sample for formulation 1 – Sieve, Atterberg and compaction test variables

Samples	Percentage of Fines (< 63 um)	Coeff. of uniformity Cu	Coeff. of curvature Cc	Liquid limit LL (%)	Plastic limit PL (%)	Plasticity index PI (%)	Max Dry density MDD (g/cm³)	Optimum Moisture content OMC (%)	Initial MC (%)	Relative moisture content (%)
A1	78.10	72.58	0.87	30.10	23.50	6.60	1.86	15.60	11.14	71.39
A2	78.10	72.58	0.87	30.10	23.50	6.60	1.86	15.60	13.72	87.96
A3	78.10	72.58	0.87	30.10	23.50	6.60	1.86	15.60	14.92	95.65
A4	78.10	72.58	0.87	30.10	23.50	6.60	1.86	15.60	18.86	120.92
A5	78.10	72.58	0.87	30.10	23.50	6.60	1.86	15.60	19.96	127.96
B1	92.52	15.65	1.15	25.70	22.66	3.04	1.84	14.60	9.33	63.90
B2	92.52	15.65	1.15	25.70	22.66	3.04	1.84	14.60	11.18	76.60
B3	92.52	15.65	1.15	25.70	22.66	3.04	1.84	14.60	14.36	98.36
B4	92.52	15.65	1.15	25.70	22.66	3.04	1.84	14.60	16.82	115.21
B5	92.52	15.65	1.15	25.70	22.66	3.04	1.84	14.60	18.77	128.56
C1	97.06	39.22	0.88	36.80	26.01	10.79	1.77	17.75	13.39	75.44
C2	97.06	39.22	0.88	36.80	26.01	10.79	1.77	17.75	16.54	93.18
C3	97.06	39.22	0.88	36.80	26.01	10.79	1.77	17.75	18.27	102.93
C4	97.06	39.22	0.88	36.80	26.01	10.79	1.77	17.75	21.21	119.51
C5	97.06	39.22	0.88	36.80	26.01	10.79	1.77	17.75	22.43	126.37
D1	38.62	109.68	0.74	23.40	17.13	6.27	1.96	11.20	8.63	77.05
D2	38.62	109.68	0.74	23.40	17.13	6.27	1.96	11.20	9.91	88.45
D3	38.62	109.68	0.74	23.40	17.13	6.27	1.96	11.20	11.27	100.63
D4	38.62	109.68	0.74	23.40	17.13	6.27	1.96	11.20	14.02	125.18
D5	38.62	109.68	0.74	23.40	17.13	6.27	1.96	11.20	16.19	144.55

Table 5.8: SPSS sample for formulation 2 – Compactive and Triaxial Variables

Samples	Dry Density (g/cm3)	Void ratio 'e0'	Degree of saturation 'Sr' (%)	Max shear stress 70 kPa	Max shear stress 140 kPa	Max shear stress 280 kPa	Initial angle of friction (o)	Cohesion (kN/m2)	Total collapse (%)	Critical Load (kPa)	Difference in Sr
A1	1.68	0.73	44.20	580.00	900.00	1650.00	43.15	50.00	**10.24**	100.00	0.43
A2	1.82	0.59	67.38	625.00	676.00	1100.00	33.00	115.00	**12.22**	100.00	0.00
A3	1.81	0.60	71.64	440.00	510.00	610.00	16.64	138.00	1.97		0.19
A4	1.73	0.67	81.68	190.00	288.00	402.00	16.56	63.00	2.39		0.03
A5	1.70	0.71	81.71	136.00	159.00	178.00	5.71	52.00	2.31		0.00
B1	1.63	0.78	34.74	670.00	880.00	1560.00	41.99	85.00	**14.10**	50.00	0.62
B2	1.78	0.63	51.57	880.00	1165.00	1800.00	42.77	120.00	**21.99**	25.00	0.38
B3	1.78	0.63	65.96	620.00	1005.00	1145.00	39.52	135.00	2.37		0.31
B4	1.78	0.63	77.27	695.00	860.00	1124.00	30.84	150.00	0.90		0.00
B5	1.73	0.67	80.93	341.00	354.00	413.00	11.31	120.00	2.43		0.00
C1	1.65	0.76	51.30	720.00	990.00	1620.00	41.28	83.00	**9.24**	100.00	0.39
C2	1.71	0.69	69.30	640.00	920.00	1040.00	29.17	170.00	**25.07**	25.00	0.05
C3	1.75	0.66	80.27	408.00	460.00	580.00	16.65	137.00	2.89		0.00
C4	1.67	0.74	83.61	318.00	355.00	460.00	14.04	108.00	2.93		0.07
C5	1.65	0.76	86.19	148.00	177.00	194.00	5.19	60.00	4.27		0.04
D1	1.79	0.62	40.58	640.00	1040.00	1450.00	38.66	105.00	1.48		0.35
D2	1.92	0.51	55.88	720.00	925.00	1400.00	38.66	110.00	4.23		0.11
D3	1.91	0.52	63.18	598.50	920.00	1280.00	36.87	100.00	5.84		0.12
D4	1.90	0.53	78.28	240.00	247.00	263.00	1.91	82.00	1.86		0.04
D5	1.83	0.58	80.64	149.00	157.00	162.00	1.82	74.00	2.20		0.05

5.3.1 Formulas generated using data from the laboratory tests.

5.3.1.1 Compaction model:

Equ5.2 gives a collapse model generated from the initial properties of the soil and proctor compaction parameters and the model summary is shown in Table 5.9.

$$CP = 3.395OMC - 4.01MCi + 0.503RMC - 75.189Ddi - 0.388Sri - 24.513Diff.Sr + 135.011 \quad \textit{Equ5.2}$$

The soil is termed collapsible when CP > 10.

The indexes represent:

CP – Collapse potential

Ddi – initial dry density in g/cm^3

MCi – initial moisture content in %

Sri – initial degree of saturation in %

Diff.Sr – Difference in saturation

MDD - Maximum dry density in g/cm^3

OMC - Optimum moisture content in %

RMC - Relative moisture content in %

Table 5.9: Compaction model from Lab data – Model summary

Model Summary[b]

Model	R	R Square	Adjusted R Square	Std. Error of the Estimate	Change Statistics				
					R Square Change	F Change	df1	df2	Sig. F Change
1	.721[a]	.520	.298	5.82347	.520	2.345	6	13	.093

a. Predictors: (Constant), Optimum Moisture Content (%), Difference between As-compacted Sr and Inundated Sr, Relative Moisture Content (%), Maximum Dry density (g/cm3), Initial degree of saturation (%), Initial Moisture Content (%)

b. Dependent Variable: Collapse Potential (%)

The model has R^2 of 52% and a statistical significant value of 0.093 is a good simulation for a less than 30 sampled model.

5.3.1.2 Sieve model:

Equ5.3 gives a collapse index created from basic properties of the soil and sieve analysis. The model summary is given in Table 5.10.

$$CP = 0.351\%fines + 0.081Cu - 1.625MCi - 11.689Diff.Sr + 1.153 \quad \textit{Equ5.3}$$

The soil is metastable when CP > 10

Where CP – collapse potential

%fines – percentage fine in %

Cu – coeffiecient of uniformity

MCi – initial moisture content in %

Diff.Sr – Difference in degree of saturation

Table 5.10: Sieve model from Lab data – Model summary

Model Summary[b]

Model	R	R Square	Adjusted R Square	Std. Error of the Estimate	Change Statistics				
					R Square Change	F Change	df1	df2	Sig. F Change
1	.657[a]	.432	.280	5.89788	.432	2.847	4	15	.061

a. Predictors: (Constant), Coeff of Uniformity, Difference between As-compacted Sr and Inundated Sr, Initial Moisture Content (%), Percentage fines (%)

b. Dependent Variable: Collapse Potential (%)

For this model, R^2 is 43.2% and statistical significant is 0.061.

5.3.1.3 Soil classification test model (Sieve, Atterberg and protor Compaction):

Equ5.4 gives the soil classification model which consists of parameters from sieve analysis, Atterberg and proctor compaction. The model summary is displayed in Table 5.11.

$$CP = 0.71\%fines + 0.131Cu + 1.18PI - 0.425Sri - 26.739Diff.Sr + 0.529RMC - 4.102MCi - 22.793 \quad \textit{Equ5.4}$$

CP is the collapse potential index. For soils with a CP > 10 they are metastable.

Where %fines – percentage fines in %

Cu – Coefficient of uniformity

PI – plasticity in %

Sri – initial degree of saturation in %

Diff.Sr – Difference in degree of saturation

RMC – Relative Moisture content in %

MCi – Initial moisture content in %

Table 5.11: Soil Classification model from Lab data – Model summary

Model Summary[b]

Model	R	R Square	Adjusted R Square	Std. Error of the Estimate	Change Statistics				
					R Square Change	F Change	df1	df2	Sig. F Change
1	.725[a]	.526	.249	6.02380	.526	1.900	7	12	.157

a. Predictors: (Constant), Coeff of Uniformity, Initial degree of saturation (%), Plasticity Index (%), Difference between As-compacted Sr and Inundated Sr, Relative Moisture Content (%), Initial Moisture Content (%), Percentage fines (%)

b. Dependent Variable: Collapse Potential (%)

For this model, R^2 is 52.6% and statistical significant is 0.157.

5.3.1.4 Atterberg model:

Equ5.5 gives the Atterberg model which consist initial properties of the soil and the plasticity index and plastic limit. The model summary is displayed in Table 5.12.

$$CP = 0.055PI + 1.692PL - 1.625MCi - 9.877Diff.Sr - 5.573 \quad \textit{Equ5.5}$$

Collapsibility is when CP is greater than 10.

Where PI – Plasticity index in %

PL – Plastic limit in %

MCi – Initial moisture content in %

Diff.Sr – Difference between degree of saturation

Table 5.12: Atterberg model from Lab data – Model summary

Model Summary[b]

Model	R	R Square	Adjusted R Square	Std. Error of the Estimate	Change Statistics				
					R Square Change	F Change	df1	df2	Sig. F Change
1	.660[a]	.435	.284	5.88027	.435	2.887	4	15	.059

a. Predictors: (Constant), Plasticity Index (%), Difference between As-compacted Sr and Inundated Sr, Plastic Limit (%), Initial Moisture Content (%)

b. Dependent Variable: Collapse Potential (%)

For this model, R^2 is 43.5% and statistical significant is 0.059.

5.3.1.5 Triaxial and Atterberg

The generated model for collapsibility is given by Equ5.6. It consist of triaxial and Atterberg parameters. The model summary is shown in Table 5.13.

$$CP = 0.031Ds_{70} - 0.361\varphi - 0.045C + 0.138LL + 1.33PL - 1.191MCi - 5.106Diff.Sr - 9.55 \quad \textit{Equ5.6}$$

When CP is greater than 10, this soil is termed collapsible.

Where Ds_{70} – maximum derivative stress at 70 kPa of confining pressure

φ – Internal friction angle in degrees

C – Cohesion in kN/m^2

LL –Liquid limit in %

PL – Plastic limit in %

MCi – Initial moisture content in %

Diff.Sr – Difference between degrees of saturation

Table 5.13: Soil triaxial and Atterberg model from Lab data – Model summary

Model Summary[b]

Model	R	R Square	Adjusted R Square	Std. Error of the Estimate	Change Statistics				
					R Square Change	F Change	df1	df2	Sig. F Change
1	.704[a]	.496	.201	6.21184	.496	1.684	7	12	.204

a. Predictors: (Constant), Cohesion (kN/m2), Liquid Limit (%), Difference between As-compacted Sr and Inundated Sr, Internal friction angle (degrees), Plastic Limit (%), Initial Moisture Content (%), Max deviator stress at 70kPa

b. Dependent Variable: Collapse Potential (%)

For this model, R^2 is 49.6% and statistical significant is 0.204.

5.3.1.6 Triaxial and Sieve:

Equ5.7 gives the collapsibility model consisting of triaxial and sieve parameters. The model summary is shown in Table 5.14.

$$CP = 0.361\%fines + 0.116Cu + 0.032Ds_{70} - 0.376\varphi - 0.046C - 1.142MCi - 5.287Diff.Sr - 11.132 \quad \textit{Equ5.7}$$

Collapsibility is when CP > 10

Where CP – collapse potential

%fines – percentage fine in %

Cu – coefficient of uniformity

Ds_{70} – maximum derivative stress at 70 kPa of confining pressure

φ – Internal friction angle in degrees

C – Cohesion in kN/m^2

MCi – Initial moisture content in %

Diff.Sr – Difference between degrees of saturation

Table 5.14: Soil triaxial and sieve model from Lab data – Model summary

Model Summary[b]

Model	R	R Square	Adjusted R Square	Std. Error of the Estimate	Change Statistics				
					R Square Change	F Change	df1	df2	Sig. F Change
1	.697[a]	.485	.185	6.27442	.485	1.617	7	12	.222

a. Predictors: (Constant), Coeff of Uniformity, Internal friction angle (degrees), Cohesion (kN/m2), Difference between As-compacted Sr and Inundated Sr, Percentage fines (%), Initial Moisture Content (%), Max deviator stress at 70kPa

b. Dependent Variable: Collapse Potential (%)

For this model, R^2 is 48.5% and statistical significant is 0.222.

5.3.1.7 Compactive variables:

Equ5.8 gives the compactive variables model which consists of parameters like degree of saturation, initial moisture, and dry density. The model summary is displayed in Table 5.15.

$$CP = 0.192\%fines - 21.53Ddi - 1.603MCi - 0.107Sr - 23.881Diff.Sr + 64.835 \quad \textit{Equ5.8}$$

Cp is collapsibility when it's greater than 10.

Where CP – collapse potential

%fines – percentage fine in %

Ddi – initial dry density in g/cm^3

MCi – initial moisture content in %

Sri – initial degree of saturation in %

Diff.Sr – Difference in saturation

Table 5.15: Compactive variable model from Lab data – Model summary

Model Summary[b]

Model	R	R Square	Adjusted R Square	Std. Error of the Estimate	Change Statistics				
					R Square Change	F Change	df1	df2	Sig. F Change
1	.659[a]	.434	.233	6.08925	.434	2.151	5	14	.119

a. Predictors: (Constant), Percentage fines (%), Difference between As-compacted Sr and Inundated Sr, Initial Dry density (g/cm3), Initial degree of saturation (%), Initial Moisture Content (%)

b. Dependent Variable: Collapse Potential (%)

For this model, R^2 is 43.4% and statistical significant is 0.119.

5.3.2 Formula generation - A combination of laboratory data and past researcher's data – Sieve parameter based

In SPSS, more samples would increase the accuracy of the model. 20 samples would give a good model, but above 30 samples would give a better model; and so, in this thesis, a further simulation is done with collected data from past research work done. The data collection and model simulation using past research works are undertake in two group- Sieve based and Compaction based.

For the sieve parameter base, data are collected from:

Laboratory results as shown previously in Table 5.7 and

Table 5.8;

Basma and Tuncer (1992) shown in Table 5.16 and Table 5.17;

Tadepalli and Fredlund (1991) shown in Table 5.18; and

Rezaei, Ajalloeian, Ghafoori (2012) shown in Table 5.19.

In all 38 samples are used in generating the model.

Table 5.16: Basma and Tuncer (1992) SPSS sample for formulation – Sieve and Atterberg

Samples: Basma and Tuncer 1992 :	Percentage of Fines (< 63 um)	Speific gravity (Gs)	Clay content (< 2um)	Coeff. of uniformity Cu	Coeff. of curvature Cc	Liquid limit LL (%)	Plastic limit PL (%)	Plasticity index PI (%)
(S1)	59.40	2.74	8.90	17.50	7.20	36.60	23.90	12.70
(S2)	52.20	2.72	5.00	25.00	1.10	29.10	17.90	11.20
(S3)	86.70	2.69	13.20	60.00	15.00	57.20	28.30	28.90
(S4)	80.40	2.77	10.00	11.50	2.90	28.00	21.00	7.00
(S5)	75.60	2.66	26.00	35.00	0.50	36.00	24.90	11.10
(S6)	57.90	2.69	15.00	100.00	0.90	28.20	17.60	10.60
(S7)	16.00	2.63	9.00	6.40	1.60	30.00	27.00	3.00
(S8)	7.80	2.65	2.00	3.40	1.10	25.00	20.00	5.00

Table 5.17: Basma and Tuncer (1992) SPSS sample for formulation 2 – Compactive Variables

Samples: Basma and Tuncer 1992	Max Dry density MDD (g/cm³)	Optimum Moisture content OMC (%)	Initial MC (%)	Relative moisture content (%)	Dry Density (g/cm3)	Void ratio 'e0'	Degree of saturation 'Sr' (%)	Total collapse (%)	Difference in Sr
(S1)	18.70	14.50	6.00	41.38	1.50	0.83	19.89	**10.00**	0.79
(S2)	19.30	13.50	6.00	44.44	1.74	0.56	28.98	5.80	0.70
(S3)	17.00	19.30	6.00	31.09	1.36	0.98	16.50	**17.50**	0.82
(S4)	17.20	14.30	6.00	41.96	1.39	0.99	16.74	**16.00**	0.82
(S5)	16.30	21.00	6.00	28.57	1.31	1.03	15.49	**22.00**	0.83
(S6)	18.30	13.70	6.00	43.80	1.65	0.63	25.61	**15.50**	0.73
(S7)			6.00		1.71	0.54	29.33	3.00	0.69
(S8)			6.00		1.63	0.63	25.41	2.50	0.73

Table 5.18: Tadepalli and Fredlund (1991) SPSS sample for formulation

Samples Tadepalli and Fredlund (1991)	Percentage of Fines (< 63 um)	Specific gravity (Gs)	Coeff. of uniformity Cu	Coeff. of curvature Cc	Liquid limit LL (%)	Plastic limit PL (%)	Plasticity index PI (%)	Initial MC (%)	Dry Density (g/cm3)	Void ratio 'e0'	Degree of saturation 'Sr' (%)	Total collapse (%)	Critical Load (kPa)	Difference in Sr
S1M	38.00	2.68	26.40	2.04	22.20	16.60	5.60	11.80	1.60	0.68	0.68	5.84	97.00	0.32
S2M	38.00	2.68	26.40	2.04	22.20	16.60	5.60	11.79	1.51	0.78	0.78	**11.64**	96.00	0.22
S3M	38.00	2.68	26.40	2.04	22.20	16.60	5.60	11.80	1.41	0.91	0.91	**15.26**	99.00	0.09
S4M	38.00	2.68	26.40	2.04	22.20	16.60	5.60	12.75	1.39	0.92	0.92	**18.62**	55.00	0.08

Table 5.19: Rezaei, Ajalloeian, Ghafoori (2012) SPSS sample for formulation

Samples Rezaei, Ajalloeian, Ghafoori (2012)	Percentage of Fines (< 63 um)	Specific gravity (Gs)	Clay content (< 2um)	Coeff. of uniformity Cu	Coeff. of curvature Cc	Liquid limit LL (%)	Plastic limit PL (%)	Plasticity index PI (%)	Initial MC (%)	Dry Density (g/cm3)	Void ratio 'e0'	Degree of saturation 'Sr' (%)	Total collapse (%)	Difference in Sr
(1) 5+700	78.00	2.68	24.00	130.00	3.89	26.16	13.73	12.43	21.12	1.61	0.66	85.17	0.50	0.13
(2) 7+000	85.00	2.68	31.00	40.00	0.40	27.89	16.89	11.00	14.19	1.21	1.21	31.30	**12.82**	0.67
(3) 8+400	56.00	2.68	31.00	1600.0	0.08	22.39	11.79	10.60	9.15	1.61	0.66	36.90	**14.96**	0.62
(4) 9+800	56.00	2.68	32.00	533.33	0.02	23.58	12.23	11.35	9.39	1.63	0.64	39.07	5.66	0.59
(5) 11+200	35.00	2.68	21.00	6000.	1.35	24.35	12.89	11.46	7.17	1.73	0.55	34.99	6.74	0.64
(6) 12+600	52.00	2.68	19.00	320.0	1.01				14.37	1.67	0.60	63.68	1.93	0.35

5.3.2.1 Sieve Model:

The generated model for collapsibility is given by Equ5.9. It consists of sieve parameters. The model summary is shown in Table 5.20.

$$CP = 0.198\%fines + 0.000457Cu - 0.783MCi - 0.183Sri - 10.637Diff.Sr + 17.558 \quad \textit{Equ5.9}$$

Collapsibility is when CP > 10

Each parameter has been previously mentioned and described.

Table 5.20: Sieve model from Lab data, and three other researchers for sieve based model – Model summary

Model Summary[b]

Model	R	R Square	Adjusted R Square	Std. Error of the Estimate	Change Statistics				
					R Square Change	F Change	df1	df2	Sig. F Change
1	.766[a]	.586	.522	4.79811	.586	9.077	5	32	.000

a. Predictors: (Constant), Coeff of Uniformity, Initial degree of saturation (%), Percentage fines (%), Difference between As-compacted Sr and Inundated Sr, Initial Moisture Content (%)

b. Dependent Variable: Collapse Potential (%)

Unlike the formulas generated from only the experimental data, these simulations would have a lower statistical significant value (Sig. F). In SPSS, the lower the sig value the more acceptable the generated statistics.

Statistics of the experimental data only, gives an acceptable index, which can be seen in the R^2 values. The R^2 value in this regression is 58.6%

5.3.2.2 Sieve (without Cu) Model:

Equ5.10 gives a similar formula as Equ5.9, except for the Cu value. But with Cu having very little effect on the formula, discarding it for this formula would have

negligible change to the new collapse index. The model summary is displayed in Table 5.21.

$$CP = 0.193\%fines - 0.781MCi - 0.179Sri - 10.142Diff.Sr + 17.498 \quad \textit{Equ5.10}$$

A soil is susceptible to collapse when CP > 10

Each parameter has been previously mentioned and described.

Table 5.21: Sieve model 2 from Lab data, and three other researchers for sieve based model – Model summary

Model Summary[b]

Model	R	R Square	Adjusted R Square	Std. Error of the Estimate	Change Statistics				
					R Square Change	F Change	df1	df2	Sig. F Change
1	.763[a]	.583	.532	4.74659	.583	11.519	4	33	.000

a. Predictors: (Constant), Percentage fines (%), Difference between As-compacted Sr and Inundated Sr, Initial degree of saturation (%), Initial Moisture Content (%)

b. Dependent Variable: Collapse Potential (%)

Sig < 0.005, and R2 = 58.3%

5.3.2.3 Atterberg Model:

Equ5.11 gives the generated collapsibility index from Atterberg tests. The model summary is displayed in Table 5.22.

$$CP = 0.155LL - 0.250PL + 0.199\%fines - 0.863MCi - 0.176Sri - 11.977Diff.Sr + 19.224 \quad \textit{Equ5.11}$$

A soil is susceptible to collapse when CP > 10

Each parameter has been previously mentioned and described.

Table 5.22: Atterberg model from Lab data, and three other researchers for sieve based model – Model summary

Model Summary[b]

Model	R	R Square	Adjusted R Square	Std. Error of the Estimate	Change Statistics				
					R Square Change	F Change	df1	df2	Sig. F Change
1	.764[a]	.584	.500	4.91334	.584	7.008	6	30	.000

a. Predictors: (Constant), Plastic Limit (%), Difference between As-compacted Sr and Inundated Sr, Percentage fines (%), Initial degree of saturation (%), Liquid Limit (%), Initial Moisture Content (%)

b. Dependent Variable: Collapse Potential (%)

Sig < 0.005 and R^2 = 58.4%

5.3.2.4 Compactive variables Model:

Equ5.12 gives the generated collapsibility index from compactive variables. The model summary is displayed in Table 5.23.

Compactive variables

$$CP = 0.17\%fines - 1.623MCi - 0.034Sri - 19.411Diff.Sr - 21.575Ddi + 61.366 \quad \textit{Equ5.12}$$

A soil is susceptible to collapse when CP > 10

Each parameter has been previously mentioned and described.

Table 5.23: Compactive variables model from lab data and three other researchers for Sieve based model – Model summary

Model Summary[b]

Model	R	R Square	Adjusted R Square	Std. Error of the Estimate	Change Statistics				
					R Square Change	F Change	df1	df2	Sig. F Change
1	.793[a]	.629	.571	4.54230	.629	10.869	5	32	.000

a. Predictors: (Constant), Percentage fines (%), Initial Dry density (g/cm3), Difference between As-compacted Sr and Inundated Sr, Initial degree of saturation (%), Initial Moisture Content (%)

b. Dependent Variable: Collapse Potential (%)

Sig < 0.005 and R^2 = 62.9%

5.3.3 Formula generation - A combination of Lab data and past researcher's data – Compaction parameter based

The data used for the compaction based model, include:

Experimental data displayed in Table 5.7 and

Table 5.8;

Basma and Tuncer (1992) data shown in Table 5.16, and Table 5.17; and

Benchouk et al (2013) data shown in Table 5.24

These data are used for simulating the collapse index of soils.

Table 5.24: Benchouk et al (2013) SPSS sample for formulation

Samples Benchouk et al (2013)	Percentage of Fines (< 63 um)	Specific gravity (Gs)	Clay content (< 2um)	Liquid limit LL (%)	Plastic limit PL (%)	Plasticity index PI (%)	Max Dry density MDD (g/cm³)	Optimum Moisture content OMC (%)	Initial MC (%)	Relative moisture content (%)	Dry Density (g/cm3)	Void ratio 'e0'	Degree of saturation 'Sr' (%)	Total collapse (%)	Difference in Sr
Test 1	54.00	2.61	30.00	50.00	22.00	28.00	1.66	20.00	20.00	100.00	1.66	0.57	91.21	0.83	0.07
Test 2	54.00	2.61	30.00	50.00	22.00	28.00	1.66	20.00	20.00	100.00	1.40	0.86	60.40	1.56	0.38
Test 3	54.00	2.61	30.00	50.00	22.00	28.00	1.66	20.00	20.00	100.00	1.20	1.18	44.43	**6.91**	0.54
Test 4	54.00	2.61	30.00	50.00	22.00	28.00	1.66	20.00	18.00	90.00	1.66	0.57	82.09	1.08	0.16
Test 5	54.00	2.61	30.00	50.00	22.00	28.00	1.66	20.00	18.00	90.00	1.40	0.86	54.36	4.83	0.44
Test 6	54.00	2.61	30.00	50.00	22.00	28.00	1.66	20.00	18.00	90.00	1.20	1.18	39.98	**9.90**	0.59
Test 7	54.00	2.61	30.00	50.00	22.00	28.00	1.66	20.00	15.00	75.00	1.66	0.57	68.41	4.96	0.30
Test 8	54.00	2.61	30.00	50.00	22.00	28.00	1.66	20.00	15.00	75.00	1.40	0.86	45.30	**12.57**	0.53
Test 9	54.00	2.61	30.00	50.00	22.00	28.00	1.66	20.00	15.00	75.00	1.20	1.18	33.32	**17.69**	0.65
Test 10	54.00	2.61	30.00	50.00	22.00	28.00	1.66	20.00	10.00	50.00	1.66	0.57	45.61	**6.37**	0.53
Test 11	54.00	2.61	30.00	50.00	22.00	28.00	1.66	20.00	10.00	50.00	1.40	0.86	30.20	**13.05**	0.68
Test 12	54.00	2.61	30.00	50.00	22.00	28.00	1.66	20.00	10.00	50.00	1.20	1.18	22.21	**18.39**	0.76

5.3.3.1 Compaction and Atterberg Model

Equ5.13 gives the generated collapsibility index from compaction and Atterberg test. The model summary is displayed in Table 5.25.

$$CP = 0.036PI - 0.936PL + 0.211\%fines - 1.194MCi - 0.476Sri - 25.402Diff.Sr + 0.008MDD + 2.007OMC + 0.168RMC + 18.282 \quad \textit{Equ5.13}$$

A soil is susceptible to collapse when CP > 10

Each parameter has been previously mentioned and described.

Table 5.25: Compaction and Atterberg model from Lab data, and two other researchers for compaction based model – Model summary

Model Summary[b]

Model	R	R Square	Adjusted R Square	Std. Error of the Estimate	Change Statistics				
					R Square Change	F Change	df1	df2	Sig. F Change
1	.810[a]	.656	.545	4.68901	.656	5.923	9	28	.000

a. Predictors: (Constant), Initial degree of saturation (%), Plastic Limit (%), Plasticity Index (%), Maximum Dry density (g/cm3), Initial Moisture Content (%), Percentage fines (%), Optimum Moisture Content (%), Difference between As-compacted Sr and Inundated Sr, Relative Moisture content (%)
b. Dependent Variable: Collapse Potential (%)

Sig < 0.005, and R^2 = 65.6% this is the highest R^2 obtained in this simulation.

5.3.3.2 Compaction and Atterber (without MDD)Model

Equ5.14 gives the generated collapsibility index from compaction and Atterberg test without the MDD. Since the index for MDD was so low, it would be negligible in this formula. The model summary is displayed in Table 5.26.

$$CP = 0.035LL - 0.963PL + 0.210\%fines - 1.192MCi - 0.474Sri - 25.203Diff.Sr + 1.995OMC + 0.166RMC + 18.281 \quad \textit{Equ5.14}$$

A soil is susceptible to collapse when CP > 10

Each parameter is previously mentioned and described.

Table 5.26: Compaction and Atterberg model from Lab data, and two other researchers for compaction based model – Model summary

Model Summary[b]

Model	R	R Square	Adjusted R Square	Std. Error of the Estimate	Change Statistics				
					R Square Change	F Change	df1	df2	Sig. F Change
1	.810[a]	.656	.561	4.60757	.656	6.901	8	29	.000

a. Predictors: (Constant), Initial degree of saturation (%), Plastic Limit (%), Liquid Limit (%), Initial Moisture Content (%), Percentage fines (%), Optimum Moisture Content (%), Difference between As-compacted Sr and Inundated Sr, Relative Moisture content (%)

b. Dependent Variable: Collapse Potential(%)

The Sig and R^2 are the same was the previous model, with Sig < 0.005 and R^2 = 65.6%

5.3.3.3 Atterberg Model:

Equ5.15 gives the generated collapsibility index from Atterberg. The model summary is displayed in Table 5.27.

$$CP = 0.216LL - 0.271PL + 0.159\%fines - 0.127MCi - 0.428Sri - 20.748Diff.Sr + 28.250 \quad \textit{Equ5.15}$$

A soil is susceptible to collapse when CP > 10

Each parameter has been previously mentioned and described.

Table 5.27: Atterberg model from Lab data and two other researchers for compaction based model – Model summary

Model Summary[b]

Model	R	R Square	Adjusted R Square	Std. Error of the Estimate	Change Statistics				
					R Square Change	F Change	df1	df2	Sig. F Change
1	.785[a]	.616	.546	4.63792	.616	8.808	6	33	.000

a. Predictors: (Constant), Liquid Limit (%), Percentage fines (%), Initial degree of saturation (%), Plastic Limit (%), Initial Moisture Content (%), Difference between As-compacted Sr and Inundated Sr

b. Dependent Variable: Collapse Potential (%)

Sig < 0.005 and R^2 = 61.6%

5.3.3.4 Compactive variables Model:

Equ5.16 gives the generated collapsibility index from compactive variables. The model summary is displayed in Table 5.28.

$$CP = 0.129\%fines - 1.104MCi - 0.149Sri - 23.009Diff.Sr - 27.330Ddi + 75.083 \quad \textit{Equ5.16}$$

A soil is susceptible to collapse when CP > 10

Each parameter is previously mentioned and described.

Table 5.28: Compactive variables model from lab data and two other researchers for compaction based model – Model summary

Model Summary[b]

Model	R	R Square	Adjusted R Square	Std. Error of the Estimate	Change Statistics				
					R Square Change	F Change	df1	df2	Sig. F Change
1	.794[a]	.630	.576	4.48209	.630	11.584	5	34	.000

a. Predictors: (Constant), Difference between As-compacted Sr and Inundated Sr, Percentage fines (%), Initial Dry density (g/cm3), Initial Moisture Content (%), Initial degree of saturation (%)

b. Dependent Variable: Collapse Potential (%)

Sig < 0.005 and R^2 = 61.6%

5.3.4 Verification of collapse-predictive model with the experimental results and past studies data

5.3.4.1 Data for the verification

The collapse predictive model generated using results of this study previously shown in Table 5.7 and

Table 5.8 has been verified against results of past studies to check whether or not the sample is metastable. The data used in the verification includes the following:

Basma and Tuncer (1992) – shown previously in Table 5.16 and Table 5.17

Tadepalli and fredlund (1991) – displayed previously in Table 5.18

Rezaei et al (2012) – previously given in Table 5.19

Benchouk et al (2013) – previously displayed in Table 5.24

Pereira, et al. (2005) and Pereira and Fredlund (2000) – shown in Table 5.29

Gaaver (2012) – displayed in Table 5.30

Nuntasarn (2011) – shown in Table 5.31

Li et al. (2014) – shown in Table 5.32

Houston, et al. (1988) – given in Table 5.33

Assallay et al. (1996) cited in Nouaouria, et al. (2008) – shown in Table 5.34

Habibagahi and Taherian (2004) – displayed in Table 5.35

These data has been used to verify the collapse-predictive model and to check the whether or not sample s metastable.

Table 5.29: Pereira, et al. (2005) and Pereira and Fredlund (2000) SPSS sample for formula verification

Samples: Pereira, et al. (2005) and Pereira and Fredlund (2000)	Percentage of Fines (< 63 um)	specific gravity (Gs)	Clay content (< 2um)	Coeff. of uniformity Cu	Coeff. of curvature Cc	Liquid limit LL (%)	Plastic limit PL (%)	Plasticity index PI (%)	Max Dry density MDD (g/cm³)	Optimum Moisture content OMC (%)	Initial MC (%)	Relative moisture content (%)	Dry Density (g/cm3)	Void ratio 'e0'	Degree of saturation 'Sr' (%)	Difference in Sr
TPT1	48.00	2.64	13.00	366.67	1.94	29.00	17.00	12.00	1.88	14.50	10.50	72.41	1.51	0.75	36.50	0.62
TPT2	48.00	2.64	13.00	366.67	1.94	29.00	17.00	12.00	1.88	14.50	10.50	72.41	1.51	0.75	36.50	0.60
TPT3	48.00	2.64	13.00	366.67	1.94	29.00	17.00	12.00	1.88	14.50	10.50	72.41	1.51	0.75	36.50	0.61
TPT4	48.00	2.64	13.00	366.67	1.94	29.00	17.00	12.00	1.88	14.50	10.50	72.41	1.51	0.75	36.50	0.59

Table 5.30: Gaaver (2012) SPSS sample for formula verification

Samples	Percentage of Fines (< 63 um)	specific gravity (Gs)	Clay content (< 2um)	Coeff. of uniformity Cu	Coeff. of curvature Cc	Liquid limit LL (%)	Plastic limit PL (%)	Plasticity index PI (%)	Initial MC (%)	Dry Density (g/cm3)	Void ratio 'e0'	Degree of saturation 'Sr' (%)	Total collapse (%)	Difference in Sr
Gaaver (2012)	70.20	2.68	16.50	52.04	2.95	28.50	13.60	14.90	11.00	1.54	0.74	39.70	Naturally collapsible	0.59

Table 5.31: Nuntasarn (2011) SPSS sample for formula verification

Samples: Nuntasarn (2011)	Percentage of Fines (< 63 um)	specific gravity (Gs)	Clay content (< 2um)	Liquid limit LL (%)	Plastic limit PL (%)	Plasticity index PI (%)	Max Dry density MDD (g/cm³)	Optimum Moisture content OMC (%)	Initial MC (%)	Relative moisture content (%)	Dry Density (g/cm3)	Void ratio 'e0'	Degree of saturation 'Sr' (%)	Max shear stress 70 kPa	Max shear stress 140 kPa	Max shear stress 280 kPa	Initial angle of friction (o)	Cohension (kN/m2)	Difference in Sr
	44.0	2.65	13.0	20.3	14.5	5.80	2.00	8.25	14.0	169.7	1.70	0.47	78.94	50.00	80.00	85.00	11.00	14.00	0.20

Table 5.32: Li, et al.(2014) SPSS sample for formula verification

Samples:	Percentage of Fines (< 63 um)	specific gravity (Gs)	Clay content (< 2um)	Liquid limit LL (%)	Plastic limit PL (%)	Plasticity index PI (%)	Max Dry density MDD (g/cm³)	Optimum Moisture content OMC (%)	Initial MC (%)	Relative moisture content (%)	Dry Density (g/cm3)	Void ratio 'e0'	Degree of saturation 'Sr' (%)	Difference in Sr
Li, et al.(2014)	98.30	2.68	31.30	36.40	18.60	17.80	1.70	16.50	16.50	100.00	1.70	0.58	76.71	0.22

Table 5.33: Houston, et al. (1988) SPSS sample for formula verification

Samples: Houston, et al. (1988)	Percentage of Fines (< 63 um)	specific gravity (Gs)	Plasticity index PI (%)	Max Dry density MDD (g/cm³)	Optimum Moisture content OMC (%)	Initial MC (%)	Relative moisture content (%)	Dry Density (g/cm3)	Void ratio 'e0'	Degree of saturation 'Sr' (%)	Total collapse (%)	Difference in Sr
1A/8-14	65.00	2.68	1.00	1.88	11.00	2.80	25.45	1.59	0.65	11.40	**9.50**	0.87
1B/15-19	65.00	2.68	1.00	1.88	11.00	3.00	27.27	1.39	0.89	9.20	**7.70**	0.89
1C/20-25	67.00	2.72	3.00	1.87	11.00	2.90	26.36	1.45	0.82	9.60	**6.40**	0.89
1D/26-31	67.00	2.72	3.00	1.87	11.00	2.80	25.45	1.43	0.83	9.20	5.60	0.89

Table 5.34: Assallay et al. (1996) cited in Nouaouria, et al. (2008) SPSS sample for formula verification

Samples Assallay et al. (1996) cited in Nouaouria, et al. (2008)	Percentage of Fines (< 63 um)	Specific gravity (Gs)	Clay content (< 2um)	Coeff. of uniformity Cu	Coeff. of curvature Cc	Liquid limit LL (%)	Plastic limit PL (%)	Plasticity index PI (%)	Initial MC (%)	Dry Density (g/cm3)	Void ratio 'e0'	Degree of saturation 'Sr' (%)	Total collapse (%)	Difference in Sr
Gharyan Loess (Libya)	62.00	2.66	11.00			27.00	19.00	8.00	6.00	1.39	1.67	9.53		0.89
Khoms Loess (Libya)	82.00	2.68	13.00			31.00	20.00	11.00	3.00	1.43	0.88	9.14		0.89
Grey Loess (Algeria)	84.00	2.68	9.00	8.13	3.08	30.00	23.00	7.00	5.00	1.42	0.89	15.06	**collapsible**	0.83
Yellow Loess (Algeria)	98.00	2.73	12.00	8.13	3.08	33.00	22.00	11.00	6.00	1.43	0.91	18.00	**collapsible**	0.81

Table 5.35: Habibagahi and Taherian (2004) SPSS sample for formula verification

Samples Habibagahi and Taherian (2004)	Percentage of Fines (< 63 um)	specific gravity (Gs)	Clay content (< 2um)	Coeff. of uniformity Cu	Coeff. of curvature Cc	Liquid limit LL (%)	Plastic limit PL (%)	Plasticity index PI (%)	Initial MC (%)	Dry Density (g/cm3)	Void ratio 'e0'	Degree of saturation 'Sr' (%)	Total collapse (%)	Difference in Sr
A (S1)	87.00	2.68	12.00	16.70	1.40	22.60	17.60	5.00	4.90	1.36	0.96	13.61	**14.10**	0.85
A (S18)	87.00	2.68	12.00	16.70	1.40	22.60	17.60	5.00	9.40	1.49	0.80	31.59	4.50	0.67
A (S37	87.00	2.68	12.00	16.70	1.40	22.60	17.60	5.00	11.60	1.31	1.05	29.51	**14.10**	0.69
A (S51)	87.00	2.68	12.00	16.70	1.40	22.60	17.60	5.00	15.70	1.66	0.62	68.37	0.10	0.30
B (S65)	68.00	2.68	16.00	50.00	1.80	24.20	16.20	8.00	5.40	1.35	0.98	14.78	**10.40**	0.84
B (S86)	68.00	2.68	16.00	50.00	1.80	24.20	16.20	8.00	9.10	1.50	0.79	31.05	9.00	0.67
B (S102)	68.00	2.68	16.00	50.00	1.80	24.20	16.20	8.00	12.40	1.45	0.85	39.29	5.60	0.59
B (S116)	68.00	2.68	16.00	50.00	1.80	24.20	16.20	8.00	16.90	1.76	0.53	86.07	0.00	0.12
C (S132)	65.00	2.68	13.00	35.00	2.40	28.20	25.20	3.00	6.00	1.76	0.52	30.76	0.80	0.68
C (S151)	65.00	2.68	13.00	35.00	2.40	28.20	25.20	3.00	9.20	1.74	0.54	45.42	0.50	0.53
C (S165)	65.00	2.68	13.00	35.00	2.40	28.20	25.20	3.00	12.20	1.45	0.85	38.66	5.50	0.60
C (S177)	65.00	2.68	13.00	35.00	2.40	28.20	25.20	3.00	15.70	1.53	0.75	55.98	1.70	0.43

5.3.4.2 Verified collapse-predictive model

The verification of the collapse-predictive model for each of the data presented herein is done in the following tables:

For experimental data - Table 5.36 and Table 5.37

For Basma and Tuncer (1992) - Table 5.38

For Tadepalli and Fredlund (1991) - Table 5.39

For Pereira, et al (2005) and Pereira and Fredlund (2000) - Table 5.40

For Gaaver (2012) - Table 5.41

For Nuntasarn (2011) - Table 5.42

For Li, et al. (2014) - Table 5.43

For Houston, et al (1988) - Table 5.44

For Rezaei, et al. (2012) - Table 5.45

For Assallay et al. (1996) cited in Nouaouria, et al. (2008) - Table 5.46

For Habibagahi and Taherian (2004) - Table 5.47

For Benchouk et al (2013) - Table 5.48

In the collapse-prediction tables:

- The values in bold text and color red represent the samples found to be collapsible by the model and also by the data collection process (compaction based and sieve based). And in cases where the research data has not stated the metastability stand, the red bold text then represents the samples found to be collapsible by the model.
- The values in italics text and color blue represent the samples that the prediction model generation are contrasting with the original data obtained from the lab or research paper.
- The values from the data are agreeing, non-metastable predictions between the model and the original data.

Table 5.36: Experimental data using the experimental data model - Collapse- predictive model verification

Experimental result		**Compaction values**	**Atterberg limits**	**Sieve analysis**	**Triaxial and Atterberg**	**Sieve and Triaxial**	**Compactive variables**
Samples	Total Potential (%)	TC = 3.395OMC - 75.189MDD - 4.01MCi + 0.503RMC - 0.388Sri - 24.513Diff.Sr + 135.011	TC = 1.692PL + 0.055PI - 1.625MCi - 9.877Diff.Sr - 5.573	TC = 0.081Cu + 0.351%fines - 1.625MCi - 11.689Diff.Sr +1.153	TC = 0.138LL + 1.331PL - 1.191Mci - 5.106Diff.Sr + 0.031Ds_{70} - 0.367ϕ - 0.045C - 9.55	TC = 0.116Cu + 0.361%fines + 0.032Ds_{70} - 0.376ϕ - 0.046C - 1.142MCi - 5.287Diff.Sr - 11.132	TC = 0.192%fines - 0.107Sri - 23.881Diff.Sr - 1.603Mci - 21.530Ddi + 64.835
A1	**10.24**	**11.34**	**12.19**	**11.30**	**10.28**	**10.52**	**10.77**
A2	**12.22**	**10.98**	**12.29**	**12.19**	**11.62**	**12.13**	**11.45**
A3	1.97	3.62	8.42	7.97	8.43	8.91	4.71
A4	2.39	0.69	3.65	3.50	0.24	0.76	2.94
A5	2.31	0.43	2.11	2.01	1.87	2.50	2.49
B1	**14.10**	**12.33**	**11.67**	**12.51**	**11.40**	**11.90**	**14.07**
B2	**21.99**	**10.50**	**10.97**	**12.24**	**15.04**	**15.84**	**11.66**
B3	2.37	4.90	6.52	7.92	4.08	4.81	6.82
B4	0.90	6.81	5.62	7.59	7.59	8.63	9.15
B5	2.43	4.23	2.43	4.39	2.80	3.79	6.60
C1	**9.24**	**17.10**	**13.38**	**12.03**	**15.60**	**14.78**	**11.58**
C2	**25.07**	**14.80**	**11.64**	**10.91**	**11.64**	**10.98**	**11.40**
C3	2.89	9.78	9.34	8.71	8.73	8.08	7.92
C4	2.93	3.41	3.91	3.16	4.37	3.81	2.98
C5	4.27	1.58	2.18	1.47	3.18	2.65	1.79
D1	1.48	5.42	6.25	5.44	5.31	4.92	7.11
D2	4.23	6.15	6.61	6.25	7.30	7.10	6.62
D3	5.84	3.63	4.26	3.88	2.95	2.72	3.44
D4	1.86	1.14	0.61	0.38	2.63	2.52	-0.39
D5	2.20	0.91	-3.06	-3.31	-2.46	-2.55	-2.95

Table 5.37: Experimental data2 - Collapse- predictive model verification

Experimental result		Sieve based - three researchers				Compaction based – two researchers			
		Sieve	Sieve (-Cu)	Atterberg (+ %fines)	Compactive variables	Atterberg (+ %fine)	Compaction & Atterberg (- MDD)	Compaction & Atterberg	Compactive variables
Samples	Total Collapse (%)	TC = 17.558 + 0.000457Cu - 0.783MCi - 0.183Sri - 10.637Diff.Sr + 0.198%fines	TC = 17.698 - 0.781MCi - 0.179Sri - 10.142Diff.Sr + 0.193%fines	TC = 28.250 - 0.127MCi - 0.428Sri - 20.748Diff.Sr - 0.271PL + 0.216LL + 0.159%fines	TC = 61.366 - 1.623MCi - 0.034Sri - 19.411Diff.Sr - 21.575Ddi + 0.17%fines	TC = 28.250 - 0.127MCi - 0.428Sri - 20.748Diff.Sr - 0.271PL + 0.216LL + 0.159%fines	TC = 1.995OMC - 1.194MCi + 0.166RMC - 0.474Sri - 25.203Diff.Sr + 0.21%fines - 0.963PL - 0.035LL + 18.281	TC = 2.007OMC + 0.008MDD - 1.194MCi + 0.168RMC - 0.476Sri - 25.402Diff.Sr + 0.211%fines - 0.936PL - 0.036PI + 18.282	TC = 75.083 - 1.104MCi - 0.149Sri - 23.009Diff.Sr - 27.33Ddi + 0.129%fines
A1	**10.24**	**11.65**	**11.78**	**11.11**	**10.44**	**11.51**	**10.97**	**10.54**	**10.94**
A2	**12.22**	**10.02**	**10.03**	**10.02**	**10.81**	**10.29**	**10.62**	**10.26**	**10.73**
A3	1.97	6.23	6.36	5.90	5.23	4.28	3.55	3.15	4.66
A4	2.39	3.07	3.16	2.72	3.37	2.93	2.47	2.13	4.73
A5	2.31	2.47	2.56	2.07	2.79	3.29	2.94	2.62	4.99
B1	**14.10**	**15.65**	**15.78**	**14.51**	**13.61**	**13.50**	**13.36**	**13.16**	**13.28**
B2	**21.99**	**13.61**	**13.70**	**12.75**	**11.33**	**10.92**	**11.19**	**11.03**	**10.01**
B3	2.37	9.26	9.37	8.34	7.15	5.86	6.02	5.88	6.10
B4	0.90	8.60	8.61	7.99	8.86	7.21	8.42	8.35	8.91
B5	2.43	6.38	6.41	5.63	6.55	5.35	6.52	6.47	7.47
C1	**9.24**	**12.73**	**12.79**	**12.56**	**11.14**	**12.75**	**12.63**	**11.92**	**11.53**
C2	**25.07**	**10.61**	**10.58**	**10.77**	**10.68**	**11.75**	**11.91**	**11.27**	**11.50**
C3	2.89	7.80	7.79	7.97	7.73	7.91	7.58	6.94	8.16
C4	2.93	4.18	4.23	4.05	3.27	4.74	3.58	2.94	5.06
C5	4.27	3.02	3.07	2.84	2.14	3.99	2.67	2.05	4.47

D1	1.48	7.32	7.57	7.56	7.07	9.01	7.43	7.02	7.96
D2	4.23	6.14	6.33	6.72	6.57	7.42	6.77	6.40	6.52
D3	5.84	3.59	3.82	4.09	3.95	3.84	3.36	2.99	3.76
D4	1.86	-0.44	-0.18	0.06	0.80	-1.24	-0.90	-1.24	0.65
D5	2.20	-2.72	-2.44	-2.40	-1.56	-2.83	-1.75	-2.06	-0.50

Table 5.38: Basma and Tuncer (1992) - Collapse- predictive model verification

Basma and Tuncer (1992)		Experimental data model			Compaction based - two researchers				Sieve based - three researchers			
		Atterberg limits	- sieve analysis	Compactive variables	Atterberg	compaction & Atterberg (-MDD)	compaction & Atterberg (+%fine - LL)	Compactive variables	Sieve	Sieve (-Cu)	Atterberg	Compactive variables
Samples	Total collapse (%)	TC = 1.692PL + 0.055PI - 1.625MCi - 9.877Diff.Sr - 5.573	TC = 0.081Cu + 0.351%fines - 1.625MCi - 11.689Diff.Sr +1.153	TC = 0.192%fines - 0.107Sri - 23.881Diff.Sr - 1.603Mci - 21.530Ddi + 64.835	TC = 0.159%fines - 0.127MCi - 0.428Sri - 20.748Diff.Sr - 0.271PL + 0.216LL + 28.250	TC = 1.995OMC - 1.194MCi + 0.166RMC - 0.474Sri - 25.203Diff.Sr + 0.21%fines - 0.963PL - 0.035LL + 18.281	TC = 2.007OMC + 0.008MDD - 1.194MCi + 0.168RMC - 0.476Sri - 25.402Diff.Sr + 0.211%fines - 0.936PL - 0.036PI + 18.282	TC = 0.129%fines - 1.104MCi - 0.149Sri - 23.009Diff.Sr - 27.33Ddi + 75.083	TC = 0.198%fines + 0.000457Cu - 0.783MCi - 0.183Sri - 10.637Diff.Sr + 17.558	TC = 0.193%fines - 0.781MCi - 0.179Sri - 10.142Diff.Sr + 17.698	TC = 0.159%fines - 0.127MCi - 0.428Sri - 20.748Diff.Sr - 0.271PL + 0.216LL + 28.250	TC = 0.17%fines - 1.623MCi - 0.034Sri - 19.411Diff.Sr - 21.575Ddi + 61.366
(S1)	**10.00**	**18.05**	*4.48*	**13.43**	**13.54**	*8.43*	*7.59*	**14.59**	**12.63**	**12.94**	**12.77**	**13.43**
(S2)	5.80	8.71	3.62	8.07	*10.40*	8.93	8.24	7.83	*10.51*	*10.85*	*11.16*	8.48
(S3)	**17.50**	**26.05**	**17.11**	**21.24**	**21.88**	**19.26**	**17.29**	**21.66**	**18.31**	**18.47**	**20.48**	**20.55**
(S4)	**16.00**	**12.52**	**11.00**	**19.41**	**16.50**	**15.72**	**15.32**	**20.05**	**17.02**	**17.24**	**16.52**	**18.87**
(S5)	**22.00**	**19.22**	**11.07**	**20.05**	**16.68**	**22.66**	**21.98**	**21.51**	**16.18**	**16.41**	**15.90**	**19.58**
(S6)	**15.50**	**7.84**	**11.31**	**10.66**	**11.93**	**11.42**	**10.77**	**10.76**	**11.93**	**12.21**	**12.42**	**10.85**
(S7)	3.00	*23.69*	-10.55	1.82	2.29			4.01	3.31	3.83	1.80	3.03
(S8)	2.50	*11.57*	-14.13	1.45	2.67			4.82	1.98	2.56	1.37	2.74

Table 5.39: Tadepalli and Fredlund (1991) - Collapse- predictive model verification

Tadepalli and Fredlund (1991)		**Experimental data model**			**Compaction based - two researchers**		**Sieve based - three researchers**			
		Atterberg limits	sieve analysis	Compactive variables	Atterberg (+ %fine)	Compactive variables (+ %fines)	Sieve	Sieve (- Cu)	Atterberg (+ %fines)	Compactive variables (+ %fines)
Samples	Total collapse (%)	TC = 1.692PL + 0.055PI - 1.625MCi - 9.877Diff. Sr - 5.573	TC = 0.081Cu + 0.351%fines - 1.625MCi - 11.689Diff.Sr +1.153	TC = 0.192%fines - 0.107Sri - 23.881Diff. Sr - 1.603Mci - 21.530Ddi + 64.835	TC = 0.159%fines - 0.127MCi - 0.428Sri - 20.748Diff.Sr - 0.271PL + 0.216LL + 28.250	TC = 0.129%fines - 1.104MCi - 0.149Sri - 23.009Diff. Sr - 27.33Ddi + 75.083	TC = 0.198%fines + 0.000457Cu - 0.783MCi - 0.183Sri - 10.637Diff. Sr + 17.558	TC = 0.193%fines - 0.781MCi - 0.179Sri - 10.142Diff .Sr + 17.698	TC = 0.159%fines - 0.127MCi - 0.428Sri - 20.748Diff. Sr - 0.271PL + 0.216LL + 28.250	TC = 0.17%fines - 1.623MCi - 0.034Sri - 19.411Diff.Sr - 21.575Ddi + 61.366
S1M	5.84	0.46	-6.32	*11.03*	*26.10*	*16.26*	*12.30*	*12.42*	*12.03*	7.91
S2M	**11.64**	*1.49*	*-5.11*	**15.46**	**28.18**	**21.13**	**13.37**	**13.45**	**13.24**	**11.89**
S3M	**15.26**	*2.73*	*-3.63*	**20.66**	**30.78**	**26.80**	**14.70**	**14.72**	**14.75**	**16.53**
S4M	**18.62**	*1.34*	*-4.99*	**19.73**	**30.97**	**26.40**	**14.12**	**14.12**	**14.10**	**15.52**

Table 5.40: Pereira, et al (2005) and Pereira and Fredlund (2000) - Collapse- predictive model verification

Pereira, et al (2005)	Experimental data model				Compaction based - two researchers				Sieve based - three researchers			
	Compaction values	Atterberg limits	sieve analysis	Compactive variables	Atterberg	compaction & Atterberg (-MDD)	compaction & Atterberg	Compactive variables	Sieve	Sieve (-Cu)	Atterberg	Compactive variables
Samples	TC = 3.395OMC - 75.189MDD - 4.01MCi + 0.503%MCOMC - 0.388Sri - 24.513Diff.Sr + 135.011	TC = 1.692PL + 0.055PI - 1.625MCi - 9.877Diff.Sr - 5.573	TC = 0.081Cu + 0.351%fines - 1.625MCi - 11.689Diff.Sr +1.153	TC = 0.192%fines - 0.107Sri - 23.881Diff.Sr - 1.603Mci - 21.530Ddi + 64.835	TC = 0.159%fines - 0.127MCi - 0.428Sri - 20.748Diff.Sr - 0.271PL + 0.216LL + 28.250	TC = 1.995OMC - 1.194MCi + 0.166RMC - 0.474Sri - 25.203Diff.Sr + 0.21%fines - 0.963PL - 0.035LL + 18.281	TC = 2.007OMC + 0.008MDD - 1.194MCi + 0.168RMC - 0.476Sri - 25.402Diff.Sr + 0.211%fines - 0.936PL - 0.036PI + 18.282	TC = 0.129%fines - 1.104MCi - 0.149Sri - 23.009Diff.Sr - 27.33Ddi + 75.083	TC = 0.198%fines + 0.000457Cu - 0.783MCi - 0.183Sri - 10.637Diff.Sr + 17.558	TC = 0.193%fines - 0.781MCi - 0.179Sri - 10.142Diff.Sr + 17.698	TC = 0.159%fines - 0.127MCi - 0.428Sri - 20.748Diff.Sr - 0.271PL + 0.216LL + 28.250	TC = 0.17%fines - 1.623MCi - 0.034Sri - 19.411Diff.Sr - 21.575Ddi + 61.366
TPT1	8.17	0.66	**23.39**	6.03	7.72	8.51	7.69	9.26	5.73	5.94	6.23	6.66
TPT2	8.73	0.89	**23.66**	6.58	8.20	9.09	8.27	9.79	5.98	6.17	6.51	7.11
TPT3	8.34	0.73	**23.47**	6.19	7.86	8.69	7.87	9.42	5.81	6.01	6.31	6.80
TPT4	8.88	0.95	**23.73**	6.72	8.32	9.24	8.42	9.92	6.04	6.23	6.58	7.22

Table 5.41: Gaaver (2012) - Collapse- predictive model verification

Gaaver (2012)	**Experimental data model**			**Compaction based - two researchers**		**Sieve based - three researchers**			
	Atterberg limits	sieve analysis	Compactive variables (+ %fines)	Atterberg (+ %fine)	Compactive variables (+ %fines)	Sieve	Sieve (-Cu)	Atterberg (+ %fines)	Compactive variables (+ %fines)
Total collapse (%)	TC = 1.692PL + 0.055PI - 1.625MCi - 9.877Diff.Sr - 5.573	TC = 0.081Cu + 0.351%fines - 1.625MCi - 11.689Diff.Sr +1.153	TC = 0.192%fines - 0.107Sri - 23.881Diff.Sr - 1.603Mci - 21.530Ddi + 64.835	TC = 0.159%fines - 0.127MCi - 0.428Sri - 20.748Diff.Sr - 0.271PL + 0.216LL + 28.250	TC = 0.129%fines - 1.104MCi - 0.149Sri - 23.009Diff.Sr - 27.33Ddi + 75.083	TC = 0.198%fines + 0.000457Cu - 0.783MCi - 0.183Sri - 10.637Diff.Sr + 17.558	TC = 0.193%fines - 0.781MCi - 0.179Sri - 10.142Diff.Sr + 17.698	TC = 0.159%fines - 0.127MCi - 0.428Sri - 20.748Diff.Sr - 0.271PL + 0.216LL + 28.250	TC = 0.17%fines - 1.623MCi - 0.034Sri - 19.411Diff.Sr - 21.575Ddi + 61.366
naturally collapsible	-5.42	5.26	9.28	**11.29**	**11.03**	9.35	9.59	**10.81**	9.50

Table 5.42: Nuntasarn (2011) - Collapse- predictive model verification

Experimental data model					**Compaction based – two researchers**				**Sieve based - three researchers**		
Compaction values	Atterberg limits	sieve analysis	(Triaxial and Atterberg - PL)	Compactive variables (+ %fines)	Atterberg (+ %fine)	compaction & Atterberg (-MDD)	compaction & Atterberg	Compactive variables (+ %fines)	Sieve (-Cu)	Atterberg (+ %fines)	Compactive variables (+ %fines)
TC = 3.395OMC - 75.189MDD - 4.01MCi + 0.503%MCOMC - 0.388Sri - 24.513Diff.Sr + 135.011	TC = 1.692PL + 0.055PI - 1.625MCi - 9.877Diff.Sr - 5.573	TC = 0.081Cu + 0.351%fines - 1.625MCi - 11.689Diff.Sr +1.153	TC = 0.138LL + 1.331PL - 1.191Mci - 5.106Diff.Sr + 0.031Ds70 - 0.367fa - 0.045C - 9.55	TC = 0.192%fines - 0.107Sri - 23.881Diff.Sr - 1.603Mci - 21.530Ddi + 64.835	TC = 0.159%fines - 0.127MCi - 0.428Sri - 20.748Diff.Sr - 0.271PL + 0.216LL + 28.250	TC = 1.995OMC - 1.194MCi + 0.166RMC - 0.474Sri - 25.203Diff.Sr + 0.21%fines - 0.963PL - 0.035LL + 18.281	TC = 2.007OMC + 0.008MDD - 1.194MCi + 0.168RMC - 0.476Sri - 25.402Diff.Sr + 0.211%fines - 0.936PL - 0.036PI + 18.282	TC = 0.129%fines - 1.104MCi - 0.149Sri - 23.009Diff.Sr - 27.33Ddi + 75.083	TC = 0.193%fines - 0.781MCi - 0.179Sri - 10.142Diff.Sr + 17.698	TC = 0.159%fines - 0.127MCi - 0.428Sri - 20.748Diff.Sr - 0.271PL + 0.216LL + 28.250	TC = 0.17%fines - 1.623MCi - 0.034Sri - 19.411Diff.Sr - 21.575Ddi + 61.366
6.44	-5.40	-8.44	-8.25	1.12	-3.92	-0.14	-0.39	3.09	-0.86	-0.70	2.97

Table 5.43: Li, et al. (2014) - Collapse- predictive model verification

Experimental data model			**Compaction based – two researchers**				**Sieve based - three researchers**		
Compaction values	Atterberg limits	Compactive variables	Atterberg (+ %fine)	compaction & Atterberg (- MDD)	compaction & Atterberg	Compactive variables	Sieve (- Cu)	Atterberg (+ %fines)	Compactive variables
TC = 3.395OMC - 75.189MDD - 4.01MCi + 0.503%MCOMC - 0.388Sri - 24.513Diff.Sr + 135.011	TC = 1.692PL + 0.055PI - 1.625MCi - 9.877Diff.Sr - 5.573	TC = 0.192%fines - 0.107Sri - 23.881Diff.Sr - 1.603Mci - 21.530Ddi + 64.835	TC = 0.159%fines - 0.127MCi - 0.428Sri - 20.748Diff.Sr - 0.271PL + 0.216LL + 28.250	TC = 1.995OMC - 1.194MCi + 0.166RMC - 0.474Sri - 25.203Diff.Sr + 0.21%fines - 0.963PL - 0.035LL + 18.281	TC = 2.007OMC + 0.008MDD - 1.194MCi + 0.168RMC - 0.476Sri - 25.402Diff.Sr + 0.211%fines - 0.936PL - 0.036PI + 18.282	TC = 0.129%fines - 1.104MCi - 0.149Sri - 23.009Diff.Sr - 27.33Ddi + 75.083	TC = 0.193%fines - 0.781MCi - 0.179Sri - 10.142Diff.Sr + 17.698	TC = 0.159%fines - 0.127MCi - 0.428Sri - 20.748Diff.Sr - 0.271PL + 0.216LL + 28.250	TC = 0.17%fines - 1.623MCi - 0.034Sri - 19.411Diff.Sr - 21.575Ddi + 61.366
12.24	-2.09	7.25	7.25	**10.28**	9.15	7.15	7.84	9.55	7.78

Table 5.44: Houston, et al (1988) - Collapse- predictive model verification

Houston, et al (1988)		**Experimental data model**			**Compaction based - Two researchers**	**Sieve based - three researchers**	
		Compaction values	Sieve analysis	Compactive variables	Compactive variables	Sieve (-Cu)	Compactive variables
Samples	Total collapse (%)	TC = 3.395OMC - 75.189MDD - 4.01MCi + 0.503%MCOMC - 0.388Sri - 24.513Diff.Sr + 135.011	TC = 0.081Cu + 0.351%fines - 1.625MCi - 11.689Diff.Sr +1.153	TC = 0.192%fines - 0.107Sri - 23.881Diff.Sr - 1.603Mci - 21.530Ddi + 64.835	TC = 0.129%fines - 1.104MCi - 0.149Sri - 23.009Diff.Sr - 27.33Ddi + 75.083	TC = 0.193%fines - 0.781MCi - 0.179Sri - 10.142Diff.Sr + 17.698	TC = 0.17%fines - 1.623MCi - 0.034Sri - 19.411Diff.Sr - 21.575Ddi + 61.366
1A/8-14	**9.50**	*6.50*	*9.24*	**16.56**	**15.68**	**17.18**	**16.26**
1B/15-19	**7.70**	*6.93*	*8.65*	**20.31**	**20.82**	**17.20**	**19.96**
1C/20-25	**6.40**	*8.00*	*9.57*	**19.66**	**19.63**	**17.63**	**19.27**
1D/26-31	5.60	8.00	9.68	*20.04*	*20.05*	*17.74*	*19.64*

Table 5.45: Rezaei, et al. (2012) - Collapse- predictive model verification

Rezaei, et al. (2012)		**Experimental data model**			**Compaction based -Two researchers**		**Sieve based - three researchers**			
		Atterberg limits	Sieve analysis	Compactive variables	Atterberg	Compactive variables	Sieve	Sieve (-Cu)	Atterberg	Compactive variables
Samples	Total collapse (%)	TC = 1.692PL + 0.055PI - 1.625MCi - 9.877Diff. Sr - 5.573	TC = 0.081Cu + 0.351%fines - 1.625MCi - 11.689Diff. Sr +1.153	TC = 0.192%fines - 0.107Sri - 23.881Diff. Sr - 1.603Mci - 21.530Ddi + 64.835	TC = 0.159%fines - 0.127MCi - 0.428Sri - 20.748Diff.Sr - 0.271PL + 0.216LL + 28.250	TC = 0.129%fines - 1.104MCi - 0.149Sri - 23.009Diff.Sr - 27.33Ddi + 75.083	TC = 0.198%fines + 0.000457Cu - 0.783MCi - 0.183Sri - 10.637Diff. Sr + 17.558	TC = 0.193%fines - 0.781MCi - 0.179Sri - 10.142Diff.Sr + 17.698	TC = 0.159%fines - 0.127MCi - 0.428Sri - 20.748Diff.Sr - 0.271PL + 0.216LL + 28.250	TC = 0.17%fines - 1.623MCi - 0.034Sri - 19.411Diff.Sr - 21.575Ddi + 61.366
(1) 5+700	0.50	-17.30	3.18	-1.00	0.68	2.58	-0.48	-0.34	0.68	0.13
(2) 7+000	**12.82**	*-6.09*	*3.31*	**12.96**	**14.07**	**17.70**	**10.42**	**10.60**	**10.56**	**12.57**
(3) 8+400	**14.96**	*-5.99*	**128.34**	7.60	*9.06*	*9.04*	*8.91*	*8.51*	*9.24*	*8.09*
(4) 9+800	5.66	-5.38	*41.80*	7.07	8.69	8.41	8.07	8.15	8.99	7.61
(5) 11+200	6.74	-1.06	*480.36*	3.90	6.52	5.09	8.46	6.15	6.91	4.84
(6) 12+600	1.93		*17.90*	0.70		3.30	1.39	1.58		1.93

Table 5.46: Assallay et al. (1996) cited in Nouaouria, et al. (2008)- Collapse- predictive model verification

Assallay et al. (1996)		Experimental data model			Compaction based -Two researchers		Sieve based - three researchers			
		Soil type - Atterberg limits	Soil type - sieve analysis	Compactive variables (+ %fines)	Atterberg (+ %fine)	Compactive variables (+ %fines)	Sieve	Sieve (-Cu)	Atterberg (+ %fines)	Compactive variables (+ %fines)
	Total collapse (%)	TC = 1.692PL + 0.055PI - 1.625MCi - 9.877Diff. Sr - 5.573	TC = 0.081Cu + 0.351%fines - 1.625MCi - 11.689Diff. Sr +1.153	TC = 0.192%fines - 0.107Sri - 23.881Diff.Sr - 1.603Mci - 21.530Ddi + 64.835	TC = 0.159%fines - 0.127MCi - 0.428Sri - 20.748Diff.Sr - 0.271PL + 0.216LL + 28.250	TC = 0.129%fines - 1.104MCi - 0.149Sri - 23.009Diff.Sr - 27.33Ddi + 75.083	TC = 0.198%fines + 0.000457Cu - 0.783MCi - 0.183Sri - 10.637Diff.Sr + 17.558	TC = 0.193%fines - 0.781MCi - 0.179Sri - 10.142Diff. Sr + 17.698	TC = 0.159%fines - 0.127MCi - 0.428Sri - 20.748Diff.Sr - 0.271PL + 0.216LL + 28.250	TC = 0.17%fines - 1.623MCi - 0.034Sri - 19.411Diff. Sr - 21.575Ddi + 61.366
Gharyan Loess (Libya)		8.48		**14.93**	**15.49**	**17.09**		**14.25**	**13.61**	**14.59**
Khoms Loess (Libya)		**15.17**		**22.66**	**19.73**	**21.85**		**20.48**	**20.57**	**21.93**
Grey Loess (Algeria)	**collapsible**	**17.36**	**13.42**	**20.84**	**17.46**	**20.66**	**18.65**	**18.85**	**18.00**	**20.19**
Yellow Loess (Algeria)	**collapsible**	**14.56**	**17.05**	**22.09**	**19.83**	**21.32**	**20.41**	**20.54**	**20.47**	**21.20**

Table 5.47: Habibagahi and Taherian (2004) - Collapse- predictive model verification

Habibagahi and Taherian (2004)		Experimental data model			Compaction based -Two researchers		Sieve based - three researchers			
		Atterberg limits	Sieve analysis	Compactive variables	Atterberg	Compactive variables	Sieve	Sieve (-Cu)	Atterberg	Compactive variables
Samples	Total collapse (%)	TC = 1.692PL + 0.055PI - 1.625MCi - 9.877Diff. Sr - 5.573	TC = 0.081Cu + 0.351%fines - 1.625MCi - 11.689Diff. Sr +1.153	TC = 0.192%fines - 0.107Sri - 23.881Diff.Sr - 1.603Mci - 21.530Ddi + 64.835	TC = 0.159%fines - 0.127MCi - 0.428Sri - 20.748Diff.Sr - 0.271PL + 0.216LL + 28.250	TC = 0.129%fines - 1.104MCi - 0.149Sri - 23.009Diff.Sr - 27.33Ddi + 75.083	TC = 0.198%fines + 0.000457Cu - 0.783MCi - 0.183Sri - 10.637Diff.Sr + 17.558	TC = 0.193%fines - 0.781MCi - 0.179Sri - 10.142Diff. Sr + 17.698	TC = 0.159%fines - 0.127MCi - 0.428Sri - 20.748Diff.Sr - 0.271PL + 0.216LL + 28.250	TC = 0.17%fines - 1.623MCi - 0.034Sri - 19.411Diff. Sr - 21.575Ddi + 61.366
A (S1)	**14.10**	*8.13*	**15.16**	**22.59**	**18.13**	**22.57**	**19.43**	**19.62**	**18.97**	**21.83**
A (S18)	4.50	2.60	9.95	*15.01*	*13.60*	*15.59*	*14.53*	*14.71*	*14.07*	*14.67*
A (S37	**14.10**	*-1.18*	*6.13*	**15.21**	**13.78**	**18.07**	**12.97**	**13.15**	**12.29**	**14.78**
A (S51)	0.10	-4.01	4.01	6.14	4.69	7.02	6.78	6.93	6.57	6.71
B (S65)	**10.40**	*5.23*	**10.51**	**18.51**	**15.52**	**19.93**	**15.21**	**15.47**	**15.29**	**18.20**
B (S86)	**9.00**	0.83	6.40	**11.56**	**11.46**	**13.15**	***11.06***	***11.32***	***11.18***	***11.62***
B (S102)	5.60	-3.72	2.00	8.41	9.22	*11.51*	7.85	8.10	7.87	8.65
B (S116)	0.00	-6.41	0.16	0.82	-1.67	2.03	0.74	0.96	1.35	2.27
C (S132)	0.80	*20.79*	9.14	*10.34*	9.86	9.08	12.91	13.18	11.64	10.51
C (S151)	0.50	*17.04*	5.65	7.63	6.23	7.37	9.28	9.54	8.06	8.16
C (S165)	5.50	*11.50*	-0.02	8.07	7.34	*11.30*	7.45	7.73	5.85	8.36
C (S177)	1.70	7.52	-3.68	3.06	3.07	6.71	3.38	3.65	1.86	3.77

Table 5.48: Benchouk et al (2013) - Collapse- predictive model verification

Benchouk et al (2013)		Experimental data model			Compaction based -Two researchers				Sieve based - three researchers		
		Compaction values	Atterberg limits	Compactive variables	Atterberg	compaction & Atterberg (-MDD)	compaction & Atterberg	Compactive variables	Sieve (-Cu)	Atterberg	Compactive variables
Samples	Total collapse (%)	TC = 3.395OMC - 75.189MDD - 4.01MCi + 0.503%MCOMC - 0.388Sri - 24.513Diff.Sr + 135.011	TC = 1.692PL + 0.055PI - 1.625MCi - 9.877Diff.Sr - 5.573	TC = 0.192%fines - 0.107Sri - 23.881Diff.Sr - 1.603Mci - 21.530Ddi + 64.835	TC = 0.159%fines - 0.127MCi - 0.428Sri - 20.748Diff.Sr - 0.271PL + 0.216LL + 28.250	TC = 1.995OMC - 1.194MCi + 0.166RMC - 0.474Sri - 25.203Diff.Sr + 0.21%fines - 0.963PL - 0.035LL + 18.281	TC = 2.007OMC + 0.008MDD - 1.194MCi + 0.168RMC - 0.476Sri - 25.402Diff.Sr + 0.211%fines - 0.936PL - 0.036PI + 18.282	TC = 0.129%fines - 1.104MCi - 0.149Sri - 23.009Diff.Sr - 27.33Ddi + 75.083	TC = 0.193%fines - 0.781MCi - 0.179Sri - 10.142Diff.Sr + 17.698	TC = 0.159%fines - 0.127MCi - 0.428Sri - 20.748Diff.Sr - 0.271PL + 0.216LL + 28.250	TC = 0.17%fines - 1.623MCi - 0.034Sri - 19.411Diff.Sr - 21.575Ddi + 61.366
Test 1	0.83	*11.02*	-0.03	-4.10	-1.42	-2.23	-4.12	-0.16	-4.57	-1.85	-2.24
Test 2	1.56	*15.42*	-3.07	-2.56	5.38	4.61	2.72	4.45	-2.18	-0.11	-1.57
Test 3	**6.91**	**17.70**	-4.65	-0.36	8.90	8.16	6.27	8.62	-0.94	0.78	0.19
Test 4	1.08	*15.31*	2.32	-2.09	0.85	0.52	-1.39	1.31	-2.30	0.39	-0.46
Test 5	4.83	*19.28*	-0.42	-0.15	6.96	6.68	4.77	6.17	-0.14	1.95	0.71
Test 6	**9.90**	**21.33**	*-1.84*	*2.26*	**10.13**	*9.87*	*7.96*	**10.47**	*0.97*	*2.76*	*2.72*
Test 7	4.96	*21.75*	5.84	0.91	*4.25*	*4.65*	*2.71*	*3.51*	1.11	3.75	2.22
Test 8	**12.57**	**25.06**	*3.56*	*3.46*	*9.34*	*9.78*	*7.84*	*8.75*	*2.90*	*5.05*	*4.13*
Test 9	**17.69**	**26.77**	*2.38*	*6.19*	**11.98**	**12.43**	**10.50**	**13.24**	*3.83*	*5.72*	*6.53*
Test 10	**6.37**	**32.49**	**11.72**	*5.92*	*9.91*	**11.52**	*9.54*	*7.19*	*6.78*	*9.35*	*6.68*
Test 11	**13.05**	**34.69**	**10.19**	*9.49*	**13.31**	**14.94**	**12.96**	**13.04**	*7.98*	**10.21**	*9.83*
Test 12	**18.39**	**35.83**	*9.41*	**12.74**	**15.07**	**16.71**	**14.74**	**17.86**	*8.60*	**10.66**	**12.86**

5.3.4.3 Findings

The verified result of the model show the model is agreeing fairly accurately with experimental data. The six samples that were collapsible from the experimental results were also collapsible using the model formulas. The verification table for experimental data is shown in Table 5.36 and Table 5.37.

For Basma and Tuncer (1992) data out of eight samples (Table 5.38) seven of the samples had the model result tally with the collected data, with five of the samples collapsible and three non-collapsible.

The data from Tadepalli and Fredlund (1991) were four in all. Three of the samples are collapsible and one non-collapsible. The nine models found all of the samples collapsible, except for the sieve and Atterberg models from the experimental data generation (Table 5.39). These two models found the samples to be non-collapsible.

Pereira, et al (2005) and Pereira and Fredlund (2000) both have the same data. The four samples were not stated to be collapsible or non-collapsible. From the model, all twelve models that were used on it found the samples non-collapsible except for the sieve model from the experimental data model (Table 5.40) which found the samples collapsible. The samples hence are non-collapsible.

One sample was taken from Gaaver (2012) of which he stated to be naturally collapsible. Nine of the models were used on the parameters and three found it collapsible whiles the other six found it non-collapsible (Table 5.41). this shows that even naturally collapsible soils can become a stable soil sample when prepared with right parameters.

One sample was collected by Nuntasarn (2011). It was checked with eleven of the models and found by all models to be non-collapsible (Table 5.42).

Li, et al. (2014)'s sample was found by eight samples to be non-collapsible and then when checked with the two compaction models from experimental data model and the compaction based model, it was found to be collapsible (Table 5.43). The compaction values (OMC, MDD and RMC), must have had numbers that make the sample collapsible. But in general the sample is non-collapsible.

Four sample were collected from Houston, et al (1988), with three collapsible and one non-collapsible. Six models were run through it, four models found all the samples collapsible and two found it non-collapsible (Table 5.44). The samples are collapsible, because even one of the two models is approaching collapsibility.

From Rezaei, et al. (2012), six samples were collected and nine models were ran. Two of the six samples were stated in the paper to be collapsible. Although from the model, only one of the samples is collapsible (Table 5.45). Also the models from Atterberg and sieve of the experimental data model were found to be fairly inaccurate.

Found samples from Assallay et al. (1996) cited in Nouaouria, et al. (2008) was collected. Two of the samples were stated to be collapsible, whiles the other two were not stated to be either collapsible or non-collapsible. All night models reflect the samples as collapsible (Table 5.46).

From Habibagahi and Taherian (2004), twelve samples were collected. They stated in their paper that four of the samples as collapsible, while the eight out of nine models revealed that five of the samples were collapsible and the others non-

collapsible (Table 5.47). The Atterberg of the experimental data model had a less than perfect result.

The twelve data samples were collected from Benchouk et al (2013). Benchouk et al (2013) stated 7 samples as collapsible while the ten models which had a lot of disagreeing gathered four of the samples as collapsible (Table 5.48).

In summary, sieve of the experimental data model is the least accurate of the fifteen models; while the compactive variables for all three based on experimental data, compaction based and sieve based are the most accurate models as compared to the others. The parameters for the compactive variable have parameters that are collapse sensitive.

6 CONCLUSION

This thesis has presented the results of an experimental work done on four geologically different soil tested at five compactive variables, to comprehensively investigate the various state parameters and geological properties that influence collapse under miscellaneous conditions. The conclusion is presented under the following four items:

1. Analysed test results.
2. Past research studies.
3. Development of collapse predictive models.
4. Test processes.

6.1 Analysed test results

The following conclusions were drawn:

- High percentage fines (< 0.063mm) and lower coefficient of uniformity (Cu) in a soil (i.e. less well-graded) would cause more collapse as revealed in Figure 5.19 in page164. This result however, disagrees with Basma and Tuncer (1992)'s conclusion; of which their results displayed the opposite due to the low ranges of Cu used in their investigation.
- Low percentage of clay binders give the soil a more stable state than high clay percentage and silt fines. In this research, it was observed that high clay content make the soil structure metastable because high clay content amass higher volumetric strain when saturated as compared to when in its as-compacted state, as found in soil C which had the highest collapse potential of 25.07 %. Silty soil B, had high collapse potential of 21.99 % also. The soil A, and soil D, which had low percentage of clay binders have the lowest collapse potentials of 12.22 % and 5.84 % respectively.

- The Atterberg limits (LL, PL, and PI) showed a direct proportion to the collapse potential of each soil, as shown in Figure 5.6 in page 147.
- Results showed that collapse decreased with increasing initial moisture content, degree of saturation, relative moisture content and initial dry density; and proportional to initial void ratio. Consequently the more stable the soil structure lesser the collapse potential.
- Result of the critical pressures varied with each soil and their compactive variable. All soils except soil D had their highest collapse potential at their 'Dry OMC'. In general soils with higher collapse potential tend to have lower critical pressure (e.g. C2 with collapse potentials 25.07 % has critical pressure of 25 kPa whilst A2 with collapse potential 12.22 % has 100 kPa of critical pressure). Hence, the higher the critical pressure, the less prone to collapse the soil would be. It is interesting to note that all the critical pressures for all the soils was under 150 kPa, which agrees with past research conclusion by Larionov (1959). See Figure 5.32 in page 180.
- The critical pressure points of each soil at moderately severe collapse (6 % collapse) show that C2 and B2 have the most collapse potential at a much lower critical pressure (25kPa) than the other samples. C2 is the most collapsible of all the soil samples. B1 is next collapsible with a critical pressure of 50 kPa. A2 has a higher collapse potential than A1 and C1 in decreasing consecutive order but they are all of the same critical pressure (100 kPa). D is however not moderately collapsible, making it the least collapsible of the 4 soils.
- From the pattern of rise or/and fall in the addition to collapse of the samples as the pressures increase, the dominating trigger, for the collapse can be stated whether it is from inundation or pressure or both.

6.2 Past research studies

The following conclusions were drawn:

- Out of the entire key past researches reviewed, the result of this study agrees with Larionov (1959) prediction (A1, A2, B1, B2, C1 and C2 as collapsible) for collapse potential. This also acknowledges Rogers (1995), who concluded that all soils should be suspected of collapse unless proved otherwise.
- In the light of these observations, this study on collapsibility of soils should not be limited to areas susceptible to natural collapse, since soils with their fabric conditions, structural properties and overburden pressures could be metastable and collapse when there is a change in the state parameter.

6.3 Development of collapse predictive models

The following conclusions were drawn:

- New collapse indexes were generated from development of collapse predictive model obtained from multiple regression analysis.
- This study provides fifteen collapse predictive models obtained from multiple regression analysis on simple laboratory test results. The models reproduced reliable and consistent results thus can be applied prior to construction for prediction of collapse.

6.4 Test processes

The following conclusions were drawn:

- The identification of soil collapsibility is a profound process which depends on the geomorphological processes combined with geological properties.
- Simple characteristics tests (PSD, Atterbergs and compaction), triaxial test and double oedometer test are suitable test methods for collapsibility identification.

- The governing state parameters in this research are initial moisture content with regard to the OMC (representing the compactive variable) and pressure before and after inundation.
- Triaxial test results without the soil suction constituent can be used to obtain collapse potential. The probable response of a soil's collapse potential can be estimated from the values of deviator stress. Increases in peak deviator stress would reflect a higher collapse potential; increase in cohesion followed with a decrease in collapse and increase in the angle of internal friction revealed an increase in the soils' collapse potential.
- Oedometer test is an effective means for collapsibility check. Where the difference between the volumetric strains of the inundated and the as-compacted states results in the calculated collapse potential of the sample. See Figure 5.16 in page 160.

7 RECOMMENDATION FOR FUTHER WORK

Time enabling the author would have wanted to expand the research.

7.1 FULL OBSERVATION OF COLLAPSIBILITY

The parameters that make a soil structure collapsible are compacted into layers of metastable soil structures where the metastable soils (gathered from general findings) are tested to see the potential, pattern and extent of collapse. Hence a relationship is drawn between the soil fabric, soil structure, critical loading and wetting of a metastable soil.

7.1.1 The Mould Specifications

Figure 7.1 shows the schematic diagram of the full mould design and features for a uniaxial loading and wetting sequence test. The mould has the following specifications:

- Full dimensions: 200mm × 400mm × 600mm height
- Detachable: one for sampling and the other for the loading and wetting test.
- Calibrated and made of a 12mm thick transparent acrylic or perspex material.
- Has two sharp thin sheets of 10 and 5mm thickness used to cut through the compacted layers to separate the sampling soils and the loading/wetting soils, after which the sampling section of the mould is removed and the loading/wetting side of the mould is made air tight with the 10mm sheet as wall and glued on to prevent leakage during soil inundation.

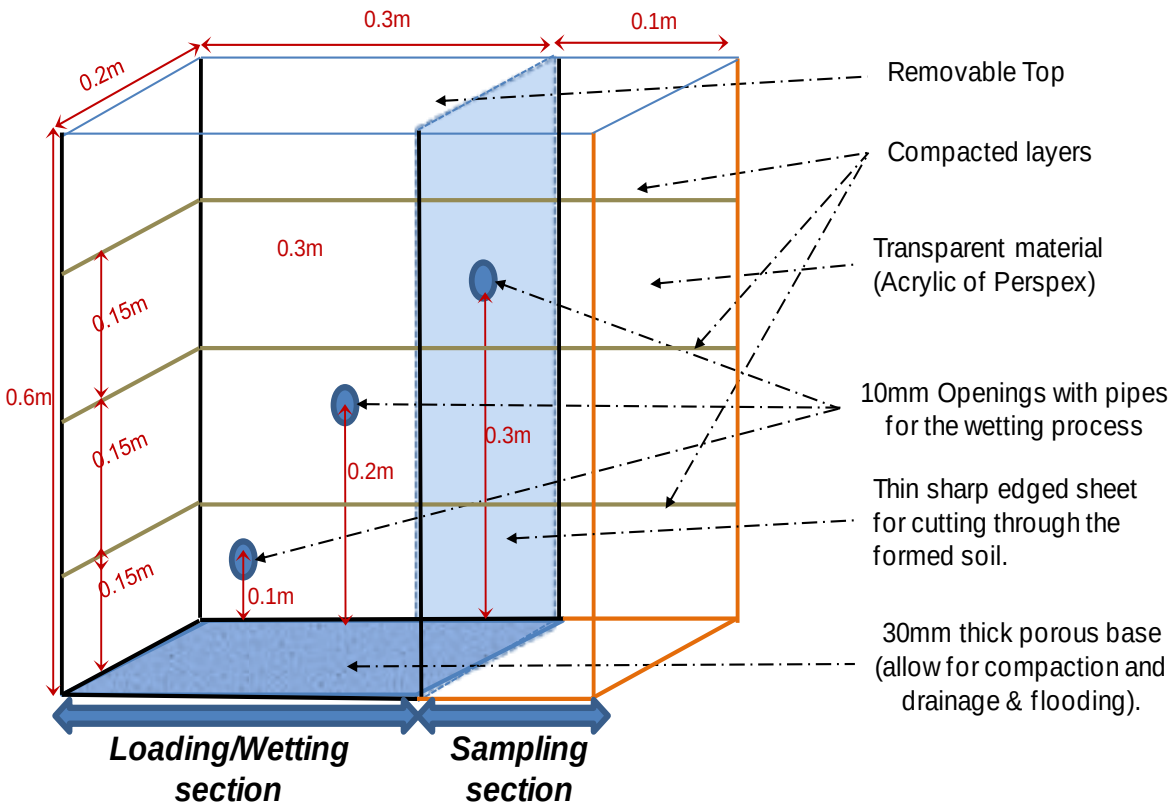

Figure 7.1 Modified uniaxial setup (citted in Okwedadi et al 2014)

7.1.2 Equipment

Fabricated calibrated mould (shown in Figure 7.1), compaction rammer, water source, weights

7.1.3 Compaction Specification

The soil is compacted into the mould by mean of a compressive machine, where the rate of compression is specified and the prepared soil is compressed at a constant rate. Hence controlling the density of the soil.

7.1.4 Wetting Fronts of the Soils

The mould is designed such that soil saturation from the bottom and other different 'near surface' wetting is possible.

7.1.5 Loading

The mould is designed to simulate structure/foundation loading. The loading is applied in two ways:

- Static loading in form of a plate loading test simulating a large scale oedometer testing.
- Incremental loading using CBR machine for the loading process.

Loading stress values within the range of a single-storey commercial/industrial/domestic structure is used with a net bearing pressure of 66.3kPa (Houston et al. 1998)

8 REFERENCES

Abelev, Y.M., (1948) *Fundamentals of Design and Construction on Macroporous Soils*. Moscow: Stroivoenmorizdat. Cited in Mansour Z.M., Chik Z. and Taha M.R. (2008) *On Soil Collapse Potential Evaluation* [online] available from <http://scialert.net/fulltext/?doi=jas.2008.4434.4439> [22 May 2010]

Al-Shayea, N.A., (2001). The combined effect of clay and moisture content on the behaviour of remoulded unsaturated soils. *Engineering geology*, **62**, 319 – 342.

Alawaji H.A. (2001) 'Settlement and bearing capacity of geogrid-reinforced sand over collapsible soil'. Geotextiles and Geomembranes 19, 75 – 88

Assalay A. M., Rogers C.D.F. and Smalley I. L. and Jefferson I. F. (1998) Silt: 2-62μm, 9-4φ. *Earth science Review* **45**, 61-88 cited in Derbyshire, E. & Meng, X.M. (2005). Loess. In: (Fookes, P.G., Lee, E.M. & Milligan, G. eds), Geomorphology for engineers, Whittles publishing, Dunbeath, Scotland, 688-728.

Assia B., Nabil A., and Said T. (2013). 'Potential Collapse for Clay soil'. International Journal of Engieering Technology and Advance Engineering, 3 (10) 43 – 47.

American Society for Testing and Materials, ASTM, Specifications.

Ayadat, T, and Hanna, A.M. (2012). Assessment of soil collapse prediction methods. *Scientific information database*, **25**, 1 – 19.

Barden, L., McGown, A. & Collins, K. (1973). The collapse mechanism in partly saturated soil. *Engineering Geology*, **7**, 49-60.

Basma, A.A. & Tuncer, E.R. (1992). Evaluation and control of collapsible soils. *Journal of Geotechnical Engineering,* 118 (**10**), 1491-1504.

Batygin V.I. (1937) "on the methods for estimate of soil subsidence." *Hydrotechnical construction* vol 7 Moscow. cited in Minkov M. (1984) "Quantitative prediction of collapsibility of loess soils." ed. by International Geological Congress, Bogdanov A.N. *Engineering geology: proceedings of the 27th International Geological congress*. The Netherland: VNU Science Press BV, **17**, 145 – 169.

Beckwith, G.H. (1995). Foundation design practices for collapsing soils in the western United States in Unsaturated soils. *In: Proceedings of the 1st International Conference on Unsaturated Soils*, Paris, France, 953 – 958.

Bell. F.G. (1992) Engineering Properties of Soils and Rocks, 3rd edition. Butterworth-Heinemann Ltd., Oxford.

Bell F.G. (2004) *Engineering geology and construction*. London: Spon Press

Blatt, H., (1970) Determination of mean sediment thickness in the crust: a sedimentologic method. Geological Society of America Bulletin 81, 255-262.

British Standards Institution (BSI). (1990). "British standard methods of test for soils for civil engineering purposes." *BS 1377-2*, London.

Catt J. A. (1978) The contributions of loess to soils in lowland Britain. In Limbrey S. and Evans J. G. (eds) The effect of man on the landscape: the lowland zone. *Council for British Archaeeology Research Report* **21**, 12-20 cited in Derbyshire, E. & Meng, X.M. (2005). Loess. In: (Fookes, P.G., Lee, E.M. & Milligan, G. eds), Geomorphology for engineers, Whittles publishing, Dunbeath, Scotland, 688-728.

Catt J. A. (2001) The agricultural importance of loess. *Earth science Reviews* **54**, 213-229 cited in Derbyshire, E. & Meng, X.M. (2005). Loess. In: (Fookes, P.G., Lee, E.M. & Milligan, G. eds), Geomorphology for engineers, Whittles publishing, Dunbeath, Scotland, 688-728.

Clevenger W.A. (1985) 'Experiences with loess as a foundation material'. Transactions American Society for Civil Engineers, 123, 51-80 cited in Rafie B., Moayed Z., and Esmaeli M. (2008) *Evaluation of Soil Collapsibility Potential: A Case Study of Semnan Railway Station* [online] available from <http://www.ejge.com/2008/Ppr0867/Ppr0867.pdf> [20 May 2010]

Conciani, W., Futai, M.M. and Soares, M.M. (1998) Plate Load Tests with Suction Measurements, in Problematic Soils, *Proceedings of the International Symposium on Problematic Soils*, E. Yanagisawa, N. Moroto, and T. Mitachi (eds), Vol. 1., Is-Tohoku,Japan, 28-30 October, A. A. Balkema, Rotterdam, pp. 301-304.

Das, S. (2004). Seismicity gaps and the shape of the seismic zone in the Banda Sea region from relocated hypocentres. Journal of Geophysical Research-Solid Earth. **10**, 1-18.

Darwell J. and Denness B. (1976) *Prediction of metastable soil collapse* [online] available from <http://iahs.info/redbooks/a121/iahs_121_0544.pdf> [20 May 2010]

Day, R.W. (2001) *Soil Testing Manual*. 1st Edn. New York: McGraw- Hill. Cited in Mansour Z.M., Chik Z. and Taha M.R. (2008) *On Soil Collapse Potential Evaluation* [online] available from <http://scialert.net/fulltext/?doi=jas.2008.4434.4439> [22 May 2010]

Denisov, N.Y. (1951) *The engineering properties of loess and loess-like soils (in Russian).* Moscow: Gosstroiizdat p.133. cited in Darwell J. and Denness B. (1976) *prediction of metastable soil collapse* [online] available from <http://iahs.info/redbooks/a121/iahs_121_0544.pdf> [20 May 2010]

Derbyshire E., Dijkstra T., Smalley J. Netherland (1995) ed *Genesis and properties of collapsible soils*. Kluwer Academic.

Derbyshire, E. & Meng, X.M. (2005). Loess. In: (Fookes, P.G., Lee, E.M. & Milligan, G. eds), Geomorphology for engineers, Whittles publishing, Dunbeath, Scotland, 688-728.

Derbyshire, E., Dijkstra, T.A., & Smalley, I.J. (eds) 1995. *Genesis and properties of collapsible soils.* Series C: Mathematical and Physical Sciences – Vol. 468. Kluwer Academic Publishers, Dordrecht.

Dudley, J.H. (1970). Review of collapsing soils. *Journal of Soil Mechanics and Foundation Division, ASCE,* 96 (3), 925-947.

El-Sohby, M. A., and Rabba, E. A. (1981). Some factors affecting swelling of clayey soils. *Geotechnical Engineering*, **12**, 19-39.

Evans, R.D., Jefferson, I., Northmore, K.J., Synac, O., and Serridge, C.J. (2004). Geophysical investigation and in-situ treatment of collapsible soils. Geotechnical Special Publication, n 126 II, Geotechnical Engineering for Transportation Projects: Proceedings of Geo-Trans, pp. 1848–1857.

Feda J. (1995) 'Mechanism of collapse of soil structure'. *Genesis and properties of collapsible soils*. eds. By Derbyshire E., Dijkstra T., Smalley J. Netherland: Kluwer Academic, 149 – 172

Feda, J. (1966). Structural stability of subsidence loess from Praha-Dejvice. *Engineering Geology*, **1**, 201-219.

Ferreira, S.R.M. and Lacerda, W.A. (1998) Volume Change Measurements in Collapsible Soils in Pernambuco Using Laboratory and Field Tests, in *Problematic Soils. In Proceedings of the International Symposium on Problematic Soils*, E. Yanagisawa, N. Moroto, and T. Mitachi (eds), Vol. 1., Is-Tohoku, Japan, 28-30, October. A. A. Balkema, Rotterdam, pp. 289-292.

Fookes, P. G. & Best, R. (1969). Consolidation characteristics of some late Pleistocene periglacial metastable soils of east Kent. Quarterly *Journal of Engineering Geology*, **2**, 103-128 cited in Derbyshire, E. & Meng, X.M. (2005). Loess. In: (Fookes, P.G., Lee, E.M. & Milligan, G. eds), Geomorphology for engineers, Whittles publishing, Dunbeath, Scotland, 688-728.

Fookes, P., and Parry, R. (1993) 'Engineering characteristics of arid soils.' Proc., 1st Int. Symp. on Engineering Characteristics of Arid Soils, Balkema, Rotterdam, The Netherlands cited in Houston, S.L., Houston, W.N. & Lawrence, C.A. (2002). Collapsible soil engineering in highway infrastructure development. *Journal of Transportation Engineering*, **3**, 295-300.

Fookes, P.G. and Parry, R.H.G., eds. (1994) Engineering Characteristics of Arid Soils, In *Proceedings of the First International Symposium on Engineering Characteristics of Arid Soils*, London, U.K., July 6-7, 1993, A. A. Balkema, Brookfield, VT.

Fredlund, D.G. and Xing, A. (1994) Equations for the soil-water characteristic curve, *Canadian Geotechnical Journal*, 31, 521-532.

Fredlund, M.,Wilson,G.W. and Fredlund,D.G. (1998) Estimation of Hydraulic Properties of an Unsaturated Soil Using a Knowledge-Based System, *In Proceedings of the Second International Conference on Unsaturated Soils*, Vol. 1, Beijing, International Academic Publisher, Beijing.

Frye J.C. (2009) 'Collapsible soils in Colorado [online] available from <http://geosurvey.state.co.us/hazards/Collapsible%20Soils/Pages/CollapsibleSoils.aspx> [22 May 2011]

Gaaver, K. E. (2012). Geotechnical properties of Egyptian collapsible soils. *Alexandria engineering journa*l, **51**, 205 – 210.

Gibbs, H.J. & Bara, J.P. (1962). Predicting surface subsidence from basic soil tests. *Special Technical Publication*, 332, ASTM, 231-247.

Gov (n.d) *sieve analysis of fine and coarse aggregates* [online] available from <http://www.in.gov/indot/files/T_27_aashtoB.pdf> [12 June 2010]

Gu, R., Chen, J., and Yuan J. (2014). Experimental analysis on influence of water content on nature of soil strength properties. *Electronic journal of geological engineering*, **19**, 3825 – 3830.

Habibagahi G. and Taherian M. (2004) 'Prediction of collapse potential for compacted soil using Artificial Neural networks'. Scientia Iranica **11**, 1 – 20

Handy, R. L. (1973). "Collapsible loess in Iowa" Soil. Sci. Soc. Am. Proc., **37**, , pp. 281-284. cited in Bell F.G. (2004) "Engineering geology and construction." London: Spon Press, pp 310.

Hong kong geology (2009) '*Weathering & erosion - Introduction to geomorphological processes*' [online] available from <http://hkss.cedd.gov.hk/hkss/eng/education/GS/eng/hkg/chapter4.htm> [6 September 2012]

Hormdee D., Ochiai H. and Yasufuku N. (2004) *Influence of stress history and socking pressure on collapsibility of Shirasu soil* [online] available from <http://www7.civil.kyushu-u.ac.jp/geotech/cd/pdf/381.pdf> [20 July 2010]

Horn, H.M., Deere, D.U., (1962). Frictional characterization of minerals. Geotechnique **12** No. 4, 319 – 335. cited in Al-Shayea, N.A., (2001). The combined effect of clay and moisture content on the behaviour of remoulded unsaturated soils. *Engineering geology*, **62**, 319 – 342.

Houston, S. L., Houston, W. N. (1997) Collapsible engineering. *Unsaturated soil engineering practice, geotechnical special publication No. 68, ASCE* (edited by Houston and fredlund).

Houston, S.L., Houston, W.N. & Lawrence, C.A. (2002). Collapsible soil engineering in highway infrastructure development. *Journal of Transportation Engineering*, 128 (3), 295-300.

Houston, S.L., Houston, W.N., Zapata, C.E. & Lawrence, C. (2001). Geotechnical engineering practice for collapsible soils. *Geotechnical and Geological Engineering,* **19**, 333-355.

Houston, S. L., Houston, W. N. & Spadola, D. J. (1988). Prediction of field collapse of soils due to wetting. *Journal of Geotechnical Engineering,* **114** (1), 40-58.

Houston, S. and El-Ehwany M. (1991) Sample Disturbance of Cemented Collapsible Soils. *J. of Geot. Division*, ASCE, 117(5), 731^752.

Iriondo M. H. (1997) Models of deposition of loess and loessoids in the Upper Quaternary of South America. *J. South American Earth sciences* **10**, 71-79 cited in Derbyshire, E. & Meng, X.M. (2005). Loess. In: (Fookes, P.G., Lee, E.M. & Milligan, G. eds), Geomorphology for engineers, Whittles publishing, Dunbeath, Scotland, 688-728.

Jardine R. J., Potts D. M. and Higgins K. G. (2004) *Advances in geotechnical engineering: the Skempton conference.* London: Thomas Telford Ltd

Jefferson, I., and Rogers, C. D. F. (2012). ICE Manual of Geotechnical Engineering Volume 1. Geotechnical Engineering Principles, *Problematic Soils and Site Investigation*, 391-411.

Jefferson, I.F., Smalley, I.J., 1999. Saltating sand erodes metastable loess: events in the impact zone. In: Skidmore, E.L., Tatarko, J. (Eds.), WERU 50 Symposium, USDA Manhattan, Kansas. </http://www.weru.ksu.edu/symposium/proceed.htmS>

Jennings, and Burland, (1962). Limitations to the use of effective stresses in partly saturated soils. *Geotechnique*, **12,** No. 2, 125–144.

Jenning J.E.B. and Knight K. (1957) 'the additional settlement of foundations due to collapse of structure of sandy subsoil on wetting.' Proc. 4th international conference on soil mechanism and foundation engineering 1, 316 -319 cited in Pererira, J.H.F. & Fredlund, D.G. (2000). Volume change behavior of collapsible compacted gneiss soil. *Journal of Geotechnical and Geoenvironmental Engineering,* 126 (10), 907-916

Jennings, J. E. and Knight, K. 1975. *A guide to construction on or with materials exhibiting additional settlement due to collapse of grain structure*. In: Proceedings of the 6th African Conference on Soil Mechanics and Foundation Engineering, Durban, 99-105.

Khattab, S.A.A., Bahhe, S.W.I., Al-Juari, K.A.K., (2007). Role of clay addiction on the stability of collapsible soil. *Al-Rafidain Engineering journal*, **15**, No. 4. 1 - 30

Lawton, E. C., Frasgaszy, R. J., and Hetherington, M. D. (1992). Review of wetting-induced collapse in compacted soil. *Journal of Geotechnical Engineering,* **118**, 1376-1394.

Lehr H. (1967) Foundation engineering problems in loess soils. Proc. 3rd Asian Reg. Conf.SMFE 1 (6), 20-24. Cited in Darwell J. and Denness B. (1976) *Prediction of metastable soil collapse* [online] available from <http://iahs.info/redbooks/a121/iahs_121_0544.pdf> [20 May 2010]

Lefebvre G. (1995). Collapse mechanisms and design considerations for some partly saturated and saturated soils. *Genesis and properties of collapsible soils*. eds. By Derbyshire E., Dijkstra T., Smalley J. Netherland: Kluwer Academic, 361 - 374.

Lin J., Tang C., Wang D., Pei X., and Shi B. (2014). 'Effect of Discrete Fibre Reinforcement on Soil Tensile Strength'. *Journal of Rock Mechanics and Geotechnical Engineering*, **6**, 133 – 137.

Lin, Z. (1995) 'Variability in collapsibility and strength of loess with age.' Genesis and properties of collapsible soils, NATO ASI Series C: Mathematical and Physical Sciences, Kluwer Academic, Dordrecht,The Netherlands, 468, 247–265 cited in Houston, S.L., Houston, W.N. & Lawrence, C.A. (2002). Collapsible soil engineering in highway infrastructure development. *Journal of Transportation Engineering*, (3), 295-300.

Livingstone, I., Warren, A., (1996) Aeolian Geomorphology. Longman, Harlow, 211

Lutenegger, A.J. and Saber, R.T. (1988). Determination of collapse potential of soils. Geotech. Test. J., 11: 173-178 cited in Mansour Z.M., Chik Z. and Taha M.R. (2008) *On Soil Collapse Potential Evaluation* [online] available from <http://scialert.net/fulltext/?doi=jas.2008.4434.4439> [22 May 2010]

Manion W. P. (2010) *Atterberg Limits: Soil Mechanics Laboratory* [online] available from <http://www.civil.umaine.edu/cie366/Atterberg_limits/default.htm> [18 June 2010]

Mansour Z.M., Chik Z. and Taha M.R. (2008) *On Soil Collapse Potential Evaluation* [online] available from <http://scialert.net/fulltext/?doi=jas.2008.4434.4439> [22 May 2010]

Maswoswe, J., 1985. Stress path for a compacted soil during collapse due to wetting. Ph.D thesis, Imperial College, London cited in Pererira, J.H.F. & Fredlund, D.G. (2000). Volume change behaviour of collapsible compacted gneiss soil. *Journal of Geotechnical and Geoenvironmental Engineering,* 126 (10), 907-916

Medero G. M., Sehnaid F., Gehling W. Y. Y. (2009) 'Oedometer behavior of an artificial cemented highly collapsible soil'. Journal of geotechnical and geoenvironmental engineering **135**, 840 – 843

Milodowski, A.E., Northmore, K.J., Kemp, S.J., McKervey, J.A., Bouch, J.E., Entwisle, D.C., Gunn, D.A., Jackson, P.D., Boardman, D.I., Zourmpakis, A., Rogers, C.D.F., Dixon, N., Jefferson, I., Smalley, I.J., 7 Clarke, M. (2012). The Mineralogy and Fabric of 'Brickearths@ and their Relationship to Engineering Properties. *Engineering Geology. (in press)*.

Minkov M. (1984) “Quantitative prediction of collapsibility of loess soils.” ed. by International Geological Congress, Bogdanov A.N. *Engineering geology: proceedings of the 27th International Geological congress*. The Netherland: VNU Science Press BV, **17**, 145 – 169.

Mitchell J.K. (1976) fundamentals of soil behaviour. New York: Wiley cited in Pererira, J.H.F. & Fredlund, D.G. (2000). Volume change behaviour of collapsible compacted gneiss soil. *Journal of Geotechnical and Geoenvironmental Engineering,* 126 (10), 907-916

Mitchell J.K. (1993) Fundamentals of soil behaviour. 2nd ed. Wiley, New York. cited in Al-Shayea, N.A., (2001). The combined effect of clay and moisture content on the behaviour of remoulded unsaturated soils. *Engineering geology*, **62**, 319 – 342.

Neemifar, O., Yasrobi, S.S., (2012). Collapse surface characteristics of clayey sands. *Geotechnical Engineering*, **165**, 379 – 390.

Northmore, K.N. Jefferson, I., Jackson PD, Entwisle DC, Milodowski AE, Raines MR, Gunn DA, Boardman DI, Zourmpakis A, Nelder LM, Rogers CDF, Dixon N, Smalley IJ, and Derbyshire E (2008). *On-Site Characterisation of Loessic Brickearth Deposits at Ospringe, Kent, UK.* Proceedings on the Institution of Civil Engineers, Geotechnical Engineering, **161**, 3-17.

Nouaouria M.S., Guenfoud M., Lafifi B. (2008) ‘Engineering properties of loess in Algeria’ in Engineering Geology **99**, 85–90.

Nuntasarn R. (2011) the Undrained shear strength Khon Kaen Loess. Unsaturated soils: Theory and Practice 2011. ed. by Jotisankasa, Sawangsuriya, Soralump and Mainraing, Thailand: Kasetsart university, 197 - 202

Okwedadi A.C., Ng'ambi S., Jefferson I. (2014) 'Laboratory Testing Regime for Quantifying Soil Collapsibility' *International Journal of Environmental, Ecological and Marine Engineering*, **8** (12), 769 -774.

Owen L.A., Derbyshire E., White B.J. and Remdell H. (1992) Loessic silt deposits in the western Himalayas: their sedimentology, genesis and age. *Catena* **19**, 493-509 cited in Derbyshire, E. & Meng, X.M. (2005). Loess. In: (Fookes, P.G., Lee, E.M. & Milligan, G. eds), Geomorphology for engineers, Whittles publishing, Dunbeath, Scotland, 688-728.

Pereira, J.H.F., Fredlund D.G., Caradao Neto M.P., and Gitirana Jr. G.F.N. (2005). Hydraulic behavior of collapsible compacted Gneiss soil. *Journal of Geotechnical and Geoenvironmental Engineering,* **131** (10) 1264 – 1273.

Pereira, J.H.F., and Fredlund, D.G. (2000). Volume change behaviour of collapsible compacted gneiss soil. *Journal of Geotechnical and Geoenvironmental Engineering,* 126 (10), 907-916

Priklonskij, V.A. (1952) *Vtoriaia Chast (Soil Science II)*. Gosgeolizdat, Moscow: Gruntovedenie. p.371. cited in Darwell J. and Denness B. (1976) *prediction of metastable soil collapse* [online] available from <http://iahs.info/redbooks/a121/iahs_121_0544.pdf> [20 May 2010]

Prokopovich, N.P. (1984) 'Validity of density – liquid limit predictions of hydrocompaction' Bulletin of the Association of Engineering Geologists. 21(2), 191-205 cited in Williams T. and Rollins K.M. (1991) *Collapsible soil hazard map for the cedar city, Utah area* [online] available from <http://ugspub.nr.utah.gov/publications/contract_reports/CR-91-10.pdf> [22 July 2010]

Pye, K., Sherwin, 1999. Loess. In: Goudie, A.S., Livingstone, I., Stokes, S. (Eds.), Aeolian Environments Sediments and Landforms. Wiley, Chichester, pp. 213–240.

Rabbi A.T.Z., Cameron D.A., and Rahman M.M. (2014). 'Role of Matric Suction On Wetting-Induced Collapse Settlement of Silty Sand'. In *Unsaturation soils: Research and Application.* ed. by Russell K. and Khoshghalb, Taylor and Francis group, 129 – 135.

Rafie, B., Moayed, Z., and Esmaeli, M. (2008). *Evaluation of Soil Collapsibility Potential: A Case Study of Semnan Railway Station.* Imam Khomeini International University of Qazvin, Iran. 13.

Rampino, C., Mancuso, C. and Vinale, F. (1998) Swelling/Collapse Behaviour of a Dynamically Compacted Silty Sand, in Problematic Soils. In *Proceedings of the International Symposium on Problematic Soils*, E. Yanagisawa, N. Moroto and T. Mitachi (eds), Vol. 1., Is-Tohoku, Japan, 28^30 October, A. A. Balkema, Rotterdam, pp. 321-324.

Rezaei, M., Ajalloeian. R., Ghafoori, M. (2012). Geotechnical properties of problematic soils emphasis on collapsible cases. *International journal of geosciences*, **3**, 105 – 110.

Reznik Y.M. (2007) 'Influence of physical properties on deformation characteristics of collapsible soils'. Engineering Geology 92, 27–37

Rogers C.D.F. (1995) 'Types and distribution of collapsible soil'. *Genesis and properties of collapsible soils*. eds. By Derbyshire E., Dijkstra T., Smalley J. Netherland: Kluwer Academic, 1-17

Sayago J. M. (1995) The Argentine neotropical loess. Quaternary Science Reviews 14, 755-766 cited in Derbyshire, E. & Meng, X.M. (2005). Loess. In: (Fookes, P.G., Lee, E.M. and Milligan, G. eds), Geomorphology for engineers, Whittles publishing, Dunbeath, Scotland, 688-728.

Seleam S. (2006). Evaluation of Collapsibility of Gypseous soils in Iraq. Journal of engineering 13 (3) 712 – 726.

SKC student (n.d) *LOESS* [online] available from <http://www.edu.pe.ca/southernkings/loesssp.htm> [14 May 2010]

Smalley, I.J., (1966). The properties of glacial loess and the formation of loess deposits. J. Sediment. Petrol. 36, 669–676.

Smalley, I.J., (1970) Cohesion of soil particles and the intrinsic resistance of simple soil systems to wind erosion. Journal of Soil Science 21, 154–161.

Smalley I.J.,. Mavlyanova N.G, Rakhmatullaev Kh.L., Shermatov M.Sh., Machalett B., O'Hara Dhand K., Jefferson I.F. (2006) 29. The formation of loess deposite in the Tashkent region and parts of central Asia; and problems with irrigation, hydrocollapse and soil erosion. Quaternary International 152–153 59–69

Steven L., And Pawlak, P.E. (n.d) *Evaluation, Design and Mitigation of Project Sites in Collapsible Soil Areas in Western Colorado* [online] available from <http://www.hpgeotech.com/pdf%20files/slp%20paper.pdf> [20 May 2010]

Swan C. C. (n.d) *Foundations on Weak and/or compressible Soils* [online] available from <http://www.icaen.uiowa.edu/~swan/courses/53139/notes/weak_compressible_soils.pdf> [12 May 2010]

Tadepalli R. and Fredlund D.G. (1991). The Collapse Behaviour of a Compacted Soil during Inundation. *Canadian Geotechnical Journal*, **28**, 477 – 488.

Tokar, R.A. (1937). "A quantitative characteristic of macro-porous loess soils". Eng. Geological studies for civil engineering purposes. No 7, Leningrad. cited in Minkov M. (1984) "Quantitative prediction of collapsibility of loess soils." ed. by International Geological Congress, Bogdanov A.N. *Engineering geology: proceedings of the 27th International Geological congress*. The Netherland: VNU Science Press BV, **17**, 145 – 169.

Torrance K. J. (1995) 'Post-deformational process in high-sensitivity fin-grained, collapsible sediments'. *Genesis and properties of collapsible soils*. eds. By Derbyshire E., Dijkstra T., Smalley J. Netherland: Kluwer Academic, 295 – 311

Uchaipichat A. (2010) 'Hydraulic hysteresis effect on compressibility of unsaturated soils'. ARPN Journal of Engineering and Applied Sciences **5**, 92 – 97

Waltham, T., Bell, F.G., Culshaw, M.G., (2005). Sinkholes and Subsidence: Karst and Cavernous Rocks in Engineering and Construction. Springer Praxis Publishing, Chichester, UK, 379.

Wang, S., Chan, D., Lam, K.C., (2009). Experimental study of the effect of fines content on dynamic compaction grouting in completely decomposed granite of Hong Kong. *Construction and building materials,* **23**, 1249 – 1264.

Wentworth C. K. (1933) fundamental limits of the sizes of classic grains. *Science* **77**, 633 – 634 cited in Derbyshire, E. & Meng, X.M. (2005). Loess. In: (Fookes, P.G., Lee, E.M. & Milligan, G. eds), Geomorphology for engineers, Whittles publishing, Dunbeath, Scotland, 688-728.

Williams T. and Rollins K.M. (1991) *Collapsible soil hazard map for the cedar city, Utah area* [online] available from <http://ugspub.nr.utah.gov/publications/contract_reports/CR-91-10.pdf> [22 July 2010]

Wright J.S. (2001a) "Desert" loess versus "glacial" loess: quartz silt formation source areas and sediment pathways in the formation of loess deposits. Geomorphology 36, 231–256.

Wright J.S. (2001b) Making loess-sized quartz silt: data from laboratory simulations and implications for sediment transport pathways and the formation of 'desert' loess deposits associated with the Sahara. Quaternary International 76/77, 7-19.

Wright J., Smith B., Whalley B., (1998) 31. Mechanism of loess-sized quartz silt production and their relationship effectiveness: laboratory simulation. Geomorphology 23, 15–34

Zapata C.E. (1999) *Uncertainty in Soil-Water Characteristic Curve and Impacts on Unsaturated Shear Strength Predictions*. PhD. Dissertation, Arizona State University, Tempe, United States.

Zur, A. And Wiseman, G. (1973). A study of collapse phenomena of an undisturbed loess. 8th CSMFE, 2.2. Moscow. cited in Minkov M. (1984) "Quantitative prediction of collapsibility of loess soils." ed. by International Geological Congress, Bogdanov A.N. *Engineering geology: proceedings of the 27th International Geological congress*. The Netherland: VNU Science Press BV, **17**, 145 – 169.

APPENDIX

A

Soils' Classification – Sieve / Hydrometer analysis test, Atterberg test and compaction test

1. Sieve / Hydrometer test

Table A.1.1: Sieve analysis of Soil A - Brown silty clay with a total sample weight of 50g

Sieve size		Weight	Percentage	Percentage
BS designation	Metric	retained	retained	passing
	(mm)	(g)	(%)	(%)
No. 7	2.36			100.00
No. 14	1.18	0.05	0.10	99.90
No. 25	0.600	0.08	0.16	99.74
No. 36	0.425	0.15	0.30	99.44
No. 52	0.300	0.44	0.88	98.56
NO. 72	0.212	1.52	3.04	95.52
No. 100	0.150	6.23	12.46	83.06
No. 200	0.075	2.48	4.96	78.10

Table A.1.2: Hydrometer analysis reading of Soil A - Brown silty clay with a total sample weight of 50g

Elapsed tme,(min)	Time (mins)	Temp (º c)	Direct hydrometer readings Rh'	Reading Rh'	Rh=Rh' + Cm	Hr (mm)	Viscosity	D (mm)	Temp Corr,Mt	Rd= Rh'-Ro'+Mt	K (%)
0.50	7:50	28.00	1.0220	22.00	22.5	111.7250	0.8279	0.0595	1.7861	20.1861	65.60
1.00	7:51	28.00	1.0210	21.00	21.5	115.6750	0.8279	0.0428	1.7861	19.1861	62.35
2.00	7:52	28.00	1.0190	19.00	19.5	123.5750	0.8279	0.0313	1.7861	17.1861	55.85
4.00	7:54	28.00	1.0180	18.00	18.5	127.5250	0.8279	0.0225	1.7861	16.1861	52.60
8.00	7:58	28.00	1.0175	17.50	18.0	129.5000	0.8279	0.0160	1.7861	15.6861	50.98
15.00	8:05	28.00	1.0155	15.50	16.0	137.4000	0.8279	0.0120	1.7861	13.6861	44.48
30.00	8:20	28.00	1.0140	14.00	14.5	143.3250	0.8279	0.0087	1.7861	12.1861	39.60
60.00	8:50	28.00	1.0125	12.50	13.0	149.2500	0.8279	0.0063	1.7861	10.6861	34.73
120.00	9:50	28.00	1.0115	11.50	12.0	153.2000	0.8279	0.0045	1.7861	9.6861	31.48
240.00	11:50	27.00	1.0100	10.00	10.5	159.1250	0.8472	0.0033	1.5249	7.9249	25.76
1440.00	7:50	25.00	1.0090	9.00	9.5	163.0750	0.8879	0.0014	1.0349	6.4348	20.91

Table A.1.3: Sieve analysis of Soil B - White silty fine sand with a total sample weight of 50g

Sieve size		Weight retained (g)	Percentage retained (%)	Percentage passing (%)
BS designation	Metric (mm)			
No. 7	2.36			100.00
No. 14	1.18	0.66	1.32	98.68
No. 25	0.600	0.43	0.86	97.82
No. 36	0.425	0.28	0.56	97.26
No. 52	0.300	0.34	0.68	96.58
NO. 72	0.212	0.48	0.96	95.62
No. 100	0.150	1.08	2.16	93.46
No. 200	0.075	0.47	0.94	92.52

Table A.1.4: Hydrometer analysis reading of Soil B - White silty fine sand with a total sample weight of 50g

Elapsed tme,(min)	Time (mins)	Temp (º c)	Direct hydrometer readings Rh'	Reading Rh'	Rh=Rh' + Cm	Hr (mm)	Viscosity	D (mm)	Temp Corr,Mt	Rd= Rh'-Ro'+Mt	K (%)
0.50	7:50	28.00	1.0275	27.50	28.0	90.0000	0.8279	0.0534	1.7861	25.6861	83.48
1.00	7:51	28.00	1.0265	26.50	27.0	93.9500	0.8279	0.0386	1.7861	24.6861	80.23
2.00	7:52	28.00	1.0255	25.50	26.0	97.9000	0.8279	0.0278	1.7861	23.6861	76.98
4.00	7:54	28.00	1.0245	24.50	25.0	101.8500	0.8279	0.0201	1.7861	22.6861	73.73
8.00	7:58	28.00	1.0240	24.00	24.5	103.8250	0.8279	0.0143	1.7861	22.1861	72.10
15.00	8:05	28.00	1.0225	22.50	23.0	109.7500	0.8279	0.0108	1.7861	20.6861	67.23
30.00	8:20	28.00	1.0220	22.00	22.5	111.7250	0.8279	0.0077	1.7861	20.1861	65.60
60.00	8:50	28.00	1.0195	19.50	20.0	121.6000	0.8279	0.0057	1.7861	17.6861	57.48
120.00	9:50	28.00	1.0167	16.70	17.2	132.6600	0.8279	0.0042	1.7861	14.8861	48.38
240.00	11:50	28.00	1.0130	13.00	13.5	147.2750	0.8279	0.0031	1.7861	11.1861	36.35
1440.00	7:50	25.00	1.0105	10.50	11.0	157.1500	0.8879	0.0014	1.0349	7.9348	25.79

Table A.1.5: Sieve analysis of Soil C - Red clay with a total sample weight of 45g

Sieve size		Weight retained (g)	Percentage retained (%)	Percentage passing (%)
BS designation	Metric (mm)			
No. 7	2.36			100.00
No. 14	1.18	0.01	0.02	99.98
No. 25	0.600	0.02	0.04	99.93
No. 36	0.425	0.02	0.04	99.89
No. 52	0.300	0.04	0.09	99.80
NO. 72	0.212	0.17	0.38	99.42
No. 100	0.150	1.64	3.64	95.78
No. 200	0.075	0.94	2.09	93.69

Table A.1.6: Hydrometer analysis reading of Soil C - Red clay with a total sample weight of 45g

Elapsed tme,(min)	Time (mins)	Temp (º c)	Direct hydrometer readings Rh'	Reading Rh'	Rh=Rh' + Cm	Hr (mm)	Viscosity	D (mm)	Temp Corr,Mt	Rd= Rh'-Ro'+Mt	K (%)
0.50	7:50	28.00	1.0250	25.00	25.5	99.8750	0.8279	0.0562	1.7861	23.1861	83.73
1.00	7:51	28.00	1.0230	23.00	23.5	107.7750	0.8279	0.0413	1.7861	21.1861	76.51
2.00	7:52	28.00	1.0210	21.00	21.5	115.6750	0.8279	0.0303	1.7861	19.1861	69.28
4.00	7:54	28.00	1.0190	19.00	19.5	123.5750	0.8279	0.0221	1.7861	17.1861	62.06
8.00	7:58	28.00	1.0180	18.00	18.5	127.5250	0.8279	0.0159	1.7861	16.1861	58.45
15.00	8:05	28.00	1.0175	17.50	18.0	129.5000	0.8279	0.0117	1.7861	15.6861	56.64
30.00	8:20	28.00	1.0160	16.00	16.5	135.4250	0.8279	0.0085	1.7861	14.1861	51.23
60.00	8:50	28.00	1.0143	14.30	14.8	142.1400	0.8279	0.0061	1.7861	12.4861	45.09
120.00	9:50	28.00	1.0130	13.00	13.5	147.2750	0.8279	0.0044	1.7861	11.1861	40.39
240.00	11:50	27.00	1.0120	12.00	12.5	151.2250	0.8472	0.0032	1.5249	9.9249	35.84
1440.00	7:50	25.00	1.0105	10.50	11.0	157.1500	0.8879	0.0014	1.0349	7.9348	28.65

Table A.1.7: Sieve analysis of Soil D - Brown clayey sand with a total sample weight of 50g

Sieve size		Weight retained (g)	Percentage retained (%)	Percentage passing (%)
BS designation	Metric (mm)			
No. 7	2.36	0.08	0.16	99.84
No. 14	1.18	4.35	8.70	91.14
No. 25	0.600	4.16	8.32	82.82
No. 36	0.425	3.79	7.58	75.24
No. 52	0.300	4.74	9.48	65.76
NO. 72	0.212	5.51	11.02	54.74
No. 100	0.150	7.08	14.16	40.58
No. 200	0.075	0.98	1.96	38.62

Table A.1.8: Hydrometer analysis reading of Soil D - Brown clayey sand with a total sample weight of 50g

Elapsed tme,(min)	Time (mins)	Temp (º c)	Direct hydrometer readings Rh'	Reading Rh'	Rh=Rh' + Cm	Hr (mm)	Viscosity	D (mm)	Temp Corr,Mt	Rd= Rh'-Ro'+Mt	K (%)
0.50	7:50	28.00	1.0115	11.50	12.0	153.2000	0.8279	0.0696	1.7861	9.6861	31.48
1.00	7:51	28.00	1.0105	10.50	11.0	157.1500	0.8279	0.0499	1.7861	8.6861	28.23
2.00	7:52	28.00	1.0100	10.00	10.5	159.1250	0.8279	0.0355	1.7861	8.1861	26.60
4.00	7:54	28.00	1.0090	9.00	9.5	163.0750	0.8279	0.0254	1.7861	7.1861	23.35
8.00	7:58	28.00	1.0089	8.90	9.4	163.4700	0.8279	0.0180	1.7861	7.0861	23.03
15.00	8:05	28.00	1.0080	8.00	8.5	167.0250	0.8279	0.0133	1.7861	6.1861	20.10
30.00	8:20	28.00	1.0075	7.50	8.0	169.0000	0.8279	0.0094	1.7861	5.6861	18.48
60.00	8:50	28.00	1.0065	6.50	7.0	172.9500	0.8279	0.0068	1.7861	4.6861	15.23
120.00	9:50	28.00	1.0060	6.00	6.5	174.9250	0.8279	0.0048	1.7861	4.1861	13.60
240.00	11:50	27.00	1.0050	5.00	5.5	178.8750	0.8472	0.0035	1.5249	2.9249	9.51
1440.00	7:50	25.00	1.0042	4.20	4.7	182.0350	0.8879	0.0015	1.0349	1.6348	5.31

Table A.1.8: Sieve / Hydrometer analysis result of Soil A - D

A - Brown silty clay		B - White silty fine sand		C - Red clay		D - Brown clayey sand	
Sieve size	**Percentage Passing**	**Sieve size**	**Percentage Passing**	**Sieve size**	**Percentage Passing**	**Sieve size**	**Percentage Passing**
(mm)	**(%)**	**(mm)**	**(%)**	**(mm)**	**(%)**	**(mm)**	**(%)**
2.360	100.00	2.360	100.00	2.360	100.00	3.18	100.0
1.180	99.90	1.180	98.68	1.180	98.82	2.360	99.84
0.600	99.74	0.600	97.82	0.600	98.22	1.180	91.14
0.425	99.44	0.425	97.26	0.425	97.80	0.600	82.82
0.300	98.56	0.300	96.58	0.300	97.50	0.425	75.24
0.212	95.52	0.212	95.62	0.212	97.28	0.300	65.76
0.150	83.06	0.150	93.46	0.150	97.13	0.212	54.74
0.075	78.10	0.075	92.52	0.075	97.06	0.150	40.58
0.059	65.60	0.053	83.48	0.056	83.73	0.075	38.62
0.043	62.35	0.039	80.23	0.041	76.51	0.070	31.48
0.031	55.85	0.028	76.98	0.030	69.28	0.050	28.23
0.022	52.60	0.020	73.73	0.022	62.06	0.035	26.60
0.016	50.98	0.014	72.10	0.016	58.45	0.025	23.35
0.012	44.48	0.011	67.23	0.012	56.64	0.018	23.03
0.0087	39.60	0.0077	65.60	0.0085	51.23	0.013	20.10
0.0063	34.73	0.0057	57.48	0.0061	45.09	0.0094	18.48
0.0045	31.48	0.0042	48.38	0.0044	40.39	0.0068	15.23
0.0033	25.76	0.0031	36.35	0.0032	35.84	0.0048	13.60
0.0014	20.91	0.0014	25.79	0.0014	28.65	0.0035	9.51
0.0003	0.00	0.0003	0.00	0.0003	0.00	0.0015	5.31
						0.0003	0.00

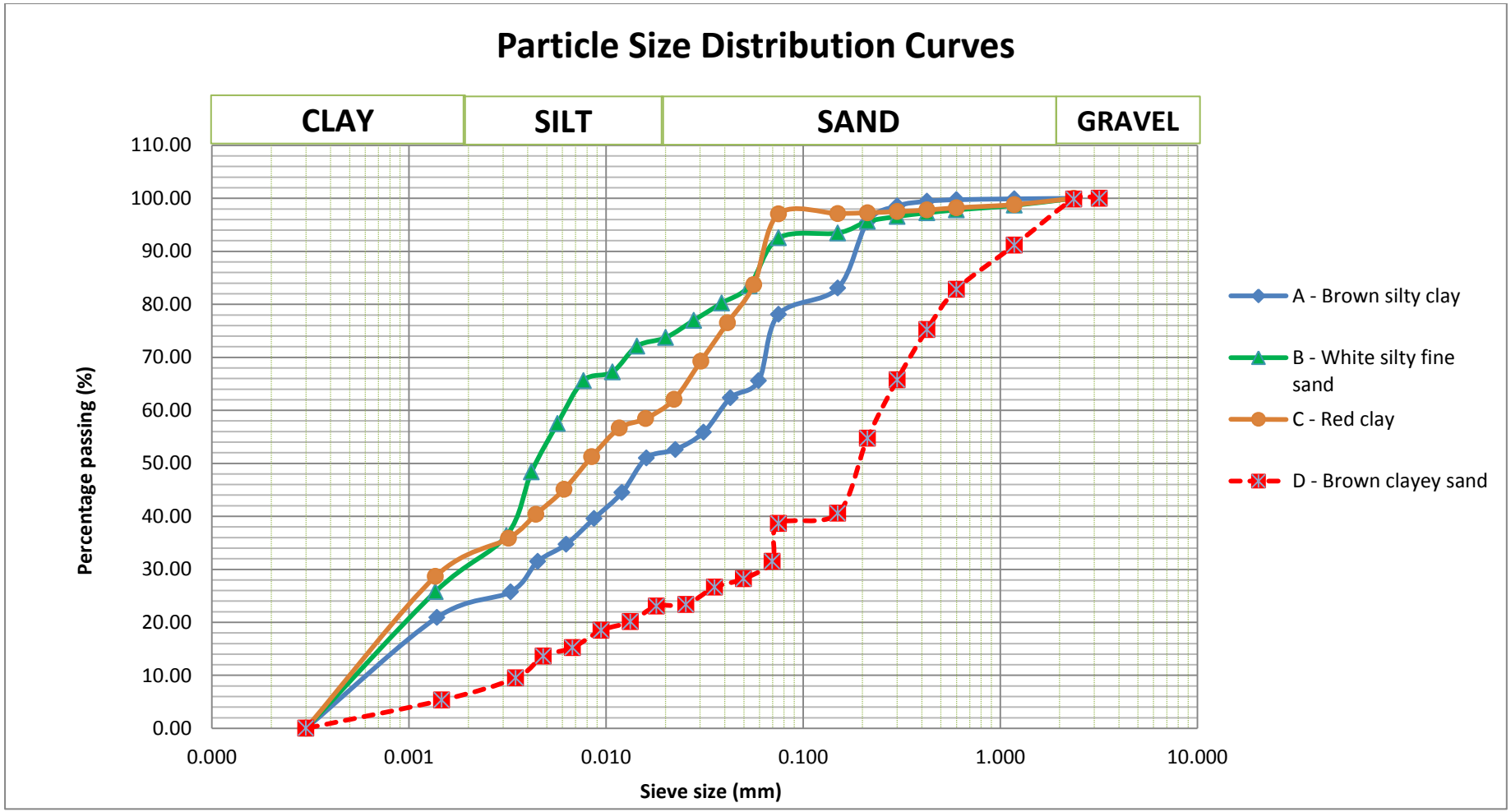

Figure A.1.1: Sieve / Hydrometer result curves of Soil A - D

2. Atterberg limits

Table A.2.1: Liquid limit values for Soil A - Brown silty clay

Liquid Limit at 20mm penetration = 30.1%									
	PENETRATION			MOISTURE CONTENT					
Test	1st readings	2nd reading	**Penetration (mm)**	Weight of container (g)	Container + Wet soil (g)	Container + Dry soil (g)	Weight of Wet soil (g)	Weight of Dry soil (g)	**Moisture content (%)**
1	0.0	117.0	**11.70**	15.80	32.70	29.30	16.90	13.50	**25.19**
2	0.0	197.0	**19.70**	15.80	32.30	28.50	16.50	12.70	**29.92**
3	0.0	237.0	**23.70**	15.80	32.60	28.40	16.80	12.60	**33.33**
4	0.0	280.0	**28.00**	15.90	44.40	37.30	28.50	21.40	**33.18**

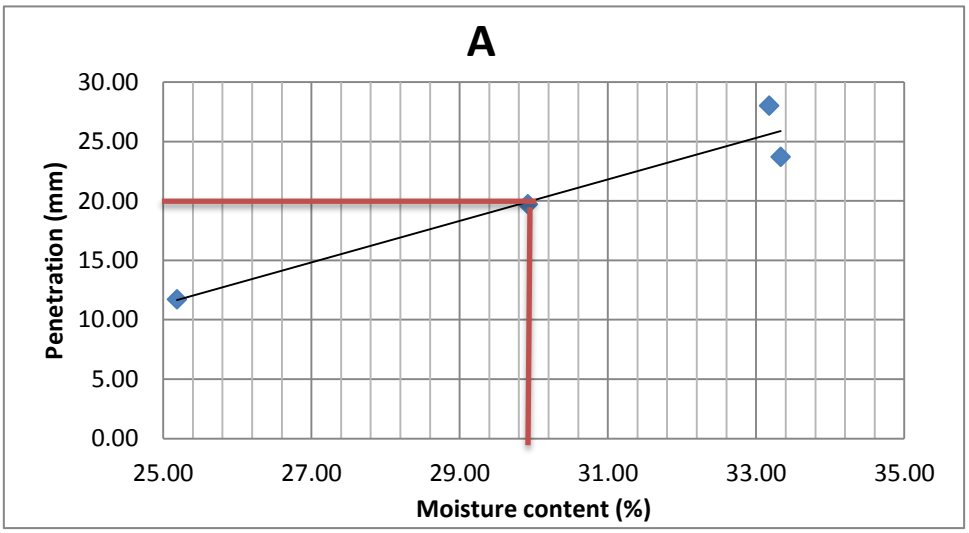

Figure A.2.1: Liquid limit linear graph for Soil A - Brown silty clay

Table A.2.2: Plastic limit values for Soil A - Brown silty clay

Plastic limit			
	Test 1	Test 2	Test 3
Weight of container (g)	15.90	15.70	17.10
Container + wet soil (g)	23.20	24.30	22.80
Container + dry soil (g)	21.80	22.70	21.70
Weight of Wet soil (g)	7.30	8.60	5.70
Weight of Dry Soil (g)	5.90	7.00	4.60
Moisture Content (%)	23.73	22.86	23.91
Av. Moisture Content (%)	23.50		

Table A.2.3: Liquid limit values for Soil B - White silty fine sand

Liquid Limit at 20mm penetration = 25.70%									
	PENETRATION			MOISTURE CONTENT					
Test	1st readings	2nd reading	**Penetration (mm)**	Weight of container (g)	Container + Wet soil (g)	Container + Dry soil (g)	Weight of Wet soil (g)	Weight of Dry soil (g)	**Moisture content (%)**
1	0.0	142.0	**14.20**	16.40	31.00	28.10	14.60	11.70	**24.79**
2	0.0	246.0	**24.60**	14.00	30.90	27.30	16.90	13.30	**27.07**
3	0.0	251.0	**25.10**	15.90	39.60	34.60	23.70	18.70	**26.74**
4	0.0	167.0	**16.70**	16.00	45.80	39.90	29.80	23.90	**24.69**
5	0.0	197.0	**19.70**	16.00	38.80	34.20	22.80	18.20	**25.27**

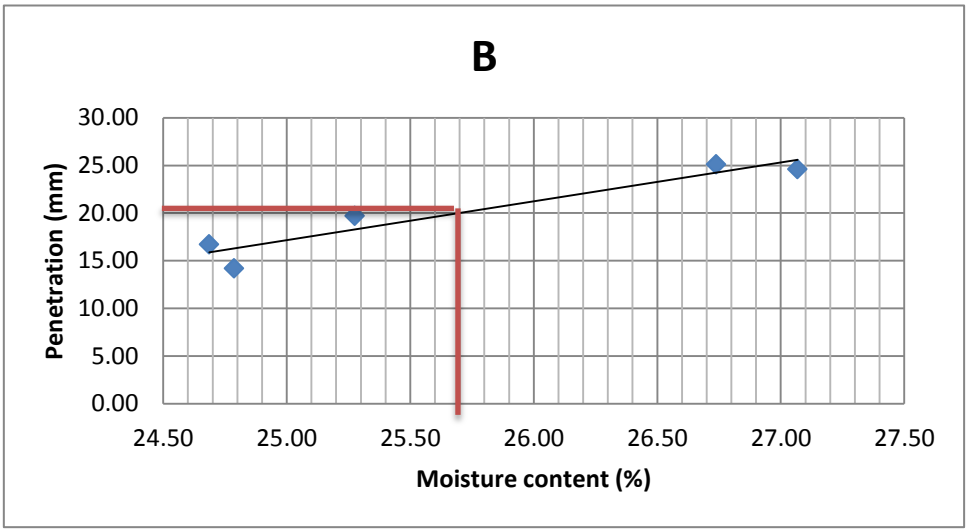

Figure A.2.2: Liquid limit linear graph for Soil B - White silty fine sand

Table A.2.4: Plastic limit values for Soil B - White silty fine sand

Plastic limit			
	Test 1	Test 2	Test 3
Weight of container (g)	16.10	15.90	16.40
Container + wet soil (g)	27.00	24.60	25.50
Container + dry soil (g)	25.00	23.00	23.80
Weight of Wet soil (g)	10.90	8.70	9.10
Weight of Dry Soil (g)	8.90	7.10	7.40
Moisture Content (%)	22.47	22.54	22.97
Av. Moisture Content (%)	22.66		

Table A.2.5: Liquid limit values for Soil C - Red clay

Liquid Limit at 20mm penetration = 36.80%									
	PENETRATION			MOISTURE CONTENT					
Test	1st readings	2nd reading	**Penetration (mm)**	Weight of container (g)	Container + Wet soil (g)	Container + Dry soil (g)	Weight of Wet soil (g)	Weight of Dry soil (g)	**Moisture content (%)**
1	0.0	132.0	**13.20**	15.80	41.90	35.70	26.10	19.90	**31.16**
2	0.0	199.0	**19.90**	16.10	51.30	41.70	35.20	25.60	**37.50**
3	0.0	225.0	**22.50**	16.60	57.30	45.80	40.70	29.20	**39.38**
4	0.0	275.0	**27.50**	17.20	63.50	49.90	46.30	32.70	**41.59**

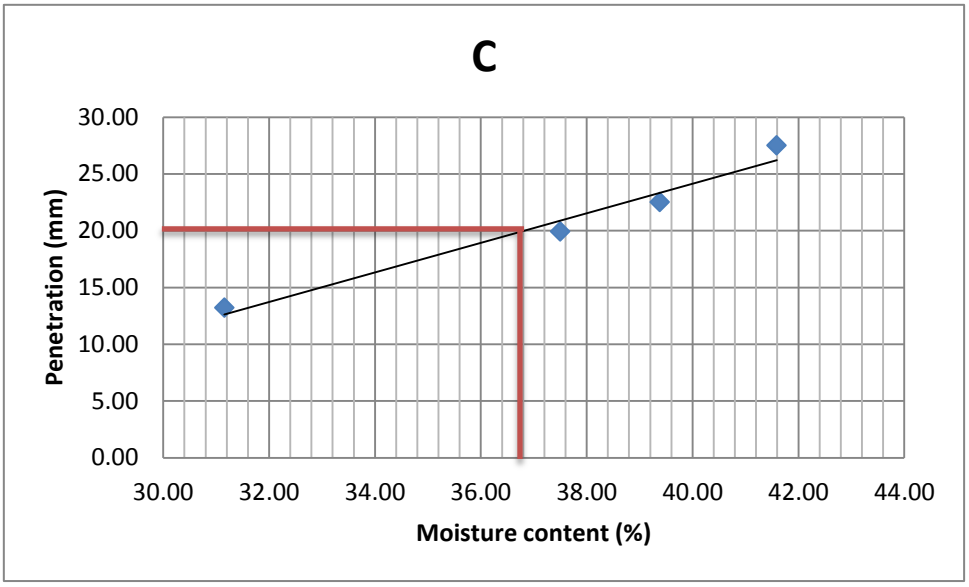

Figure A.2.3: Liquid limit linear graph for Soil C - Red clay

Table A.2.6: Plastic limit values for Soil C - Red clay

Plastic limit			
	Test 1	Test 2	Test 3
Weight of container (g)	15.90	15.60	16.30
Container + wet soil (g)	26.20	27.70	27.80
Container + dry soil (g)	24.10	25.20	25.40
Weight of Wet soil (g)	10.30	12.10	11.50
Weight of Dry Soil (g)	8.20	9.60	9.10
Moisture Content (%)	25.61	26.04	26.37
Av. Moisture Content (%)	26.01		

Table A.2.7: Liquid limit values for Soil D - Brown clayey sand

Liquid Limit at 20mm penetration = 23.40%									
	PENETRATION			MOISTURE CONTENT					
Test	1st readings	2nd reading	**Penetration (mm)**	Weight of container (g)	Container + Wet soil (g)	Container + Dry soil (g)	Weight of Wet soil (g)	Weight of Dry soil (g)	**Moisture content (%)**
1	0.0	109.0	**10.90**	15.70	39.00	35.20	23.30	19.50	**19.49**
2	0.0	172.0	**17.20**	16.60	47.70	41.90	31.10	25.30	**22.92**
3	0.0	260.0	**26.00**	15.80	48.40	41.90	32.60	26.10	**24.90**
4	0.0	265.0	**26.50**	16.20	43.90	38.10	27.70	21.90	**26.48**

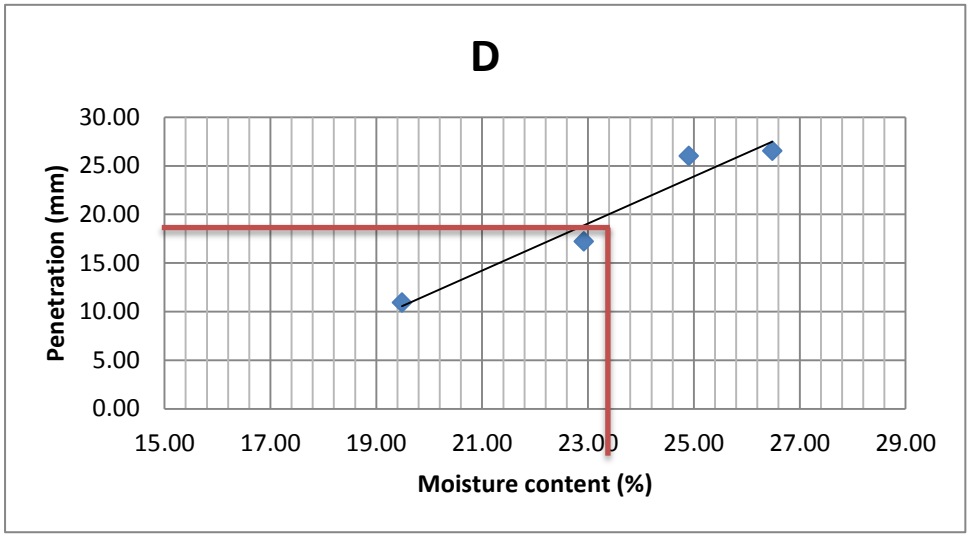

Figure A.2.4: Liquid limit linear graph for Soil D - Brown clayey sand

Table A.2.8: Plastic limit values for Soil D - Brown clayey sand

Plastic limit			
	Test 1	Test 2	Test 3
Weight of container (g)	14.40	15.90	17.30
Container + wet soil (g)	28.40	30.10	31.50
Container + dry soil (g)	26.40	28.00	29.40
Weight of Wet soil (g)	14.00	14.20	14.20
Weight of Dry Soil (g)	12.00	12.10	12.10
Moisture Content (%)	16.67	17.36	17.36
Av. Moisture Content (%)	17.13		

Table A.2.8: Liquid limit, Plastic limit and Plasticity index values for Soil A, B, C and D.

Soils	ATTERBERG LIMITS (%)		
	LIQUID LIMIT	PLASTIC LIMIT	PLASTICITY INDEX
A	30.10	23.50	6.60
B	25.70	22.66	3.04
C	36.80	26.01	10.79
D	23.40	17.13	6.27

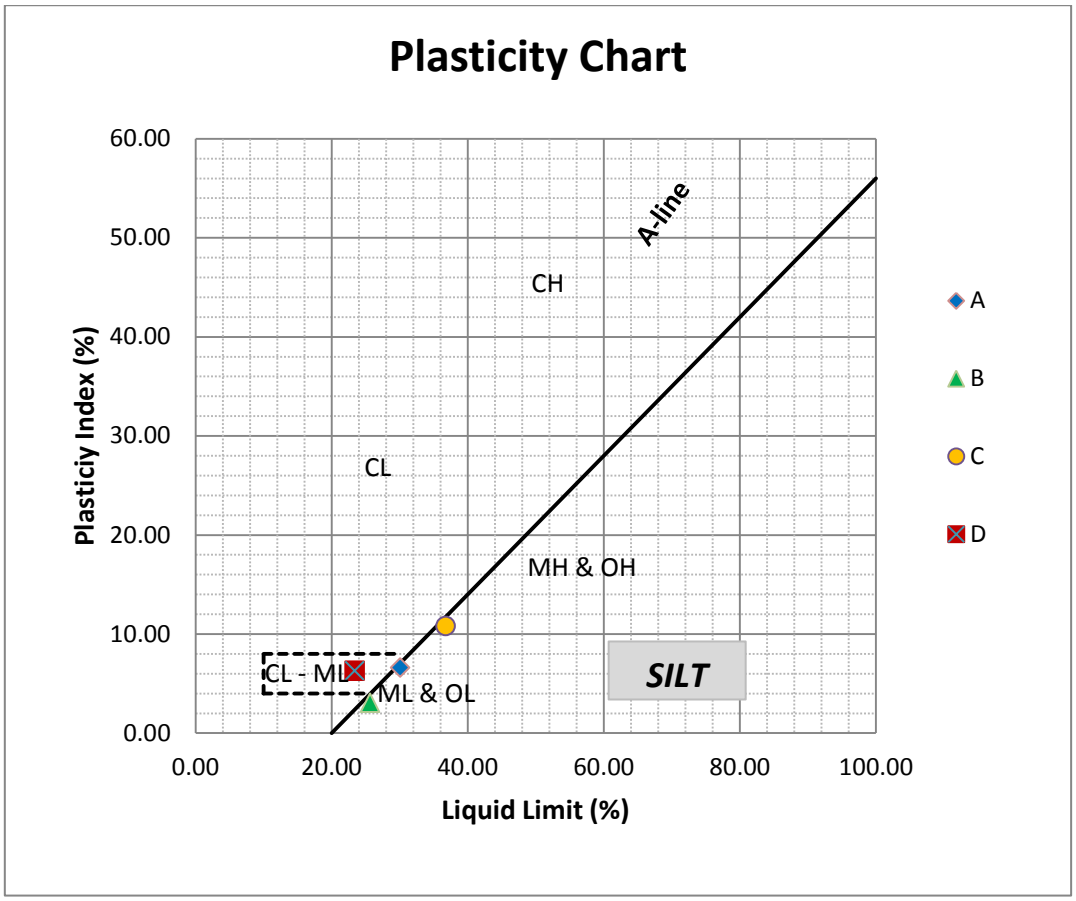

Figure A.2.5: Graph of Plasticity index for Soils A, B, C and D.

3. Compaction

Table A.3.1: Compaction values for Soil A - Brown silty clay

	Compaction 1	Compaction 2	Compaction 3	Compaction 4	Compaction 5
Mass of cylinder + wet sample(g)	5167.3	5355.2	5475	5390.3	5341.8
Mass of cylinder (g)	3340	3340	3340	3340	3340
Mass of wet sample(g)	1827.3	2015.2	2135	2050.3	2001.8
Volume of Mould (cm^3)	1000	1000	1000	1000	1000
Bulk Density(g/cm^3)	1.8273	2.0152	2.135	2.0503	2.0018
Mass of container + wet sample(g)	64.00	68.60	68.70	89.90	106.90
Mass of container + dry sample(g)	60.40	62.80	61.70	77.90	90.10
Mass of container (g)	15.70	15.80	15.90	15.90	15.90
Mass of wet soil (g)	48.30	52.80	52.80	74.00	91.00
Mass of dry soil (g)	44.70	47.00	45.80	62.00	74.20
Mass of water (g)	3.60	5.80	7.00	12.00	16.80
Water content (%)	8.05	12.34	15.28	19.35	22.64
Dry density (g/cm^3)	1.69	1.79	1.85	1.72	1.63

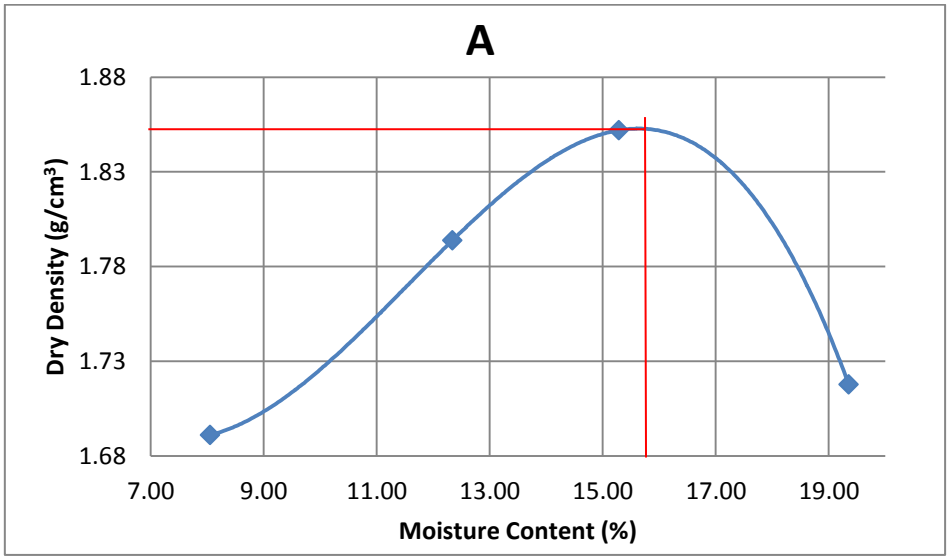

Fig A.3.1: Compaction graph of Soil A - Brown silty clay

Table A.3.2: Compaction values for Soil B - White silty fine sand

	Compaction 1	Compaction 2	Compaction 3	Compaction 4
Mass of cylinder + wet sample(g)	5058.9	5316.9	5373.3	5341.2
Mass of cylinder (g)	3340.6	3340.6	3340.6	3340.6
Mass of wet sample(g)	1718.3	1976.3	2032.7	2000.6
Volume of Mould (cm^3)	1000	1000	1000	1000
Bulk Density(g/cm^3)	1.7183	1.9763	2.0327	2.0006
mass of container+wet sample(g)	48.90	56.40	73.70	80.00
mass of container+dry sample(g)	46.30	52.20	64.20	67.90
mass of container (g)	17.20	17.00	17.10	15.60
mass of wet soil (g)	31.70	39.40	56.60	64.40
mass of dry soil (g)	29.10	35.20	47.10	52.30
mass of water (g)	2.60	4.20	9.50	12.10
water content (%)	8.93	11.93	20.17	23.14
dry density (g/cm^3)	1.58	1.77	1.69	1.62

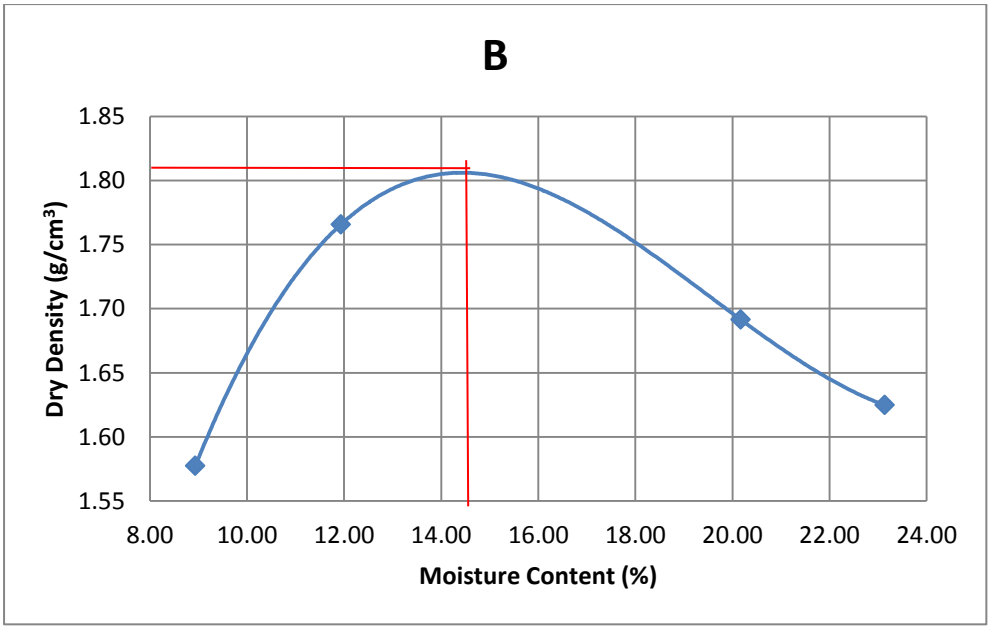

Fig A.3.2: Compaction graph of Soil B - White silty fine sand

Table A.3.3: Compaction values for Soil C - Red clay

	Compaction 1	Compaction 2	Compaction 3	Compaction 4
Mass of cylinder + wet sample(g)	5216.5	5438.6	5471.8	5400.4
Mass of cylinder (g)	3408.5	3408.5	3408.5	3408.5
Mass of wet sample(g)	1808	2030.1	2063.3	1991.9
Volume of Mould (cm^3)	1000	1000	1000	1000
Bulk Density(g/cm^3)	1.808	2.0301	2.0633	1.9919
Mass of container + wet sample(g)	59.80	59.20	68.90	82.80
Mass of container + dry sample(g)	55.20	53.40	59.70	69.90
Mass of container (g)	16.50	15.80	15.50	16.20
Mass of wet soil (g)	43.30	43.40	53.40	66.60
Mass of dry soil (g)	38.70	37.60	44.20	53.70
Mass of water (g)	4.60	5.80	9.20	12.90
Water content (%)	11.89	15.43	20.81	24.02
Dry density (g/cm^3)	1.62	1.76	1.71	1.61

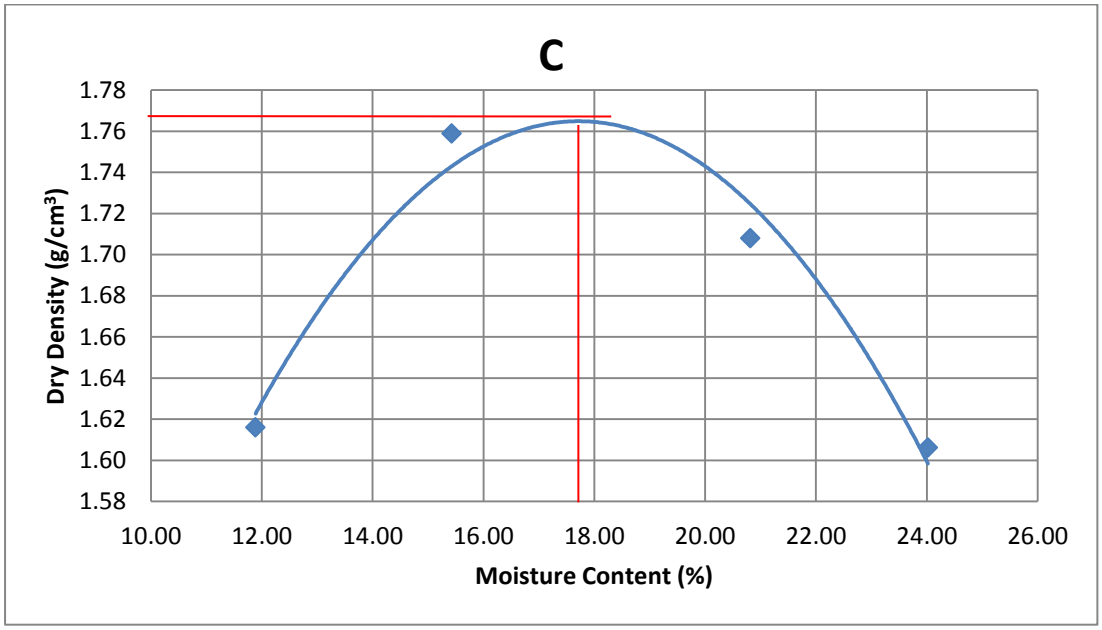

Fig A.3.3: Compaction graph of Soil C - Red clay

Table A.3.3: Compaction values for Soil D - Brown clayey sand

	Compaction 1	Compaction 2	Compaction 3	Compaction 4	Compaction 5
Mass of cylinder + wet sample(g)	5202.2	5316	5528.3	5477.8	5417.9
Mass of cylinder (g)	3341.7	3341.7	3341.7	3341.7	3341.7
Mass of wet sample(g)	1860.5	1974.3	2186.6	2136.1	2076.2
Volume of Mould (cm^3)	1000	1000	1000	1000	1000
Bulk Density(g/cm^3)	1.8605	1.9743	2.1866	2.1361	2.0762
Mass of container + wet sample(g)	62.30	59.60	72.00	98.30	98.00
Mass of container + dry sample(g)	60.20	56.30	66.20	87.80	85.40
Mass of container (g)	16.10	16.00	16.00	16.40	15.90
Mass of wet soil (g)	46.20	43.60	56.00	81.90	82.10
Mass of dry soil (g)	44.10	40.30	50.20	71.40	69.50
Mass of water (g)	2.10	3.30	5.80	10.50	12.60
Water content (%)	4.76	8.19	11.55	14.71	18.13
Dry density(g/cm^3)	1.78	1.82	1.96	1.86	1.76

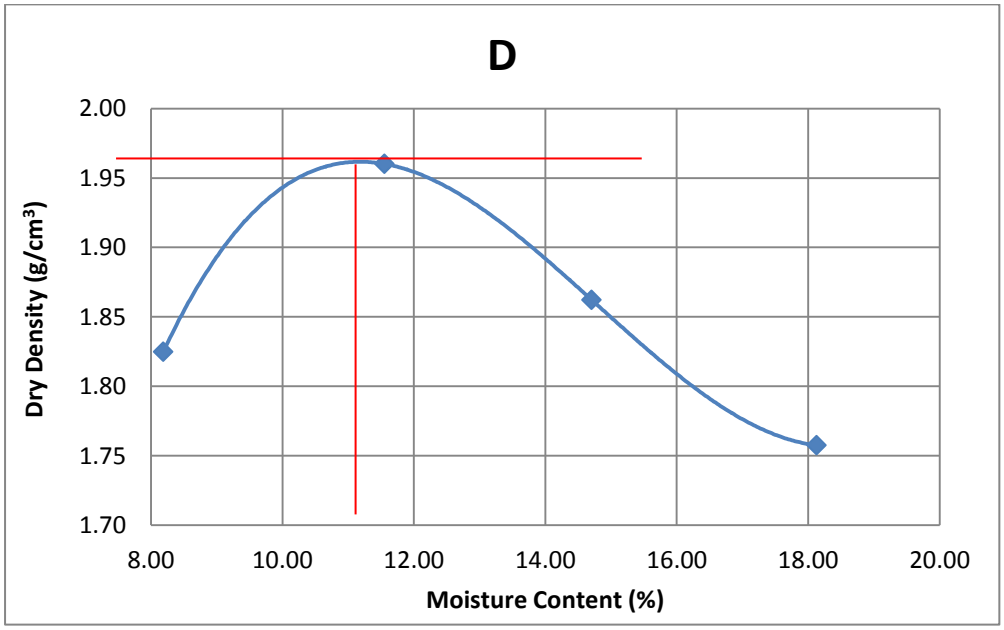

Fig A.3.3: Compaction graph of Soil D - Brown clayey sand

B

Triaxial Tests

1. *Soil A at Low dry of OMC (1)*

Table B.1.1: Initial parameters from preparation of sample A1.

Compaction test		
Mass of Mould + base (g)	3668.60	
Mass of Mould + base + soil (g)	5530.90	
Mass Soil (g)	1862.30	
Weight of container (g)	15.60	15.50
Container + wet soil (g)	55.70	64.40
Container + dry soil (g)	51.60	59.60
Moisture Content (%)	11.39	10.88
Av. Moisture Content (%)	11.14	
Volume of mould (cm^3)	1000	
Bulk Density (g/cm^3)	1.86	
Dry density (g/cm^3)	1.68	
Void ratio 'e_0' = $[(Gs*\rho_w/\rho_d)-1]$	0.731	
Degree of saturation 'Sr_i' (%)	44.203	

Table B.1.2: Initial parameters for sample A1 at confining pressure 'σ3' 70kPa.

Diameter of sample 'D_0' (mm)	37.60
Length of sample 'L_0' (mm)	72.40
20% strain of length (%)	14.48
Mass of Sample 'M_0' (g)	155.70
Area of sample 'A_0' (mm^2)	1110.81
Moisture content (%)	12.15
Young's modulus for latex membrane 'E_m' (kN/m^2)	1400.00
Thickness of membrane (0.1 - 0.2mm) 't_m' (mm)	0.15

Table B.1.3: Initial parameters for sample A1 at confining pressure 'σ3' 140kPa.

Diameter of sample 'D_0' (mm)	37.90
Length of sample 'L_0' (mm)	76.90
20% strain of length (%)	15.38
Mass of Sample 'M_0' (g)	166.20
Area of sample 'A_0' (mm^2)	1128.61
Moisture content (%)	11.84
Young's modulus for latex membrane 'E_m' (kN/m^2)	1400.00
Thickness of membrane (0.1 - 0.2mm) 't_m' (mm)	0.15

Table B.1.4: Initial parameters for sample A1 at confining pressure 'σ3' 280kPa.

Diameter of sample 'D_0' (mm)	38.00
Length of sample 'L_0' (mm)	76.20
20% strain of length (%)	15.24
Mass of Sample 'M_0' (g)	169.90
Area of sample 'A_0' (mm^2)	1134.57
Moisture content (%)	11.73
Young's modulus for latex membrane 'E_m' (kN/m^2)	1400.00
Thickness of membrane (0.1 - 0.2mm) 't_m' (mm)	0.15

Table B.1.5: Triaxial test values for sample A1 at confining pressure 'σ3' 70kPa.

Strain guage reading (yellow (bottom) gauge)	Force guage reading (white (top) gauge)	Change in sample length 'ΔL' (mm)	Axial strain 'Ea'	Corrected Area 'Ac' (mm^2)	Axial Force 'P' (N)	Axial Stress 'σ_1-σ_3' (KN/m^2)	Rubber membrane 'R_m' (KN/m^2)	Corrected Axial Stress 'σ_1-σ_3' (KN/m^2)	Axial strain 'Ea' (%)
Sr	**Fr**	Sr*0.01	$\Delta L/L_0$	$A_0/(1+Ea)$	(100/37)*Fr	P/Ac	$(4.E_m.t_m.Ea)/D_0$	σ_1-σ_3' -R_m	Ea*100%
0.00	0.00	0.00	0.0000	1110.81	0.00	0.00	0.00	0.00	0.00
50.00	59.00	0.50	0.0069	1103.19	159.46	144.54	0.15	144.39	0.69
100.00	96.00	1.00	0.0138	1095.68	259.46	236.80	0.31	236.49	1.38
200.00	140.00	2.00	0.0276	1080.95	378.38	350.04	0.62	349.43	2.76
300.00	172.00	3.00	0.0414	1066.61	464.86	435.83	0.93	434.91	4.14
400.00	179.00	4.00	0.0552	1052.65	483.78	459.58	1.23	458.35	5.52
500.00	170.00	5.00	0.0691	1039.05	459.46	442.19	1.54	440.65	6.91
600.00	178.00	6.00	0.0829	1025.80	481.08	468.98	1.85	467.13	8.29
700.00	188.00	7.00	0.0967	1012.88	508.11	501.65	2.16	499.49	9.67
800.00	185.00	8.00	0.1105	1000.28	500.00	499.86	2.47	497.39	11.05
900.00	190.00	9.00	0.1243	987.99	513.51	519.75	2.78	516.98	12.43
1000.00	195.00	10.00	0.1381	976.00	527.03	539.98	3.09	536.90	13.81
1100.00	192.00	11.00	0.1519	964.30	518.92	538.13	3.39	534.74	15.19
1200.00	193.00	12.00	0.1657	952.88	521.62	547.42	3.70	543.72	16.57
1300.00	196.00	13.00	0.1796	941.72	529.73	562.51	4.01	558.50	17.96
1400.00	196.00	14.00	0.1934	930.82	529.73	569.10	4.32	564.78	19.34
1500.00	199.00	15.00	0.2072	920.17	537.84	584.50	4.63	579.87	20.72

Table B.1.6: Triaxial test values for sample A1 at confining pressure 'σ3' 140kPa.

Strain guage reading (yellow (bottom) gauge)	Force guage reading (white (top) gauge)	Change in sample length 'ΔL' (mm)	Axial strain 'Ea'	Corrected Area 'Ac' (mm^2)	Axial Force 'P' (N)	Axial Stress 'σ_1-σ_3' (KN/m^2)	Rubber membrane 'R_m' (KN/m^2)	Corrected Axial Stress 'σ_1-σ_3' (KN/m^2)	Axial strain 'Ea' (%)
Sr	**Fr**	Sr*0.01	$\Delta L/L_0$	$A_0/(1+Ea)$	(100/37)*Fr	P/Ac	$(4.E_m.t_m.Ea)/D_0$	σ_1-σ_3' -R_m	Ea*100%
0.00	0.00	0.00	0.0000	1110.81	0.00	0.00	0.00	0.00	0.00
50.00	78.00	0.50	0.0069	1103.19	210.81	191.09	0.15	190.94	0.69
100.00	127.00	1.00	0.0138	1095.68	343.24	313.27	0.31	312.96	1.38
200.00	186.00	2.00	0.0276	1080.95	502.70	465.06	0.62	464.44	2.76
300.00	218.00	3.00	0.0414	1066.61	589.19	552.39	0.93	551.47	4.14
400.00	242.00	4.00	0.0552	1052.65	654.05	621.34	1.23	620.10	5.52
500.00	258.00	5.00	0.0691	1039.05	697.30	671.09	1.54	669.55	6.91
600.00	270.00	6.00	0.0829	1025.80	729.73	711.38	1.85	709.52	8.29
700.00	280.00	7.00	0.0967	1012.88	756.76	747.13	2.16	744.97	9.67
800.00	288.00	8.00	0.1105	1000.28	778.38	778.16	2.47	775.69	11.05
900.00	294.00	9.00	0.1243	987.99	794.59	804.25	2.78	801.47	12.43
1000.00	298.00	10.00	0.1381	976.00	805.41	825.21	3.09	822.12	13.81
1100.00	302.00	11.00	0.1519	964.30	816.22	846.43	3.39	843.04	15.19
1200.00	305.00	12.00	0.1657	952.88	824.32	865.09	3.70	861.39	16.57
1300.00	305.00	13.00	0.1796	941.72	824.32	875.34	4.01	871.33	17.96
1400.00	306.00	14.00	0.1934	930.82	827.03	888.49	4.32	884.17	19.34
1500.00	307.00	15.00	0.2072	920.17	829.73	901.71	4.63	897.09	20.72
1600.00	308.00	16.00	0.2210	909.76	832.43	915.00	4.94	910.07	22.10

Table B.1.7: Triaxial test values for sample A1 at confining pressure 'σ3' 280kPa.

Strain guage reading (yellow (bottom) gauge)	Force guage reading (white (top) gauge)	Change in sample length 'ΔL' (mm)	Axial strain 'Ea'	Corrected Area 'Ac' (mm^2)	Axial Force 'P' (N)	Axial Stress 'σ_1-σ_3' (KN/m^2)	Rubber membrane 'R_m' (KN/m^2)	Corrected Axial Stress 'σ_1-σ_3' (KN/m^2)	Axial strain 'Ea' (%)
Sr	**Fr**	Sr*0.01	$\Delta L/L_0$	$A_0/(1+Ea)$	(100/37)*Fr	P/Ac	$(4.E_m.t_m.Ea)/D_0$	σ_1-σ_3' -R_m	Ea*100%
0.00	0.00	0.00	0.0000	1110.81	0.00	0.00	0.00	0.00	0.00
50.00	80.00	0.50	0.0069	1103.19	216.22	195.99	0.15	195.84	0.69
100.00	165.00	1.00	0.0138	1095.68	445.95	407.00	0.31	406.70	1.38
200.00	263.00	2.00	0.0276	1080.95	710.81	657.58	0.62	656.96	2.76
300.00	312.00	3.00	0.0414	1066.61	843.24	790.58	0.93	789.65	4.14
400.00	360.00	4.00	0.0552	1052.65	972.97	924.30	1.23	923.07	5.52
500.00	394.00	5.00	0.0691	1039.05	1064.86	1024.84	1.54	1023.30	6.91
600.00	426.00	6.00	0.0829	1025.80	1151.35	1122.39	1.85	1120.54	8.29
700.00	455.00	7.00	0.0967	1012.88	1229.73	1214.09	2.16	1211.93	9.67
800.00	480.00	8.00	0.1105	1000.28	1297.30	1296.93	2.47	1294.46	11.05
900.00	502.00	9.00	0.1243	987.99	1356.76	1373.24	2.78	1370.47	12.43
1000.00	522.00	10.00	0.1381	976.00	1410.81	1445.50	3.09	1442.41	13.81
1100.00	537.00	11.00	0.1519	964.30	1451.35	1505.08	3.39	1501.69	15.19
1200.00	549.00	12.00	0.1657	952.88	1483.78	1557.16	3.70	1553.46	16.57
1300.00	556.00	13.00	0.1796	941.72	1502.70	1595.70	4.01	1591.69	17.96
1400.00	558.50	14.00	0.1934	930.82	1509.46	1621.65	4.32	1617.33	19.34
1500.00	562.00	15.00	0.2072	920.17	1518.92	1650.70	4.63	1646.07	20.72
1600.00	567.00	16.00	0.2210	909.76	1532.43	1684.44	4.94	1679.50	22.10

Fig B.1.1: Triaxial test graph for Sample A1

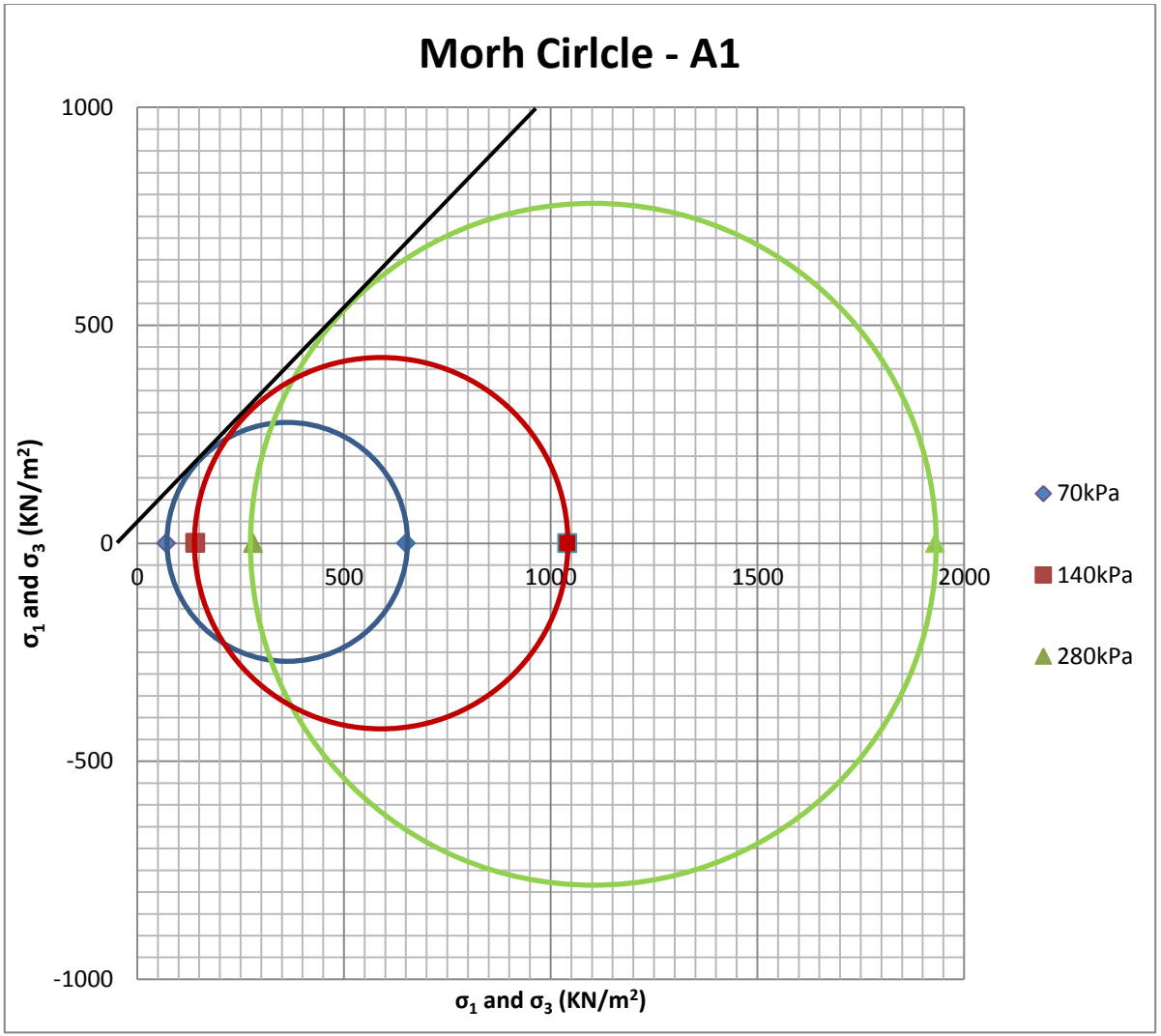

Fig B.1.2: Morh circle graph for Sample A1

Table B.1.18: Stress strength parameters for sample A1.

Result from graph	0	70kPa	140kPa	280kPa
Deviator stress (max) $'\sigma_1-\sigma_3'$ (KN/m^2)	0	580	900	1650
Normal stress $'\sigma_3'$ (KN/m^2)	0	70	140	280
Shear stress $'\sigma_1'$ (KN/m^2)	0	650	1040	1930
Mean Stress $'[1/3('\sigma_1+2\sigma_3]'$ (KN/m2)	0.0	263.3	440.0	830.0
Internal angle of friction (^{o})	43.15			
Cohesion (KN/m2)	50			

2. *Soil A at High dry of OMC (2)*

Table B.2.1: Initial parameters from preparation of sample A2.

Compaction test		
Mass of Mould + base (g)	3665.80	
Mass of Mould + base + soil (g)	5739.20	
Mass Soil (g)	2073.40	
Weight of container (g)	15.80	15.50
Container + wet soil (g)	43.00	38.00
Container + dry soil (g)	39.70	35.30
Moisture Content (%)	13.81	13.64
Av. Moisture Content (%)	13.72	
Volume of mould (cm^3)	1000	
Bulk Density (g/cm^3)	2.07	
Dry density (g/cm^3)	1.82	
Void ratio $'e_0' = [(Gs*\rho_w/\rho_d)-1]$	0.591	
Degree of saturation $'Sr_i'$ (%)	67.379	

Table B.2.2: Initial parameters for sample A2 at confining pressure 'σ3' 70kPa.

Diameter of sample 'D_0' (mm)	37.3
Length of sample 'L_0' (mm)	77.2
20% strain of length (%)	15.44
Mass of Sample 'M_0' (g)	182.9
Area of sample 'A_0' (mm^2)	1093.16
Moisture content (%)	14.05
Young's modulus for latex membrane 'E_m' (kN/m^2)	1400
Thickness of membrane (0.1 - 0.2mm) 't_m' (mm)	0.15

Table B.2.3: Initial parameters for sample A2 at confining pressure 'σ3' 140kPa.

Diameter of sample 'D_0' (mm)	35.4
Length of sample 'L_0' (mm)	76.4
20% strain of length (%)	15.28
Mass of Sample 'M_0' (g)	164.6
Area of sample 'A_0' (mm^2)	984.63
Moisture content (%)	13.61
Young's modulus for latex membrane 'E_m' (kN/m^2)	1400
Thickness of membrane (0.1 - 0.2mm) 't_m' (mm)	0.15

Table B.2.4: Initial parameters for sample A2 at confining pressure 'σ3' 280kPa.

Diameter of sample 'D_0' (mm)	36.8
Length of sample 'L_0' (mm)	76.1
20% strain of length (%)	15.22
Mass of Sample 'M_0' (g)	186.9
Area of sample 'A_0' (mm^2)	1064.05
Moisture content (%)	14.25
Young's modulus for latex membrane 'E_m' (kN/m^2)	1400
Thickness of membrane (0.1 - 0.2mm) 't_m' (mm)	0.15

Table B.2.5: Triaxial test values for sample A2 at confining pressure 'σ3' 70kPa.

Strain guage reading (yellow (bottom) gauge)	Force guage reading (white (top) gauge)	Change in sample length 'ΔL' (mm)	Axial strain 'Ea'	Corrected Area 'Ac' (mm^2)	Axial Force 'P' (N)	Axial Stress 'σ_1-σ_3' (KN/m^2)	Rubber membrane 'R_m' (KN/m^2)	Corrected Axial Stress 'σ_1-σ_3' (KN/m^2)	Axial strain 'Ea' (%)
Sr	**Fr**	Sr*0.01	$\Delta L/L_0$	$A_0/(1+Ea)$	(100/37)*Fr	P/Ac	$(4.E_m.t_m.Ea)/D_0$	σ_1-σ_3' -R_m	Ea*100%
0.00	0.00	0.00	0.0000	1093.16	0.00	0.00	0.00	0.00	0.00
50.00	45.00	0.50	0.0065	1086.12	121.62	111.98	0.15	111.83	0.65
100.00	70.00	1.00	0.0130	1079.18	189.19	175.31	0.29	175.02	1.30
200.00	110.00	2.00	0.0259	1065.55	297.30	279.01	0.58	278.42	2.59
300.00	138.00	3.00	0.0389	1052.27	372.97	354.45	0.88	353.57	3.89
400.00	161.00	4.00	0.0518	1039.31	435.14	418.68	1.17	417.51	5.18
500.00	178.00	5.00	0.0648	1026.66	481.08	468.59	1.46	467.13	6.48
600.00	190.00	6.00	0.0777	1014.32	513.51	506.26	1.75	504.51	7.77
700.00	194.00	7.00	0.0907	1002.28	524.32	523.13	2.04	521.09	9.07
800.00	188.00	8.00	0.1036	990.51	508.11	512.97	2.33	510.64	10.36
900.00	185.00	9.00	0.1166	979.02	500.00	510.71	2.63	508.09	11.66
1000.00	194.00	10.00	0.1295	967.79	524.32	541.77	2.92	538.86	12.95
1100.00	199.00	11.00	0.1425	956.82	537.84	562.11	3.21	558.90	14.25
1200.00	204.00	12.00	0.1554	946.10	551.35	582.77	3.50	579.26	15.54
1300.00	205.00	13.00	0.1684	935.61	554.05	592.19	3.79	588.40	16.84
1400.00	205.00	14.00	0.1813	925.35	554.05	598.75	4.08	594.67	18.13
1500.00	207.00	15.00	0.1943	915.31	559.46	611.22	4.38	606.85	19.43
1600.00	210.00	16.00	0.2073	905.49	567.57	626.81	4.67	622.14	20.73

Table B.2.6: Triaxial test values for sample A2 at confining pressure 'σ3' 140kPa.

Strain guage reading (yellow (bottom) gauge)	Force guage reading (white (top) gauge)	Change in sample length 'ΔL' (mm)	Axial strain 'Ea'	Corrected Area 'Ac' (mm^2)	Axial Force 'P' (N)	Axial Stress 'σ_1-σ_3' (KN/m^2)	Rubber membrane 'R_m' (KN/m^2)	Corrected Axial Stress 'σ_1-σ_3' (KN/m^2)	Axial strain 'Ea' (%)
Sr	**Fr**	Sr*0.01	$\Delta L/L_0$	$A_0/(1+Ea)$	(100/37)*Fr	P/Ac	$(4.E_m.t_m.Ea)/D_0$	σ_1-σ_3' -R_m	Ea*100%
0.00	0.00	0.00	0.0000	1093.16	0.00	0.00	0.00	0.00	0.00
50.00	35.00	0.50	0.0065	1086.12	94.59	87.09	0.15	86.95	0.65
100.00	43.00	1.00	0.0130	1079.18	116.22	107.69	0.29	107.40	1.30
200.00	56.00	2.00	0.0259	1065.55	151.35	142.04	0.58	141.46	2.59
300.00	67.00	3.00	0.0389	1052.27	181.08	172.09	0.88	171.21	3.89
400.00	80.00	4.00	0.0518	1039.31	216.22	208.04	1.17	206.87	5.18
500.00	94.00	5.00	0.0648	1026.66	254.05	247.46	1.46	246.00	6.48
600.00	113.00	6.00	0.0777	1014.32	305.41	301.09	1.75	299.34	7.77
700.00	127.00	7.00	0.0907	1002.28	343.24	342.46	2.04	340.42	9.07
800.00	143.00	8.00	0.1036	990.51	386.49	390.19	2.33	387.85	10.36
900.00	157.00	9.00	0.1166	979.02	424.32	433.42	2.63	430.79	11.66
1000.00	179.00	10.00	0.1295	967.79	483.78	499.88	2.92	496.97	12.95
1100.00	190.00	11.00	0.1425	956.82	513.51	536.69	3.21	533.48	14.25
1200.00	204.00	12.00	0.1554	946.10	551.35	582.77	3.50	579.26	15.54
1300.00	213.00	13.00	0.1684	935.61	575.68	615.30	3.79	611.50	16.84
1400.00	221.00	14.00	0.1813	925.35	597.30	645.48	4.08	641.40	18.13
1500.00	225.00	15.00	0.1943	915.31	608.11	664.37	4.38	660.00	19.43
1600.00	226.00	16.00	0.2073	905.49	610.81	674.56	4.67	669.90	20.73

Table B.2.7: Triaxial test values for sample A2 at confining pressure 'σ3' 280kPa.

Strain guage reading (yellow (bottom) gauge)	Force guage reading (white (top) gauge)	Change in sample length 'ΔL' (mm)	Axial strain 'Ea'	Corrected Area 'Ac' (mm^2)	Axial Force 'P' (N)	Axial Stress 'σ_1-σ_3' (KN/m^2)	Rubber membrane 'R_m' (KN/m^2)	Corrected Axial Stress 'σ_1-σ_3' (KN/m^2)	Axial strain 'Ea' (%)
Sr	**Fr**	Sr*0.01	$\Delta L/L_0$	$A_0/(1+Ea)$	(100/37)*Fr	P/Ac	$(4.E_m.t_m.Ea)/D_0$	σ_1-σ_3' -R_m	Ea*100%
0.00	0.00	0.00	0.0000	1093.16	0.00	0.00	0.00	0.00	0.00
50.00	75.00	0.50	0.0065	1086.12	202.70	186.63	0.15	186.48	0.65
100.00	125.00	1.00	0.0130	1079.18	337.84	313.05	0.29	312.76	1.30
200.00	181.00	2.00	0.0259	1065.55	489.19	459.09	0.58	458.51	2.59
300.00	213.00	3.00	0.0389	1052.27	575.68	547.08	0.88	546.21	3.89
400.00	238.00	4.00	0.0518	1039.31	643.24	618.92	1.17	617.75	5.18
500.00	256.00	5.00	0.0648	1026.66	691.89	673.92	1.46	672.46	6.48
600.00	273.00	6.00	0.0777	1014.32	737.84	727.42	1.75	725.67	7.77
700.00	289.00	7.00	0.0907	1002.28	781.08	779.31	2.04	777.27	9.07
800.00	302.00	8.00	0.1036	990.51	816.22	824.03	2.33	821.70	10.36
900.00	315.00	9.00	0.1166	979.02	851.35	869.59	2.63	866.97	11.66
1000.00	326.00	10.00	0.1295	967.79	881.08	910.40	2.92	907.48	12.95
1100.00	337.00	11.00	0.1425	956.82	910.81	951.91	3.21	948.70	14.25
1200.00	346.00	12.00	0.1554	946.10	935.14	988.42	3.50	984.92	15.54
1300.00	352.00	13.00	0.1684	935.61	951.35	1016.83	3.79	1013.04	16.84
1400.00	359.00	14.00	0.1813	925.35	970.27	1048.55	4.08	1044.46	18.13
1500.00	364.00	15.00	0.1943	915.31	983.78	1074.81	4.38	1070.43	19.43
1600.00	370.00	16.00	0.2073	905.49	1000.00	1104.37	4.67	1099.71	20.73

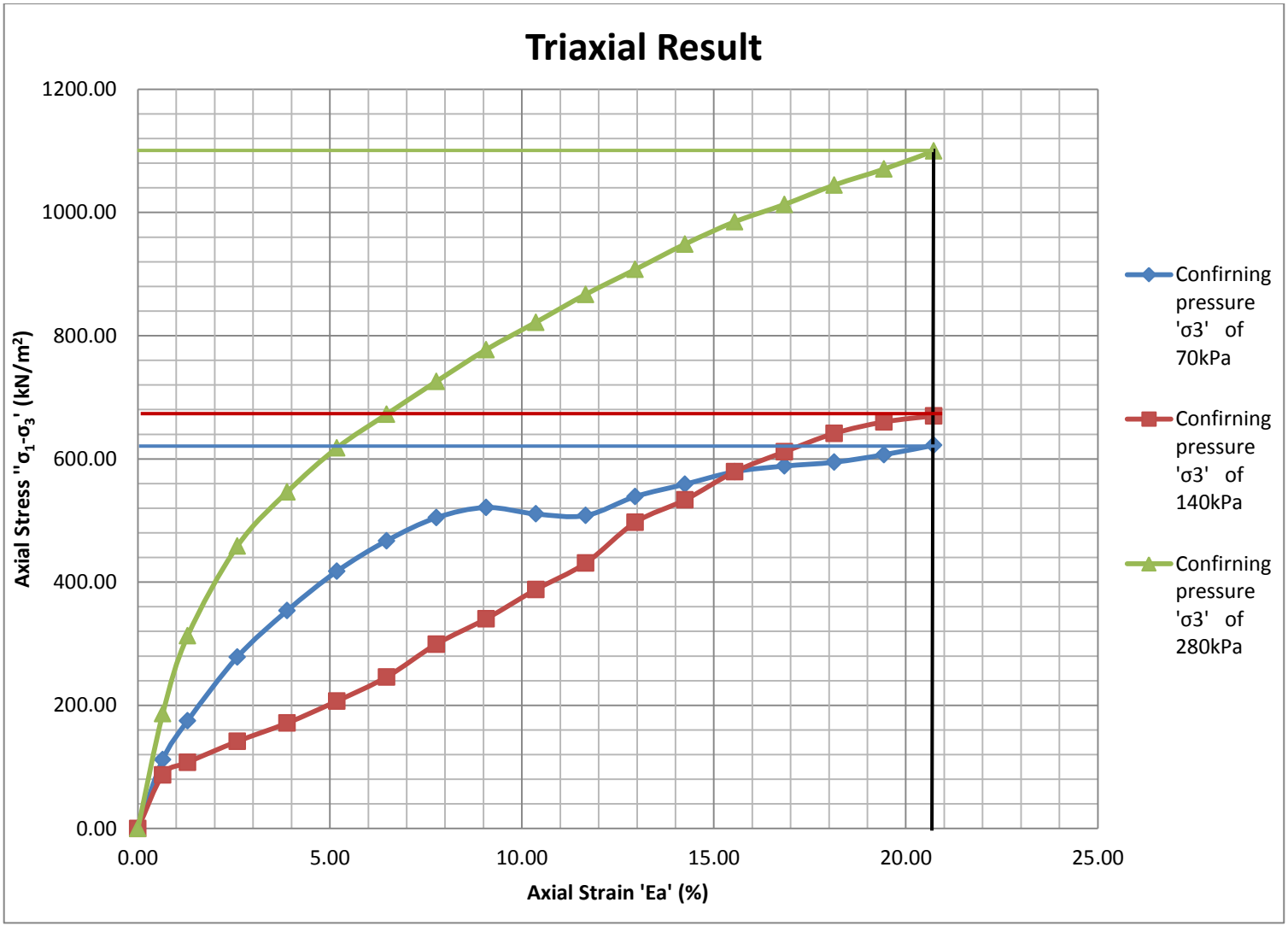

Fig B.2.1: Triaxial test graph for Sample A2

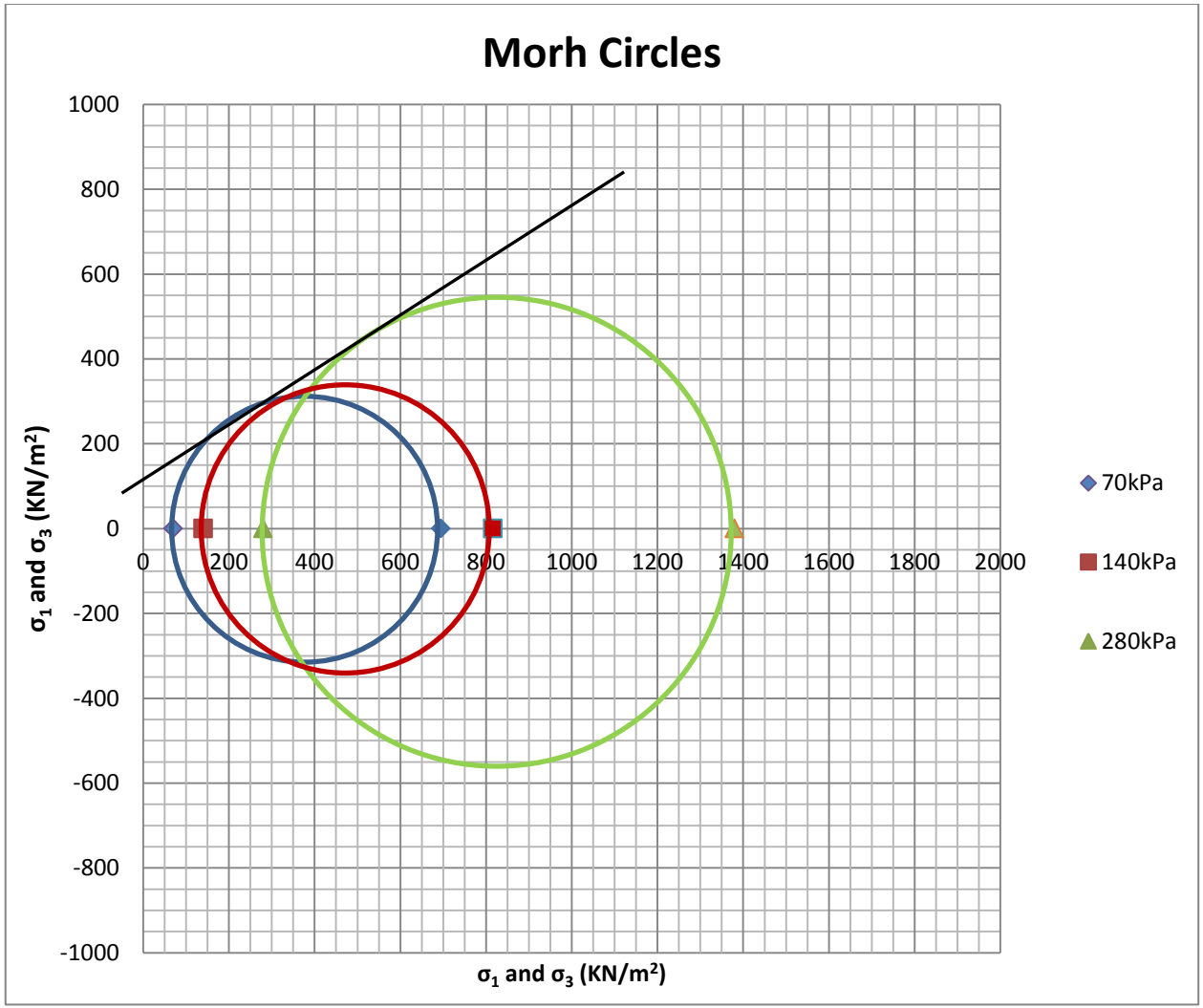

Fig B.2.2: Morh circle graph for Sample A2

Table B.1.8: Stress strength parameters for sample A1.

Result from graph	0	70kPa	140kPa	280kPa
Deviator stress (max) $'\sigma_1-\sigma_3'$ (KN/m^2)	0	625	676	1100
Normal stress $'\sigma_3'$ (KN/m^2)	0	70	140	280
Shear stress $'\sigma_1'$ (KN/m^2)	0	695	816	1380
Mean Stress $'[1/3('\sigma_1+2\sigma_3]'$ (KN/m2)	0.0	278.3	365.3	646.7
Internal angle of friction (^{o})	33.00			
Cohesion (KN/m2)	115			

3. Soil A at At-OMC (3)

Table B.3.1: Initial parameters from preparation of sample A3.

Compaction test		
Mass of Mould + base (g)	3667.90	
Mass of Mould + base + soil (g)	5745.60	
Mass Soil (g)	2077.70	
Weight of container (g)	16.00	16.30
Container + wet soil (g)	62.90	61.80
Container + dry soil (g)	56.70	56.00
Moisture Content (%)	15.23	14.61
Av. Moisture Content (%)	14.92	
Volume of mould (cm^3)	1000	
Bulk Density (g/cm^3)	2.08	
Dry density (g/cm^3)	1.81	
Void ratio $'e_0' = [(Gs*\rho_w/\rho_d)-1]$	0.604	
Degree of saturation $'Sr_i'$ (%)	71.638	

Table B.3.2: Initial parameters for sample A3 at confining pressure 'σ3' 70kPa.

Diameter of sample 'D_0' (mm)	38.3
Length of sample 'L_0' (mm)	77.0
20% strain of length (%)	15.40
Mass of Sample 'M_0' (g)	184.9
Area of sample 'A_0' (mm^2)	1152.56
Moisture content (%)	16.13
Young's modulus for latex membrane 'E_m' (kN/m^2)	1400
Thickness of membrane (0.1 - 0.2mm) 't_m' (mm)	0.15

Table B.3.3: Initial parameters for sample A3 at confining pressure 'σ3' 140kPa.

Diameter of sample 'D_0' (mm)	38.0
Length of sample 'L_0' (mm)	77.0
20% strain of length (%)	15.40
Mass of Sample 'M_0' (g)	184.9
Area of sample 'A_0' (mm^2)	1134.57
Moisture content (%)	15.98
Young's modulus for latex membrane 'E_m' (kN/m^2)	1400
Thickness of membrane (0.1 - 0.2mm) 't_m' (mm)	0.15

Table B.3.4: Initial parameters for sample A3 at confining pressure 'σ3' 280kPa.

Diameter of sample 'D_0' (mm)	38.3
Length of sample 'L_0' (mm)	76.7
20% strain of length (%)	15.34
Mass of Sample 'M_0' (g)	187.3
Area of sample 'A_0' (mm^2)	1152.56
Moisture content (%)	15.97
Young's modulus for latex membrane 'E_m' (kN/m^2)	1400
Thickness of membrane (0.1 - 0.2mm) 't_m' (mm)	0.15

Table B.3.5: Triaxial test values for sample A3 at confining pressure 'σ3' 70kPa.

Strain guage reading (yellow (bottom) gauge)	Force guage reading (white (top) gauge)	Change in sample length 'ΔL' (mm)	Axial strain 'Ea'	Corrected Area 'Ac' (mm^2)	Axial Force 'P' (N)	Axial Stress 'σ_1-σ_3' (KN/m^2)	Rubber membrane 'R_m' (KN/m^2)	Corrected Axial Stress 'σ_1-σ_3' (KN/m^2)	Axial strain 'Ea' (%)
Sr	**Fr**	Sr*0.01	$\Delta L/L_0$	$A_0/(1+Ea)$	(100/37)*Fr	P/Ac	$(4.E_m.t_m.Ea)/D_0$	σ_1-σ_3' -R_m	Ea*100%
0.00	0.00	0.00	0.0000	1152.56	0.00	0.00	0.00	0.00	0.00
50.00	19.00	0.50	0.0065	1145.12	51.35	44.84	0.14	44.70	0.65
100.00	29.00	1.00	0.0130	1137.78	78.38	68.89	0.28	68.60	1.30
200.00	49.00	2.00	0.0260	1123.38	132.43	117.89	0.57	117.32	2.60
300.00	64.50	3.00	0.0390	1109.34	174.32	157.14	0.85	156.29	3.90
400.00	80.00	4.00	0.0519	1095.64	216.22	197.34	1.14	196.20	5.19
500.00	93.80	5.00	0.0649	1082.28	253.51	234.24	1.42	232.82	6.49
600.00	105.00	6.00	0.0779	1069.24	283.78	265.41	1.71	263.70	7.79
700.00	115.20	7.00	0.0909	1056.51	311.35	294.70	1.99	292.70	9.09
800.00	125.00	8.00	0.1039	1044.08	337.84	323.57	2.28	321.30	10.39
900.00	132.00	9.00	0.1169	1031.94	356.76	345.71	2.56	343.15	11.69
1000.00	139.00	10.00	0.1299	1020.08	375.68	368.28	2.85	365.43	12.99
1100.00	145.00	11.00	0.1429	1008.49	391.89	388.59	3.13	385.46	14.29
1200.00	149.50	12.00	0.1558	997.16	404.05	405.21	3.42	401.79	15.58
1300.00	153.00	13.00	0.1688	986.08	413.51	419.35	3.70	415.65	16.88
1400.00	157.00	14.00	0.1818	975.24	424.32	435.10	3.99	431.11	18.18
1500.00	157.00	15.00	0.1948	964.64	424.32	439.88	4.27	435.61	19.48
1600.00	157.00	16.00	0.2078	954.27	424.32	444.66	4.56	440.10	20.78

Table B.3.6: Triaxial test values for sample A3 at confining pressure 'σ3' 140kPa.

Strain guage reading (yellow (bottom) gauge)	Force guage reading (white (top) gauge)	Change in sample length 'ΔL' (mm)	Axial strain 'Ea'	Corrected Area 'Ac' (mm^2)	Axial Force 'P' (N)	Axial Stress 'σ_1-σ_3' (KN/m^2)	Rubber membrane 'R_m' (KN/m^2)	Corrected Axial Stress 'σ_1-σ_3' (KN/m^2)	Axial strain 'Ea' (%)
Sr	**Fr**	Sr*0.01	$\Delta L/L_0$	$A_0/(1+Ea)$	(100/37)*Fr	P/Ac	$(4.E_m.t_m.Ea)/D_0$	σ_1-σ_3' -R_m	Ea*100%
0.00	0.00	0.00	0.0000	1152.56	0.00	0.00	0.00	0.00	0.00
50.00	20.00	0.50	0.0065	1145.12	54.05	47.20	0.14	47.06	0.65
100.00	32.00	1.00	0.0130	1137.78	86.49	76.01	0.28	75.73	1.30
200.00	51.50	2.00	0.0260	1123.38	139.19	123.90	0.57	123.33	2.60
300.00	69.50	3.00	0.0390	1109.34	187.84	169.32	0.85	168.47	3.90
400.00	86.00	4.00	0.0519	1095.64	232.43	212.14	1.14	211.00	5.19
500.00	99.00	5.00	0.0649	1082.28	267.57	247.23	1.42	245.80	6.49
600.00	110.50	6.00	0.0779	1069.24	298.65	279.31	1.71	277.60	7.79
700.00	121.00	7.00	0.0909	1056.51	327.03	309.54	1.99	307.54	9.09
800.00	131.00	8.00	0.1039	1044.08	354.05	339.11	2.28	336.83	10.39
900.00	139.00	9.00	0.1169	1031.94	375.68	364.05	2.56	361.48	11.69
1000.00	148.00	10.00	0.1299	1020.08	400.00	392.13	2.85	389.28	12.99
1100.00	155.50	11.00	0.1429	1008.49	420.27	416.73	3.13	413.60	14.29
1200.00	161.00	12.00	0.1558	997.16	435.14	436.38	3.42	432.96	15.58
1300.00	168.00	13.00	0.1688	986.08	454.05	460.47	3.70	456.76	16.88
1400.00	174.00	14.00	0.1818	975.24	470.27	482.21	3.99	478.22	18.18
1500.00	177.00	15.00	0.1948	964.64	478.38	495.91	4.27	491.64	19.48
1600.00	181.00	16.00	0.2078	954.27	489.19	512.63	4.56	508.08	20.78

Table B.3.6: Triaxial test values for sample A3 at confining pressure 'σ3' 140kPa.

Strain guage reading (yellow (bottom) gauge)	Force guage reading (white (top) gauge)	Change in sample length 'ΔL' (mm)	Axial strain 'Ea'	Corrected Area 'Ac' (mm^2)	Axial Force 'P' (N)	Axial Stress 'σ_1-σ_3' (KN/m^2)	Rubber membrane 'R_m' (KN/m^2)	Corrected Axial Stress 'σ_1-σ_3' (KN/m^2)	Axial strain 'Ea' (%)
Sr	**Fr**	Sr*0.01	$\Delta L/L_0$	$A_0/(1+Ea)$	(100/37)*Fr	P/Ac	$(4.E_m.t_m.Ea)/D_0$	σ_1-σ_3' -R_m	Ea*100%
0.00	0.00	0.00	0.0000	1152.56	0.00	0.00	0.00	0.00	0.00
50.00	20.00	0.50	0.0065	1145.09	54.05	47.21	0.14	47.06	0.65
100.00	61.00	1.00	0.0130	1137.72	164.86	144.91	0.29	144.62	1.30
200.00	97.00	2.00	0.0261	1123.27	262.16	233.39	0.57	232.82	2.61
300.00	115.00	3.00	0.0391	1109.17	310.81	280.22	0.86	279.36	3.91
400.00	127.50	4.00	0.0522	1095.43	344.59	314.58	1.14	313.43	5.22
500.00	139.00	5.00	0.0652	1082.02	375.68	347.20	1.43	345.77	6.52
600.00	149.00	6.00	0.0782	1068.94	402.70	376.73	1.72	375.02	7.82
700.00	157.00	7.00	0.0913	1056.17	424.32	401.76	2.00	399.76	9.13
800.00	166.50	8.00	0.1043	1043.70	450.00	431.16	2.29	428.87	10.43
900.00	174.00	9.00	0.1173	1031.52	470.27	455.90	2.57	453.33	11.73
1000.00	179.00	10.00	0.1304	1019.62	483.78	474.47	2.86	471.61	13.04
1100.00	189.00	11.00	0.1434	1007.99	510.81	506.76	3.15	503.61	14.34
1200.00	196.00	12.00	0.1565	996.63	529.73	531.52	3.43	528.09	15.65
1300.00	202.00	13.00	0.1695	985.52	545.95	553.97	3.72	550.25	16.95
1400.00	207.00	14.00	0.1825	974.65	559.46	574.01	4.00	570.01	18.25
1500.00	211.50	15.00	0.1956	964.02	571.62	592.95	4.29	588.66	19.56
1600.00	216.00	16.00	0.2086	953.63	583.78	612.17	4.58	607.60	20.86

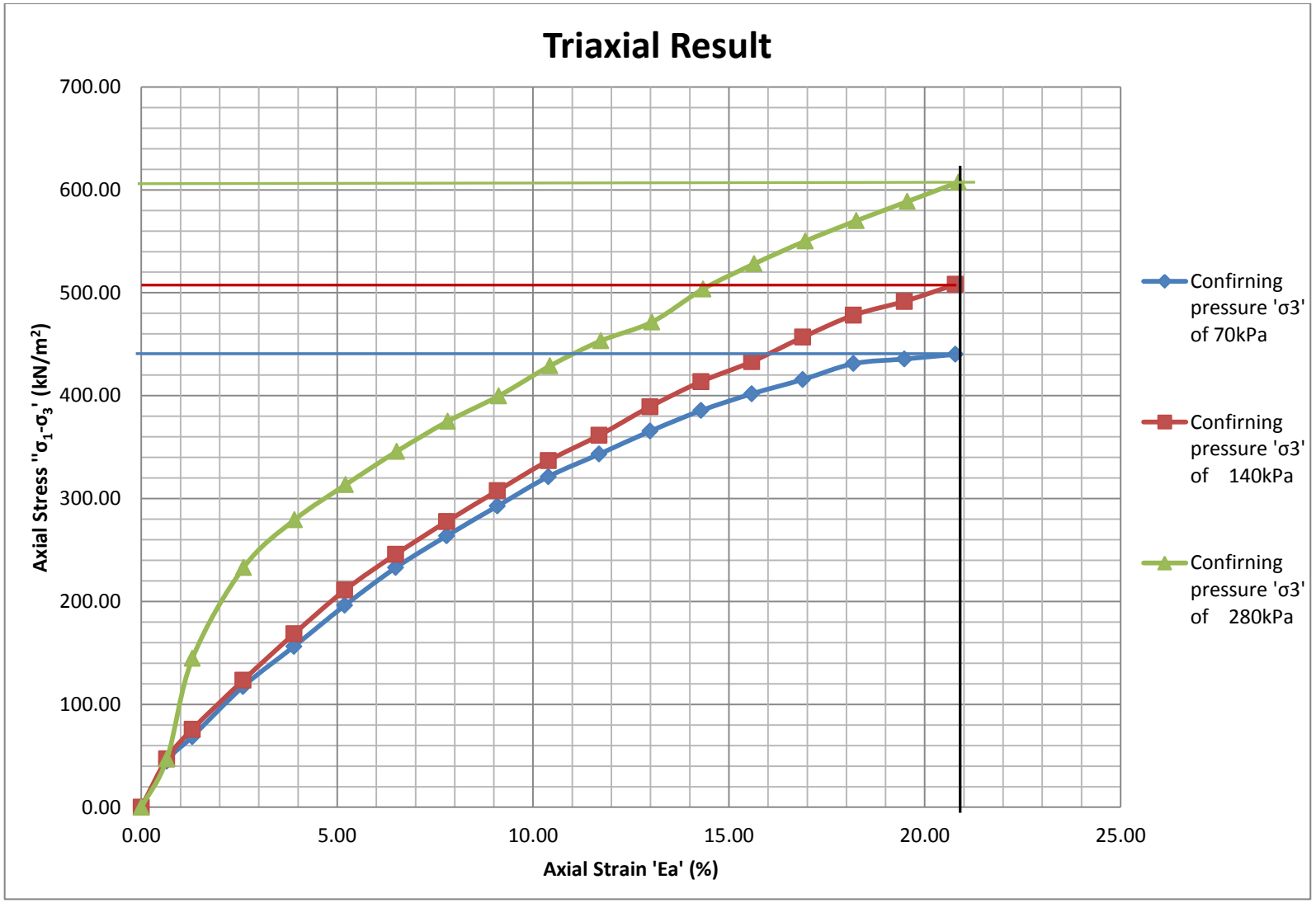

Fig B.3.1: Triaxial test graph for Sample A3

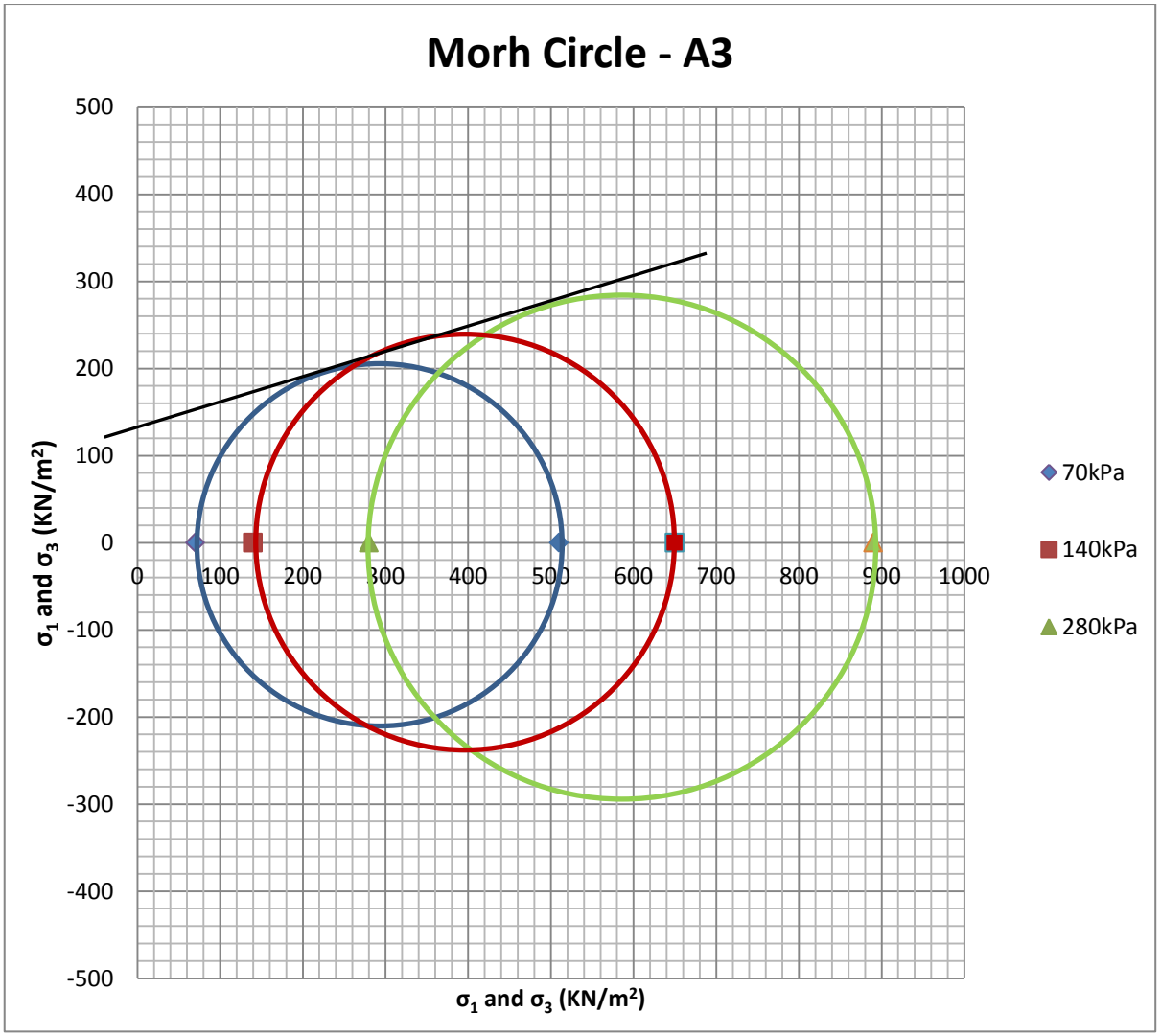

Fig B.3.2: Morh circle graph for Sample A3

Table B.3.8: Stress strength parameters for sample A3.

Result from graph	0	70kPa	140kPa	280kPa
Deviator stress (max) 'σ_1-σ_3' (KN/m^2)	0	440	510	610
Normal stress 'σ_3' (KN/m^2)	0	70	140	280
Shear stress 'σ_1' (KN/m^2)	0	510	650	890
Mean Stress '[1/3('σ_1+2σ_3]' (KN/m2)	0.0	216.7	310.0	483.3
Internal angle of friction (^{o})	16.64			
Cohesion (KN/m2)	138			

4. Soil A at Low wet of OMC (4)

Table B.4.1: Initial parameters from preparation of sample A4.

Compaction test		
Mass of Mould + base (g)	3664.80	
Mass of Mould + base + soil (g)	5729.20	
Mass Soil (g)	2064.40	
Weight of container (g)	15.90	16.10
Container + wet soil (g)	52.80	43.40
Container + dry soil (g)	46.90	39.10
Moisture Content (%)	19.03	18.70
Av. Moisture Content (%)	18.86	
Volume of mould (cm^3)	1000	
Bulk Density (g/cm^3)	2.06	
Dry density (g/cm^3)	1.74	
Void ratio 'e_0' = [(Gs*ρ_w/ρ_d)-1]	0.670	
Degree of saturation 'Sr_i' (%)	81.679	

Table B.4.2: Initial parameters for sample A4 at confining pressure 'σ3' 70kPa.

Diameter of sample 'D_0' (mm)	37.3
Length of sample 'L_0' (mm)	76.4
20% strain of length (%)	15.28
Mass of Sample 'M_0' (g)	172.5
Area of sample 'A_0' (mm^2)	1093.16
Moisture content (%)	18.83
Young's modulus for latex membrane 'E_m' (kN/m^2)	1400
Thickness of membrane (0.1 - 0.2mm) 't_m' (mm)	0.15

Table B.4.3: Initial parameters for sample A4 at confining pressure 'σ3' 140kPa.

Diameter of sample 'D_0' (mm)	37.9
Length of sample 'L_0' (mm)	76.1
20% strain of length (%)	15.22
Mass of Sample 'M_0' (g)	175.8
Area of sample 'A_0' (mm^2)	1128.61
Moisture content (%)	19.19
Young's modulus for latex membrane 'E_m' (kN/m^2)	1400
Thickness of membrane (0.1 - 0.2mm) 't_m' (mm)	0.15

Table B.4.4: Initial parameters for sample A4 at confining pressure 'σ3' 280kPa.

Diameter of sample 'D_0' (mm)	37.7
Length of sample 'L_0' (mm)	76.4
20% strain of length (%)	15.28
Mass of Sample 'M_0' (g)	177.6
Area of sample 'A_0' (mm^2)	1116.73
Moisture content (%)	18.71
Young's modulus for latex membrane 'E_m' (kN/m^2)	1400
Thickness of membrane (0.1 - 0.2mm) 't_m' (mm)	0.15

Table B.4.5: Triaxial test values for sample A4 at confining pressure 'σ3' 70kPa.

Strain guage reading (yellow (bottom) gauge)	Force guage reading (white (top) gauge)	Change in sample length 'ΔL' (mm)	Axial strain 'Ea'	Corrected Area 'Ac' (mm^2)	Axial Force 'P' (N)	Axial Stress 'σ_1-σ_3' (KN/m^2)	Rubber membrane 'R_m' (KN/m^2)	Corrected Axial Stress 'σ_1-σ_3' (KN/m^2)	Axial strain 'Ea' (%)
Sr	**Fr**	Sr*0.01	$\Delta L/L_0$	$A_0/(1+Ea)$	(100/37)*Fr	P/Ac	$(4.E_m.t_m.Ea)/D_0$	σ_1-σ_3' -R_m	Ea*100%
0.00	0.00	0.00	0.0000	1093.16	0.00	0.00	0.00	0.00	0.00
50.00	6.00	0.50	0.0065	1086.05	16.22	14.93	0.15	14.78	0.65
100.00	12.00	1.00	0.0131	1079.03	32.43	30.06	0.29	29.76	1.31
200.00	16.00	2.00	0.0262	1065.27	43.24	40.59	0.59	40.00	2.62
300.00	20.00	3.00	0.0393	1051.85	54.05	51.39	0.88	50.51	3.93
400.00	27.00	4.00	0.0524	1038.77	72.97	70.25	1.18	69.07	5.24
500.00	31.00	5.00	0.0654	1026.01	83.78	81.66	1.47	80.19	6.54
600.00	37.00	6.00	0.0785	1013.56	100.00	98.66	1.77	96.89	7.85
700.00	40.00	7.00	0.0916	1001.40	108.11	107.96	2.06	105.89	9.16
800.00	44.00	8.00	0.1047	989.54	118.92	120.18	2.36	117.82	10.47
900.00	47.00	9.00	0.1178	977.95	127.03	129.89	2.65	127.24	11.78
1000.00	49.00	10.00	0.1309	966.63	132.43	137.00	2.95	134.06	13.09
1100.00	53.00	11.00	0.1440	955.57	143.24	149.90	3.24	146.66	14.40
1200.00	55.00	12.00	0.1571	944.76	148.65	157.34	3.54	153.80	15.71
1300.00	58.00	13.00	0.1702	934.20	156.76	167.80	3.83	163.97	17.02
1400.00	60.00	14.00	0.1832	923.86	162.16	175.53	4.13	171.40	18.32
1500.00	63.00	15.00	0.1963	913.75	170.27	186.34	4.42	181.92	19.63
1600.00	65.00	16.00	0.2094	903.87	175.68	194.36	4.72	189.64	20.94

Table B.4.6: Triaxial test values for sample A4 at confining pressure 'σ3' 140kPa.

Strain guage reading (yellow (bottom) gauge)	Force guage reading (white (top) gauge)	Change in sample length 'ΔL' (mm)	Axial strain 'Ea'	Corrected Area 'Ac' (mm^2)	Axial Force 'P' (N)	Axial Stress 'σ_1-σ_3' (KN/m^2)	Rubber membrane 'R_m' (KN/m^2)	Corrected Axial Stress 'σ_1-σ_3' (KN/m^2)	Axial strain 'Ea' (%)
Sr	**Fr**	Sr*0.01	$\Delta L/L_0$	$A_0/(1+Ea)$	(100/37)*Fr	P/Ac	$(4.E_m.t_m.Ea)/D_0$	σ_1-σ_3' -R_m	Ea*100%
0.00	0.00	0.00	0.0000	1093.16	0.00	0.00	0.00	0.00	0.00
50.00	22.00	0.50	0.0065	1086.05	59.46	54.75	0.15	54.60	0.65
100.00	29.00	1.00	0.0131	1079.03	78.38	72.64	0.29	72.34	1.31
200.00	34.00	2.00	0.0262	1065.27	91.89	86.26	0.59	85.67	2.62
300.00	42.00	3.00	0.0393	1051.85	113.51	107.92	0.88	107.03	3.93
400.00	49.00	4.00	0.0524	1038.77	132.43	127.49	1.18	126.31	5.24
500.00	55.00	5.00	0.0654	1026.01	148.65	144.88	1.47	143.41	6.54
600.00	61.00	6.00	0.0785	1013.56	164.86	162.66	1.77	160.89	7.85
700.00	66.00	7.00	0.0916	1001.40	178.38	178.13	2.06	176.06	9.16
800.00	71.00	8.00	0.1047	989.54	191.89	193.92	2.36	191.56	10.47
900.00	76.00	9.00	0.1178	977.95	205.41	210.04	2.65	207.38	11.78
1000.00	80.00	10.00	0.1309	966.63	216.22	223.68	2.95	220.73	13.09
1100.00	83.00	11.00	0.1440	955.57	224.32	234.75	3.24	231.51	14.40
1200.00	88.00	12.00	0.1571	944.76	237.84	251.74	3.54	248.21	15.71
1300.00	90.00	13.00	0.1702	934.20	243.24	260.38	3.83	256.55	17.02
1400.00	92.00	14.00	0.1832	923.86	248.65	269.14	4.13	265.01	18.32
1500.00	95.00	15.00	0.1963	913.75	256.76	280.99	4.42	276.57	19.63
1600.00	98.00	16.00	0.2094	903.87	264.86	293.04	4.72	288.32	20.94

Table B.4.7: Triaxial test values for sample A4 at confining pressure 'σ3' 280kPa.

Strain guage reading (yellow (bottom) gauge)	Force guage reading (white (top) gauge)	Change in sample length 'ΔL' (mm)	Axial strain 'Ea'	Corrected Area 'Ac' (mm^2)	Axial Force 'P' (N)	Axial Stress 'σ_1-σ_3' (KN/m^2)	Rubber membrane 'R_m' (KN/m^2)	Corrected Axial Stress 'σ_1-σ_3' (KN/m^2)	Axial strain 'Ea' (%)
Sr	**Fr**	Sr*0.01	$\Delta L/L_0$	$A_0/(1+Ea)$	(100/37)*Fr	P/Ac	$(4.E_m.t_m.Ea)/D_0$	σ_1-σ_3' -R_m	Ea*100%
0.00	0.00	0.00	0.0000	1093.16	0.00	0.00	0.00	0.00	0.00
50.00	61.00	0.50	0.0065	1086.05	164.86	151.80	0.15	151.66	0.65
100.00	72.00	1.00	0.0131	1079.03	194.59	180.34	0.29	180.05	1.31
200.00	82.00	2.00	0.0262	1065.27	221.62	208.04	0.59	207.45	2.62
300.00	89.00	3.00	0.0393	1051.85	240.54	228.68	0.88	227.80	3.93
400.00	93.00	4.00	0.0524	1038.77	251.35	241.97	1.18	240.79	5.24
500.00	99.00	5.00	0.0654	1026.01	267.57	260.78	1.47	259.31	6.54
600.00	103.00	6.00	0.0785	1013.56	278.38	274.65	1.77	272.89	7.85
700.00	107.00	7.00	0.0916	1001.40	289.19	288.78	2.06	286.72	9.16
800.00	111.00	8.00	0.1047	989.54	300.00	303.17	2.36	300.81	10.47
900.00	115.00	9.00	0.1178	977.95	310.81	317.82	2.65	315.16	11.78
1000.00	119.00	10.00	0.1309	966.63	321.62	332.72	2.95	329.78	13.09
1100.00	122.00	11.00	0.1440	955.57	329.73	345.06	3.24	341.82	14.40
1200.00	125.00	12.00	0.1571	944.76	337.84	357.59	3.54	354.05	15.71
1300.00	128.00	13.00	0.1702	934.20	345.95	370.31	3.83	366.48	17.02
1400.00	132.00	14.00	0.1832	923.86	356.76	386.16	4.13	382.03	18.32
1500.00	135.00	15.00	0.1963	913.75	364.86	399.30	4.42	394.88	19.63
1600.00	137.00	16.00	0.2094	903.87	370.27	409.65	4.72	404.94	20.94

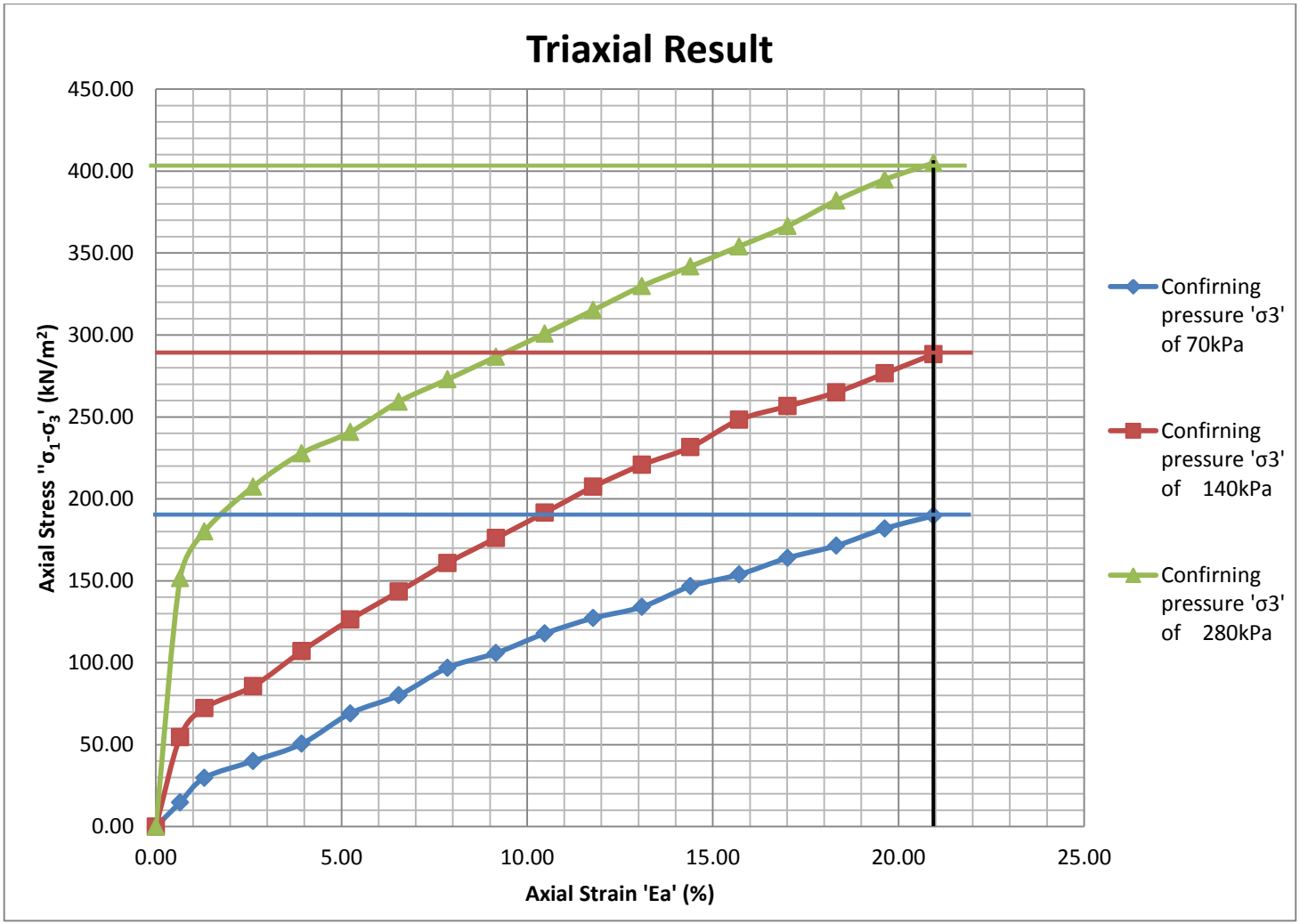

Fig B.4.1: Triaxial test graph for Sample A4

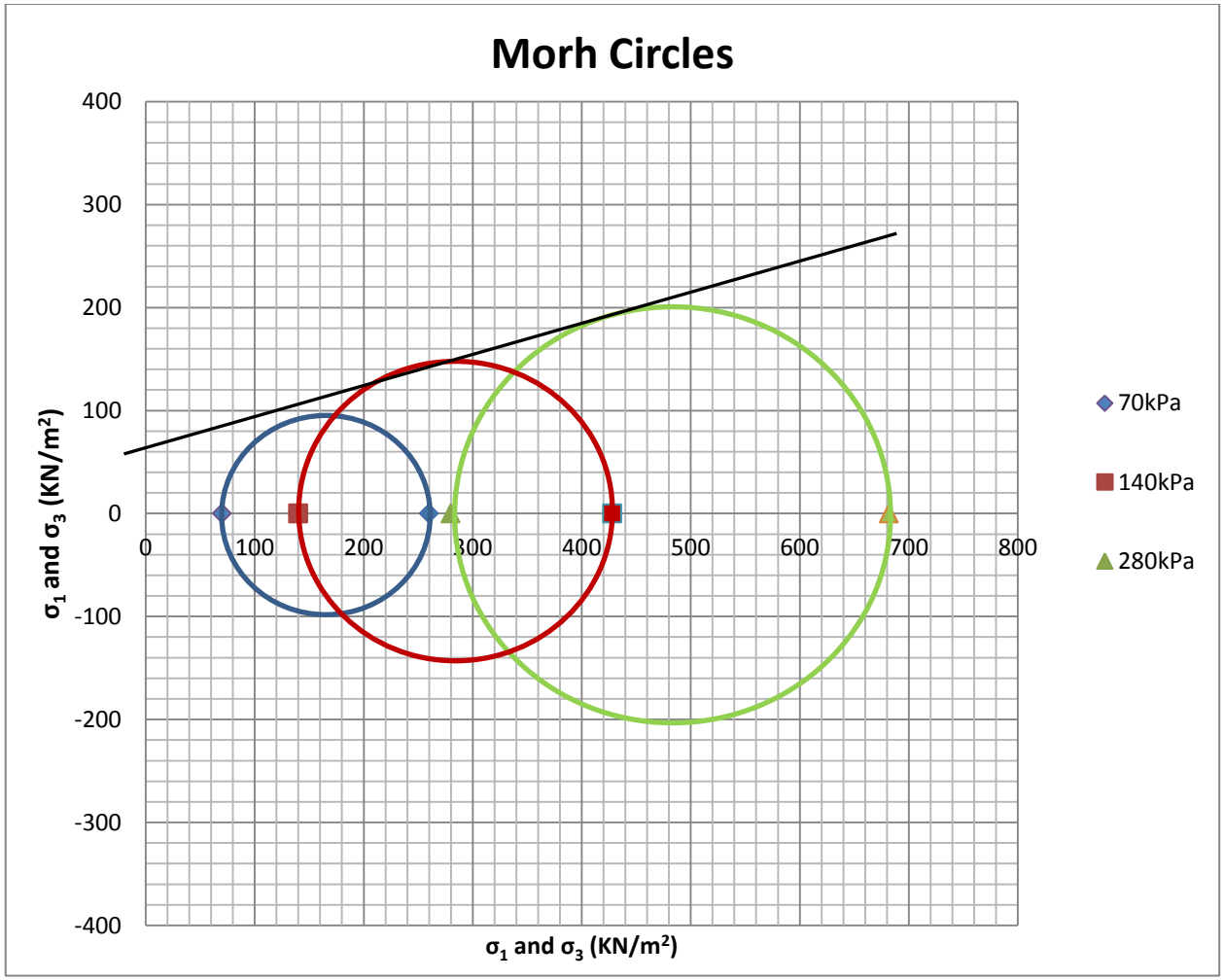

Fig B.4.2: Morh circle graph for Sample A4

Table B.4.8: Stress strength parameters for sample A4.

Result from graph	0	70kPa	140kPa	280kPa
Deviator stress (max) 'σ_1-σ_3' (KN/m^2)	0	190	288	402
Normal stress 'σ_3' (KN/m^2)	0	70	140	280
Shear stress 'σ_1' (KN/m^2)	0	260	428	682
Mean Stress '[1/3('σ_1+2σ_3]' (KN/m2)	0.0	133.3	236.0	414.0
Internal angle of friction (^{o})	16.56			
Cohesion (KN/m2)	62			

5. Soil A at High wet of OMC (5)

Table B.5.1: Initial parameters from preparation of sample A5.

Compaction test		
Mass of Mould + base (g)	3340.60	
Mass of Mould + base + soil (g)	5376.90	
Mass Soil (g)	2036.30	
Weight of container (g)	15.70	16.10
Container + wet soil (g)	61.10	78.00
Container + dry soil (g)	53.40	67.90
Moisture Content (%)	20.42	19.50
Av. Moisture Content (%)	19.96	
Volume of mould (cm^3)	1000	
Bulk Density (g/cm^3)	2.04	
Dry density (g/cm^3)	1.70	
Void ratio 'e_0' = [(Gs*ρ_w/ρ_d)-1]	0.708	
Degree of saturation 'Sr_i' (%)	81.713	

Table B.5.2: Initial parameters for sample A5 at confining pressure 'σ3' 70kPa.

Diameter of sample 'D_0' (mm)	38.3
Length of sample 'L_0' (mm)	77.6
20% strain of length (%)	15.52
Mass of Sample 'M_0' (g)	181.4
Area of sample 'A_0' (mm^2)	1152.56
Moisture content (%)	18.39
Young's modulus for latex membrane 'E_m' (kN/m^2)	1400
Thickness of membrane (0.1 - 0.2mm) 't_m' (mm)	0.15

Table B.5.3: Initial parameters for sample A5 at confining pressure 'σ3' 140kPa.

Diameter of sample 'D_0' (mm)	37.6
Length of sample 'L_0' (mm)	77.3
20% strain of length (%)	15.46
Mass of Sample 'M_0' (g)	177.4
Area of sample 'A_0' (mm^2)	1110.81
Moisture content (%)	19.02
Young's modulus for latex membrane 'E_m' (kN/m^2)	1400
Thickness of membrane (0.1 - 0.2mm) 't_m' (mm)	0.15

Table B.5.4: Initial parameters for sample A5 at confining pressure 'σ3' 280kPa.

Diameter of sample 'D_0' (mm)	38.0
Length of sample 'L_0' (mm)	77.8
20% strain of length (%)	15.56
Mass of Sample 'M_0' (g)	179.4
Area of sample 'A_0' (mm^2)	1134.57
Moisture content (%)	18.63
Young's modulus for latex membrane 'E_m' (kN/m^2)	1400
Thickness of membrane (0.1 - 0.2mm) 't_m' (mm)	0.15

Table B.5.5: Triaxial test values for sample A5 at confining pressure 'σ3' 70kPa.

Strain guage reading (yellow (bottom) gauge) **Sr**	Force guage reading (white (top) gauge) **Fr**	Change in sample length '***ΔL***' (mm) Sr*0.01	Axial strain '***Ea***' $\Delta L/L_0$	Corrected Area '***Ac***' (mm^2) $A_0/(1+Ea)$	Axial Force '***P***' (N) (100/37)*Fr	Axial Stress 'σ_1-σ_3' (KN/m^2) P/Ac	Rubber membrane 'R_m' (KN/m^2) $(4.E_m.t_m.Ea)/D_0$	Corrected Axial Stress 'σ_1-σ_3' (KN/m^2) σ_1-σ_3' -R_m	Axial strain '***Ea***' (%) Ea*100%
0.00	0.00	0.00	0.0000	1152.56	0.00	0.00	0.00	0.00	0.00
50.00	11.00	0.50	0.0064	1145.18	29.73	25.96	0.14	25.82	0.64
100.00	13.00	1.00	0.0129	1137.89	35.14	30.88	0.28	30.59	1.29
200.00	16.00	2.00	0.0258	1123.60	43.24	38.49	0.57	37.92	2.58
300.00	18.00	3.00	0.0387	1109.66	48.65	43.84	0.85	42.99	3.87
400.00	20.00	4.00	0.0515	1096.06	54.05	49.32	1.13	48.19	5.15
500.00	23.00	5.00	0.0644	1082.79	62.16	57.41	1.41	56.00	6.44
600.00	26.00	6.00	0.0773	1069.84	70.27	65.68	1.70	63.99	7.73
700.00	28.50	7.00	0.0902	1057.19	77.03	72.86	1.98	70.88	9.02
800.00	31.50	8.00	0.1031	1044.84	85.14	81.48	2.26	79.22	10.31
900.00	34.50	9.00	0.1160	1032.78	93.24	90.28	2.54	87.74	11.60
1000.00	37.50	10.00	0.1289	1020.99	101.35	99.27	2.83	96.44	12.89
1100.00	40.50	11.00	0.1418	1009.46	109.46	108.43	3.11	105.32	14.18
1200.00	43.00	12.00	0.1546	998.20	116.22	116.43	3.39	113.03	15.46
1300.00	45.00	13.00	0.1675	987.18	121.62	123.20	3.67	119.53	16.75
1400.00	46.50	14.00	0.1804	976.40	125.68	128.71	3.96	124.76	18.04
1500.00	48.50	15.00	0.1933	965.86	131.08	135.71	4.24	131.48	19.33
1600.00	49.50	16.00	0.2062	955.54	133.78	140.01	4.52	135.49	20.62

Table B.5.6: Triaxial test values for sample A5 at confining pressure 'σ3' 140kPa.

Strain guage reading (yellow (bottom) gauge)	Force guage reading (white (top) gauge)	Change in sample length 'ΔL' (mm)	Axial strain 'Ea'	Corrected Area 'Ac' (mm^2)	Axial Force 'P' (N)	Axial Stress 'σ_1-σ_3' (KN/m^2)	Rubber membrane 'R_m' (KN/m^2)	Corrected Axial Stress 'σ_1-σ_3' (KN/m^2)	Axial strain 'Ea' (%)
Sr	**Fr**	Sr*0.01	$\Delta L/L_0$	$A_0/(1+Ea)$	(100/37)*Fr	P/Ac	$(4.E_m.t_m.Ea)/D_0$	σ_1-σ_3' -R_m	Ea*100%
0.00	0.00	0.00	0.0000	1152.56	0.00	0.00	0.00	0.00	0.00
50.00	12.00	0.50	0.0064	1145.18	32.43	28.32	0.14	28.18	0.64
100.00	16.00	1.00	0.0129	1137.89	43.24	38.00	0.28	37.72	1.29
200.00	19.00	2.00	0.0258	1123.60	51.35	45.70	0.57	45.14	2.58
300.00	24.00	3.00	0.0387	1109.66	64.86	58.45	0.85	57.61	3.87
400.00	27.00	4.00	0.0515	1096.06	72.97	66.58	1.13	65.45	5.15
500.00	31.00	5.00	0.0644	1082.79	83.78	77.38	1.41	75.96	6.44
600.00	35.00	6.00	0.0773	1069.84	94.59	88.42	1.70	86.72	7.73
700.00	38.50	7.00	0.0902	1057.19	104.05	98.43	1.98	96.45	9.02
800.00	41.50	8.00	0.1031	1044.84	112.16	107.35	2.26	105.09	10.31
900.00	44.00	9.00	0.1160	1032.78	118.92	115.14	2.54	112.60	11.60
1000.00	47.00	10.00	0.1289	1020.99	127.03	124.42	2.83	121.59	12.89
1100.00	49.00	11.00	0.1418	1009.46	132.43	131.19	3.11	128.08	14.18
1200.00	51.00	12.00	0.1546	998.20	137.84	138.09	3.39	134.70	15.46
1300.00	54.00	13.00	0.1675	987.18	145.95	147.84	3.67	144.17	16.75
1400.00	55.00	14.00	0.1804	976.40	148.65	152.24	3.96	148.28	18.04
1500.00	56.00	15.00	0.1933	965.86	151.35	156.70	4.24	152.46	19.33
1600.00	58.00	16.00	0.2062	955.54	156.76	164.05	4.52	159.53	20.62

Table B.5.7: Triaxial test values for sample A5 at confining pressure 'σ3' 280kPa.

Strain guage reading (yellow (bottom) gauge)	Force guage reading (white (top) gauge)	Change in sample length 'ΔL' (mm)	Axial strain 'Ea'	Corrected Area 'Ac' (mm^2)	Axial Force 'P' (N)	Axial Stress 'σ_1-σ_3' (KN/m^2)	Rubber membrane 'R_m' (KN/m^2)	Corrected Axial Stress 'σ_1-σ_3' (KN/m^2)	Axial strain 'Ea' (%)
Sr	**Fr**	Sr*0.01	$\Delta L/L_0$	$A_0/(1+Ea)$	(100/37)*Fr	P/Ac	$(4.E_m.t_m.Ea)/D_0$	σ_1-σ_3' -R_m	Ea*100%
0.00	0.00	0.00	0.0000	1152.56	0.00	0.00	0.00	0.00	0.00
50.00	15.00	0.50	0.0064	1145.18	40.54	35.40	0.14	35.26	0.64
100.00	20.00	1.00	0.0129	1137.89	54.05	47.50	0.28	47.22	1.29
200.00	24.50	2.00	0.0258	1123.60	66.22	58.93	0.57	58.37	2.58
300.00	28.00	3.00	0.0387	1109.66	75.68	68.20	0.85	67.35	3.87
400.00	31.50	4.00	0.0515	1096.06	85.14	77.67	1.13	76.54	5.15
500.00	35.00	5.00	0.0644	1082.79	94.59	87.36	1.41	85.95	6.44
600.00	39.00	6.00	0.0773	1069.84	105.41	98.52	1.70	96.83	7.73
700.00	42.00	7.00	0.0902	1057.19	113.51	107.37	1.98	105.39	9.02
800.00	45.50	8.00	0.1031	1044.84	122.97	117.70	2.26	115.43	10.31
900.00	49.00	9.00	0.1160	1032.78	132.43	128.23	2.54	125.69	11.60
1000.00	51.00	10.00	0.1289	1020.99	137.84	135.00	2.83	132.18	12.89
1100.00	54.00	11.00	0.1418	1009.46	145.95	144.58	3.11	141.47	14.18
1200.00	56.00	12.00	0.1546	998.20	151.35	151.62	3.39	148.23	15.46
1300.00	58.00	13.00	0.1675	987.18	156.76	158.79	3.67	155.12	16.75
1400.00	60.00	14.00	0.1804	976.40	162.16	166.08	3.96	162.12	18.04
1500.00	62.50	15.00	0.1933	965.86	168.92	174.89	4.24	170.65	19.33
1600.00	64.00	16.00	0.2062	955.54	172.97	181.02	4.52	176.50	20.62

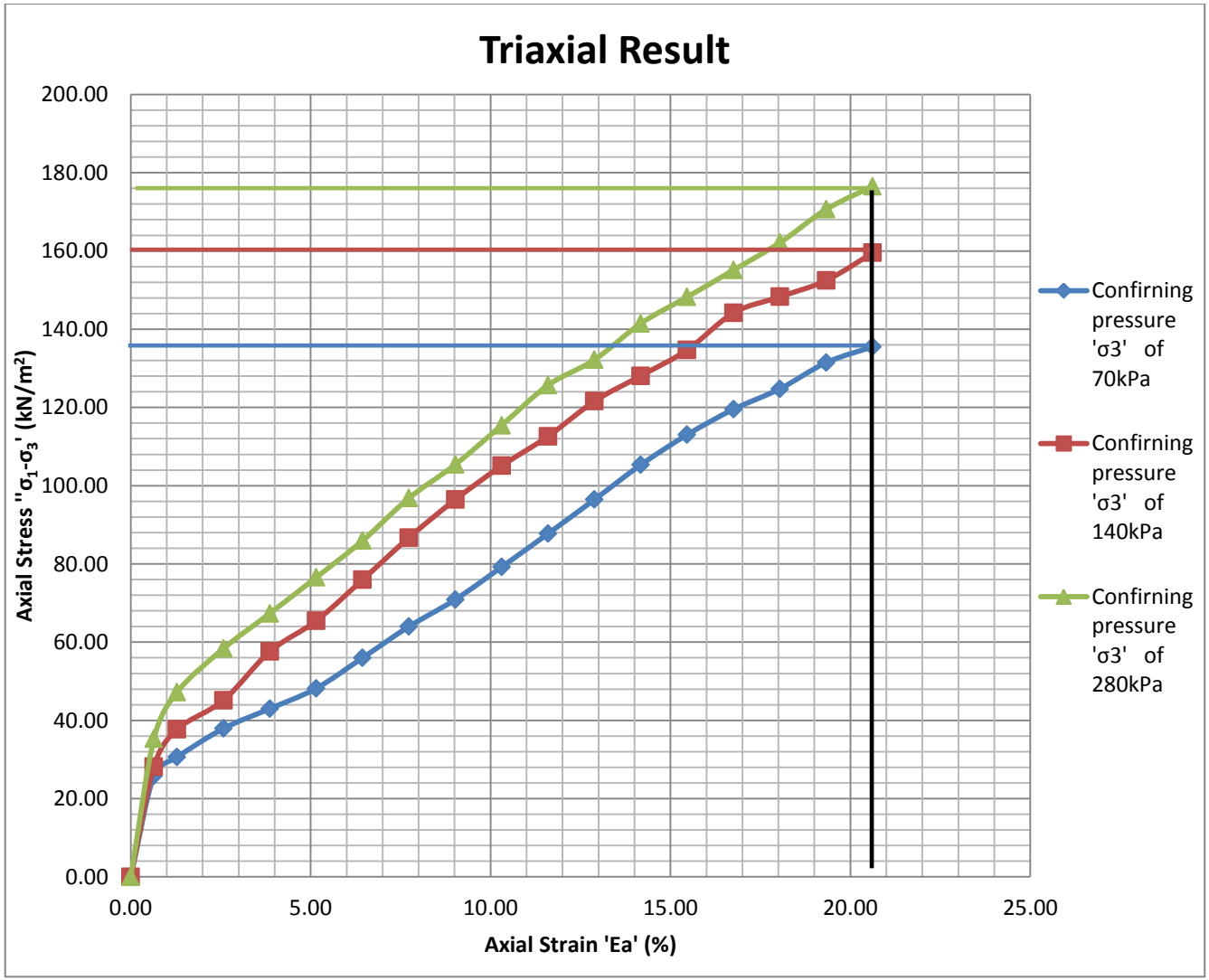

Fig B.5.1: Triaxial test graph for Sample A5

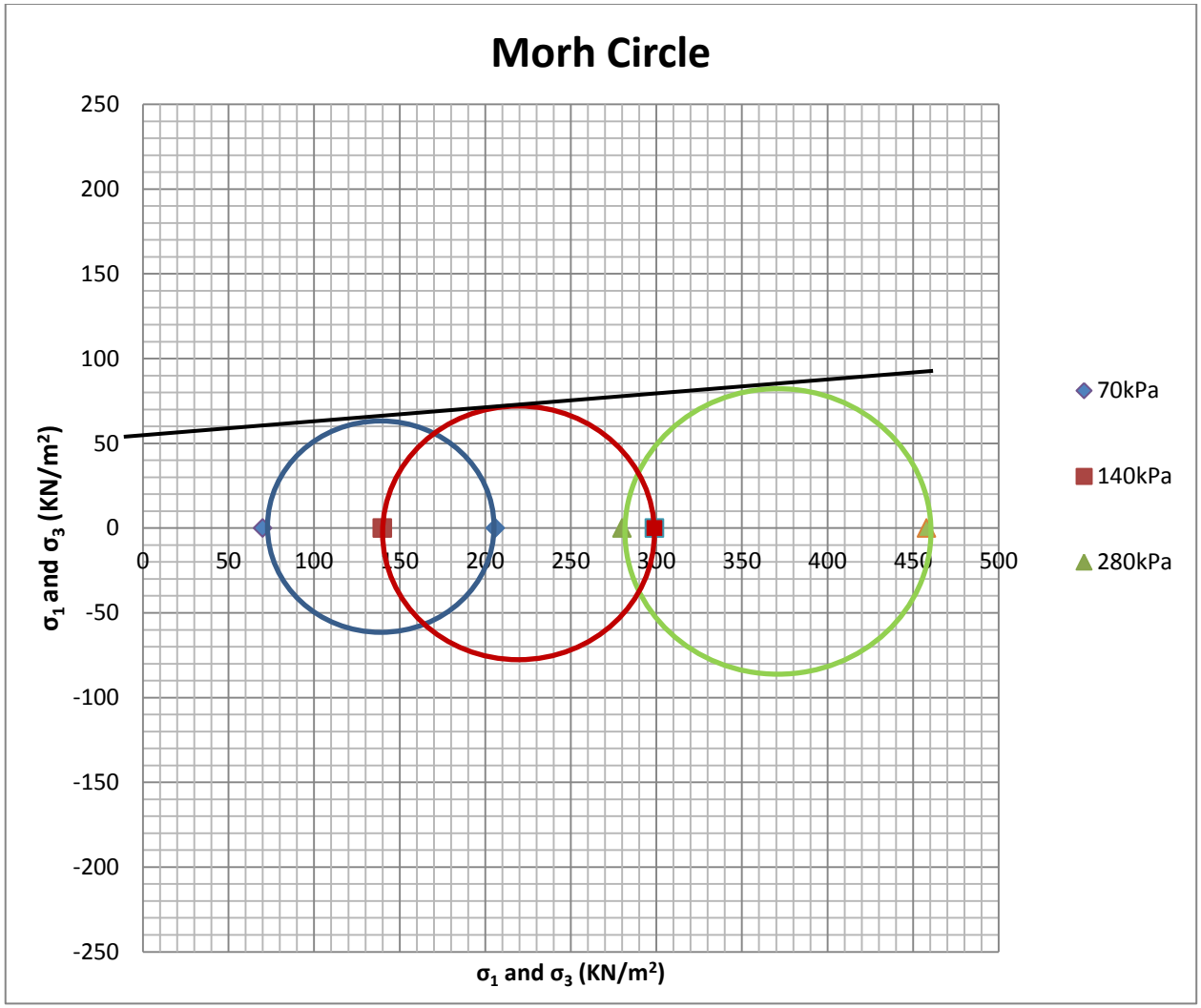

Fig B.5.2: Morh circle graph for Sample A5

Table B.5.8: Stress strength parameters for sample A5.

Result from graph	0	70kPa	140kPa	280kPa
Deviator stress (max) 'σ_1-σ_3' (KN/m^2)	0	136	159	178
Normal stress 'σ_3' (KN/m^2)	0	70	140	280
Shear stress 'σ_1' (KN/m^2)	0	206	299	458
Mean Stress '[1/3('σ_1+2σ_3]' (KN/m2)	0.0	115.3	193.0	339.3
Internal angle of friction (^{o})	5.71			
Cohesion (KN/m2)	52			

6. *Soil B at Low dry of OMC (1)*

Table B.6.1: Initial parameters from preparation of sample B1.

Compaction test		
Mass of Mould + base (g)	3600.20	
Mass of Mould + base + soil (g)	5382.50	
Mass Soil (g)	1782.30	
Weight of container (g)	15.90	16.00
Container + wet soil (g)	62.80	56.70
Container + dry soil (g)	58.60	53.40
Moisture Content (%)	9.84	8.82
Av. Moisture Content (%)	9.33	
Volume of mould (cm^3)	1000	
Bulk Density (g/cm^3)	1.78	
Dry density (g/cm^3)	1.63	
Void ratio 'e_0' = [(Gs*ρ_w/ρ_d)-1]	0.779	
Degree of saturation 'Sr_i' (%)	34.736	

Table B.6.2: Initial parameters for sample B1 at confining pressure 'σ3' 70kPa.

Diameter of sample 'D_0' (mm)	37.8
Length of sample 'L_0' (mm)	68.9
20% strain of length (%)	13.78
Mass of Sample 'M_0' (g)	136.2
Area of sample 'A_0' (mm^2)	1122.66
Moisture content (%)	12.33
Young's modulus for latex membrane 'E_m' (kN/m^2)	1400
Thickness of membrane (0.1 - 0.2mm) 't_m' (mm)	0.15

Table B.6.3: Initial parameters for sample B1 at confining pressure 'σ3' 140kPa.

Diameter of sample 'D_0' (mm)	37.9
Length of sample 'L_0' (mm)	77.9
20% strain of length (%)	15.58
Mass of Sample 'M_0' (g)	157.7
Area of sample 'A_0' (mm^2)	1128.61
Moisture content (%)	12.05
Young's modulus for latex membrane 'E_m' (kN/m^2)	1400
Thickness of membrane (0.1 - 0.2mm) 't_m' (mm)	0.15

Table B.6.4: Initial parameters for sample B1 at confining pressure 'σ3' 280kPa.

Diameter of sample 'D_0' (mm)	38.2
Length of sample 'L_0' (mm)	73.1
20% strain of length (%)	14.62
Mass of Sample 'M_0' (g)	148.8
Area of sample 'A_0' (mm^2)	1146.55
Moisture content (%)	11.73
Young's modulus for latex membrane 'E_m' (kN/m^2)	1400
Thickness of membrane (0.1 - 0.2mm) 't_m' (mm)	0.15

Table B.6.5: Triaxial test values for sample B1 at confining pressure 'σ3' 70kPa.

Strain guage reading (yellow (bottom) gauge) **Sr**	Force guage reading (white (top) gauge) **Fr**	Change in sample length 'ΔL' (mm) Sr*0.01	Axial strain 'Ea' $\Delta L/L_0$	Corrected Area 'Ac' (mm^2) $A_0/(1+Ea)$	Axial Force 'P' (N) (100/37)*Fr	Axial Stress 'σ_1-σ_3' (KN/m^2) P/Ac	Rubber membrane 'R_m' (KN/m^2) $(4.E_m.t_m.Ea)/D_0$	Corrected Axial Stress 'σ_1-σ_3' (KN/m^2) σ_1-σ_3' -R_m	Axial strain 'Ea' (%) Ea*100%
0.00	0.00	0.00	0.0000	1122.66	0.00	0.00	0.00	0.00	0.00
50.00	16.00	0.50	0.0073	1114.57	43.24	38.80	0.16	38.64	0.73
100.00	64.00	1.00	0.0145	1106.60	172.97	156.31	0.32	155.99	1.45
200.00	133.00	2.00	0.0290	1090.99	359.46	329.48	0.65	328.83	2.90
300.00	178.00	3.00	0.0435	1075.82	481.08	447.18	0.97	446.21	4.35
400.00	205.00	4.00	0.0581	1061.06	554.05	522.17	1.29	520.88	5.81
500.00	213.00	5.00	0.0726	1046.70	575.68	549.99	1.61	548.38	7.26
600.00	214.00	6.00	0.0871	1032.73	578.38	560.05	1.94	558.11	8.71
700.00	213.50	7.00	0.1016	1019.12	577.03	566.20	2.26	563.94	10.16
800.00	214.00	8.00	0.1161	1005.87	578.38	575.00	2.58	572.42	11.61
900.00	215.00	9.00	0.1306	992.96	581.08	585.20	2.90	582.30	13.06
1000.00	217.50	10.00	0.1451	980.37	587.84	599.61	3.23	596.38	14.51
1100.00	218.50	11.00	0.1597	968.10	590.54	610.00	3.55	606.45	15.97
1200.00	219.00	12.00	0.1742	956.13	591.89	619.05	3.87	615.18	17.42
1300.00	222.50	13.00	0.1887	944.46	601.35	636.71	4.19	632.52	18.87
1400.00	225.50	14.00	0.2032	933.07	609.46	653.18	4.52	648.66	20.32
1500.00	225.50	15.00	0.2177	921.95	609.46	661.06	4.84	656.22	21.77
1600.00	228.00	16.00	0.2322	911.09	616.22	676.35	5.16	671.19	23.22

Table B.6.6: Triaxial test values for sample B1 at confining pressure 'σ3' 140kPa.

Strain guage reading (yellow (bottom) gauge) **Sr**	Force guage reading (white (top) gauge) **Fr**	Change in sample length 'ΔL' (mm) Sr*0.01	Axial strain 'Ea' $\Delta L/L_0$	Corrected Area 'Ac' (mm^2) $A_0/(1+Ea)$	Axial Force 'P' (N) (100/37)*Fr	Axial Stress 'σ_1-σ_3' (KN/m^2) P/Ac	Rubber membrane 'R_m' (KN/m^2) $(4.E_m.t_m.Ea)/D_0$	Corrected Axial Stress 'σ_1-σ_3' (KN/m^2) σ_1-σ_3' -R_m	Axial strain 'Ea' (%) Ea*100%
0.00	0.00	0.00	0.0000	1122.66	0.00	0.00	0.00	0.00	0.00
50.00	90.00	0.50	0.0073	1114.57	243.24	218.24	0.16	218.08	0.73
100.00	158.00	1.00	0.0145	1106.60	427.03	385.89	0.32	385.57	1.45
200.00	221.00	2.00	0.0290	1090.99	597.30	547.48	0.65	546.84	2.90
300.00	251.00	3.00	0.0435	1075.82	678.38	630.57	0.97	629.60	4.35
400.00	269.00	4.00	0.0581	1061.06	727.03	685.19	1.29	683.90	5.81
500.00	279.00	5.00	0.0726	1046.70	754.05	720.41	1.61	718.80	7.26
600.00	281.00	6.00	0.0871	1032.73	759.46	735.39	1.94	733.46	8.71
700.00	283.50	7.00	0.1016	1019.12	766.22	751.84	2.26	749.58	10.16
800.00	285.50	8.00	0.1161	1005.87	771.62	767.12	2.58	764.54	11.61
900.00	287.50	9.00	0.1306	992.96	777.03	782.54	2.90	779.64	13.06
1000.00	290.00	10.00	0.1451	980.37	783.78	799.48	3.23	796.25	14.51
1100.00	291.50	11.00	0.1597	968.10	787.84	813.80	3.55	810.25	15.97
1200.00	292.50	12.00	0.1742	956.13	790.54	826.81	3.87	822.94	17.42
1300.00	294.00	13.00	0.1887	944.46	794.59	841.32	4.19	837.13	18.87
1400.00	297.50	14.00	0.2032	933.07	804.05	861.73	4.52	857.22	20.32
1500.00	299.50	15.00	0.2177	921.95	809.46	877.99	4.84	873.15	21.77
1600.00	301.00	16.00	0.2322	911.09	813.51	892.90	5.16	887.74	23.22

Table B.6.7: Triaxial test values for sample B1 at confining pressure 'σ3' 280kPa.

Strain guage reading (yellow (bottom) gauge) **Sr**	Force guage reading (white (top) gauge) **Fr**	Change in sample length '***ΔL***' (mm) Sr*0.01	Axial strain '***Ea***' $\Delta L/L_0$	Corrected Area '***Ac***' (mm^2) $A_0/(1+Ea)$	Axial Force '***P***' (N) (100/37)*Fr	Axial Stress 'σ_1-σ_3' (KN/m^2) P/Ac	Rubber membrane 'R_m' (KN/m^2) $(4.E_m.t_m.Ea)/D_0$	Corrected Axial Stress 'σ_1-σ_3' (KN/m^2) σ_1-σ_3' -R_m	Axial strain '***Ea***' (%) Ea*100%
0.00	0.00	0.00	0.0000	1122.66	0.00	0.00	0.00	0.00	0.00
50.00	23.00	0.50	0.0073	1114.57	62.16	55.77	0.16	55.61	0.73
100.00	137.00	1.00	0.0145	1106.60	370.27	334.60	0.32	334.28	1.45
200.00	272.00	2.00	0.0290	1090.99	735.14	673.82	0.65	673.18	2.90
300.00	352.00	3.00	0.0435	1075.82	951.35	884.31	0.97	883.34	4.35
400.00	401.00	4.00	0.0581	1061.06	1083.78	1021.42	1.29	1020.13	5.81
500.00	435.00	5.00	0.0726	1046.70	1175.68	1123.22	1.61	1121.61	7.26
600.00	458.00	6.00	0.0871	1032.73	1237.84	1198.61	1.94	1196.68	8.71
700.00	473.00	7.00	0.1016	1019.12	1278.38	1254.39	2.26	1252.14	10.16
800.00	485.00	8.00	0.1161	1005.87	1310.81	1303.16	2.58	1300.58	11.61
900.00	494.50	9.00	0.1306	992.96	1336.49	1345.97	2.90	1343.06	13.06
1000.00	500.00	10.00	0.1451	980.37	1351.35	1378.41	3.23	1375.18	14.51
1100.00	505.00	11.00	0.1597	968.10	1364.86	1409.84	3.55	1406.29	15.97
1200.00	509.00	12.00	0.1742	956.13	1375.68	1438.79	3.87	1434.92	17.42
1300.00	513.00	13.00	0.1887	944.46	1386.49	1468.02	4.19	1463.83	18.87
1400.00	517.50	14.00	0.2032	933.07	1398.65	1498.98	4.52	1494.46	20.32
1500.00	522.50	15.00	0.2177	921.95	1412.16	1531.72	4.84	1526.88	21.77
1600.00	529.00	16.00	0.2322	911.09	1429.73	1569.26	5.16	1564.10	23.22

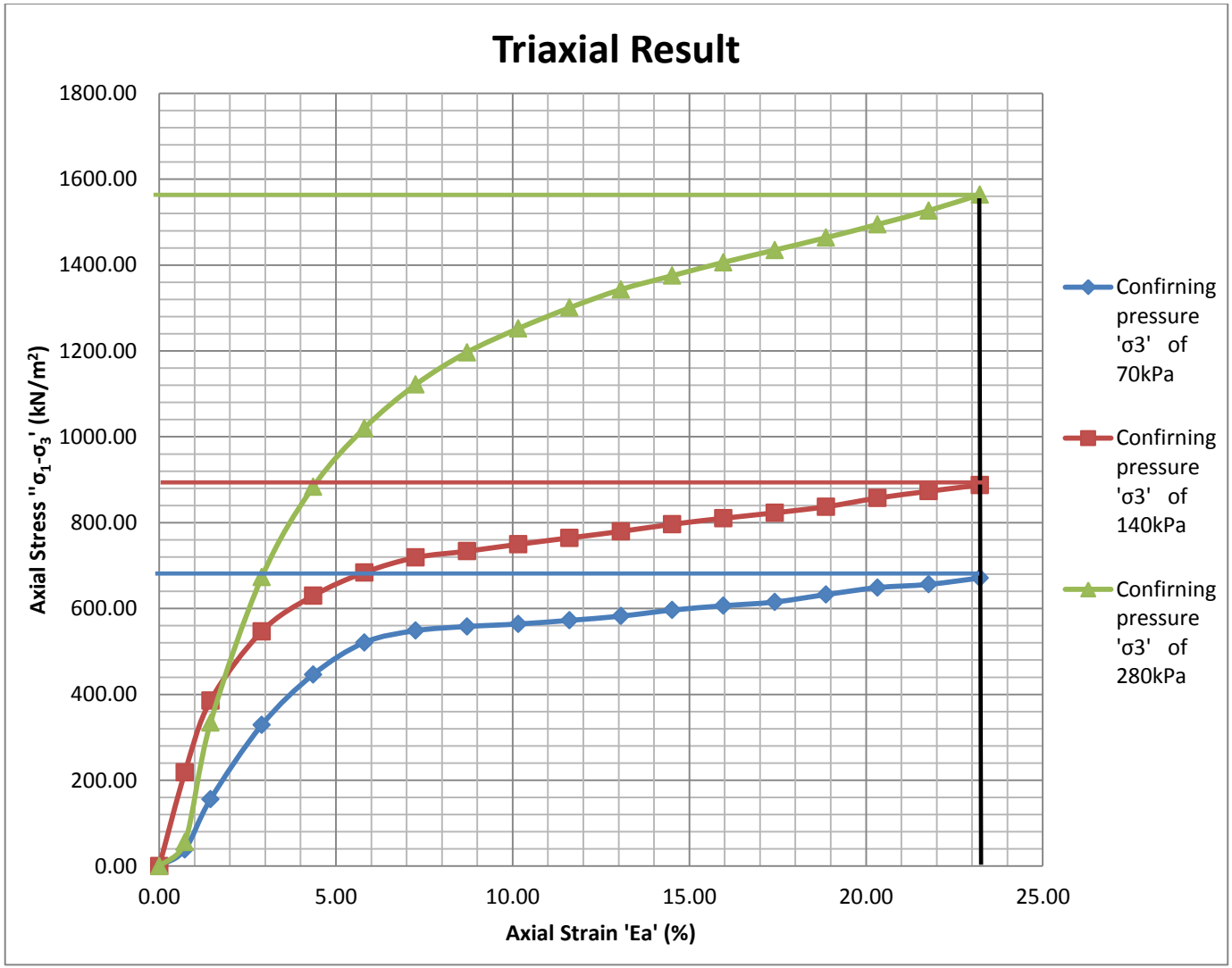

Fig B.6.1: Triaxial test graph for Sample B1

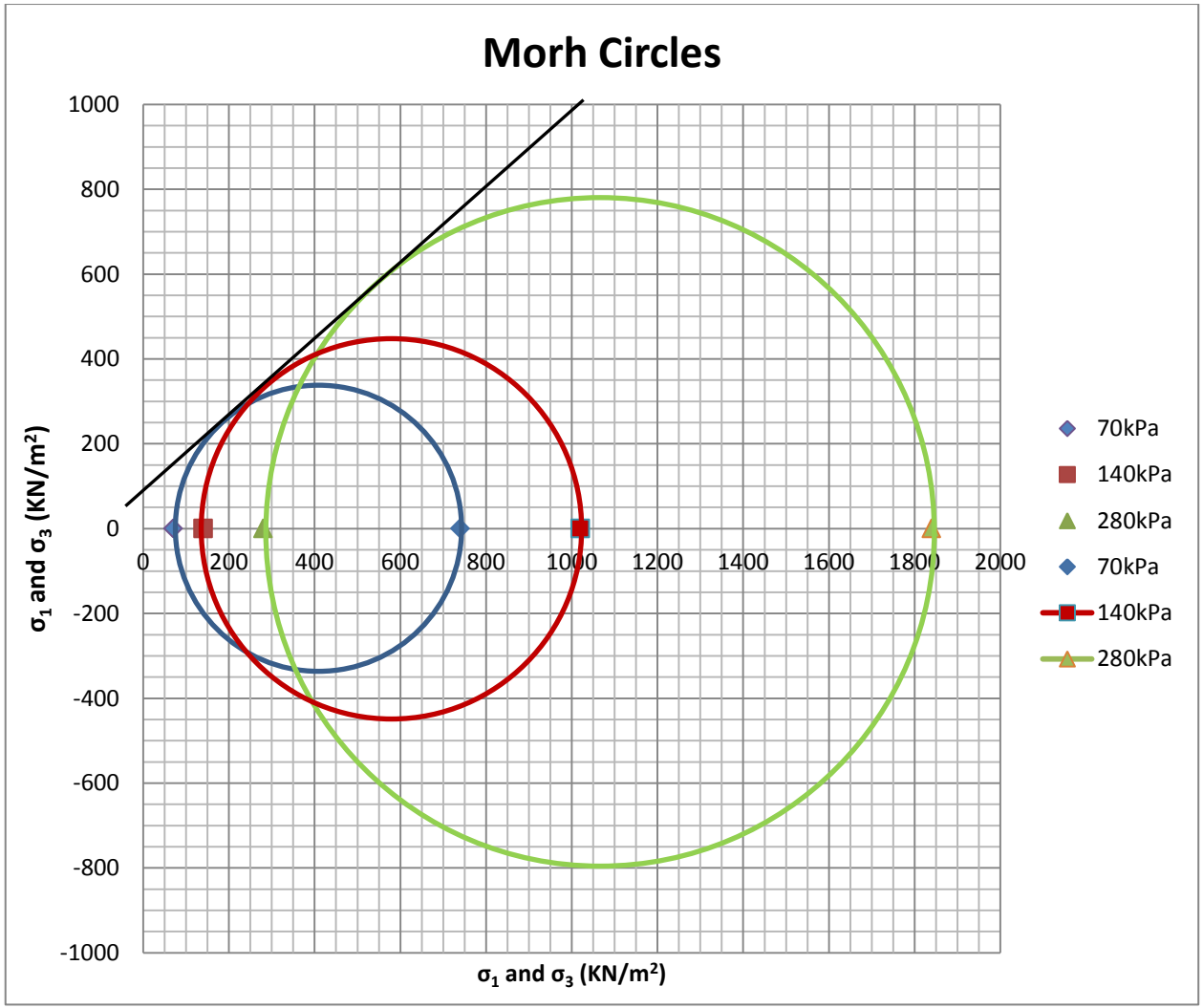

Fig B.6.2: Morh circle graph for Sample B1

Table B.6.8: Stress strength parameters for sample B1

Result from graph	0	70kPa	140kPa	280kPa
Deviator stress (max) 'σ_1-σ_3' (KN/m^2)	0	670	880	1560
Normal stress 'σ_3' (KN/m^2)	0	70	140	280
Shear stress 'σ_1' (KN/m^2)	0	740	1020	1840
Mean Stress '[1/3('σ_1+2σ_3]' (KN/m2)	0.0	293.3	433.3	800.0
Internal angle of friction (^{o})	41.99			
Cohesion (KN/m2)	85			

1. *Soil B at High dry of OMC (2)*

Table B.7.1: Initial parameters from preparation of sample B2.

Compaction test		
Mass of Mould + base (g)	3665.40	
Mass of Mould + base + soil (g)	5644.80	
Mass Soil (g)	1979.40	
Weight of container (g)	16.40	15.80
Container + wet soil (g)	34.00	34.00
Container + dry soil (g)	32.20	32.20
Moisture Content (%)	11.39	10.98
Av. Moisture Content (%)	11.18	
Volume of mould (cm^3)	1000	
Bulk Density (g/cm^3)	1.98	
Dry density (g/cm^3)	1.78	
Void ratio 'e_0' = [(Gs*ρ_w/ρ_d)-1]	0.63	
Degree of saturation 'Sr_i' (%)	51.57	

Table B.7.2: Initial parameters for sample B2 at confining pressure 'σ3' 70kPa.

Diameter of sample 'D_0' (mm)	38.0
Length of sample 'L_0' (mm)	77.6
20% strain of length (%)	15.52
Mass of Sample 'M_0' (g)	180.9
Area of sample 'A_0' (mm^2)	1134.57
Moisture content (%)	12.86
Young's modulus for latex membrane 'E_m' (kN/m^2)	1400
Thickness of membrane (0.1 - 0.2mm) 't_m' (mm)	0.15

Table B.7.3: Initial parameters for sample B2 at confining pressure 'σ3' 140kPa.

Diameter of sample 'D_0' (mm)	37.9
Length of sample 'L_0' (mm)	76.9
20% strain of length (%)	15.38
Mass of Sample 'M_0' (g)	177.3
Area of sample 'A_0' (mm^2)	1128.61
Moisture content (%)	13.63
Young's modulus for latex membrane 'E_m' (kN/m^2)	1400
Thickness of membrane (0.1 - 0.2mm) 't_m' (mm)	0.15

Table B.7.4: Initial parameters for sample B2 at confining pressure 'σ3' 140kPa.

Diameter of sample 'D_0' (mm)	37.8
Length of sample 'L_0' (mm)	78.1
20% strain of length (%)	15.62
Mass of Sample 'M_0' (g)	176.9
Area of sample 'A_0' (mm^2)	1122.66
Moisture content (%)	12.15
Young's modulus for latex membrane 'E_m' (kN/m^2)	1400
Thickness of membrane (0.1 - 0.2mm) 't_m' (mm)	0.15

Table B.7.5: Triaxial test values for sample B2 at confining pressure 'σ3' 70kPa.

Strain guage reading (yellow (bottom) gauge) **Sr**	Force guage reading (white (top) gauge) **Fr**	Change in sample length '***ΔL***' (mm) Sr*0.01	Axial strain '***Ea***' $\Delta L/L_0$	Corrected Area '***Ac***' (mm^2) $A_0/(1+Ea)$	Axial Force '***P***' (N) (100/37)*Fr	Axial Stress 'σ_1-σ_3' (KN/m^2) P/Ac	Rubber membrane 'R_m' (KN/m^2) $(4.E_m.t_m.Ea)/D_0$	Corrected Axial Stress 'σ_1-σ_3' (KN/m^2) σ_1-σ_3' -R_m	Axial strain '***Ea***' (%) Ea*100%
0.00	0.00	0.00	0.0000	1134.57	0.00	0.00	0.00	0.00	0.00
50.00	80.00	0.50	0.0064	1127.31	216.22	191.80	0.14	191.66	0.64
100.00	229.00	1.00	0.0129	1120.14	618.92	552.54	0.28	552.25	1.29
200.00	302.00	2.00	0.0258	1106.06	816.22	737.95	0.57	737.38	2.58
300.00	278.00	3.00	0.0387	1092.34	751.35	687.84	0.85	686.98	3.87
400.00	280.00	4.00	0.0515	1078.96	756.76	701.38	1.14	700.24	5.15
500.00	283.00	5.00	0.0644	1065.89	764.86	717.58	1.42	716.16	6.44
600.00	284.00	6.00	0.0773	1053.14	767.57	728.84	1.71	727.13	7.73
700.00	287.00	7.00	0.0902	1040.69	775.68	745.34	1.99	743.35	9.02
800.00	291.00	8.00	0.1031	1028.54	786.49	764.67	2.28	762.39	10.31
900.00	293.00	9.00	0.1160	1016.66	791.89	778.92	2.56	776.35	11.60
1000.00	296.00	10.00	0.1289	1005.05	800.00	795.98	2.85	793.13	12.89
1100.00	301.00	11.00	0.1418	993.71	813.51	818.66	3.13	815.53	14.18
1200.00	304.00	12.00	0.1546	982.62	821.62	836.15	3.42	832.74	15.46
1300.00	306.00	13.00	0.1675	971.77	827.03	851.05	3.70	847.35	16.75
1400.00	306.00	14.00	0.1804	961.17	827.03	860.44	3.99	856.45	18.04
1500.00	307.00	15.00	0.1933	950.79	829.73	872.68	4.27	868.41	19.33
1600.00	307.00	16.00	0.2062	940.63	829.73	882.10	4.56	877.54	20.62

Table B.7.6: Triaxial test values for sample B2 at confining pressure 'σ3' 140kPa.

Strain guage reading (yellow (bottom) gauge) **Sr**	Force guage reading (white (top) gauge) **Fr**	Change in sample length '***ΔL***' (mm) Sr*0.01	Axial strain '***Ea***' $\Delta L/L_0$	Corrected Area '***Ac***' (mm^2) $A_0/(1+Ea)$	Axial Force '***P***' (N) (100/37)*Fr	Axial Stress 'σ_1-σ_3' (KN/m^2) P/Ac	Rubber membrane 'R_m' (KN/m^2) $(4.E_m.t_m.Ea)/D_0$	Corrected Axial Stress 'σ_1-σ_3' (KN/m^2) σ_1-σ_3' -R_m	Axial strain '***Ea***' (%) Ea*100%
0.00	0.00	0.00	0.0000	1134.57	0.00	0.00	0.00	0.00	0.00
50.00	134.00	0.50	0.0064	1127.31	362.16	321.26	0.14	321.12	0.64
100.00	246.00	1.00	0.0129	1120.14	664.86	593.56	0.28	593.27	1.29
200.00	362.00	2.00	0.0258	1106.06	978.38	884.56	0.57	883.99	2.58
300.00	374.00	3.00	0.0387	1092.34	1010.81	925.36	0.85	924.51	3.87
400.00	384.00	4.00	0.0515	1078.96	1037.84	961.89	1.14	960.75	5.15
500.00	394.00	5.00	0.0644	1065.89	1064.86	999.04	1.42	997.61	6.44
600.00	394.00	6.00	0.0773	1053.14	1064.86	1011.13	1.71	1009.42	7.73
700.00	396.00	7.00	0.0902	1040.69	1070.27	1028.42	1.99	1026.43	9.02
800.00	403.00	8.00	0.1031	1028.54	1089.19	1058.97	2.28	1056.69	10.31
900.00	405.00	9.00	0.1160	1016.66	1094.59	1076.66	2.56	1074.09	11.60
1000.00	396.00	10.00	0.1289	1005.05	1070.27	1064.89	2.85	1062.04	12.89
1100.00	396.50	11.00	0.1418	993.71	1071.62	1078.40	3.13	1075.27	14.18
1200.00	400.00	12.00	0.1546	982.62	1081.08	1100.20	3.42	1096.78	15.46
1300.00	401.00	13.00	0.1675	971.77	1083.78	1115.26	3.70	1111.56	16.75
1400.00	401.00	14.00	0.1804	961.17	1083.78	1127.57	3.99	1123.58	18.04
1500.00	404.00	15.00	0.1933	950.79	1091.89	1148.41	4.27	1144.14	19.33
1600.00	410.00	16.00	0.2062	940.63	1108.11	1178.05	4.56	1173.49	20.62

Table B.7.7: Triaxial test values for sample B2 at confining pressure 'σ3' 280kPa.

Strain guage reading (yellow (bottom) gauge) **Sr**	Force guage reading (white (top) gauge) **Fr**	Change in sample length '***ΔL***' (mm) Sr*0.01	Axial strain '***Ea***' $\Delta L/L_0$	Corrected Area '***Ac***' (mm^2) $A_0/(1+Ea)$	Axial Force '***P***' (N) (100/37)*Fr	Axial Stress 'σ_1-σ_3' (KN/m^2) P/Ac	Rubber membrane 'R_m' (KN/m^2) $(4.E_m.t_m.Ea)/D_0$	Corrected Axial Stress 'σ_1-σ_3' (KN/m^2) σ_1-σ_3' -R_m	Axial strain '***Ea***' (%) Ea*100%
0.00	0.00	0.00	0.0000	1134.57	0.00	0.00	0.00	0.00	0.00
50.00	250.00	0.50	0.0064	1127.31	675.68	599.37	0.14	599.23	0.64
100.00	390.00	1.00	0.0129	1120.14	1054.05	941.00	0.28	940.72	1.29
200.00	515.00	2.00	0.0258	1106.06	1391.89	1258.42	0.57	1257.85	2.58
300.00	568.00	3.00	0.0387	1092.34	1535.14	1405.36	0.85	1404.51	3.87
400.00	590.00	4.00	0.0515	1078.96	1594.59	1477.91	1.14	1476.77	5.15
500.00	600.00	5.00	0.0644	1065.89	1621.62	1521.37	1.42	1519.95	6.44
600.00	609.00	6.00	0.0773	1053.14	1645.95	1562.89	1.71	1561.18	7.73
700.00	612.00	7.00	0.0902	1040.69	1654.05	1589.38	1.99	1587.38	9.02
800.00	611.00	8.00	0.1031	1028.54	1651.35	1605.53	2.28	1603.26	10.31
900.00	613.00	9.00	0.1160	1016.66	1656.76	1629.61	2.56	1627.04	11.60
1000.00	614.00	10.00	0.1289	1005.05	1659.46	1651.11	2.85	1648.27	12.89
1100.00	614.00	11.00	0.1418	993.71	1659.46	1669.96	3.13	1666.83	14.18
1200.00	619.00	12.00	0.1546	982.62	1672.97	1702.56	3.42	1699.15	15.46
1300.00	622.00	13.00	0.1675	971.77	1681.08	1729.91	3.70	1726.21	16.75
1400.00	625.00	14.00	0.1804	961.17	1689.19	1757.44	3.99	1753.45	18.04
1500.00	629.00	15.00	0.1933	950.79	1700.00	1788.00	4.27	1783.72	19.33
1600.00	632.00	16.00	0.2062	940.63	1708.11	1815.92	4.56	1811.37	20.62

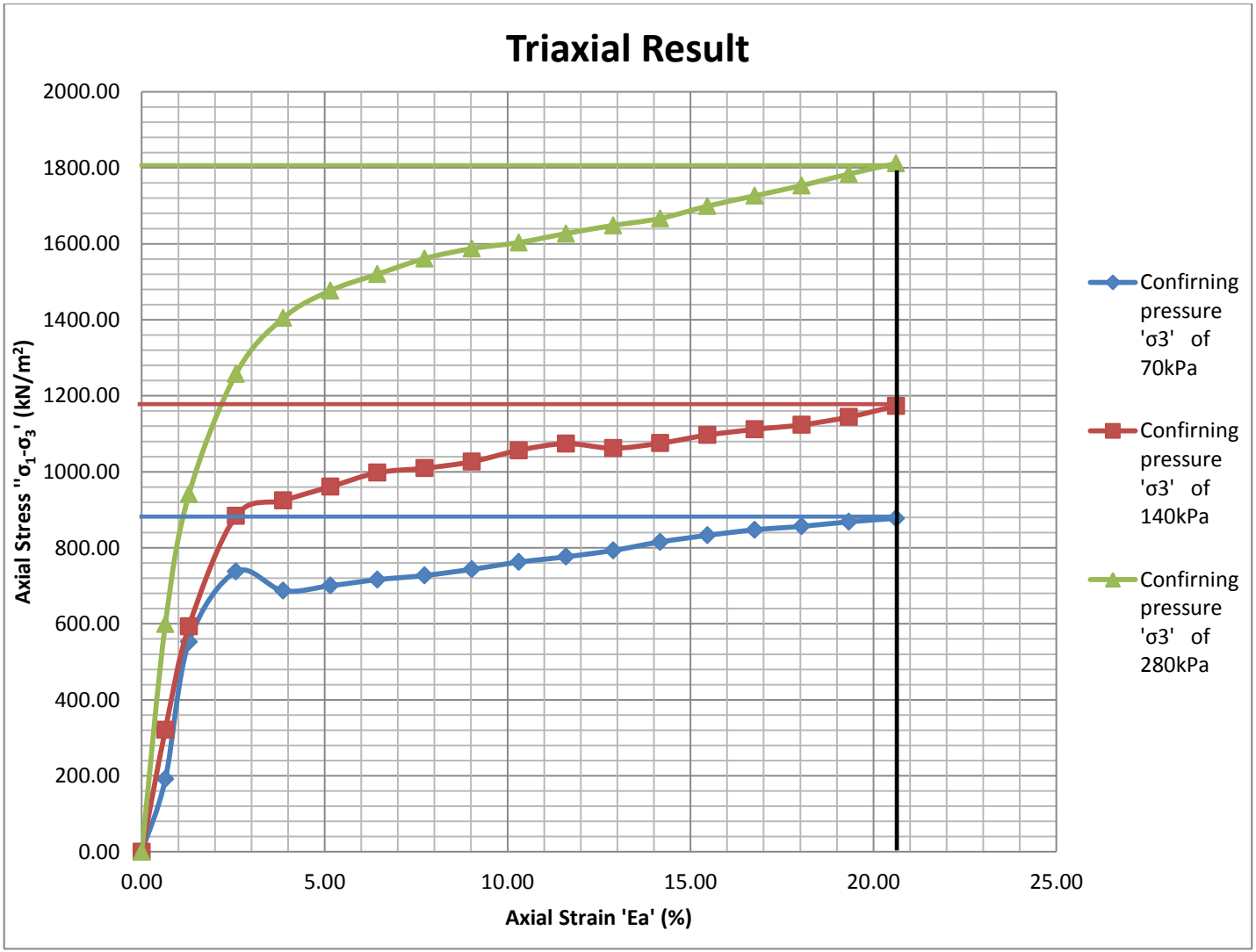

Fig B.7.1: Triaxial test graph for Sample B2

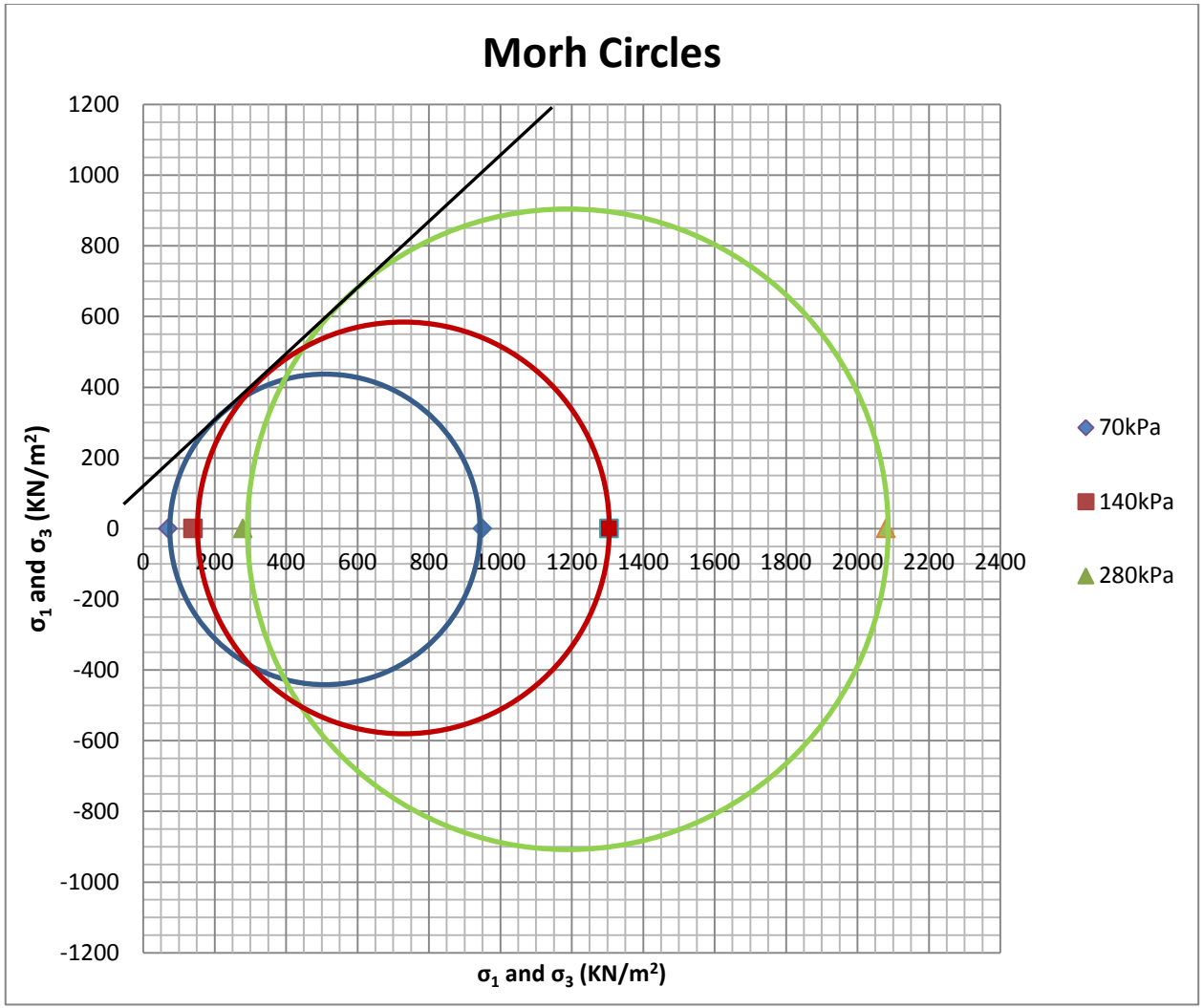

Fig B.7.2: Morh circle graph for Sample B2

Table B.7.8: Stress strength parameters for sample B2

Result from graph	0	70kPa	140kPa	280kPa
Deviator stress (max) 'σ_1-σ_3' (KN/m^2)	0	880	1165	1800
Normal stress 'σ_3' (KN/m^2)	0	70	140	280
Shear stress 'σ_1' (KN/m^2)	0	950	1305	2080
Mean Stress '[1/3('σ_1+2σ_3]' (KN/m2)	0.0	363.3	528.3	880.0
Internal angle of friction (^{o})	42.77			
Cohesion (KN/m2)	120			

C

Oedometer Test

Oedometer

1. Soil A at Low dry of OMC (1)

Table C.1.1: initial parameter of sample A1 (As-compacted)

Dimensions			**Initial specimen**	**Final specimen**
Diameter	'D'	(cm)	7.640	7.640
Area	'A'	(cm^2)	45.843	45.843
Height	'H'	(cm)	1.810	1.769
Volume	'V'	(cm^3)	82.976	81.118
Weights				
Ring		(g)	97.600	97.600
Ring + Sample in ring		(g)	272.500	272.285
Sample in ring	'M'	(g)	174.900	174.685
Moisture content 'W'		(%)	0.101	0.099
Calculated				
Assumed specific gravity 'Gs'			2.900	2.900
Density of water 'ρ_w'		(g/cm^3)	1.000	1.000
bulk density	'ρ' = [M/(A*H)]	(g/cm^3)	2.108	2.153
Dry Density	'ρ_d' = [ρ/(1+W)]	(g/cm^3)	1.915	1.959
Void ratio	'e_0' = [(Gs*ρ_w/ρ_d)-1]		0.515	0.481
Degree of saturation 'Sr_i'	= [Gs*W/e_0]		0.568	0.600
Mass of solids in sample 'M_s'	=[M/(W+1)]	(g)	158.884	158.884
Height of solids in sample 'H_s'	=[H/(1+e_0)]	(cm)	1.195	1.195

Table C.1.2: Consolidation data for sample A1 (As-compacted)

Time		Pressure at 5kPa		Pressure at 25kPa		Pressure at 50kPa		Pressure at 100kPa		Pressure at 200kPa		Pressure at 300kPa	
		Gauge reading	Consolidation settlement 'Δh'	Gauge reading	Consolidation settlement 'Δh'	Gauge reading	Consolidation settlement 'Δh'	Gauge reading	Consolidation settlement 'Δh'	Gauge reading	Consolidation settlement 'Δh'	Gauge reading	Consolidation settlement 'Δh'
t	√t	Gr	$(Gr_1 - Gr)$ *0.002	Gr	$(Gr_1 - Gr)$ *0.002	Gr	$(Gr_1 - Gr)$ *0.002	Gr	$(Gr_1 - Gr)$ *0.002	Gr	$(Gr_1 - Gr)$ *0.002	Gr	$(Gr_1 - Gr)$ *0.002
(mins)	(√mins)	(div)	(mm)	(div)	(mm)	(div)	(mm)	(div)	(mm)	(div)	(mm)	(div)	(mm)
0.00	0.00	1200.0	0.000	1187.9	0.024	1157.8	0.084	1137.1	0.126	1092.8	0.214	997.3	0.405
0.13	0.37	1190.5	0.019	1160.5	0.079	1144.0	0.112	1109.0	0.182	1025.0	0.350	958.0	0.484
0.25	0.50	1190.2	0.020	1160.2	0.080	1142.5	0.115	1107.2	0.186	1019.8	0.360	953.0	0.494
0.50	0.71	1190.0	0.020	1160.1	0.080	1141.8	0.116	1104.0	0.192	1015.8	0.368	949.5	0.501
1.00	1.00	1189.8	0.020	1159.6	0.081	1140.9	0.118	1102.2	0.196	1012.3	0.375	946.2	0.508
2.00	1.41	1189.2	0.022	1159.0	0.082	1140.0	0.120	1101.5	0.197	1009.0	0.382	942.9	0.514
4.00	2.00	1189.0	0.022	1158.7	0.083	1139.2	0.122	1098.6	0.203	1005.8	0.388	939.6	0.521
8.00	2.83	1188.8	0.022	1158.1	0.084	1138.8	0.122	1096.8	0.206	1002.7	0.395	936.9	0.526
15.00	3.87	1188.1	0.024	1157.9	0.084	1137.9	0.124	1094.9	0.210	999.8	0.400	934.0	0.532
30.00	5.48	1187.9	0.024	1157.8	0.084	1137.1	0.126	1092.8	0.214	997.3	0.405	931.1	0.538

Table C.1.3: Consolidation calculated parameter for sample A1 (As-compacted)

Pressures	**(kPa)**	**0**	**5**	**25**	**50**	**100**	**200**	**300**
Δh_{90}	(mm)		0.020	0.080	0.116	0.186	0.362	0.49
Δh_0	(mm)		0.000	0.024	0.088	0.126	0.214	0.405
$\Delta h_{100} = [((\Delta h_{90} - \Delta h_0)/0.9) + \Delta h_0]$	(mm)		0.022	0.086	0.119	0.193	0.378	0.499
Δh_f	(mm)		0.024	0.084	0.126	0.214	0.405	0.538
Initial Compression ratio $r_i = [\Delta h_0/\Delta h_f]$			0.000	0.284	0.703	0.588	0.528	0.753
Primary Compression ratio $r_p = [(\Delta h_{100}-\Delta h_0)/\Delta h_f]$			0.914	0.737	0.244	0.311	0.406	0.176
Secondary Compression ratio 'r_{sec}' $= [(\Delta h_f - \Delta h_{100})/\Delta h_f]$			0.086	-0.022	0.054	0.101	0.066	0.071
√t90	(√min)		0.540	0.460	0.590	0.480	0.500	0.560
t_{90}	(mins)		0.292	0.212	0.348	0.230	0.250	0.314
T_{90}			0.848	0.848	0.848	0.848	0.848	0.848
drainage path 'd' $= [h_i/2]$	(mm)		9.050	9.038	9.006	8.987	8.943	8.848
Initial void ratio 'e_i' $=[(H-\Delta h_0-Hs)/Hs]$			0.515	0.513	0.507	0.504	0.497	0.481
Final void ratio 'e_f' $=[(H-\Delta h_f-Hs)/Hs]$		0.515	0.512	0.507	0.504	0.497	0.481	0.470
Total change in void ratio 'Δe' $= e_i - e_f$			0.002	0.005	0.003	0.007	0.016	0.011
Change of stress/pressure 'Δσ' $= \sigma_t - \sigma_p$	(kPa) or (kN/m^2)		5	20	25	50	100	100
Volume Compressibility 'Mv' $= [(1/1+e_0)*(\Delta e/\Delta\sigma')]$	(m^2/MN)		0.267	0.167	0.083	0.098	0.106	0.073
Volumetric Strain $= (\Delta hi/H)*100\%$	(%)	0.000	0.134	0.466	0.695	1.185	2.240	2.971
Coefficient of consolidation 'Cv' $= [(T_{90}*d^2)/t_{90}]$	(mm^2/min)		238.2	327.4	197.6	297.3	271.3	211.7
Coefficient of Permeability 'k' $= C_v*M_v*\gamma_w$	(m/yr)		0.320	0.275	0.082	0.146	0.144	0.078

Table C.1.4: initial parameter of sample A1 (Inundated)

Dimensions			Initial specimen	Final specimen
Diameter	'D'	(cm)	7.670	7.670
Area	'A'	(cm^2)	46.204	46.204
Height	'H'	(cm)	1.800	1.728
Volume	'V'	(cm^3)	83.167	79.821
Weights				
Ring		(g)	76.400	76.400
Ring + Sample in ring		(g)	252.100	261.758
Sample in ring	'M'	(g)	175.700	185.358
Moisture content 'W'		(%)	0.100	0.1758
Calculated				
Assumed specific gravity 'Gs'			2.900	2.900
Density of water 'ρ_w'		(g/cm^3)	1.000	1.000
bulk density	'ρ' = [M/(A*H)]	(g/cm^3)	2.113	2.322
Dry Density	'ρ_d' = [ρ/(1+W)]	(g/cm^3)	1.921	1.921
Void ratio	'e_0' = [(Gs*ρ_w/ρ_d)-1]		0.510	0.510
Degree of saturation	'Sr_i' = [Gs*W/e_0]		0.568	1.000
Mass of solids in sample	'M_s' =[M/(W+1)]	(g)	159.745	159.745
Height of solids in sample	'H_s' =[H/(1+e_0)]	(cm)	1.192	1.192

Table C.1.5: Consolidation data for sample A1 (Inundated)

Time		Pressure at 5kPa		Pressure at 25kPa		Pressure at 50kPa		Pressure at 100kPa		Pressure at 200kPa		Pressure at 300kPa	
		Gauge reading	Consolidation settlement 'Δh'	Gauge reading	Consolidation settlement 'Δh'	Gauge reading	Consolidation settlement 'Δh'	Gauge reading	Consolidation settlement 'Δh'	Gauge reading	Consolidation settlement 'Δh'	Gauge reading	Consolidation settlement 'Δh'
t	√t	Gr	$(Gr_1 - Gr)$ *0.002	Gr	$(Gr_1 – Gr)$ *0.002	Gr	$(Gr_1 - Gr)$ *0.002	Gr	$(Gr_1 - Gr)$ *0.002	Gr	$(Gr_1 - Gr)$ *0.002	Gr	$(Gr_1 - Gr)$ *0.002
(mins)	(√mins)	(div)	(mm)	(div)	(mm)	(div)	(mm)	(div)	(mm)	(div)	(mm)	(div)	(mm)
0.00	0.00	1100.0	0.000	1003.6	0.193	897.8	0.404	846.8	0.506	793.0	0.614	737.9	0.724
0.13	0.37	1065.0	0.070	954.0	0.292	876.0	0.448	828.0	0.544	768.0	0.664	726.0	0.748
0.25	0.50	1057.0	0.086	946.0	0.308	873.0	0.454	822.0	0.556	764.0	0.672	723.5	0.753
0.50	0.71	1048.0	0.104	936.0	0.328	869.0	0.462	816.3	0.567	758.5	0.683	721.0	0.758
1.00	1.00	1038.0	0.124	927.0	0.346	863.8	0.472	810.2	0.580	753.0	0.694	718.0	0.764
2.00	1.41	1025.5	0.149	915.2	0.370	858.2	0.484	804.2	0.592	747.8	0.704	714.1	0.772
4.00	2.00	1015.0	0.170	906.5	0.387	853.1	0.494	799.5	0.601	743.5	0.713	711.1	0.778
8.00	2.83	1008.1	0.184	901.1	0.398	850.0	0.500	796.8	0.606	741.0	0.718	708.9	0.782
15.00	3.87	1005.1	0.190	899.0	0.402	848.1	0.504	794.6	0.611	739.1	0.722	708.0	0.784
30.00	5.48	1003.6	0.193	897.8	0.404	846.8	0.506	793.2	0.614	737.9	0.724	706.7	0.787

Table C.1.6: Consolidation calculated parameter for sample A1 (Inundated)

Pressures (kPa)	0	5	25	50	100	200	300
Δh_{90} (mm)		0.190	0.321	0.455	0.572	0.678	0.756
Δh_0 (mm)		0.000	0.193	0.404	0.506	0.614	0.724
$\Delta h_{100} = [((\Delta h_{90} - \Delta h_0)/0.9) + \Delta h_0]$ (mm)		0.211	0.335	0.461	0.579	0.685	0.760
Δh_f (mm)		0.193	0.404	0.506	0.614	0.724	0.787
Initial Compression ratio $r_i = [\Delta h_0/\Delta h_f]$		0.000	0.477	0.798	0.825	0.848	0.920
Primary Compression ratio $r_p = [(\Delta h_{100}-\Delta h_0)/\Delta h_f]$		1.095	0.352	0.112	0.120	0.098	0.045
Secondary Compression ratio 'r_{sec}' $= [(\Delta h_f - \Delta h_{100})/\Delta h_f]$		-0.095	0.171	0.090	0.056	0.054	0.034
√t90 (√min)		0.700	0.620	0.740	0.800	0.600	0.610
t_{90} (mins)		0.490	0.384	0.548	0.640	0.360	0.372
T_{90}		0.848	0.848	0.848	0.848	0.848	0.848
drainage path 'd' $= [h_i/2]$ (mm)		9.000	8.904	8.798	8.747	8.693	8.688
Initial void ratio 'e_i' $=[(H-\Delta h_0-Hs)/Hs]$		0.510	0.494	0.476	0.467	0.458	0.454
Final void ratio 'e_f' $=[(H-\Delta h_f-Hs)/Hs]$	0.510	0.494	0.476	0.467	0.458	0.449	0.449
Total change in void ratio 'Δe' $= e_i - e_f$		0.016	0.018	0.009	0.009	0.009	0.005
Change of stress/pressure '$\Delta\sigma$' $= \sigma_t - \sigma_p$ (kPa) or (kN/m^2)		5	20	25	50	100	100
Volume Compressibility 'Mv' $= [(1/1+e_0)*(\Delta e/\Delta\sigma')]$ (m^2/MN)		2.142	0.587	0.228	0.120	0.061	0.035
Volumetric Strain $= (\Delta hi/H)*100\%$ (%)	0.000	1.071	2.247	2.813	3.409	4.023	4.370
coefficient of consolidation 'Cv' $= [(T_{90}*d^2)/t_{90}]$ (mm^2/min)		140.2	174.9	119.9	101.4	178.0	172.0
Coefficient of Permeability 'k' $= C_v*M_v*\gamma_w$ (m/yr)		1.510	0.516	0.137	0.061	0.055	0.030

2. Soil A at High dry of OMC (2)

Table C.2.1: initial parameter of sample A2 (As-compacted)

Dimensions			Initial specimen	Final specimen
Diameter	'D'	(cm)	7.710	7.710
Area	'A'	(cm^2)	46.687	46.687
Height	'H'	(cm)	1.777	1.734
Volume	'V'	(cm^3)	82.963	80.957
Weights				
Ring		(g)	76.200	76.200
Ring + Sample in ring		(g)	273.100	270.270
Sample in ring	'M'	(g)	196.900	194.070
Moisture content 'W'		(%)	0.133	0.117
Calculated				
Assumed specific gravity 'Gs'			2.900	2.900
Density of water 'ρ_w'		(g/cm^3)	1.000	1.000
bulk density	'ρ' = [M/(A*H)]	(g/cm^3)	2.373	2.397
Dry Density	'ρ_d' = [ρ/(1+W)]	(g/cm^3)	2.095	2.147
Void ratio	'e_0' = [(Gs*ρ_w/ρ_d)-1]		0.384	0.351
Degree of saturation 'Sr_i'	= [Gs*W/e_0]		1.003	0.965
Mass of solids in sample 'M_s'	=[M/(W+1)]	(g)	173.784	173.784
Height of solids in sample 'H_s'	=[H/(1+e_0)]	(cm)	1.284	1.284

Table C.2.2: Consolidation data for sample A2 (As-compacted)

Time		Pressure at 5kPa		Pressure at 25kPa		Pressure at 50kPa		Pressure at 100kPa		Pressure at 200kPa		Pressure at 300kPa	
		Gauge reading	Consolidation settlement 'Δh'	Gauge reading	Consolidation settlement 'Δh'	Gauge reading	Consolidation settlement 'Δh'	Gauge reading	Consolidation settlement 'Δh'	Gauge reading	Consolidation settlement 'Δh'	Gauge reading	Consolidation settlement 'Δh'
t	√t	Gr	$(Gr_1 - Gr)$ *0.002	Gr	$(Gr_1 - Gr)$ *0.002	Gr	$(Gr_1 - Gr)$ *0.002	Gr	$(Gr_1 - Gr)$ *0.002	Gr	$(Gr_1 - Gr)$ *0.002	Gr	$(Gr_1 - Gr)$ *0.002
(mins)	(√mins)	(div)	(mm)	(div)	(mm)	(div)	(mm)	(div)	(mm)	(div)	(mm)	(div)	(mm)
0.00	0.00	928.0	0.000	892.0	0.072	835.0	0.186	798.8	0.258	758.1	0.340	713.1	0.430
0.13	0.37	899.0	0.058	847.0	0.162	810.0	0.236	771.0	0.314	729.5	0.397	699.0	0.458
0.25	0.50	898.8	0.058	845.5	0.165	809.0	0.238	770.2	0.316	728.1	0.400	697.8	0.460
0.50	0.71	898.1	0.060	844.5	0.167	808.0	0.240	768.8	0.318	726.2	0.404	696.4	0.463
1.00	1.00	897.3	0.061	843.0	0.170	806.2	0.244	767.9	0.320	724.0	0.408	694.4	0.467
2.00	1.41	896.7	0.063	841.3	0.173	804.6	0.247	764.9	0.326	721.1	0.414	692.2	0.472
4.00	2.00	895.7	0.065	839.7	0.177	802.5	0.251	762.6	0.331	718.3	0.419	690.1	0.476
8.00	2.83	894.5	0.067	838.8	0.178	801.0	0.254	760.9	0.334	716.1	0.424	688.0	0.480
15.00	3.87	893.5	0.069	836.3	0.183	800.0	0.256	759.2	0.338	714.8	0.426	686.5	0.483
30.00	5.48	892.0	0.072	835.0	0.186	798.8	0.258	758.1	0.340	713.1	0.430	685.0	0.486

Table C.2.3: Consolidation calculated parameter for sample A2 (As-compacted)

Pressures	**(kPa)**	**0**	**5**	**25**	**50**	**100**	**200**	**300**
Δh_{90}	(mm)		0.059	0.167	0.239	0.316	0.401	0.461
Δh_0	(mm)		0.000	0.072	0.186	0.258	0.340	0.43
Δh_{100} = $[((\Delta h_{90} - \Delta h_0)/0.9)+ \Delta h_0]$	(mm)		0.066	0.178	0.244	0.322	0.408	0.464
Δh_f	(mm)		0.072	0.186	0.258	0.340	0.430	0.486
Initial Compression ratio $r_i = [\Delta h_0/\Delta h_f]$			0.000	0.387	0.720	0.759	0.791	0.885
Primary Compression ratio $r_p = [(\Delta h_{100}-\Delta h_0)/\Delta h_f]$			0.910	0.568	0.226	0.190	0.158	0.071
Secondary Compression ratio 'r_{sec}' = $[(\Delta h_f - \Delta h_{100})/\Delta h_f]$			0.090	0.045	0.054	0.051	0.051	0.044
√t90	(√min)		0.490	0.490	0.490	0.480	0.460	0.500
t_{90}	(mins)		0.240	0.240	0.240	0.230	0.212	0.250
T_{90}			0.848	0.848	0.848	0.848	0.848	0.848
drainage path 'd' = $[h_i/2]$	(mm)		8.885	8.849	8.792	8.756	8.715	8.670
Initial void ratio 'e_i' =$[(H-\Delta h_0-Hs)/Hs]$			0.384	0.379	0.370	0.364	0.358	0.351
Final void ratio 'e_f' =$[(H-\Delta h_f-Hs)/Hs]$		0.384	0.379	0.370	0.364	0.358	0.351	0.347
Total change in void ratio 'Δe' = $e_i - e_f$			0.006	0.009	0.006	0.006	0.007	0.004
Change of stress/pressure 'Δσ' = $\sigma_t - \sigma_p$	(kPa) or (kN/m^2)		5	20	25	50	100	100
Volume Compressibility 'Mv' = $[(1/1+e_0)*(\Delta e/\Delta\sigma')]$	(m^2/MN)		0.810	0.321	0.163	0.092	0.051	0.032
Volumetric Strain = (Δhi/H)*100%	(%)	0.000	0.405	1.047	1.454	1.912	2.419	2.735
coefficient of consolidation 'Cv' = $[(T_{90}*d^2)/t_{90}]$	(mm^2/min)		278.8	276.6	273.0	282.2	304.4	255.0
Coefficient of Permeability 'k' = $C_v*M_v*\gamma_w$	(m/yr)		1.136	0.446	0.224	0.131	0.077	0.040

Table C.2.4: initial parameter of sample A2 (Inundated)

Dimensions			Initial specimen	Final specimen
Diameter	'D'	(cm)	7.690	7.690
Area	'A'	(cm^2)	46.445	46.445
Height	'H'	(cm)	1.810	1.732
Volume	'V'	(cm^3)	84.066	80.426
Weights				
Ring		(g)	76.900	76.900
Ring + Sample in ring		(g)	269.000	271.276
Sample in ring	'M'	(g)	192.100	194.376
Moisture content 'W'		(%)	0.137	0.153
Calculated				
Assumed specific gravity 'Gs'			2.900	2.900
Density of water 'ρ_w'		(g/cm^3)	1.000	1.000
bulk density	'ρ' = [M/(A*H)]	(g/cm^3)	2.285	2.417
Dry Density	'ρ_d' = [ρ/(1+W)]	(g/cm^3)	2.010	2.010
Void ratio	'e_0' = [(Gs*ρ_w/ρ_d)-1]		0.443	0.443
Degree of saturation 'Sr_i'	= [Gs*W/e_0]		0.896	1.000
Mass of solids in sample 'M_s'	=[M/(W+1)]	(g)	169.003	169.003
Height of solids in sample 'H_s'	=[H/(1+e_0)]	(cm)	1.255	1.255

Table C.2.5: Consolidation data for sample A2 (Inundated)

Time		Pressure at 5kPa		Pressure at 25kPa		Pressure at 50kPa		Pressure at 100kPa		Pressure at 200kPa		Pressure at 300kPa	
		Gauge reading	Consolidation settlement 'Δh'	Gauge reading	Consolidation settlement 'Δh'	Gauge reading	Consolidation settlement 'Δh'	Gauge reading	Consolidation settlement 'Δh'	Gauge reading	Consolidation settlement 'Δh'	Gauge reading	Consolidation settlement 'Δh'
t	√t	Gr	$(Gr_1 - Gr)$ *0.002	Gr	$(Gr_1 - Gr)$ *0.002	Gr	$(Gr_1 - Gr)$ *0.002	Gr	$(Gr_1 - Gr)$ *0.002	Gr	$(Gr_1 - Gr)$ *0.002	Gr	$(Gr_1 - Gr)$ *0.002
(mins)	(√mins)	(div)	(mm)	(div)	(mm)	(div)	(mm)	(div)	(mm)	(div)	(mm)	(div)	(mm)
0.00	0.00	856.0	0.000	653.8	0.404	586.1	0.540	550.2	0.612	509.2	0.694	464.1	0.928
0.13	0.37	719.0	0.274	622.0	0.468	569.2	0.574	528.0	0.656	483.0	0.746	451.0	0.954
0.25	0.50	711.0	0.290	615.3	0.481	567.0	0.578	525.7	0.661	481.3	0.749	449.0	0.958
0.50	0.71	705.0	0.302	609.0	0.494	565.2	0.582	523.8	0.664	479.0	0.754	448.0	0.960
1.00	1.00	693.0	0.326	605.0	0.502	562.2	0.588	520.9	0.670	475.0	0.762	446.0	0.964
2.00	1.41	679.1	0.354	598.8	0.514	558.9	0.594	517.5	0.677	472.5	0.767	444.1	0.968
4.00	2.00	666.8	0.378	593.1	0.526	555.5	0.601	514.4	0.683	469.6	0.773	441.0	0.974
8.00	2.83	658.6	0.395	589.3	0.533	553.0	0.606	512.0	0.688	467.1	0.778	439.1	0.978
15.00	3.87	655.3	0.401	587.2	0.538	551.5	0.609	510.5	0.691	465.8	0.780	437.6	0.981
30.00	5.48	653.8	0.404	586.1	0.540	550.2	0.612	509.2	0.694	464.1	0.784	436.1	0.984

Table C.2.6: Consolidation calculated parameter for sample A2 (Inundated)

Pressures **(kPa)**	**0**	**5**	**25**	**50**	**100**	**200**	**300**
Δh_{90} (mm)		0.295	0.494	0.578	0.662	0.750	0.9585
Δh_0 (mm)		0.000	0.404	0.504	0.612	0.694	0.928
$\Delta h_{100} = [((\Delta h_{90} - \Delta h_0)/0.9) + \Delta h_0]$ (mm)		0.328	0.504	0.586	0.668	0.756	0.962
Δh_f (mm)		0.404	0.540	0.612	0.694	0.784	0.984
Initial Compression ratio $r_i = [\Delta h_0/\Delta h_f]$		0.000	0.748	0.824	0.882	0.885	0.943
Primary Compression ratio $r_p = [(\Delta h_{100}-\Delta h_0)/\Delta h_f]$		0.811	0.185	0.134	0.080	0.079	0.034
Secondary Compression ratio 'r_{sec}' $= [(\Delta h_f - \Delta h_{100})/\Delta h_f]$		0.189	0.066	0.041	0.038	0.035	0.022
√t90 (√min)		0.500	0.690	0.520	0.520	0.490	0.560
t_{90} (mins)		0.250	0.476	0.270	0.270	0.240	0.314
T_{90}		0.848	0.848	0.848	0.848	0.848	0.848
drainage path 'd' $= [h_i/2]$ (mm)		9.050	8.848	8.798	8.744	8.703	8.586
Initial void ratio 'e_i' $=[(H-\Delta h_0-Hs)/Hs]$		0.443	0.410	0.402	0.394	0.387	0.369
Final void ratio 'e_f' $=[(H-\Delta h_f-Hs)/Hs]$	0.443	0.410	0.400	0.394	0.387	0.380	0.364
Total change in void ratio 'Δe' $= e_i - e_f$		0.032	0.011	0.009	0.007	0.007	0.004
Change of stress/pressure 'Δσ' $= \sigma_t - \sigma_p$ (kPa) or (kN/m^2)		5	20	25	50	100	100
Volume Compressibility 'Mv' $= [(1/1+e_0)*(\Delta e/\Delta\sigma')]$ (m^2/MN)		4.469	0.375	0.238	0.090	0.050	0.031
Volumetric Strain $= (\Delta hi/H)*100\%$ (%)	0.000	2.234	2.982	3.379	3.832	4.330	5.435
coefficient of consolidation 'Cv' $= [(T_{90}*d^2)/t_{90}]$ (mm^2/min)		277.8	139.4	242.7	239.8	267.5	199.3
Coefficient of Permeability 'k' $= C_v*M_v*\gamma_w$ (m/yr)		6.243	0.263	0.290	0.109	0.067	0.031

3. Soil A at 'At OMC' (3)

Table C.3.1: initial parameter of sample A3 (As-compacted)

Dimensions			Initial specimen	Final specimen
Diameter	'D'	(cm)	7.640	7.640
Area	'A'	(cm^2)	45.843	45.843
Height	'H'	(cm)	1.810	1.778
Volume	'V'	(cm^3)	82.976	81.501
Weights				
Ring		(g)	97.600	97.600
Ring + Sample in ring		(g)	277.800	275.299
Sample in ring	'M'	(g)	180.200	177.699
Moisture content 'W'		(%)	0.149	0.133
Calculated				
Assumed specific gravity 'Gs'			2.900	2.900
Density of water 'ρ_w'		(g/cm^3)	1.000	1.000
bulk density 'ρ' = [M/(A*H)]		(g/cm^3)	2.172	2.180
Dry Density 'ρ_d' = [ρ/(1+W)]		(g/cm^3)	1.890	1.924
Void ratio 'e_0' = [(Gs*ρ_w/ρ_d)-1]			0.534	0.507
Degree of saturation 'Sr_i' = [Gs*W/e_0]			0.809	0.761
Mass of solids in sample 'M_s' =[M/(W+1)]		(g)	156.823	156.823
Height of solids in sample 'H_s' =[H/(1+e_0)]		(cm)	1.180	1.180

Table C.3.2: Consolidation data for sample A3 (As-compacted)

Time		Pressure at 5kPa		Pressure at 25kPa		Pressure at 50kPa		Pressure at 100kPa		Pressure at 200kPa		Pressure at 300kPa	
		Gauge reading	Consolidation settlement 'Δh'	Gauge reading	Consolidation settlement 'Δh'	Gauge reading	Consolidation settlement 'Δh'	Gauge reading	Consolidation settlement 'Δh'	Gauge reading	Consolidation settlement 'Δh'	Gauge reading	Consolidation settlement 'Δh'
t	√t	Gr	$(Gr_1 - Gr)$ *0.002	Gr	$(Gr_1 - Gr)$ *0.002	Gr	$(Gr_1 - Gr)$ *0.002	Gr	$(Gr_1 - Gr)$ *0.002	Gr	$(Gr_1 - Gr)$ *0.002	Gr	$(Gr_1 - Gr)$ *0.002
(mins)	(√mins)	(div)	(mm)	(div)	(mm)	(div)	(mm)	(div)	(mm)	(div)	(mm)	(div)	(mm)
0.00	0.00	1000.0	0.000	978.8	0.042	939.1	0.122	912.8	0.174	879.1	0.242	839.1	0.322
0.13	0.37	985.7	0.029	950.4	0.099	923.0	0.154	892.0	0.216	856.5	0.287	827.0	0.346
0.25	0.50	984.8	0.030	949.0	0.102	921.0	0.158	890.5	0.219	854.0	0.292	825.2	0.350
0.50	0.71	983.9	0.032	947.8	0.104	920.5	0.159	889.1	0.222	852.5	0.295	823.9	0.352
1.00	1.00	983.0	0.034	946.1	0.108	919.1	0.162	887.5	0.225	850.0	0.300	822.1	0.356
2.00	1.41	982.1	0.036	944.8	0.110	917.9	0.164	885.8	0.228	847.1	0.306	820.0	0.360
4.00	2.00	981.1	0.038	943.0	0.114	916.1	0.168	883.6	0.233	844.3	0.311	817.9	0.364
8.00	2.83	980.2	0.040	941.0	0.118	914.8	0.170	881.5	0.237	842.1	0.316	815.8	0.368
15.00	3.87	979.3	0.041	940.0	0.120	913.5	0.173	880.1	0.240	840.7	0.319	814.1	0.372
30.00	5.48	978.8	0.042	939.1	0.122	912.8	0.174	879.1	0.242	839.1	0.322	813.0	0.374

Table C.3.3: Consolidation calculated parameter for sample A3 (As-compacted)

Pressures	**(kPa)**	**0**	**5**	**25**	**50**	**100**	**200**	**300**
Δh_{90}	(mm)		0.031	0.102	0.158	0.220	0.293	0.355
Δh_0	(mm)		0.000	0.042	0.122	0.174	0.242	0.322
Δh_{100} = $[((\Delta h_{90} - \Delta h_0)/0.9)+ \Delta h_0]$	(mm)		0.035	0.109	0.162	0.225	0.298	0.359
Δh_f	(mm)		0.042	0.122	0.174	0.242	0.322	0.374
Initial Compression ratio $r_i = [\Delta h_0/\Delta h_f]$			0.000	0.345	0.700	0.720	0.752	0.861
Primary Compression ratio $r_p = [(\Delta h_{100}-\Delta h_0)/\Delta h_f]$			0.818	0.547	0.231	0.211	0.174	0.098
Secondary Compression ratio 'r_{sec}' = $[(\Delta h_f - \Delta h_{100})/\Delta h_f]$			0.182	0.108	0.069	0.069	0.074	0.041
√t90	(√min)		0.580	0.510	0.560	0.510	0.570	0.590
t_{90}	(mins)		0.336	0.260	0.314	0.260	0.325	0.348
T_{90}			0.848	0.848	0.848	0.848	0.848	0.848
drainage path 'd' = $[h_i/2]$	(mm)		9.050	9.029	8.989	8.963	8.929	8.889
Initial void ratio 'e_i' =$[(H-\Delta h_0-Hs)/Hs]$			0.534	0.531	0.524	0.520	0.514	0.507
Final void ratio 'e_f' =$[(H-\Delta h_f-Hs)/Hs]$		0.534	0.531	0.524	0.520	0.514	0.507	0.503
Total change in void ratio 'Δe' = $e_i - e_f$			0.004	0.007	0.004	0.006	0.007	0.004
Change of stress/pressure 'Δσ' = $\sigma_t - \sigma_p$	(kPa) or (kN/m^2)		5	20	25	50	100	100
Volume Compressibility 'Mv' = $[(1/1+e_0)*(\Delta e/\Delta\sigma')]$	(m^2/MN)		0.469	0.220	0.116	0.075	0.044	0.029
Volumetric Strain = (Δhi/H)*100%	(%)	0.000	0.234	0.673	0.964	1.336	1.778	2.066
coefficient of consolidation 'Cv' = $[(T_{90}*d^2)/t_{90}]$	(mm^2/min)		206.5	265.8	218.5	261.9	208.1	192.5
Coefficient of Permeability 'k' = $C_v*M_v*\gamma_w$	(m/yr)		0.486	0.295	0.127	0.099	0.046	0.028

Table C.3.4: initial parameter of sample A3 (Inundated)

Dimensions			Initial specimen	Final specimen
Diameter	'D'	(cm)	7.620	7.620
Area	'A'	(cm^2)	45.604	45.604
Height	'H'	(cm)	1.830	1.789
Volume	'V'	(cm^3)	83.455	81.574
Weights				
Ring		(g)	99.300	99.300
Ring + Sample in ring		(g)	289.500	286.684
Sample in ring	'M'	(g)	190.200	187.384
Moisture content 'W'		(%)	0.149	0.1591
Calculated				
Assumed specific gravity 'Gs'			2.900	2.900
Density of water 'ρ_w'		(g/cm^3)	1.000	1.000
bulk density	'ρ' = [M/(A*H)]	(g/cm^3)	2.279	2.297
Dry Density	'ρ_d' = [ρ/(1+W)]	(g/cm^3)	1.984	1.984
Void ratio	'e_0' = [(Gs*ρ_w/ρ_d)-1]		0.462	0.462
Degree of saturation 'Sr_i'	= [Gs*W/e_0]		0.934	1.000
Mass of solids in sample 'M_s'	=[M/(W+1)]	(g)	165.595	165.595
Height of solids in sample 'H_s'	=[H/(1+e_0)]	(cm)	1.252	1.252

Table C.3.5: Consolidation data for sample A3 (Inundated)

Time		Pressure at 5kPa		Pressure at 25kPa		Pressure at 50kPa		Pressure at 100kPa		Pressure at 200kPa		Pressure at 300kPa	
		Gauge reading	Consolidation settlement 'Δh'	Gauge reading	Consolidation settlement 'Δh'	Gauge reading	Consolidation settlement 'Δh'	Gauge reading	Consolidation settlement 'Δh'	Gauge reading	Consolidation settlement 'Δh'	Gauge reading	Consolidation settlement 'Δh'
t	√t	Gr	$(Gr_1 - Gr)$ *0.002	Gr	$(Gr_1 - Gr)$ *0.002	Gr	$(Gr_1 - Gr)$ *0.002	Gr	$(Gr_1 - Gr)$ *0.002	Gr	$(Gr_1 - Gr)$ *0.002	Gr	$(Gr_1 - Gr)$ *0.002
(mins)	(√mins)	(div)	(mm)	(div)	(mm)	(div)	(mm)	(div)	(mm)	(div)	(mm)	(div)	(mm)
0.00	0.00	1200.0	0.000	1167.0	0.066	1118.9	0.162	1088.9	0.222	1045.1	0.310	993.8	0.412
0.13	0.37	1181.0	0.038	1133.0	0.134	1100.5	0.199	1060.0	0.280	1012.0	0.376	976.0	0.448
0.25	0.50	1179.3	0.041	1131.0	0.138	1099.0	0.202	1058.0	0.284	1009.8	0.380	974.5	0.451
0.50	0.71	1178.0	0.044	1129.1	0.142	1097.8	0.204	1056.8	0.286	1007.1	0.386	973.0	0.454
1.00	1.00	1175.6	0.049	1127.0	0.146	1096.0	0.208	1054.5	0.291	1004.7	0.391	970.3	0.459
2.00	1.41	1173.5	0.053	1125.0	0.150	1094.2	0.212	1052.1	0.296	1001.9	0.396	968.2	0.464
4.00	2.00	1171.6	0.057	1122.9	0.154	1092.6	0.215	1049.9	0.300	998.9	0.402	965.9	0.468
8.00	2.83	1169.7	0.061	1120.9	0.158	1090.9	0.218	1047.5	0.305	996.2	0.408	964.6	0.471
15.00	3.87	1168.1	0.064	1119.5	0.161	1089.8	0.220	1046.1	0.308	994.9	0.410	962.0	0.476
30.00	5.48	1167.0	0.066	1118.9	0.162	1088.9	0.222	1045.1	0.310	993.8	0.412	960.9	0.478

Table C.3.6: Consolidation calculated parameter for sample A3 (Inundated)

Pressures	**(kPa)**	**0**	**5**	**25**	**50**	**100**	**200**	**300**
Δh_{90}	(mm)		0.042	0.140	0.202	0.284	0.382	0.4517
Δh_0	(mm)		0.000	0.066	0.162	0.222	0.310	0.412
Δh_{100} = $[((\Delta h_{90} - \Delta h_0)/0.9)+ \Delta h_0]$	(mm)		0.047	0.148	0.207	0.291	0.390	0.456
Δh_f	(mm)		0.066	0.162	0.222	0.310	0.412	0.478
Initial Compression ratio $r_i = [\Delta h_0/\Delta h_f]$			0.000	0.407	0.729	0.717	0.752	0.862
Primary Compression ratio $r_p = [(\Delta h_{100}-\Delta h_0)/\Delta h_f]$			0.707	0.507	0.201	0.222	0.194	0.092
Secondary Compression ratio 'r_{sec}' = $[(\Delta h_f - \Delta h_{100})/\Delta h_f]$			0.293	0.086	0.070	0.061	0.055	0.046
√t90	(√min)		0.570	0.500	0.540	0.500	0.520	0.510
t_{90}	(mins)		0.325	0.250	0.292	0.250	0.270	0.260
T_{90}			0.848	0.848	0.848	0.848	0.848	0.848
drainage path 'd' = $[h_i/2]$	(mm)		9.150	9.117	9.069	9.039	8.995	8.844
Initial void ratio 'e_i' =$[(H-\Delta h_0-Hs)/Hs]$			0.462	0.456	0.449	0.444	0.437	0.429
Final void ratio 'e_f' =$[(H-\Delta h_f-Hs)/Hs]$		0.462	0.456	0.449	0.444	0.437	0.429	0.423
Total change in void ratio 'Δe' = $e_i - e_f$			0.005	0.008	0.005	0.007	0.008	0.005
Change of stress/pressure 'Δσ' = $\sigma_t - \sigma_p$	(kPa) or (kN/m^2)		5	20	25	50	100	100
Volume Compressibility 'Mv' = $[(1/1+e_0)*(\Delta e/\Delta\sigma')]$	(m^2/MN)		0.721	0.263	0.132	0.096	0.056	0.034
Volumetric Strain = (Δhi/H)*100%	(%)	0.000	0.361	0.886	1.214	1.693	2.254	2.613
coefficient of consolidation 'Cv' = $[(T_{90}*d^2)/t_{90}]$	(mm^2/min)		218.5	281.9	239.2	277.1	253.7	255.0
Coefficient of Permeability 'k' = $C_v*M_v*\gamma_w$	(m/yr)		0.793	0.373	0.158	0.134	0.071	0.044

4. Soil A at 'Low wet of OMC' (4)

Table C.4.1: initial parameter of sample A4 (As-compacted)

Dimensions			Initial specimen	Final specimen
Diameter	'D'	(cm)	7.650	7.650
Area	'A'	(cm^2)	45.963	45.963
Height	'H'	(cm)	1.780	1.740
Volume	'V'	(cm^3)	81.815	79.979
Weights				
Ring		(g)	97.400	97.400
Ring + Sample in ring		(g)	279.000	272.465
Sample in ring	'M'	(g)	181.600	175.065
Moisture content 'W'		(%)	0.184	0.141
Calculated				
Assumed specific gravity 'Gs'			2.900	2.900
Density of water 'ρ_w'		(g/cm^3)	1.000	1.000
bulk density 'ρ' = [M/(A*H)]		(g/cm^3)	2.220	2.189
Dry Density 'ρ_d' = [ρ/(1+W)]		(g/cm^3)	1.875	1.918
Void ratio 'e_0' = [(Gs*ρ_w/ρ_d)-1]			0.547	0.512
Degree of saturation 'Sr_i' = [Gs*W/e_0]			0.975	0.800
Mass of solids in sample 'M_s' =[M/(W+1)]		(g)	153.409	153.409
Height of solids in sample 'H_s' =[H/(1+e_0)]		(cm)	1.151	1.151

Table C.4.2: Consolidation data for sample A4 (As-compacted)

Time		Pressure at 5kPa		Pressure at 25kPa		Pressure at 50kPa		Pressure at 100kPa		Pressure at 200kPa		Pressure at 300kPa	
		Gauge reading	Consolidation settlement 'Δh'	Gauge reading	Consolidation settlement 'Δh'	Gauge reading	Consolidation settlement 'Δh'	Gauge reading	Consolidation settlement 'Δh'	Gauge reading	Consolidation settlement 'Δh'	Gauge reading	Consolidation settlement 'Δh'
t	√t	Gr	$(Gr_1 - Gr)$ *0.002	Gr	$(Gr_1 - Gr)$ *0.002	Gr	$(Gr_1 - Gr)$ *0.002	Gr	$(Gr_1 - Gr)$ *0.002	Gr	$(Gr_1 - Gr)$ *0.002	Gr	$(Gr_1 - Gr)$ *0.002
(mins)	(√mins)	(div)	(mm)	(div)	(mm)	(div)	(mm)	(div)	(mm)	(div)	(mm)	(div)	(mm)
0.00	0.00	555.3	0.000	517.2	0.076	467.0	0.177	438.3	0.234	400.4	0.310	355.6	0.399
0.13	0.37	539.1	0.032	484.0	0.143	451.0	0.209	416.0	0.279	373.7	0.363	342.8	0.425
0.25	0.50	538.0	0.035	482.6	0.145	450.0	0.211	414.5	0.282	372.0	0.367	341.1	0.428
0.50	0.71	536.5	0.038	480.9	0.149	448.5	0.214	412.5	0.286	369.5	0.372	339.4	0.432
1.00	1.00	534.3	0.042	478.2	0.154	446.6	0.217	410.2	0.290	365.9	0.379	337.0	0.437
2.00	1.41	530.4	0.050	475.2	0.160	444.7	0.221	407.3	0.296	362.9	0.385	334.2	0.442
4.00	2.00	528.0	0.055	472.1	0.166	442.2	0.226	404.5	0.302	359.9	0.391	332.0	0.447
8.00	2.83	522.1	0.066	469.1	0.172	440.2	0.230	402.3	0.306	357.9	0.395	330.1	0.450
15.00	3.87	518.8	0.073	467.8	0.175	439.1	0.232	401.2	0.308	356.5	0.398	328.9	0.453
30.00	5.48	517.2	0.076	467.0	0.177	438.3	0.234	400.4	0.310	355.6	0.399	328.0	0.455

Table C.4.3: Consolidation calculated parameter for sample A4 (As-compacted)

Pressures	**(kPa)**	**0**	**5**	**25**	**50**	**100**	**200**	**300**
Δh_{90}	(mm)		0.035	0.146	0.211	0.282	0.367	0.429
Δh_0	(mm)		0.000	0.076	0.177	0.234	0.310	0.399
Δh_{100} = $[((\Delta h_{90} - \Delta h_0)/0.9)+ \Delta h_0]$	(mm)		0.039	0.154	0.215	0.287	0.373	0.432
Δh_f	(mm)		0.076	0.177	0.234	0.310	0.399	0.455
Initial Compression ratio $r_i = [\Delta h_0/\Delta h_f]$			0.000	0.430	0.756	0.755	0.776	0.878
Primary Compression ratio $r_p = [(\Delta h_{100}-\Delta h_0)/\Delta h_f]$			0.507	0.440	0.163	0.172	0.159	0.073
Secondary Compression ratio 'r_{sec}' = $[(\Delta h_f - \Delta h_{100})/\Delta h_f]$			0.493	0.129	0.080	0.073	0.065	0.049
√t90	(√min)		0.500	0.460	0.500	0.480	0.440	0.560
t_{90}	(mins)		0.250	0.212	0.250	0.230	0.194	0.314
T_{90}			0.848	0.848	0.848	0.848	0.848	0.848
drainage path 'd' = $[h_i/2]$	(mm)		8.900	8.862	8.812	8.783	8.745	8.701
Initial void ratio 'e_i' =$[(H-\Delta h_0-Hs)/Hs]$			0.547	0.540	0.531	0.526	0.520	0.512
Final void ratio 'e_f' =$[(H-\Delta h_f-Hs)/Hs]$		0.547	0.540	0.531	0.526	0.520	0.512	0.507
Total change in void ratio 'Δe' = $e_i - e_f$			0.007	0.009	0.005	0.007	0.008	0.005
Change of stress/pressure 'Δσ' = $\sigma_t - \sigma_p$	(kPa) or (kN/m^2)		5	20	25	50	100	100
Volume Compressibility 'Mv' = $[(1/1+e_0)*(\Delta e/\Delta\sigma')]$	(m^2/MN)		0.856	0.283	0.128	0.085	0.050	0.031
Volumetric Strain = (Δhi/H)*100%	(%)	0.000	0.428	0.992	1.315	1.740	2.244	2.554
coefficient of consolidation 'Cv' = $[(T_{90}*d^2)/t_{90}]$	(mm^2/min)		268.7	314.7	263.4	283.9	335.0	204.7
Coefficient of Permeability 'k' = $C_v*M_v*\gamma_w$	(m/yr)		1.157	0.447	0.170	0.122	0.085	0.032

Table C.4.4: initial parameter of sample A4 (Inundated)

Dimensions			Initial specimen	Final specimen
Diameter	'D'	(cm)	7.640	7.640
Area	'A'	(cm^2)	45.843	45.843
Height	'H'	(cm)	1.800	1.751
Volume	'V'	(cm^3)	82.518	80.253
Weights				
Ring		(g)	79.900	79.900
Ring + Sample in ring		(g)	263.100	256.434
Sample in ring	'M'	(g)	183.200	176.534
Moisture content 'W'		(%)	0.189	0.191
Calculated				
Assumed specific gravity 'Gs'			2.900	2.900
Density of water 'ρ_w'		(g/cm^3)	1.000	1.000
bulk density	'ρ' = [M/(A*H)]	(g/cm^3)	2.220	2.200
Dry Density	'ρ_d' = [ρ/(1+W)]	(g/cm^3)	1.867	1.867
Void ratio	'e_0' = [(Gs*ρ_w/ρ_d)-1]		0.554	0.554
Degree of saturation 'Sr_i'	= [Gs*W/e_0]		0.992	1.000
Mass of solids in sample 'M_s'	=[M/(W+1)]	(g)	154.032	154.032
Height of solids in sample 'H_s'	=[H/(1+e_0)]	(cm)	1.159	1.159

Table C.4.5: Consolidation data for sample A4 (Inundated)

Time		Pressure at 5kPa		Pressure at 25kPa		Pressure at 50kPa		Pressure at 100kPa		Pressure at 200kPa		Pressure at 300kPa	
		Gauge reading	Consolidation settlement 'Δh'	Gauge reading	Consolidation settlement 'Δh'	Gauge reading	Consolidation settlement 'Δh'	Gauge reading	Consolidation settlement 'Δh'	Gauge reading	Consolidation settlement 'Δh'	Gauge reading	Consolidation settlement 'Δh'
t	√t	Gr	$(Gr_1 - Gr)$ *0.002	Gr	$(Gr_1 - Gr)$ *0.002	Gr	$(Gr_1 - Gr)$ *0.002	Gr	$(Gr_1 - Gr)$ *0.002	Gr	$(Gr_1 - Gr)$ *0.002	Gr	$(Gr_1 - Gr)$ *0.002
(mins)	(√mins)	(div)	(mm)	(div)	(mm)	(div)	(mm)	(div)	(mm)	(div)	(mm)	(div)	(mm)
0.00	0.00	715.0	0.000	659.8	0.110	597.5	0.235	559.8	0.310	516.0	0.398	468.0	0.494
0.13	0.37	690.8	0.048	622.2	0.186	578.6	0.273	537.0	0.356	491.6	0.447	455.2	0.520
0.25	0.50	688.3	0.053	619.8	0.190	576.5	0.277	535.2	0.360	489.5	0.451	454.0	0.522
0.50	0.71	685.3	0.059	616.8	0.196	574.3	0.281	532.8	0.364	485.9	0.458	451.7	0.527
1.00	1.00	681.5	0.067	613.0	0.204	571.5	0.287	528.9	0.372	481.1	0.468	449.0	0.532
2.00	1.41	676.3	0.077	607.9	0.214	568.0	0.294	524.0	0.382	476.2	0.478	445.9	0.538
4.00	2.00	670.0	0.090	603.2	0.224	564.3	0.301	520.5	0.389	472.9	0.484	443.2	0.544
8.00	2.83	664.1	0.102	600.0	0.230	562.0	0.306	518.2	0.394	470.5	0.489	441.3	0.547
15.00	3.87	661.2	0.108	598.8	0.232	560.5	0.309	517.0	0.396	469.2	0.492	439.9	0.550
30.00	5.48	659.8	0.110	597.8	0.234	559.8	0.310	516.0	0.398	468.0	0.494	438.6	0.553

Table C.4.6: Consolidation calculated parameter for sample A4 (Inundated)

Pressures	**(kPa)**	**0**	**5**	**25**	**50**	**100**	**200**	**300**
Δh_{90}	(mm)		0.055	0.191	0.278	0.360	0.452	0.5233
Δh_0	(mm)		0.000	0.110	0.235	0.310	0.398	0.494
Δh_{100} = $[((\Delta h_{90} - \Delta h_0)/0.9)+ \Delta h_0]$	(mm)		0.061	0.199	0.283	0.366	0.457	0.527
Δh_f	(mm)		0.110	0.234	0.310	0.398	0.494	0.553
Initial Compression ratio $r_i = [\Delta h_0/\Delta h_f]$			0.000	0.469	0.757	0.779	0.806	0.894
Primary Compression ratio $r_p = [(\Delta h_{100}-\Delta h_0)/\Delta h_f]$			0.554	0.382	0.154	0.140	0.120	0.059
Secondary Compression ratio 'r_{sec}' = $[(\Delta h_f - \Delta h_{100})/\Delta h_f]$			0.446	0.149	0.089	0.082	0.074	0.047
√t90	(√min)		0.520	0.500	0.560	0.490	0.500	0.560
t_{90}	(mins)		0.270	0.250	0.314	0.240	0.250	0.314
T_{90}			0.848	0.848	0.848	0.848	0.848	0.848
drainage path 'd' = $[h_i/2]$	(mm)		9.000	8.945	8.883	8.845	8.801	8.753
Initial void ratio 'e_i' =$[(H-\Delta h_0-Hs)/Hs]$			0.554	0.544	0.533	0.527	0.519	0.511
Final void ratio 'e_f' =$[(H-\Delta h_f-Hs)/Hs]$		0.554	0.544	0.533	0.527	0.519	0.511	0.506
Total change in void ratio 'Δe' = $e_i - e_f$			0.010	0.011	0.007	0.008	0.008	0.005
Change of stress/pressure 'Δσ' = $\sigma_t - \sigma_p$	(kPa) or (kN/m^2)		5	20	25	50	100	100
Volume Compressibility 'Mv' = $[(1/1+e_0)*(\Delta e/\Delta\sigma')]$	(m^2/MN)		1.227	0.346	0.168	0.098	0.053	0.033
Volumetric Strain = (Δhi/H)*100%	(%)	0.000	0.613	1.302	1.724	2.211	2.744	3.071
coefficient of consolidation 'Cv' = $[(T_{90}*d^2)/t_{90}]$	(mm^2/min)		254.0	271.4	213.3	276.3	262.7	207.2
Coefficient of Permeability 'k' = $C_v*M_v*\gamma_w$	(m/yr)		1.567	0.472	0.180	0.136	0.070	0.034

5. Soil A at 'High wet of OMC' (5)

Table C.5.1: initial parameter of sample A5 (As-compacted)

Dimensions			Initial specimen	Final specimen
Diameter	'D'	(cm)	7.650	7.650
Area	'A'	(cm^2)	45.963	45.963
Height	'H'	(cm)	1.780	1.736
Volume	'V'	(cm^3)	81.815	79.780
Weights				
Ring		(g)	76.300	76.300
Ring + Sample in ring		(g)	258.300	250.759
Sample in ring	'M'	(g)	182.000	174.459
Moisture content 'W'		(%)	0.195	0.145
Calculated				
Assumed specific gravity 'Gs'			2.900	2.900
Density of water 'ρ_w'		(g/cm^3)	1.000	1.000
bulk density	'ρ' = [M/(A*H)]	(g/cm^3)	2.225	2.187
Dry Density	'ρ_d' = [ρ/(1+W)]	(g/cm^3)	1.862	1.910
Void ratio	'e_0' = [(Gs*ρ_w/ρ_d)-1]		0.557	0.519
Degree of saturation 'Sr_i'	= [Gs*W/e_0]		1.012	0.811
Mass of solids in sample 'M_s'	=[M/(W+1)]	(g)	152.357	152.357
Height of solids in sample 'H_s'	=[H/(1+e_0)]	(cm)	1.143	1.143

Table C.5.2: Consolidation data for sample A5 (As-compacted)

Time		Pressure at 5kPa		Pressure at 25kPa		Pressure at 50kPa		Pressure at 100kPa		Pressure at 200kPa		Pressure at 300kPa	
		Gauge reading	Consolidation settlement 'Δh'	Gauge reading	Consolidation settlement 'Δh'	Gauge reading	Consolidation settlement 'Δh'	Gauge reading	Consolidation settlement 'Δh'	Gauge reading	Consolidation settlement 'Δh'	Gauge reading	Consolidation settlement 'Δh'
t	√t	Gr	$(Gr_1 - Gr)$ *0.002	Gr	$(Gr_1 - Gr)$ *0.002	Gr	$(Gr_1 - Gr)$ *0.002	Gr	$(Gr_1 - Gr)$ *0.002	Gr	$(Gr_1 - Gr)$ *0.002	Gr	$(Gr_1 - Gr)$ *0.002
(mins)	(√mins)	(div)	(mm)	(div)	(mm)	(div)	(mm)	(div)	(mm)	(div)	(mm)	(div)	(mm)
0.00	0.00	1000.0	0.000	971.7	0.057	912.0	0.176	874.6	0.251	829.2	0.342	778.6	0.443
0.13	0.37	988.6	0.023	940.0	0.120	895.2	0.210	855.0	0.290	806.0	0.388	767.0	0.466
0.25	0.50	988.0	0.024	937.0	0.126	893.8	0.212	852.0	0.296	804.5	0.391	765.5	0.469
0.50	0.71	987.0	0.026	934.0	0.132	891.2	0.218	845.0	0.310	799.9	0.400	763.5	0.473
1.00	1.00	985.2	0.030	930.4	0.139	888.9	0.222	840.5	0.319	795.0	0.410	760.8	0.478
2.00	1.41	983.1	0.034	926.0	0.148	885.2	0.230	835.0	0.330	790.0	0.420	757.5	0.485
4.00	2.00	980.0	0.040	921.1	0.158	881.2	0.238	832.8	0.334	785.8	0.428	754.5	0.491
8.00	2.83	976.2	0.048	916.2	0.168	878.0	0.244	831.0	0.338	782.0	0.436	752.3	0.495
15.00	3.87	973.5	0.053	913.5	0.173	876.0	0.248	830.9	0.338	780.0	0.440	750.5	0.499
30.00	5.48	971.7	0.057	912.0	0.176	874.6	0.251	829.2	0.342	778.6	0.443	749.1	0.502

Table C.5.3: Consolidation calculated parameter for sample A5 (As-compacted)

Pressures	**(kPa)**	**0**	**5**	**25**	**50**	**100**	**200**	**300**
Δh_{90}	(mm)		0.024	0.128	0.214	0.313	0.392	0.47
Δh_0	(mm)		0.000	0.057	0.176	0.251	0.342	0.443
Δh_{100} = $[((\Delta h_{90} - \Delta h_0)/0.9)+ \Delta h_0]$	(mm)		0.027	0.136	0.218	0.320	0.398	0.473
Δh_f	(mm)		0.057	0.176	0.251	0.342	0.443	0.502
Initial Compression ratio $r_i = [\Delta h_0/\Delta h_f]$			0.000	0.324	0.702	0.735	0.772	0.883
Primary Compression ratio $r_p = [(\Delta h_{100}-\Delta h_0)/\Delta h_f]$			0.475	0.448	0.168	0.202	0.126	0.060
Secondary Compression ratio 'r_{sec}' = $[(\Delta h_f - \Delta h_{100})/\Delta h_f]$			0.525	0.228	0.130	0.064	0.101	0.057
√t90	(√min)		0.540	0.480	0.510	0.800	0.550	0.580
t_{90}	(mins)		0.292	0.230	0.260	0.640	0.303	0.336
T_{90}			0.848	0.848	0.848	0.848	0.848	0.848
drainage path 'd' = $[h_i/2]$	(mm)		8.900	8.872	8.812	8.775	8.729	8.679
Initial void ratio 'e_i' =$[(H-\Delta h_0-Hs)/Hs]$			0.557	0.552	0.542	0.535	0.527	0.519
Final void ratio 'e_f' =$[(H-\Delta h_f-Hs)/Hs]$		0.557	0.552	0.542	0.535	0.527	0.519	0.513
Total change in void ratio 'Δe' = $e_i - e_f$			0.005	0.010	0.007	0.008	0.009	0.005
Change of stress/pressure 'Δσ' = $\sigma_t - \sigma_p$	(kPa) or (kN/m^2)		5	20	25	50	100	100
Volume Compressibility 'Mv' = $[(1/1+e_0)*(\Delta e/\Delta\sigma')]$	(m^2/MN)		0.636	0.334	0.168	0.102	0.057	0.033
Volumetric Strain = (Δhi/H)*100%	(%)	0.000	0.318	0.989	1.409	1.919	2.488	2.819
coefficient of consolidation 'Cv' = $[(T_{90}*d^2)/t_{90}]$	(mm^2/min)		230.4	289.7	253.2	102.0	213.6	189.9
Coefficient of Permeability 'k' = $C_v*M_v*\gamma_w$	(m/yr)		0.737	0.487	0.214	0.052	0.061	0.032

Table C.5.4: initial parameter of sample A5 (Inundated)

Dimensions			Initial specimen	Final specimen
Diameter	'D'	(cm)	7.680	7.680
Area	'A'	(cm^2)	46.325	46.325
Height	'H'	(cm)	1.820	1.768
Volume	'V'	(cm^3)	84.311	81.879
Weights				
Ring		(g)	99.300	99.300
Ring + Sample in ring		(g)	281.400	274.027
Sample in ring	'M'	(g)	182.100	174.727
Moisture content 'W'		(%)	0.193	0.2077
Calculated				
Assumed specific gravity 'Gs'			2.900	2.900
Density of water 'ρ_w'		(g/cm^3)	1.000	1.000
bulk density	'ρ' = [M/(A*H)]	(g/cm^3)	2.160	2.134
Dry Density	'ρ_d' = [ρ/(1+W)]	(g/cm^3)	1.810	1.810
Void ratio	'e_0' = [(Gs*ρ_w/ρ_d)-1]		0.602	0.602
Degree of saturation 'Sr_i'	= [Gs*W/e_0]		0.931	1.000
Mass of solids in sample 'M_s'	=[M/(W+1)]	(g)	152.578	152.578
Height of solids in sample 'H_s'	=[H/(1+e_0)]	(cm)	1.136	1.136

Table C.5.5: Consolidation data for sample A5 (Inundated)

Time		Pressure at 5kPa		Pressure at 25kPa		Pressure at 50kPa		Pressure at 100kPa		Pressure at 200kPa		Pressure at 300kPa	
		Gauge reading	Consolidation settlement 'Δh'	Gauge reading	Consolidation settlement 'Δh'	Gauge reading	Consolidation settlement 'Δh'	Gauge reading	Consolidation settlement 'Δh'	Gauge reading	Consolidation settlement 'Δh'	Gauge reading	Consolidation settlement 'Δh'
t	√t	Gr	$(Gr_1 - Gr)$ *0.002	Gr	$(Gr_1 - Gr)$ *0.002	Gr	$(Gr_1 – Gr)$ *0.002	Gr	$(Gr_1 - Gr)$ *0.002	Gr	$(Gr_1 - Gr)$ *0.002	Gr	$(Gr_1 - Gr)$ *0.002
(mins)	(√mins)	(div)	(mm)	(div)	(mm)	(div)	(mm)	(div)	(mm)	(div)	(mm)	(div)	(mm)
0.00	0.00	1200.0	0.000	1140.9	0.118	1074.5	0.251	1036.1	0.328	990.0	0.420	937.5	0.525
0.13	0.37	1179.0	0.042	1106.8	0.186	1057.0	0.286	1014.0	0.372	965.0	0.470	924.5	0.551
0.25	0.50	1176.6	0.047	1103.5	0.193	1055.2	0.290	1012.2	0.376	963.0	0.474	923.0	0.554
0.50	0.71	1174.2	0.052	1099.7	0.201	1053.0	0.294	1009.3	0.381	958.7	0.483	920.0	0.560
1.00	1.00	1170.9	0.058	1095.0	0.210	1050.3	0.299	1005.5	0.389	953.1	0.494	917.9	0.564
2.00	1.41	1165.2	0.070	1090.2	0.220	1046.7	0.307	1001.1	0.398	948.1	0.504	914.7	0.571
4.00	2.00	1158.1	0.084	1084.2	0.232	1042.8	0.314	997.0	0.406	943.7	0.513	911.9	0.576
8.00	2.83	1150.1	0.100	1079.1	0.242	1039.4	0.321	993.5	0.413	940.9	0.518	909.5	0.581
15.00	3.87	1144.0	0.112	1076.2	0.248	1037.8	0.324	991.3	0.417	938.9	0.522	907.5	0.585
30.00	5.48	1140.9	0.118	1074.5	0.251	1036.1	0.328	990.0	0.420	937.5	0.525	906.1	0.588

Table C.5.6: Consolidation calculated parameter for sample A5 (Inundated)

Pressures **(kPa)**	**0**	**5**	**25**	**50**	**100**	**200**	**300**
Δh_{90} (mm)		0.048	0.192	0.290	0.376	0.475	0.556
Δh_0 (mm)		0.000	0.118	0.251	0.328	0.420	0.525
Δh_{100} = $[((\Delta h_{90} - \Delta h_0)/0.9)+ \Delta h_0]$ (mm)		0.054	0.200	0.294	0.381	0.481	0.559
Δh_f (mm)		0.118	0.251	0.328	0.420	0.525	0.588
Initial Compression ratio $r_i = [\Delta h_0/\Delta h_f]$		0.000	0.470	0.766	0.781	0.800	0.893
Primary Compression ratio $r_p = [(\Delta h_{100}-\Delta h_0)/\Delta h_f]$		0.454	0.328	0.132	0.127	0.116	0.059
Secondary Compression ratio 'r_{sec}' = $[(\Delta h_f - \Delta h_{100})/\Delta h_f]$		0.546	0.202	0.102	0.092	0.084	0.048
√t90 (√min)		0.590	0.520	0.520	0.490	0.460	0.590
t_{90} (mins)		0.348	0.270	0.270	0.240	0.212	0.348
T_{90}		0.848	0.848	0.848	0.848	0.848	0.848
drainage path 'd' = $[h_i/2]$ (mm)		9.100	9.041	8.975	8.936	8.890	8.638
Initial void ratio 'e_i' =$[(H-\Delta h_0-Hs)/Hs]$		0.602	0.592	0.580	0.574	0.565	0.511
Final void ratio 'e_f' =$[(H-\Delta h_f-Hs)/Hs]$	0.602	0.592	0.580	0.574	0.565	0.556	0.506
Total change in void ratio 'Δe' = $e_i - e_f$		0.010	0.012	0.007	0.008	0.009	0.005
Change of stress/pressure 'Δσ' = $\sigma_t - \sigma_p$ (kPa) or (kN/m^2)		5	20	25	50	100	100
Volume Compressibility 'Mv' = $[(1/1+e_0)*(\Delta e/\Delta\sigma')]$ (m^2/MN)		1.299	0.365	0.169	0.101	0.058	0.035
Volumetric Strain = (Δhi/H)*100% (%)	0.000	0.649	1.379	1.801	2.308	2.885	3.230
coefficient of consolidation 'Cv' = $[(T_{90}*d^2)/t_{90}]$ (mm^2/min)		201.7	256.3	252.6	282.0	316.7	181.7
Coefficient of Permeability 'k' = $C_v*M_v*\gamma_w$ (m/yr)		1.318	0.471	0.214	0.143	0.092	0.032

6. Soil B at 'High dry of OMC' (1)

Table C.6.1: initial parameter of sample B1 (As-compacted)

Dimensions			Initial specimen	Final specimen
Diameter	'D'	(cm)	7.630	7.630
Area	'A'	(cm^2)	45.723	45.723
Height	'H'	(cm)	1.800	1.774
Volume	'V'	(cm^3)	82.302	81.104
Weights				
Ring		(g)	76.300	76.300
Ring + Sample in ring		(g)	234.100	233.892
Sample in ring	'M'	(g)	157.800	157.592
Moisture content 'W'		(%)	0.084	0.083
Calculated				
Assumed specific gravity 'Gs'			2.900	2.900
Density of water 'ρ_w'		(g/cm^3)	1.000	1.000
bulk density	'ρ' = [M/(A*H)]	(g/cm^3)	1.917	1.943
Dry Density	'ρ_d' = [ρ/(1+W)]	(g/cm^3)	1.768	1.794
Void ratio	'e_0' = [(Gs*ρ_w/ρ_d)-1]		0.640	0.616
Degree of saturation 'Sr_i'	= [Gs*W/e_0]		0.382	0.390
Mass of solids in sample 'M_s'	=[M/(W+1)]	(g)	145.526	145.526
Height of solids in sample 'H_s'	=[H/(1+e_0)]	(cm)	1.097	1.097

Table C.6.2: Consolidation data for sample B1 (As-compacted)

Time		Pressure at 5kPa		Pressure at 25kPa		Pressure at 50kPa		Pressure at 100kPa		Pressure at 200kPa		Pressure at 300kPa	
		Gauge reading	Consolidation settlement 'Δh'	Gauge reading	Consolidation settlement 'Δh'	Gauge reading	Consolidation settlement 'Δh'	Gauge reading	Consolidation settlement 'Δh'	Gauge reading	Consolidation settlement 'Δh'	Gauge reading	Consolidation settlement 'Δh'
t	√t	Gr	$(Gr_1 - Gr)$ *0.002	Gr	$(Gr_1 - Gr)$ *0.002	Gr	$(Gr_1 - Gr)$ *0.002	Gr	$(Gr_1 - Gr)$ *0.002	Gr	$(Gr_1 - Gr)$ *0.002	Gr	$(Gr_1 - Gr)$ *0.002
(mins)	(√mins)	(div)	(mm)	(div)	(mm)	(div)	(mm)	(div)	(mm)	(div)	(mm)	(div)	(mm)
0.00	0.00	1100.0	0.000	1086.8	0.026	1057.2	0.086	1037.1	0.126	1008.9	0.182	969.0	0.262
0.13	0.37	1089.5	0.021	1061.5	0.077	1042.8	0.114	1018.0	0.164	981.8	0.236	952.0	0.296
0.25	0.50	1089.2	0.022	1061.0	0.078	1042.0	0.116	1016.0	0.168	979.5	0.241	950.0	0.300
0.50	0.71	1089.0	0.022	1060.1	0.080	1041.1	0.118	1014.5	0.171	977.8	0.244	948.5	0.303
1.00	1.00	1088.6	0.023	1059.8	0.080	1040.5	0.119	1013.5	0.173	976.0	0.248	946.8	0.306
2.00	1.41	1088.1	0.024	1059.1	0.082	1039.9	0.120	1012.2	0.176	974.2	0.252	944.0	0.312
4.00	2.00	1087.8	0.024	1058.7	0.083	1039.0	0.122	1011.2	0.178	972.9	0.254	943.1	0.314
8.00	2.83	1087.2	0.026	1058.0	0.084	1038.5	0.123	1010.3	0.179	971.4	0.257	941.8	0.316
15.00	3.87	1087.0	0.026	1057.8	0.084	1037.9	0.124	1009.7	0.181	970.0	0.260	940.0	0.320
30.00	5.48	1086.8	0.026	1057.2	0.086	1037.1	0.126	1008.9	0.182	969.0	0.262	938.8	0.322

Table C.6.3: Consolidation calculated parameter for sample B1 (As-compacted)

Pressures	**(kPa)**	**0**	**5**	**25**	**50**	**100**	**200**	**300**
Δh_{90}	(mm)		0.022	0.079	0.116	0.169	0.242	0.301
Δh_0	(mm)		0.000	0.026	0.086	0.126	0.182	0.262
Δh_{100} = $[((\Delta h_{90} - \Delta h_0)/0.9)+ \Delta h_0]$	(mm)		0.024	0.085	0.119	0.174	0.249	0.305
Δh_f	(mm)		0.026	0.086	0.126	0.182	0.262	0.322
Initial Compression ratio $r_i = [\Delta h_0/\Delta h_f]$			0.000	0.304	0.684	0.692	0.695	0.813
Primary Compression ratio $r_p = [(\Delta h_{100}-\Delta h_0)/\Delta h_f]$			0.922	0.685	0.265	0.262	0.254	0.134
Secondary Compression ratio 'r_{sec}' = $[(\Delta h_f - \Delta h_{100})/\Delta h_f]$			0.078	0.011	0.051	0.046	0.051	0.053
√t90	(√min)		0.480	0.480	0.510	0.560	0.580	0.560
t_{90}	(mins)		0.230	0.230	0.260	0.314	0.336	0.314
T_{90}			0.848	0.848	0.848	0.848	0.848	0.848
drainage path 'd' = $[h_i/2]$	(mm)		9.000	8.987	8.957	8.937	8.909	8.869
Initial void ratio 'e_i' =$[(H-\Delta h_0-Hs)/Hs]$			0.640	0.638	0.632	0.629	0.624	0.616
Final void ratio 'e_f' =$[(H-\Delta h_f-Hs)/Hs]$		0.640	0.638	0.632	0.629	0.623	0.616	0.611
Total change in void ratio 'Δe' = $e_i - e_f$			0.002	0.005	0.004	0.005	0.007	0.006
Change of stress/pressure 'Δσ' = $\sigma_t - \sigma_p$	(kPa) or (kN/m^2)		5	20	25	50	100	100
Volume Compressibility 'Mv' = $[(1/1+e_0)*(\Delta e/\Delta\sigma')]$	(m^2/MN)		0.293	0.166	0.088	0.062	0.044	0.034
Volumetric Strain = (Δhi/H)*100%	(%)	0.000	0.147	0.476	0.699	1.012	1.456	1.791
coefficient of consolidation 'Cv' = $[(T_{90}*d^2)/t_{90}]$	(mm^2/min)		298.1	297.3	261.6	216.0	200.1	212.7
Coefficient of Permeability 'k' = $C_v*M_v*\gamma_w$	(m/yr)		0.440	0.247	0.116	0.068	0.045	0.036

Table C.6.4: initial parameter of sample B1 (Inundated)

Dimensions			Initial specimen	Final specimen
Diameter	'D'	(cm)	7.610	7.610
Area	'A'	(cm^2)	45.484	45.484
Height	'H'	(cm)	1.810	1.741
Volume	'V'	(cm^3)	82.326	79.167
Weights				
Ring		(g)	97.500	97.500
Ring + Sample in ring		(g)	254.400	270.781
Sample in ring	'M'	(g)	156.900	173.281
Moisture content 'W'		(%)	0.087	0.2256
Calculated				
Assumed specific gravity 'Gs'			2.900	2.900
Density of water 'ρ_w'		(g/cm^3)	1.000	1.000
bulk density	'ρ' = [M/(A*H)]	(g/cm^3)	1.906	2.189
Dry Density	'ρ_d' = [ρ/(1+W)]	(g/cm^3)	1.753	1.753
Void ratio	'e_0' = [(Gs*ρ_w/ρ_d)-1]		0.654	0.654
Degree of saturation 'Sr_i'	= [Gs*W/e_0]		0.387	1.000
Mass of solids in sample 'M_s'	=[M/(W+1)]	(g)	144.312	144.312
Height of solids in sample 'H_s'	=[H/(1+e_0)]	(cm)	1.094	1.094

Table C.6.5: Consolidation data for sample B1 (Inundated)

Time		Pressure at 5kPa		Pressure at 25kPa		Pressure at 50kPa		Pressure at 100kPa		Pressure at 200kPa		Pressure at 300kPa	
		Gauge reading	Consolidation settlement 'Δh'	Gauge reading	Consolidation settlement 'Δh'	Gauge reading	Consolidation settlement 'Δh'	Gauge reading	Consolidation settlement 'Δh'	Gauge reading	Consolidation settlement 'Δh'	Gauge reading	Consolidation settlement 'Δh'
t	√t	Gr	$(Gr_1 - Gr)$ *0.002	Gr	$(Gr_1 - Gr)$ *0.002	Gr	$(Gr_1 - Gr)$ *0.002	Gr	$(Gr_1 - Gr)$ *0.002	Gr	$(Gr_1 - Gr)$ *0.002	Gr	$(Gr_1 - Gr)$ *0.002
(mins)	(√mins)	(div)	(mm)	(div)	(mm)	(div)	(mm)	(div)	(mm)	(div)	(mm)	(div)	(mm)
0.00	0.00	1000.0	0.000	810.7	0.379	730.3	0.539	708.2	0.584	683.0	0.634	652.7	0.695
0.13	0.37	839.0	0.322	744.0	0.512	716.0	0.568	690.0	0.620	663.0	0.674	642.5	0.715
0.25	0.50	829.0	0.342	739.5	0.521	714.8	0.570	689.0	0.622	661.1	0.678	641.1	0.718
0.50	0.71	821.0	0.358	736.1	0.528	713.9	0.572	688.2	0.624	659.5	0.681	640.7	0.719
1.00	1.00	815.6	0.369	734.5	0.531	712.5	0.575	687.5	0.625	658.1	0.684	639.9	0.720
2.00	1.41	813.0	0.374	733.2	0.534	711.6	0.577	686.8	0.626	657.0	0.686	638.9	0.722
4.00	2.00	811.9	0.376	732.2	0.536	710.5	0.579	685.8	0.628	655.9	0.688	637.7	0.725
8.00	2.83	811.1	0.378	731.8	0.536	709.9	0.580	684.7	0.631	654.6	0.691	636.5	0.727
15.00	3.87	810.9	0.378	731.0	0.538	709.0	0.582	683.9	0.632	653.7	0.693	635.2	0.730
30.00	5.48	810.7	0.379	730.3	0.539	708.2	0.584	683.0	0.634	652.7	0.695	634.2	0.732

Table C.6.6: Consolidation calculated parameter for sample B1 (Inundated)

Pressures **(kPa)**	**0**	**5**	**25**	**50**	**100**	**200**	**300**
Δh_{90} (mm)		0.346	0.538	0.569	0.623	0.679	0.7185
Δh_0 (mm)		0.000	0.379	0.539	0.584	0.634	0.695
$\Delta h_{100} = [((\Delta h_{90} - \Delta h_0)/0.9) + \Delta h_0]$ (mm)		0.384	0.556	0.572	0.627	0.684	0.721
Δh_f (mm)		0.379	0.539	0.584	0.634	0.695	0.732
Initial Compression ratio $r_i = [\Delta h_0/\Delta h_f]$		0.000	0.703	0.924	0.921	0.913	0.950
Primary Compression ratio $r_p = [(\Delta h_{100}-\Delta h_0)/\Delta h_f]$		1.015	0.328	0.057	0.067	0.073	0.036
Secondary Compression ratio 'r_{sec}' $= [(\Delta h_f - \Delta h_{100})/\Delta h_f]$		-0.015	-0.030	0.019	0.011	0.015	0.014
√t90 (√min)		0.480	0.500	0.520	0.560	0.590	0.600
t_{90} (mins)		0.230	0.250	0.270	0.314	0.348	0.360
T_{90}		0.848	0.848	0.848	0.848	0.848	0.848
drainage path 'd' $= [h_i/2]$ (mm)		9.050	8.861	8.781	8.758	8.733	8.653
Initial void ratio 'e_i' $=[(H-\Delta h_0-Hs)/Hs]$		0.654	0.620	0.605	0.601	0.596	0.577
Final void ratio 'e_f' $=[(H-\Delta h_f-Hs)/Hs]$	0.654	0.620	0.605	0.601	0.596	0.591	0.573
Total change in void ratio 'Δe' $= e_i - e_f$		0.035	0.015	0.004	0.005	0.006	0.003
Change of stress/pressure 'Δσ' $= \sigma_t - \sigma_p$ (kPa) or (kN/m^2)		5	20	25	50	100	100
Volume Compressibility 'Mv' $= [(1/1+e_0)*(\Delta e/\Delta\sigma')]$ (m^2/MN)		4.183	0.443	0.099	0.055	0.033	0.020
Volumetric Strain $= (\Delta hi/H)*100\%$ (%)	0.000	2.092	2.980	3.224	3.503	3.838	4.042
coefficient of consolidation 'Cv' $= [(T_{90}*d^2)/t_{90}]$ (mm^2/min)		301.4	266.3	241.8	207.4	185.8	176.4
Coefficient of Permeability 'k' $= C_v*M_v*\gamma_w$ (m/yr)		6.342	0.593	0.120	0.058	0.031	0.018

7. Soil B at 'Low dry of OMC' (2)

Table C.7.1: initial parameter of sample B2 (As-compacted)

Dimensions			Initial specimen	Final specimen
Diameter	'D'	(cm)	7.650	7.650
Area	'A'	(cm^2)	45.963	45.963
Height	'H'	(cm)	1.800	1.768
Volume	'V'	(cm^3)	82.734	81.257
Weights				
Ring		(g)	97.600	97.600
Ring + Sample in ring		(g)	274.400	276.623
Sample in ring	'M'	(g)	176.800	179.023
Moisture content 'W'		(%)	0.107	0.121
Calculated				
Assumed specific gravity 'Gs'			2.900	2.900
Density of water 'ρ_w'		(g/cm^3)	1.000	1.000
bulk density	'ρ' = [M/(A*H)]	(g/cm^3)	2.137	2.203
Dry Density	'ρ_d' = [ρ/(1+W)]	(g/cm^3)	1.931	1.966
Void ratio	'e_0' = [(Gs*ρ_w/ρ_d)-1]		0.502	0.475
Degree of saturation 'Sr_i'	= [Gs*W/e_0]		0.616	0.736
Mass of solids in sample 'M_s'	=[M/(W+1)]	(g)	159.761	159.761
Height of solids in sample 'H_s'	=[H/(1+e_0)]	(cm)	1.199	1.199

Table C.7.2: Consolidation data for sample B2 (As-compacted)

Time		Pressure at 5kPa		Pressure at 25kPa		Pressure at 50kPa		Pressure at 100kPa		Pressure at 200kPa		Pressure at 300kPa	
		Gauge reading	Consolidation settlement 'Δh'	Gauge reading	Consolidation settlement 'Δh'	Gauge reading	Consolidation settlement 'Δh'	Gauge reading	Consolidation settlement 'Δh'	Gauge reading	Consolidation settlement 'Δh'	Gauge reading	Consolidation settlement 'Δh'
t	√t	Gr	$(Gr_1 - Gr)$ *0.002	Gr	$(Gr_1 - Gr)$ *0.002	Gr	$(Gr_1 - Gr)$ *0.002	Gr	$(Gr_1 – Gr)$ *0.002	Gr	$(Gr_1 - Gr)$ *0.002	Gr	$(Gr_1 - Gr)$ *0.002
(mins)	(√mins)	(div)	(mm)	(div)	(mm)	(div)	(mm)	(div)	(mm)	(div)	(mm)	(div)	(mm)
0.00	0.00	761.5	0.000	730.0	0.063	686.2	0.151	662.2	0.199	634.9	0.253	600.8	0.321
0.13	0.37	735.6	0.052	694.0	0.135	668.0	0.187	641.8	0.239	609.5	0.304	588.2	0.347
0.25	0.50	735.0	0.053	692.9	0.137	667.1	0.189	640.8	0.241	608.7	0.306	587.4	0.348
0.50	0.71	734.5	0.054	691.5	0.140	666.2	0.191	640.0	0.243	607.5	0.308	586.8	0.349
1.00	1.00	733.9	0.055	690.4	0.142	665.7	0.192	639.2	0.245	606.4	0.310	585.9	0.351
2.00	1.41	733.0	0.057	689.4	0.144	665.0	0.193	638.2	0.247	605.2	0.313	584.8	0.353
4.00	2.00	732.2	0.059	688.7	0.146	664.1	0.195	637.2	0.249	604.1	0.315	583.8	0.355
8.00	2.83	731.6	0.060	687.8	0.147	663.5	0.196	636.3	0.250	602.5	0.318	582.3	0.358
15.00	3.87	730.9	0.061	687.0	0.149	662.9	0.197	635.7	0.252	601.8	0.319	581.5	0.360
30.00	5.48	730.0	0.063	686.2	0.151	662.2	0.199	634.9	0.253	600.8	0.321	580.6	0.362

Table C.7.3: Consolidation calculated parameter for sample B2 (As-compacted)

Pressures **(kPa)**	**0**	**5**	**25**	**50**	**100**	**200**	**300**
Δh_{90} (mm)		0.053	0.138	0.189	0.242	0.306	0.3485
Δh_0 (mm)		0.000	0.063	0.151	0.199	0.253	0.321
Δh_{100} = $[((\Delta h_{90} - \Delta h_0)/0.9)+ \Delta h_0]$ (mm)		0.059	0.146	0.193	0.247	0.312	0.352
Δh_f (mm)		0.063	0.151	0.199	0.253	0.321	0.362
Initial Compression ratio $r_i = [\Delta h_0/\Delta h_f]$		0.000	0.418	0.760	0.786	0.787	0.887
Primary Compression ratio $r_p = [(\Delta h_{100}-\Delta h_0)/\Delta h_f]$		0.935	0.553	0.213	0.189	0.183	0.084
Secondary Compression ratio 'r_{sec}' = $[(\Delta h_f - \Delta h_{100})/\Delta h_f]$		0.065	0.028	0.027	0.025	0.030	0.028
√t90 (√min)		0.480	0.480	0.490	0.490	0.500	0.480
t_{90} (mins)		0.230	0.230	0.240	0.240	0.250	0.230
T_{90}		0.848	0.848	0.848	0.848	0.848	0.848
drainage path 'd' = $[h_i/2]$ (mm)		9.000	8.969	8.925	8.901	8.874	8.840
Initial void ratio 'e_i' =$[(H-\Delta h_0-Hs)/Hs]$		0.502	0.497	0.489	0.485	0.481	0.475
Final void ratio 'e_f' =$[(H-\Delta h_f-Hs)/Hs]$	0.502	0.497	0.489	0.485	0.481	0.475	0.472
Total change in void ratio 'Δe' = $e_i - e_f$		0.005	0.007	0.004	0.005	0.006	0.003
Change of stress/pressure 'Δσ' = $\sigma_t - \sigma_p$ (kPa) or (kN/m^2)		5	20	25	50	100	100
Volume Compressibility 'Mv' = $[(1/1+e_0)*(\Delta e/\Delta\sigma')]$ (m^2/MN)		0.650	0.226	0.098	0.056	0.035	0.021
Volumetric Strain = (Δhi/H)*100% (%)	0.000	0.350	0.837	1.103	1.407	1.786	2.010
coefficient of consolidation 'Cv' = $[(T_{90}*d^2)/t_{90}]$ (mm^2/min)		298.1	296.0	281.3	279.8	267.1	287.6
Coefficient of Permeability 'k' = $C_v*M_v*\gamma_w$ (m/yr)		0.975	0.337	0.139	0.079	0.047	0.030

Table C.7.4: initial parameter of sample B2 (Inundated)

Dimensions			Initial specimen	Final specimen
Diameter	'D'	(cm)	7.660	7.660
Area	'A'	(cm^2)	46.084	46.084
Height	'H'	(cm)	1.825	1.726
Volume	'V'	(cm^3)	84.103	79.549
Weights				
Ring		(g)	99.400	99.400
Ring + Sample in ring		(g)	277.000	287.160
Sample in ring	'M'	(g)	177.600	187.760
Moisture content 'W'		(%)	0.105	0.179
Calculated				
Assumed specific gravity 'Gs'			2.900	2.900
Density of water 'ρ_w'		(g/cm^3)	1.000	1.000
bulk density	'ρ' = [M/(A*H)]	(g/cm^3)	2.112	2.360
Dry Density	'ρ_d' = [ρ/(1+W)]	(g/cm^3)	1.910	1.910
Void ratio	'e_0' = [(Gs*ρ_w/ρ_d)-1]		0.518	0.518
Degree of saturation 'Sr_i'	= [Gs*W/e_0]		0.590	1.000
Mass of solids in sample 'M_s'	=[M/(W+1)]	(g)	160.667	160.667
Height of solids in sample 'H_s'	=[H/(1+e_0)]	(cm)	1.202	1.202

Table C.7.5: Consolidation data for sample B2 (Inundated)

Time		Pressure at 5kPa		Pressure at 25kPa		Pressure at 50kPa		Pressure at 100kPa		Pressure at 200kPa		Pressure at 300kPa	
		Gauge reading	Consolidation settlement 'Δh'	Gauge reading	Consolidation settlement 'Δh'	Gauge reading	Consolidation settlement 'Δh'	Gauge reading	Consolidation settlement 'Δh'	Gauge reading	Consolidation settlement 'Δh'	Gauge reading	Consolidation settlement 'Δh'
t	√t	Gr	$(Gr_1 - Gr)$ *0.002	Gr	$(Gr_1 - Gr)$ *0.002	Gr	$(Gr_1 - Gr)$ *0.002	Gr	$(Gr_1 - Gr)$ *0.002	Gr	$(Gr_1 - Gr)$ *0.002	Gr	$(Gr_1 - Gr)$ *0.002
(mins)	(√mins)	(div)	(mm)	(div)	(mm)	(div)	(mm)	(div)	(mm)	(div)	(mm)	(div)	(mm)
0.00	0.00	980.0	0.000	628.4	0.703	557.6	0.845	536.8	0.886	512.9	0.934	485.9	0.988
0.13	0.37	712.0	0.536	583.0	0.794	543.0	0.874	522.0	0.916	494.0	0.972	475.2	1.010
0.25	0.50	700.0	0.560	572.0	0.816	542.0	0.876	519.8	0.920	492.2	0.976	474.8	1.010
0.50	0.71	678.0	0.604	566.0	0.828	541.0	0.878	518.2	0.924	491.5	0.977	474.0	1.012
1.00	1.00	652.0	0.656	562.0	0.836	539.7	0.881	517.0	0.926	490.6	0.979	473.0	1.014
2.00	1.41	634.5	0.691	559.5	0.841	539.0	0.882	516.0	0.928	489.7	0.981	471.9	1.016
4.00	2.00	630.5	0.699	559.1	0.842	538.2	0.884	515.0	0.930	488.4	0.983	470.9	1.018
8.00	2.83	629.2	0.702	558.4	0.843	537.9	0.884	514.1	0.932	487.6	0.985	470.0	1.020
15.00	3.87	628.9	0.702	558.0	0.844	537.2	0.886	513.5	0.933	486.8	0.986	469.0	1.022
30.00	5.48	628.4	0.703	557.6	0.845	536.8	0.886	512.9	0.934	485.9	0.988	468.0	1.024

Table C.7.6: Consolidation calculated parameter for sample B2 (Inundated)

Pressures	**(kPa)**	**0**	**5**	**25**	**50**	**100**	**200**	**300**
Δh_{90}	(mm)		0.580	0.824	0.876	0.922	0.976	1.011
Δh_0	(mm)		0.000	0.703	0.845	0.886	0.934	0.988
Δh_{100} = $[((\Delta h_{90} - \Delta h_0)/0.9)+ \Delta h_0]$	(mm)		0.644	0.837	0.879	0.926	0.981	1.014
Δh_f	(mm)		0.703	0.845	0.886	0.934	0.988	1.024
Initial Compression ratio $r_i = [\Delta h_0/\Delta h_f]$			0.000	0.832	0.953	0.948	0.945	0.965
Primary Compression ratio $r_p = [(\Delta h_{100}-\Delta h_0)/\Delta h_f]$			0.916	0.159	0.039	0.043	0.047	0.025
Secondary Compression ratio 'r_{sec}' = $[(\Delta h_f - \Delta h_{100})/\Delta h_f]$			0.084	0.009	0.008	0.009	0.008	0.010
√t90	(√min)		0.440	0.600	0.520	0.560	0.500	0.500
t_{90}	(mins)		0.194	0.360	0.270	0.314	0.250	0.250
T_{90}			0.848	0.848	0.848	0.848	0.848	0.848
drainage path 'd' = $[h_i/2]$	(mm)		9.125	8.774	8.703	8.682	8.658	8.631
Initial void ratio 'e_i' =$[(H-\Delta h_0-Hs)/Hs]$			0.518	0.460	0.448	0.444	0.440	0.436
Final void ratio 'e_f' =$[(H-\Delta h_f-Hs)/Hs]$		0.518	0.460	0.448	0.444	0.440	0.436	0.433
Total change in void ratio 'Δe' = $e_i - e_f$			0.058	0.012	0.003	0.004	0.005	0.003
Change of stress/pressure 'Δσ' = $\sigma_t - \sigma_p$	(kPa) or (kN/m^2)		5	20	25	50	100	100
Volume Compressibility 'Mv' = $[(1/1+e_0)*(\Delta e/\Delta\sigma')]$	(m^2/MN)		7.237	0.365	0.085	0.050	0.028	0.019
Volumetric Strain = (Δhi/H)*100%	(%)	0.000	3.853	4.629	4.857	5.119	5.415	5.611
coefficient of consolidation 'Cv' = $[(T_{90}*d^2)/t_{90}]$	(mm^2/min)		364.7	181.3	237.5	203.8	254.3	252.7
Coefficient of Permeability 'k' = $C_v*M_v*\gamma_w$	(m/yr)		13.275	0.333	0.102	0.051	0.036	0.024

8. Soil B at 'At OMC' (3)

Table C.8.1: initial parameter of sample B3 (As-compacted)

Dimensions			Initial specimen	Final specimen
Diameter	'D'	(cm)	7.660	7.660
Area	'A'	(cm^2)	46.084	46.084
Height	'H'	(cm)	1.830	1.798
Volume	'V'	(cm^3)	84.333	82.876
Weights				
Ring		(g)	101.200	101.200
Ring + Sample in ring		(g)	277.500	273.038
Sample in ring	'M'	(g)	176.300	171.838
Moisture content 'W'		(%)	0.137	0.108
Calculated				
Assumed specific gravity 'Gs'			2.900	2.900
Density of water 'ρ_w'		(g/cm^3)	1.000	1.000
bulk density	'ρ' = [M/(A*H)]	(g/cm^3)	2.091	2.073
Dry Density	'ρ_d' = [ρ/(1+W)]	(g/cm^3)	1.838	1.871
Void ratio	'e_0' = [(Gs*ρ_w/ρ_d)-1]		0.577	0.550
Degree of saturation 'Sr_i'	= [Gs*W/e_0]		0.689	0.571
Mass of solids in sample 'M_s'	=[M/(W+1)]	(g)	155.037	155.037
Height of solids in sample 'H_s'	=[H/(1+e_0)]	(cm)	1.160	1.160

Table C.8.2: Consolidation data for sample B3 (As-compacted)

Time		Pressure at 5kPa		Pressure at 25kPa		Pressure at 50kPa		Pressure at 100kPa		Pressure at 200kPa		Pressure at 300kPa	
		Gauge reading	Consolidation settlement 'Δh'	Gauge reading	Consolidation settlement 'Δh'	Gauge reading	Consolidation settlement 'Δh'	Gauge reading	Consolidation settlement 'Δh'	Gauge reading	Consolidation settlement 'Δh'	Gauge reading	Consolidation settlement 'Δh'
t	√t	Gr	$(Gr_1 - Gr)$ *0.002	Gr	$(Gr_1 - Gr)$ *0.002	Gr	$(Gr_1 – Gr)$ *0.002	Gr	$(Gr_1 - Gr)$ *0.002	Gr	$(Gr_1 - Gr)$ *0.002	Gr	$(Gr_1 - Gr)$ *0.002
(mins)	(√mins)	(div)	(mm)	(div)	(mm)	(div)	(mm)	(div)	(mm)	(div)	(mm)	(div)	(mm)
0.00	0.00	1300.0	0.000	1274.9	0.050	1234.0	0.132	1209.7	0.181	1178.5	0.243	1141.9	0.316
0.13	0.37	1279.8	0.040	1240.2	0.120	1218.0	0.164	1191.0	0.218	1154.0	0.292	1127.5	0.345
0.25	0.50	1278.9	0.042	1239.7	0.121	1215.9	0.168	1187.0	0.226	1153.2	0.294	1126.0	0.348
0.50	0.71	1278.2	0.044	1238.9	0.122	1214.8	0.170	1186.0	0.228	1150.3	0.299	1124.8	0.350
1.00	1.00	1277.8	0.044	1238.0	0.124	1213.8	0.172	1184.8	0.230	1148.8	0.302	1123.2	0.354
2.00	1.41	1277.0	0.046	1237.0	0.126	1212.9	0.174	1183.7	0.233	1147.1	0.306	1121.9	0.356
4.00	2.00	1276.6	0.047	1236.2	0.128	1211.9	0.176	1182.4	0.235	1145.5	0.309	1120.2	0.360
8.00	2.83	1276.0	0.048	1235.5	0.129	1211.1	0.178	1181.5	0.237	1144.1	0.312	1118.9	0.362
15.00	3.87	1275.3	0.049	1234.9	0.130	1210.5	0.179	1180.7	0.239	1143.9	0.312	1117.5	0.365
30.00	5.48	1274.9	0.050	1234.0	0.132	1209.7	0.181	1178.5	0.243	1141.9	0.316	1116.1	0.368

Table C.8.3: Consolidation calculated parameter for sample B3 (As-compacted)

Pressures	**(kPa)**	**0**	**5**	**25**	**50**	**100**	**200**	**300**
Δh_{90}	(mm)		0.043	0.122	0.169	0.228	0.294	0.3484
Δh_0	(mm)		0.000	0.050	0.132	0.181	0.243	0.316
Δh_{100} = $[((\Delta h_{90} - \Delta h_0)/0.9)+ \Delta h_0]$	(mm)		0.047	0.130	0.173	0.233	0.300	0.352
Δh_f	(mm)		0.050	0.132	0.181	0.243	0.316	0.368
Initial Compression ratio $r_i = [\Delta h_0/\Delta h_f]$			0.000	0.379	0.731	0.745	0.769	0.859
Primary Compression ratio $r_p = [(\Delta h_{100}-\Delta h_0)/\Delta h_f]$			0.941	0.604	0.228	0.215	0.179	0.098
Secondary Compression ratio 'r_{sec}' = $[(\Delta h_f - \Delta h_{100})/\Delta h_f]$			0.059	0.017	0.041	0.040	0.052	0.043
√t90	(√min)		0.540	0.500	0.570	0.640	0.510	0.580
t_{90}	(mins)		0.292	0.250	0.325	0.410	0.260	0.336
T_{90}			0.848	0.848	0.848	0.848	0.848	0.848
drainage path 'd' = $[h_i/2]$	(mm)		9.150	9.125	9.084	9.060	9.029	8.992
Initial void ratio 'e_i' =$[(H-\Delta h_0-Hs)/Hs]$			0.577	0.573	0.566	0.562	0.557	0.550
Final void ratio 'e_f' =$[(H-\Delta h_f-Hs)/Hs]$		0.577	0.573	0.566	0.562	0.557	0.550	0.546
Total change in void ratio 'Δe' = $e_i - e_f$			0.004	0.007	0.004	0.005	0.006	0.004
Change of stress/pressure 'Δσ' = $\sigma_t - \sigma_p$	(kPa) or (kN/m^2)		5	20	25	50	100	100
Volume Compressibility 'Mv' = $[(1/1+e_0)*(\Delta e/\Delta\sigma')]$	(m^2/MN)		0.549	0.224	0.106	0.068	0.040	0.028
Volumetric Strain = (Δhi/H)*100%	(%)	0.000	0.274	0.721	0.987	1.328	1.728	2.010
coefficient of consolidation 'Cv' = $[(T_{90}*d^2)/t_{90}]$	(mm^2/min)		243.5	282.4	215.4	169.9	265.8	203.8
Coefficient of Permeability 'k' = $C_v*M_v*\gamma_w$	(m/yr)		0.672	0.318	0.115	0.058	0.053	0.029

Table C.8.4: initial parameter of sample B3 (Inundated)

Dimensions			Initial specimen	Final specimen
Diameter	'D'	(cm)	7.650	7.650
Area	'A'	(cm^2)	45.963	45.963
Height	'H'	(cm)	1.800	1.763
Volume	'V'	(cm^3)	82.734	81.036
Weights				
Ring		(g)	97.500	97.500
Ring + Sample in ring		(g)	275.400	280.701
Sample in ring	'M'	(g)	177.900	183.201
Moisture content 'W'		(%)	0.141	0.1858
Calculated				
Assumed specific gravity 'Gs'			2.900	2.900
Density of water 'ρ_w'		(g/cm^3)	1.000	1.000
bulk density	'ρ' = [M/(A*H)]	(g/cm^3)	2.150	2.261
Dry Density	'ρ_d' = [ρ/(1+W)]	(g/cm^3)	1.885	1.885
Void ratio	'e_0' = [(Gs*ρ_w/ρ_d)-1]		0.539	0.539
Degree of saturation 'Sr_i'	= [Gs*W/e_0]		0.759	1.000
Mass of solids in sample 'M_s'	=[M/(W+1)]	(g)	155.919	155.919
Height of solids in sample 'H_s'	=[H/(1+e_0)]	(cm)	1.170	1.170

Table C.8.5: Consolidation data for sample B3 (Inundated)

Time		Pressure at 5kPa		Pressure at 25kPa		Pressure at 50kPa		Pressure at 100kPa		Pressure at 200kPa		Pressure at 300kPa	
		Gauge reading	Consolidation settlement 'Δh'	Gauge reading	Consolidation settlement 'Δh'	Gauge reading	Consolidation settlement 'Δh'	Gauge reading	Consolidation settlement 'Δh'	Gauge reading	Consolidation settlement 'Δh'	Gauge reading	Consolidation settlement 'Δh'
t	√t	Gr	$(Gr_1 - Gr)$ *0.002	Gr	$(Gr_1 - Gr)$ *0.002	Gr	$(Gr_1 - Gr)$ *0.002	Gr	$(Gr_1 - Gr)$ *0.002	Gr	$(Gr_1 - Gr)$ *0.002	Gr	$(Gr_1 - Gr)$ *0.002
(mins)	(√mins)	(div)	(mm)	(div)	(mm)	(div)	(mm)	(div)	(mm)	(div)	(mm)	(div)	(mm)
0.00	0.00	1000.0	0.000	943.0	0.114	887.0	0.226	866.5	0.267	842.0	0.316	815.3	0.369
0.13	0.37	969.0	0.062	899.0	0.202	874.5	0.251	850.0	0.300	825.0	0.350	806.2	0.388
0.25	0.50	965.0	0.070	896.0	0.208	873.0	0.254	848.5	0.303	823.5	0.353	805.8	0.388
0.50	0.71	959.1	0.082	893.0	0.214	871.6	0.257	847.2	0.306	822.5	0.355	805.1	0.390
1.00	1.00	952.0	0.096	890.8	0.218	870.3	0.259	846.2	0.308	820.5	0.359	804.1	0.392
2.00	1.41	947.9	0.104	889.5	0.221	869.2	0.262	845.2	0.310	819.5	0.361	803.1	0.394
4.00	2.00	945.0	0.110	888.7	0.223	868.5	0.263	844.3	0.311	818.2	0.364	802.1	0.396
8.00	2.83	944.0	0.112	888.0	0.224	867.8	0.264	843.5	0.313	817.1	0.366	801.0	0.398
15.00	3.87	943.7	0.113	887.2	0.226	867.0	0.266	842.9	0.314	816.2	0.368	800.0	0.400
30.00	5.48	943.0	0.114	887.0	0.226	866.5	0.267	842.0	0.316	815.3	0.369	798.9	0.402

Table C.8.6: Consolidation calculated parameter for sample B3 (Inundated)

Pressures	**(kPa)**	**0**	**5**	**25**	**50**	**100**	**200**	**300**
Δh_{90}	(mm)		0.072	0.210	0.255	0.304	0.354	0.389
Δh_0	(mm)		0.000	0.114	0.226	0.267	0.316	0.369
Δh_{100} = $[((\Delta h_{90} - \Delta h_0)/0.9)+ \Delta h_0]$	(mm)		0.080	0.221	0.258	0.308	0.358	0.391
Δh_f	(mm)		0.114	0.226	0.267	0.316	0.369	0.402
Initial Compression ratio $r_i = [\Delta h_0/\Delta h_f]$			0.000	0.504	0.846	0.845	0.855	0.917
Primary Compression ratio $r_p = [(\Delta h_{100}-\Delta h_0)/\Delta h_f]$			0.702	0.472	0.121	0.130	0.113	0.055
Secondary Compression ratio 'r_{sec}' = $[(\Delta h_f - \Delta h_{100})/\Delta h_f]$			0.298	0.024	0.033	0.025	0.032	0.027
√t90	(√min)		0.560	0.570	0.590	0.580	0.540	0.540
t_{90}	(mins)		0.314	0.325	0.348	0.336	0.292	0.292
T_{90}			0.848	0.848	0.848	0.848	0.848	0.848
drainage path 'd' = $[h_i/2]$	(mm)		9.000	8.943	8.887	8.867	8.842	8.816
Initial void ratio 'e_i' =$[(H-\Delta h_0-Hs)/Hs]$			0.539	0.529	0.519	0.516	0.512	0.507
Final void ratio 'e_f' =$[(H-\Delta h_f-Hs)/Hs]$		0.539	0.529	0.519	0.516	0.512	0.507	0.504
Total change in void ratio 'Δe' = $e_i - e_f$			0.010	0.010	0.004	0.004	0.005	0.003
Change of stress/pressure 'Δσ' = $\sigma_t - \sigma_p$	(kPa) or (kN/m^2)		5	20	25	50	100	100
Volume Compressibility 'Mv' = $[(1/1+e_0)*(\Delta e/\Delta\sigma')]$	(m^2/MN)		1.267	0.311	0.091	0.054	0.030	0.018
Volumetric Strain = (Δhi/H)*100%	(%)	0.000	0.633	1.256	1.483	1.756	2.052	2.234
coefficient of consolidation 'Cv' = $[(T_{90}*d^2)/t_{90}]$	(mm^2/min)		219.0	208.7	192.4	198.2	227.4	226.0
Coefficient of Permeability 'k' = $C_v*M_v*\gamma_w$	(m/yr)		1.395	0.327	0.088	0.054	0.034	0.021

9. Soil B at 'Low wet of OMC' (4)

Table C.9.1: initial parameter of sample B4 (As-compacted)

Dimensions			Initial specimen	Final specimen
Diameter	'D'	(cm)	7.630	7.630
Area	'A'	(cm^2)	45.723	45.723
Height	'H'	(cm)	1.820	1.790
Volume	'V'	(cm^3)	83.217	81.857
Weights				
Ring		(g)	99.200	99.200
Ring + Sample in ring		(g)	291.300	286.949
Sample in ring	'M'	(g)	192.100	187.749
Moisture content 'W'		(%)	0.162	0.136
Calculated				
Assumed specific gravity 'Gs'			2.900	2.900
Density of water 'ρ_w'		(g/cm^3)	1.000	1.000
bulk density 'ρ' = [M/(A*H)]		(g/cm^3)	2.308	2.294
Dry Density 'ρ_d' = [ρ/(1+W)]		(g/cm^3)	1.986	2.019
Void ratio 'e_0' = [(Gs*ρ_w/ρ_d)-1]			0.460	0.436
Degree of saturation 'Sr_i' = [Gs*W/e_0]			1.023	0.904
Mass of solids in sample 'M_s' =[M/(W+1)]		(g)	165.256	165.256
Height of solids in sample 'H_s' =[H/(1+e_0)]		(cm)	1.246	1.246

Table C.9.2: Consolidation data for sample B4 (As-compacted)

Time		Pressure at 5kPa		Pressure at 25kPa		Pressure at 50kPa		Pressure at 100kPa		Pressure at 200kPa		Pressure at 300kPa	
		Gauge reading	Consolidation settlement 'Δh'	Gauge reading	Consolidation settlement 'Δh'	Gauge reading	Consolidation settlement 'Δh'	Gauge reading	Consolidation settlement 'Δh'	Gauge reading	Consolidation settlement 'Δh'	Gauge reading	Consolidation settlement 'Δh'
t	√t	Gr	$(Gr_1 - Gr)$ *0.002	Gr	$(Gr_1 - Gr)$ *0.002	Gr	$(Gr_1 - Gr)$ *0.002	Gr	$(Gr_1 - Gr)$ *0.002	Gr	$(Gr_1 - Gr)$ *0.002	Gr	$(Gr_1 - Gr)$ *0.002
(mins)	(√mins)	(div)	(mm)	(div)	(mm)	(div)	(mm)	(div)	(mm)	(div)	(mm)	(div)	(mm)
0.00	0.00	444.0	0.000	414.1	0.060	375.2	0.138	354.1	0.180	326.1	0.236	295.3	0.297
0.13	0.37	433.0	0.022	386.0	0.116	362.8	0.162	335.6	0.217	312.0	0.264	287.6	0.313
0.25	0.50	426.0	0.036	384.9	0.118	361.8	0.164	334.7	0.219	307.8	0.272	286.6	0.315
0.50	0.71	424.5	0.039	383.2	0.122	360.8	0.166	333.3	0.221	304.3	0.279	285.8	0.316
1.00	1.00	422.8	0.042	381.6	0.125	359.2	0.170	332.0	0.224	302.5	0.283	284.7	0.319
2.00	1.41	420.5	0.047	380.0	0.128	358.0	0.172	330.4	0.227	301.0	0.286	283.2	0.322
4.00	2.00	418.0	0.052	378.0	0.132	356.8	0.174	329.0	0.230	299.2	0.290	282.0	0.324
8.00	2.83	415.8	0.056	376.9	0.134	355.8	0.176	328.0	0.232	298.0	0.292	280.3	0.327
15.00	3.87	414.9	0.058	376.0	0.136	355.0	0.178	327.0	0.234	296.7	0.295	279.1	0.330
30.00	5.48	414.1	0.060	375.2	0.138	354.1	0.180	326.1	0.236	295.3	0.297	277.4	0.333

Table C.9.3: Consolidation calculated parameter for sample B4 (As-compacted)

Pressures	**(kPa)**	**0**	**5**	**25**	**50**	**100**	**200**	**300**
Δh_{90}	(mm)		0.039	0.118	0.164	0.219	0.280	0.315
Δh_0	(mm)		0.000	0.060	0.138	0.180	0.236	0.297
$\Delta h_{100} = [((\Delta h_{90} - \Delta h_0)/0.9) + \Delta h_0]$	(mm)		0.043	0.125	0.167	0.223	0.285	0.317
Δh_f	(mm)		0.060	0.138	0.180	0.236	0.297	0.333
Initial Compression ratio $r_i = [\Delta h_0/\Delta h_f]$			0.000	0.436	0.768	0.763	0.794	0.891
Primary Compression ratio $r_p = [(\Delta h_{100}-\Delta h_0)/\Delta h_f]$			0.725	0.470	0.163	0.184	0.164	0.060
Secondary Compression ratio 'r_{sec}' $= [(\Delta h_f - \Delta h_{100})/\Delta h_f]$			0.275	0.094	0.069	0.053	0.042	0.049
√t90	(√min)		0.760	0.490	0.520	0.500	0.780	0.520
t_{90}	(mins)		0.578	0.240	0.270	0.250	0.608	0.270
T_{90}			0.848	0.848	0.848	0.848	0.848	0.848
drainage path 'd' $= [h_i/2]$	(mm)		9.100	9.070	9.031	9.010	8.982	8.952
Initial void ratio 'e_i' $=[(H-\Delta h_0-Hs)/Hs]$			0.460	0.456	0.449	0.446	0.441	0.436
Final void ratio 'e_f' $=[(H-\Delta h_f-Hs)/Hs]$		0.460	0.456	0.449	0.446	0.441	0.436	0.434
Total change in void ratio 'Δe' $= e_i - e_f$			0.005	0.006	0.003	0.004	0.005	0.003
Change of stress/pressure 'Δσ' $= \sigma_t - \sigma_p$	(kPa) or (kN/m^2)		5	20	25	50	100	100
Volume Compressibility 'Mv' $= [(1/1+e_0)*(\Delta e/\Delta \sigma')]$	(m^2/MN)		0.474	0.154	0.066	0.044	0.024	0.014
Volumetric Strain $= (\Delta hi/H)*100\%$	(%)	0.000	0.329	0.756	0.988	1.296	1.634	1.831
coefficient of consolidation 'Cv' $= [(T_{90}*d^2)/t_{90}]$	(mm^2/min)		121.6	290.5	255.8	275.4	112.4	251.3
Coefficient of Permeability 'k' $= C_v*M_v*\gamma_w$	(m/yr)		0.290	0.225	0.085	0.061	0.014	0.018

Table C.9.4: initial parameter of sample B4 (Inundated)

Dimensions			Initial specimen	Final specimen
Diameter	'D'	(cm)	7.610	7.610
Area	'A'	(cm^2)	45.484	45.484
Height	'H'	(cm)	1.790	1.757
Volume	'V'	(cm^3)	81.416	79.928
Weights				
Ring		(g)	76.100	76.100
Ring + Sample in ring		(g)	259.700	255.990
Sample in ring	'M'	(g)	183.600	179.890
Moisture content 'W'		(%)	0.171	0.175
Calculated				
Assumed specific gravity 'Gs'			2.900	2.900
Density of water 'ρ_w'		(g/cm^3)	1.000	1.000
bulk density	'ρ' = [M/(A*H)]	(g/cm^3)	2.255	2.251
Dry Density	'ρ_d' = [ρ/(1+W)]	(g/cm^3)	1.925	1.925
Void ratio	'e_0' = [(Gs*ρ_w/ρ_d)-1]		0.506	0.506
Degree of saturation 'Sr_i'	= [Gs*W/e_0]		0.981	1.000
Mass of solids in sample 'M_s'	=[M/(W+1)]	(g)	156.759	156.759
Height of solids in sample 'H_s'	=[H/(1+e_0)]	(cm)	1.188	1.188

Table C.9.5: Consolidation data for sample B4 (Inundated)

Time		Pressure at 5kPa		Pressure at 25kPa		Pressure at 50kPa		Pressure at 100kPa		Pressure at 200kPa		Pressure at 300kPa	
		Gauge reading	Consolidation settlement 'Δh'	Gauge reading	Consolidation settlement 'Δh'	Gauge reading	Consolidation settlement 'Δh'	Gauge reading	Consolidation settlement 'Δh'	Gauge reading	Consolidation settlement 'Δh'	Gauge reading	Consolidation settlement 'Δh'
t	√t	Gr	$(Gr_1 - Gr)$ *0.002	Gr	$(Gr_1 – Gr)$ *0.002	Gr	$(Gr_1 - Gr)$ *0.002	Gr	$(Gr_1 - Gr)$ *0.002	Gr	$(Gr_1 - Gr)$ *0.002	Gr	$(Gr_1 - Gr)$ *0.002
(mins)	(√mins)	(div)	(mm)	(div)	(mm)	(div)	(mm)	(div)	(mm)	(div)	(mm)	(div)	(mm)
0.00	0.00	600.0	0.000	562.5	0.075	521.5	0.157	499.2	0.202	469.8	0.260	436.4	0.327
0.13	0.37	580.7	0.039	533.0	0.134	508.9	0.182	481.3	0.237	448.4	0.303	428.2	0.344
0.25	0.50	579.2	0.042	532.0	0.136	507.5	0.185	480.0	0.240	447.1	0.306	427.8	0.344
0.50	0.71	577.1	0.046	530.2	0.140	506.5	0.187	478.3	0.243	445.5	0.309	426.8	0.346
1.00	1.00	573.8	0.052	528.0	0.144	506.0	0.188	476.1	0.248	443.6	0.313	425.8	0.348
2.00	1.41	570.0	0.060	526.0	0.148	503.3	0.193	474.7	0.251	442.0	0.316	424.1	0.352
4.00	2.00	566.3	0.067	524.2	0.152	502.1	0.196	473.2	0.254	440.5	0.319	422.8	0.354
8.00	2.83	564.2	0.072	523.1	0.154	501.0	0.198	472.0	0.256	439.0	0.322	421.1	0.358
15.00	3.87	563.2	0.074	522.1	0.156	500.1	0.200	471.0	0.258	437.9	0.324	420.0	0.360
30.00	5.48	562.5	0.075	521.5	0.157	499.2	0.202	469.8	0.260	436.4	0.327	418.2	0.364

Table C.9.6: Consolidation calculated parameter for sample B4 (Inundated)

Pressures	**(kPa)**	**0**	**5**	**25**	**50**	**100**	**200**	**300**
Δh_{90}	(mm)		0.042	0.136	0.185	0.240	0.306	0.3445
Δh_0	(mm)		0.000	0.075	0.157	0.202	0.260	0.327
Δh_{100} = $[((\Delta h_{90} - \Delta h_0)/0.9)+ \Delta h_0]$	(mm)		0.047	0.143	0.188	0.244	0.311	0.346
Δh_f	(mm)		0.075	0.157	0.202	0.260	0.327	0.364
Initial Compression ratio $r_i = [\Delta h_0/\Delta h_f]$			0.000	0.478	0.779	0.776	0.795	0.899
Primary Compression ratio $r_p = [(\Delta h_{100}-\Delta h_0)/\Delta h_f]$			0.625	0.432	0.154	0.162	0.156	0.053
Secondary Compression ratio 'r_{sec}' = $[(\Delta h_f - \Delta h_{100})/\Delta h_f]$			0.375	0.091	0.067	0.062	0.049	0.047
√t90	(√min)		0.470	0.490	0.500	0.460	0.500	0.500
t_{90}	(mins)		0.221	0.240	0.250	0.212	0.250	0.250
T_{90}			0.848	0.848	0.848	0.848	0.848	0.848
drainage path 'd' = $[h_i/2]$	(mm)		8.950	8.913	8.872	8.849	8.820	8.787
Initial void ratio 'e_i' =$[(H-\Delta h_0-Hs)/Hs]$			0.506	0.500	0.493	0.489	0.484	0.479
Final void ratio 'e_f' =$[(H-\Delta h_f-Hs)/Hs]$		0.506	0.500	0.493	0.489	0.484	0.479	0.476
Total change in void ratio 'Δe' = $e_i - e_f$			0.006	0.007	0.004	0.005	0.006	0.003
Change of stress/pressure 'Δσ' = $\sigma_t - \sigma_p$	(kPa) or (kN/m^2)		5	20	25	50	100	100
Volume Compressibility 'Mv' = $[(1/1+e_0)*(\Delta e/\Delta\sigma')]$	(m^2/MN)		0.624	0.171	0.074	0.049	0.028	0.015
Volumetric Strain = (Δhi/H)*100%	(%)	0.000	0.419	0.877	1.126	1.455	1.828	2.031
coefficient of consolidation 'Cv' = $[(T_{90}*d^2)/t_{90}]$	(mm^2/min)		307.5	280.5	267.0	313.8	263.9	261.9
Coefficient of Permeability 'k' = $C_v*M_v*\gamma_w$	(m/yr)		0.965	0.241	0.100	0.077	0.037	0.020

10. Soil B at 'High wet of OMC' (5)

Table C.10.1: initial parameter of sample B5 (As-compacted)

Dimensions			Initial specimen	Final specimen
Diameter	'D'	(cm)	7.650	7.650
Area	'A'	(cm^2)	45.963	45.963
Height	'H'	(cm)	1.800	1.771
Volume	'V'	(cm^3)	82.734	81.393
Weights				
Ring		(g)	97.500	97.500
Ring + Sample in ring		(g)	287.300	282.269
Sample in ring	'M'	(g)	189.800	184.769
Moisture content 'W'		(%)	0.184	0.152
Calculated				
Assumed specific gravity 'Gs'			2.900	2.900
Density of water 'ρ_w'		(g/cm^3)	1.000	1.000
bulk density	'ρ' = [M/(A*H)]	(g/cm^3)	2.294	2.270
Dry Density	'ρ_d' = [ρ/(1+W)]	(g/cm^3)	1.938	1.970
Void ratio	'e_0' = [(Gs*ρ_w/ρ_d)-1]		0.496	0.472
Degree of saturation 'Sr_i'	= [Gs*W/e_0]		1.074	0.936
Mass of solids in sample 'M_s'	=[M/(W+1)]	(g)	160.334	160.334
Height of solids in sample 'H_s'	=[H/(1+e_0)]	(cm)	1.203	1.203

Table C.10.2: Consolidation data for sample B5 (As-compacted)

Time		Pressure at 5kPa		Pressure at 25kPa		Pressure at 50kPa		Pressure at 100kPa		Pressure at 200kPa		Pressure at 300kPa	
		Gauge reading	Consolidation settlement 'Δh'	Gauge reading	Consolidation settlement 'Δh'	Gauge reading	Consolidation settlement 'Δh'	Gauge reading	Consolidation settlement 'Δh'	Gauge reading	Consolidation settlement 'Δh'	Gauge reading	Consolidation settlement 'Δh'
t	√t	Gr	$(Gr_1 - Gr)$ *0.002	Gr	$(Gr_1 - Gr)$ *0.002	Gr	$(Gr_1 - Gr)$ *0.002	Gr	$(Gr_1 - Gr)$ *0.002	Gr	$(Gr_1 - Gr)$ *0.002	Gr	$(Gr_1 - Gr)$ *0.002
(mins)	(√mins)	(div)	(mm)	(div)	(mm)	(div)	(mm)	(div)	(mm)	(div)	(mm)	(div)	(mm)
0.00	0.00	1200.0	0.000	1170.1	0.060	1132.0	0.136	1112.1	0.176	1085.8	0.228	1054.1	0.292
0.13	0.37	1178.0	0.044	1138.0	0.124	1117.2	0.166	1092.2	0.216	1060.9	0.278	1038.0	0.324
0.25	0.50	1176.5	0.047	1136.8	0.126	1116.2	0.168	1091.7	0.217	1060.0	0.280	1037.2	0.326
0.50	0.71	1175.0	0.050	1135.8	0.128	1115.8	0.168	1090.7	0.219	1059.3	0.281	1036.6	0.327
1.00	1.00	1173.0	0.054	1134.9	0.130	1115.1	0.170	1089.2	0.222	1058.2	0.284	1035.9	0.328
2.00	1.41	1171.9	0.056	1134.0	0.132	1114.2	0.172	1088.6	0.223	1057.5	0.285	1035.1	0.330
4.00	2.00	1171.2	0.058	1133.5	0.133	1113.8	0.172	1087.9	0.224	1056.5	0.287	1034.2	0.332
8.00	2.83	1170.8	0.058	1133.0	0.134	1113.1	0.174	1087.0	0.226	1055.8	0.288	1033.3	0.333
15.00	3.87	1170.3	0.059	1132.5	0.135	1112.8	0.174	1086.4	0.227	1055.0	0.290	1032.7	0.335
30.00	5.48	1170.1	0.060	1132.0	0.136	1112.1	0.176	1085.8	0.228	1054.1	0.292	1031.8	0.336

Table C.10.3: Consolidation calculated parameter for sample B5 (As-compacted)

Pressures	**(kPa)**	**0**	**5**	**25**	**50**	**100**	**200**	**300**
Δh_{90}	(mm)		0.048	0.127	0.168	0.218	0.281	0.326
Δh_0	(mm)		0.000	0.060	0.136	0.176	0.228	0.292
Δh_{100} = $[((\Delta h_{90} - \Delta h_0)/0.9)+ \Delta h_0]$	(mm)		0.053	0.134	0.172	0.222	0.286	0.330
Δh_f	(mm)		0.060	0.136	0.176	0.228	0.292	0.336
Initial Compression ratio $r_i = [\Delta h_0/\Delta h_f]$			0.000	0.441	0.774	0.771	0.781	0.868
Primary Compression ratio $r_p = [(\Delta h_{100}-\Delta h_0)/\Delta h_f]$			0.892	0.547	0.203	0.203	0.200	0.112
Secondary Compression ratio 'r_{sec}' = $[(\Delta h_f - \Delta h_{100})/\Delta h_f]$			0.108	0.011	0.024	0.026	0.018	0.020
√t90	(√min)		0.560	0.500	0.510	0.520	0.490	0.560
t_{90}	(mins)		0.314	0.250	0.260	0.270	0.240	0.314
T_{90}			0.848	0.848	0.848	0.848	0.848	0.848
drainage path 'd' = $[h_i/2]$	(mm)		9.000	8.970	8.932	8.912	8.886	8.854
Initial void ratio 'e_i' =$[(H-\Delta h_0-Hs)/Hs]$			0.496	0.491	0.485	0.482	0.477	0.472
Final void ratio 'e_f' =$[(H-\Delta h_f-Hs)/Hs]$		0.496	0.491	0.485	0.482	0.477	0.472	0.468
Total change in void ratio 'Δe' = $e_i - e_f$			0.005	0.006	0.003	0.004	0.005	0.004
Change of stress/pressure 'Δσ' = $\sigma_t - \sigma_p$	(kPa) or (kN/m^2)		5	20	25	50	100	100
Volume Compressibility 'Mv' = $[(1/1+e_0)*(\Delta e/\Delta\sigma')]$	(m^2/MN)		0.664	0.211	0.088	0.058	0.035	0.025
Volumetric Strain = (Δhi/H)*100%	(%)	0.000	0.332	0.756	0.977	1.269	1.621	1.869
coefficient of consolidation 'Cv' = $[(T_{90}*d^2)/t_{90}]$	(mm^2/min)		219.0	272.9	260.1	249.1	278.9	212.0
Coefficient of Permeability 'k' = $C_v*M_v*\gamma_w$	(m/yr)		0.732	0.290	0.116	0.073	0.050	0.026

Table C.10.4: initial parameter of sample B5 (Inundated)

Dimensions			Initial specimen	Final specimen
Diameter	'D'	(cm)	7.660	7.660
Area	'A'	(cm^2)	46.084	46.084
Height	'H'	(cm)	1.830	1.794
Volume	'V'	(cm^3)	84.333	82.682
Weights				
Ring		(g)	101.200	101.200
Ring + Sample in ring		(g)	292.600	288.398
Sample in ring	'M'	(g)	191.400	187.198
Moisture content 'W'		(%)	0.190	0.1795
Calculated				
Assumed specific gravity 'Gs'			2.900	2.900
Density of water 'ρ_w'		(g/cm^3)	1.000	1.000
bulk density	'ρ' = [M/(A*H)]	(g/cm^3)	2.270	2.264
Dry Density	'ρ_d' = [ρ/(1+W)]	(g/cm^3)	1.907	1.907
Void ratio	'e_0' = [(Gs*ρ_w/ρ_d)-1]		0.521	0.521
Degree of saturation 'Sr_i'	= [Gs*W/e_0]		1.058	1.000
Mass of solids in sample 'M_s'	=[M/(W+1)]	(g)	160.842	160.842
Height of solids in sample 'H_s'	=[H/(1+e_0)]	(cm)	1.204	1.204

Table C.10.5: Consolidation data for sample B5 (Inundated)

Time		Pressure at 5kPa		Pressure at 25kPa		Pressure at 50kPa		Pressure at 100kPa		Pressure at 200kPa		Pressure at 300kPa	
		Gauge reading	Consolidation settlement 'Δh'	Gauge reading	Consolidation settlement 'Δh'	Gauge reading	Consolidation settlement 'Δh'	Gauge reading	Consolidation settlement 'Δh'	Gauge reading	Consolidation settlement 'Δh'	Gauge reading	Consolidation settlement 'Δh'
t	√t	Gr	$(Gr_1 - Gr)$ *0.002	Gr	$(Gr_1 - Gr)$ *0.002	Gr	$(Gr_1 - Gr)$ *0.002	Gr	$(Gr_1 - Gr)$ *0.002	Gr	$(Gr_1 - Gr)$ *0.002	Gr	$(Gr_1 - Gr)$ *0.002
(mins)	(√mins)	(div)	(mm)	(div)	(mm)	(div)	(mm)	(div)	(mm)	(div)	(mm)	(div)	(mm)
0.00	0.00	1100.0	0.000	1030.9	0.138	984.5	0.231	967.1	0.266	944.4	0.311	920.9	0.358
0.13	0.37	1062.0	0.076	994.0	0.212	974.0	0.252	951.0	0.298	929.2	0.342	912.2	0.376
0.25	0.50	1056.4	0.087	991.5	0.217	972.8	0.254	950.1	0.300	928.0	0.344	912.0	0.376
0.50	0.71	1049.5	0.101	989.9	0.220	971.7	0.257	949.2	0.302	926.8	0.346	911.4	0.377
1.00	1.00	1041.0	0.118	987.9	0.224	970.6	0.259	948.2	0.304	925.5	0.349	910.8	0.378
2.00	1.41	1035.1	0.130	986.8	0.226	969.9	0.260	947.5	0.305	924.6	0.351	909.9	0.380
4.00	2.00	1032.9	0.134	986.0	0.228	969.0	0.262	946.8	0.306	923.5	0.353	908.9	0.382
8.00	2.83	1031.9	0.136	985.5	0.229	968.2	0.264	945.1	0.310	922.5	0.355	907.9	0.384
15.00	3.87	1031.2	0.138	985.0	0.230	967.9	0.264	945.0	0.310	921.4	0.357	906.9	0.386
30.00	5.48	1030.9	0.138	984.5	0.231	967.1	0.266	944.4	0.311	920.9	0.358	905.9	0.388

Table C.10.6: Consolidation calculated parameter for sample B5 (Inundated)

Pressures	**(kPa)**	**0**	**5**	**25**	**50**	**100**	**200**	**300**
Δh_{90}	(mm)		0.096	0.218	0.255	0.300	0.345	0.3765
Δh_0	(mm)		0.000	0.138	0.231	0.266	0.311	0.358
Δh_{100} = $[((\Delta h_{90} - \Delta h_0)/0.9)+ \Delta h_0]$	(mm)		0.107	0.227	0.258	0.304	0.348	0.379
Δh_f	(mm)		0.138	0.231	0.266	0.311	0.358	0.388
Initial Compression ratio $r_i = [\Delta h_0/\Delta h_f]$			0.000	0.597	0.869	0.855	0.868	0.922
Primary Compression ratio $r_p = [(\Delta h_{100}-\Delta h_0)/\Delta h_f]$			0.772	0.385	0.100	0.121	0.104	0.053
Secondary Compression ratio 'r_{sec}' = $[(\Delta h_f - \Delta h_{100})/\Delta h_f]$			0.228	0.018	0.031	0.024	0.028	0.025
√t90	(√min)		0.620	0.520	0.540	0.500	0.520	0.540
t_{90}	(mins)		0.384	0.270	0.292	0.250	0.270	0.292
T_{90}			0.848	0.848	0.848	0.848	0.848	0.848
drainage path 'd' = $[h_i/2]$	(mm)		9.150	9.081	9.035	9.017	8.995	8.821
Initial void ratio 'e_i' =$[(H-\Delta h_0-Hs)/Hs]$			0.521	0.509	0.501	0.498	0.495	0.467
Final void ratio 'e_f' =$[(H-\Delta h_f-Hs)/Hs]$		0.521	0.509	0.501	0.498	0.495	0.491	0.464
Total change in void ratio 'Δe' = $e_i - e_f$			0.011	0.008	0.003	0.004	0.004	0.003
Change of stress/pressure 'Δσ' = $\sigma_t - \sigma_p$	(kPa) or (kN/m^2)		5	20	25	50	100	100
Volume Compressibility 'Mv' = $[(1/1+e_0)*(\Delta e/\Delta\sigma')]$	(m^2/MN)		1.510	0.254	0.076	0.049	0.026	0.017
Volumetric Strain = (Δhi/H)*100%	(%)	0.000	0.755	1.262	1.452	1.701	1.957	2.121
coefficient of consolidation 'Cv' = $[(T_{90}*d^2)/t_{90}]$	(mm^2/min)		184.7	258.6	237.4	275.8	253.7	226.3
Coefficient of Permeability 'k' = $C_v*M_v*\gamma_w$	(m/yr)		1.403	0.330	0.091	0.069	0.033	0.019

11. Soil C at 'High dry of OMC' (1)

Table C.11.1: initial parameter of sample C1 (As-compacted)

Dimensions			Initial specimen	Final specimen
Diameter	'D'	(cm)	7.670	7.670
Area	'A'	(cm^2)	46.204	46.204
Height	'H'	(cm)	1.830	1.787
Volume	'V'	(cm^3)	84.553	82.587
Weights				
Ring		(g)	99.400	99.400
Ring + Sample in ring		(g)	271.000	270.517
Sample in ring	'M'	(g)	171.600	171.117
Moisture content 'W'		(%)	0.128	0.125
Calculated				
Assumed specific gravity 'Gs'			2.900	2.900
Density of water 'ρ_w'		(g/cm^3)	1.000	1.000
bulk density	'ρ' = [M/(A*H)]	(g/cm^3)	2.029	2.072
Dry Density	'ρ_d' = [ρ/(1+W)]	(g/cm^3)	1.799	1.842
Void ratio	'e_0' = [(Gs*ρ_w/ρ_d)-1]		0.612	0.574
Degree of saturation 'Sr_i'	= [Gs*W/e_0]		0.606	0.630
Mass of solids in sample 'M_s'	=[M/(W+1)]	(g)	152.142	152.142
Height of solids in sample 'H_s'	=[H/(1+e_0)]	(cm)	1.135	1.135

Table C.11.2: Consolidation data for sample C1 (As-compacted)

Time		Pressure at 5kPa		Pressure at 25kPa		Pressure at 50kPa		Pressure at 100kPa		Pressure at 200kPa		Pressure at 300kPa	
		Gauge reading	Consolidation settlement 'Δh'	Gauge reading	Consolidation settlement 'Δh'	Gauge reading	Consolidation settlement 'Δh'	Gauge reading	Consolidation settlement 'Δh'	Gauge reading	Consolidation settlement 'Δh'	Gauge reading	Consolidation settlement 'Δh'
t	√t	Gr	$(Gr_1 - Gr)$ *0.002	Gr	$(Gr_1 - Gr)$ *0.002	Gr	$(Gr_1 - Gr)$ *0.002	Gr	$(Gr_1 - Gr)$ *0.002	Gr	$(Gr_1 - Gr)$ *0.002	Gr	$(Gr_1 - Gr)$ *0.002
(mins)	(√mins)	(div)	(mm)	(div)	(mm)	(div)	(mm)	(div)	(mm)	(div)	(mm)	(div)	(mm)
0.00	0.00	1200.0	0.000	1190.0	0.020	1166.0	0.068	1130.0	0.140	1088.0	0.224	987.0	0.426
0.13	0.37	1195.2	0.010	1173.0	0.054	1150.0	0.100	1109.0	0.182	1015.0	0.370	858.0	0.684
0.25	0.50	1195.0	0.010	1170.0	0.060	1139.0	0.122	1102.0	0.196	1006.0	0.388	850.0	0.700
0.50	0.71	1194.8	0.010	1169.0	0.062	1137.0	0.126	1099.0	0.202	1004.0	0.392	847.0	0.706
1.00	1.00	1194.7	0.011	1169.2	0.062	1135.9	0.128	1096.0	0.208	1001.0	0.398	842.0	0.716
2.00	1.41	1194.3	0.011	1168.9	0.062	1135.0	0.130	1094.1	0.212	996.1	0.408	837.0	0.726
4.00	2.00	1194.0	0.012	1168.0	0.064	1134.1	0.132	1092.9	0.214	993.5	0.413	834.9	0.730
8.00	2.83	1193.0	0.014	1167.5	0.065	1133.6	0.133	1091.2	0.218	991.0	0.418	832.9	0.734
15.00	3.87	1192.9	0.014	1167.0	0.066	1132.9	0.134	1090.1	0.220	989.0	0.422	831.0	0.738
30.00	5.48	1192.9	0.014	1166.0	0.068	1132.0	0.136	1089.0	0.222	987.2	0.426	829.5	0.741

Table C.11.3: Consolidation calculated parameter for sample C1 (As-compacted)

Pressures	**(kPa)**	**0**	**5**	**25**	**50**	**100**	**200**	**300**
Δh_{90}	(mm)		0.010	0.062	0.127	0.203	0.390	0.702
Δh_0	(mm)		0.000	0.020	0.068	0.140	0.224	0.426
Δh_{100} = $[((\Delta h_{90} - \Delta h_0)/0.9)+ \Delta h_0]$	(mm)		0.011	0.066	0.134	0.210	0.408	0.733
Δh_f	(mm)		0.014	0.068	0.136	0.222	0.426	0.741
Initial Compression ratio $r_i = [\Delta h_0/\Delta h_f]$			0.000	0.294	0.500	0.631	0.526	0.575
Primary Compression ratio $r_p = [(\Delta h_{100}-\Delta h_0)/\Delta h_f]$			0.798	0.683	0.482	0.315	0.433	0.414
Secondary Compression ratio 'r_{sec}' = $[(\Delta h_f - \Delta h_{100})/\Delta h_f]$			0.202	0.023	0.018	0.054	0.040	0.011
√t90	(√min)		0.500	0.570	0.800	0.770	0.590	0.580
t_{90}	(mins)		0.250	0.325	0.640	0.593	0.348	0.336
T_{90}			0.848	0.848	0.848	0.848	0.848	0.848
drainage path 'd' = $[h_i/2]$	(mm)		9.150	9.140	9.116	9.080	9.038	8.937
Initial void ratio 'e_i' =$[(H-\Delta h_0-Hs)/Hs]$			0.612	0.610	0.606	0.599	0.592	0.574
Final void ratio 'e_f' =$[(H-\Delta h_f-Hs)/Hs]$		0.612	0.610	0.606	0.600	0.592	0.574	0.546
Total change in void ratio 'Δe' = $e_i - e_f$			0.001	0.004	0.006	0.007	0.018	0.028
Change of stress/pressure 'Δσ' = $\sigma_t - \sigma_p$	(kPa) or (kN/m^2)		5	20	25	50	100	100
Volume Compressibility 'Mv' = $[(1/1+e_0)*(\Delta e/\Delta\sigma')]$	(m^2/MN)		0.155	0.131	0.149	0.090	0.110	0.172
Volumetric Strain = (Δhi/H)*100%	(%)	0.000	0.078	0.372	0.743	1.213	2.326	4.049
coefficient of consolidation 'Cv' = $[(T_{90}*d^2)/t_{90}]$	(mm^2/min)		284.0	218.0	110.1	117.9	199.0	201.3
Coefficient of Permeability 'k' = $C_v*M_v*\gamma_w$	(m/yr)		0.222	0.144	0.082	0.053	0.110	0.174

Table C.11.4: initial parameter of sample C1 (Inundated)

Dimensions			Initial specimen	Final specimen
Diameter	'D'	(cm)	7.610	7.610
Area	'A'	(cm^2)	45.484	45.484
Height	'H'	(cm)	1.790	1.717
Volume	'V'	(cm^3)	81.416	78.085
Weights				
Ring		(g)	76.400	76.400
Ring + Sample in ring		(g)	239.500	244.450
Sample in ring	'M'	(g)	163.100	168.050
Moisture content 'W'		(%)	0.125	0.2169
Calculated				
Assumed specific gravity 'Gs'			2.900	2.900
Density of water 'ρ_w'		(g/cm^3)	1.000	1.000
bulk density	'ρ' = [M/(A*H)]	(g/cm^3)	2.003	2.152
Dry Density	'ρ_d' = [ρ/(1+W)]	(g/cm^3)	1.780	1.780
Void ratio	'e_0' = [(Gs*ρ_w/ρ_d)-1]		0.629	0.629
Degree of saturation 'Sr_i'	= [Gs*W/e_0]		0.578	1.000
Mass of solids in sample 'M_s'	=[M/(W+1)]	(g)	144.939	144.939
Height of solids in sample 'H_s'	=[H/(1+e_0)]	(cm)	1.099	1.099

Table C.11.5: Consolidation data for sample C1 (Inundated)

Time		Pressure at 5kPa		Pressure at 25kPa		Pressure at 50kPa		Pressure at 100kPa		Pressure at 200kPa		Pressure at 300kPa	
		Gauge reading	Consolidation settlement 'Δh'	Gauge reading	Consolidation settlement 'Δh'	Gauge reading	Consolidation settlement 'Δh'	Gauge reading	Consolidation settlement 'Δh'	Gauge reading	Consolidation settlement 'Δh'	Gauge reading	Consolidation settlement 'Δh'
t	√t	Gr	$(Gr_1 - Gr)$ *0.002	Gr	$(Gr_1 - Gr)$ *0.002	Gr	$(Gr_1 - Gr)$ *0.002	Gr	$(Gr_1 - Gr)$ *0.002	Gr	$(Gr_1 - Gr)$ *0.002	Gr	$(Gr_1 - Gr)$ *0.002
(mins)	(√mins)	(div)	(mm)	(div)	(mm)	(div)	(mm)	(div)	(mm)	(div)	(mm)	(div)	(mm)
0.00	0.00	1100.0	0.000	1006.0	0.188	901.0	0.398	849.1	0.502	790.0	0.620	733.8	0.732
0.13	0.37	1064.0	0.072	965.0	0.270	886.0	0.428	830.0	0.540	770.0	0.660	726.0	0.748
0.25	0.50	1063.0	0.074	958.0	0.284	882.0	0.436	827.0	0.546	768.0	0.664	724.0	0.752
0.50	0.71	1058.0	0.084	952.0	0.296	878.0	0.444	822.5	0.555	763.0	0.674	722.0	0.756
1.00	1.00	1051.0	0.098	944.5	0.311	874.0	0.452	817.0	0.566	758.0	0.684	720.0	0.760
2.00	1.41	1041.5	0.117	935.0	0.330	868.0	0.464	810.0	0.580	750.0	0.700	715.5	0.769
4.00	2.00	1030.0	0.140	923.3	0.353	861.5	0.477	802.0	0.596	743.0	0.714	712.0	0.776
8.00	2.83	1018.0	0.164	911.1	0.378	855.1	0.490	795.7	0.609	738.0	0.724	709.0	0.782
15.00	3.87	1010.1	0.180	904.1	0.392	851.5	0.497	792.1	0.616	735.4	0.729	707.0	0.786
30.00	5.48	1006.0	0.188	901.0	0.398	849.1	0.502	790.0	0.620	733.8	0.732	707.0	0.786

Table C.11.6: Consolidation calculated parameter for sample C1 (Inundated)

Pressures	**(kPa)**	**0**	**5**	**25**	**50**	**100**	**200**	**300**
Δh_{90}	(mm)		0.076	0.293	0.450	0.553	0.672	0.7575
Δh_0	(mm)		0.000	0.188	0.398	0.502	0.602	0.732
Δh_{100} = $[((\Delta h_{90} - \Delta h_0)/0.9)+ \Delta h_0]$	(mm)		0.084	0.305	0.456	0.559	0.680	0.760
Δh_f	(mm)		0.188	0.398	0.502	0.620	0.732	0.786
Initial Compression ratio $r_i = [\Delta h_0/\Delta h_f]$			0.000	0.472	0.793	0.810	0.822	0.931
Primary Compression ratio $r_p = [(\Delta h_{100}-\Delta h_0)/\Delta h_f]$			0.449	0.293	0.115	0.091	0.106	0.036
Secondary Compression ratio 'r_{sec}' = $[(\Delta h_f - \Delta h_{100})/\Delta h_f]$			0.551	0.235	0.092	0.099	0.072	0.033
√t90	(√min)		0.540	0.620	0.900	0.640	0.620	0.800
t_{90}	(mins)		0.292	0.384	0.810	0.410	0.384	0.640
T_{90}			0.848	0.848	0.848	0.848	0.848	0.848
drainage path 'd' = $[h_i/2]$	(mm)		8.950	8.856	8.751	8.699	8.649	8.784
Initial void ratio 'e_i' =$[(H-\Delta h_0-Hs)/Hs]$			0.629	0.612	0.593	0.583	0.574	0.547
Final void ratio 'e_f' =$[(H-\Delta h_f-Hs)/Hs]$		0.629	0.612	0.593	0.583	0.573	0.562	0.542
Total change in void ratio 'Δe' = $e_i - e_f$			0.017	0.019	0.009	0.011	0.012	0.005
Change of stress/pressure 'Δσ' = $\sigma_t - \sigma_p$	(kPa) or (kN/m^2)		5	20	25	50	100	100
Volume Compressibility 'Mv' = $[(1/1+e_0)*(\Delta e/\Delta\sigma')]$	(m^2/MN)		2.101	0.587	0.232	0.132	0.073	0.030
Volumetric Strain = (Δhi/H)*100%	(%)	0.000	1.050	2.223	2.803	3.464	4.092	4.391
coefficient of consolidation 'Cv' = $[(T_{90}*d^2)/t_{90}]$	(mm^2/min)		232.9	173.0	80.2	156.7	165.0	102.2
Coefficient of Permeability 'k' = $C_v*M_v*\gamma_w$	(m/yr)		2.461	0.510	0.094	0.104	0.060	0.015

12. Soil C at 'Low dry of OMC' (2)

Table C.12.1: initial parameter of sample C2 (As-compacted)

Dimensions			Initial specimen	Final specimen
Diameter	'D'	(cm)	7.650	7.650
Area	'A'	(cm^2)	45.963	45.963
Height	'H'	(cm)	1.800	1.759
Volume	'V'	(cm^3)	82.734	80.843
Weights				
Ring		(g)	97.600	97.600
Ring + Sample in ring		(g)	284.600	282.671
Sample in ring	'M'	(g)	187.000	185.071
Moisture content 'W'		(%)	0.159	0.147
Calculated				
Assumed specific gravity 'Gs'			2.900	2.900
Density of water 'ρ_w'		(g/cm^3)	1.000	1.000
bulk density	'ρ' = [M/(A*H)]	(g/cm^3)	2.260	2.289
Dry Density	'ρ_d' = [ρ/(1+W)]	(g/cm^3)	1.950	1.995
Void ratio	'e_0' = [(Gs*ρ_w/ρ_d)-1]		0.488	0.454
Degree of saturation 'Sr_i'	= [Gs*W/e_0]		0.948	0.943
Mass of solids in sample 'M_s'	=[M/(W+1)]	(g)	161.294	161.294
Height of solids in sample 'H_s'	=[H/(1+e_0)]	(cm)	1.210	1.210

Table C.12.2: Consolidation data for sample C2 (As-compacted)

Time		Pressure at 5kPa		Pressure at 25kPa		Pressure at 50kPa		Pressure at 100kPa		Pressure at 200kPa		Pressure at 300kPa	
		Gauge reading	Consolidation settlement 'Δh'	Gauge reading	Consolidation settlement 'Δh'	Gauge reading	Consolidation settlement 'Δh'	Gauge reading	Consolidation settlement 'Δh'	Gauge reading	Consolidation settlement 'Δh'	Gauge reading	Consolidation settlement 'Δh'
t	√t	Gr	$(Gr_1 - Gr)$ *0.002	Gr	$(Gr_1 - Gr)$ *0.002	Gr	$(Gr_1 - Gr)$ *0.002	Gr	$(Gr_1 - Gr)$ *0.002	Gr	$(Gr_1 - Gr)$ *0.002	Gr	$(Gr_1 - Gr)$ *0.002
(mins)	(√mins)	(div)	(mm)	(div)	(mm)	(div)	(mm)	(div)	(mm)	(div)	(mm)	(div)	(mm)
0.00	0.00	675.0	0.000	654.5	0.041	598.0	0.154	563.6	0.223	522.2	0.306	469.3	0.411
0.13	0.37	659.0	0.032	606.0	0.138	572.1	0.206	540.5	0.269	498.9	0.352	457.2	0.436
0.25	0.50	658.5	0.033	605.1	0.140	571.2	0.208	538.5	0.273	496.5	0.357	456.0	0.438
0.50	0.71	657.9	0.034	604.0	0.142	570.3	0.209	536.5	0.277	494.8	0.360	453.9	0.442
1.00	1.00	657.2	0.036	602.9	0.144	569.2	0.212	534.2	0.282	489.0	0.372	450.8	0.448
2.00	1.41	656.6	0.037	601.9	0.146	568.0	0.214	531.9	0.286	483.9	0.382	446.3	0.457
4.00	2.00	655.8	0.038	600.8	0.148	566.5	0.217	528.7	0.293	477.9	0.394	442.6	0.465
8.00	2.83	655.3	0.039	599.6	0.151	565.2	0.220	525.3	0.299	473.6	0.403	439.0	0.472
15.00	3.87	654.8	0.040	598.9	0.152	564.3	0.221	523.5	0.303	471.0	0.408	436.8	0.476
30.00	5.48	654.5	0.041	598.0	0.154	563.6	0.223	522.2	0.306	469.3	0.411	435.0	0.480

Table C.12.3: Consolidation calculated parameter for sample C2 (As-compacted)

Pressures	**(kPa)**	**0**	**5**	**25**	**50**	**100**	**200**	**300**
Δh_{90}	(mm)		0.033	0.141	0.208	0.274	0.358	0.439
Δh_0	(mm)		0.000	0.041	0.154	0.223	0.306	0.411
Δh_{100} = $[((\Delta h_{90} - \Delta h_0)/0.9)+ \Delta h_0]$	(mm)		0.037	0.152	0.214	0.280	0.364	0.442
Δh_f	(mm)		0.041	0.154	0.223	0.306	0.411	0.480
Initial Compression ratio $r_i = [\Delta h_0/\Delta h_f]$			0.000	0.266	0.691	0.730	0.744	0.856
Primary Compression ratio $r_p = [(\Delta h_{100}-\Delta h_0)/\Delta h_f]$			0.894	0.722	0.269	0.185	0.140	0.065
Secondary Compression ratio 'r_{sec}' = $[(\Delta h_f - \Delta h_{100})/\Delta h_f]$			0.106	0.012	0.039	0.085	0.116	0.079
√t90	(√min)		0.500	0.500	0.480	0.540	0.500	0.560
t_{90}	(mins)		0.250	0.250	0.230	0.292	0.250	0.314
T_{90}			0.848	0.848	0.848	0.848	0.848	0.848
drainage path 'd' = $[h_i/2]$	(mm)		9.000	8.980	8.923	8.889	8.847	8.795
Initial void ratio 'e_i' =$[(H-\Delta h_0-Hs)/Hs]$			0.488	0.484	0.475	0.469	0.462	0.454
Final void ratio 'e_f' =$[(H-\Delta h_f-Hs)/Hs]$		0.488	0.484	0.475	0.469	0.462	0.454	0.448
Total change in void ratio 'Δe' = $e_i - e_f$			0.003	0.009	0.006	0.007	0.009	0.006
Change of stress/pressure 'Δσ' = $\sigma_t - \sigma_p$	(kPa) or (kN/m^2)		5	20	25	50	100	100
Volume Compressibility 'Mv' = $[(1/1+e_0)*(\Delta e/\Delta\sigma')]$	(m^2/MN)		0.348	0.240	0.117	0.070	0.045	0.029
Volumetric Strain = (Δhi/H)*100%	(%)	0.000	0.228	0.856	1.238	1.698	2.286	2.667
coefficient of consolidation 'Cv' = $[(T_{90}*d^2)/t_{90}]$	(mm^2/min)		274.8	273.5	293.0	229.8	265.5	209.1
Coefficient of Permeability 'k' = $C_v*M_v*\gamma_w$	(m/yr)		0.481	0.330	0.172	0.081	0.060	0.031

Table C.12.4: initial parameter of sample C2 (Inundated)

Dimensions			Initial specimen	Final specimen
Diameter	'D'	(cm)	7.660	7.660
Area	'A'	(cm^2)	46.084	46.084
Height	'H'	(cm)	1.825	1.702
Volume	'V'	(cm^3)	84.103	78.426
Weights				
Ring		(g)	99.400	99.400
Ring + Sample in ring		(g)	296.000	294.791
Sample in ring	'M'	(g)	196.600	195.391
Moisture content 'W'		(%)	0.156	0.150
Calculated				
Assumed specific gravity 'Gs'			2.900	2.900
Density of water 'ρ_w'		(g/cm^3)	1.000	1.000
bulk density	'ρ' = [M/(A*H)]	(g/cm^3)	2.338	2.491
Dry Density	'ρ_d' = [ρ/(1+W)]	(g/cm^3)	2.022	2.022
Void ratio	'e_0' = [(Gs*ρ_w/ρ_d)-1]		0.434	0.434
Degree of saturation 'Sr_i'	= [Gs*W/e_0]		1.042	1.000
Mass of solids in sample 'M_s'	=[M/(W+1)]	(g)	170.060	170.060
Height of solids in sample 'H_s'	=[H/(1+e_0)]	(cm)	1.273	1.273

Table C.12.5: Consolidation data for sample C2 (Inundated)

Time		Pressure at 5kPa		Pressure at 25kPa		Pressure at 50kPa		Pressure at 100kPa		Pressure at 200kPa		Pressure at 300kPa	
		Gauge reading	Consolidation settlement 'Δh'	Gauge reading	Consolidation settlement 'Δh'	Gauge reading	Consolidation settlement 'Δh'	Gauge reading	Consolidation settlement 'Δh'	Gauge reading	Consolidation settlement 'Δh'	Gauge reading	Consolidation settlement 'Δh'
t	√t	Gr	$(Gr_1 - Gr)$ *0.002	Gr	$(Gr_1 - Gr)$ *0.002	Gr	$(Gr_1 - Gr)$ *0.002	Gr	$(Gr_1 - Gr)$ *0.002	Gr	$(Gr_1 - Gr)$ *0.002	Gr	$(Gr_1 - Gr)$ *0.002
(mins)	(√mins)	(div)	(mm)	(div)	(mm)	(div)	(mm)	(div)	(mm)	(div)	(mm)	(div)	(mm)
0.00	0.00	790.0	0.000	451.2	0.678	341.5	0.897	292.0	0.996	235.0	1.110	174.1	1.232
0.13	0.37	657.0	0.266	412.0	0.756	327.5	0.925	272.0	1.036	212.0	1.156	163.5	1.253
0.25	0.50	653.0	0.274	408.4	0.763	324.7	0.931	270.0	1.040	209.5	1.161	162.0	1.256
0.50	0.71	646.0	0.288	403.5	0.773	322.0	0.936	267.8	1.044	205.2	1.170	158.0	1.264
1.00	1.00	633.0	0.314	396.0	0.788	317.9	0.944	261.1	1.058	199.6	1.181	156.0	1.268
2.00	1.41	610.5	0.359	385.9	0.808	312.0	0.956	254.1	1.072	192.0	1.196	151.8	1.276
4.00	2.00	573.4	0.433	371.9	0.836	305.0	0.970	246.3	1.087	184.2	1.212	147.1	1.286
8.00	2.83	525.0	0.530	356.8	0.866	298.0	0.984	240.0	1.100	179.1	1.222	143.7	1.293
15.00	3.87	481.4	0.617	346.5	0.887	294.2	0.992	237.0	1.106	176.2	1.228	141.5	1.297
30.00	5.48	451.2	0.678	341.5	0.897	292.0	0.996	235.0	1.110	174.1	1.232	139.8	1.300

Table C.12.6: Consolidation calculated parameter for sample C2 (Inundated)

Pressures	**(kPa)**	**0**	**5**	**25**	**50**	**100**	**200**	**300**
Δh_{90}	(mm)		0.208	0.765	0.934	1.045	1.163	1.264
Δh_0	(mm)		0.000	0.678	0.897	0.996	1.110	1.232
$\Delta h_{100} = [((\Delta h_{90} - \Delta h_0)/0.9) + \Delta h_0]$	(mm)		0.231	0.775	0.938	1.050	1.168	1.268
Δh_f	(mm)		0.678	0.897	0.996	1.110	1.232	1.300
Initial Compression ratio $r_i = [\Delta h_0/\Delta h_f]$			0.000	0.756	0.901	0.897	0.901	0.947
Primary Compression ratio $r_p = [(\Delta h_{100}-\Delta h_0)/\Delta h_f]$			0.341	0.108	0.041	0.049	0.047	0.027
Secondary Compression ratio 'r_{sec}' $= [(\Delta h_f - \Delta h_{100})/\Delta h_f]$			0.659	0.136	0.058	0.054	0.052	0.025
√t90	(√min)		0.480	0.500	0.620	0.520	0.580	0.700
t_{90}	(mins)		0.230	0.250	0.384	0.270	0.336	0.490
T_{90}			0.848	0.848	0.848	0.848	0.848	0.848
drainage path 'd' $= [h_i/2]$	(mm)		9.125	8.786	8.677	8.627	8.570	8.509
Initial void ratio 'e_i' $=[(H-\Delta h_0-Hs)/Hs]$			0.434	0.381	0.364	0.356	0.347	0.337
Final void ratio 'e_f' $=[(H-\Delta h_f-Hs)/Hs]$		0.434	0.381	0.364	0.356	0.347	0.337	0.332
Total change in void ratio 'Δe' $= e_i - e_f$			0.053	0.017	0.008	0.009	0.010	0.005
Change of stress/pressure 'Δσ' $= \sigma_t - \sigma_p$	(kPa) or (kN/m^2)		5	20	25	50	100	100
Volume Compressibility 'Mv' $= [(1/1+e_0)*(\Delta e/\Delta\sigma')]$	(m^2/MN)		5.467	0.442	0.160	0.092	0.049	0.028
Volumetric Strain $= (\Delta hi/H)*100\%$	(%)	0.000	3.713	4.915	5.458	6.082	6.750	7.125
coefficient of consolidation 'Cv' $= [(T_{90}*d^2)/t_{90}]$	(mm^2/min)		306.5	261.8	166.1	233.4	185.1	125.3
Coefficient of Permeability 'k' $= C_v*M_v*\gamma_w$	(m/yr)		8.426	0.582	0.133	0.108	0.046	0.017

13. Soil C at 'At OMC' (3)

Table C.13.1: initial parameter of sample C3 (As-compacted)

Dimensions			Initial specimen	Final specimen
Diameter	'D'	(cm)	7.640	7.640
Area	'A'	(cm^2)	45.843	45.843
Height	'H'	(cm)	1.805	1.763
Volume	'V'	(cm^3)	82.747	80.810
Weights				
Ring		(g)	97.600	97.600
Ring + Sample in ring		(g)	286.000	281.301
Sample in ring	'M'	(g)	188.400	183.701
Moisture content 'W'		(%)	0.177	0.147
Calculated				
Assumed specific gravity 'Gs'			2.900	2.900
Density of water 'ρ_w'		(g/cm^3)	1.000	1.000
bulk density	'ρ' = [M/(A*H)]	(g/cm^3)	2.277	2.273
Dry Density	'ρ_d' = [ρ/(1+W)]	(g/cm^3)	1.935	1.981
Void ratio	'e_0' = [(Gs*ρ_w/ρ_d)-1]		0.499	0.464
Degree of saturation 'Sr_i'	= [Gs*W/e_0]		1.027	0.921
Mass of solids in sample 'M_s'	=[M/(W+1)]	(g)	160.123	160.123
Height of solids in sample 'H_s'	=[H/(1+e_0)]	(cm)	1.204	1.204

Table C.13.2: Consolidation data for sample C3 (As-compacted)

Time		Pressure at 5kPa		Pressure at 25kPa		Pressure at 50kPa		Pressure at 100kPa		Pressure at 200kPa		Pressure at 300kPa	
		Gauge reading	Consolidation settlement 'Δh'	Gauge reading	Consolidation settlement 'Δh'	Gauge reading	Consolidation settlement 'Δh'	Gauge reading	Consolidation settlement 'Δh'	Gauge reading	Consolidation settlement 'Δh'	Gauge reading	Consolidation settlement 'Δh'
t	√t	Gr	$(Gr_1 - Gr)$ *0.002	Gr	$(Gr_1 - Gr)$ *0.002	Gr	$(Gr_1 - Gr)$ *0.002	Gr	$(Gr_1 - Gr)$ *0.002	Gr	$(Gr_1 - Gr)$ *0.002	Gr	$(Gr_1 - Gr)$ *0.002
(mins)	(√mins)	(div)	(mm)	(div)	(mm)	(div)	(mm)	(div)	(mm)	(div)	(mm)	(div)	(mm)
0.00	0.00	1200.0	0.000	1174.2	0.052	1123.0	0.154	1090.0	0.220	1045.0	0.310	988.7	0.423
0.13	0.37	1189.5	0.021	1149.0	0.102	1113.0	0.174	1081.0	0.238	1031.0	0.338	980.0	0.440
0.25	0.50	1188.5	0.023	1147.0	0.106	1112.0	0.176	1078.0	0.244	1028.0	0.344	978.0	0.444
0.50	0.71	1187.2	0.026	1145.0	0.110	1110.5	0.179	1074.0	0.252	1023.0	0.354	975.0	0.450
1.00	1.00	1186.0	0.028	1142.3	0.115	1108.2	0.184	1069.5	0.261	1018.0	0.364	972.5	0.455
2.00	1.41	1184.0	0.032	1139.2	0.122	1105.0	0.190	1064.1	0.272	1011.0	0.378	967.8	0.464
4.00	2.00	1181.2	0.038	1134.9	0.130	1100.3	0.199	1057.8	0.284	1002.2	0.396	962.0	0.476
8.00	2.83	1178.6	0.043	1130.0	0.140	1095.5	0.209	1051.8	0.296	995.0	0.410	958.0	0.484
15.00	3.87	1176.0	0.048	1126.0	0.148	1092.0	0.216	1047.3	0.305	991.0	0.418	954.8	0.490
30.00	5.48	1174.2	0.052	1123.2	0.154	1090.0	0.220	1045.0	0.310	988.7	0.423	952.8	0.494

Table C.13.3: Consolidation calculated parameter for sample C3 (As-compacted)

Pressures	**(kPa)**	**0**	**5**	**25**	**50**	**100**	**200**	**300**
Δh_{90}	(mm)		0.024	0.108	0.177	0.274	0.365	0.452
Δh_0	(mm)		0.000	0.052	0.154	0.220	0.310	0.423
Δh_{100} = $[((\Delta h_{90} - \Delta h_0)/0.9)+ \Delta h_0]$	(mm)		0.027	0.114	0.179	0.280	0.371	0.455
Δh_f	(mm)		0.052	0.154	0.220	0.310	0.423	0.494
Initial Compression ratio $r_i = [\Delta h_0/\Delta h_f]$			0.000	0.339	0.700	0.710	0.734	0.856
Primary Compression ratio $r_p = [(\Delta h_{100}-\Delta h_0)/\Delta h_f]$			0.517	0.405	0.115	0.194	0.145	0.065
Secondary Compression ratio 'r_{sec}' = $[(\Delta h_f - \Delta h_{100})/\Delta h_f]$			0.483	0.256	0.185	0.097	0.122	0.079
√t90	(√min)		0.590	0.590	0.590	1.520	1.000	0.800
t_{90}	(mins)		0.348	0.348	0.348	2.310	1.000	0.640
T_{90}			0.848	0.848	0.848	0.848	0.848	0.848
drainage path 'd' = $[h_i/2]$	(mm)		9.025	8.999	8.948	8.915	8.870	8.814
Initial void ratio 'e_i' =$[(H-\Delta h_0-Hs)/Hs]$			0.499	0.494	0.486	0.480	0.473	0.464
Final void ratio 'e_f' =$[(H-\Delta h_f-Hs)/Hs]$		0.499	0.494	0.486	0.480	0.473	0.464	0.458
Total change in void ratio 'Δe' = $e_i - e_f$			0.004	0.008	0.005	0.007	0.009	0.006
Change of stress/pressure 'Δσ' = $\sigma_t - \sigma_p$	(kPa) or (kN/m^2)		5	20	25	50	100	100
Volume Compressibility 'Mv' = $[(1/1+e_0)*(\Delta e/\Delta\sigma')]$	(m^2/MN)		0.572	0.281	0.146	0.100	0.062	0.040
Volumetric Strain = (Δhi/H)*100%	(%)	0.000	0.286	0.851	1.219	1.717	2.341	2.739
coefficient of consolidation 'Cv' = $[(T_{90}*d^2)/t_{90}]$	(mm^2/min)		198.4	197.3	195.0	29.2	66.7	102.9
Coefficient of Permeability 'k' = $C_v*M_v*\gamma_w$	(m/yr)		0.571	0.279	0.143	0.015	0.021	0.020

Table C.13.4: initial parameter of sample C3 (Inundated)

Dimensions			Initial specimen	Final specimen
Diameter	'D'	(cm)	7.640	7.640
Area	'A'	(cm^2)	45.843	45.843
Height	'H'	(cm)	1.820	1.769
Volume	'V'	(cm^3)	83.435	81.076
Weights				
Ring		(g)	99.200	99.200
Ring + Sample in ring		(g)	287.800	286.075
Sample in ring	'M'	(g)	188.600	186.875
Moisture content 'W'		(%)	0.176	0.1752
Calculated				
Assumed specific gravity 'Gs'			2.900	2.900
Density of water 'ρ_w'		(g/cm^3)	1.000	1.000
bulk density	'ρ' = [M/(A*H)]	(g/cm^3)	2.260	2.305
Dry Density	'ρ_d' = [ρ/(1+W)]	(g/cm^3)	1.923	1.923
Void ratio	'e_0' = [(Gs*ρ_w/ρ_d)-1]		0.508	0.508
Degree of saturation 'Sr_i'	= [Gs*W/e_0]		1.002	1.027
Mass of solids in sample 'M_s'	=[M/(W+1)]	(g)	160.437	160.437
Height of solids in sample 'H_s'	=[H/(1+e_0)]	(cm)	1.207	1.207

Table C.13.5: Consolidation data for sample C3 (Inundated)

Time		Pressure at 5kPa		Pressure at 25kPa		Pressure at 50kPa		Pressure at 100kPa		Pressure at 200kPa		Pressure at 300kPa	
		Gauge reading	Consolidation settlement 'Δh'	Gauge reading	Consolidation settlement 'Δh'	Gauge reading	Consolidation settlement 'Δh'	Gauge reading	Consolidation settlement 'Δh'	Gauge reading	Consolidation settlement 'Δh'	Gauge reading	Consolidation settlement 'Δh'
t	√t	Gr	$(Gr_1 - Gr)$ *0.002	Gr	$(Gr_1 - Gr)$ *0.002	Gr	$(Gr_1 - Gr)$ *0.002	Gr	$(Gr_1 - Gr)$ *0.002	Gr	$(Gr_1 - Gr)$ *0.002	Gr	$(Gr_1 - Gr)$ *0.002
(mins)	(√mins)	(div)	(mm)	(div)	(mm)	(div)	(mm)	(div)	(mm)	(div)	(mm)	(div)	(mm)
0.00	0.00	1100.0	0.000	1044.0	0.112	975.0	0.250	937.8	0.324	893.0	0.414	842.7	0.515
0.13	0.37	1081.5	0.037	1017.0	0.166	965.0	0.270	926.0	0.348	881.0	0.438	834.0	0.532
0.25	0.50	1079.4	0.041	1014.5	0.171	963.0	0.274	924.0	0.352	877.0	0.446	832.5	0.535
0.50	0.71	1076.9	0.046	1011.0	0.178	961.3	0.277	921.5	0.357	874.0	0.452	830.8	0.538
1.00	1.00	1073.0	0.054	1007.0	0.186	958.8	0.282	917.8	0.364	869.1	0.462	828.0	0.544
2.00	1.41	1069.2	0.062	1001.3	0.197	954.5	0.291	912.8	0.374	863.0	0.474	824.0	0.552
4.00	2.00	1063.8	0.072	994.8	0.210	950.0	0.300	906.0	0.388	855.5	0.489	819.8	0.560
8.00	2.83	1057.0	0.086	986.8	0.226	944.0	0.312	900.0	0.400	849.0	0.502	815.2	0.570
15.00	3.87	1050.2	0.100	979.9	0.240	940.2	0.320	896.0	0.408	845.1	0.510	812.6	0.575
30.00	5.48	1044.0	0.112	975.5	0.249	937.8	0.324	893.5	0.413	842.7	0.515	810.5	0.579

Table C.13.6: Consolidation calculated parameter for sample C3 (Inundated)

Pressures **(kPa)**	**0**	**5**	**25**	**50**	**100**	**200**	**300**
Δh_{90} (mm)		0.042	0.172	0.276	0.356	0.462	0.538
Δh_0 (mm)		0.000	0.112	0.250	0.324	0.414	0.515
$\Delta h_{100} = [((\Delta h_{90} - \Delta h_0)/0.9) + \Delta h_0]$ (mm)		0.047	0.179	0.279	0.360	0.467	0.541
Δh_f (mm)		0.112	0.249	0.324	0.413	0.515	0.579
Initial Compression ratio $r_i = [\Delta h_0/\Delta h_f]$		0.000	0.450	0.771	0.785	0.805	0.889
Primary Compression ratio $r_p = [(\Delta h_{100}-\Delta h_0)/\Delta h_f]$		0.417	0.268	0.089	0.086	0.104	0.044
Secondary Compression ratio 'r_{sec}' $= [(\Delta h_f - \Delta h_{100})/\Delta h_f]$		0.583	0.282	0.140	0.129	0.092	0.066
√t90 (√min)		0.560	0.560	0.600	0.640	1.020	0.650
t_{90} (mins)		0.314	0.314	0.360	0.410	1.040	0.423
T_{90}		0.848	0.848	0.848	0.848	0.848	0.848
drainage path 'd' $= [h_i/2]$ (mm)		9.100	9.044	8.975	8.938	8.893	8.768
Initial void ratio 'e_i' $=[(H-\Delta h_0-Hs)/Hs]$		0.508	0.499	0.487	0.481	0.474	0.456
Final void ratio 'e_f' $=[(H-\Delta h_f-Hs)/Hs]$	0.508	0.499	0.488	0.481	0.474	0.465	0.451
Total change in void ratio 'Δe' $= e_i - e_f$		0.009	0.011	0.006	0.007	0.008	0.005
Change of stress/pressure 'Δσ' $= \sigma_t - \sigma_p$ (kPa) or (kN/m^2)		5	20	25	50	100	100
Volume Compressibility 'Mv' $= [(1/1+e_0)*(\Delta e/\Delta\sigma')]$ (m^2/MN)		1.231	0.376	0.164	0.098	0.055	0.035
Volumetric Strain $= (\Delta hi/H)*100\%$ (%)	0.000	0.615	1.368	1.782	2.269	2.827	3.181
coefficient of consolidation 'Cv' $= [(T_{90}*d^2)/t_{90}]$ (mm^2/min)		223.9	221.2	189.7	165.4	64.5	154.3
Coefficient of Permeability 'k' $= C_v*M_v*\gamma_w$ (m/yr)		1.386	0.419	0.156	0.081	0.018	0.028

14. Soil C at 'Low wet of OMC' (4)

Table C.14.1: initial parameter of sample C4 (As-compacted)

Dimensions			Initial specimen	Final specimen
Diameter	'D'	(cm)	7.660	7.660
Area	'A'	(cm^2)	46.084	46.084
Height	'H'	(cm)	1.825	1.781
Volume	'V'	(cm^3)	84.103	82.066
Weights				
Ring		(g)	99.400	99.400
Ring + Sample in ring		(g)	276.700	270.738
Sample in ring	'M'	(g)	177.300	171.338
Moisture content 'W'		(%)	0.217	0.176
Calculated				
Assumed specific gravity 'Gs'			2.900	2.900
Density of water 'ρ_w'		(g/cm^3)	1.000	1.000
bulk density	'ρ' = [M/(A*H)]	(g/cm^3)	2.108	2.088
Dry Density	'ρ_d' = [ρ/(1+W)]	(g/cm^3)	1.732	1.775
Void ratio	'e_0' = [(Gs*ρ_w/ρ_d)-1]		0.674	0.634
Degree of saturation 'Sr_i'	= [Gs*W/e_0]		0.934	0.807
Mass of solids in sample 'M_s'	=[M/(W+1)]	(g)	145.656	145.656
Height of solids in sample 'H_s'	=[H/(1+e_0)]	(cm)	1.090	1.090

Table C.14.2: Consolidation data for sample C4 (As-compacted)

Time		Pressure at 5kPa		Pressure at 25kPa		Pressure at 50kPa		Pressure at 100kPa		Pressure at 200kPa		Pressure at 300kPa	
		Gauge reading	Consolidation settlement 'Δh'	Gauge reading	Consolidation settlement 'Δh'	Gauge reading	Consolidation settlement 'Δh'	Gauge reading	Consolidation settlement 'Δh'	Gauge reading	Consolidation settlement 'Δh'	Gauge reading	Consolidation settlement 'Δh'
t	√t	Gr	$(Gr_1 - Gr)$ *0.002	Gr	$(Gr_1 - Gr)$ *0.002	Gr	$(Gr_1 - Gr)$ *0.002	Gr	$(Gr_1 - Gr)$ *0.002	Gr	$(Gr_1 - Gr)$ *0.002	Gr	$(Gr_1 - Gr)$ *0.002
(mins)	(√mins)	(div)	(mm)	(div)	(mm)	(div)	(mm)	(div)	(mm)	(div)	(mm)	(div)	(mm)
0.00	0.00	535.0	0.000	513.4	0.043	462.0	0.146	422.9	0.224	372.2	0.326	314.0	0.442
0.13	0.37	522.6	0.025	480.5	0.109	442.5	0.185	398.0	0.274	349.3	0.371	302.0	0.466
0.25	0.50	522.0	0.026	479.0	0.112	441.0	0.188	396.2	0.278	346.5	0.377	300.2	0.470
0.50	0.71	521.2	0.028	477.1	0.116	439.0	0.192	393.9	0.282	342.4	0.385	297.8	0.474
1.00	1.00	520.1	0.030	474.8	0.120	436.2	0.198	390.0	0.290	336.9	0.396	294.0	0.482
2.00	1.41	519.1	0.032	471.8	0.126	432.2	0.206	385.2	0.300	329.6	0.411	289.2	0.492
4.00	2.00	517.9	0.034	468.5	0.133	429.5	0.211	380.0	0.310	323.0	0.424	284.5	0.501
8.00	2.83	516.1	0.038	465.1	0.140	426.2	0.218	376.0	0.318	318.6	0.433	281.0	0.508
15.00	3.87	514.8	0.040	463.3	0.143	424.3	0.221	373.9	0.322	316.0	0.438	278.8	0.512
30.00	5.48	513.4	0.043	462.0	0.146	422.9	0.224	372.2	0.326	314.0	0.442	276.9	0.516

Table C.14.3: Consolidation calculated parameter for sample C4 (As-compacted)

Pressures	**(kPa)**	**0**	**5**	**25**	**50**	**100**	**200**	**300**
Δh_{90}	(mm)		0.027	0.113	0.187	0.279	0.377	0.474
Δh_0	(mm)		0.000	0.043	0.146	0.224	0.326	0.442
Δh_{100} = $[((\Delta h_{90} - \Delta h_0)/0.9)+ \Delta h_0]$	(mm)		0.029	0.121	0.191	0.285	0.383	0.478
Δh_f	(mm)		0.043	0.146	0.224	0.326	0.442	0.516
Initial Compression ratio $r_i = [\Delta h_0/\Delta h_f]$			0.000	0.295	0.651	0.688	0.738	0.856
Primary Compression ratio $r_p = [(\Delta h_{100}-\Delta h_0)/\Delta h_f]$			0.682	0.533	0.202	0.188	0.128	0.069
Secondary Compression ratio 'r_{sec}' = $[(\Delta h_f - \Delta h_{100})/\Delta h_f]$			0.318	0.173	0.147	0.124	0.134	0.075
√t90	(√min)		0.500	0.460	0.480	0.530	0.460	0.600
t_{90}	(mins)		0.250	0.212	0.230	0.281	0.212	0.360
T_{90}			0.848	0.848	0.848	0.848	0.848	0.848
drainage path 'd' = $[h_i/2]$	(mm)		9.125	9.104	9.052	9.013	8.962	8.904
Initial void ratio 'e_i' =$[(H-\Delta h_0-Hs)/Hs]$			0.674	0.671	0.661	0.654	0.645	0.634
Final void ratio 'e_f' =$[(H-\Delta h_f-Hs)/Hs]$		0.674	0.671	0.661	0.654	0.645	0.634	0.627
Total change in void ratio 'Δe' = $e_i - e_f$			0.004	0.009	0.007	0.009	0.011	0.007
Change of stress/pressure 'Δσ' = $\sigma_t - \sigma_p$	(kPa) or (kN/m^2)		5	20	25	50	100	100
Volume Compressibility 'Mv' = $[(1/1+e_0)*(\Delta e/\Delta\sigma')]$	(m^2/MN)		0.410	0.244	0.148	0.096	0.055	0.035
Volumetric Strain = (Δhi/H)*100%	(%)	0.000	0.237	0.800	1.228	1.784	2.422	2.828
coefficient of consolidation 'Cv' = $[(T_{90}*d^2)/t_{90}]$	(mm^2/min)		282.4	332.1	301.6	245.2	321.9	186.8
Coefficient of Permeability 'k' = $C_v*M_v*\gamma_w$	(m/yr)		0.582	0.408	0.225	0.119	0.089	0.033

Table C.14.4: initial parameter of sample C4 (Inundated)

Dimensions			Initial specimen	Final specimen
Diameter	'D'	(cm)	7.650	7.650
Area	'A'	(cm^2)	45.963	45.963
Height	'H'	(cm)	1.800	1.747
Volume	'V'	(cm^3)	82.734	80.316
Weights				
Ring		(g)	97.600	97.600
Ring + Sample in ring		(g)	276.600	272.510
Sample in ring	'M'	(g)	179.000	174.910
Moisture content 'W'		(%)	0.216	0.217
Calculated				
Assumed specific gravity 'Gs'			2.900	2.900
Density of water 'ρ_w'		(g/cm^3)	1.000	1.000
bulk density	'ρ' = [M/(A*H)]	(g/cm^3)	2.164	2.178
Dry Density	'ρ_d' = [ρ/(1+W)]	(g/cm^3)	1.780	1.780
Void ratio	'e_0' = [(Gs*ρ_w/ρ_d)-1]		0.629	0.629
Degree of saturation 'Sr_i'	= [Gs*W/e_0]		0.993	1.000
Mass of solids in sample 'M_s'	=[M/(W+1)]	(g)	147.252	147.252
Height of solids in sample 'H_s'	=[H/(1+e_0)]	(cm)	1.105	1.105

Table C.14.5: Consolidation data for sample C4 (Inundated)

Time		Pressure at 5kPa		Pressure at 25kPa		Pressure at 50kPa		Pressure at 100kPa		Pressure at 200kPa		Pressure at 300kPa	
		Gauge reading	Consolidation settlement 'Δh'	Gauge reading	Consolidation settlement 'Δh'	Gauge reading	Consolidation settlement 'Δh'	Gauge reading	Consolidation settlement 'Δh'	Gauge reading	Consolidation settlement 'Δh'	Gauge reading	Consolidation settlement 'Δh'
t	√t	Gr	$(Gr_1 - Gr)$ *0.002	Gr	$(Gr_1 - Gr)$ *0.002	Gr	$(Gr_1 - Gr)$ *0.002	Gr	$(Gr_1 - Gr)$ *0.002	Gr	$(Gr_1 - Gr)$ *0.002	Gr	$(Gr_1 - Gr)$ *0.002
(mins)	(√mins)	(div)	(mm)	(div)	(mm)	(div)	(mm)	(div)	(mm)	(div)	(mm)	(div)	(mm)
0.00	0.00	669.0	0.000	614.1	0.110	550.5	0.237	510.7	0.317	462.0	0.414	406.0	0.526
0.13	0.37	649.0	0.040	586.5	0.165	536.0	0.266	493.7	0.351	442.0	0.454	394.0	0.550
0.25	0.50	646.0	0.046	583.4	0.171	534.5	0.269	491.9	0.354	439.0	0.460	391.5	0.555
0.50	0.71	642.0	0.054	580.0	0.178	532.0	0.274	488.0	0.362	434.6	0.469	389.8	0.558
1.00	1.00	637.2	0.064	575.0	0.188	528.9	0.280	483.0	0.372	428.9	0.480	386.5	0.565
2.00	1.41	632.0	0.074	568.8	0.200	524.3	0.289	477.2	0.384	421.2	0.496	382.0	0.574
4.00	2.00	626.0	0.086	562.0	0.214	519.3	0.299	471.0	0.396	413.5	0.511	377.5	0.583
8.00	2.83	620.2	0.098	556.0	0.226	514.9	0.308	466.0	0.406	410.0	0.518	374.0	0.590
15.00	3.87	616.3	0.105	552.5	0.233	512.4	0.313	463.9	0.410	407.9	0.522	372.0	0.594
30.00	5.48	614.1	0.110	550.5	0.237	510.7	0.317	462.0	0.414	406.0	0.526	370.0	0.598

Table C.14.6: Consolidation calculated parameter for sample C4 (Inundated)

Pressures	**(kPa)**	**0**	**5**	**25**	**50**	**100**	**200**	**300**
Δh_{90}	(mm)		0.048	0.172	0.270	0.356	0.466	0.554
Δh_0	(mm)		0.000	0.110	0.237	0.317	0.414	0.526
Δh_{100} = $[((\Delta h_{90} - \Delta h_0)/0.9)+ \Delta h_0]$	(mm)		0.053	0.179	0.274	0.360	0.472	0.557
Δh_f	(mm)		0.110	0.237	0.317	0.414	0.526	0.598
Initial Compression ratio $r_i = [\Delta h_0/\Delta h_f]$			0.000	0.464	0.749	0.766	0.787	0.880
Primary Compression ratio $r_p = [(\Delta h_{100}-\Delta h_0)/\Delta h_f]$			0.486	0.291	0.116	0.105	0.110	0.052
Secondary Compression ratio 'r_{sec}' = $[(\Delta h_f - \Delta h_{100})/\Delta h_f]$			0.514	0.245	0.136	0.130	0.103	0.068
√t90	(√min)		0.550	0.540	0.500	0.580	0.620	0.600
t_{90}	(mins)		0.303	0.292	0.250	0.336	0.384	0.360
T_{90}			0.848	0.848	0.848	0.848	0.848	0.848
drainage path 'd' = $[h_i/2]$	(mm)		9.000	8.945	8.882	8.842	8.793	8.737
Initial void ratio 'e_i' =$[(H-\Delta h_0-Hs)/Hs]$			0.629	0.619	0.608	0.601	0.592	0.582
Final void ratio 'e_f' =$[(H-\Delta h_f-Hs)/Hs]$		0.629	0.619	0.608	0.601	0.592	0.582	0.575
Total change in void ratio 'Δe' = $e_i - e_f$			0.010	0.011	0.007	0.009	0.010	0.007
Change of stress/pressure 'Δσ' = $\sigma_t - \sigma_p$	(kPa) or (kN/m^2)		5	20	25	50	100	100
Volume Compressibility 'Mv' = $[(1/1+e_0)*(\Delta e/\Delta\sigma')]$	(m^2/MN)		1.028	0.297	0.149	0.091	0.052	0.034
Volumetric Strain = (Δhi/H)*100%	(%)	0.000	0.610	1.317	1.759	2.300	2.922	3.322
coefficient of consolidation 'Cv' = $[(T_{90}*d^2)/t_{90}]$	(mm^2/min)		227.1	232.7	267.6	197.1	170.6	179.8
Coefficient of Permeability 'k' = $C_v*M_v*\gamma_w$	(m/yr)		1.174	0.348	0.201	0.090	0.045	0.030

15. Soil C at 'High wet of OMC' (5)

Table C.15.1: initial parameter of sample C5 (As-compacted)

Dimensions			Initial specimen	Final specimen
Diameter	'D'	(cm)	7.650	7.650
Area	'A'	(cm^2)	45.963	45.963
Height	'H'	(cm)	1.850	1.793
Volume	'V'	(cm^3)	85.032	82.423
Weights				
Ring		(g)	76.300	76.300
Ring + Sample in ring		(g)	256.000	246.786
Sample in ring	'M'	(g)	179.700	170.486
Moisture content 'W'		(%)	0.225	0.163
Calculated				
Assumed specific gravity 'Gs'			2.900	2.900
Density of water 'ρ_w'		(g/cm^3)	1.000	1.000
bulk density	'ρ' = [M/(A*H)]	(g/cm^3)	2.113	2.068
Dry Density	'ρ_d' = [ρ/(1+W)]	(g/cm^3)	1.725	1.779
Void ratio	'e_0' = [(Gs*ρ_w/ρ_d)-1]		0.681	0.630
Degree of saturation 'Sr_i'	= [Gs*W/e_0]		0.959	0.748
Mass of solids in sample 'M_s'	=[M/(W+1)]	(g)	146.651	146.651
Height of solids in sample 'H_s'	=[H/(1+e_0)]	(cm)	1.100	1.100

Table C.15.2: Consolidation data for sample C5 (As-compacted)

Time		Pressure at 5kPa		Pressure at 25kPa		Pressure at 50kPa		Pressure at 100kPa		Pressure at 200kPa		Pressure at 300kPa	
		Gauge reading	Consolidation settlement 'Δh'	Gauge reading	Consolidation settlement 'Δh'	Gauge reading	Consolidation settlement 'Δh'	Gauge reading	Consolidation settlement 'Δh'	Gauge reading	Consolidation settlement 'Δh'	Gauge reading	Consolidation settlement 'Δh'
t	√t	Gr	$(Gr_1 - Gr)$ *0.002	Gr	$(Gr_1 - Gr)$ *0.002	Gr	$(Gr_1 - Gr)$ *0.002	Gr	$(Gr_1 - Gr)$ *0.002	Gr	$(Gr_1 - Gr)$ *0.002	Gr	$(Gr_1 - Gr)$ *0.002
(mins)	(√mins)	(div)	(mm)	(div)	(mm)	(div)	(mm)	(div)	(mm)	(div)	(mm)	(div)	(mm)
0.00	0.00	1100.0	0.000	1057.0	0.086	977.7	0.245	930.0	0.340	876.0	0.448	816.1	0.568
0.13	0.37	1081.5	0.037	1023.0	0.154	963.0	0.274	914.0	0.372	860.0	0.480	808.0	0.584
0.25	0.50	1080.2	0.040	1019.0	0.162	961.5	0.277	911.0	0.378	857.9	0.484	806.0	0.588
0.50	0.71	1079.0	0.042	1016.0	0.168	958.9	0.282	908.0	0.384	852.5	0.495	803.0	0.594
1.00	1.00	1077.0	0.046	1011.4	0.177	955.0	0.290	903.0	0.394	846.5	0.507	799.0	0.602
2.00	1.41	1075.0	0.050	1005.8	0.188	950.3	0.299	897.0	0.406	838.3	0.523	794.2	0.612
4.00	2.00	1071.5	0.057	998.3	0.203	944.0	0.312	888.0	0.424	829.5	0.541	788.9	0.622
8.00	2.83	1067.1	0.066	990.0	0.220	937.4	0.325	882.0	0.436	822.5	0.555	784.3	0.631
15.00	3.87	1062.1	0.076	982.2	0.236	932.9	0.334	879.0	0.442	818.5	0.563	781.9	0.636
30.00	5.48	1057.0	0.086	977.7	0.245	930.0	0.340	876.2	0.448	816.1	0.568	780.0	0.640

Table C.15.3: Consolidation calculated parameter for sample C5 (As-compacted)

Pressures	**(kPa)**	**0**	**5**	**25**	**50**	**100**	**200**	**300**
Δh_{90}	(mm)		0.040	0.164	0.280	0.381	0.494	0.604
Δh_0	(mm)		0.000	0.086	0.245	0.340	0.448	0.568
Δh_{100} = $[((\Delta h_{90} - \Delta h_0)/0.9)+ \Delta h_0]$	(mm)		0.044	0.173	0.284	0.386	0.499	0.608
Δh_f	(mm)		0.086	0.245	0.340	0.448	0.568	0.640
Initial Compression ratio $r_i = [\Delta h_0/\Delta h_f]$			0.000	0.352	0.721	0.760	0.789	0.888
Primary Compression ratio $r_p = [(\Delta h_{100}-\Delta h_0)/\Delta h_f]$			0.517	0.354	0.114	0.102	0.090	0.063
Secondary Compression ratio 'r_{sec}' = $[(\Delta h_f - \Delta h_{100})/\Delta h_f]$			0.483	0.294	0.165	0.139	0.121	0.050
√t90	(√min)		0.540	0.580	0.610	0.600	0.700	1.080
t_{90}	(mins)		0.292	0.336	0.372	0.360	0.490	1.166
T_{90}			0.848	0.848	0.848	0.848	0.848	0.848
drainage path 'd' = $[h_i/2]$	(mm)		9.250	9.207	9.128	9.080	9.026	8.966
Initial void ratio 'e_i' =$[(H-\Delta h_0-Hs)/Hs]$			0.681	0.674	0.659	0.651	0.641	0.630
Final void ratio 'e_f' =$[(H-\Delta h_f-Hs)/Hs]$		0.681	0.674	0.659	0.651	0.641	0.630	0.623
Total change in void ratio 'Δe' = $e_i - e_f$			0.008	0.014	0.009	0.010	0.011	0.007
Change of stress/pressure 'Δσ' = $\sigma_t - \sigma_p$	(kPa) or (kN/m^2)		5	20	25	50	100	100
Volume Compressibility 'Mv' = $[(1/1+e_0)*(\Delta e/\Delta\sigma')]$	(m^2/MN)		0.930	0.429	0.205	0.116	0.065	0.039
Volumetric Strain = (Δhi/H)*100%	(%)	0.000	0.465	1.322	1.838	2.419	3.069	3.459
coefficient of consolidation 'Cv' = $[(T_{90}*d^2)/t_{90}]$	(mm^2/min)		248.8	213.7	189.9	194.2	141.0	58.4
Coefficient of Permeability 'k' = $C_v*M_v*\gamma_w$	(m/yr)		1.163	0.461	0.196	0.114	0.046	0.011

Table C.15.4: initial parameter of sample C5 (Inundated)

Dimensions			Initial specimen	Final specimen
Diameter	'D'	(cm)	7.640	7.640
Area	'A'	(cm^2)	45.843	45.843
Height	'H'	(cm)	1.790	1.720
Volume	'V'	(cm^3)	82.060	78.858
Weights				
Ring		(g)	97.500	97.500
Ring + Sample in ring		(g)	279.500	268.932
Sample in ring	'M'	(g)	182.000	171.432
Moisture content 'W'		(%)	0.223	0.2068
Calculated				
Assumed specific gravity 'Gs'			2.900	2.900
Density of water 'ρ_w'		(g/cm^3)	1.000	1.000
bulk density	'ρ' = [M/(A*H)]	(g/cm^3)	2.218	2.174
Dry Density	'ρ_d' = [ρ/(1+W)]	(g/cm^3)	1.813	1.813
Void ratio	'e_0' = [(Gs*ρ_w/ρ_d)-1]		0.600	0.600
Degree of saturation 'Sr_i'	= [Gs*W/e_0]		1.000	1.000
Mass of solids in sample 'M_s'	=[M/(W+1)]	(g)	148.768	148.768
Height of solids in sample 'H_s'	=[H/(1+e_0)]	(cm)	1.119	1.119

Table C.15.5: Consolidation data for sample C5 (Inundated)

Time		Pressure at 5kPa		Pressure at 25kPa		Pressure at 50kPa		Pressure at 100kPa		Pressure at 200kPa		Pressure at 300kPa	
		Gauge reading	Consolidation settlement 'Δh'	Gauge reading	Consolidation settlement 'Δh'	Gauge reading	Consolidation settlement 'Δh'	Gauge reading	Consolidation settlement 'Δh'	Gauge reading	Consolidation settlement 'Δh'	Gauge reading	Consolidation settlement 'Δh'
t	√t	Gr	$(Gr_1 - Gr)$ *0.002	Gr	$(Gr_1 - Gr)$ *0.002	Gr	$(Gr_1 - Gr)$ *0.002	Gr	$(Gr_1 - Gr)$ *0.002	Gr	$(Gr_1 - Gr)$ *0.002	Gr	$(Gr_1 - Gr)$ *0.002
(mins)	(√mins)	(div)	(mm)	(div)	(mm)	(div)	(mm)	(div)	(mm)	(div)	(mm)	(div)	(mm)
0.00	0.00	1200.0	0.000	1117.5	0.165	1025.1	0.350	975.0	0.450	911.1	0.578	850.8	0.698
0.13	0.37	1176.0	0.048	1081.0	0.238	1013.0	0.374	958.0	0.484	896.0	0.608	841.0	0.718
0.25	0.50	1171.0	0.058	1078.0	0.244	1010.0	0.380	955.0	0.490	892.0	0.616	838.0	0.724
0.50	0.71	1168.0	0.064	1073.2	0.254	1006.5	0.387	951.0	0.498	887.0	0.626	835.5	0.729
1.00	1.00	1163.8	0.072	1067.5	0.265	1002.2	0.396	945.5	0.509	880.0	0.640	831.5	0.737
2.00	1.41	1158.0	0.084	1059.6	0.281	996.0	0.408	938.0	0.524	873.0	0.654	826.2	0.748
4.00	2.00	1148.0	0.104	1049.2	0.302	989.2	0.422	929.9	0.540	863.5	0.673	820.9	0.758
8.00	2.83	1138.2	0.124	1038.2	0.324	982.1	0.436	922.2	0.556	856.2	0.688	816.5	0.767
15.00	3.87	1127.9	0.144	1029.6	0.341	977.9	0.444	918.5	0.563	853.0	0.694	814.0	0.772
30.00	5.48	1117.5	0.165	1025.1	0.350	975.0	0.450	911.1	0.578	850.8	0.698	812.8	0.774

Table C.15.6: Consolidation calculated parameter for sample C5 (Inundated)

Pressures	**(kPa)**	**0**	**5**	**25**	**50**	**100**	**200**	**300**
Δh_{90}	(mm)		0.064	0.248	0.394	0.501	0.645	0.743
Δh_0	(mm)		0.000	0.165	0.350	0.450	0.578	0.698
Δh_{100} = $[((\Delta h_{90} - \Delta h_0)/0.9)+ \Delta h_0]$	(mm)		0.071	0.257	0.399	0.507	0.652	0.748
Δh_f	(mm)		0.165	0.350	0.450	0.578	0.698	0.774
Initial Compression ratio $r_i = [\Delta h_0/\Delta h_f]$			0.000	0.472	0.778	0.779	0.828	0.901
Primary Compression ratio $r_p = [(\Delta h_{100}-\Delta h_0)/\Delta h_f]$			0.428	0.264	0.109	0.098	0.107	0.065
Secondary Compression ratio 'r_{sec}' = $[(\Delta h_f - \Delta h_{100})/\Delta h_f]$			0.572	0.265	0.114	0.123	0.066	0.034
√t90	(√min)		0.620	0.580	0.980	0.990	1.140	1.230
t_{90}	(mins)		0.384	0.336	0.960	0.980	1.300	1.513
T_{90}			0.848	0.848	0.848	0.848	0.848	0.848
drainage path 'd' = $[h_i/2]$	(mm)		8.950	8.868	8.775	8.725	8.661	8.601
Initial void ratio 'e_i' =$[(H-\Delta h_0-Hs)/Hs]$			0.600	0.585	0.568	0.559	0.548	0.537
Final void ratio 'e_f' =$[(H-\Delta h_f-Hs)/Hs]$		0.600	0.585	0.568	0.559	0.548	0.537	0.530
Total change in void ratio 'Δe' = $e_i - e_f$			0.015	0.017	0.009	0.011	0.011	0.007
Change of stress/pressure 'Δσ' = $\sigma_t - \sigma_p$	(kPa) or (kN/m^2)		5	20	25	50	100	100
Volume Compressibility 'Mv' = $[(1/1+e_0)*(\Delta e/\Delta\sigma')]$	(m^2/MN)		1.844	0.516	0.223	0.143	0.067	0.043
Volumetric Strain = (Δhi/H)*100%	(%)	0.000	0.922	1.954	2.514	3.228	3.902	4.326
coefficient of consolidation 'Cv' = $[(T_{90}*d^2)/t_{90}]$	(mm^2/min)		176.7	198.2	68.0	65.9	48.9	41.5
Coefficient of Permeability 'k' = $C_v*M_v*\gamma_w$	(m/yr)		1.638	0.515	0.076	0.047	0.017	0.009

16. Soil D at 'High dry of OMC' (1)

Table C.16.1: initial parameter of sample D1 (As-compacted)

Dimensions			Initial specimen	Final specimen
Diameter	'D'	(cm)	7.650	7.650
Area	'A'	(cm^2)	45.963	45.963
Height	'H'	(cm)	1.800	1.739
Volume	'V'	(cm^3)	82.734	79.939
Weights				
Ring		(g)	76.200	76.200
Ring + Sample in ring		(g)	262.400	262.180
Sample in ring	'M'	(g)	186.200	185.980
Moisture content 'W'		(%)	0.090	0.089
Calculated				
Assumed specific gravity 'Gs'			2.900	2.900
Density of water 'ρ_w'		(g/cm^3)	1.000	1.000
bulk density	'ρ' = [M/(A*H)]	(g/cm^3)	2.251	2.327
Dry Density	'ρ_d' = [ρ/(1+W)]	(g/cm^3)	2.064	2.136
Void ratio	'e_0' = [(Gs*ρ_w/ρ_d)-1]		0.405	0.357
Degree of saturation 'Sr_i'	= [Gs*W/e_0]		0.647	0.722
Mass of solids in sample 'M_s'	=[M/(W+1)]	(g)	170.775	170.775
Height of solids in sample 'H_s'	=[H/(1+e_0)]	(cm)	1.281	1.281

Table C.16.2: Consolidation data for sample D1 (As-compacted)

Time		Pressure at 5kPa		Pressure at 25kPa		Pressure at 50kPa		Pressure at 100kPa		Pressure at 200kPa		Pressure at 300kPa	
		Gauge reading	Consolidation settlement 'Δh'	Gauge reading	Consolidation settlement 'Δh'	Gauge reading	Consolidation settlement 'Δh'	Gauge reading	Consolidation settlement 'Δh'	Gauge reading	Consolidation settlement 'Δh'	Gauge reading	Consolidation settlement 'Δh'
t	√t	Gr	$(Gr_1 - Gr)$ *0.002	Gr	$(Gr_1 - Gr)$ *0.002	Gr	$(Gr_1 - Gr)$ *0.002	Gr	$(Gr_1 - Gr)$ *0.002	Gr	$(Gr_1 - Gr)$ *0.002	Gr	$(Gr_1 - Gr)$ *0.002
(mins)	(√mins)	(div)	(mm)	(div)	(mm)	(div)	(mm)	(div)	(mm)	(div)	(mm)	(div)	(mm)
0.00	0.00	1200.0	0.000	1154.1	0.092	1079.9	0.240	1028.2	0.344	967.1	0.466	895.9	0.608
0.13	0.37	1162.6	0.075	1090.2	0.220	1040.5	0.319	978.2	0.444	907.6	0.585	860.5	0.679
0.25	0.50	1162.0	0.076	1089.3	0.221	1038.8	0.322	977.1	0.446	906.1	0.588	858.8	0.682
0.50	0.71	1161.1	0.078	1088.2	0.224	1036.9	0.326	975.2	0.450	904.8	0.590	856.7	0.687
1.00	1.00	1160.1	0.080	1087.9	0.224	1035.4	0.329	974.0	0.452	903.2	0.594	854.8	0.690
2.00	1.41	1159.0	0.082	1085.7	0.229	1034.0	0.332	972.0	0.456	901.9	0.596	853.0	0.694
4.00	2.00	1157.9	0.084	1084.3	0.231	1032.8	0.334	971.0	0.458	900.3	0.599	851.3	0.697
8.00	2.83	1156.6	0.087	1082.9	0.234	1031.1	0.338	970.0	0.460	898.9	0.602	849.7	0.701
15.00	3.87	1155.3	0.089	1081.6	0.237	1029.9	0.340	968.8	0.462	897.4	0.605	848.0	0.704
30.00	5.48	1154.1	0.092	1079.9	0.240	1028.2	0.344	967.1	0.466	895.9	0.608	846.3	0.707

Table C.16.3: Consolidation calculated parameter for sample D1 (As-compacted)

Pressures	**(kPa)**	**0**	**5**	**25**	**50**	**100**	**200**	**300**
Δh_{90}	(mm)		0.076	0.222	0.323	0.447	0.588	0.683
Δh_0	(mm)		0.000	0.092	0.240	0.344	0.466	0.608
Δh_{100} = $[((\Delta h_{90} - \Delta h_0)/0.9)+ \Delta h_0]$	(mm)		0.084	0.236	0.332	0.458	0.602	0.691
Δh_f	(mm)		0.092	0.240	0.344	0.466	0.608	0.707
Initial Compression ratio $r_i = [\Delta h_0/\Delta h_f]$			0.000	0.383	0.698	0.739	0.766	0.859
Primary Compression ratio $r_p = [(\Delta h_{100}-\Delta h_0)/\Delta h_f]$			0.920	0.601	0.268	0.246	0.223	0.118
Secondary Compression ratio 'r_{sec}' = $[(\Delta h_f - \Delta h_{100})/\Delta h_f]$			0.080	0.016	0.033	0.016	0.011	0.023
√t90	(√min)		0.540	0.480	0.500	0.500	0.500	0.520
t_{90}	(mins)		0.292	0.230	0.250	0.250	0.250	0.270
T_{90}			0.848	0.848	0.848	0.848	0.848	0.848
drainage path 'd' = $[h_i/2]$	(mm)		9.000	8.954	8.880	8.828	8.767	8.696
Initial void ratio 'e_i' =$[(H-\Delta h_0-Hs)/Hs]$			0.405	0.398	0.386	0.378	0.369	0.357
Final void ratio 'e_f' =$[(H-\Delta h_f-Hs)/Hs]$		0.405	0.398	0.386	0.378	0.369	0.357	0.350
Total change in void ratio 'Δe' = $e_i - e_f$			0.007	0.012	0.008	0.010	0.011	0.008
Change of stress/pressure 'Δσ' = $\sigma_t - \sigma_p$	(kPa) or (kN/m^2)		5	20	25	50	100	100
Volume Compressibility 'Mv' = $[(1/1+e_0)*(\Delta e/\Delta\sigma')]$	(m^2/MN)		1.020	0.412	0.230	0.135	0.079	0.055
Volumetric Strain = (Δhi/H)*100%	(%)	0.000	0.510	1.334	1.909	2.588	3.379	3.930
coefficient of consolidation 'Cv' = $[(T_{90}*d^2)/t_{90}]$	(mm^2/min)		235.6	295.1	267.5	264.4	260.7	237.2
Coefficient of Permeability 'k' = $C_v*M_v*\gamma_w$	(m/yr)		1.208	0.611	0.310	0.180	0.104	0.066

Table C.16.4: initial parameter of sample D1 (Inundated)

Dimensions			Initial specimen	Final specimen
Diameter	'D'	(cm)	7.630	7.630
Area	'A'	(cm^2)	45.723	45.723
Height	'H'	(cm)	1.790	1.730
Volume	'V'	(cm^3)	81.845	79.079
Weights				
Ring		(g)	97.500	97.500
Ring + Sample in ring		(g)	263.700	270.139
Sample in ring	'M'	(g)	166.200	172.639
Moisture content 'W'		(%)	0.078	0.1858
Calculated				
Assumed specific gravity 'Gs'			2.900	2.900
Density of water 'ρ_w'		(g/cm^3)	1.000	1.000
bulk density	'ρ' = [M/(A*H)]	(g/cm^3)	2.031	2.183
Dry Density	'ρ_d' = [ρ/(1+W)]	(g/cm^3)	1.885	1.885
Void ratio	'e_0' = [(Gs*ρ_w/ρ_d)-1]		0.539	0.539
Degree of saturation 'Sr_i'	= [Gs*W/e_0]		0.417	1.000
Mass of solids in sample 'M_s'	=[M/(W+1)]	(g)	154.246	154.246
Height of solids in sample 'H_s'	=[H/(1+e_0)]	(cm)	1.163	1.163

Table C.16.5: Consolidation data for sample D1 (Inundated)

Time		Pressure at 5kPa		Pressure at 25kPa		Pressure at 50kPa		Pressure at 100kPa		Pressure at 200kPa		Pressure at 300kPa	
		Gauge reading	Consolidation settlement 'Δh'	Gauge reading	Consolidation settlement 'Δh'	Gauge reading	Consolidation settlement 'Δh'	Gauge reading	Consolidation settlement 'Δh'	Gauge reading	Consolidation settlement 'Δh'	Gauge reading	Consolidation settlement 'Δh'
t	√t	Gr	$(Gr_1 - Gr)$ *0.002	Gr	$(Gr_1 - Gr)$ *0.002	Gr	$(Gr_1 - Gr)$ *0.002	Gr	$(Gr_1 - Gr)$ *0.002	Gr	$(Gr_1 - Gr)$ *0.002	Gr	$(Gr_1 - Gr)$ *0.002
(mins)	(√mins)	(div)	(mm)	(div)	(mm)	(div)	(mm)	(div)	(mm)	(div)	(mm)	(div)	(mm)
0.00	0.00	900.0	0.000	809.2	0.182	733.8	0.332	690.8	0.418	647.1	0.506	597.5	0.605
0.13	0.37	877.0	0.046	757.9	0.284	705.0	0.390	658.5	0.483	610.5	0.579	577.1	0.646
0.25	0.50	871.0	0.058	754.9	0.290	703.8	0.392	657.5	0.485	608.9	0.582	576.2	0.648
0.50	0.71	860.0	0.080	751.6	0.297	701.5	0.397	656.2	0.488	606.8	0.586	575.0	0.650
1.00	1.00	844.0	0.112	747.0	0.306	699.0	0.402	654.7	0.491	605.1	0.590	573.8	0.652
2.00	1.41	829.9	0.140	741.9	0.316	696.9	0.406	652.9	0.494	603.1	0.594	572.2	0.656
4.00	2.00	819.8	0.160	738.2	0.324	694.9	0.410	651.1	0.498	601.5	0.597	571.0	0.658
8.00	2.83	813.8	0.172	735.9	0.328	692.9	0.414	649.2	0.502	600.0	0.600	569.5	0.661
15.00	3.87	810.8	0.178	734.7	0.331	691.8	0.416	648.1	0.504	598.8	0.602	568.4	0.663
30.00	5.48	809.2	0.182	733.8	0.332	690.8	0.418	647.1	0.506	597.5	0.605	567.1	0.666

Table C.16.6: Consolidation calculated parameter for sample D1 (Inundated)

Pressures **(kPa)**	**0**	**5**	**25**	**50**	**100**	**200**	**300**
Δh_{90} (mm)		0.158	0.290	0.393	0.486	0.583	0.648
Δh_0 (mm)		0.000	0.182	0.332	0.418	0.506	0.605
Δh_{100} = $[((\Delta h_{90} - \Delta h_0)/0.9)+ \Delta h_0]$ (mm)		0.176	0.302	0.400	0.494	0.592	0.653
Δh_f (mm)		0.182	0.332	0.418	0.506	0.605	0.666
Initial Compression ratio $r_i = [\Delta h_0/\Delta h_f]$		0.000	0.548	0.793	0.826	0.836	0.909
Primary Compression ratio $r_p = [(\Delta h_{100}-\Delta h_0)/\Delta h_f]$		0.967	0.361	0.162	0.149	0.141	0.072
Secondary Compression ratio 'r_{sec}' = $[(\Delta h_f - \Delta h_{100})/\Delta h_f]$		0.033	0.091	0.045	0.024	0.022	0.020
√t90 (√min)		1.900	0.500	0.530	0.560	0.530	0.470
t_{90} (mins)		3.610	0.250	0.281	0.314	0.281	0.221
T_{90}		0.848	0.848	0.848	0.848	0.848	0.848
drainage path 'd' = $[h_i/2]$ (mm)		8.950	8.859	8.784	8.741	8.697	8.648
Initial void ratio 'e_i' =$[(H-\Delta h_0-Hs)/Hs]$		0.539	0.523	0.510	0.503	0.495	0.487
Final void ratio 'e_f' =$[(H-\Delta h_f-Hs)/Hs]$	0.539	0.523	0.510	0.503	0.495	0.487	0.482
Total change in void ratio 'Δe' = $e_i - e_f$		0.016	0.013	0.007	0.008	0.009	0.005
Change of stress/pressure 'Δσ' = $\sigma_t - \sigma_p$ (kPa) or (kN/m^2)		5	20	25	50	100	100
Volume Compressibility 'Mv' = $[(1/1+e_0)*(\Delta e/\Delta\sigma')]$ (m^2/MN)		2.029	0.420	0.193	0.098	0.055	0.034
Volumetric Strain = (Δhi/H)*100% (%)	0.000	1.015	1.857	2.337	2.826	3.380	3.720
coefficient of consolidation 'Cv' = $[(T_{90}*d^2)/t_{90}]$ (mm^2/min)		18.8	266.2	232.9	206.6	228.3	287.1
Coefficient of Permeability 'k' = $C_v*M_v*\gamma_w$ (m/yr)		0.192	0.562	0.226	0.102	0.064	0.049

17. Soil D at 'Low dry of OMC' (2)

Table C.17.1: initial parameter of sample D2 (As-compacted)

Dimensions			Initial specimen	Final specimen
Diameter	'D'	(cm)	7.660	7.660
Area	'A'	(cm^2)	46.084	46.084
Height	'H'	(cm)	1.825	1.781
Volume	'V'	(cm^3)	84.103	82.060
Weights				
Ring		(g)	99.400	99.400
Ring + Sample in ring		(g)	300.500	299.554
Sample in ring	'M'	(g)	201.100	200.154
Moisture content 'W'		(%)	0.105	0.100
Calculated				
Assumed specific gravity 'Gs'			2.900	2.900
Density of water 'ρ_w'		(g/cm^3)	1.000	1.000
bulk density	'ρ' = [M/(A*H)]	(g/cm^3)	2.391	2.439
Dry Density	'ρ_d' = [ρ/(1+W)]	(g/cm^3)	2.164	2.218
Void ratio	'e_0' = [(Gs*ρ_w/ρ_d)-1]		0.340	0.307
Degree of saturation 'Sr_i'	= [Gs*W/e_0]		0.894	0.939
Mass of solids in sample 'M_s'	=[M/(W+1)]	(g)	182.031	182.031
Height of solids in sample 'H_s'	=[H/(1+e_0)]	(cm)	1.362	1.362

Table C.17.2: Consolidation data for sample D2 (As-compacted)

Time		Pressure at 5kPa		Pressure at 25kPa		Pressure at 50kPa		Pressure at 100kPa		Pressure at 200kPa		Pressure at 300kPa	
		Gauge reading	Consolidation settlement 'Δh'	Gauge reading	Consolidation settlement 'Δh'	Gauge reading	Consolidation settlement 'Δh'	Gauge reading	Consolidation settlement 'Δh'	Gauge reading	Consolidation settlement 'Δh'	Gauge reading	Consolidation settlement 'Δh'
t	√t	Gr	$(Gr_1 - Gr)$ *0.002	Gr	$(Gr_1 - Gr)$ *0.002	Gr	$(Gr_1 - Gr)$ *0.002	Gr	$(Gr_1 - Gr)$ *0.002	Gr	$(Gr_1 - Gr)$ *0.002	Gr	$(Gr_1 - Gr)$ *0.002
(mins)	(√mins)	(div)	(mm)	(div)	(mm)	(div)	(mm)	(div)	(mm)	(div)	(mm)	(div)	(mm)
0.00	0.00	666.2	0.000	642.3	0.048	593.1	0.146	553.1	0.226	504.1	0.324	444.6	0.443
0.13	0.37	647.2	0.038	601.2	0.130	563.1	0.206	515.0	0.302	456.8	0.419	420.3	0.492
0.25	0.50	646.5	0.039	600.3	0.132	562.2	0.208	513.8	0.305	455.5	0.421	419.4	0.494
0.50	0.71	646.0	0.040	599.5	0.133	561.0	0.210	512.3	0.308	454.0	0.424	418.0	0.496
1.00	1.00	645.5	0.041	598.5	0.135	559.8	0.213	511.0	0.310	452.2	0.428	416.5	0.499
2.00	1.41	644.9	0.043	597.3	0.138	558.2	0.216	509.6	0.313	450.9	0.431	415.1	0.502
4.00	2.00	644.2	0.044	596.2	0.140	557.0	0.218	508.1	0.316	449.1	0.434	414.3	0.504
8.00	2.83	643.9	0.045	595.3	0.142	555.8	0.221	506.8	0.319	448.8	0.435	411.8	0.509
15.00	3.87	643.1	0.046	594.2	0.144	554.8	0.223	505.8	0.321	446.1	0.440	410.3	0.512
30.00	5.48	642.3	0.048	593.1	0.146	553.1	0.226	504.1	0.324	444.6	0.443	408.7	0.515

Table C.17.3: Consolidation calculated parameter for sample D2 (As-compacted)

Pressures	**(kPa)**	**0**	**5**	**25**	**50**	**100**	**200**	**300**
Δh_{90}	(mm)		0.038	0.133	0.208	0.306	0.423	0.494
Δh_0	(mm)		0.000	0.048	0.146	0.226	0.324	0.443
Δh_{100} = $[((\Delta h_{90} - \Delta h_0)/0.9)+ \Delta h_0]$	(mm)		0.042	0.142	0.215	0.315	0.434	0.500
Δh_f	(mm)		0.048	0.146	0.226	0.324	0.443	0.515
Initial Compression ratio $r_i = [\Delta h_0/\Delta h_f]$			0.000	0.328	0.645	0.697	0.731	0.860
Primary Compression ratio $r_p = [(\Delta h_{100}-\Delta h_0)/\Delta h_f]$			0.883	0.646	0.305	0.274	0.248	0.110
Secondary Compression ratio 'r_{sec}' = $[(\Delta h_f - \Delta h_{100})/\Delta h_f]$			0.117	0.026	0.050	0.029	0.021	0.030
√t90	(√min)		0.510	0.440	0.420	0.490	0.470	0.510
t_{90}	(mins)		0.260	0.194	0.176	0.240	0.221	0.260
T_{90}			0.848	0.848	0.848	0.848	0.848	0.848
drainage path 'd' = $[h_i/2]$	(mm)		9.125	9.101	9.052	9.012	8.963	8.904
Initial void ratio 'e_i' =$[(H-\Delta h_0-Hs)/Hs]$			0.340	0.336	0.329	0.323	0.316	0.307
Final void ratio 'e_f' =$[(H-\Delta h_f-Hs)/Hs]$		0.340	0.336	0.329	0.323	0.316	0.307	0.302
Total change in void ratio 'Δe' = $e_i - e_f$			0.004	0.007	0.006	0.007	0.009	0.005
Change of stress/pressure 'Δσ' = $\sigma_t - \sigma_p$	(kPa) or (kN/m^2)		5	20	25	50	100	100
Volume Compressibility 'Mv' = $[(1/1+e_0)*(\Delta e/\Delta\sigma')]$	(m^2/MN)		0.371	0.190	0.124	0.076	0.046	0.028
Volumetric Strain = (Δhi/H)*100%	(%)	0.000	0.262	0.801	1.239	1.776	2.428	2.822
coefficient of consolidation 'Cv' = $[(T_{90}*d^2)/t_{90}]$	(mm^2/min)		271.5	362.8	393.9	286.8	308.4	258.5
Coefficient of Permeability 'k' = $C_v*M_v*\gamma_w$	(m/yr)		0.506	0.347	0.246	0.110	0.072	0.036

Table C.17.4: initial parameter of sample D2 (Inundated)

Dimensions			Initial specimen	Final specimen
Diameter	'D'	(cm)	7.710	7.710
Area	'A'	(cm^2)	46.687	46.687
Height	'H'	(cm)	1.770	1.718
Volume	'V'	(cm^3)	82.636	80.213
Weights				
Ring		(g)	76.200	76.200
Ring + Sample in ring		(g)	280.500	282.327
Sample in ring	'M'	(g)	204.300	206.127
Moisture content 'W'		(%)	0.097	0.099
Calculated				
Assumed specific gravity 'Gs'			2.900	2.900
Density of water 'ρ_w'		(g/cm^3)	1.000	1.000
bulk density	'ρ' = [M/(A*H)]	(g/cm^3)	2.472	2.570
Dry Density	'ρ_d' = [ρ/(1+W)]	(g/cm^3)	2.254	2.254
Void ratio	'e_0' = [(Gs*ρ_w/ρ_d)-1]		0.287	0.287
Degree of saturation 'Sr_i'	= [Gs*W/e_0]		0.981	1.000
Mass of solids in sample 'M_s'	=[M/(W+1)]	(g)	186.243	186.243
Height of solids in sample 'H_s'	=[H/(1+e_0)]	(cm)	1.376	1.376

Table C.17.5: Consolidation data for sample D2 (Inundated)

Time		Pressure at 5kPa		Pressure at 25kPa		Pressure at 50kPa		Pressure at 100kPa		Pressure at 200kPa		Pressure at 300kPa	
		Gauge reading	Consolidation settlement 'Δh'	Gauge reading	Consolidation settlement 'Δh'	Gauge reading	Consolidation settlement 'Δh'	Gauge reading	Consolidation settlement 'Δh'	Gauge reading	Consolidation settlement 'Δh'	Gauge reading	Consolidation settlement 'Δh'
t	√t	Gr	$(Gr_1 - Gr)$ *0.002	Gr	$(Gr_1 - Gr)$ *0.002	Gr	$(Gr_1 - Gr)$ *0.002	Gr	$(Gr_1 - Gr)$ *0.002	Gr	$(Gr_1 - Gr)$ *0.002	Gr	$(Gr_1 - Gr)$ *0.002
(mins)	(√mins)	(div)	(mm)	(div)	(mm)	(div)	(mm)	(div)	(mm)	(div)	(mm)	(div)	(mm)
0.00	0.00	606.0	0.000	540.1	0.132	468.0	0.276	431.8	0.348	390.7	0.431	346.5	0.639
0.13	0.37	583.0	0.046	497.2	0.218	446.0	0.320	404.8	0.402	359.1	0.494	330.0	0.672
0.25	0.50	579.0	0.054	495.3	0.221	444.0	0.324	403.1	0.406	358.0	0.496	329.2	0.674
0.50	0.71	576.0	0.060	491.3	0.229	443.1	0.326	401.8	0.408	357.0	0.498	328.0	0.676
1.00	1.00	569.5	0.073	486.6	0.239	441.2	0.330	399.5	0.413	355.0	0.502	326.9	0.679
2.00	1.41	560.5	0.091	481.1	0.250	438.9	0.334	397.2	0.418	352.8	0.506	325.1	0.682
4.00	2.00	552.5	0.107	475.8	0.260	436.5	0.339	395.0	0.422	351.1	0.510	323.5	0.685
8.00	2.83	545.9	0.120	471.8	0.268	434.4	0.343	393.1	0.426	349.1	0.514	322.0	0.688
15.00	3.87	542.1	0.128	469.8	0.272	432.8	0.346	391.8	0.428	347.8	0.516	320.8	0.691
30.00	5.48	540.1	0.132	468.0	0.276	431.8	0.348	390.7	0.431	346.5	0.519	319.3	0.694

Table C.17.6: Consolidation calculated parameter for sample D2 (Inundated)

Pressures	**(kPa)**	**0**	**5**	**25**	**50**	**100**	**200**	**300**
Δh_{90}	(mm)		0.058	0.223	0.325	0.407	0.497	0.675
Δh_0	(mm)		0.000	0.132	0.276	0.348	0.431	0.639
Δh_{100} = $[((\Delta h_{90} - \Delta h_0)/0.9)+ \Delta h_0]$	(mm)		0.064	0.233	0.330	0.414	0.504	0.679
Δh_f	(mm)		0.132	0.276	0.348	0.431	0.519	0.694
Initial Compression ratio $r_i = [\Delta h_0/\Delta h_f]$			0.000	0.478	0.792	0.808	0.830	0.921
Primary Compression ratio $r_p = [(\Delta h_{100}-\Delta h_0)/\Delta h_f]$			0.489	0.366	0.156	0.152	0.141	0.058
Secondary Compression ratio 'r_{sec}' = $[(\Delta h_f - \Delta h_{100})/\Delta h_f]$			0.511	0.155	0.052	0.040	0.028	0.021
√t90	(√min)		0.600	0.510	0.590	0.480	0.500	0.540
t_{90}	(mins)		0.360	0.260	0.348	0.230	0.250	0.292
T_{90}			0.848	0.848	0.848	0.848	0.848	0.848
drainage path 'd' = $[h_i/2]$	(mm)		8.850	8.784	8.712	8.676	8.635	8.531
Initial void ratio 'e_i' =$[(H-\Delta h_0-Hs)/Hs]$			0.287	0.277	0.267	0.261	0.255	0.240
Final void ratio 'e_f' =$[(H-\Delta h_f-Hs)/Hs]$		0.287	0.277	0.267	0.261	0.255	0.249	0.236
Total change in void ratio 'Δe' = $e_i - e_f$			0.010	0.010	0.005	0.006	0.006	0.004
Change of stress/pressure 'Δσ' = $\sigma_t - \sigma_p$	(kPa) or (kN/m^2)		5	20	25	50	100	100
Volume Compressibility 'Mv' = $[(1/1+e_0)*(\Delta e/\Delta\sigma')]$	(m^2/MN)		1.012	0.276	0.111	0.063	0.034	0.021
Volumetric Strain = (Δhi/H)*100%	(%)	0.000	0.745	1.559	1.968	2.433	2.932	3.920
coefficient of consolidation 'Cv' = $[(T_{90}*d^2)/t_{90}]$	(mm^2/min)		184.5	251.6	184.9	277.0	252.9	211.6
Coefficient of Permeability 'k' = $C_v*M_v*\gamma_w$	(m/yr)		0.939	0.350	0.103	0.088	0.043	0.022

18. Soil D at 'At OMC' (3)

Table C.18.1: initial parameter of sample D3 (As-compacted)

Dimensions			Initial specimen	Final specimen
Diameter	'D'	(cm)	7.670	7.670
Area	'A'	(cm^2)	46.204	46.204
Height	'H'	(cm)	1.820	1.774
Volume	'V'	(cm^3)	84.091	81.968
Weights				
Ring		(g)	99.300	99.300
Ring + Sample in ring		(g)	297.300	296.480
Sample in ring	'M'	(g)	198.000	197.180
Moisture content 'W'		(%)	0.112	0.108
Calculated				
Assumed specific gravity 'Gs'			2.900	2.900
Density of water 'ρ_w'		(g/cm^3)	1.000	1.000
bulk density	'ρ' = [M/(A*H)]	(g/cm^3)	2.355	2.406
Dry Density	'ρ_d' = [ρ/(1+W)]	(g/cm^3)	2.117	2.172
Void ratio	'e_0' = [(Gs*ρ_w/ρ_d)-1]		0.370	0.335
Degree of saturation 'Sr_i'	= [Gs*W/e_0]		0.880	0.931
Mass of solids in sample 'M_s'	=[M/(W+1)]	(g)	178.005	178.005
Height of solids in sample 'H_s'	=[H/(1+e_0)]	(cm)	1.328	1.328

Table C.18.2: Consolidation data for sample D3 (As-compacted)

Time		Pressure at 5kPa		Pressure at 25kPa		Pressure at 50kPa		Pressure at 100kPa		Pressure at 200kPa		Pressure at 300kPa	
		Gauge reading	Consolidation settlement 'Δh'	Gauge reading	Consolidation settlement 'Δh'	Gauge reading	Consolidation settlement 'Δh'	Gauge reading	Consolidation settlement 'Δh'	Gauge reading	Consolidation settlement 'Δh'	Gauge reading	Consolidation settlement 'Δh'
t	√t	Gr	$(Gr_1 - Gr)$ *0.002	Gr	$(Gr_1 - Gr)$ *0.002	Gr	$(Gr_1 - Gr)$ *0.002	Gr	$(Gr_1 - Gr)$ *0.002	Gr	$(Gr_1 - Gr)$ *0.002	Gr	$(Gr_1 - Gr)$ *0.002
(mins)	(√mins)	(div)	(mm)	(div)	(mm)	(div)	(mm)	(div)	(mm)	(div)	(mm)	(div)	(mm)
0.00	0.00	1100.0	0.000	1037.5	0.125	993.5	0.213	961.5	0.277	918.9	0.362	870.2	0.460
0.13	0.37	1042.5	0.115	1001.0	0.198	971.3	0.257	927.6	0.345	880.5	0.439	847.4	0.505
0.25	0.50	1041.9	0.116	1000.4	0.199	970.1	0.260	926.8	0.346	879.0	0.442	846.4	0.507
0.50	0.71	1041.2	0.118	999.7	0.201	968.9	0.262	925.8	0.348	877.7	0.445	845.2	0.510
1.00	1.00	1040.7	0.119	998.9	0.202	967.4	0.265	924.8	0.350	876.3	0.447	844.1	0.512
2.00	1.41	1040.0	0.120	997.9	0.204	966.1	0.268	923.6	0.353	875.1	0.450	842.8	0.514
4.00	2.00	1039.2	0.122	996.9	0.206	965.0	0.270	922.4	0.355	873.8	0.452	841.3	0.517
8.00	2.83	1038.9	0.122	995.8	0.208	963.9	0.272	921.1	0.358	872.3	0.455	840.4	0.519
15.00	3.87	1038.2	0.124	994.9	0.210	962.7	0.275	920.3	0.359	871.1	0.458	838.9	0.522
30.00	5.48	1037.5	0.125	993.5	0.213	961.5	0.277	918.9	0.362	870.2	0.460	837.5	0.525

Table C.18.3: Consolidation calculated parameter for sample D3 (As-compacted)

Pressures	**(kPa)**	**0**	**5**	**25**	**50**	**100**	**200**	**300**
Δh_{90}	(mm)		0.118	0.200	0.260	0.347	0.443	0.508
Δh_0	(mm)		0.000	0.125	0.213	0.277	0.362	0.46
$\Delta h_{100} = [((\Delta h_{90} - \Delta h_0)/0.9) + \Delta h_0]$	(mm)		0.131	0.208	0.265	0.355	0.452	0.513
Δh_f	(mm)		0.125	0.213	0.277	0.362	0.460	0.525
Initial Compression ratio $r_i = [\Delta h_0/\Delta h_f]$			0.000	0.587	0.769	0.765	0.788	0.876
Primary Compression ratio $r_p = [(\Delta h_{100}-\Delta h_0)/\Delta h_f]$			1.049	0.391	0.189	0.215	0.196	0.102
Secondary Compression ratio 'r_{sec}' = $[(\Delta h_f - \Delta h_{100})/\Delta h_f]$			-0.049	0.022	0.043	0.020	0.017	0.022
√t90	(√min)		0.500	0.460	0.490	0.500	0.500	0.510
t_{90}	(mins)		0.250	0.212	0.240	0.250	0.250	0.260
T_{90}			0.848	0.848	0.848	0.848	0.848	0.848
drainage path 'd' = $[h_i/2]$	(mm)		9.100	9.038	8.994	8.962	8.919	8.870
Initial void ratio 'e_i' =$[(H-\Delta h_0-Hs)/Hs]$			0.370	0.361	0.354	0.349	0.343	0.335
Final void ratio 'e_f' =$[(H-\Delta h_f-Hs)/Hs]$		0.370	0.361	0.354	0.349	0.343	0.335	0.330
Total change in void ratio 'Δe' = $e_i - e_f$			0.009	0.007	0.005	0.006	0.007	0.005
Change of stress/pressure 'Δσ' = $\sigma_t - \sigma_p$	(kPa) or (kN/m^2)		5	20	25	50	100	100
Volume Compressibility 'Mv' = $[(1/1+e_0)*(\Delta e/\Delta \sigma')]$	(m^2/MN)		1.374	0.242	0.141	0.094	0.054	0.036
Volumetric Strain = (Δhi/H)*100%	(%)	0.000	0.687	1.170	1.522	1.990	2.525	2.885
coefficient of consolidation 'Cv' = $[(T_{90}*d^2)/t_{90}]$	(mm^2/min)		280.9	327.3	285.7	272.4	269.8	256.5
Coefficient of Permeability 'k' = $C_v*M_v*\gamma_w$	(m/yr)		1.940	0.398	0.202	0.128	0.073	0.046

Table C.18.4: initial parameter of sample D3 (Inundated)

Dimensions			Initial specimen	Final specimen
Diameter	'D'	(cm)	7.640	7.640
Area	'A'	(cm^2)	45.843	45.843
Height	'H'	(cm)	1.790	1.727
Volume	'V'	(cm^3)	82.060	79.174
Weights				
Ring		(g)	76.300	76.300
Ring + Sample in ring		(g)	268.600	271.323
Sample in ring	'M'	(g)	192.300	195.023
Moisture content 'W'		(%)	0.101	0.1249
Calculated				
Assumed specific gravity 'Gs'			2.900	2.900
Density of water 'ρ_w'		(g/cm^3)	1.000	1.000
bulk density	'ρ' = [M/(A*H)]	(g/cm^3)	2.343	2.463
Dry Density	'ρ_d' = [ρ/(1+W)]	(g/cm^3)	2.129	2.129
Void ratio	'e_0' = [(Gs*ρ_w/ρ_d)-1]		0.362	0.362
Degree of saturation 'Sr_i'	= [Gs*W/e_0]		0.807	1.000
Mass of solids in sample 'M_s'	=[M/(W+1)]	(g)	174.700	174.700
Height of solids in sample 'H_s'	=[H/(1+e_0)]	(cm)	1.314	1.314

Table C.18.5: Consolidation data for sample D3 (Inundated)

Time		Pressure at 5kPa		Pressure at 25kPa		Pressure at 50kPa		Pressure at 100kPa		Pressure at 200kPa		Pressure at 300kPa	
		Gauge reading	Consolidation settlement 'Δh'	Gauge reading	Consolidation settlement 'Δh'	Gauge reading	Consolidation settlement 'Δh'	Gauge reading	Consolidation settlement 'Δh'	Gauge reading	Consolidation settlement 'Δh'	Gauge reading	Consolidation settlement 'Δh'
t	√t	Gr	$(Gr_1 - Gr)$ *0.002	Gr	$(Gr_1 - Gr)$ *0.002	Gr	$(Gr_1 - Gr)$ *0.002	Gr	$(Gr_1 - Gr)$ *0.002	Gr	$(Gr_1 - Gr)$ *0.002	Gr	$(Gr_1 - Gr)$ *0.002
(mins)	(√mins)	(div)	(mm)	(div)	(mm)	(div)	(mm)	(div)	(mm)	(div)	(mm)	(div)	(mm)
0.00	0.00	1100.0	0.000	984.2	0.232	901.2	0.398	856.2	0.488	821.4	0.557	785.3	0.629
0.13	0.37	1054.0	0.092	931.5	0.337	870.1	0.460	833.5	0.533	798.0	0.604	773.5	0.653
0.25	0.50	1044.0	0.112	927.8	0.344	869.0	0.462	832.0	0.536	795.6	0.609	772.6	0.655
0.50	0.71	1029.5	0.141	922.8	0.354	867.1	0.466	830.5	0.539	794.0	0.612	771.4	0.657
1.00	1.00	1014.5	0.171	917.7	0.365	864.8	0.470	828.7	0.543	792.1	0.616	770.1	0.660
2.00	1.41	1002.2	0.196	912.4	0.375	862.1	0.476	826.3	0.547	790.1	0.620	768.9	0.662
4.00	2.00	995.1	0.210	907.5	0.385	860.0	0.480	824.5	0.551	788.1	0.624	767.2	0.666
8.00	2.83	988.0	0.224	904.2	0.392	858.0	0.484	822.9	0.554	786.5	0.627	765.9	0.668
15.00	3.87	985.9	0.228	902.3	0.395	856.9	0.486	821.6	0.557	785.4	0.629	764.5	0.671
30.00	5.48	984.2	0.232	901.2	0.398	856.2	0.488	821.4	0.557	785.3	0.629	764.1	0.672

Table C.18.6: Consolidation calculated parameter for sample D3 (Inundated)

Pressures	**(kPa)**	**0**	**5**	**25**	**50**	**100**	**200**	**300**
Δh_{90}	(mm)		0.153	0.346	0.463	0.537	0.609	0.655
Δh_0	(mm)		0.000	0.232	0.398	0.488	0.557	0.629
$\Delta h_{100} = [((\Delta h_{90} - \Delta h_0)/0.9) + \Delta h_0]$	(mm)		0.170	0.359	0.470	0.542	0.615	0.658
Δh_f	(mm)		0.232	0.398	0.488	0.557	0.629	0.672
Initial Compression ratio $r_i = [\Delta h_0/\Delta h_f]$			0.000	0.584	0.816	0.876	0.885	0.936
Primary Compression ratio $r_p = [(\Delta h_{100}-\Delta h_0)/\Delta h_f]$			0.734	0.319	0.148	0.098	0.092	0.043
Secondary Compression ratio 'r_{sec}' = $[(\Delta h_f - \Delta h_{100})/\Delta h_f]$			0.266	0.098	0.036	0.026	0.023	0.021
√t90	(√min)		0.840	0.540	0.560	0.530	0.540	0.500
t_{90}	(mins)		0.706	0.292	0.314	0.281	0.292	0.250
T_{90}			0.848	0.848	0.848	0.848	0.848	0.848
drainage path 'd' = $[h_i/2]$	(mm)		8.950	8.834	8.751	8.706	8.672	8.636
Initial void ratio 'e_i' =$[(H-\Delta h_0-Hs)/Hs]$			0.362	0.345	0.332	0.325	0.320	0.314
Final void ratio 'e_f' =$[(H-\Delta h_f-Hs)/Hs]$		0.362	0.345	0.332	0.325	0.320	0.314	0.311
Total change in void ratio 'Δe' = $e_i - e_f$			0.018	0.013	0.007	0.005	0.006	0.003
Change of stress/pressure 'Δσ' = $\sigma_t - \sigma_p$	(kPa) or (kN/m^2)		5	20	25	50	100	100
Volume Compressibility 'Mv' = $[(1/1+e_0)*(\Delta e/\Delta \sigma')]$	(m^2/MN)		2.588	0.463	0.200	0.077	0.040	0.024
Volumetric Strain = (Δhi/H)*100%	(%)	0.000	1.294	2.221	2.724	3.113	3.516	3.753
coefficient of consolidation 'Cv' = $[(T_{90}*d^2)/t_{90}]$	(mm^2/min)		96.3	226.9	207.1	228.8	218.7	252.9
Coefficient of Permeability 'k' = $C_v*M_v*\gamma_w$	(m/yr)		1.253	0.528	0.209	0.089	0.044	0.030

19. Soil D at 'Low wet of OMC' (4)

Table C.19.1: initial parameter of sample D4 (As-compacted)

Dimensions			Initial specimen	Final specimen
Diameter	'D'	(cm)	7.610	7.610
Area	'A'	(cm^2)	45.484	45.484
Height	'H'	(cm)	1.790	1.750
Volume	'V'	(cm^3)	81.416	79.606
Weights				
Ring		(g)	76.100	76.100
Ring + Sample in ring		(g)	265.500	259.528
Sample in ring	'M'	(g)	189.400	183.428
Moisture content 'W'		(%)	0.140	0.104
Calculated				
Assumed specific gravity 'Gs'			2.900	2.900
Density of water 'ρ_w'		(g/cm^3)	1.000	1.000
bulk density	'ρ' = [M/(A*H)]	(g/cm^3)	2.326	2.304
Dry Density	'ρ_d' = [ρ/(1+W)]	(g/cm^3)	2.041	2.087
Void ratio	'e_0' = [(Gs*ρ_w/ρ_d)-1]		0.421	0.389
Degree of saturation 'Sr_i'	= [Gs*W/e_0]		0.963	0.774
Mass of solids in sample 'M_s'	=[M/(W+1)]	(g)	166.168	166.168
Height of solids in sample 'H_s'	=[H/(1+e_0)]	(cm)	1.260	1.260

Table C.19.2: Consolidation data for sample D4 (As-compacted)

Time		Pressure at 5kPa		Pressure at 25kPa		Pressure at 50kPa		Pressure at 100kPa		Pressure at 200kPa		Pressure at 300kPa	
		Gauge reading	Consolidation settlement 'Δh'	Gauge reading	Consolidation settlement 'Δh'	Gauge reading	Consolidation settlement 'Δh'	Gauge reading	Consolidation settlement 'Δh'	Gauge reading	Consolidation settlement 'Δh'	Gauge reading	Consolidation settlement 'Δh'
t	√t	Gr	$(Gr_1 - Gr)$ *0.002	Gr	$(Gr_1 - Gr)$ *0.002	Gr	$(Gr_1 - Gr)$ *0.002	Gr	$(Gr_1 - Gr)$ *0.002	Gr	$(Gr_1 - Gr)$ *0.002	Gr	$(Gr_1 - Gr)$ *0.002
(mins)	(√mins)	(div)	(mm)	(div)	(mm)	(div)	(mm)	(div)	(mm)	(div)	(mm)	(div)	(mm)
0.00	0.00	648.0	0.000	604.5	0.087	556.8	0.182	526.9	0.242	490.8	0.314	449.0	0.398
0.13	0.37	627.6	0.041	572.0	0.152	542.0	0.212	503.2	0.290	462.9	0.370	434.5	0.427
0.25	0.50	626.4	0.043	570.8	0.154	537.0	0.222	502.1	0.292	462.0	0.372	433.7	0.429
0.50	0.71	624.8	0.046	569.4	0.157	535.8	0.224	500.8	0.294	460.0	0.376	432.6	0.431
1.00	1.00	622.7	0.051	567.5	0.161	534.5	0.227	499.2	0.298	458.2	0.380	431.0	0.434
2.00	1.41	619.3	0.057	565.2	0.166	533.0	0.230	497.3	0.301	456.0	0.384	429.1	0.438
4.00	2.00	615.1	0.066	562.4	0.171	531.0	0.234	495.1	0.306	453.7	0.389	427.2	0.442
8.00	2.83	610.4	0.075	559.8	0.176	529.0	0.238	493.0	0.310	452.5	0.391	425.8	0.444
15.00	3.87	606.8	0.082	558.0	0.180	527.8	0.240	491.8	0.312	450.0	0.396	424.6	0.447
30.00	5.48	604.5	0.087	556.8	0.182	526.9	0.242	490.8	0.314	449.0	0.398	423.0	0.450

Table C.19.3: Consolidation calculated parameter for sample D4 (As-compacted)

Pressures	**(kPa)**	**0**	**5**	**25**	**50**	**100**	**200**	**300**
Δh_{90}	(mm)		0.044	0.155	0.224	0.292	0.372	0.429
Δh_0	(mm)		0.000	0.087	0.182	0.242	0.314	0.398
$\Delta h_{100} = [((\Delta h_{90} - \Delta h_0)/0.9) + \Delta h_0]$	(mm)		0.049	0.163	0.229	0.298	0.379	0.432
Δh_f	(mm)		0.087	0.182	0.242	0.314	0.398	0.450
Initial Compression ratio $r_i = [\Delta h_0/\Delta h_f]$			0.000	0.477	0.751	0.770	0.789	0.884
Primary Compression ratio $r_p = [(\Delta h_{100}-\Delta h_0)/\Delta h_f]$			0.562	0.414	0.193	0.177	0.162	0.077
Secondary Compression ratio 'r_{sec}' $= [(\Delta h_f - \Delta h_{100})/\Delta h_f]$			0.438	0.109	0.055	0.053	0.049	0.039
√t90	(√min)		0.500	0.470	0.620	0.500	0.480	0.470
t_{90}	(mins)		0.250	0.221	0.384	0.250	0.230	0.221
T_{90}			0.848	0.848	0.848	0.848	0.848	0.848
drainage path 'd' $= [h_i/2]$	(mm)		8.950	8.907	8.859	8.829	8.793	8.751
Initial void ratio 'e_i' $=[(H-\Delta h_0-Hs)/Hs]$			0.421	0.414	0.406	0.402	0.396	0.389
Final void ratio 'e_f' $=[(H-\Delta h_f-Hs)/Hs]$		0.421	0.414	0.406	0.402	0.396	0.389	0.385
Total change in void ratio 'Δe' $= e_i - e_f$			0.007	0.008	0.005	0.006	0.007	0.004
Change of stress/pressure 'Δσ' $= \sigma_t - \sigma_p$	(kPa) or (kN/m^2)		5	20	25	50	100	100
Volume Compressibility 'Mv' $= [(1/1+e_0)*(\Delta e/\Delta \sigma')]$	(m^2/MN)		0.704	0.193	0.097	0.059	0.034	0.021
Volumetric Strain $= (\Delta hi/H)*100\%$	(%)	0.000	0.486	1.019	1.353	1.756	2.223	2.514
coefficient of consolidation 'Cv' $= [(T_{90}*d^2)/t_{90}]$	(mm^2/min)		271.7	304.5	173.1	264.4	284.6	294.0
Coefficient of Permeability 'k' $= C_v*M_v*\gamma_w$	(m/yr)		0.961	0.295	0.085	0.078	0.049	0.031

Table C.19.4: initial parameter of sample D4 (Inundated)

Dimensions			Initial specimen	Final specimen
Diameter	'D'	(cm)	7.640	7.640
Area	'A'	(cm^2)	45.843	45.843
Height	'H'	(cm)	1.800	1.753
Volume	'V'	(cm^3)	82.518	80.385
Weights				
Ring		(g)	79.900	79.900
Ring + Sample in ring		(g)	256.200	252.027
Sample in ring	'M'	(g)	176.300	172.127
Moisture content 'W'		(%)	0.141	0.189
Calculated				
Assumed specific gravity 'Gs'			2.900	2.900
Density of water 'ρ_w'		(g/cm^3)	1.000	1.000
bulk density	'ρ' = [M/(A*H)]	(g/cm^3)	2.137	2.141
Dry Density	'ρ_d' = [ρ/(1+W)]	(g/cm^3)	1.873	1.873
Void ratio	'e_0' = [(Gs*ρ_w/ρ_d)-1]		0.548	0.548
Degree of saturation 'Sr_i'	= [Gs*W/e_0]		0.744	1.000
Mass of solids in sample 'M_s'	=[M/(W+1)]	(g)	154.561	154.561
Height of solids in sample 'H_s'	=[H/(1+e_0)]	(cm)	1.163	1.163

Table C.19.5: Consolidation data for sample D4 (Inundated)

Time		Pressure at 5kPa		Pressure at 25kPa		Pressure at 50kPa		Pressure at 100kPa		Pressure at 200kPa		Pressure at 300kPa	
		Gauge reading	Consolidation settlement 'Δh'	Gauge reading	Consolidation settlement 'Δh'	Gauge reading	Consolidation settlement 'Δh'	Gauge reading	Consolidation settlement 'Δh'	Gauge reading	Consolidation settlement 'Δh'	Gauge reading	Consolidation settlement 'Δh'
t	√t	Gr	$(Gr_1 - Gr)$ *0.002	Gr	$(Gr_1 - Gr)$ *0.002	Gr	$(Gr_1 - Gr)$ *0.002	Gr	$(Gr_1 - Gr)$ *0.002	Gr	$(Gr_1 - Gr)$ *0.002	Gr	$(Gr_1 - Gr)$ *0.002
(mins)	(√mins)	(div)	(mm)	(div)	(mm)	(div)	(mm)	(div)	(mm)	(div)	(mm)	(div)	(mm)
0.00	0.00	610.0	0.000	555.5	0.109	491.2	0.238	456.5	0.307	418.0	0.384	377.4	0.465
0.13	0.37	584.0	0.052	512.0	0.196	471.2	0.278	432.0	0.356	391.6	0.437	362.5	0.495
0.25	0.50	581.3	0.057	510.0	0.200	469.2	0.282	431.0	0.358	390.2	0.440	361.9	0.496
0.50	0.71	578.5	0.063	507.5	0.205	467.2	0.286	429.0	0.362	388.2	0.444	360.3	0.499
1.00	1.00	574.3	0.071	504.0	0.212	465.5	0.289	427.5	0.365	386.2	0.448	359.1	0.502
2.00	1.41	569.2	0.082	500.2	0.220	463.3	0.293	426.5	0.367	383.8	0.452	357.4	0.505
4.00	2.00	563.1	0.094	496.7	0.227	460.7	0.299	424.1	0.372	381.3	0.457	355.7	0.509
8.00	2.83	559.0	0.102	494.0	0.232	459.2	0.302	421.8	0.376	379.5	0.461	354.1	0.512
15.00	3.87	557.0	0.106	492.7	0.235	457.8	0.304	420.0	0.380	378.5	0.463	353.0	0.514
30.00	5.48	555.5	0.109	491.2	0.238	456.5	0.307	418.0	0.384	377.4	0.465	351.9	0.516

Table C.19.6: Consolidation calculated parameter for sample D4 (Inundated)

Pressures	**(kPa)**	**0**	**5**	**25**	**50**	**100**	**200**	**300**
Δh_{90}	(mm)		0.058	0.200	0.282	0.359	0.440	0.4965
Δh_0	(mm)		0.000	0.109	0.238	0.307	0.384	0.465
Δh_{100} = $[((\Delta h_{90} - \Delta h_0)/0.9)+ \Delta h_0]$	(mm)		0.064	0.210	0.287	0.365	0.446	0.500
Δh_f	(mm)		0.109	0.238	0.307	0.384	0.465	0.516
Initial Compression ratio $r_i = [\Delta h_0/\Delta h_f]$			0.000	0.459	0.775	0.799	0.825	0.901
Primary Compression ratio $r_p = [(\Delta h_{100}-\Delta h_0)/\Delta h_f]$			0.591	0.426	0.159	0.150	0.134	0.068
Secondary Compression ratio 'r_{sec}' = $[(\Delta h_f - \Delta h_{100})/\Delta h_f]$			0.409	0.116	0.066	0.050	0.041	0.031
√t90	(√min)		0.500	0.460	0.520	0.480	0.500	0.500
t_{90}	(mins)		0.250	0.212	0.270	0.230	0.250	0.250
T_{90}			0.848	0.848	0.848	0.848	0.848	0.848
drainage path 'd' = $[h_i/2]$	(mm)		9.000	8.946	8.881	8.847	8.808	8.768
Initial void ratio 'e_i' =$[(H-\Delta h_0-Hs)/Hs]$			0.548	0.539	0.528	0.522	0.515	0.508
Final void ratio 'e_f' =$[(H-\Delta h_f-Hs)/Hs]$		0.548	0.539	0.528	0.522	0.515	0.508	0.504
Total change in void ratio 'Δe' = $e_i - e_f$			0.009	0.011	0.006	0.007	0.007	0.004
Change of stress/pressure 'Δσ' = $\sigma_t - \sigma_p$	(kPa) or (kN/m^2)		5	20	25	50	100	100
Volume Compressibility 'Mv' = $[(1/1+e_0)*(\Delta e/\Delta\sigma')]$	(m^2/MN)		0.955	0.282	0.121	0.067	0.036	0.022
Volumetric Strain = (Δhi/H)*100%	(%)	0.000	0.606	1.320	1.706	2.133	2.584	2.868
coefficient of consolidation 'Cv' = $[(T_{90}*d^2)/t_{90}]$	(mm^2/min)		274.8	320.7	247.4	288.0	263.2	260.7
Coefficient of Permeability 'k' = $C_v*M_v*\gamma_w$	(m/yr)		1.320	0.454	0.150	0.098	0.047	0.029

20. Soil B at 'High wet of OMC' (5)

Table C.20.1: initial parameter of sample D5 (As-compacted)

Dimensions			Initial specimen	Final specimen
Diameter	'D'	(cm)	7.660	7.660
Area	'A'	(cm^2)	46.084	46.084
Height	'H'	(cm)	1.830	1.788
Volume	'V'	(cm^3)	84.333	82.408
Weights				
Ring		(g)	99.300	99.300
Ring + Sample in ring		(g)	290.300	283.020
Sample in ring	'M'	(g)	191.000	183.720
Moisture content 'W'		(%)	0.158	0.114
Calculated				
Assumed specific gravity 'Gs'			2.900	2.900
Density of water 'ρ_w'		(g/cm^3)	1.000	1.000
bulk density	'ρ' = [M/(A*H)]	(g/cm^3)	2.265	2.229
Dry Density	'ρ_d' = [ρ/(1+W)]	(g/cm^3)	1.956	2.001
Void ratio	'e_0' = [(Gs*ρ_w/ρ_d)-1]		0.483	0.449
Degree of saturation 'Sr_i'	= [Gs*W/e_0]		0.949	0.736
Mass of solids in sample 'M_s'	=[M/(W+1)]	(g)	164.937	164.937
Height of solids in sample 'H_s'	=[H/(1+e_0)]	(cm)	1.234	1.234

Table C.20.2: Consolidation data for sample D5 (As-compacted)

Time		Pressure at 5kPa		Pressure at 25kPa		Pressure at 50kPa		Pressure at 100kPa		Pressure at 200kPa		Pressure at 300kPa	
		Gauge reading	Consolidation settlement 'Δh'	Gauge reading	Consolidation settlement 'Δh'	Gauge reading	Consolidation settlement 'Δh'	Gauge reading	Consolidation settlement 'Δh'	Gauge reading	Consolidation settlement 'Δh'	Gauge reading	Consolidation settlement 'Δh'
t	√t	Gr	$(Gr_1 - Gr)$ *0.002	Gr	$(Gr_1 - Gr)$ *0.002	Gr	$(Gr_1 - Gr)$ *0.002	Gr	$(Gr_1 - Gr)$ *0.002	Gr	$(Gr_1 - Gr)$ *0.002	Gr	$(Gr_1 - Gr)$ *0.002
(mins)	(√mins)	(div)	(mm)	(div)	(mm)	(div)	(mm)	(div)	(mm)	(div)	(mm)	(div)	(mm)
0.00	0.00	900.0	0.000	864.5	0.071	809.9	0.180	776.2	0.248	736.0	0.328	691.9	0.416
0.13	0.37	884.8	0.030	828.5	0.143	791.0	0.218	751.8	0.296	707.5	0.385	676.5	0.447
0.25	0.50	884.1	0.032	826.2	0.148	789.5	0.221	750.0	0.300	706.3	0.387	675.9	0.448
0.50	0.71	882.0	0.036	825.5	0.149	788.1	0.224	748.3	0.303	704.5	0.391	674.7	0.451
1.00	1.00	880.0	0.040	822.9	0.154	786.2	0.228	746.1	0.308	702.2	0.396	673.1	0.454
2.00	1.41	877.1	0.046	819.9	0.160	784.1	0.232	743.8	0.312	699.7	0.401	671.1	0.458
4.00	2.00	873.8	0.052	816.7	0.167	781.5	0.237	741.0	0.318	697.0	0.406	669.0	0.462
8.00	2.83	869.3	0.061	813.1	0.174	779.1	0.242	738.5	0.323	694.7	0.411	667.1	0.466
15.00	3.87	866.1	0.068	811.1	0.178	777.8	0.244	737.1	0.326	693.1	0.414	665.9	0.468
30.00	5.48	864.5	0.071	809.9	0.180	776.2	0.248	736.0	0.328	691.1	0.418	664.5	0.471

Table C.20.3: Consolidation calculated parameter for sample D5 (As-compacted)

Pressures	**(kPa)**	**0**	**5**	**25**	**50**	**100**	**200**	**300**
Δh_{90}	(mm)		0.032	0.148	0.221	0.301	0.388	0.449
Δh_0	(mm)		0.000	0.071	0.180	0.248	0.328	0.416
Δh_{100} = $[((\Delta h_{90} - \Delta h_0)/0.9)+ \Delta h_0]$	(mm)		0.036	0.157	0.226	0.307	0.395	0.453
Δh_f	(mm)		0.071	0.180	0.248	0.328	0.418	0.471
Initial Compression ratio $r_i = [\Delta h_0/\Delta h_f]$			0.000	0.394	0.727	0.756	0.785	0.883
Primary Compression ratio $r_p = [(\Delta h_{100}-\Delta h_0)/\Delta h_f]$			0.501	0.475	0.184	0.180	0.160	0.078
Secondary Compression ratio 'r_{sec}' = $[(\Delta h_f - \Delta h_{100})/\Delta h_f]$			0.499	0.131	0.089	0.064	0.055	0.039
√t90	(√min)		0.490	0.540	0.510	0.560	0.500	0.550
t_{90}	(mins)		0.240	0.292	0.260	0.314	0.250	0.303
T_{90}			0.848	0.848	0.848	0.848	0.848	0.848
drainage path 'd' = $[h_i/2]$	(mm)		9.150	9.115	9.060	9.026	8.986	8.942
Initial void ratio 'e_i' =$[(H-\Delta h_0-Hs)/Hs]$			0.483	0.477	0.468	0.463	0.456	0.449
Final void ratio 'e_f' =$[(H-\Delta h_f-Hs)/Hs]$		0.483	0.477	0.468	0.463	0.456	0.449	0.445
Total change in void ratio 'Δe' = $e_i - e_f$			0.006	0.009	0.005	0.006	0.007	0.004
Change of stress/pressure 'Δσ' = $\sigma_t - \sigma_p$	(kPa) or (kN/m^2)		5	20	25	50	100	100
Volume Compressibility 'Mv' = $[(1/1+e_0)*(\Delta e/\Delta\sigma')]$	(m^2/MN)		0.776	0.298	0.148	0.087	0.049	0.030
Volumetric Strain = (Δhi/H)*100%	(%)	0.000	0.388	0.985	1.353	1.792	2.283	2.574
coefficient of consolidation 'Cv' = $[(T_{90}*d^2)/t_{90}]$	(mm^2/min)		295.7	241.6	267.6	220.3	273.9	224.2
Coefficient of Permeability 'k' = $C_v*M_v*\gamma_w$	(m/yr)		1.154	0.362	0.199	0.097	0.068	0.034

Table C.20.4: initial parameter of sample D5 (Inundated)

Dimensions			Initial specimen	Final specimen
Diameter	'D'	(cm)	7.650	7.650
Area	'A'	(cm^2)	45.963	45.963
Height	'H'	(cm)	1.780	1.733
Volume	'V'	(cm^3)	81.815	79.655
Weights				
Ring		(g)	97.500	97.500
Ring + Sample in ring		(g)	284.300	279.238
Sample in ring	'M'	(g)	186.800	181.738
Moisture content 'W'		(%)	0.156	0.1613
Calculated				
Assumed specific gravity 'Gs'			2.900	2.900
Density of water 'ρ_w'		(g/cm^3)	1.000	1.000
bulk density	'ρ' = [M/(A*H)]	(g/cm^3)	2.283	2.282
Dry Density	'ρ_d' = [ρ/(1+W)]	(g/cm^3)	1.976	1.976
Void ratio	'e_0' = [(Gs*ρ_w/ρ_d)-1]		0.468	0.468
Degree of saturation 'Sr_i'	= [Gs*W/e_0]		0.965	1.000
Mass of solids in sample 'M_s'	=[M/(W+1)]	(g)	161.652	161.652
Height of solids in sample 'H_s'	=[H/(1+e_0)]	(cm)	1.213	1.213

Table C.20.5: Consolidation data for sample D5 (Inundated)

Time		Pressure at 5kPa		Pressure at 25kPa		Pressure at 50kPa		Pressure at 100kPa		Pressure at 200kPa		Pressure at 300kPa	
		Gauge reading	Consolidation settlement 'Δh'	Gauge reading	Consolidation settlement 'Δh'	Gauge reading	Consolidation settlement 'Δh'	Gauge reading	Consolidation settlement 'Δh'	Gauge reading	Consolidation settlement 'Δh'	Gauge reading	Consolidation settlement 'Δh'
t	√t	Gr	$(Gr_1 - Gr)$ *0.002	Gr	$(Gr_1 - Gr)$ *0.002	Gr	$(Gr_1 - Gr)$ *0.002	Gr	$(Gr_1 - Gr)$ *0.002	Gr	$(Gr_1 - Gr)$ *0.002	Gr	$(Gr_1 - Gr)$ *0.002
(mins)	(√mins)	(div)	(mm)	(div)	(mm)	(div)	(mm)	(div)	(mm)	(div)	(mm)	(div)	(mm)
0.00	0.00	1500.0	0.000	1434.9	0.130	1378.0	0.244	1345.9	0.308	1308.1	0.384	1265.0	0.470
0.13	0.37	1476.5	0.047	1401.6	0.197	1362.0	0.276	1324.0	0.352	1284.4	0.431	1251.0	0.498
0.25	0.50	1474.5	0.051	1400.0	0.200	1360.5	0.279	1323.0	0.354	1281.2	0.438	1250.0	0.500
0.50	0.71	1471.2	0.058	1398.5	0.203	1359.0	0.282	1321.5	0.357	1279.6	0.441	1249.0	0.502
1.00	1.00	1465.9	0.068	1394.5	0.211	1356.9	0.286	1319.2	0.362	1277.0	0.446	1247.5	0.505
2.00	1.41	1459.7	0.081	1390.2	0.220	1354.1	0.292	1317.0	0.366	1274.1	0.452	1245.8	0.508
4.00	2.00	1450.8	0.098	1385.6	0.229	1351.2	0.298	1313.9	0.372	1271.0	0.458	1244.7	0.511
8.00	2.83	1442.2	0.116	1381.5	0.237	1348.8	0.302	1311.1	0.378	1268.1	0.464	1241.3	0.517
15.00	3.87	1437.1	0.126	1379.2	0.242	1347.1	0.306	1309.5	0.381	1266.6	0.467	1239.8	0.520
30.00	5.48	1434.9	0.130	1378.0	0.244	1345.9	0.308	1308.1	0.384	1265.0	0.470	1238.1	0.524

Table C.20.6: Consolidation calculated parameter for sample D5 (Inundated)

Pressures	**(kPa)**	**0**	**5**	**25**	**50**	**100**	**200**	**300**
Δh_{90}	(mm)		0.052	0.200	0.280	0.355	0.438	0.501
Δh_0	(mm)		0.000	0.130	0.244	0.308	0.384	0.47
Δh_{100} = $[((\Delta h_{90} - \Delta h_0)/0.9)+ \Delta h_0]$	(mm)		0.058	0.208	0.284	0.360	0.444	0.504
Δh_f	(mm)		0.130	0.244	0.308	0.384	0.470	0.524
Initial Compression ratio $r_i = [\Delta h_0/\Delta h_f]$			0.000	0.533	0.792	0.803	0.817	0.897
Primary Compression ratio $r_p = [(\Delta h_{100}-\Delta h_0)/\Delta h_f]$			0.444	0.319	0.130	0.135	0.128	0.066
Secondary Compression ratio 'r_{sec}' = $[(\Delta h_f - \Delta h_{100})/\Delta h_f]$			0.556	0.148	0.079	0.063	0.055	0.037
√t90	(√min)		0.580	0.520	0.560	0.490	0.560	0.560
t_{90}	(mins)		0.336	0.270	0.314	0.240	0.314	0.314
T_{90}			0.848	0.848	0.848	0.848	0.848	0.848
drainage path 'd' = $[h_i/2]$	(mm)		8.900	8.835	8.778	8.746	8.708	8.665
Initial void ratio 'e_i' =$[(H-\Delta h_0-Hs)/Hs]$			0.468	0.457	0.448	0.442	0.436	0.429
Final void ratio 'e_f' =$[(H-\Delta h_f-Hs)/Hs]$		0.468	0.457	0.448	0.442	0.436	0.429	0.425
Total change in void ratio 'Δe' = $e_i - e_f$			0.011	0.009	0.005	0.006	0.007	0.004
Change of stress/pressure 'Δσ' = $\sigma_t - \sigma_p$	(kPa) or (kN/m^2)		5	20	25	50	100	100
Volume Compressibility 'Mv' = $[(1/1+e_0)*(\Delta e/\Delta\sigma')]$	(m^2/MN)		1.463	0.320	0.144	0.085	0.048	0.030
Volumetric Strain = (Δhi/H)*100%	(%)	0.000	0.731	1.371	1.731	2.156	2.640	2.943
coefficient of consolidation 'Cv' = $[(T_{90}*d^2)/t_{90}]$	(mm^2/min)		199.7	244.8	208.4	270.2	205.0	203.0
Coefficient of Permeability 'k' = $C_v*M_v*\gamma_w$	(m/yr)		1.469	0.394	0.151	0.116	0.050	0.031

D

COLLAPSE PREDICTIVE MODEL

1. Formulas generated using data from the laboratory tests

1.a Compaction model

Table D.1.a.1: Compactive model Summary

Model Summary

Model	R	R Square	Adjusted R Square	Std. Error of the Estimate	Change Statistics				
					R Square Change	F Change	df1	df2	Sig. F Change
1	.721[a]	.520	.298	5.82347	.520	2.345	6	13	.093

a. Predictors: (Constant), Optimum Moisture Content (%), Difference between As-compacted Sr and Inundated Sr, Relative Moisture Content (%), Maximum Dry density (g/cm3), Initial degree of saturation (%), Initial Moisture Content (%)

b. Dependent Variable: Collapse Potential (%)

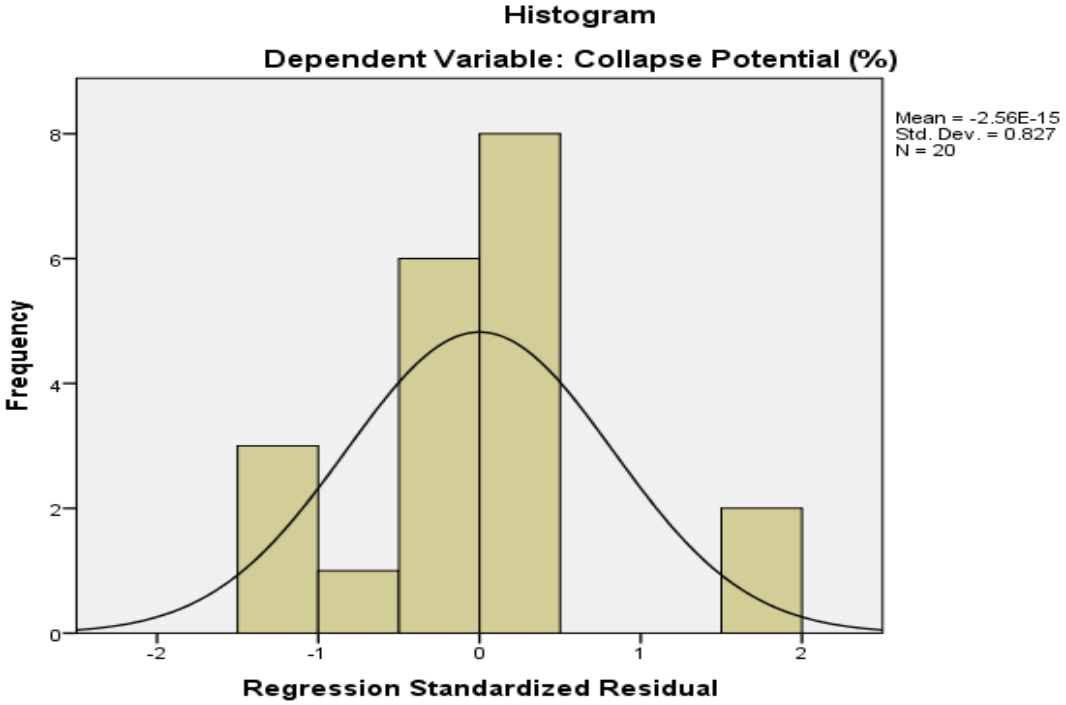

Figure D.1.a.1: Histogram of the Compactive model regression

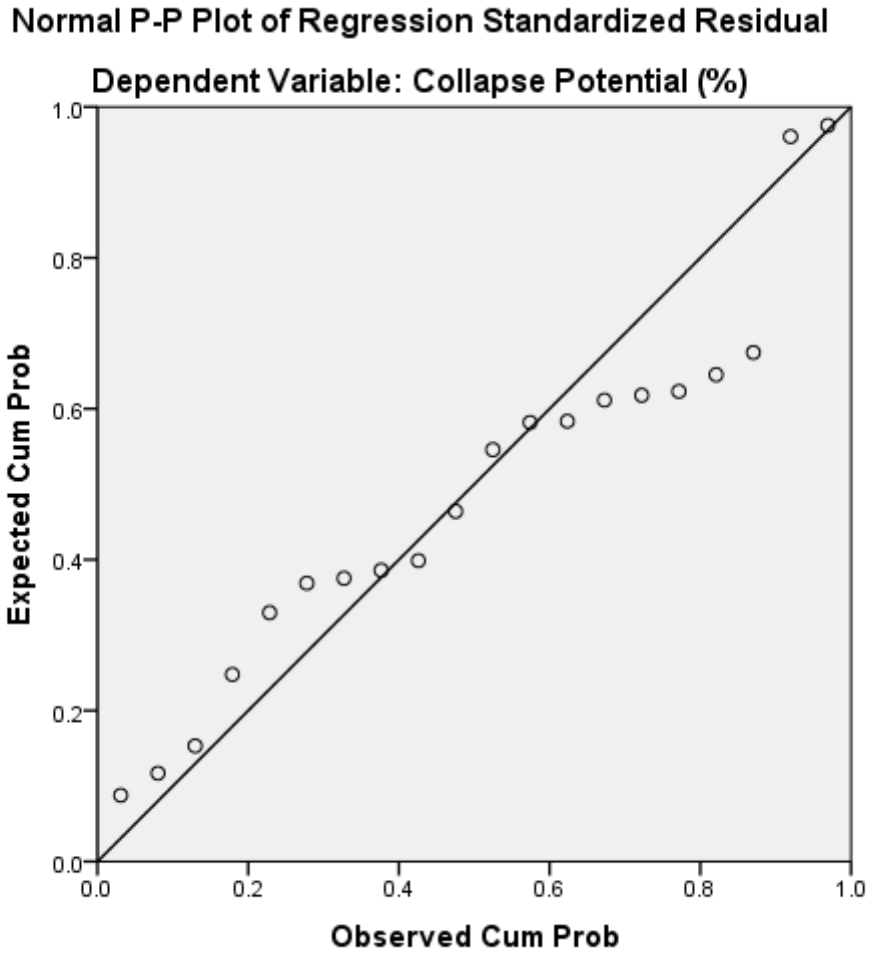

Figure D.1.a.2: Normal P-P Plot of the Compactive model regression

Table D.1.a.2: Compactive model Coefficients

Coefficients

Model		Unstandardized Coefficients		Standardized Coefficients			95.0% Confidence Interval for B		Correlations			Collinearity Statistics	
		B	Std. Error	Beta	t	Sig.	Lower Bound	Upper Bound	Zero-order	Partial	Part	Tolerance	VIF
1	(Constant)	135.011	172.190		.784	.447	-236.984	507.006					
	Initial Moisture Content (%)	-4.010	2.591	-2.342	-1.547	.146	-9.609	1.588	-.306	-.394	-.297	.016	61.975
	Relative Moisture Content (%)	.503	.421	1.664	1.197	.253	-.405	1.412	-.557	.315	.230	.019	52.361
	Initial degree of saturation (%)	-.388	.463	-.884	-.837	.418	-1.389	.613	-.440	-.226	-.161	.033	30.213
	Difference between As-compacted Sr and Inundated Sr	-24.513	19.521	-.659	-1.256	.231	-66.684	17.659	.368	-.329	-.241	.134	7.448
	Maximum Dry density (g/cm3)	-75.189	73.570	-.766	-1.022	.325	-234.127	83.749	-.322	-.273	-.196	.066	15.192
	Optimum Moisture Content (%)	3.395	3.430	1.184	.990	.340	-4.016	10.805	.285	.265	.190	.026	38.762

a. Dependent Variable: Collapse Potential (%)

1.b Sieve Model

Table D.1.b.1: Sieve model Summary

Model Summary

Model	R	R Square	Adjusted R Square	Std. Error of the Estimate	Change Statistics				
					R Square Change	F Change	df1	df2	Sig. F Change
1	.657[a]	.432	.280	5.89788	.432	2.847	4	15	.061

a. Predictors: (Constant), Coeff of Uniformity, Difference between As-compacted Sr and Inundated Sr, Initial Moisture Content (%), Percentage fines (%)

b. Dependent Variable: Collapse Potential (%)

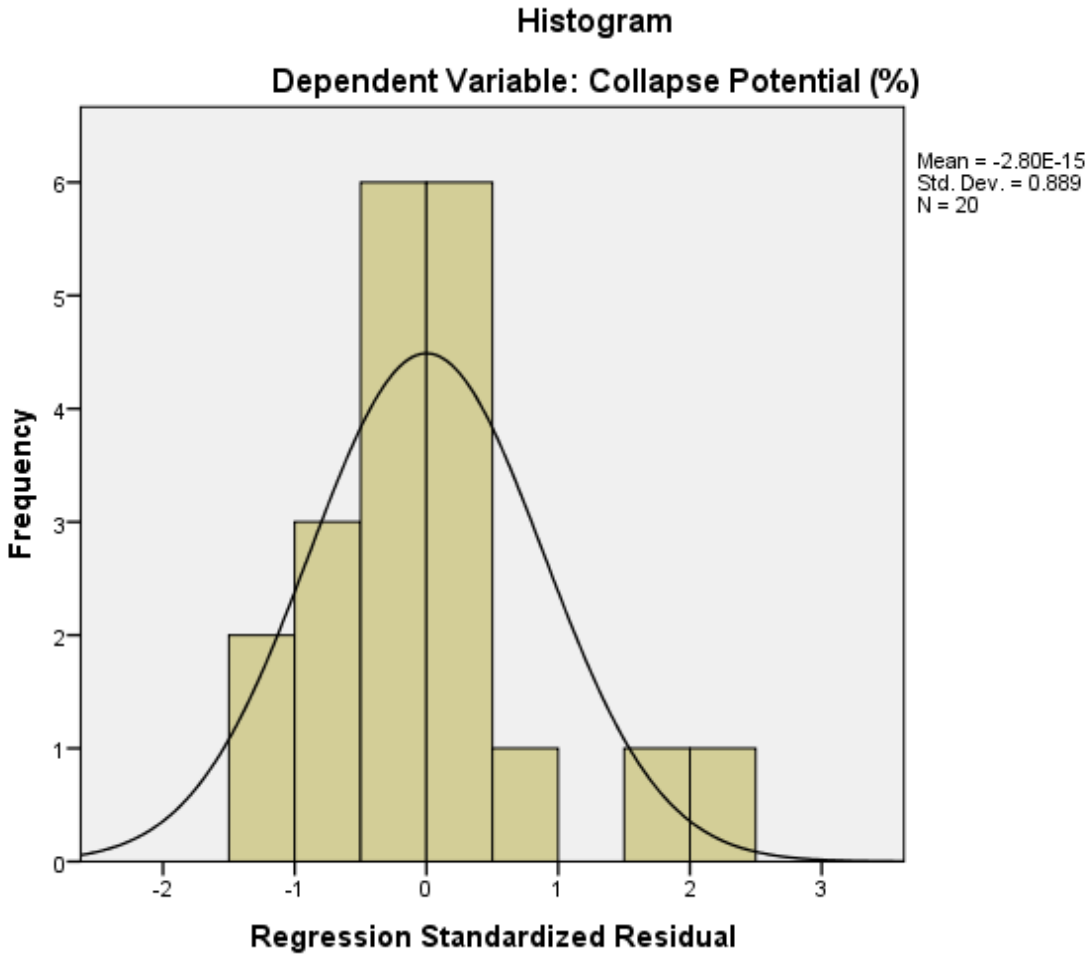

Figure D.1.b.1: Histogram of the Sieve model regression

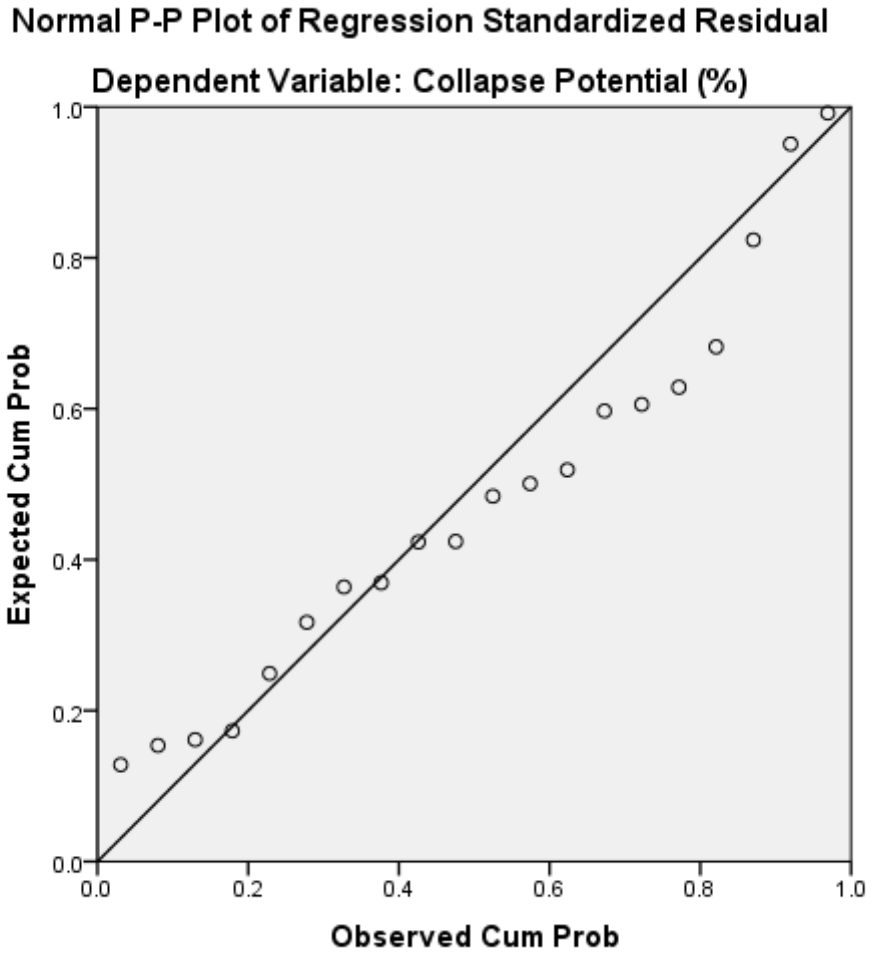

Figure D.1.b.2: Normal P-P Plot of the Sieve model regression

Table D.1.b.2: Sieve model Coefficients

Coefficients

Model		Unstandardized Coefficients		Standardized Coefficients			95.0% Confidence Interval for B		Correlations			Collinearity Statistics	
		B	Std. Error	Beta	t	Sig.	Lower Bound	Upper Bound	Zero-order	Partial	Part	Tolerance	VIF
1	(Constant)	1.153	17.883		.064	.949	-36.963	39.269					
	Difference between As-compacted Sr and Inundated Sr	-11.689	13.167	-.314	-.888	.389	-39.754	16.376	.368	-.223	-.173	.303	3.303
	Initial Moisture Content (%)	-1.625	.698	-.949	-2.327	.034	-3.114	-.137	-.306	-.515	-.453	.228	4.388
	Percentage fines (%)	.351	.178	1.192	1.970	.068	-.029	.731	.330	.453	.384	.104	9.659
	Coeff of Uniformity	.081	.102	.425	.799	.437	-.136	.298	-.321	.202	.155	.134	7.478

a. Dependent Variable: Collapse Potential (%)

1.c Soil classification test model (Sieve, Atterberg and protor Compaction)

Table D.1.c.1: Classification model Summary

Model Summary[b]

Model	R	R Square	Adjusted R Square	Std. Error of the Estimate	Change Statistics				
					R Square Change	F Change	df1	df2	Sig. F Change
1	.725[a]	.526	.249	6.02380	.526	1.900	7	12	.157

a. Predictors: (Constant), Coeff of Uniformity, Initial degree of saturation (%), Plasticity Index (%), Difference between As-compacted Sr and Inundated Sr, Relative Moisture Content (%), Initial Moisture Content (%), Percentage fines (%)

b. Dependent Variable: Collapse Potential (%)

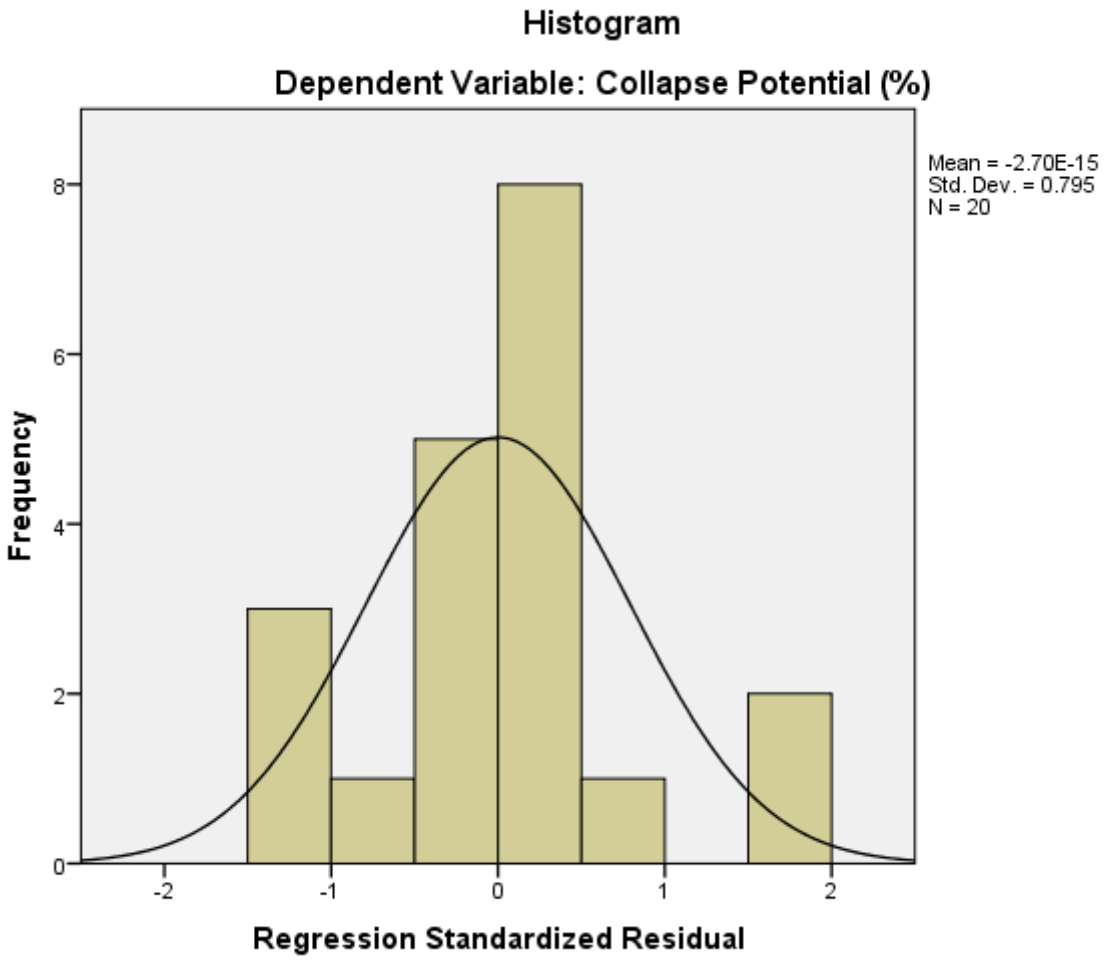

Figure D.1.c.1: Histogram of the Classification model regression

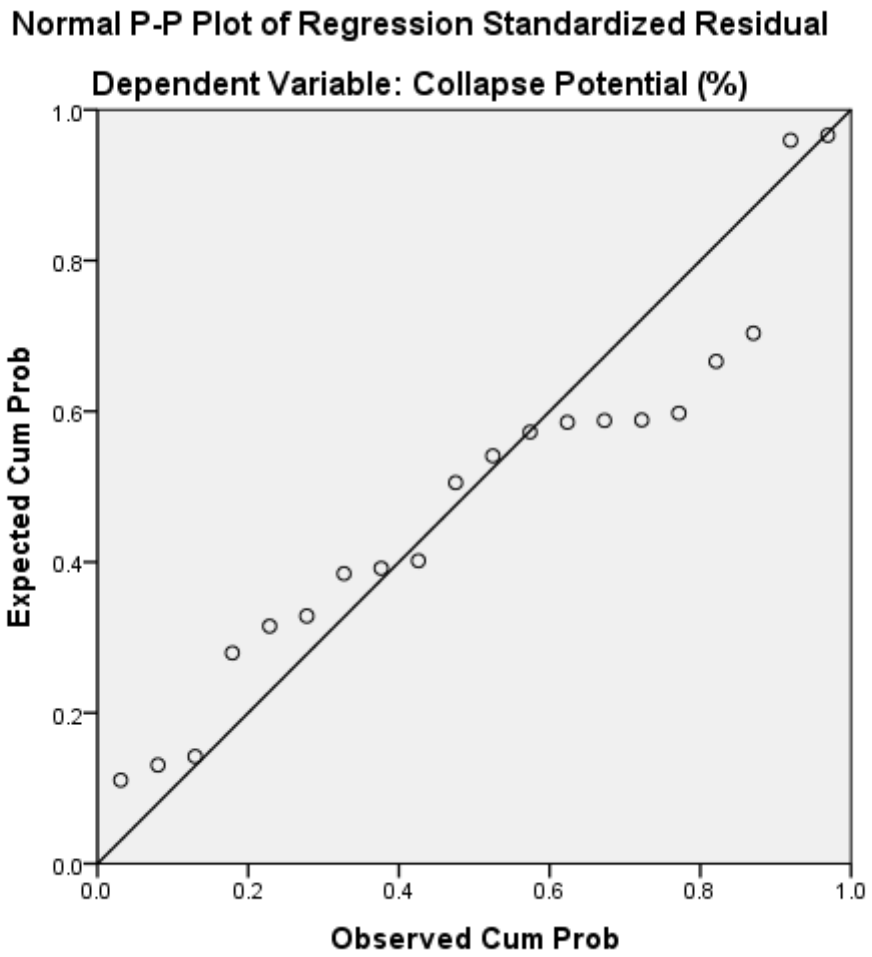

Figure D.1.c.2: Normal P-P Plot of the Classification model regression

Table D.1.c.2: Classification model Coefficients

Coefficients[a]

Model		Unstandardized Coefficients		Standardized Coefficients			95.0% Confidence Interval for B		Correlations			Collinearity Statistics	
		B	Std. Error	Beta	t	Sig.	Lower Bound	Upper Bound	Zero-order	Partial	Part	Tolerance	VIF
1	(Constant)	-22.793	48.041		-.474	.644	-127.467	81.880					
	Difference between As-compacted Sr and Inundated Sr	-26.739	21.100	-.719	-1.267	.229	-72.712	19.235	.368	-.344	-.252	.123	8.133
	Initial Moisture Content (%)	-4.102	2.690	-2.395	-1.525	.153	-9.963	1.759	-.306	-.403	-.303	.016	62.411
	Relative Moisture Content (%)	.529	.439	1.748	1.203	.252	-.428	1.485	-.557	.328	.239	.019	53.344
	Initial degree of saturation (%)	-.425	.488	-.969	-.871	.401	-1.488	.638	-.440	-.244	-.173	.032	31.319
	Plasticity Index (%)	1.180	.906	.480	1.302	.217	-.794	3.154	.060	.352	.259	.292	3.430
	Percentage fines (%)	.710	.502	2.412	1.415	.183	-.384	1.804	.330	.378	.281	.014	73.523
	Coeff of Uniformity	.131	.196	.683	.666	.518	-.297	.558	-.321	.189	.132	.038	26.615

a. Dependent Variable: Collapse Potential (%)

1.d Atterberg model

Table D.1.d.1: Atterberg model Summary

Model Summary

Model	R	R Square	Adjusted R Square	Std. Error of the Estimate	Change Statistics				
					R Square Change	F Change	df1	df2	Sig. F Change
1	.660[a]	.435	.284	5.88027	.435	2.887	4	15	.059

a. Predictors: (Constant), Plasticity Index (%), Difference between As-compacted Sr and Inundated Sr, Plastic Limit (%), Initial Moisture Content (%)

b. Dependent Variable: Collapse Potential (%)

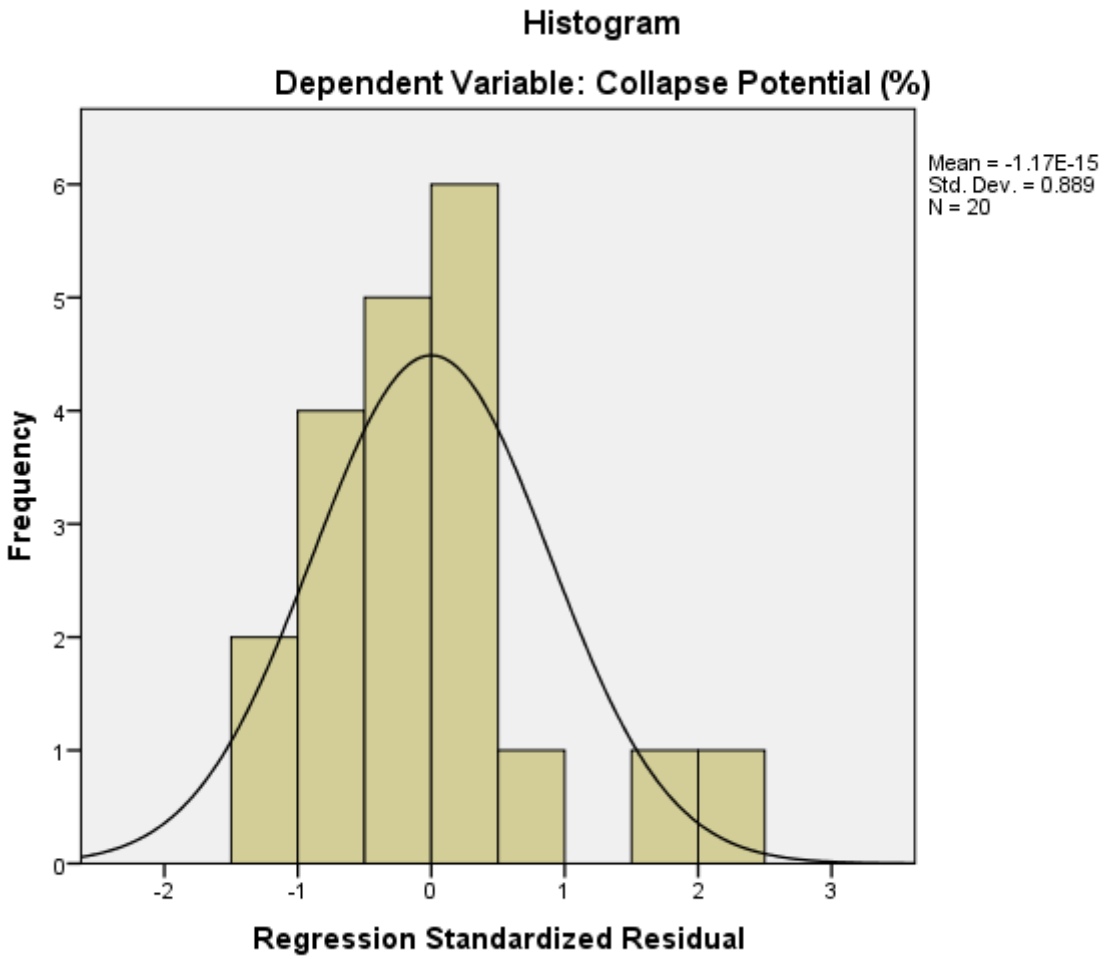

Figure D.1.d.1: Histogram of the Atterberg model regression

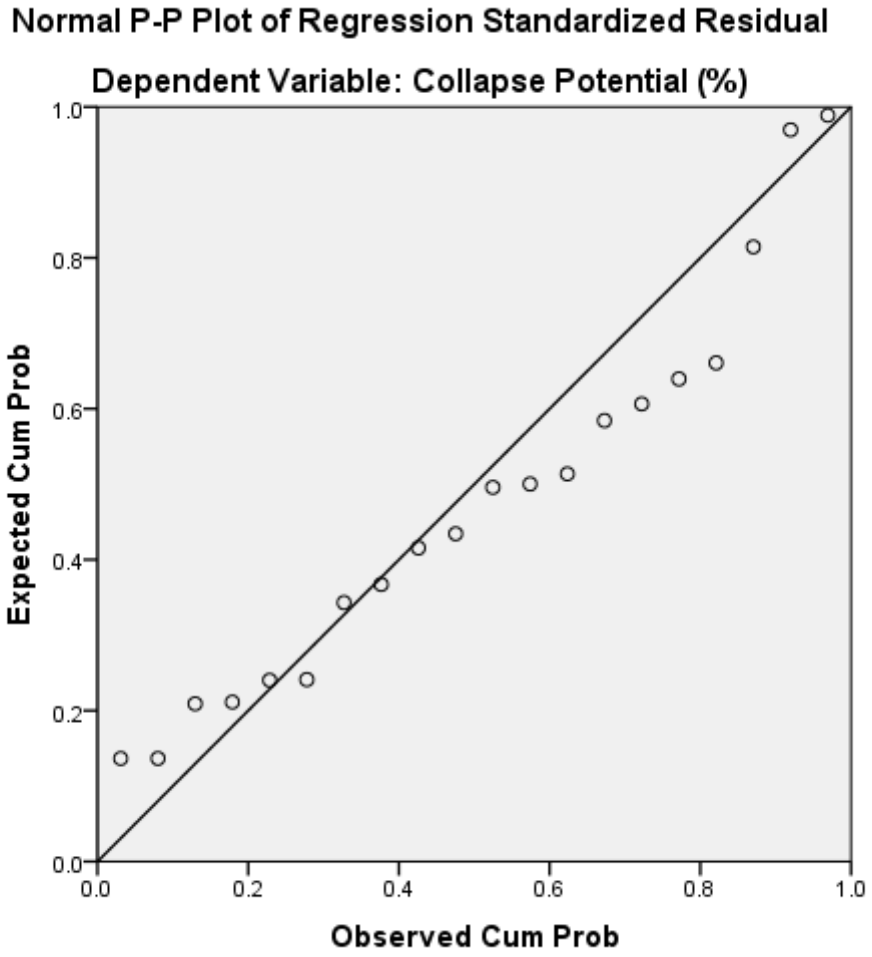

Figure D.1.d.2: Normal P-P Plot of the Atterberg model regression

Table D.1.d.2: Atterberg model Coefficients

Coefficients

Model		Unstandardized Coefficients		Standardized Coefficients			95.0% Confidence Interval for B		Correlations			Collinearity Statistics	
		B	Std. Error	Beta	t	Sig.	Lower Bound	Upper Bound	Zero-order	Partial	Part	Tolerance	VIF
1	(Constant)	-5.573	9.435		-.591	.564	-25.682	14.536					
	Difference between As-compacted Sr and Inundated Sr	-9.877	12.819	-.265	-.771	.453	-37.200	17.446	.368	-.195	-.150	.317	3.150
	Initial Moisture Content (%)	-1.625	.695	-.949	-2.338	.034	-3.106	-.144	-.306	-.517	-.454	.229	4.372
	Plastic Limit (%)	1.692	.653	.810	2.591	.020	.300	3.083	.297	.556	.503	.386	2.592
	Plasticity Index (%)	.055	.561	.022	.099	.923	-1.139	1.250	.060	.025	.019	.726	1.378

a. Dependent Variable: Collapse Potential (%)

1.e Triaxial and Atterberg model

Table D.1.e.1: Triaxial and Atterberg model Summary

Model Summary

Model	R	R Square	Adjusted R Square	Std. Error of the Estimate	Change Statistics				
					R Square Change	F Change	df1	df2	Sig. F Change
1	.704[a]	.496	.201	6.21184	.496	1.684	7	12	.204

a. Predictors: (Constant), Cohesion (kN/m2), Liquid Limit (%), Difference between As-compacted Sr and Inundated Sr, Internal friction angle (degrees), Plastic Limit (%), Initial Moisture Content (%), Max deviator stress at 70kPa

b. Dependent Variable: Collapse Potential (%)

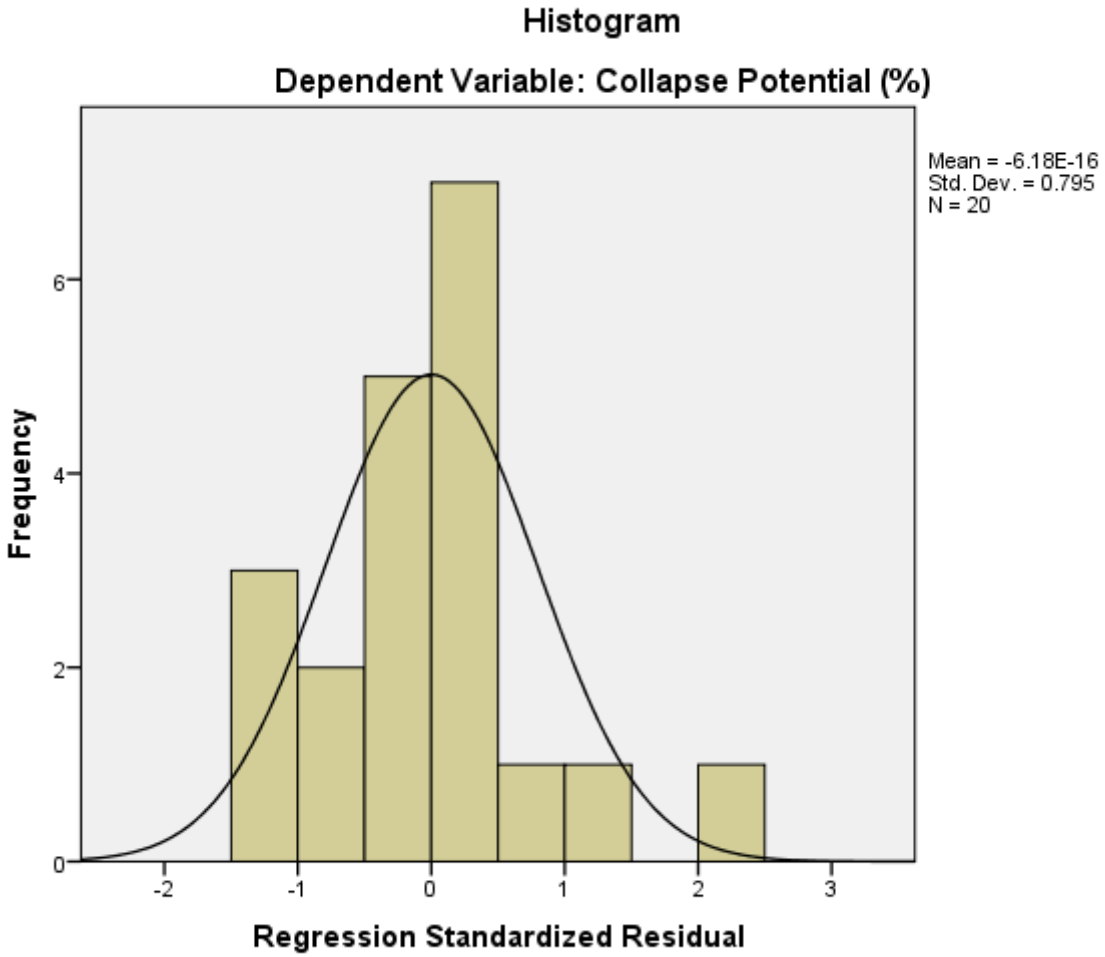

Figure D.1.e.1: Histogram of the Triaxial and Atterberg model regression

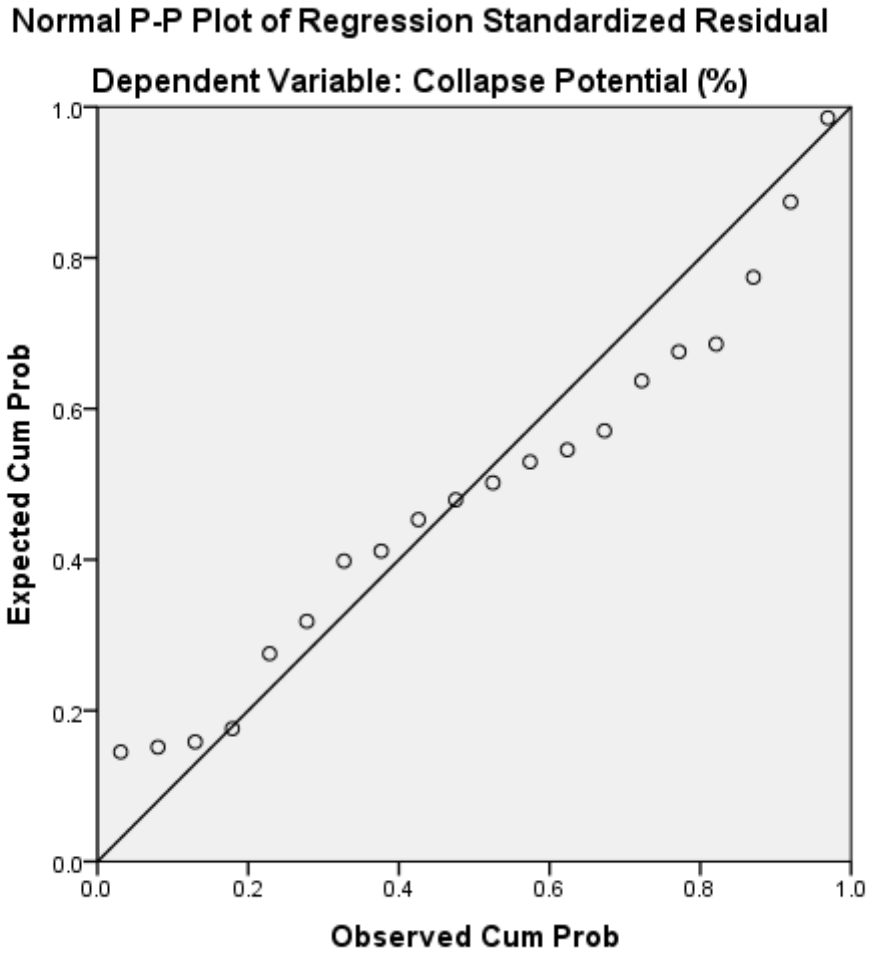

Figure D.1.e.2: Normal P-P Plot of the Triaxial and Atterberg model regression

Table D.1.e.2: Triaxial and Atterberg model Coefficients

Coefficients

Model		Unstandardized Coefficients		Standardized Coefficients			95.0% Confidence Interval for B		Correlations			Collinearity Statistics	
		B	Std. Error	Beta	t	Sig.	Lower Bound	Upper Bound	Zero-order	Partial	Part	Tolerance	VIF
1	(Constant)	-9.550	13.060		-.731	.479	-38.006	18.906					
	Difference between As-compacted Sr and Inundated Sr	-5.106	16.448	-.137	-.310	.762	-40.944	30.732	.368	-.089	-.064	.215	4.647
	Initial Moisture Content (%)	-1.191	1.351	-.695	-.881	.395	-4.134	1.753	-.306	-.247	-.181	.068	14.805
	Plastic Limit (%)	1.330	1.454	.637	.915	.378	-1.837	4.497	.297	.255	.188	.087	11.514
	Liquid Limit (%)	.138	.630	.104	.219	.831	-1.235	1.510	.221	.063	.045	.186	5.363
	Max deviator stress at 70kPa	.031	.027	1.018	1.144	.275	-.028	.089	.552	.314	.235	.053	18.850
	Internal friction angle (degrees)	-.367	.345	-.803	-1.065	.308	-1.118	.384	.482	-.294	-.218	.074	13.518
	Cohesion (kN/m2)	-.045	.073	-.218	-.611	.553	-.205	.115	.245	-.174	-.125	.329	3.040

a. Dependent Variable: Collapse Potential (%)

1.f Triaxial and Sieve Model

Table D.1.f.1: Triaxial and Sieve *model Summary*

Model Summary[b]

Model	R	R Square	Adjusted R Square	Std. Error of the Estimate	Change Statistics				
					R Square Change	F Change	df1	df2	Sig. F Change
1	.697[a]	.485	.185	6.27442	.485	1.617	7	12	.222

a. Predictors: (Constant), Coeff of Uniformity, Internal friction angle (degrees), Cohesion (kN/m2), Difference between As-compacted Sr and Inundated Sr, Percentage fines (%), Initial Moisture Content (%), Max deviator stress at 70kPa

b. Dependent Variable: Collapse Potential (%)

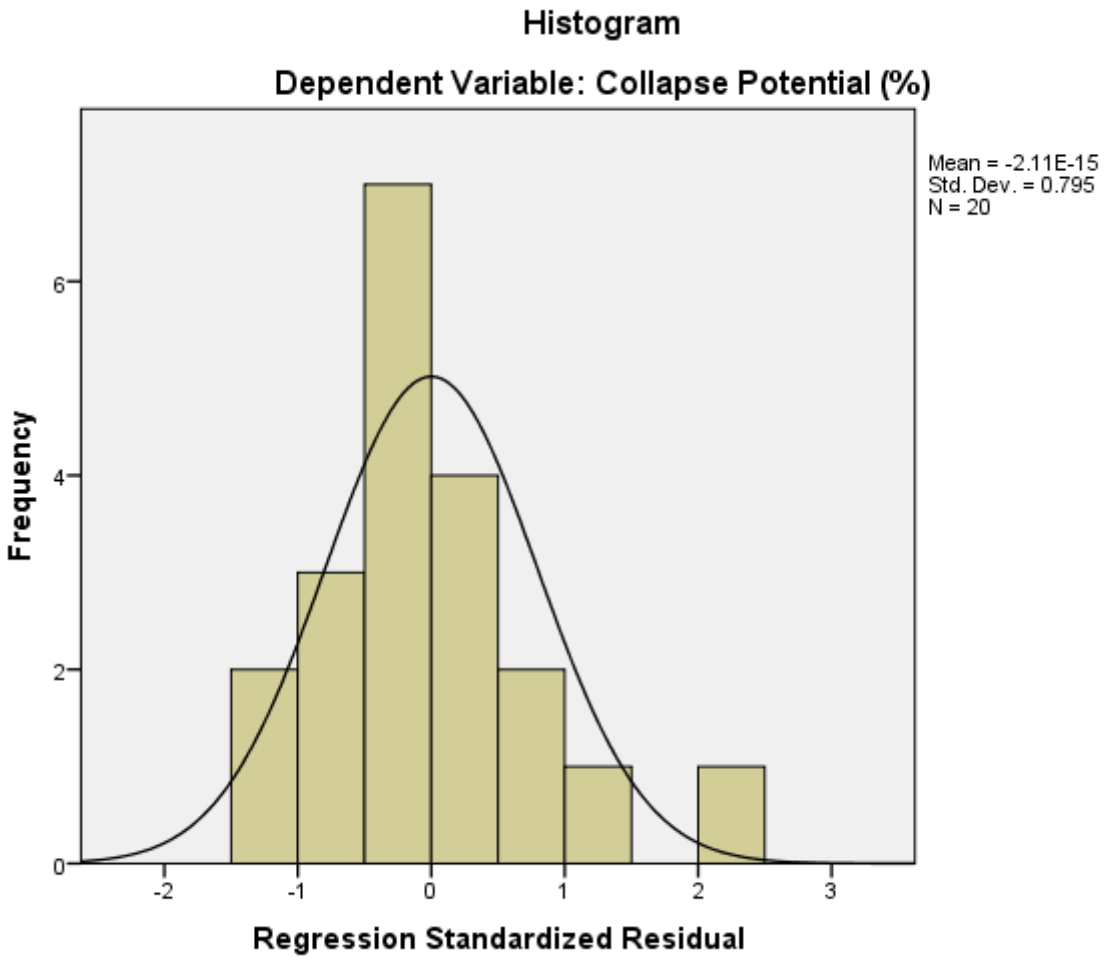

Figure D.1.f.1: Histogram of the Triaxial and Sieve *model regression*

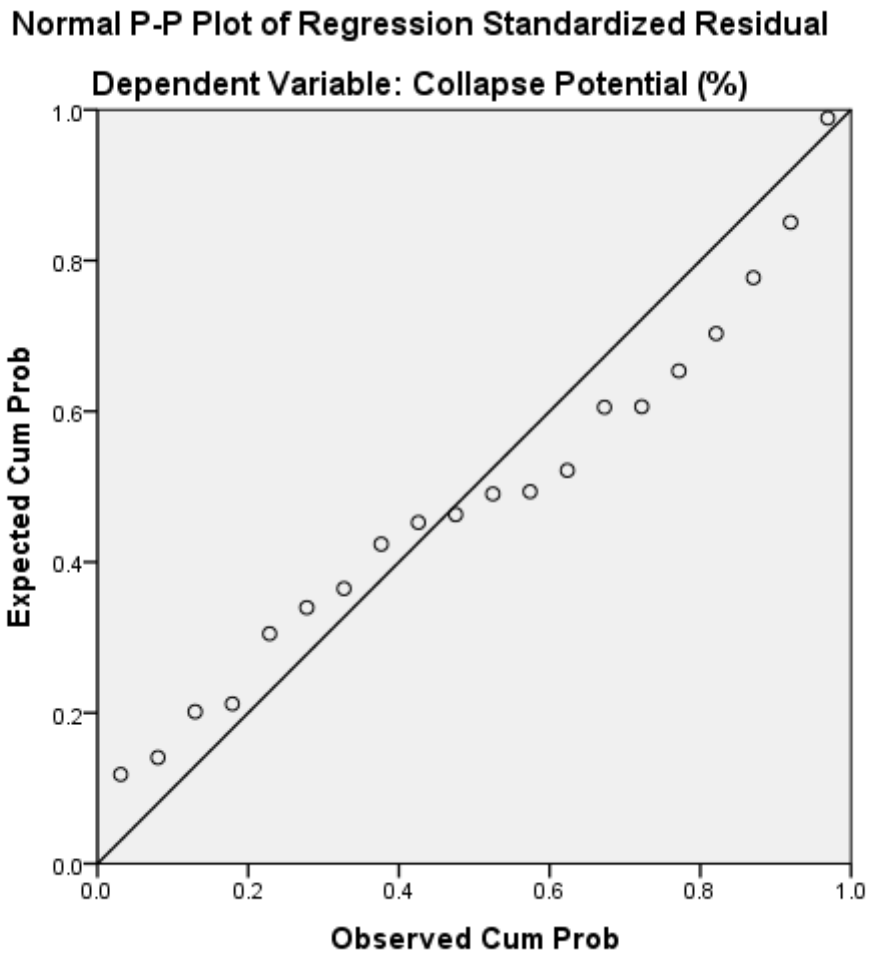

Figure D.1.f.2: Normal P-P Plot of the Triaxial and Sieve *model regression*

Table D.1.f.2: Triaxial and Sieve *model Coefficients*

Coefficients

Model		Unstandardized Coefficients		Standardized Coefficients			95.0% Confidence Interval for B		Correlations			Collinearity Statistics	
		B	Std. Error	Beta	t	Sig.	Lower Bound	Upper Bound	Zero-order	Partial	Part	Tolerance	VIF
1	(Constant)	-11.132	34.887		-.319	.755	-87.145	64.881					
	Difference between As-compacted Sr and Inundated Sr	-5.287	21.364	-.142	-.247	.809	-51.836	41.262	.368	-.071	-.051	.130	7.685
	Initial Moisture Content (%)	-1.142	1.701	-.667	-.671	.515	-4.849	2.565	-.306	-.190	-.139	.043	23.015
	Max deviator stress at 70kPa	.032	.030	1.045	1.041	.319	-.035	.098	.552	.288	.215	.043	23.508
	Internal friction angle (degrees)	-.376	.355	-.822	-1.059	.310	-1.149	.397	.482	-.292	-.219	.071	14.047
	Cohesion (kN/m2)	-.046	.076	-.225	-.611	.553	-.211	.118	.245	-.174	-.127	.316	3.160
	Percentage fines (%)	.361	.226	1.226	1.599	.136	-.131	.853	.330	.419	.331	.073	13.700
	Coeff of Uniformity	.116	.121	.608	.958	.357	-.148	.381	-.321	.267	.198	.106	9.394

a. Dependent Variable: Collapse Potential (%)

1.g Compactive Variables Model

Table D.1.g.1: Compactive Variables *model Summary*

Model Summary

Model	R	R Square	Adjusted R Square	Std. Error of the Estimate	Change Statistics				
					R Square Change	F Change	df1	df2	Sig. F Change
1	.659[a]	.434	.233	6.08925	.434	2.151	5	14	.119

a. Predictors: (Constant), Percentage fines (%), Difference between As-compacted Sr and Inundated Sr, Initial Dry density (g/cm3), Initial degree of saturation (%), Initial Moisture Content (%)

b. Dependent Variable: Collapse Potential (%)

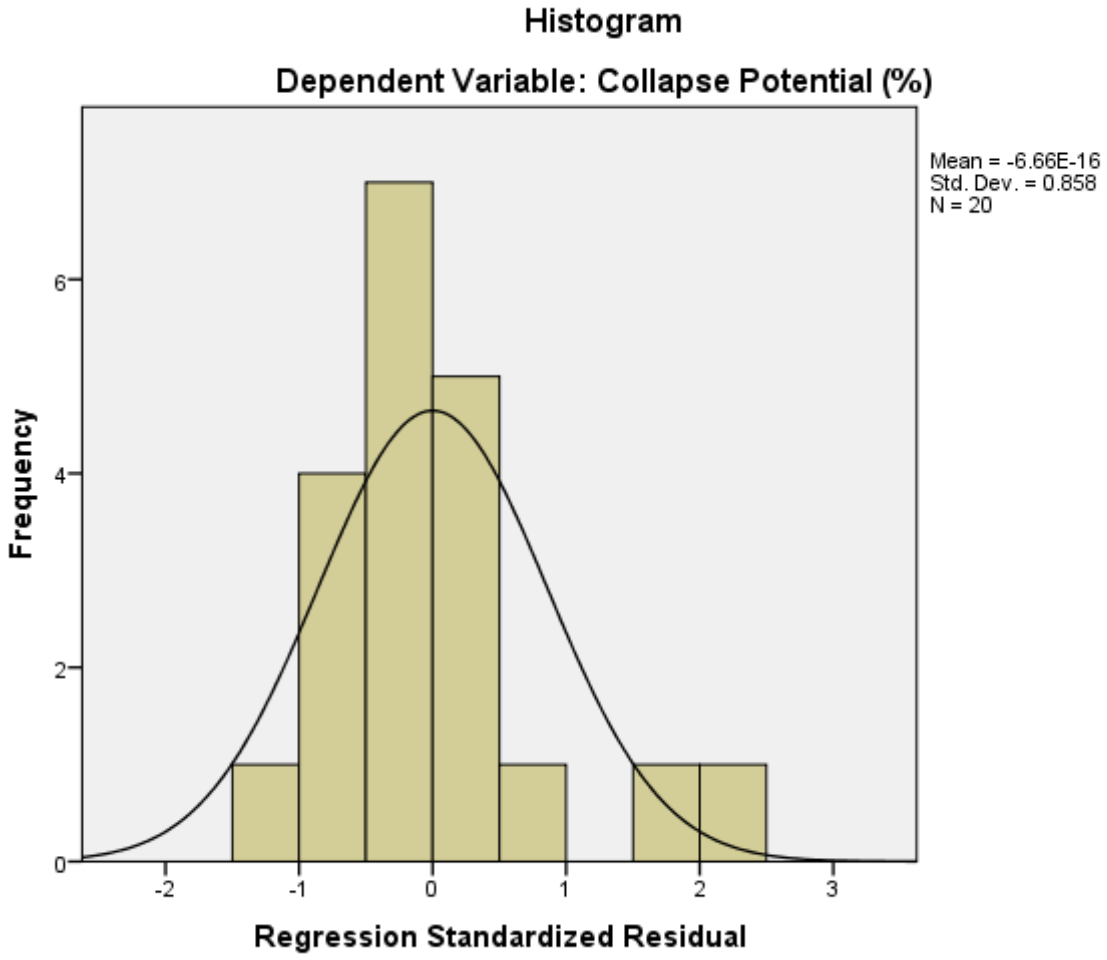

Figure D.1.g.1: Histogram of the Compactive Variables *model regression*

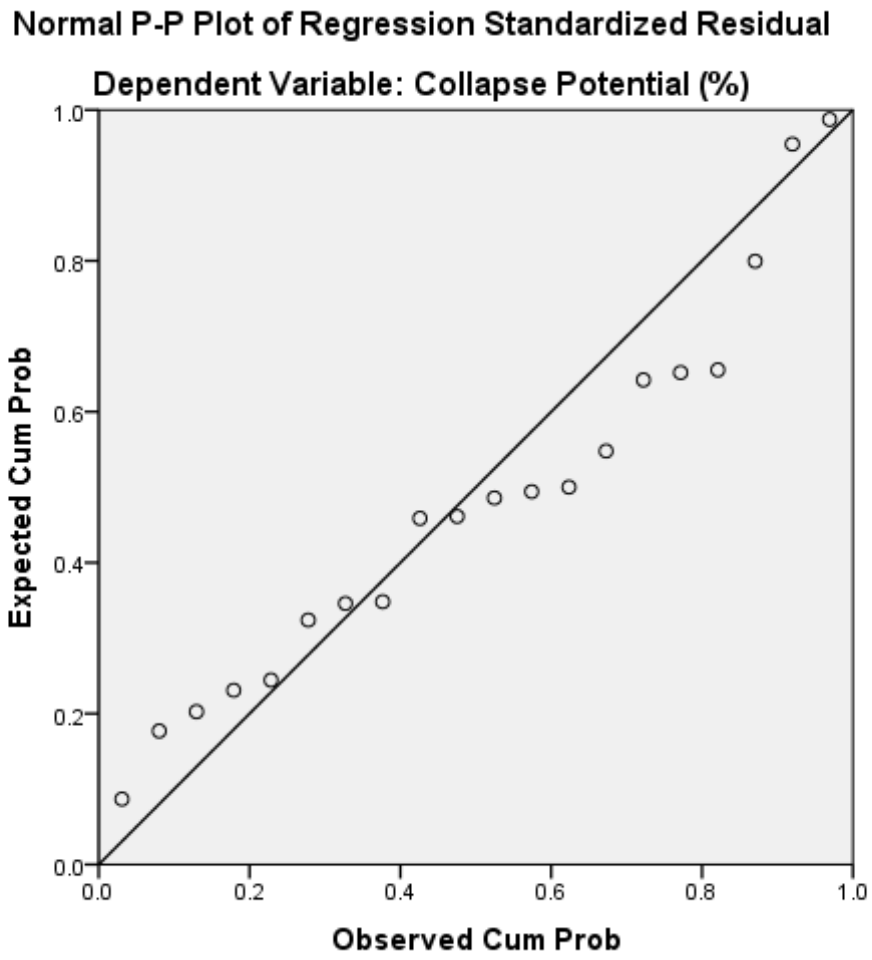

Figure D.1.g.2: Normal P-P Plot of the Compactive Variables *model regression*

Table D.1.g.2: Compactive Variables *model Coefficients*

Coefficients

Model		Unstandardized Coefficients		Standardized Coefficients			95.0% Confidence Interval for B		Correlations			Collinearity Statistics	
		B	Std. Error	Beta	t	Sig.	Lower Bound	Upper Bound	Zero-order	Partial	Part	Tolerance	VIF
1	(Constant)	64.835	152.660		.425	.678	-262.587	392.257					
	Difference between As-compacted Sr and Inundated Sr	-23.881	20.761	-.642	-1.150	.269	-68.409	20.646	.368	-.294	-.231	.130	7.705
	Initial Moisture Content (%)	-1.603	3.631	-.936	-.442	.666	-9.390	6.184	-.306	-.117	-.089	.009	111.271
	Initial Dry density (g/cm3)	-21.530	82.803	-.268	-.260	.799	-199.125	156.065	-.231	-.069	-.052	.038	26.367
	Initial degree of saturation (%)	-.107	.816	-.243	-.131	.898	-1.856	1.643	-.440	-.035	-.026	.012	85.602
	Percentage fines (%)	.192	.098	.652	1.970	.069	-.017	.401	.330	.466	.396	.368	2.716

a. Dependent Variable: Collapse Potential (%)

2. Formula generation - A combination of laboratory data and past researcher's data – Sieve parameter based

2.a Sieve Model

Table D.2.a.1: Sieve model Summary

Model Summary

Model	R	R Square	Adjusted R Square	Std. Error of the Estimate	Change Statistics				
					R Square Change	F Change	df1	df2	Sig. F Change
1	.766[a]	.586	.522	4.79811	.586	9.077	5	32	.000

a. Predictors: (Constant), Coeff of Uniformity, Initial degree of saturation (%), Percentage fines (%), Difference between As-compacted Sr and Inundated Sr, Initial Moisture Content (%)

b. Dependent Variable: Collapse Potential (%)

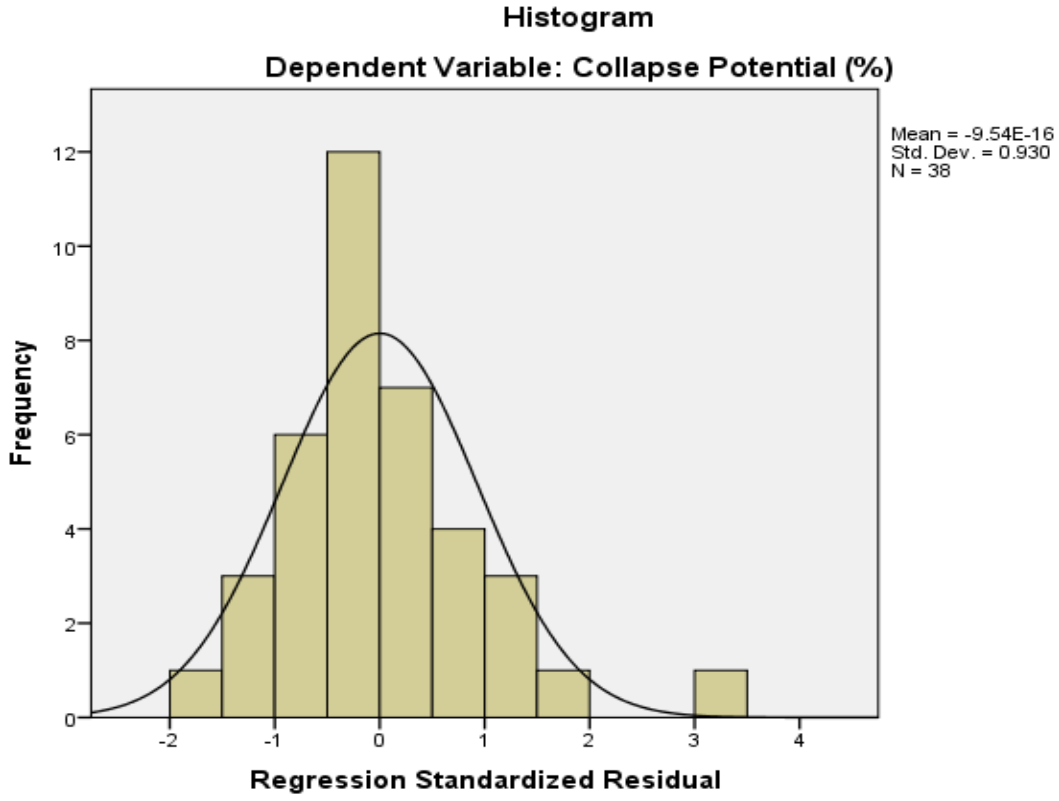

Figure D.2.a.1: Histogram of the Sieve model regression

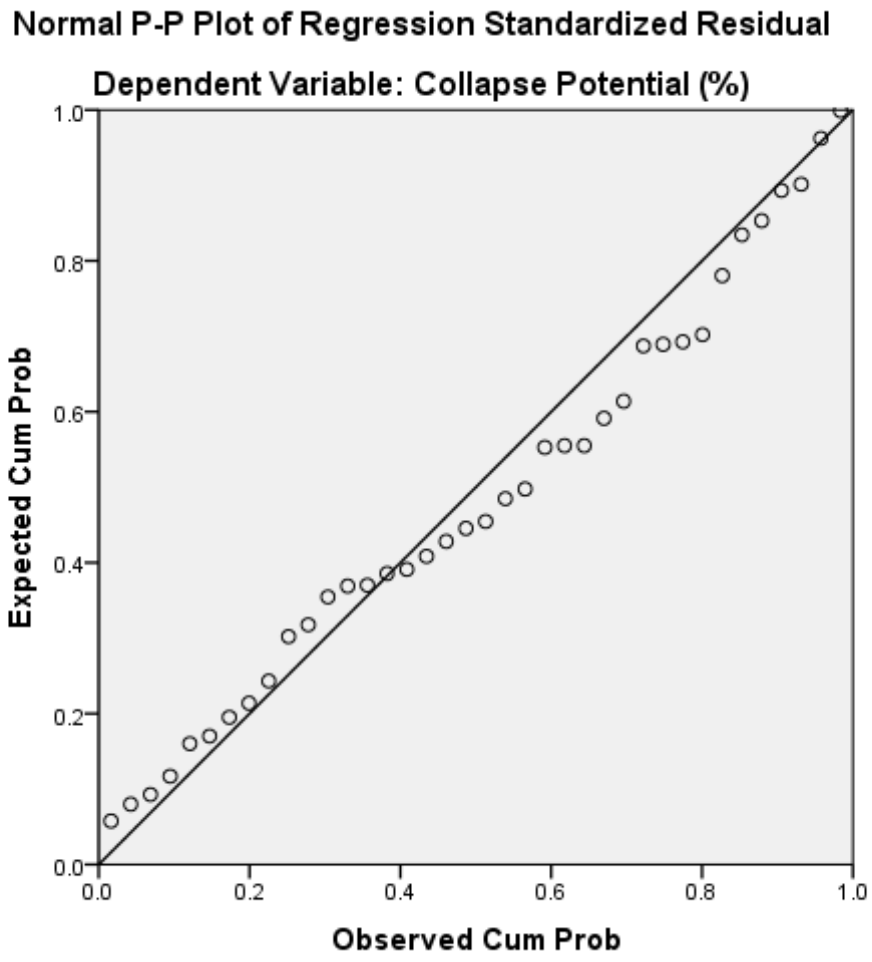

Figure D.2.a.2: Normal P-P Plot of the Sieve model regression

Table D.2.a.2: Sieve model Coefficients

Coefficients[a]

Model		Unstandardized Coefficients		Standardized Coefficients			95.0% Confidence Interval for B		Correlations			Collinearity Statistics	
		B	Std. Error	Beta	t	Sig.	Lower Bound	Upper Bound	Zero-order	Partial	Part	Tolerance	VIF
1	(Constant)	17.558	5.131		3.398	.002	6.986	27.890					
	Difference between As-compacted Sr and Inundated Sr	-10.637	5.464	-.458	-1.947	.060	-21.768	.494	.362	-.325	-.221	.234	4.278
	Initial degree of saturation (%)	-.183	.046	-.737	-4.014	.000	-.276	-.090	-.537	-.579	-.456	.383	2.608
	Initial Moisture Content (%)	-.783	.394	-.560	-1.988	.055	-1.585	.019	-.394	-.332	-.226	.163	6.141
	Percentage fines (%)	.198	.042	.736	4.746	.000	.113	.282	.187	.643	.539	.538	1.860
	Coeff of Uniformity	.000	.001	.065	.543	.591	-.001	.002	-.019	.096	.062	.897	1.115

a. Dependent Variable: Collapse Potential (%)

2.b Sieve (without Cu) Model

Table D.2.b.1: Sieve (without Cu) *model Summary*

Model Summary

Model	R	R Square	Adjusted R Square	Std. Error of the Estimate	Change Statistics				
					R Square Change	F Change	df1	df2	Sig. F Change
1	.763[a]	.583	.532	4.74659	.583	11.519	4	33	.000

a. Predictors: (Constant), Percentage fines (%), Difference between As-compacted Sr and Inundated Sr, Initial degree of saturation (%), Initial Moisture Content (%)

b. Dependent Variable: Collapse Potential (%)

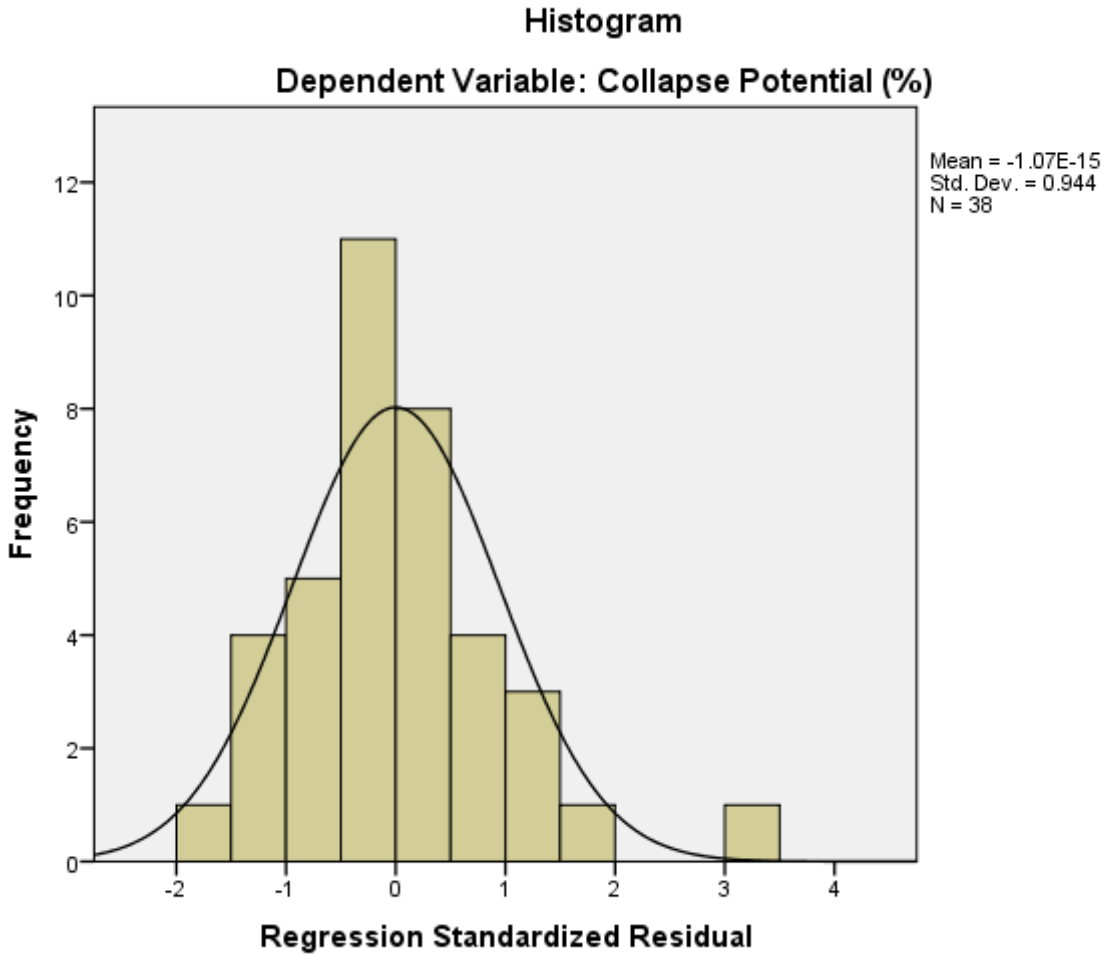

Figure D.2.b.1: Histogram of the Sieve (without Cu) *model regression*

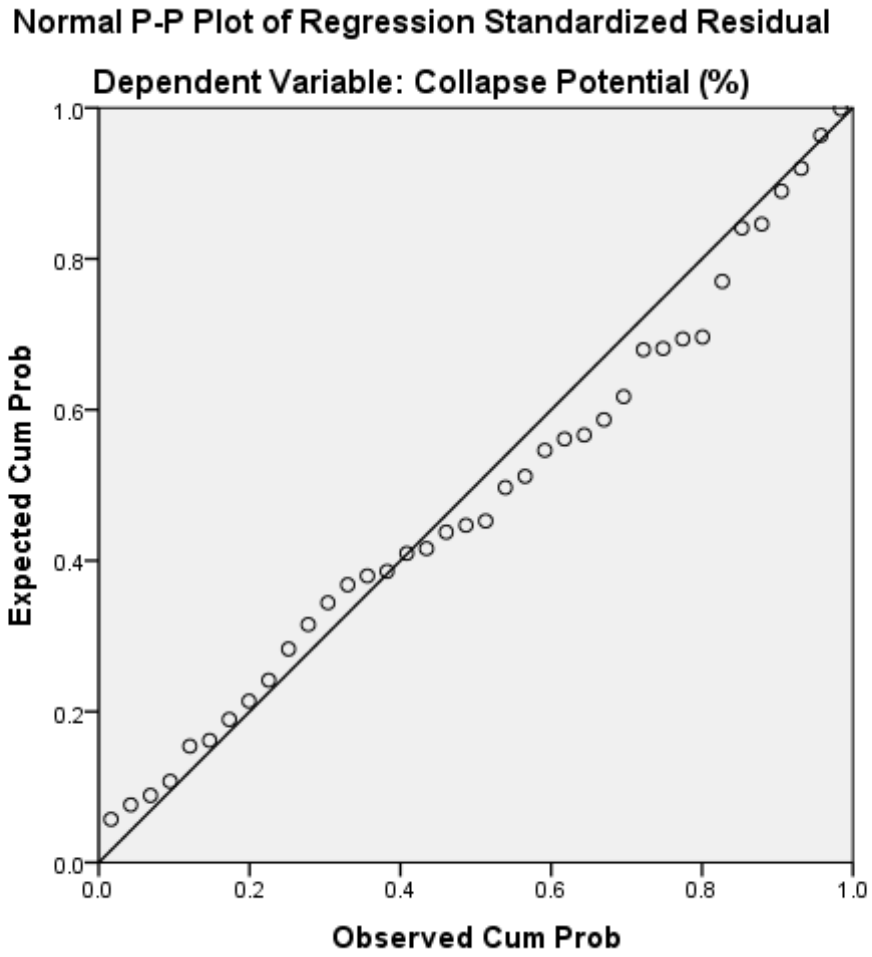

Figure D.2.b.2: Normal P-P Plot of the Sieve (without Cu) *model regression*

Table D.2.b.2: Sieve (without Cu) *model Coefficients*

Coefficients

Model		Unstandardized Coefficients		Standardized Coefficients			95.0% Confidence Interval for B		Correlations			Collinearity Statistics	
		B	Std. Error	Beta	t	Sig.	Lower Bound	Upper Bound	Zero-order	Partial	Part	Tolerance	VIF
1	(Constant)	17.498	5.075		3.448	.002	7.173	27.824					
	Difference between As-compacted Sr and Inundated Sr	-10.142	5.330	-.436	-1.903	.066	-20.986	.702	.362	-.314	-.214	.240	4.159
	Initial degree of saturation (%)	-.179	.044	-.721	-4.021	.000	-.269	-.088	-.537	-.573	-.452	.394	2.539
	Initial Moisture Content (%)	-.781	.389	-.559	-2.005	.053	-1.573	.012	-.394	-.329	-.225	.163	6.141
	Percentage fines (%)	.193	.040	.717	4.794	.000	.111	.274	.187	.641	.539	.565	1.770

a. Dependent Variable: Collapse Potential (%)

2.c Atterberg Model

Table D.2.c.1: Atterberg *model Summary*

Model Summary

Model	R	R Square	Adjusted R Square	Std. Error of the Estimate	Change Statistics				
					R Square Change	F Change	df1	df2	Sig. F Change
1	.764[a]	.584	.500	4.91334	.584	7.008	6	30	.000

a. Predictors: (Constant), Plastic Limit (%), Difference between As-compacted Sr and Inundated Sr, Percentage fines (%), Initial degree of saturation (%), Liquid Limit (%), Initial Moisture Content (%)

b. Dependent Variable: Collapse Potential (%)

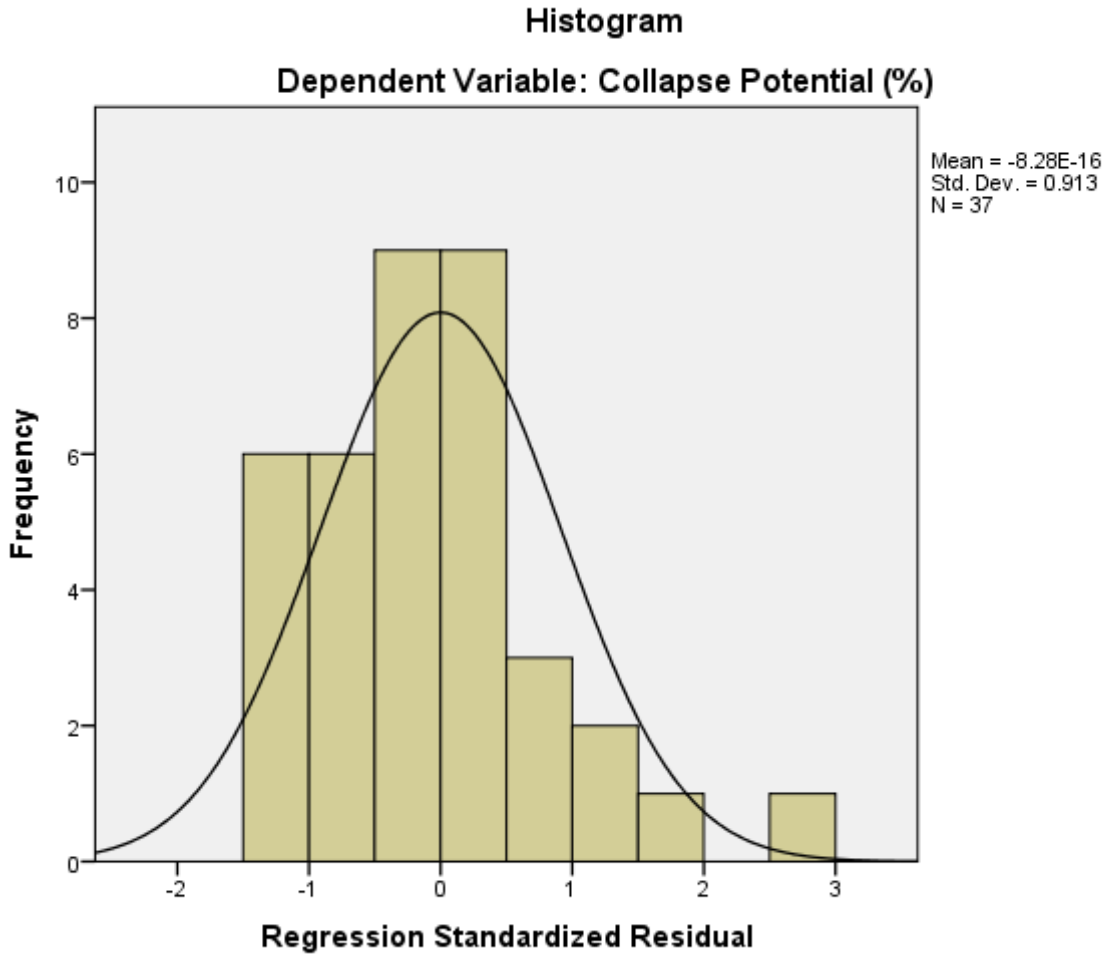

Figure D.2.c.1: Histogram of the Atterberg *model regression*

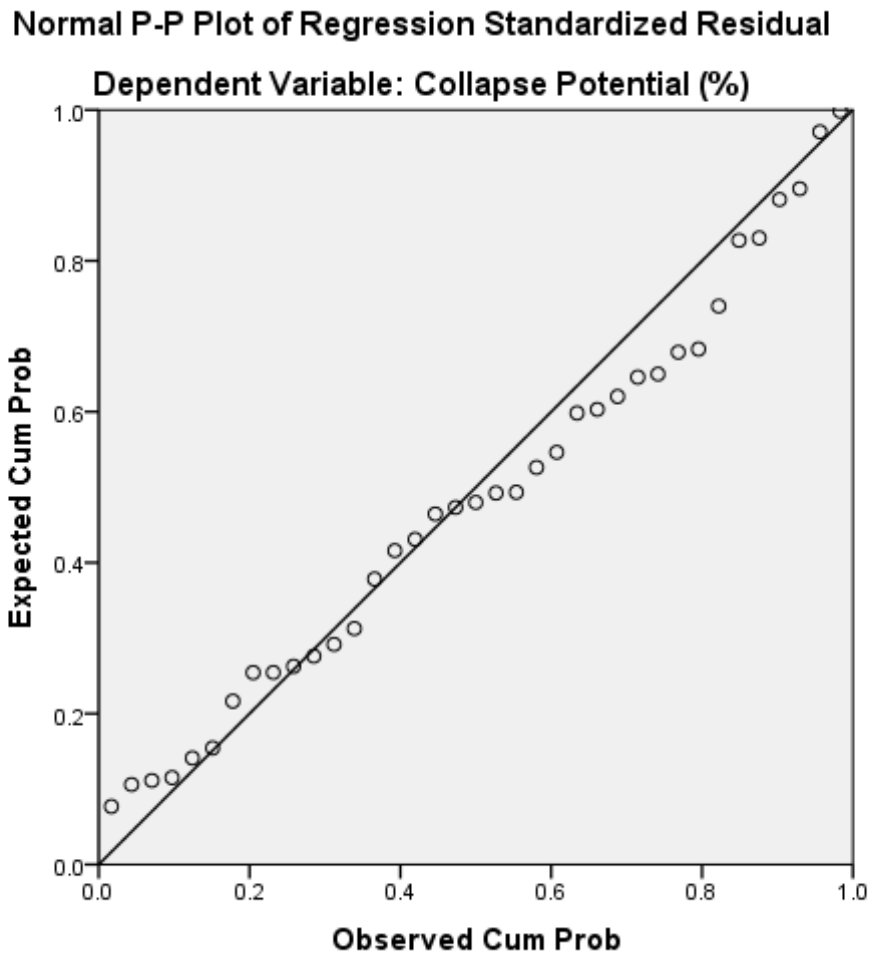

Figure D.2.c.2: Normal P-P Plot of the Atterberg *model regression*

Table D.2.c.2: Atterberg *model Coefficients*

Coefficients[a]

Model		Unstandardized Coefficients		Standardized Coefficients			95.0% Confidence Interval for B		Correlations			Collinearity Statistics	
		B	Std. Error	Beta	t	Sig.	Lower Bound	Upper Bound	Zero-order	Partial	Part	Tolerance	VIF
1	(Constant)	19.244	6.522		2.951	.006	5.925	32.564					
	Difference between As-compacted Sr and Inundated Sr	-11.977	5.966	-.522	-2.007	.054	-24.162	.208	.367	-.344	-.237	.206	4.863
	Initial degree of saturation (%)	-.176	.047	-.715	-3.776	.001	-.271	-.081	-.531	-.568	-.445	.387	2.583
	Initial Moisture Content (%)	-.863	.420	-.624	-2.055	.049	-1.721	-.006	-.389	-.351	-.242	.151	6.636
	Percentage fines (%)	.199	.050	.748	3.954	.000	.096	.302	.176	.585	.466	.388	2.578
	Liquid Limit (%)	.155	.199	.155	.781	.441	-.251	.562	.230	.141	.092	.353	2.833
	Plastic Limit (%)	-.250	.300	-.164	-.833	.411	-.862	.362	.090	-.150	-.098	.359	2.786

a. Dependent Variable: Collapse Potential (%)

2.d Compactive Variables

Table D.2.d.1: Compactive Variables *model Summary*

Model Summary[b]

Model	R	R Square	Adjusted R Square	Std. Error of the Estimate	Change Statistics				
					R Square Change	F Change	df1	df2	Sig. F Change
1	.793[a]	.629	.571	4.54230	.629	10.869	5	32	.000

a. Predictors: (Constant), Percentage fines (%), Initial Dry density (g/cm3), Difference between As-compacted Sr and Inundated Sr, Initial degree of saturation (%), Initial Moisture Content (%)

b. Dependent Variable: Collapse Potential (%)

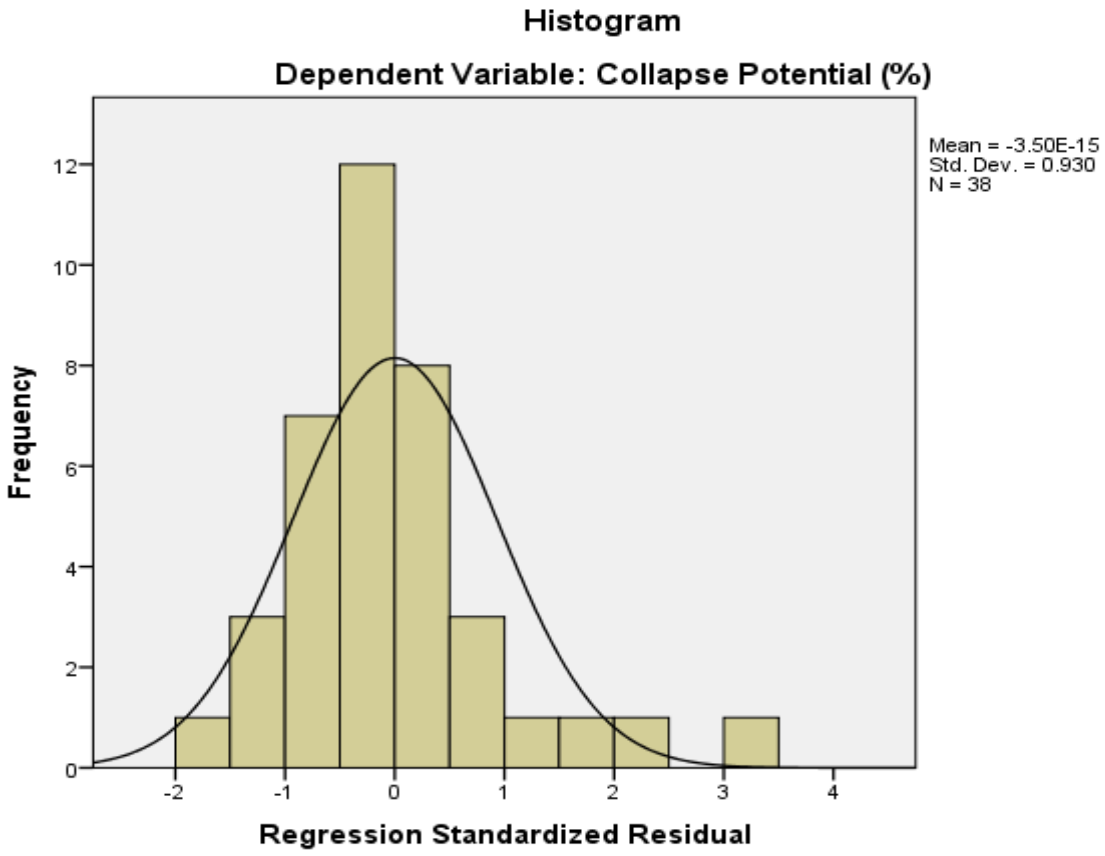

Figure D.2.d.1: Histogram of the Compactive Variables *model regression*

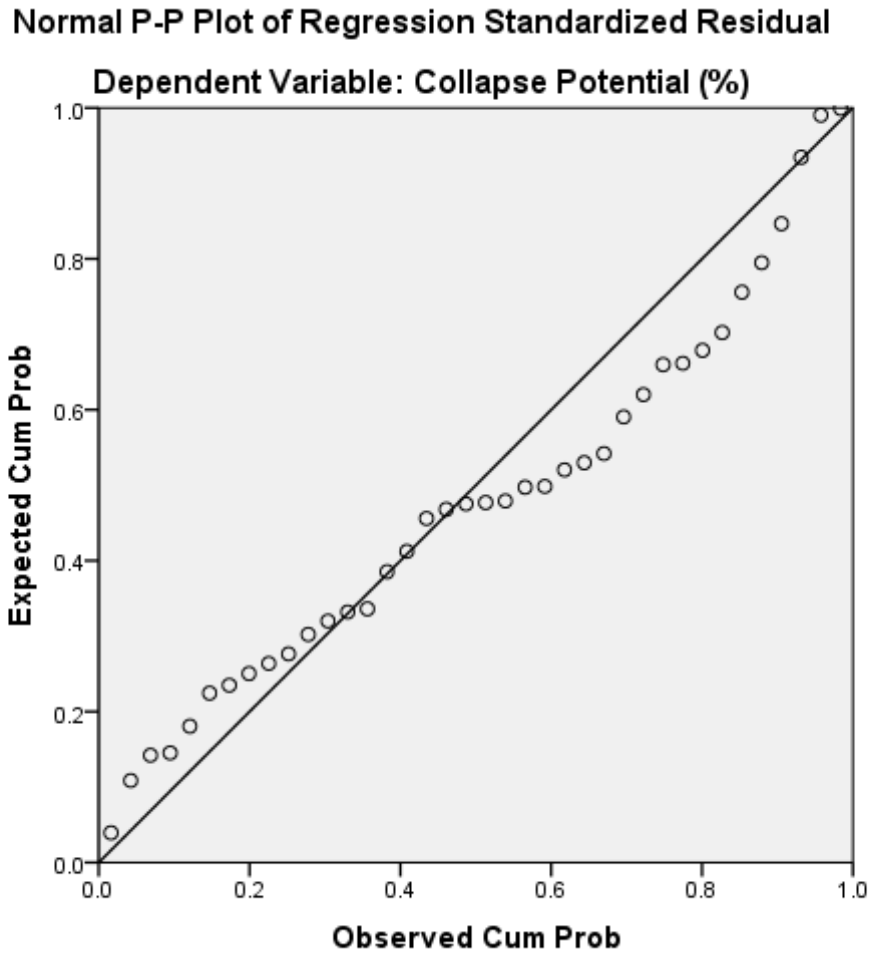

Figure D.2.d.2: Normal P-P Plot of the Compactive Variables *model regression*

Table D.2.d.2: Compactive Variables *model Coefficients*

Coefficients[a]

Model		Unstandardized Coefficients		Standardized Coefficients			95.0% Confidence Interval for B		Correlations			Collinearity Statistics	
		B	Std. Error	Beta	t	Sig.	Lower Bound	Upper Bound	Zero-order	Partial	Part	Tolerance	VIF
1	(Constant)	61.366	22.371		2.743	.010	15.797	106.935					
	Difference between As-compacted Sr and Inundated Sr	-19.411	6.878	-.835	-2.822	.008	-33.420	-5.401	.362	-.446	-.304	.132	7.562
	Initial degree of saturation (%)	-.034	.084	-.136	-.403	.690	-.204	.137	-.537	-.071	-.043	.102	9.851
	Initial Moisture Content (%)	-1.623	.561	-1.161	-2.893	.007	-2.766	-.480	-.394	-.455	-.311	.072	13.916
	Initial Dry density (g/cm3)	-21.575	10.741	-.522	-2.009	.053	-43.453	.302	-.543	-.335	-.216	.171	5.835
	Percentage fines (%)	.170	.040	.634	4.249	.000	.089	.252	.187	.601	.457	.521	1.919

a. Dependent Variable: Collapse Potential (%)

3. Formula generation - A combination of Lab data and past researcher's data – Compaction parameter based

3.a Compaction and Atterberg Model

Table D.3.a.1: Compaction and Atterberg *model Summary*

Model Summary

Model	R	R Square	Adjusted R Square	Std. Error of the Estimate	Change Statistics				
					R Square Change	F Change	df1	df2	Sig. F Change
1	.810[a]	.656	.545	4.68901	.656	5.923	9	28	.000

a. Predictors: (Constant), Initial degree of saturation (%), Plastic Limit (%), Plasticity Index (%), Maximum Dry density (g/cm3), Initial Moisture Content (%), Percentage fines (%), Optimum Moisture Content (%), Difference between As-compacted Sr and Inundated Sr, Relative Moisture content (%)

b. Dependent Variable: Collapse Potential (%)

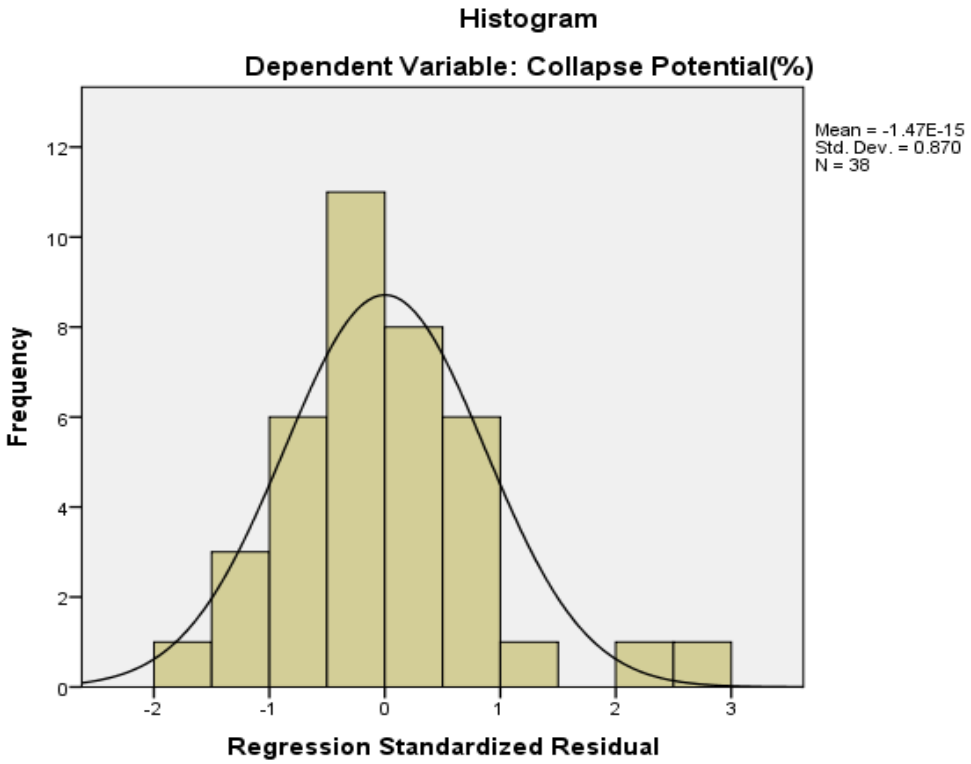

Figure D.3.a.1: Histogram of the Compaction and Atterberg *model regression*

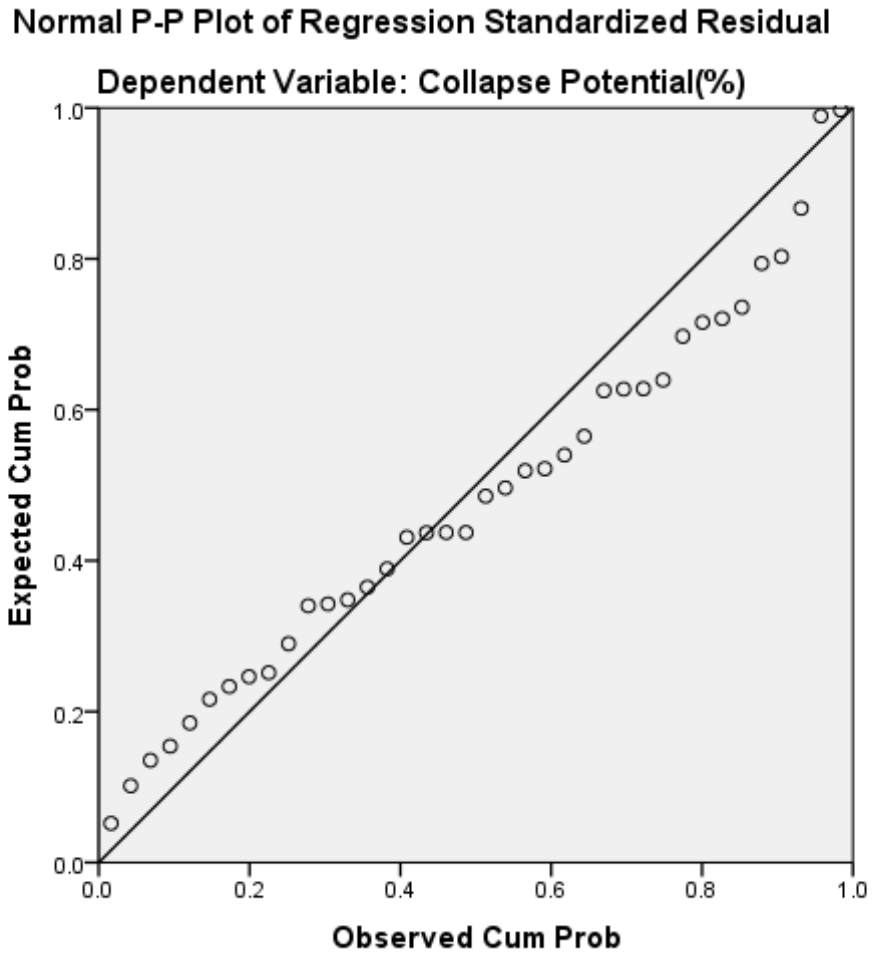

Figure D.3.a.2: Normal P-P Plot of the Compaction and Atterberg *model regression*

Table D.3.a.2: Compaction and Atterberg *model Coefficients*

Model		Unstandardized Coefficients		Standardized Coefficients			95.0% Confidence Interval for B		Correlations			Collinearity Statistics	
		B	Std. Error	Beta	t	Sig.	Lower Bound	Upper Bound	Zero-order	Partial	Part	Tolerance	VIF
1	(Constant)	18.282	18.178		1.006	.323	-18.954	55.518					
	Difference between As-compacted Sr and Inundated Sr	-25.402	13.186	-1.070	-1.927	.064	-52.412	1.607	.599	-.342	-.214	.040	25.065
	Initial Moisture Content (%)	-1.194	.887	-.859	-1.346	.189	-3.012	.623	-.519	-.247	-.149	.030	33.109
	Percentage fines (%)	.211	.126	.618	1.667	.107	-.048	.470	.204	.300	.185	.089	11.185
	Maximum Dry density (g/cm3)	.008	.212	.007	.037	.971	-.426	.442	.364	.007	.004	.376	2.659
	Optimum Moisture Content (%)	2.007	1.031	.913	1.946	.062	-.106	4.119	.247	.345	.216	.056	17.920
	Relative Moisture content (%)	.168	.153	.728	1.099	.281	-.145	.480	-.643	.203	.122	.028	35.720
	Plastic Limit (%)	-.936	.834	-.383	-1.123	.271	-2.645	.772	.261	-.208	-.125	.106	9.476
	Plasticity Index (%)	.036	.267	.053	.135	.893	-.512	.584	.107	.026	.015	.079	12.580
	Initial degree of saturation (%)	-.476	.167	-1.591	-2.852	.008	-.817	-.134	-.665	-.474	-.316	.040	25.316

a. Dependent Variable: Collapse Potential(%)

3.b Compaction + Atterberg (without MDD)

Table D.3.b.1: Compaction and Atterberg (without MDD) *model Summary*

Model Summary

Model	R	R Square	Adjusted R Square	Std. Error of the Estimate	Change Statistics				
					R Square Change	F Change	df1	df2	Sig. F Change
1	.810[a]	.656	.561	4.60757	.656	6.901	8	29	.000

a. Predictors: (Constant), Initial degree of saturation (%), Plastic Limit (%), Liquid Limit (%), Initial Moisture Content (%), Percentage fines (%), Optimum Moisture Content (%), Difference between As-compacted Sr and Inundated Sr, Relative Moisture content (%)

b. Dependent Variable: Collapse Potential(%)

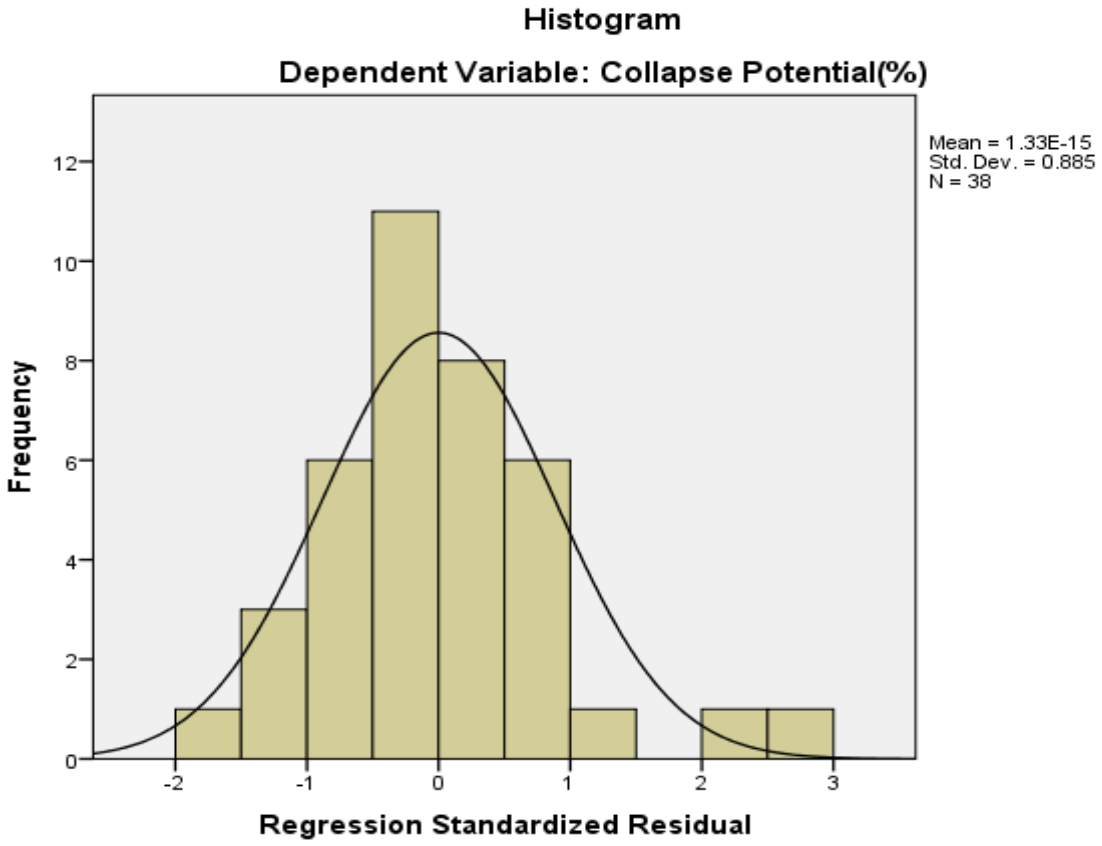

Figure D.3.b.1: Histogram of the Compaction and Atterberg (without MDD) *model regression*

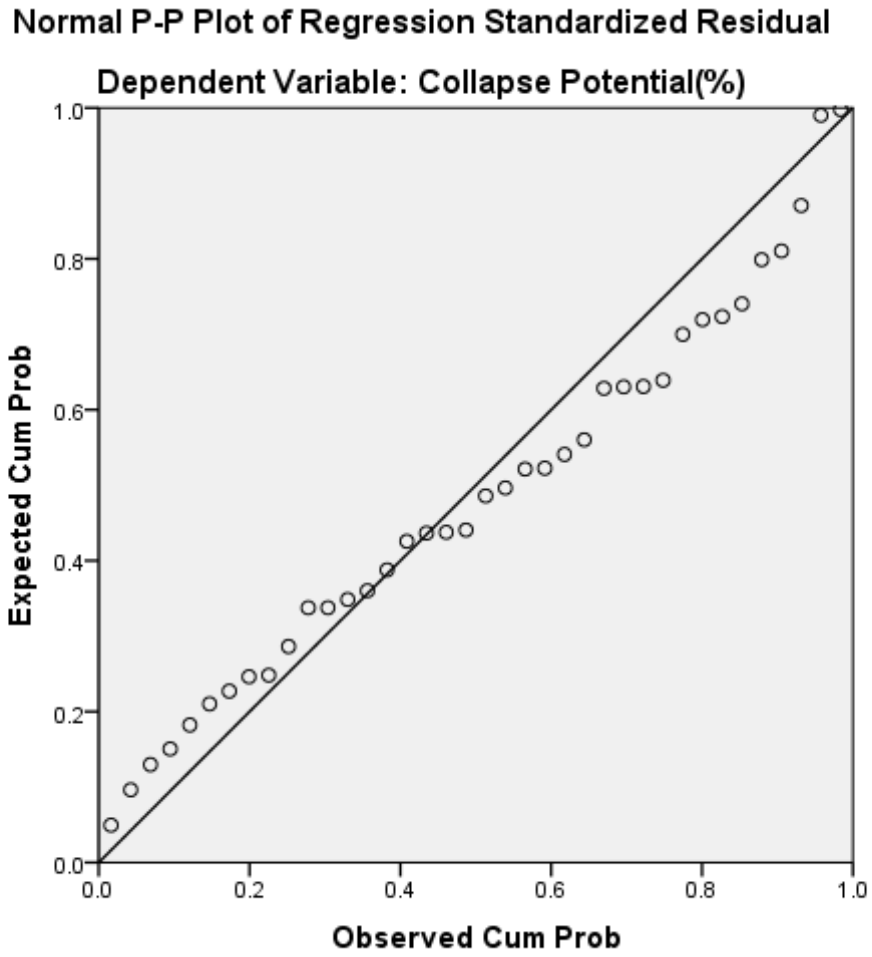

Figure D.3.b.2: Normal P-P Plot of the Compaction and Atterberg (without MDD) *model regression*

Table D.3.b.2: Compaction and Atterberg (without MDD) *model Coefficients*

Coefficients

Model		Unstandardized Coefficients		Standardized Coefficients	t	Sig.	95.0% Confidence Interval for B		Correlations			Collinearity Statistics	
		B	Std. Error	Beta			Lower Bound	Upper Bound	Zero-order	Partial	Part	Tolerance	VIF
1	(Constant)	18.281	17.862		1.023	.315	-18.252	54.813					
	Difference between As-compacted Sr and Inundated Sr	-25.203	11.835	-1.061	-2.130	.042	-49.408	-.998	.599	-.368	-.232	.048	20.913
	Initial Moisture Content (%)	-1.192	.868	-.857	-1.372	.181	-2.968	.585	-.519	-.247	-.150	.030	32.860
	Percentage fines (%)	.210	.122	.616	1.715	.097	-.040	.460	.204	.303	.187	.092	10.862
	Optimum Moisture Content (%)	1.995	.963	.908	2.070	.047	.024	3.965	.247	.359	.226	.062	16.198
	Relative Moisture content (%)	.166	.146	.723	1.142	.263	-.132	.464	-.643	.207	.124	.030	33.709
	Liquid Limit (%)	.035	.262	.056	.135	.894	-.500	.571	.168	.025	.015	.070	14.375
	Plastic Limit (%)	-.963	.894	-.394	-1.077	.290	-2.791	.866	.261	-.196	-.117	.089	11.281
	Initial degree of saturation (%)	-.474	.156	-1.585	-3.042	.005	-.792	-.155	-.665	-.492	-.331	.044	22.868

a. Dependent Variable: Collapse Potential (%)

3.c Atterberg (+%fines)

Table D.3.c.1: Atterberg *model Summary*

Model Summary

Model	R	R Square	Adjusted R Square	Std. Error of the Estimate	Change Statistics				
					R Square Change	F Change	df1	df2	Sig. F Change
1	.785[a]	.616	.546	4.63792	.616	8.808	6	33	.000

a. Predictors: (Constant), Liquid Limit (%), Percentage fines (%), Initial degree of saturation (%), Plastic Limit (%), Initial Moisture Content (%), Difference between As-compacted Sr and Inundated Sr

b. Dependent Variable: Collapse Potential (%)

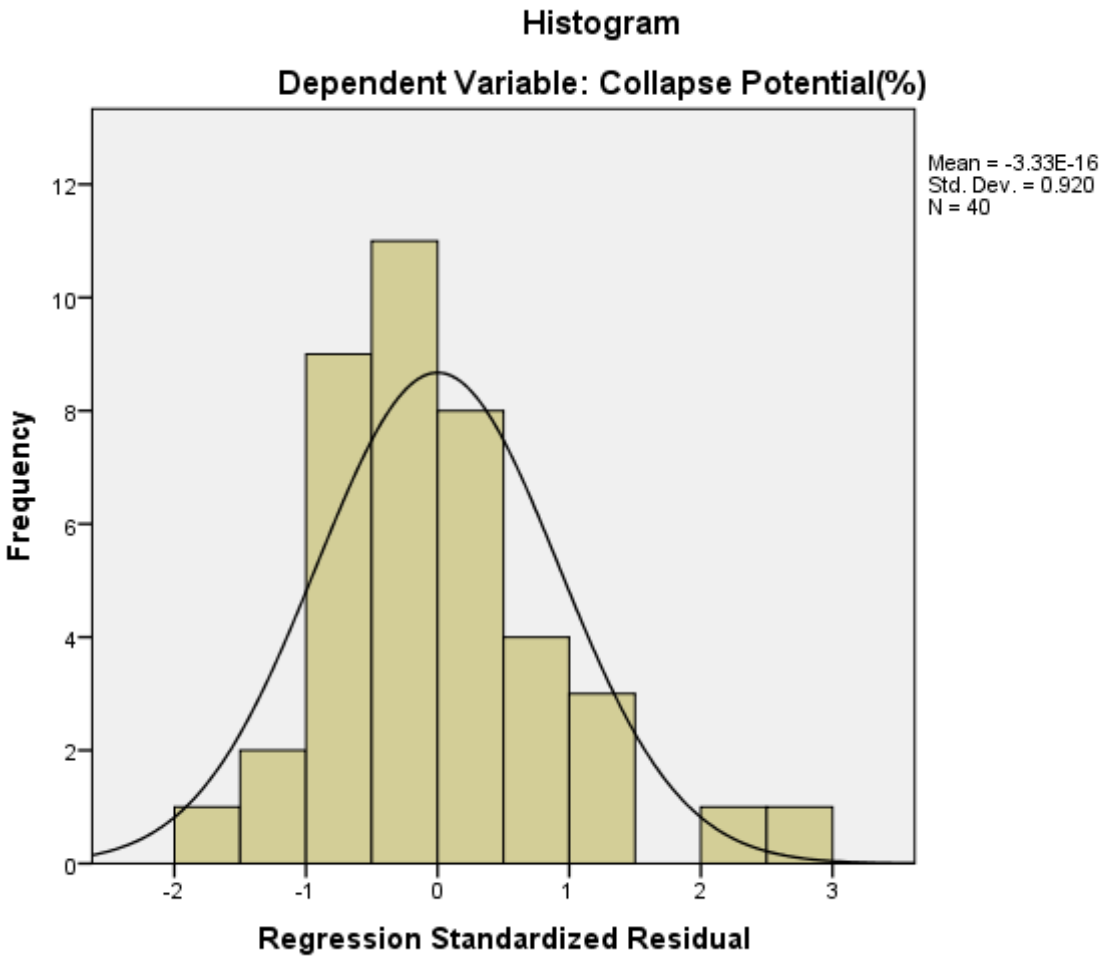

Figure D.3.c.1: Histogram of the Atterberg *model regression*

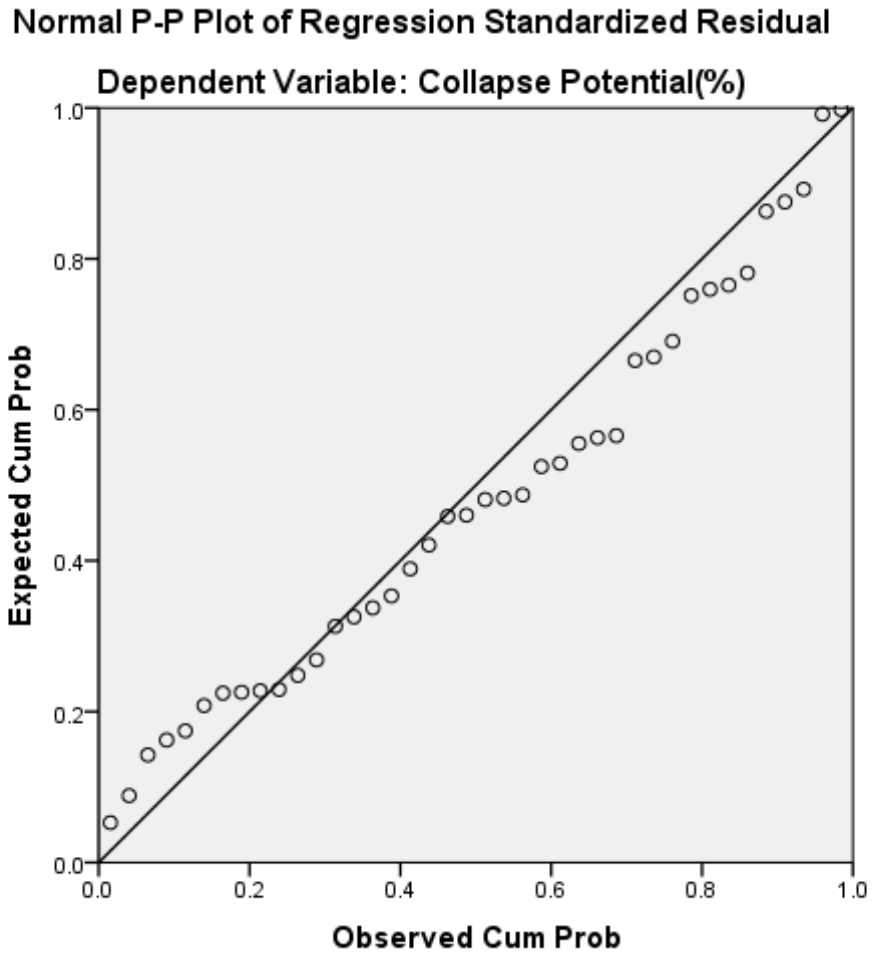

Figure D.3.c.2: Normal P-P Plot of the Atterberg *model regression*

Table D.3.c.2: Atterberg *model Coefficients*

Coefficients

Model		Unstandardized Coefficients		Standardized Coefficients			95.0% Confidence Interval for B		Correlations			Collinearity Statistics	
		B	Std. Error	Beta	t	Sig.	Lower Bound	Upper Bound	Zero-order	Partial	Part	Tolerance	VIF
1	(Constant)	28.250	10.946		2.581	.014	5.979	50.521					
	Difference between As-compacted Sr and Inundated Sr	-20.748	10.654	-.892	-1.947	.060	-42.423	.928	.520	-.321	-.210	.056	18.003
	Initial Moisture Content (%)	-.127	.344	-.095	-.368	.715	-.827	.574	-.422	-.064	-.040	.174	5.734
	Percentage fines (%)	.159	.045	.541	3.541	.001	.068	.250	.265	.525	.382	.499	2.005
	Plastic Limit (%)	-.271	.365	-.114	-.741	.464	-1.014	.473	.230	-.128	-.080	.492	2.032
	Initial degree of saturation (%)	-.428	.149	-1.461	-2.875	.007	-.732	-.125	-.586	-.448	-.310	.045	22.168
	Liquid Limit (%)	.216	.108	.341	1.993	.055	-.004	.436	.196	.328	.215	.397	2.519

a. Dependent Variable: Collapse Potential (%)

3.d Compactive Variables Model

Table D.3.d.1: Compactive Variables *model Summary*

Model Summary

Model	R	R Square	Adjusted R Square	Std. Error of the Estimate	Change Statistics				
					R Square Change	F Change	df1	df2	Sig. F Change
1	.794[a]	.630	.576	4.48209	.630	11.584	5	34	.000

a. Predictors: (Constant), Difference between As-compacted Sr and Inundated Sr, Percentage fines (%), Initial Dry density (g/cm3), Initial Moisture Content (%), Initial degree of saturation (%)

b. Dependent Variable: Collapse Potential(%)

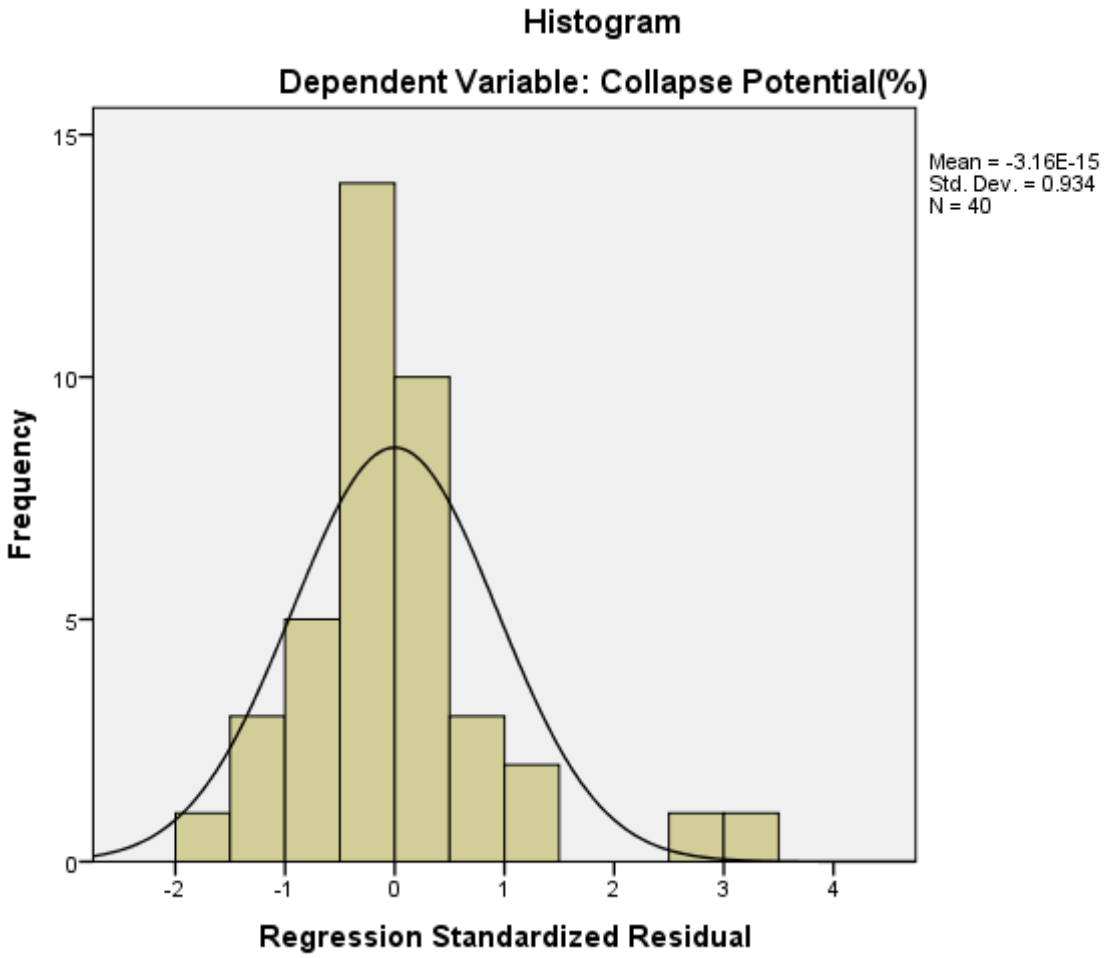

Figure D.3.d.1: Histogram of the Compactive Variables *model regression*

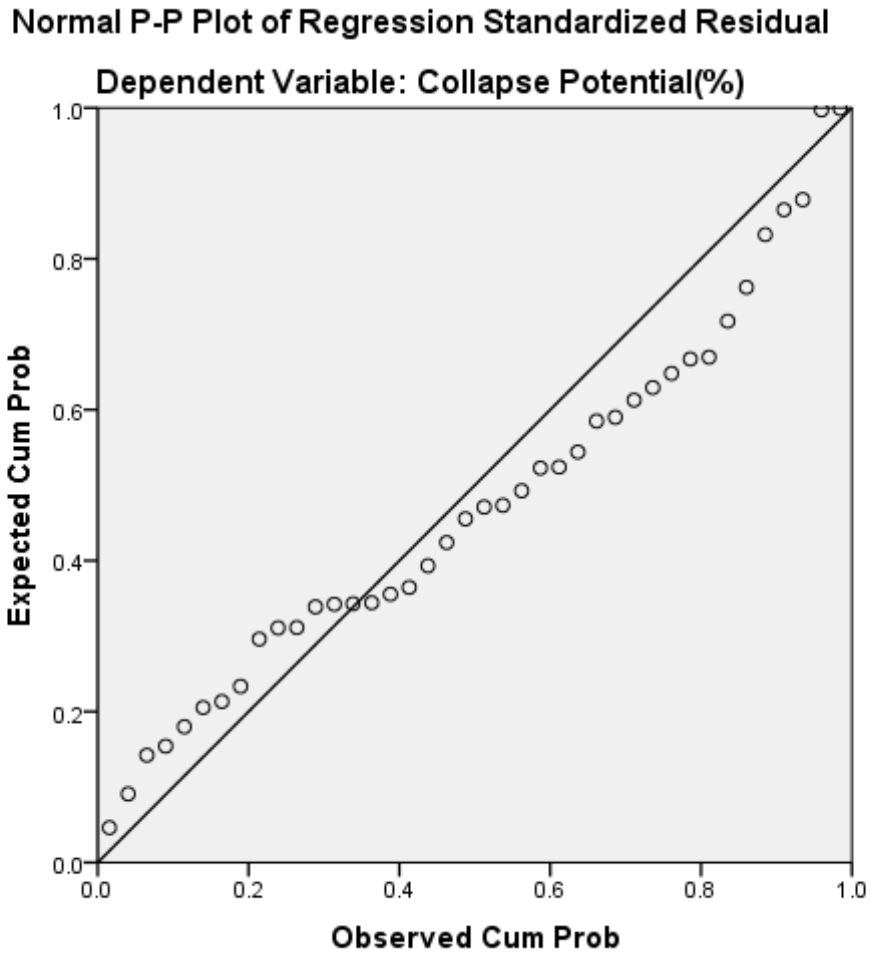

Figure D.3.d.2: Normal P-P Plot of the Compactive Variables *model regression*

Table D.3.c.2: Compactive Variables *model Coefficients*

Coefficients

Model	Unstandardized Coefficients		Standardized Coefficients			95.0% Confidence Interval for B		Correlations			Collinearity Statistics	
	B	Std. Error	Beta	t	Sig.	Lower Bound	Upper Bound	Zero-order	Partial	Part	Tolerance	VIF
1 (Constant)	75.083	24.086		3.117	.004	26.134	124.032					
Percentage fines (%)	.129	.033	.441	3.961	.000	.063	.196	.265	.562	.413	.877	1.141
Initial Moisture Content (%)	-1.104	.634	-.830	-1.743	.090	-2.392	.183	-.422	-.286	-.182	.048	20.822
Initial Dry density (g/cm3)	-27.330	11.558	-.829	-2.365	.024	-50.819	-3.842	-.459	-.376	-.247	.088	11.300
Initial degree of saturation (%)	-.149	.180	-.508	-.826	.414	-.515	.217	-.586	-.140	-.086	.029	34.740
Difference between As-compacted Sr and Inundated Sr	-23.009	10.246	-.989	-2.246	.031	-43.831	-2.186	.520	-.359	-.234	.056	17.829

a. Dependent Variable: Collapse Potential (%)